NEW PERSPECTIVES IN BENTHIC-PELAGIC COUPLING IN MARINE AND TRANSITIONAL COASTAL AREAS

EDITED BY: Tamara Cibic, Martina Orlando-Bonaca and Fernando Rubino
PUBLISHED IN: Frontiers in Marine Science

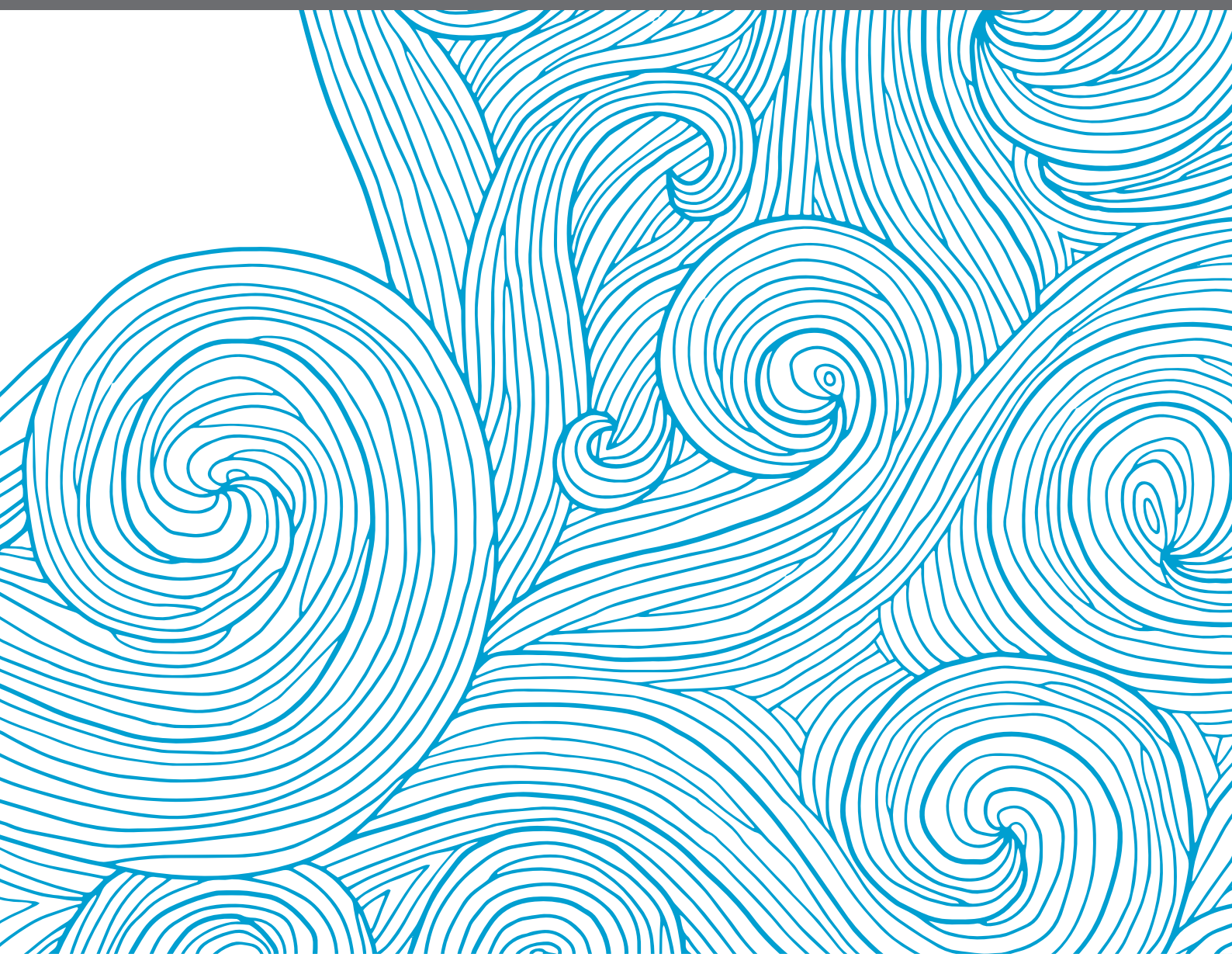

frontiers Research Topics

frontiers

ISSN 1664-8714
ISBN 978-2-83250-170-2
DOI 10.3389/978-2-83250-170-2

About Frontiers

Frontiers is more than just an open-access publisher of scholarly articles: it is a pioneering approach to the world of academia, radically improving the way scholarly research is managed. The grand vision of Frontiers is a world where all people have an equal opportunity to seek, share and generate knowledge. Frontiers provides immediate and permanent online open access to all its publications, but this alone is not enough to realize our grand goals.

Frontiers Journal Series

The Frontiers Journal Series is a multi-tier and interdisciplinary set of open-access, online journals, promising a paradigm shift from the current review, selection and dissemination processes in academic publishing. All Frontiers journals are driven by researchers for researchers; therefore, they constitute a service to the scholarly community. At the same time, the Frontiers Journal Series operates on a revolutionary invention, the tiered publishing system, initially addressing specific communities of scholars, and gradually climbing up to broader public understanding, thus serving the interests of the lay society, too.

Dedication to Quality

Each Frontiers article is a landmark of the highest quality, thanks to genuinely collaborative interactions between authors and review editors, who include some of the world's best academicians. Research must be certified by peers before entering a stream of knowledge that may eventually reach the public - and shape society; therefore, Frontiers only applies the most rigorous and unbiased reviews.
Frontiers revolutionizes research publishing by freely delivering the most outstanding research, evaluated with no bias from both the academic and social point of view. By applying the most advanced information technologies, Frontiers is catapulting scholarly publishing into a new generation.

What are Frontiers Research Topics?

Frontiers Research Topics are very popular trademarks of the Frontiers Journals Series: they are collections of at least ten articles, all centered on a particular subject. With their unique mix of varied contributions from Original Research to Review Articles, Frontiers Research Topics unify the most influential researchers, the latest key findings and historical advances in a hot research area! Find out more on how to host your own Frontiers Research Topic or contribute to one as an author by contacting the Frontiers Editorial Office: frontiersin.org/about/contact

NEW PERSPECTIVES IN BENTHIC-PELAGIC COUPLING IN MARINE AND TRANSITIONAL COASTAL AREAS

Topic Editors:
Tamara Cibic, Istituto Nazionale di Oceanografia e di Geofisica Sperimentale (Italy), Italy
Martina Orlando-Bonaca, National Institute of Biology (Slovenia), Slovenia
Fernando Rubino, National Research Council (CNR), Italy

Citation: Cibic, T., Orlando-Bonaca, M., Rubino, F., eds. (2022). New Perspectives in Benthic-Pelagic Coupling in Marine and Transitional Coastal Areas. Lausanne: Frontiers Media SA. doi: 10.3389/978-2-83250-170-2

Table of Contents

frontiers | Frontiers in Marine Science

TYPE Editorial
PUBLISHED 25 August 2022
DOI 10.3389/fmars.2022.1009078

OPEN ACCESS

EDITED AND REVIEWED BY
Angel Borja,
Technological Center Expert in Marine and Food Innovation (AZTI), Spain

*CORRESPONDENCE
Tamara Cibic
tcibic@ogs.it

SPECIALTY SECTION
This article was submitted to Marine Ecosystem Ecology, a section of the journal Frontiers in Marine Science

RECEIVED 01 August 2022
ACCEPTED 12 August 2022
PUBLISHED 25 August 2022

CITATION
Cibic T, Orlando-Bonaca M and Rubino F (2022) Editorial: New perspectives in benthic-pelagic coupling in marine and transitional coastal areas. *Front. Mar. Sci.* 9:1009078. doi: 10.3389/fmars.2022.1009078

Editorial: New perspectives in benthic-pelagic coupling in marine and transitional coastal areas

Tamara Cibic[1]*, Martina Orlando-Bonaca[2] and Fernando Rubino[3]

[1]National Institute of Oceanography and Applied Geophysics - OGS, Oceanography Section, Trieste, Italy, [2]National Institute of Biology, Marine Biology Station, Piran, Slovenia, [3]Water Research Institute, Unit Talassografico "A. Cerruti", National Research Council CNR-IRSA, Taranto, Italy

KEYWORDS

marine coastal environment, plankton, benthos, life cycle, biological processes, ecosystem functioning, ecosystem services

Editorial on the Research Topic
New perspectives in benthic-pelagic coupling in marine and transitional coastal areas

Shallow environments and transitional habitats are among the world's most productive ecosystems (Odum, 1983; Cloern et al., 2014) where light penetration to the bottom and nutrient availability fuel multiple primary producers including phytoplankton, benthic microalgae, macroalgae and seagrasses (Kirk, 2000; Sundbäck et al., 2000; Sala et al., 2012; Papathanasiou et al., 2015; Orfanidis et al., 2021) that sustain higher trophic levels and provide important ecosystem services (Barbier et al., 2011; Queirós et al., 2019). In these ecosystems, pelagos and benthos have been classically studied as distinct domains of the marine environment, although they cannot be considered as separate entities (Boero et al., 1996; Marcus & Boero, 1998). The compartmentalization of these ecosystems into their benthic and pelagic components in experimental studies and models often limits our understanding of the scope and strength of interactions between these habitats, their role in maintaining the ecosystem function, and their sensitivity to future change (Griffiths et al., 2017). The benthic–pelagic coupling involves all those processes that connect the bottom and water column habitats through the exchange of mass, energy, and nutrients. Matter and energy flow between the two domains in both directions, along food webs, involving the movement of planktonic and benthic organisms at different life stages (Kiljunen et al., 2020). Indeed, many physical, chemical and biological processes bind these two domains, where benthic-pelagic coupling concurs to maintain high rates of primary production and decomposition (Kennish et al., 2014). While primary producers compete for the same resources (light and nutrients), benthic filter feeders are well adapted to efficiently filter bacteria, phytoplankton and zooplankton, dissolved organic matter

(Hughes et al., 2005; Karuza et al., 2016), as well as pollutants from the water column (Giandomenico et al., 2016). An in-depth knowledge of the life cycles of meroplanktonic species is an indispensable prerequisite for understanding the functioning of the ecosystem in shallow areas. Besides this, benthic primary producers and invertebrates provide several ecosystem services and drive important processes such as nutrient cycling, bio-irrigation and organic matter decomposition in coastal areas (Bremner et al., 2006; Olsgard et al., 2008).

Lately, efforts have increased to describe and understand the diversity of processes that couple benthic and pelagic habitats, especially those mediated by biota (Griffiths et al., 2017), but many aspects of the "benthic-pelagic unicum" are still to be discovered. Moreover, anthropogenic pressures like organic enrichment, eutrophication, hypoxia events and contamination (Mozetič et al., 2012), are increasingly affecting the status and functioning of these highly biodiverse, shallow water environments (Kennish et al., 2014). Given the pressing goal of sustainable management of natural marine resources, there is an urgent need to advance our knowledge of the overall picture of processes and flows between pelagos and benthos.

This Research Topic aims to update the current knowledge on benthic-pelagic coupling in shallow marine and transitional waters, covering recent investigations on biologically mediated processes that interconnect benthic and pelagic habitats. The Research Topic comprises a collection of 9 contributions, 8 of which include original research and one is a review article.

One paper is focused on the function and structure of eukaryotic phototrophs. In the publication by Cibic et al., the benthic and pelagic contributions to total primary production were estimated experimentally at a 17-m deep site in the Gulf of Trieste, northern Adriatic Sea. The authors found that the mean benthic contribution to the total primary production was 11.3% but reached 43% when phytoplankton in the water column was scarce. Further, they reported that the seasonal development of pelagic and benthic phototrophs and primary production was more affected by nutrients availability than the physical variables, except for the surface layer of the water column where temperature and salinity were the main drivers.

Two articles present data on angiosperms and macrophytes, and their use as bioindicators to assess the environmental status of coastal areas, formerly or still affected by eutrophication and hypoxia events. In the paper by Sfriso et al. the latest results on the environmental recovery of aquatic angiosperms in the Venice Lagoon and their net primary production are presented. A decrease of anthropogenic impacts, such as eutrophication and clam harvesting, favored a sharp decline of Ulvaceae that were replaced by species of higher ecological value. Surveys carried out by the authors in 2021 revealed that the recolonization of aquatic angiosperms is further expanding, leading to increased biodiversity and production of both macroalgae and aquatic angiosperms, and improving the overall ecological conditions of the Venice Lagoon. In the second article, Gerakaris et al. used a large dataset from three Mediterranean sub-basins (Adriatic, Ionian and Aegean Seas) with different trophic conditions to investigate, on a large scale, the coupled responses of benthic and pelagic primary producers (phytoplankton as Chl *a*, and macrophytes) to eutrophication. Their results show that increasing nutrient concentrations lead to increased coverage of opportunistic macroalgal species at the expense of canopy-forming species. Further, structural traits of *Posidonia oceanica* showed opposite trends to increasing levels of pressure indicators such as ammonium, nitrate, phosphate, Chl-*a*, and light attenuation. Overall, they found that the coupling of pelagic and benthic primary producers across trophic gradients showed consistent patterns at subregional scales.

The next two articles cover the aspects on the life cycle of some specific planktonic organisms, on their dormant phase or the subsequent germination/rejuvenation stages. In the paper by Ishii et al., the life cycle strategies of centric diatoms from a shallow area of Ago Bay (central Japan) were studied using the plankton emergence trap/chamber (PET chamber). The authors compared their experimental data on geminated/rejuvenated cells to the vegetative cells sampled in the water column but did not find a clear relationship. Their findings indicate that the magnitude of the vegetative population depends on the vegetative cells' growth rather than on the recruitment of cells from the surface sediment. They also proposed different patterns of life cycle strategies of centric diatoms in shallow coastal waters. The article by Dzhembekova et al. investigated the distribution of some cyst morphotypes of the dinoflagellate *Scrippsiella acuminata* in surface sediments of the Black Sea. The authors followed a basin scale approach, collecting samples from 34 sites, and linked the spatial distribution and abundance of cyst morphotypes to some selected physical and chemical variables measured in the water column. They found that salinity, temperature, and nutrients, particularly nitrates and phosphates, were the most important drivers of the occurrence, density, and geographical distribution of *Scrippsiella acuminata* in the Black Sea.

The article by Matsuoka et al. reports on the marine environmental changes induced by anthropogenic activities recorded in the sediments of Beppu Bay, western Japan, by analyzing the palynomorph assemblages (microfossils of dinoflagellate cysts and other planktonic organisms with organic walls). The authors' stratigraphic analysis of these assemblages preserved in the sediments, together with the age determination of the cores, revealed a rapid eutrophication due to anthropogenic activities from the mid-1960s in the area, that induced the most drastic change in the biota over the past 1000 years in Beppu Bay.

The next paper relates to the use of foraminifera as bioindicators in a contaminated port area. Rožič et al. applied a multiparametric approach to link the geoenvironmental variables in the sediments of the Bay of Koper (north-eastern

Adriatic Sea) to the benthic foraminifera assemblage. They reported moderate to high species diversity, and a dominance of pollution tolerant species. Their findings revealed a possible influence of some potentially toxic heavy metals on the foraminifera diversity and taxonomic composition. The authors further evaluated the ecological status by using the Foram-AMBI and EcoQs indices; the first highlighted a good to moderate quality of ecological conditions, whereas the second a high to poor ecological status.

The review article by Dimitriou et al. is a synthesis of the results of the project HYPOXIA "Benthic–pelagic coupling and regime shifts". The aim of this project was to investigate how nutrient input in the water column leads to ecological processes of eutrophication, which may in turn lead to significant, irreversible changes in the eastern Mediterranean ecosystems. The project included analysis of historical water and benthos data, field sampling, and mesocosm experiments. After reanalyzing the project results, the authors reported that, unlike other regions of the world, eutrophication did not cause water hypoxia or benthic dead zones in the eastern Mediterranean coastal ecosystems. They concluded that this region shows high resilience to the adverse effects of eutrophication, preventing hypoxia and azoic conditions when eutrophication is the only source of environmental disturbance.

The last paper presents the main outputs of the food web modelling in two areas of the northern Ionian Sea. The study by Ricci et al. investigated the contribution of intermediate and high trophic level species to benthic-pelagic coupling in a region subjected to large-scale oceanographic changes, e.g., the Adriatic-Ionian Bimodal Oscillating Systems (BiOS), that might result in relevant spatial and temporal changes in the benthic-pelagic coupling. The authors' findings highlight the pivotal role of deep faunal communities, in which demersal and benthopelagic species sustain upward energy flows towards the pelagic domain and shelf faunal communities. They also reported that temporal changes driven by BiOS affect the trophic state of the deep communities resulting in considerable variations in their amount of consumption flows.

In summary, this Research Topic contributes to the advancement of our knowledge of biologically mediated processes that interconnect shallow-water benthic and pelagic habitats. These sensitive ecosystems are often subjected to management policies designed to improve their ecological status, or to enhance the ecosystem services they provide. Yet, the environmental quality targets and the ecosystem approach to the management of these ecosystems are often based upon the current compartmentalization of benthic and pelagic habitats. Environmental quality indicators, such as those used in the European Water Framework Directive (WFD; Directive 2000/60/EC) and the Marine Strategy Framework Directive (MSFD; EU Directive 2008/56/EC), commonly describe the status of pelagic or benthic habitats separately. However, many anthropogenic activities affect fundamental benthic–pelagic linkages and disrupt the flow of ecosystem services in shallow coastal and transitional ecosystems (Griffiths et al., 2017). Thus, understanding the interdependence between benthos and pelagos, and the processes involved in the benthic-pelagic unicum, is pivotal to help maintain the function of these shallow water ecosystems and ensure the services they will continue providing under increasing anthropogenic pressure. Therefore, it is of paramount importance to consider benthic and pelagic habitats as a unicum and include them as such in future management frameworks.

Author contributions

TC: conceptualization, original draft, editing; MO-B and FR: conceptualization, writing, review. All authors contributed to the article and approved the submitted version.

Acknowledgments

We thank the contributing authors, reviewers, and the editorial staff at Frontiers in Marine Science for their support in producing this Research Topic.

Conflict of interest

The authors declare that the research was conducted in the absence of any commercial or financial relationships that could be construed as a potential conflict of interest.

Publisher's note

References

Barbier, E. B., Hacker, S. D., Kennedy, C., Koch, E. W., Stier, A. C., and Silliman, B. R. (2011). The value of estuarine and coastal ecosystem services. *Ecol. Monogr.* 81 (2), 169–193. doi: 10.1890/10-1510.1

Boero, F., Belmonte, G., Fanelli, G., Piraino, S., and Rubino, F. (1996). The continuity of living matter and the discontinuities of its constituents: Do plankton and benthos really exist? *Trends Ecol. Evol.* 11, 177–180. doi: 10.1016/0169-5347(96)20007-2

Bremner, J., Rogers, S. I., and Frid, C. L. J. (2006). Methods for describing ecological functioning of marine benthic assemblages using biological traits analysis (BTA). *Ecol. Indicat.* 6, 609–622. doi: 10.1016/j.ecolind.2005.08.026

Cloern, J. E., Foster, S. Q., and Kleckner, A. E. (2014). Phytoplankton primary production in the world's estuarine-coastal ecosystems. *Biogeosciences* 11, 2477–2501. doi: 10.5194/bg-11-2477-2014

Giandomenico, S., Cardellicchio, N., Spada, L., Annicchiarico, C., and Di Leo, A. (2016). Metals and PCB levels in some edible marine organisms from the Ionian Sea: dietary intake evaluation and risk for consumers. *Environ. Sci. Pollut. Res.* 23, 12596–12612. doi: 10.1007/s11356-015-5280-2

Griffiths, J. R., Kadin, M., Nascimento, F. J. A., Tamelander, T., Törnroos, A., Bonaglia, S., et al. (2017). The importance of benthic–pelagic coupling for marine ecosystem functioning in a changing world. *Global Change Biol.* 23, 2179–2196. doi: 10.1111/gcb.13642

Hughes, D. J., Cottier-Cook, E. J., and Sawyer, M. D. (2005). "Biofiltration and biofouling on artificial structures in Europe: the potential for mitigating organic impacts," in *Oceanography and marine biology, an annual review*, vol. 43 . Eds. R. N. Gibson, R. J. A. Atkinson and J. D. M. Gordon (Boca Raton: CRC press), 123–172.

Karuza, A., Caroppo, C., Camatti, E., Di Poi, E., Monti, M., Stabili, L., et al. (2016). 'End to end' planktonic trophic web and its implications for the mussel farms in the mar piccolo of taranto (Ionian Sea, Italy). *Environ. Sci. Pollut. Res.* 23, 12707–12724. doi: 10.1007/s11356-015-5621-1

Kennish, M., Brush, M., and Moore, K. (2014). Drivers of change in shallow coastal photic systems: An introduction to a special issue. *Estuaries Coasts* 37, 3–19. doi: 10.1007/s12237-014-9779-4

Kiljunen, M., Peltonen, H., Lehtiniemi, M., Uusitalo, L., Sinisalo, T., Norkko, J., et al. (2020). Benthic-pelagic coupling and trophic relationships in northern Baltic Sea food webs. *Limnol. Oceanogr.* 65, 1706–1722. doi: 10.1002/lno.11413

Kirk, J. T. O. (2000). *Light and photosynthesis in aquatic ecosystems* (U.K.: Cambridge University Press), 509 pp.

Marcus, N. H., and Boero, F. (1998). Minireview: the importance of benthic-pelagic coupling and the forgotten role of life cycles in coastal aquatic systems. *Limnol. Oceanography* 43, 763–768. doi: 10.4319/lo.1998.43.5.0763

Mozetič, P., Francé, J., Kogovšek, T., Talaber, I., and Malej, A. (2012). Plankton trends and community changes in a coastal sea (northern adriatic): bottom-up vs. top-down control in relation to environmental drivers. *Estuar. Coast. Shelf. Sci.* 115, 138–148. doi: 10.1016/j.ecss.2012.02.009

Odum, E. P. (1983). *Basic ecology* (Philadelphia: Saunders College Pub.), 613 pp.

Olsgard, F., Schaanning, M. T., Widdicombe, S., Kendall, M. A., and Austen, M. C. (2008). Effects of bottom trawling on ecosystem functioning. *J. Exp. Mar. Biol. Ecol.* 366, 123–133. doi: 10.1016/j.jembe.2008.07.036

Orfanidis, S., Rindi, F., Cebrian, E., Fraschetti, S., Nasto, I., Taskin, E., et al. (2021). Effects of natural and anthropogenic stressors on fucalean brown seaweeds across different spatial scales in the Mediterranean Sea. *Front. Mar. Sci.* 8. doi: 10.3389/fmars.2021.658417

Papathanasiou, V., Orfanidis, S., and Brown, M. T. (2015). Intra-specific responses of *Cymodocea nodosa* to macro-nutrient, irradiance and copper exposure. *J. Exp. Mar. Biol. Ecol.* 469, 113–122. doi: 10.1016/j.jembe.2015.04.022

Queirós, A. M., Stephens, N., Widdicombe, S., Tait, K., McCoy, S. J., Ingels, J., et al. (2019). Connected macroalgal-sediment systems: blue carbon and food webs in the deep coastal ocean. *Ecol. Monogr.* 89, e01366. doi: 10.1002/ecm.1366

Sala, E., Ballesteros, E., Dendrinos, P., Di Franco, A., Ferretti, F., Foley, D., et al. (2012). The structure of Mediterranean rocky reef ecosystems across environmental and human gradients, and conservation implications. *PloS One* 7, e0032742. doi: 10.1371/journal.pone.0032742

Sundbäck, K., Miles, A., and Gőrnasson, E. (2000). Nitrogen fluxes, denitrification and the role of microphytobenthos in microtidal shallow-water sediments: an annual study. *Mar. Ecol. Prog. Ser.* 200, 59–76. doi: 10.3354/meps200059

frontiers in Marine Science

ORIGINAL RESEARCH
published: 28 March 2022
doi: 10.3389/fmars.2022.843824

Marine Environmental Change Induced by Anthropogenic Activities – From a Viewpoint of Aquatic Palynomorph Assemblages Preserved in Sediment Cores of Beppu Bay, West Japan

Kazumi Matsuoka[1], Natsuhiko Kojima[2] and Michinobu Kuwae[3]*

[1] Osaka Museum of Natural History and C/O Institute for East China Sea, Nagasaki University, Nagasaki, Japan, [2] Department of Biology, Osaka Institute of Technology, Osaka, Japan, [3] Center for Marine Environmental Studies, Ehime University, Ehime, Japan

OPEN ACCESS

Edited by:
Fernando Rubino, Water Research Institute (IRSA) (CNR), Italy

Reviewed by:
Haifeng Gu, Third Institute of Oceanography, State Oceanic Administration, China
Hilal Aydin, Manisa Celal Bayar University, Turkey
Audrey Limoges, University of New Brunswick, Canada

***Correspondence:**
Kazumi Matsuoka
kazu-mtk@nagasaki-u.ac.jp

Specialty section:
This article was submitted to Marine Ecosystem Ecology, a section of the journal Frontiers in Marine Science

Received: *27 December 2021*
Accepted: *16 February 2022*
Published: *28 March 2022*

Citation:
Matsuoka K, Kojima N and Kuwae M (2022) Marine Environmental Change Induced by Anthropogenic Activities – From a Viewpoint of Aquatic Palynomorph Assemblages Preserved in Sediment Cores of Beppu Bay, West Japan. Front. Mar. Sci. 9:843824. doi: 10.3389/fmars.2022.843824

Stratigraphic cluster analysis using aquatic palynomorphs preserved in the core sediments revealed a rapid eutrophication due to anthropogenic activities from the mid 1960s in Beppu Bay, East Kyushu, Japan. These assemblages were divided into three major units: BP-I, BP-II and BP-III, and also only dinoflagellate cyst assemblages were divided into the following four units in Beppu Bay: BP-A, BP-B, BP-C, and BP-D. Unit boundaries based on aquatic palynomorphs and dinoflagellate cysts were different except in the upper part, BP-III and BP-D, both of which clearly indicated anthropogenic eutrophication in both sea water and bottom sediments. On the other hand, in dinoflagellate cyst assemblages, Unit BP-A was characterized by stable occurrence of *Spiniferites bulloideus* and *Spiniferites hyperacanthus, Lingulodinium machaerophorum* of Gonyaulacales, and reduction of heterotrophic Peridinioid *Brigantedinium* spp. In Unit BP-C there was a clear decrease of *L. machaerophorum.* Unit BP-B was characterized by decreases of *S. bulloideus*, *S. hyperacanthus,* and *L. machaerophorum*, and little increase of *Spniferites bentori.* Unit BP-C was characterized by an increase in *S. bulloideus* and heterotrophic Peridinioid *Echinidinium* spp. Unit BP-D was subdivided into Subunit BP-D1 where dinoflagellate cysts showed a marked increase in *S. bulloideus* accompanied by the appearance of *L. machaerophorum* and *Tuberculodinium vancampoae*, and Subunit PB-D2 where there was a decrease of total dinoflagellate cysts. From the dinoflagellate cyst assemblages, the marine environment of the period of BP-A Unit was suggested to be warm and stable. However, *L. machaerophorum* started to decrease in BP-B. The clear decrease of *L. machaerophorum* suggest that the marine environment became cooler than that of Unit BP-A. Significant increases of *S. bulloideus, S. hypearcanthus, L. machaerophorum, T. vancampoae, Brigantedinium* spp., and *Polykrikos kofoidii* were characteristic of Unit BP-D. The increase in total dinoflagellate cyst density and

the increase of the ratio of heterotrophic dinoflagellate cysts in Subunit BP-D1 are manifestations of the Oslo fjord Signal and Heterotroph Signal, respectively. In addition, the decrease in microforaminiferal lining that continued from Unit BP-C to Unit BP-D might indicate deterioration of the bottom sediment environment.

Keywords: aquatic palynomorph, dinoflagellate cyst, microforaminiferal lining, anthropogenic eutrophication, Beppu Bay, Anthropocene

INTRODUCTION

The remains of organisms that live by aquatic environments are transported and preserved in the sediments in coastal areas. In particular, large amounts of microscopic biological remains (microfossils) are preserved. Among these, microfossils with organic walls are collectively called palynomorphs (Travers, 2007). Among palynomorphs, dinoflagellate cysts appeared in the Triassic period of the Mesozoic era and from then onward and have contributed greatly to the establishment of biostratigraphy and the elucidation of changes in the paleo-ocean environment, as well as diatoms, foraminifera, and coccoliths, which have mineral shells (e.g., Guiot and de Vernal, 2007; Fensome et al., 2009; Zonneveld et al., 2013; Williams et al., 2017; Penaud et al., 2018).

Dinoflagellate cysts are dormant zygotes formed by sexual reproduction with a size of 10–100 μm (Matsuoka and Fukuyo, 2000) and have a cell wall composed of a cellulose-based biopolymer (Kokinos et al., 1998; Versteegh et al., 2012). Since this cell wall is physically and chemically resistant, it is conserved in various fine-grained sediments (Zonneveld et al., 1997), especially in coastal sediments. Due to these characteristics, it has been used to elucidate changes in oceanic climate and biological production on the order of decades to hundreds of years (Thorsen and Dale, 1998; Harland et al., 2013). Focusing on the characteristics of production of dinoflagellates, which are primary producers and also include various heterotrophic species, has also contributed to clarifying changes in lower-order ecosystems associated with changes in nutrient levels (eutrophication) based on changes of dinoflagellate cyst assemblages (Dale et al., 1999; Matsuoka, 1999; Matsuoka et al., 2003; Pospelova et al., 2005).

In recent years, research on palynomorphs other than dinoflagellate cysts, including microforaminiferal linings, crustacean resting eggs, resting cysts and lorica of ciliates, turbellarian egg capsules, testate amoebas, and others has progressed (Belmonte and Rubino, 2019; McCarthy et al., 2021; Mudie et al., 2021; Shumilovskikh et al., 2021). Research on these microfossils is expected to play an important role in studying coastal environmental changes.

The coastal area is the main location for ocean-related human activities, and it responds sensitively to environmental changes in the land and sea areas. Recently, harmful algal blooms have occurred frequently, and their damage to human health and role in decreased biological production are of great concern (IOC[1]). Marine coastal ecosystems are changing, and it is argued that such changes have been accelerating in recent years (e.g., Clarke et al., 2006; Köster et al., 2007; Maier et al., 2009; Caffrey and Murrell, 2016). Thus, it is necessary to know the changes in ecosystems over time in order to clarify when and to what extent they have progressed. Since the changes in the ecosystem in the coastal areas are extremely regional phenomena, we must clarify them locally.

In order to clarify the beginning of the change in the ecosystem and the actual condition of the change, we investigated the aquatic palynomorphs preserved in the sediment cores collected in Beppu Bay, Western Japan. Beppu Bay is one of most investigated regions for clarifying human-induced environmental changes from the view point of environmental sciences and is regarded as one of candities for GSSP (global boundary stratotype section and point) (Anthropocene Working Group, 2020; Kuwae et al., 2022). However, although there are many related studies of sediment cores from a view point of geochemistry, only stratigraphic changes of the environments using diatoms were investigated at this point in time (Kuwae et al., 2022). In this article, we try to clarify the historical changes of coastal marine environments based on the findings about aquatic palynomorph assemblages and to discuss the primary factors leading to these changes in Beppu Bay for understanding how and when anthropogenic activities affected the low-trophic ecosystems. In addition, important aquatic palynomorphs which are not so much familiar to other than palynologists are briefly introduced for future study.

MATERIALS AND METHODS

Environmental Setting

Beppu Bay, in the western Seto Inland Sea, northeast Kyushu, Japan (**Figure 1**) is one of the enclosed bays indirectly affected by the warm Kuroshio Current through Bungo Channel and Hyuga Nada. This bay also is the only basin located within the Japanese coastal zone which exhibits clear autumnal oxygen depletions in bottom waters (0–0.2 mg L^{-1}) (Kameda and Fujiwara, 1995) as well as annual varve sedimentation during the late Holocene in the deepest area (Kuwae et al., 2013). Sediments in the area are continuously deposited with relatively high sedimentation rates (of 0.23–0.30 cm $year^{-1}$) (Kuwae et al., 2013; Yamada et al., 2016). The high sedimentation rates have allowed for the precise dating of surface sediments using lead-210 (^{210}Pb) (Takahashi et al., 2020) and the reconstruction of excellent proxy records of anthropogenic markers, including increases in concentrations of cesium-137 (^{137}Cs) (Kuwae et al., 2013; Takahashi et al., 2020), polychlorinated biphenyls (PCB; Takahashi et al., 2020), dichloro-diphenyl-trichloroethane (DDT;

[1]http://hab.ioc-unesco.org/

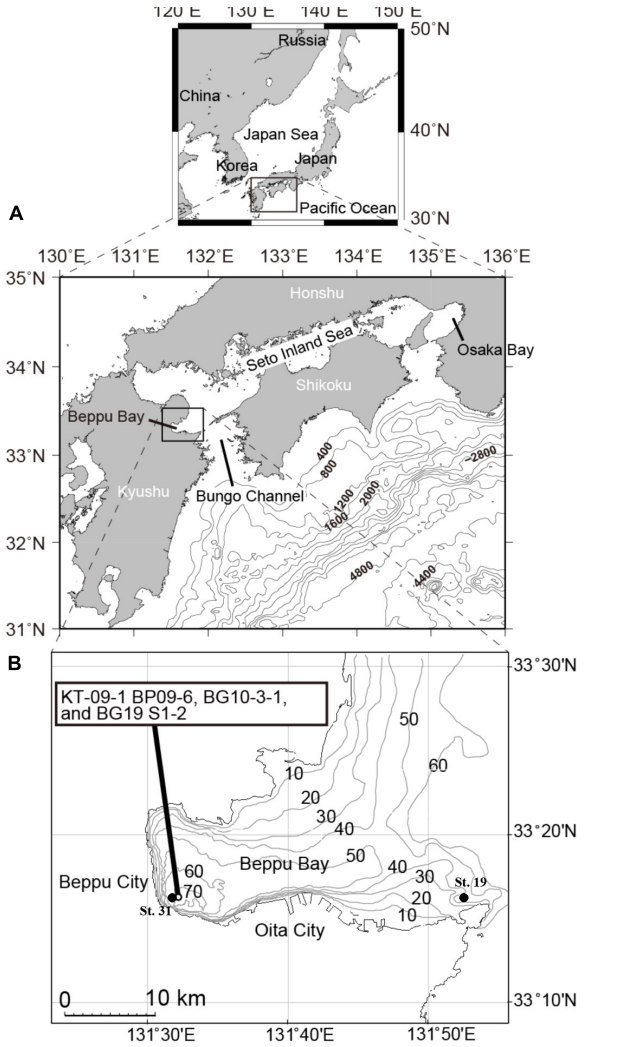

FIGURE 1 | (A,B) Sampling location map and operation points for the shallow sea constant line survey (Senkai Teisen Chosa (STC) in Japanese) carried out by the Oita Prefectural Fisheries Research Department.

Nishimuta et al., 2020), brominated fire retardants (Hoang et al., 2021) and microplastics (Masumoto et al., 2018) since year 1950. There are cities in the coastal area around Beppu Bay, Oita City in the south and Beppu City in the west, and an orchard area in the north (Kuwae et al., 2022). The Ohno and Oita Rivers, which drain the Oita Plain, are major rivers discharging to Beppu Bay (Yamada et al., 2016). Thus, this bay is one of most well-investigated sites for understanding anthropogenic activities in the world (Anthropocene Working Group, 2020).

Sampling of Sediment Cores

Three cores, namely KT-09-1 BP09-6, BG10-3-1, and BG19 S1-2, collected at the innermost part of Beppu Bay on 2009/3/8, 2010/9/10, 2019/9/10, respectively (**Figure 1** and **Supplementary Material 1**) were obtained for palynomorph analysis. The respective cores were collected using a 10-m-long piston core, a 100-cm-long gravity core (HRL, RIGO Co., Ltd., Saitama, Japan), and a 100-cm-long multiple corer (Ashra, RIGO Co., Ltd., Saitama, Japan).

All of the cores consisted primarily of hemipelagic silty to clayey sediments and a few millimeters or centimeters thickness-event layers with high-density, high-magnetic susceptibility, and coarser grains than those in hemipelagic layers (i.e., turbidites, which were probably formed by flooding and earthquakes). Since the event stratigraphy and chronology at the deepest site in Beppu Bay is well known, these event layers could be correlated between cores at the deepest site in Beppu Bay by lithological features and stratigraphy on visual inspection, CT images, and magnetic susceptibility and each event layer was named as a specific identification code (e.g., event (Ev) 0, 1, 2, 0a, 0b, and so on, in **Supplementary Material 2**; Kuwae et al., 2013). The ages of these event layers in the sediment (**Supplementary Material 3**) were determined in previous studies (Kuwae et al., 2013; Takahashi et al., 2020), and were used as time markers and for dating the core samples used in this study.

Samples for the palynomorph analysis were obtained from the stratigraphic sequence which was dated back to 1000 years using core samples from event (Ev) 8c to Ev 0 for BP09-6, Ev 0 to Ev 0c for BG10-3-1, and from Ev 0c to Ev -1cU.

Palynomorph Analysis

Each sample was divided into portions that were then treated according to the method of Matsuoka and Fukuyo (2000) described below to prepare a concentrated sample for observation of palynomorphs.

About 1 to 2 g of a wet sample was picked up from the divided samples and transferred to a 15-ml chemical-resistant plastic tube. After desalting with distilled water, the sample was treated with hydrochloric acid (37%) and hydrofluoric acid (46%) for 24 h to remove calcareous and siliceous particles, respectively. The sample was fractionated using a sieve with a mesh size of 125 μm and then a mesh size of 10 μm, and distilled water was added to the residue on the sieve with a mesh size of 10 μm to prepare a purified sample for observing palynomorphs. All processes were carried out at the room temperature.

A part of the concentrated sample for observation was taken with a micropipette (GILSON, PIPETMAN, P-1000), dropped onto a slide glass, and palynomorphs were identified and counted using an upright microscope (ASONE Digital Biological Microscope, DN-107T) with 400 to 1000 x magnification.

For calculating water content of the samples, the collected columnar sediment cores were cut in half vertically, and a 1cc cube was pushed into the cross section to collect samples. And then their wet weight was measured. After drying the cube at 50°C for 2 days in dry oven, the dry weight of the cub was measured.

A minimum of 200 palynomorphs were counted per sample to obtain homogeneous data for the statistical analyses.

Age Determination of the Cores

Ages of event layers (**Supplementary Material 3**) have been determined in previous studies using the constant rate of supply (CRS) model of ^{210}Pb dating (Appleby and Oldfield, 1978) for

sediments above Event 0a (R7) (Takahashi et al., 2020) and ^{14}C wiggle match-dating methods (Kuwae et al., 2013) below Event 0a and were used to date the core samples in this study. The ages of events determined by the CRS model were 2005 ± < 1 for Event -1c (R11), 1994 ± < 1 for Event -1b (R9), 1968 ± 4 for Event -1a (R8), and 1925 ± 10 to 30 for Event 0a (R7) (Takahashi et al., 2020). The uncertainty of ^{14}C wiggle match-based age was less than 25 years (Kuwae et al., 2013). The age of each sample was determined by linear-interpolation of the ages and depths of two successive events.

Data of Dissolved Oxygen and Chemical Oxygen Demand

Data of Dissolved Oxygen (DO) and Chemical Oxygen Demand (COD) in the inner and mouth parts of Beppu Bay (St. 31 and St. 19 of the shallow sea constant line survey (Senkai Teisen Chosa; STC) in Japanese) respectively measured at STC carried out by the Oita Prefectural Fisheries Research Department was employed, however, these data were left from year 1972 onward only.

Statistical Analysis

In order to determine temporal changes in coastal aquatic biota of Beppu Bay, stratigraphic changes in aquatic palynomorph assemblages were statistically analyzed using total count numbers of each palynomorphs and total numbers of major palynomorphs including dinoflagellate cysts with software Past 4[2] under stratigraphic clustering of paired group with Bray-Curtis similarity index. In the case of dinoflagellate cyst assemblages, relative abundances of each species were statistically analyzed in the same way independently. Also, to know temporal change of dissolved oxygen at the bottom layer of sea water, the original data were analyzed with PC-ORD 7[3].

RESULTS

Aquatic Palynomorph Assemblage

Major aquatic palynomorphs preserved in sediments are summarized in **Table 1** and specific species needed further study are introduced in **Supplementary Material 4**. The main components of aquatic palynomorphs in Beppu Bay were dinoflagellate cysts, microforaminiferal linings, and crustacean resting eggs, which accounted for more than 90% of the total aquatic palynomorph assemblages as shown in **Figure 2**, **Table 2**, and **Supplementary Material 5**. Microforaminiferal linings sometimes accounted for more than 50% of total palynomorphs in the middle and lower depth (for example, year 1395 and 1933), but they decreased rapidly after year 1969. Dinoflagellate cysts were 40 to 50% in the lower middle depth and 60% or more in the upper depth (1979 and 2003). The maximum output of aquatic palynomorphs was 8863 palynomorphs/g in year 1771, the minimum was 2203 palynomorphs/g in year 1960, and the average was 4878 palynomorphs/g. After the maximum output was recorded in year 1771, it decreased significantly after year 1824. After a slight increase from year 1880 to 1933, the minimum output was recorded in year 1960. Furthermore, it increased toward year 1979 and decreased after that. These increases and decreases were mainly due to the production of dinoflagellate cysts and microforaminiferal linings.

The results of the cluster analysis using the aquatic palynomorph assemblage data of Beppu Bay core revealed that these palynomorph assemblages were stratigraphically divided into three major units: BP- I Unit, BP- II Unit, and BP- III Unit. The boundaries were placed at year 1771 between BP- I Unit and BP- II Unit, and year 1964 between BP- II Unit and BP- III Unit (**Figure 2**).

Dinoflagellate Cysts (Figures 3, 4(1-11), 5, 6))

The average concentration of dinoflagellate cysts appearing throughout all samples was 1954 cysts/g, accounting for about 20% (year 1933) to about 70% (year 2003) of the total aquatic palynomorph assemblage. The maximum number of dinoflagellate cysts was 3546 cysts/g in year 1984, and the minimum number was 661 cysts/g in year 1955. There was a marked decrease in dinoflagellate cysts between year 1854 and 1873, and an increase between year 1960 and 1979.

The photosynthetic group mainly includes species belonging to Gonyaulacales, Peridiniales such as *Scrippsiella** and Gymnodiniales such as *Levanderina fissa**, *Pseudocochlodinium profundisulcus** and *Gymnodinium catenatum**. The relative contribution of all dinoflagellate cysts was 61% (year 1979) to 12% (year 1890) of the total palynomorphs observed. In the heterotrophic group, other Peridiniales (Protoperidinioid, Diplopsalid) and *Polykrikos** of Gymnodiniales were the main components, and they accounted for more than 50% of all dinoflagellate cysts except for a few samples with lower counts.

In Gonyaulacales, *Spiniferites* (mainly *S. bulloideus* and *S. hyperacanthus)* were dominant, accounting for more than 90% of Gonyaulacales in year 1979. In addition, *S. bentori* constituted nearly 20% from year 1964 to 1984. *Lingulodinium machaerophorum* was abundant before year 1824, accounting for more than 40% of Gonyaulacales in year 1222 and 1557. *Tuberculodinium vancampoae* was also observed in almost all samples, although its densities were relatively low. The appearance of *Operculodinium centrocarpum* sensu Wall and Dale was very low.

In the Peridiniales, *Brigantedinium* spp. which accounted for about 70% of Peridiniales throughout this taxon, occurred in all samples. In *Brigantedinium*, species that could be identified based on the archeopyle morphology and cyst size were *B. simplex, B. cariacoense, B. majusculum,* and *B. irregulare.* In other Peridiniales, various cysts belonging to the family Protoperidiniaceae occurred. These were *Lejeunecysta subrina, Quinquecuspis concreta, Selenopemphix nephroides, S. quanta, Stelladinium abei*, *S. robustus, Trinovantedinium applanatum, Votadinium spinosum, V. rhomboideum*, *Echinidinium aculeatum*, *Echinidinium* spp., and others. They constituted around 10% of dinoflagellate cyst assemblages and did not become dominant. In addition, *Dubridinium cavatum*, *Niea*

[2]https://www.nhm.uio.no/english/research/infrastructure/past/

[3]https://www.wildblueberrymedia.net/pcord

TABLE 1 | Aquatic palynomorphs.

Taxa	Habitat	Life mode	Mode of nutrition	Common remaining parts	Morphological types and features	Representative fossil name (example)	References
Cyanobacteria	**freshwater, blackish water, marine**		**photosynthetic**	**heterocyst akinete sheath**	**elongatedly rectangular, ellipsoidal, fusiform, subspherical with tail**		van Geel, 2001
Dinophyta	**abundantly marine (commonly blackish, freshwater)**	**mainly planktonic**	**photosynthetic, heterotrophic** (bacteria, diatoms, other phototrophic dinoflagellates, ciliates, non-noflagellates, colorless detrital particles) **mixotrophic**	**resting cyst**	**spherical to subspherical type ellipsoidal type peridinioid type ovoidal type with various surface ornamentations transverse and longitudinal furrows archeopyle**	***Spiniferites Brigantedinium***	Wall and Dale, 1968; Jacobson and Anderson, 1986; Hansen, 1991
Acritarch	**mainly marine (commonly brackish water, freshwater)**	**probably planktonic autotrophic, heterotrophic, mixotrophic (?)**	**mainly photosynthetic, heterotrophic (?) mixotrophic (?)**	**resting cell?**	**spherical to subspherical type ellipsoidal type peridinioid type ovoidal type ornamented with various appendages and openings**	***Baltisphaeridium Micrhystridium***	Downie et al., 1963
Chlorophyta	**mainly freshwater, blackish water, marine**	**planktonic, benthic**	**photosynthetic**	**resting cell**		**Oedogoniaceae (*Oedogonium*) Botryococcaceae *(Botryococcus*) Hydrodictyaceae (*Pediastrum*) Scenedesmaceae (*Scenedesmus*)**	Shumilovskikh et al., 2021
Charophyta	**mainly freshwater, blackish water, marine**	**planktonic, benthic**	**photosynthetic**	**zygospore aplanospore**	**spherical, ovoidal, elongatedly ovoidal, square, dome-shaped**	**Zygnemataceae (*Spitogyra*) Desmidiales (*Cosmarium*) *Ovoidites***	van Geel, 2001
Prasinophyta	**mainly marine**	**planktonic**	**photosynthetic**	**resting phycoma**	**spherical to subspherical type with or without fenestrate walls and membranous surface ornaments**	***Tasmanites, Cymatiosphaera Pleurozonaria, Pterosperma Pterospermella***	Wall, 1962; Park et al., 1978
Euglenophyta	**mainly freshwater**	**planktonic**	**photosynthetic**	**loricate**		***Trachelomonas***	Shumilovskikh et al., 2019
Ciliophora	**marine, fresh water, blackish water**	**planktonic**	**heterotrophic** bacteria, diatoms, dinoflagellates, microflagellates (chlorophytes, chrysophytes, pelagophytes, prasiophytes, pyrenomonadaceae), raphidophytes, other ciliates, small organic particles)	**lorica**	**circular cylindrical inverted frustum**	***Strombidium Hexasterias Halodinium Radiosperma***	Taniguchi, 1975; Reid and John, 1978; Dolan et al., 2013; Gurdebeke et al., 2018

(Continued)

TABLE 1 | (Continued)

Taxa	Habitat	Life mode	Mode of nutrition	Common remaining parts	Morphological types and features	Representative fossil name (example)	References
				resting cyst	**spherical type elliptical type spindle type disk-shaped type**		
Amoebozoa	**freshwater to blackish water**	**benthic**	**heterotrophic (**organic detritus?)	**organic shell**	**discoidal, cup-shaped and elongated ellipsoidal with simple opening**		Meisterfeld, 2002
Foraminifera (microforaminiferal linings)	**marine, blackish water**	**benthic**	**heterotrophic (**bacteria, pennate diatoms, micro-algae, other protozoans, and dead organic material)	**organic inner lining**	**single chamber type uniserial type biserial type coiled type compound type**		Kitazato, 1981; Stancliffe, 1989; Topping et al., 2006; Armstrong and Brasier, 2007
Fungi	**freshwater, blackish water, marine**	**synbiont**	**heterotrophic**		**spore, fruiting bodies, hyphae**	**Chlamydospore conidiophore**	van Geel, 2001; Travers, 2007
Crustaceae	**marine, freshwater, blackish water**	**planktonic heterotrophic**	**heterotrophic (**diatoms, dinoflagellates, ciliates, fecal pellets, organic detritus)	**exoskeleton**	**intercoxal plate tail sternite appendage, etc.**		van Waveren, 1993
				egg envelope	**discoid type folded discoid type double saucer shaped type fissured sphere type hemisphere type ellipse type fusiform type double fusiform type**	***Cobricosphaeridium***	Sherr and Sherr, 1988; Uye and Takamatsu, 1990; McMinn et al., 1992; van Waveren, 1993
Ostracod	**marine, freshwater, blackish water**	**benthic**	**heterotrophic**	**mandibles and carapace linings**			Mudie et al., 2021
Polychaeta	**freshwater, blackish water, marine**	**benthic**	**heterotrophic**	**mouth-lining parts scolecodont**			Travers, 2007; Mudie et al., 2021
Turbellaria	**Fresh water Freshwater, blackish water, marine**	**benthic**	**heterotrophic**	**egg capsule**	**stalk Group** ellipsoidal type cup-shaped type spherical type n**on-Stalk Group** ellipsoidal/cup-shaped type sp. spherical type	***Palaeocystoptosis***	Matsuoka and Ando, 2021; Mudie et al., 2021

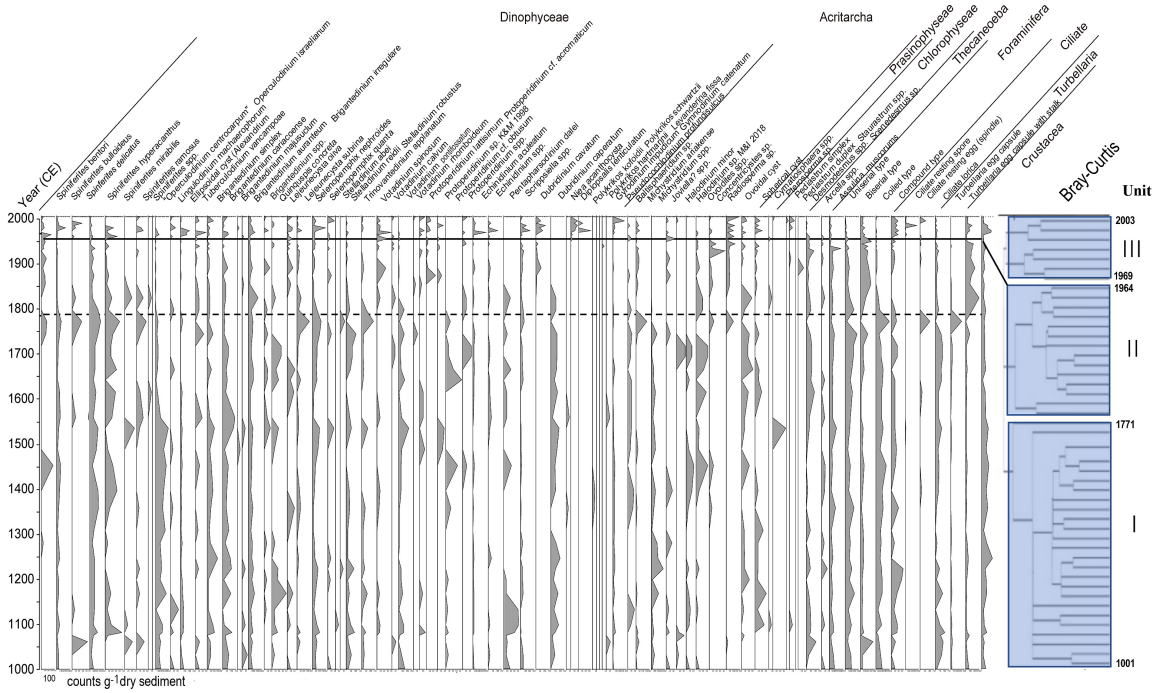

FIGURE 2 | Stratigraphic distribution of all aquatic palynomorphs observed in the core samples of Beppu Bay and Unit division based on stratigraphic cluster analysis using Bray-Curtis method.

TABLE 2 | List of aquatic palynomorphs observed in sediments of Beppu Bay.

Algae
Dinophyta (Dinoflagellate cyst)
Gonyaulacales; *Spiniferites, Hiddenocysta, Operculodinium, Lingulodinium, Impagidinium, Tuberculodinium, Alexandrium**
Peridiniales; *Brigantedinium, Quinquecuspis, Lejeunecysta, Selenopemphix, Stelladinium, Trinovantedinium, Votadinium, Echinidinium, Protoperidinium*, Pentapharsodinium*, Scrippsiella*, Dubridinium, Niea*, Diplopsalis**
Gymnodiniales; *Polykrikos*, Gymnodinium*, Pseudocochlodinium*, Levanderina**
Prasinophyta; *Cymatiosphaera*, Pterosperma*
Chlorophyta; *Pediastrum, Staurastrum, Desmodesmus, Scenedesmus*
Protozoa
Ameboza; *Arcella, Assulina*
Ciliophora; *Cyrtostrombidium, Strombidium,* (resting cyst), *Dadayiella, Favella*
Foraminifera (foraminiferal linings)
Uniserial type (cf. *Reophax*), Biserial type (cf. *Textularia, Bolivina*),
Coiled type (cf. *Buccella, Ammonia*), Compound type
Metazoa
Crustacea; copepod (resting egg), body, appendages, Cladocea (resting egg)
Turbellaria; *Palaeostomocystes* (egg?), *Aegla*-type, *Wahlia*-type, *Syndesmis*-type (egg capsule)
Acritarcha (Unknown origin)
Baltisphaeridium, *Micrhystridium, Ovoidites*, *Concentricystes, Joviella?*, *Halodinium*# , *Radiosperma*# (#: possibly resting cyst of Ciliophora suggested by Gurdebeke et al., 2018)

*In this study, paleontological names for dinoflagellate cysts were used, but in the case of dinoflagellate cysts which do not have paleontological names, names of plankton or biological were adopted with a * mark after their name.*

*acanthocysta**, and others frequently appeared in the Diplopsalid group, although they constituted only a few percent.

In the Gymnodiniales, a small amount of *Polykrikos hartmannii** appeared in year 1395 and year 1452, but after year 1955, it occurred in a few percent of all dinoflagellate cyst assemblages. There were many heterotrophic *Polykrikos kofoidii** (**Figure 5**).

The ratio between the photosynthetic group (auto-mixotroph) mainly composed of Gonyaulacales and calciodinellid and the heterotrophic group mainly composed of Protoperidinid and

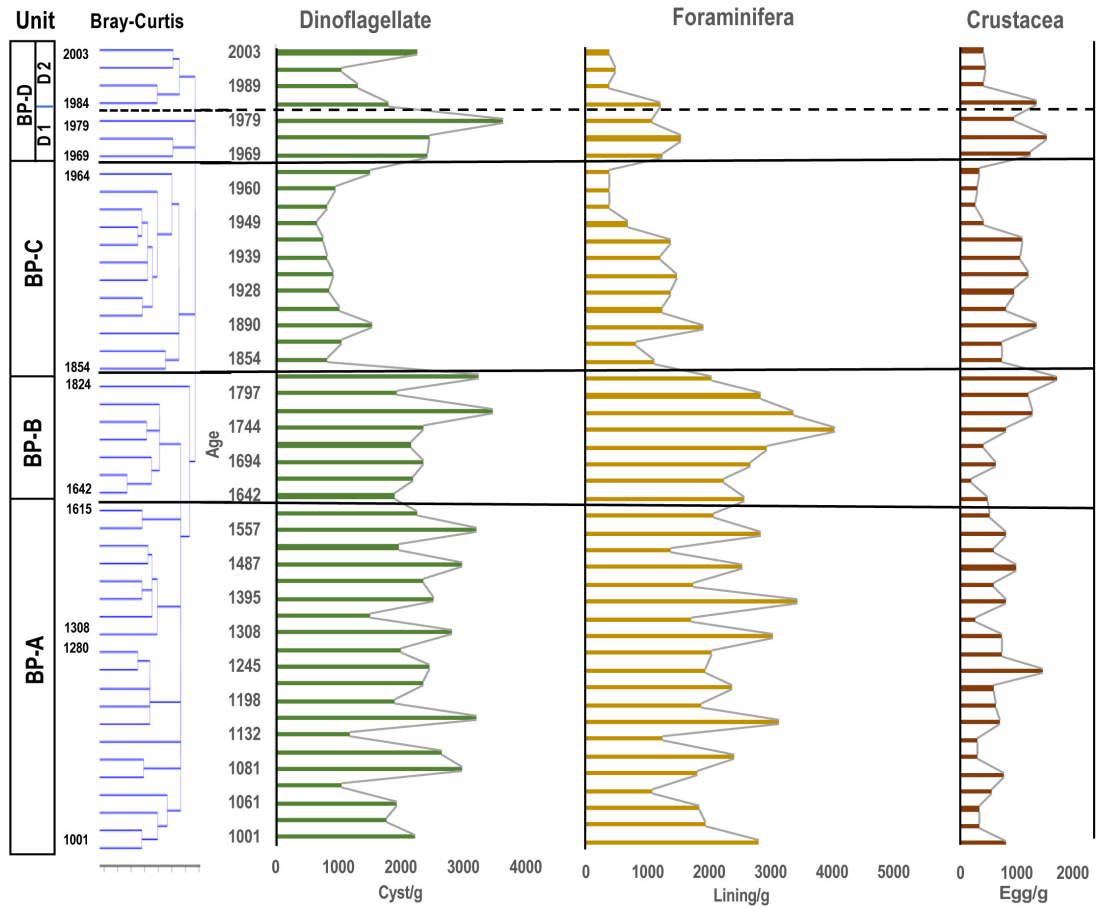

FIGURE 3 | Stratigraphic distribution of major aquatic palynomorphs (dinoflagellate cysts, microforaminiferal linings and crustacean resting eggs) observed in the core samples of Beppu Bay. Unit division in the left column based on the result for dinoflagellate cyst assemblages according to stratigraphic cluster analysis using Bray-Curtis method.

Diplopsalid was ranged between 80% (year 1824) to 40% (year 1989). Except for year 1960 to 1979, when the photosynthetic group increased to 50% or more, the heterotroph group was dominant throughout the cores.

Microforaminiferal Linings (Figures 3, 7(2-4))

Microforaminiferal linings were the next most abundant after dinoflagellate cysts with an average of 1802 linings/g in all samples, and the highest number being 4055 linings/g in year 1744, and the minimum number being 366 linings/g in year 1989 (**Figure 8**). After a rapid decrease after year 1744, the number increased slightly from year 1854 to 1955, except in year 1933, but was nearly constant (1158 linings/g), and then after year 1960 it increased slightly until year 1984 (929 linings/g). However, it decreased (412 linings/g) almost continuously from then until year 2003.

Among microforaminiferal linings, the biserial type was dominant, followed by the uniserial type. Before year 1744, the average number of the biserial type (**Figure 7(7)**) was 1281 linings/g, but after then it dropped sharply to 866 linings/g until year 1955 and 195 linings/g until year 2003. The uniserial type (**Figure 7(2)**) showed an average of 495 linings/g before year 1744, but thereafter their occurrence did not change (465 linings/g until year 1955), but it decreased sharply to 159 linings/g until year 2003. The number of the coiled type linings was smaller than that of uniserial and biserial types, and although they did not dominate in all samples, they also decreased after year 1960.

Ciliates (Figures 7(5-6))

Ciliophora were present in very low percentages throughout all samples, but 711 cells/g were recorded in year 1984 and 147 cells/g in year 1995. This was due to the abundance of loricae of *Dadayiella**. In other samples, resting cysts of *Favella** and *Cyrtostrombidium** sometimes occurred.

Crustaceans (Figures 3, 7(7-10))

Crustacean resting eggs were the most abundant after dinoflagellate cysts and microforaminiferal linings. The average number of resting eggs was 751 eggs/g in all samples; the highest was 1709 eggs/g (year 1709), and the lowest was 284 eggs/g.

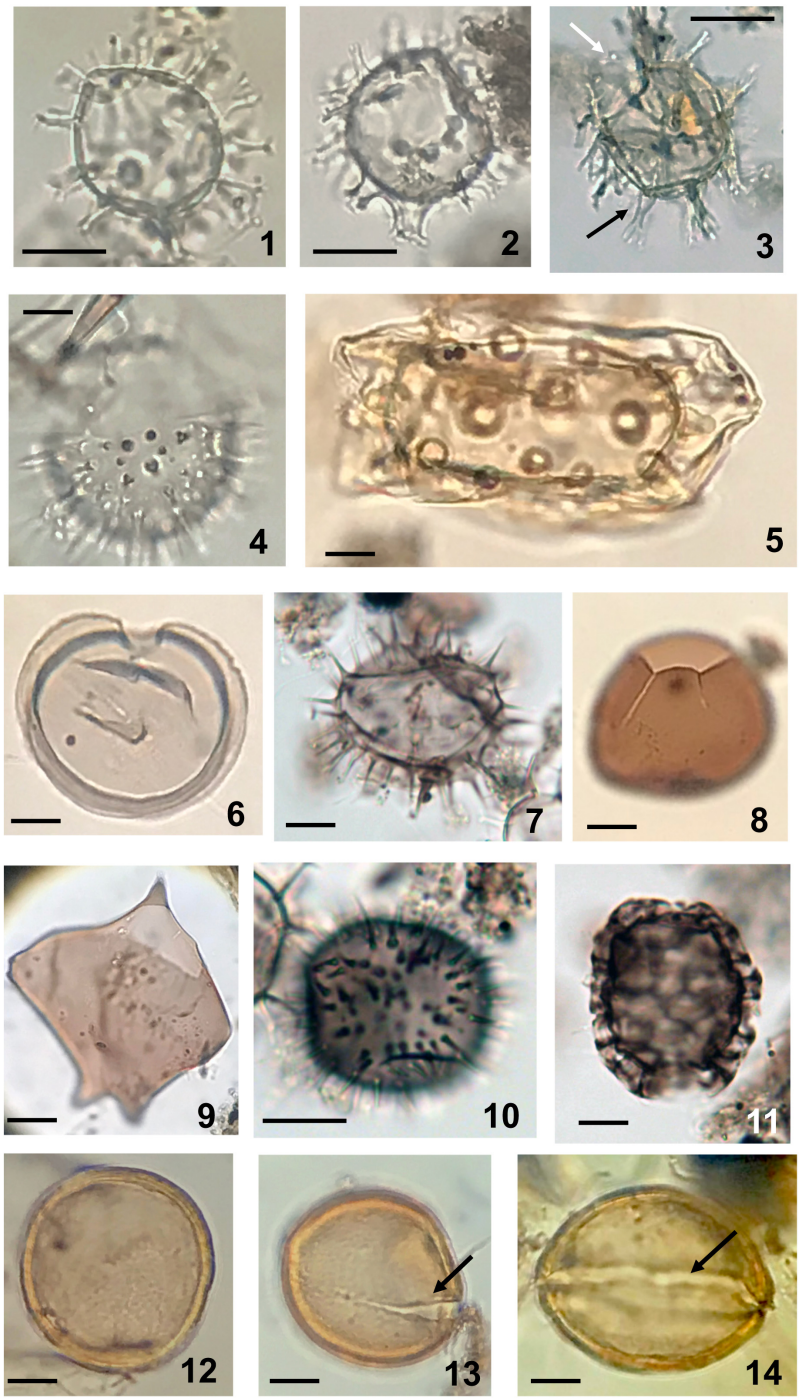

FIGURE 4 | Dinoflagellate cysts (1-11) and acritarch (112-14) observed in sediments of Beppu Bay. (1) *Spiniferites bulloideus* (Deflandre and Cookson) Sarjeant; photosynthetic. Sample BG19 St 1 2 10-11. (2) *Spiniferites delicatus* Reid; photosynthetic. Sample BG19 St 1-2 10-11. (3) *Hiddenocysta matsuokae* P. *Gurdebeke, V. Pospelova, K.N. Mertens*, and *S. Louwye*; probably photosynthetic, black arrow indicating fenestrate process, white arrow indicating larger precingular archeopyle. In statistical analysis this species is included in *Spiniferites* spp. Sample BG19 St 1-2 14-15. (4) *Lingulodinium machaerophorum* (Deflandre and Cookson) Wall; photosynthetic. Sample BG19 St 1-2 14-15. (5) *Tuberculodinium vancampoae* Rossignol; photosynthetic. Sample BG19 St 1-2 28-29. (6) *Selenopemphix nephroides* Benedeck; heterotrophic. Sample BG19 St 1-2 10-11. (7) *Selenopemphix quanta* (M.R. Bradford) Matsuoka; heterotrophic. Sample BG19 St 1-2 14-15. (8) *Votadinium calvum* Reid; heterotrophic. Sample BG19 St 1-2 64-65. (9) Cyst of *Protoperidinium latissimum** (Kofoid) Balech; heterotrophic. Sample BP09-6 3-22. (10) Cyst of *Niea acanthocysta** (H. *Kawami, M. Iwataki*, and *K. Matsuoka*) T. Liu, K.N. Mertens, and H. Gu; heterotrophic. Sample BG19 St 1-2 14-15. (11) Cyst of *Polykrikos kofoidii** Chatton; heterotrophic. Sample BG 19 St1-2 14-15. (12-14) Acritarch, *Joviella*? sp.; 12; Sample BP 09 4-53, 13; Sample BP 09 4-60, 14; Sample BP 09 4-81. Scale bars; 20 μm.

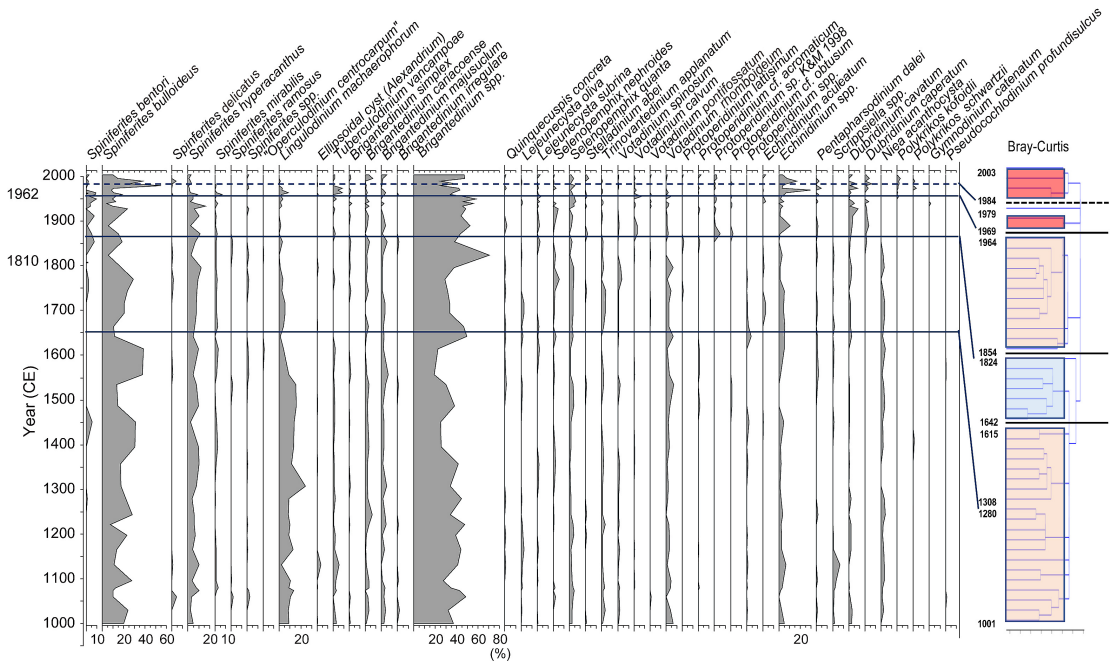

FIGURE 5 | Stratigraphic distribution of major groups of dinoflagellate cysts and Unit division based on stratigraphic cluster analysis using Bray-Curtis method.

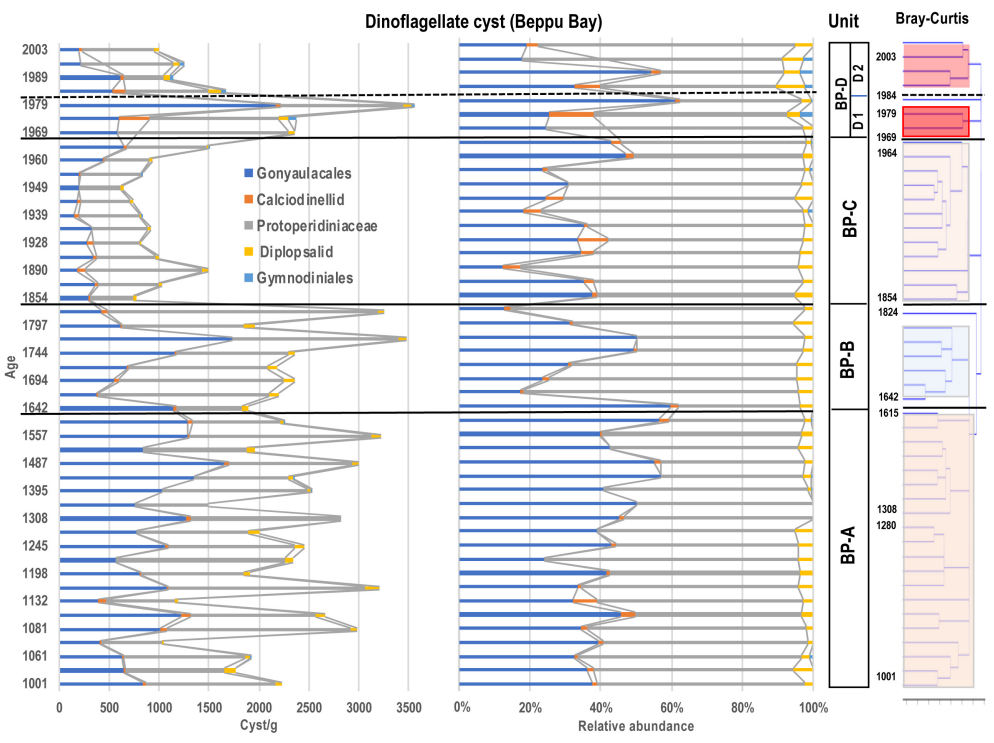

FIGURE 6 | Stratigraphic abundances of dinoflagellate cysts and Unit division based on stratigraphic cluster analysis using Bray-Curtis method.

However, their occurrence patterns were different from those of dinoflagellate cysts and microforaminiferal linings. Until year 1665, the output was almost constant (615 eggs/g on average), but after that, it increased (1005 eggs/g) until year 1944, and then decreased sharply until year 1960 (336 eggs/g). After that, it started to increase again (913 eggs/g).

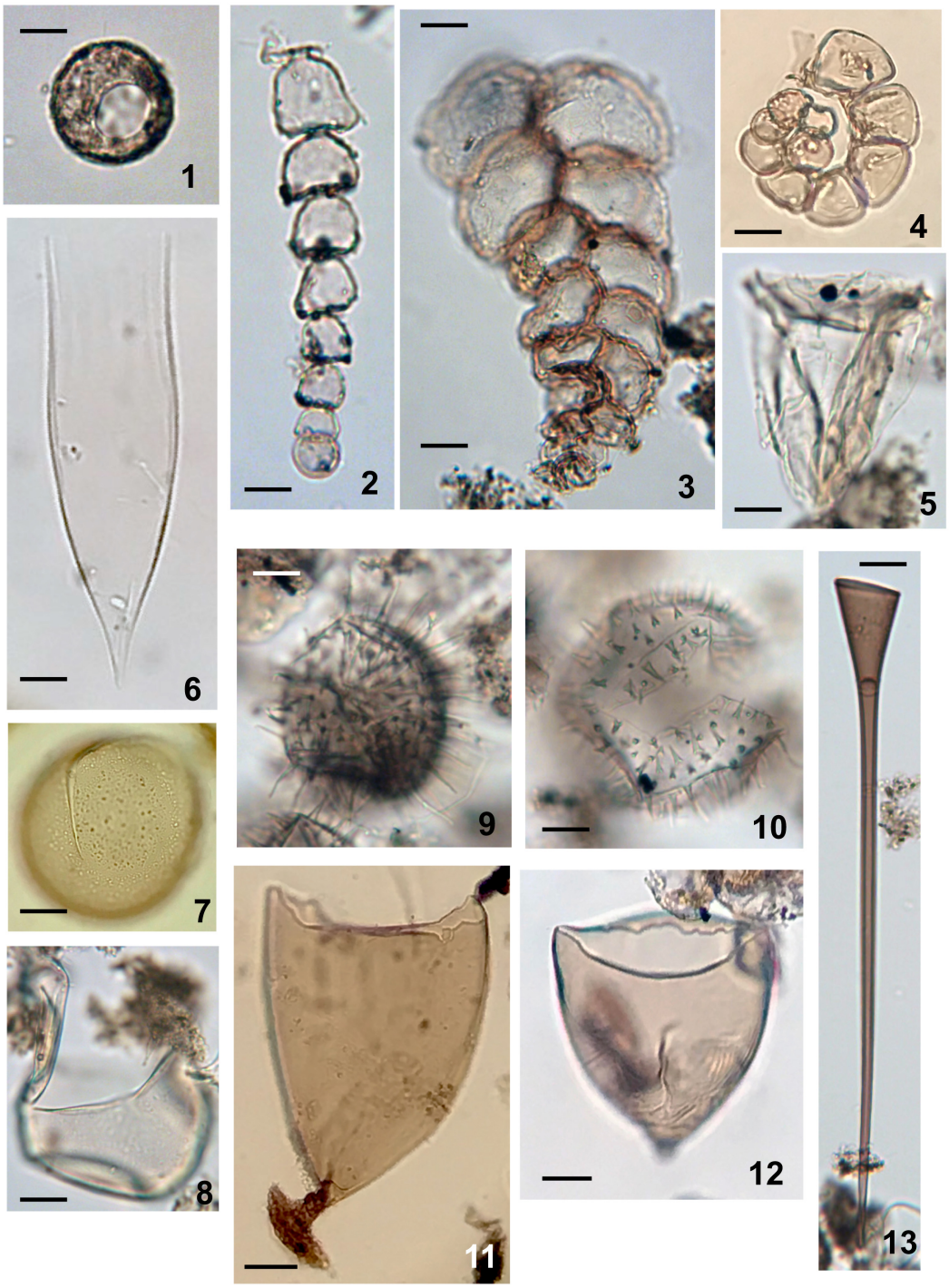

FIGURE 7 | Aquatic palynomorphs except for dinoflagellate cysts and acritarchs observed in sediments of Beppu Bay. (1) Testate amoeba; *Arcella* sp. Sample BG19 St 1-2 14-15. (2) Microforaminiferal lining uniserial type (*Reophax* sp.). Sample BG 19 St 1-2 14-15. (3) Microforaminiferal lining biserial type (*Textularia* cf. *tenuissima*). Sample BG 19 St 1-2 14-15. (4) Microforaminiferal lining coiled type (*Buccella* sp.). Sample BG 19 St 1-2 10-11. (5) Ciliate; *Favella* sp. Sample BG 19 St 1-2 14-15. (6) Ciliate; damaged lorica of *Dadayiella* sp. Sample BG 19 St 1-2 14-15. (7) Crustacean resting egg with finely granular surface. Arrow indicating rupture for hatching. Sample BG 19 St 1-2 14-15. (8) Crustacean resting egg with smooth surface. Arrow indicating rupture for hatching. Sample BG 19 St 1-2 14-15. (9) Crustacean resting egg ornamented with long flexuous spines. Sample BG 19 St 1-2 14-15. (10) Crustacean resting egg ornamented with short and solid spines. Arrow indicating rupture for hatching. Sample BG 19 St 1-2 14-15. (11) Turbellarian egg capsule with short and stout stalk. Arrow indicating basal attachment. Sample BP 09-6 3-89. (12) Turbellarian egg capsule with very short stalk. Sample BP 09-6 5-45. (13) Turbellarian egg capsule with very long stalk. Sample BG 19 St 1-2. (14-15) Scale bars; 20 μm.

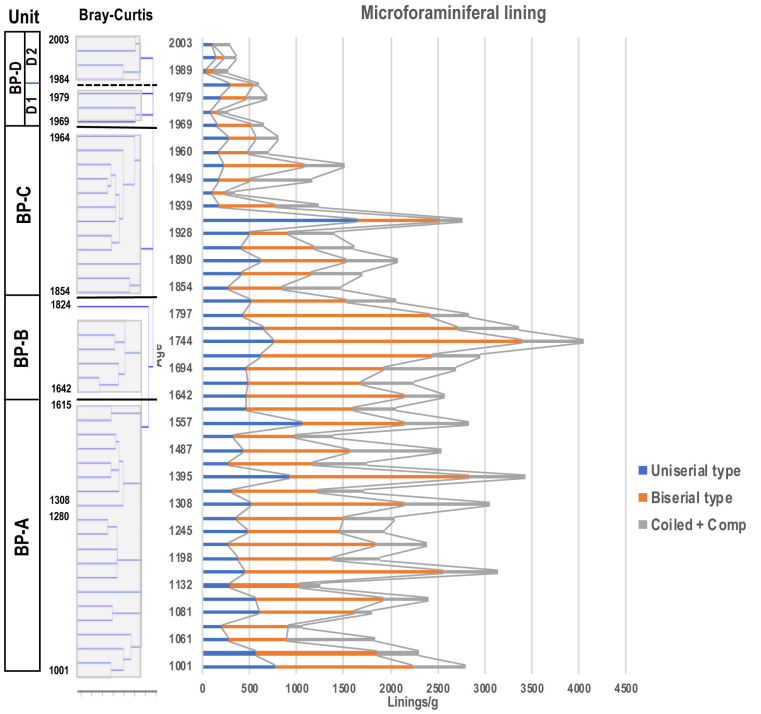

FIGURE 8 | Stratigraphic distribution of microforaminiferal linings. Unit division in the left column based on the result for dinoflagellate cyst assemblages resulting from stratigraphic cluster analysis using Bray-Curtis method.

Other Aquatic Palynomorphs

Testate amoebae (**Figure 7(1)**) were also obtained from almost all samples, but did not dominate. Their occurrence was a little higher in the sample before year 1771.

Turbellarian egg capsules (**Figures 7(11-13)**) occurred in almost all samples with various morphologies, consisting of less than a few percent of all palynomorphs, but were relatively abundant in the samples before year 1771 (263 capsules/g; highest value) and decreased thereafter.

Acritarchs (Figures 4(12-14) Is *Joviella*? sp.)

Acritarchs were also obtained from all samples, but always constituted less than 10% of all palynomorphs and never dominated. After year 1771, they decreased from about 200 to 146 cells/g.

Stratigraphic Divisions of Dinoflagellate Cyst Assemblage

Since the eco-physiological characteristics of palynomorphs except dinoflagellate cysts have not been well investigated so far, dinoflagellate cyst assemblages were statistically analyzed using a stratigraphic and Bray-Curtis method. As the results of the cluster analysis for the dinoflagellate cyst assemblage data dominated in the Beppu Bay core, the dinoflagellate cyst assemblages were divided into four major units.; BP-A Unit (year 1001–1615) from the bottom, BP-B Unit (year 1642–1824), BP-C Unit (year 1854–1964), and BP-D Unit (year 1969–2003). BP-D Unit was further subdivided into BP-D 1 Subunit (year 1969–1979) and BP-D 2 Subunit (year 1984–2003) (**Figure 5**).

BP- A Unit

Palynomorphs ranged from 2957 to 7583 (5440 on average) palynomorphs/g. Dinoflagellates dominated by *Spiniferites hyperacanthus, S, mirabilis, Lingulodinium machaerophorum* and *Brigantedinium* spp. were present at 2268 cysts/g on average, and constituted ca. 40% of the total palynomorphs. The foraminiferal linings were also dominant at 2165 linings/g on average, and constituted more than 40% of total palynomorphs. Crustacean resting eggs were present as 642 eggs/g on average and constituted ca. 10% of total palynomorphs.

BP- B Unit

Palynomorphs slightly increased to within the range of 4968–8863 (6556 on average) palynomorphs/g. The density of dinoflagellate cysts was approximately the same as the density of BP- A Unit, being 2458 cysts/g on average, however, *L. machaerophorum* remarkably decreased in this unit. The microforaminiferal linings slightly increased in concentration, with 2845 linings/g on average, and represented 40–50% of total palynomorphs; however, toward the upper parts they decreased.

BP- C Unit

Palynomorphs clearly decreased to within the range of 2957–7583 (3380 on average) palynomorphs/g. Dinoflagellate cysts

also decreased to 986 cysts/g on average, but their relative proportion among total palynomorphs was over 50% in the upper strata, and 1517 cysts/g were recorded in year 1964. The microforaminiferal linings were present at 1492 linings/g, however, they showed a clear decrease from 20% to 40% of the total palynomorphs in the upper layer. The crustacean resting eggs were present at 777 palynomorphs/g on average and increased their relative proportion to 40% (2070 palynomorphs/g) of total palynomorphs at year 1890.

BP- D Unit

Palynomorphs were present as 2325–5546 palynomorphs/g(3751 on average). Dinoflagellate cysts remarkably increased to 2141cysts/g on average and constituted ca. 40% of total palynomorphs. *Spiniferites bulloideus* was dominant in this unit. The microforaminiferal linings constituted 40–50% of total palynomorphs; however, both uniserial and biserial types continuously decreased to 449 linings/g on average. The crustacean resting eggs slightly increased to 913 palynomorphs/g.

Dissolved Oxygen and Chemical Oxygen Dissolved After Year 1972

The DO at the bottom layer of the inner part of the bay (St. 31) near the core sampling point was the highest in year 1973 (4.2 mg/L). After this, it once dropped to around 2 mg/L, but increased to nearly 3 mg/L around year 2010. The COD at 0 m decreased from the maximum value of 1.5 mg/L in year 1974 to 0.5 to 1 mg/L. At St. 19 of the mouth of the bay, the DO of the bottom layer was 5 mg/L, but it increased slightly after year 2000, and the COD at 0 m reached a maximum of 1.8 mg/L in year 1974. It decreased to 0.5 mg/L in year 1978, but slightly increased 0.7 mg/L until around year 2000, and has remained at 0.5 mg/L since then 1 (**Figure 9**).

DISCUSSION

Marine Environmental Changes Recorded in Dinoflagellate Cysts and Other Palynomorph Assemblages

Although the palynomorph assemblages do not represent all organisms that inhabit in and around Beppu Bay, the changes of these assemblages seemed to reflect the change of ecosystem (biota) in Beppu Bay. The unit boundaries were concordant in BP- III Unit of all palynomorphs and Unit BP-D of dinoflagellate cysts only, although others were slightly different. This means that the change of aquatic biota in this period seems to be larger than that in other periods. As discussed later, these changes were induced by eutrophication due to human activities. Except in the upper part of the Unit, the boundaries suggested by all aquatic palynomorphs and dinoflagellate cysts were different. This might be due to the use of different data sets for statistical analysis. As shown in **Table 1**, all aquatic palynomorphs included the remains of organisms inhabiting freshwater, brackish water and marine environments, as well as water column and bottom sediments. For example, dinoflagellate cysts originated from planktonic dinoflagellates whereas microforaminiferal linings were from benthic foraminifers. Therefore, the unit divisions resulting from total aquatic palynomorphs might be proxies for wider biota of Beppu Bay (**Supplementary Material 6**).

In the cluster analysis, BP-D Unit had a lower similarity between each sample than those of other Units, and it is specific that the year 1979 sample did not belong to any cluster. This was only due to extremely dominant *Spiniferites bulloideus* in the year 1979 sample, but this tendency did not continue. In addition, the cysts of heterotrophic species were common to each sample, but their relative ratios were not constant. The production of such unstable occurrence of dinoflagellate cysts suggested that the coastal marine environment became unstable after year 1964.

Marine Environmental Changes Recorded in Dinoflagellate Cyst Assemblages at Millennium Scale in Beppu Bay

As previously pointed out, dinoflagellate cysts were most dominant in the aquatic palynomorphs, and their eco-physiologies were well investigated. Therefore, for understanding the environmental changes of Beppu Bay, the temporal changes of dinoflagellate cyst assemblages should be clarified. As results of statistical analysis, dinoflagellate cyst assemblages were divided into four major units as shown previously.

BP-A Unit (Year 1001 to 1615): Warm Period

In BP-A Unit, the occurrence of all palynomorphs fluctuated, but it was within a certain range and nearly stable. The number of aquatic palynomorphs in this unit is 5759 palynomorphs/g, which is abundant in the core sample. Dinoflagellate cysts and microforaminiferal linings account for 80 to 90% of all palynomorph assemblages. In BP-A Unit, dinoflagellate cysts, foraminifera linings, and crustacean resting eggs also fluctuated. The relationship between these fluctuations and the rapid tide of the Kuroshio, which has a relatively short cycle and affects the marine environment of the Bungo Channel, is an important topic for further study.

Harada et al. (1994) presented the nearly 9,000 years' evolution of the dinoflagellate cyst assemblages in the core samples collected in the inner part of Beppu Bay, which was north of the core samping site in this study. After Harada et al. (1994), the study of dinoflagellates cysts, especially those of heterotrophic species, has greatly progressed, and many cyst species have been described thereafter, so it is difficult to quote the data at that time as they were, but the species of photosynthetic *Spiniferites bulloideus* and *Lingulodinium machaerophorum* have been consistent. Therefore, the occurrence patterns of *L. machaerophorum* in the core sample of Harada et al. (1994) seemed to be rather constant at 100 cysts/ml of wet sediment for the past 2000 years. According to Zonneveld et al. (2013), *L. machaerophorum* is a warm water species. Based on these data, it appears that the marine environment of BP-A Unit was rather stable and warm judging from the dinoflagellate cyst assemblages.

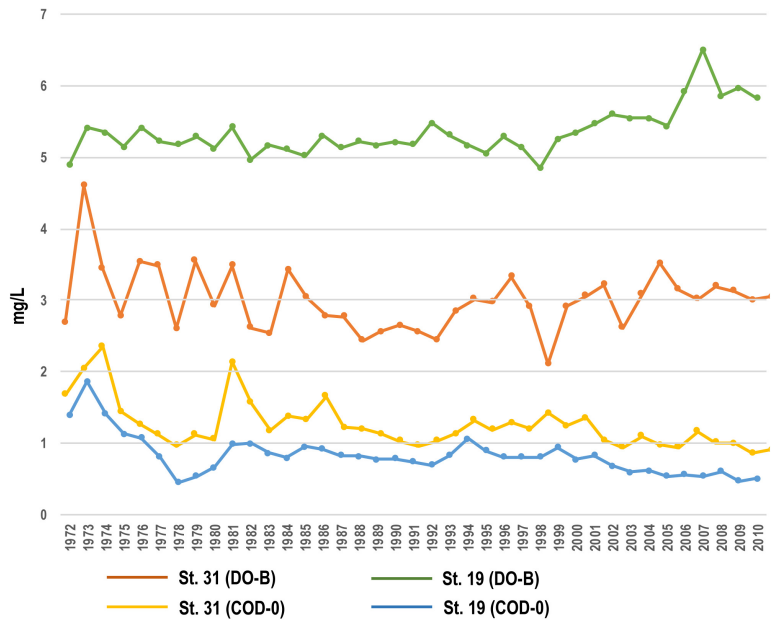

FIGURE 9 | Temporal changes of DO and COD at the inner (St. 31) and mouth (St. 19) parts of Beppu Bay.

This warm period might correspond to the Medieval Warm Period suggested in Marcott et al. (2013).

BP-B Unit (Year 1642 to 1824): Cool Period

The biserial type of microforaminiferal lining has been decreasing since its highest appearance value was recorded in year 1744. This suggests that the bottom environments of Beppu Bay started to deteriorate in this period. A remarkable decrease of *L. machaerophorum* characterizing BP-B Unit suggested that the water temperature in Beppu Bay might have become lower than that of BP-A Unit. The heterotrophic *Protoperidinium* species consisting of *Brigantedinium* spp., *Selenopenphix quanta, Votadinium rhomboideum*, and *Echinidinium* spp. suggested that dominant phytoplankton might shift from photosynthetic dinoflagellates to diatoms which are prey for heterotrophic dinoflagellates, mainly *Protoperidinium* species (Gaines and Taylor, 1984; Jacobson and Anderson, 1986).

BP-C Unit (Year 1854 to 1964): Warmer Period

In BP- C Unit, the total count of palynomorphs was 3543 palynomorphs/g, which was lower than that in BP-A Unit and BP-B Unit. Among them, dinoflagellate cysts and microforaminiferal linings decreased to about 70% of all palynomorphs, and crustacean resting eggs increased instead. The decrease of *Spiniferites* spp. and *Lingulodinium machaerophorum* did not mean that the biological productivity in the inner part of Beppu Bay had decreased, because the increase in crustacean resting eggs indicated that it was possible that there was a change in phytoplankton as primary producers, for example from dinoflagellates to diatoms during this period. In Kuwae et al. (2022), diatom flora also changed around year 1850 in their D2a zone of Beppu Bay core sediments.

Increase of *S. bentori,* a warm water species discussed in Zonneveld et al. (2013) with sporadic appearance of *Tuberclodinium vancampoae* suggested a climatic change toward warmer conditions in the upper layer. On the other hand, the decrease in microforaminiferal linings of the uniserial type (e.g., *Reophax* spp.) and the Biserial type (e.g., *Texturalia* spp.) inhabiting the surface layer of sediments might indicate degraded bottom environments in Beppu Bay (Names of foraminifera inferred from Sugaya and Nakao, 1983). In year 1854, a tsunami of about 2 m height due to the Ansei Nankai Earthquake struck Beppu Bay[4]. Since the sediments in the shallow waters along the Sanriku coast were much disturbed when this region was hit by the Chile Tsunami and the Great East Japan Earthquake (e.g., Matsuoka et al., 2018), there is no doubt that Beppu Bay was also affected by the tsunami caused by the Ansei Nankai Earthquake. However, how much the bottom habitats were affected cannot be evaluated at this time. In addition to this, Shimada et al. (2012) suggested that the vegetation around Beppu Bay was changed from a poor to a rich forest condition covered with *Pinus* (*Diploxylon*) and *Cryptomeria* around year 1850, based on pollen analysis. This change of the vegetation on the land might have influenced the transport of sediment into the coasts of Beppu Bay and then changed the coastal environments.

BP-D Unit (Year 1969 to 2003): Anthropogenic Eutrophication

In the dinoflagellate cyst assemblage of BP-D Unit, the photosynthetic species *Spiniferites bulloideus* prominently

[4]https://www.pref.oita.jp/soshiki/13550/jishinkiroku.html

proliferated to 2011 cysts/g in year 1979, and *Lingulodinium machaerophorum* and *Tuberclodinium vancampoae* also increased to near the level of BP-A Unit. This is a manifestation of the "Oslo fjord signal" of Dale (2009), which suggested an increase in photosynthetic species, indicating cultural eutrophication reflected by the dinoflagellate cyst assemblages. In addition, the increase of heterotrophic dinoflagellate cysts named as "Heterotroph signal" of Matsuoka (1999); Dale (2009) also showed eutrophication. This period coincides with the period of frequent large-scale red tides of a raphidophycean, *Chattonella marina*, and a dinoflagellate, *Karenia mikimotoi* (late 1960s to 1970s) in the Seto Inland Sea. Interestingly, Kuwae et al. (2022) showed that the dominant pigment preserved in the core sediments of Beppu Bay changed from fucoxanthin to diatoxanthin around the 1960s. This result suggests that dominant primary producers might change from diatoms to phytoflagellates including dinoflagellates. It has been pointed out that the cause of such a large-scale red tide was the load of nutrients from the land, that is, the progress of artificial eutrophication (Okaichi, 1997).

Therefore, BP-D1 Subunit (year 1964 to 1979) of the dinoflagellate cyst assemblages seemed to reflect the anthropogenic eutrophication caused by the increase of the population around Beppu Bay since the 1950s (Beppu City data[5]). Furthermore, it is speculated that the total nitrogen and total phosphate supplied from the land to the bay in the 1960s and 1970s reached 800 ton/day and 80 ton/day, respectively, which might have contributed to increasing the primary productivity (Tsugeki et al., 2016). In the subsequent BP-D2 Subunit, dinoflagellate cysts, microforaminiferal linings, and crustacean eggs decreased to the level of the BP-C Unit. This may reflect the reduction in nutrient load due to the improvement of drainage regulation and purification function from the land, as mentioned by Tsugeki et al. (2016).

BP-D1 Unit was characterized by the increase of Gymnodinialean *Polykrikos kofoidii** and *Polykrikos schwartzii**. These *Polykrikos** species are heterotrophic, and use nematocysts to capture prey organisms such as *Alexandrium catenella*, *Gymnodinium catenatum*, *Karenia mikimotoi*, *Prorocentrum sigmoides*, and other flagellates and engulf them at the ventral area (Cho and Matsuoka, 2000; Matsuoka et al., 2000). This way of feeding is different from that of *Protoperidinium* species, which use a capture membrane called as the feeding veil, to wrap prey organisms such as diatoms and assimilate their cytoplasm (Gaines and Taylor, 1984; Jacobson and Anderson, 1986, Jeong, 1994). That is, the appearance of *Polykrikos** suggests an increase in swimming-powered prey organisms such as flagellar microalgae. In other words, since the increases of *P. kofoidii** and *P. schwartzii** cysts suggest the emergence of flagellates such as *C. marina* and *K. mikimotoi*, which favor the environment of stratified seawater, the primary production in the BP-D1 Subunit might be dependent on flagellates rather than diatoms.

The existence of BP-D1 and -D2 Subunits could be controlled by the eutrophication of seawater due to the reclamation of tidal flats and the increase of urban wastewater by the regulation of the discharge of nutrients by law and the increase of sewage treatment capacity. This strongly suggests that it is difficult to improve the bottom sediment over a wide area.

Observational data are only available after year 1972, but COD around year 1974 suggest that the entire bay was rich in nutrients, which coincides with the frequent red tides in the entire Seto Inland Sea. DO of the bottom layer has remained almost unchanged since year 1972 at the mouth of the bay, but it shows that oxygen consumption was predominant at the inner part of the bay until around year 1990. This reflects the fact that organic matter in the water was deposited on the seafloor and its decomposition promoted oxygen consumption. Summarizing the above, it can be judged that eutrophication was progressing around year 1972 included BP-D1 Unit, and once the water quality improved slightly, but the improvement of the bottom layer environment in the inner part of the bay was not remarkable. The environment of seawater and sediment in the inner part of the bay shown in the observation data is consistent with the environmental change inferred from the aquatic palynomorph community (BP-III Unit and BP-D1 Unit).

Deterioration of Bottom Environments Reflected by Microforaminiferal Linings in Beppu Bay

In Beppu Bay core samples, the biserial type and the uniserial type dominated, and the coiled type was rather few as mentioned above. The foraminiferal community indicated that the bottom sediments of the inner part of Beppu Bay consisted of mud with rich organic substance. Kuwae et al. (2022) suggested that total sulfur in sediments clearly increased after year 1968. This increase induced hypoxia bottom sediments and then decreased microforaminiferal linings.

The remarkable deterioration of the bottom habitats suggested by the decrease of microforaminiferal linings in BP-D1 Subunit, especially the biserial type and uniserial type, continued to BP-D2 Subunit and progressed further in BP-C Unit. This deterioration of sediments may be due to the rapid decrease in tidal flat area due to reclamation on the southern coast of Beppu Bay during the BP-D1 Subunit period (1970s)[6], when industrialization along the southern coast of this Bay started. As in Ariake Sound of Western Kyushu discussed below, similar bottom environmental changes occurred in Beppu Bay.

Other Coastal Regions Around Japanese Islands

The analysis of dinoflagellate cyst and other aquatic microfossil assemblages in coastal sediments in Japan has revealed that artificial eutrophication has progressed since the 1960s and that the lower trophic system has changed significantly, including the occurrence of large-scale red tides.

In Tokyo Bay, the dinoflagellate cyst density decreased once in the mid-1940s (The Second World War), but then increased sharply after the 1960s, and the proportion of heterotrophic

[5]https://www.city.beppu.oita.jp/doc/sisei/kakusyukeikaku/sousei/2ki/vision.pdf

[6]https://www.biodic.go.jp/reports/4-11/q211.html

species cysts, mainly Protoperidinioid cysts and accompanied by considerable amount of *Polykrikos** cysts, contributed to that increase. These changes, as the Heterotroph signal in dinoflagellate cyst assemblages, reflected the nutrient enrichment caused by the urbanization around Tokyo Bay (Matsuoka, 1999).

In Ariake Sound located on the opposite side of Kyushu respect to Beppu Bay, changes in the dinoflagellate cyst assemblages in core samples of Isahaya Bay and the inner part of Ariake Sound were investigated. According to Matsuoka (2004), Shin et al. (2010a,b), the density of dinoflagellate cysts increased sharply in Isahaya Bay and the inner part of Ariake Sound after the 1960s, and the proportion of heterotrophic species cysts, mainly *Protoperidinium** species, clearly increased in Isahaya Bay (Matsuoka, 2004). The cause was that the disappearance of tidal flats by artificial reclamation reduced the processing capacity of organic matter carried from the land by the organisms inhabiting there, and the construction of vertical embankments by reclamation reduced vertical mixing and enhanced stratification of sea water (Manda and Matsuoka, 2006). The resultant stratification due to a sharp reduction in speed of bottom current, promoted the decomposition of organic matter in the seafloor, resulting in an anoxic condition at the boundary between seawater and sediments (Matsuoka, 2006). The cause of artificial eutrophication in the Ariake Sound was not urbanization but large-scale tidal flat reclamation after the 1960s. As introduced above, similar artificial eutrophication progressed around Beppu Bay after the 1960s.

In Osaka Bay, paleoenvironmental studies were conducted on materials other than dinoflagellate cysts using diatoms (Hirose et al., 2008), ostracods (Yasuhara et al., 2003), and benthic foraminifera (Tsujimoto et al., 2006). Taken together, these results showed that the marine environment recovered once in the latter half of the 1940s after a slight increase in nutrient load in the 1900s, but since the 1960s, the artificial nutrient load has increased sharply until the present. The factors that led to such environmental changes are thought to be the reclamation of tidal flats, population growth, industrialization and urbanization around Osaka Bay.

Therefore, it can be concluded that artificial eutrophication around the western Japanese archipelago was caused by the period of high economic growth accompanied with reclamation of tidal flats, urbanization, and industrialization after the 1960s. However, as a result of subsequent restrictions on the influx of nutrients that lead to eutrophication, oligotrophic conditions in coastal areas are progressing now and biological production is declining for example in the Seto Inland Sea (Abo and Yamamoto, 2019).

Consequently, such coastal environmental changes have been well preserved in not only dinoflagellate cyst but also other aquatic palynomorph assemblages. Therefore, further eco-physiological investigations for these aquatic palynomorph groups are needed.

Summary

The sediment cores collected at the innermost part of Beppu Bay included various planktonic and benthic aquatic palynomorphs consisting of dinoflagellate cysts, prasinophycean phycoma, algal cells of chlorophyceae, organic shells of testate ameboae, resting cysts and lorica of ciliates, microforaminiferal linings, crustacean resting eggs and fragments of bodies, turbellarian egg capsules, and acritarchs. Among them, dinoflagellate cysts, microforaminiferal linings, and crustacean resting eggs dominated.

As results of stratigraphic cluster analysis for all aquatic palynomorph assemblages and dinoflagellate cyst assemblages, these palynomorphs and dinoflagellate cysts were divided into several units respectively.

The boundary of both upper units, BP-III Unit for all palynomorphs and BP-D Unit for dinoflagellate cysts, was the same era between year 1964 and 1969. However, other boundaries were different. This might have been caused by their different ecological components, since microforaniniferal linings represent a benthic life form, whereas dinoflagellate cysts and Crustaean resting eggs indicated planktonic life form.

Results from BP-III and BP-D Units suggested that artificial eutrophication started in year 1964 and in 1969, and this change of biota in Beppu Bay was the most drastic in the past 1000 years.

The eutrophication might have been induced by anthropogenic activities such as reclamation of tidal flats, urbanization due to increased population, and industrialization involving the development of larger plants around Beppu Bay.

Since non-dinoflagellate aquatic palynomorphs like microforaminiferal linings, crustacean resting eggs, turbellarian egg capsules and other micro-remains will be useful for reconstructing paleoenvironments, further taxonomical and eco-physiological studies of these palynomorphs are needed.

DATA AVAILABILITY STATEMENT

The raw data supporting the conclusions of this article will be made available by the authors, without undue reservation.

AUTHOR CONTRIBUTIONS

KM and MK planned the basic design of the project. MK collected the samples and contributed to making an age model. KM and NK analyzed the samples and observed the palynomorphs and revised the earlier draft of the manuscript. KM wrote a draft of the article. All authors approved the submitted version.

FUNDING

This study was supported financially by Grants-in-Aid for Scientific Research (22340155, 21244073, and 18H01292) from the Japan Society for the Promotion of Science and a research grant from the Mitsui and Co., Ltd., Environment Fund (R09-B022). The cooperative research program (09A043, 10A020, and 19A007) of the Center for Advanced Marine Core Research, Kochi University, also supported this study.

ACKNOWLEDGMENTS

We thank Hidejiro Onishi for conducting sampling with E/R/V ISANA of Ehime University and the crew of the R/V Tansei-Maru (cruises KT-09-01) of the Ocean Research Institute, University of Tokyo, for sampling. We also appreciate Wen Liu for his technical support in statistical analysis and Oita Prefectural Fisheries Research Department for kindly providing the data of STC. We also thank three reviewers and Fernando Rubio whose constructive suggestions and comments were very useful for improving the earlier manuscript.

SUPPLEMENTARY MATERIAL

The Supplementary Material for this article can be found online at: https://www.frontiersin.org/articles/10.3389/fmars.2022.843824/full#supplementary-material

REFERENCES

Abo, K., and Yamamoto, T. (2019). Oligotrophocation and its measures in the Seto Inland Sea. *Jpn. Fish. Res. Educ. Agen.* 49, 21–26.

Anthropocene Working Group (2020). *Report of activities 2020, Newsletter of the Anthropocene Working Group*. California: Anthropocene Working Group, 31.

Appleby, P. G., and Oldfield, F. (1978). The Calculation of Lead-210 Dates Assuming a Constant Rate of Supply of Unsupported ^{210}Pb to the Sediment. *CATENA* 5, 1–8.

Armstrong, H. A., and Brasier, M. D. (2007). *Microfossils*, 2nd Edn. London: Blackwell publishing Ltd, viii+296.

Belmonte, G., and Rubino, F. (2019). "Resting cysts from coastal marine plankton," in *Oceanography and Marine Biology: Annual Review*, Vol. 57, eds S. J. Hawkins, A. L. Allcock, A. E. Bates, L. B. Firth, I. P. Smith, S. E. Swearer, et al. (Boca Raton: CRC Press), 1–186.

Caffrey, J. M., and Murrell, M. C. (2016). "A historical perspective on eutrophication in the Pensacola Bay Estuary, FL, USA," in *Aquat. Microb. Ecol. Biogeochem.: A dual perspective*, eds P. M. Gilbert and T. M. Kana, (Switzerland: Springer International Publishing), 199–213. doi: 10.1007/978-3-319-30259-1_16

Cho, H.-J., and Matsuoka, K. (2000). Cell lyses of a phagotrophic dinoflagellate, *Polykrikos fokoidii* feeding on *Alexandrium tamarense*. *Plank Biol. Ecol.* 47, 134–136.

Clarke, A. L., Conle, Y. D. J., Anderson, N. J., Adser, F., Andren, E., de Jonge, V. N., et al. (2006). Long-term trends in eutrophication and nutrients in the coastal zone. *Limnol. Oceanol.* 51, 385–397.

Dale, B. (2009). Eutrophication signals in the sedimentary record of dinoflagellate cysts in coastal waters. *J. Sea Res.* 61, 103–113. doi: 10.1016/j.scitotenv.2003.08.003

Dale, B., Thorsen, T. A., and Fjellsa, A. (1999). Dinoflagellate cysts as indicators of cultural eutrophication in the Oslofjord, Norway. *Est. Coast. Shelf Sci.* 48, 371–382.

Dolan, J. R., Montagnes, D. J. S., Agatha, S., Wayne Coats, D., and Diane, K. (2013). "Introduction to tintinnids," in *The Biology and Ecology of Tinntinid Ciliates*, eds J. R. Dolan, D. J. S. Montagnes, S. Agatha, W. Coats, and D. K. Stoecker (United Kingdom: Wiley-Blackwell), 1–16.

Downie, C., Evitt, W. R., and Sarjeant, W. A. S. (1963). Dinoflagellates, hystrichospheres, and the classification of the acritarchs. *Stanford Univ. Publ. Geosci.* 7, 1–16.

Fensome, R. A., Williams, G. L., and MacRae, R. A. (2009). Late Cretaceous and Cenozoic fossil dinoflagellates and other palynomorphs from the Scotian Margin off shore eastern Canada. *J. System. Palaeont.* 7, 1–79.

Gaines, G., and Taylor, F. J. R. (1984). Extracellular digestion in marine dinoflagellates. *J. Plank. Res.* 6, 1057–1061.

Guiot, J., and de Vernal, A. (2007). "Chapter Thirteen Transfer Functions: Methods for Quantitative Paleoceanography based on microfossils," in *Developments in Marine Geology*, eds C. Hillaire-Marcel and A. Vernal (Amsterdam: Elsevier), 523–563.

Gurdebeke, P. R., Mertens, K. N., Takano, Y., Yamaguchi, A., Bogus, K., Micah Dunthorn, M., et al. (2018). The affiliation of *Hexasterias problematica* and *Halodinium verrucatum* sp. nov. to ciliate cysts based on molecular phylogeny and cyst wall composition. *Europ. J. Protistol.* 66, 115–135. doi: 10.1016/j.ejop.2018.09.002

Hansen, P. J. (1991). Quantitative importance and trophic role of heterotrophic dinoflagellates in a coastal pelagical food web. *MEPS* 73, 253–261.

Harada, K., Endo, A., and Matsuoka, K. (1994). Uzubennmousou Kaseki wo Mochiita Beppuwann ni okeru Kohyouki no Kaiyoukannkyou Hennsenn no Fukugen (Reconstruction of the post glacial marine environments using dinoflagellate cysts in Beppu Bay). *Gekkan Chikyu* 16, 709–716.

Harland, R., Asteman, I. P., and Nordberg, K. (2013). A two-millennium dinoflagellate cyst record from Gullmar Fjord, a Swedish Skagerrak sill fjord. *Palaeogeogr. Palaeoclimatol. Palaeoecol.* 392, 247–260. doi: 10.1016/j.palaeo.2013.09.006

Hirose, K., Yasuhara, M., Tsujimoto, A., Yamazaki, H., and Yoshikawa, S. (2008). The succession of diatom assemblages and anthropogenically-induced environmental changes over the last 120 years, Osaka Bay, Japan. *Daiyonki Kenkyu* 47, 287–296. doi: 10.4116/jaqua.47.287

Hoang, A. Q., Aono, D., Watanabe, I., Kuwae, M., Kunisue, T., and Takahashi, S. (2021). Contamination levels and temporal trends of legacy and current-use brominated flame retardants in a dated sediment core from Beppu Bay, southwestern Japan. *Chemosphere* 266:129180. doi: 10.1016/j.chemosphere.2020.129180

Jacobson, D. M., and Anderson, D. M. (1986). Thecate heterotrophic dinoflagellates: feeding behavior and mechanism. *J. Phycol.* 22, 249–258.

Jeong, H.-J. (1994). Predation by the heterotrophic dinoflagellate *Protoperidinium* cf. *divergens* on copepod eggs and early naupliar stages. *MEPS* 114, 203–208. doi: 10.3354/meps114203

Kameda, T., and Fujiwara, T. (1995). Ventilation time and anoxia of the Benthic cold water in Beppu Bay. *Bull. Coast. Oceanogr.* 33, 59–68.

Kitazato, H. (1981). Observation of behavior and mode of life of benthic foraminifera in laboratory. *Bull. Earth Sci. Shizuoka Univ.* 6, 61–71.

Kokinos, J. P., Eglinton, T. I., Goni, M. A., Boon, J. J., Martog, A., and Anderson, D. M. (1998). Characterization of a highly resistant biomacromolecular material in the cell wall of a marine dinoflagellate resting cyst. *Org. Geochem.* 28, 265–288.

Köster, D., Lichter, J., Lea, P. D., and Nurse, A. (2007). Historical eutrophication in a river-estuary complex in mid-coast Maine. *Ecol. Appl.* 17, 765–778. doi: 10.1890/06-0815

Kuwae, M., Tsugeki, N. K., Amano, A., Agusa, T., Suzuki, Y., Tsutsumi, J., et al. (2022). Evidence of human-induced marine degradation in anoxic coastal sediments of Beppu Bay, Japan, as an Anthropocene marker in East Asia. *Anthropocene* 37:100318.

Kuwae, M., Yamamoto, M., Ikehara, K., Irino, T., Takemura, K., Sagawa, T., et al. (2013). Stratigraphy and wiggle-matching-based age-depth model of late Holocene marine sediments in Beppu Bay, southwest Japan. *J. Asian Earth Sci.* 69, 133–148. doi: 10.1016/j.jseaes.2012.07.002

Maier, G., Nimmo-Smith, J., Glegg, G. A., Tappin, A. D., and Worsfold, P. J. (2009). Estuarine eutrophication in the UK: current incidence and future trends. *Mar. Freshw. Ecosyst.* 19, 43–56. doi: 10.1002/aqc.982

Manda, A., and Matsuoka, K. (2006). Changes in tidal currents in the Ariake Sound due to reclamation. *Estuar. Coast.* 29, 645–652. doi: 10.1007/bf02784289

Marcott, S. A., Shakun, J. D., Clark, P. U., and Mix, A. C. (2013). A reconstruction of regional and global temperature for the past 11,300 years. *Science* 339:1198.1228026 doi: 10.1126/science

Masumoto, M., Kuwae, M., and Hinata, H. (2018). Flux of sedimentary microplastics in Beppu Bay, Japan. *Proc. Jpn. Soc. Civil Engin. B* 2, 1321–1326.

Matsuoka, K. (1999). Eutrophication recorded in dinoflagellate cyst assemblages - a case of Yokohama Port, Tokyo Bay, Japan. *Sci. Total Environ.* 231, 17–35. doi: 10.1016/s0048-9697(99)00087-x

Matsuoka, K. (2004). Changes in the Aquatic Environment of Isahaya Bay, Ariake Sound, West Japan: from the view point of dinoflagellate cyst assemblage. *Bull. Coast. Oceanog.* 42, 55–59.

Matsuoka, K. (2006). Medium- to long-term environmental changes in the inner part of Ariake Sound recorded in the dinoflagellate cyst assemblages. *Sci. Tot. Environ.* 264, 65–93.

Matsuoka, K., and Ando, T. (2021). Review-Turbellarian egg capsule as one type of aquatic palynomorph; reconsideration of Tintinnomorph. *Laguna* 28, 15–35. doi: 10.1002/jmor.1051880103

Matsuoka, K., Cho, H.-J., and Jacobson, D. M. (2000). Observations of the feeding behavior and growth rates of the heterotrophic dinoflagellate *Polykrikos kofoidii* (Polykrikaceae, Dinophyceae). *Phycologia* 39, 82–86. doi: 10.2216/i0031-8884-39-1-82.1

Matsuoka, K., and Fukuyo, Y. (2000). *Technical Guide for modern dinoflagellate cyst study. i+ 29pp, 17 figures, 7 tables, 22 plates*. Tokyo: Japan Society for the Promotion of Science.

Matsuoka, K., Ikeda, Y., Kaga, S., Kaga, M., and Ogata, T. (2018). Repercussions of the Great East Japan Earthquake tsunami on ellipsoidal *Alexandrium* cysts (Dinophyceae) in Ofunato Bay, Japan. *Mar. Environ. Res.* 135, 123–135. doi: 10.1016/j.marenvres.2018.01.001

Matsuoka, K., Joyce, B. L., Kotani, Y., and Matsuyama, Y. (2003). Modern dinoflagellate cysts in hypertrophic coastal waters of Tokyo, Bay, Japan. *J. Plank. Res.* 25, 1461–1470.

McCarthy, F. M. G., Pilkington, P. M., Volik, O., Heyde, A., and Cocker, S. L. (2021). "Non-pollen palynomorphs in freshwater sediments and their palaeolimnological potential and selected applications," in *Applications of Non-Pollen Palynomorphs: from Palaeoenvironmental Reconstructions to Biostratigraphy*, Vol. 511, eds F. Marret, J. O'Keefe, P. Osterloff, M. Pound, and L. Shumilovskikh (London: Geological Society), 1144/SP511-2020-2109 doi: 10

McMinn, A., Bolch, C., and Hallegraeff, G. (1992). *Cobricosphaeridium* Harland and Sarjeant: Dinoflagellate cyst or copepod egg? *Micropaleontol.* 38, 315–316.

Meisterfeld, R. (2002). "Order Arcellinida Kent, 1880," in *The Illustrated Guide to the Protozoa. Vol. 2, Second edition*, eds J. J. Lee, G. F. Leedale, and P. Bradbury (Kansas: Society of Protozoologists), 827–860. doi: 10.1016/j.protis.2005.03.002

Mudie, P. J., Marret, F., Gurdbeke, P. R., Hartman, J. D., and Reid, P. C. (2021). "Marine dinocysts, acritarchs and less well-known NPP: tintinnids, ostracod and foraminiferal linings, copepod and worm remains," in *Applications of Non-Pollen Palynomorphs: from Palaeoenvironmental Reconstructions to Biostratigraphy*, eds F. Marret, J. O'Keefe, P. Osterloff, M. Pound, and L. Shumilovskikh (London: Geological Society), 511. SP511-2020-55 doi: 10.1144/

Nishimuta, K., Ueno, D., Takahashi, S., Kuwae, M., Kadokami, K., Miyawaki, T., et al. (2020). Use of comprehensive target analysis for determination of contaminants of emerging concern in a sediment core collected from Beppu Bay, Japan. *Environ. Pollut.* 272:115587. doi: 10.1016/j.envpol.2020.115587

Okaichi, T. (1997). *Science of Red Tides (Akashio no Kagaku)*, 2nd Edn. Tokyo: Koseisha-Koseikaku, 337.

Park, M., Boalch, G. T., Jowett, R., and Harbour, D. S. (1978). The genus *Peterosperma* (Prasinophyceae): species with a single equatorial ala. *J. Mar. Bio. Ass. U.K.* 58, 239–276.

Penaud, A., Hardy, W., Lambert, C., Marret, F., Masure, E., Servais, T., et al. (2018). Dinoflagellate fossils: Geological and biological applications. *Rev. Micropaléont.* 61, 235–254.

Pospelova, V., Chmura, G. L., Boothman, W., and Latimer, J. S. (2005). Spatial distribution of modern dinoflagellate cysts in polluted estuarine sediments from Buzzards Bay (Massachusetts, USA) embayments. *MEPS* 292, 23–40.

Reid, P. C., and John, A. W. G. (1978). Tintinnid cysts. *J. Mar. Boil. Assoc. U.K.* 58, 551–557.

Sherr, E., and Sherr, B. (1988). Role of microbes in pelagic food webs: a revised concept. *Limnol. Oceanog.* 33, 187–197.

Shimada, M., Takahara, H., Kuwae, M., Yamamoto, M., Ikehara, K., Irino, T., et al. (2012). Late Holocene human impact on vegetation changes around Beppu Bay in northeast Kyushu, southwest Japan based on the influx pollen data dated by a wiggle-matching. *Jpn. J. Palynol.* 58, 212–213.

Shin, H. H., Matsuoka, K., Yoon, Y. H., and Kim, Y.-O. (2010a). Response of dinoflagellate cyst assemblages to salinity changes in Yeoja Bay, Korea. *Mar. Micropaleont.* 77, 15–24.

Shin, H. H., Mizushima, K., Oh, S. J., Park, J. S., Noh, I. H., Iwataki, M., et al. (2010b). Reconstruction of historical nutrient levels in Korean and Japanese coastal areas based on dinoflagellate cyst assemblages. *Mar. Pol. Bull.* 60, 1243–1258. doi: 10.1016/j.marpolbul.2010.03.019

Shumilovskikh, L. S., O'Keefe, J. M. K., and Marret, F. (2021). "An overview of the taxonomic groups of NPPs. In Applications of Non-pollen Palynomorphs: from palaeoenvironmental reconstructions to biostratigraphy," in *Applications of Non-Pollen Palynomorphs: from Palaeoenvironmental Reconstructions to Biostratigraphy*, eds F. Marret, J. O'Keefe, P. Osterloff, M. Pound, and L. Shumilovskikh (London: Geological Society), 511.

Shumilovskikh, L. S., Schlütz, F., Lorenz, M., and Tomaselli, B. (2019). Non-pollen palynomorphs notes: 3. Phototrophic loricate euglenoids in palaeoecology and the effect of acetolysis on Trachelomonas loricae. *Rev. Palaeobot. Palynol.* 270, 1–7.

Stancliffe, R. P. W. (1989). Microforaminiferal linings: Their classification, biostratigraphy and paleoecology, with special reference to specimens from British Oxfordian sediments. *Micropaleont.* 35, 337–352. doi: 10.2307/1485676

Sugaya, M., and Nakao, S. (1983). Distribution of recent shallow water foraminifera of Bungo Suido. *Bull. Geol. Surv. Jpn.* 34, 483–496.

Takahashi, S., Anh, H. Q., Watanabe, I., Aono, D., Kuwae, M., and Kunisue, T. (2020). Characterization of mono- to deca-chlorinated biphenyls in a well-preserved sediment core from Beppu Bay, Southwestern Japan: Historical profiles, emission sources, and inventory. *Sci. Total Environ.* 743:140767. doi: 10.1016/j.scitotenv.2020.140767

Taniguchi, A. (1975). "A role and position of zooplankton in marine ecosystem," in *Marine Science Basic Series 6*, ed. S. Motoda (Tokyo: Tokai University Press), 119–235.

Thorsen, T., and Dale, B. (1998). Climatically influenced distribution of *Gymnodinium catenatum* during the past 2000 years in coastal sediments of southern Norway. *Palaeog. Palaeoc. Palaeoecol.* 143, 159–177.

Topping, J. N., Murray, J. W., and Pond, D. Z. W. (2006). Sewage effects on the food source and diet of benthic formaninifera living in anoxic sediment: a microcosm experiment. *J. Exp. Mar. Biol. Ecol.* 329, 239–250.

Travers, A. (2007). *Paleopalynology*, 2nd Edn. The Netherland: Springer, xii+813.

Tsugeki, N. K., Kuwae, M., Tani, Y., Guo, X.-Y., Omori, K., and Takeoka, H. (2016). Temporal variations in phytoplankton biomass over the past 150 years in the western Seto Inland Sea, Japan. *J. Oceanog.* 73, 309–320. doi: 10.1007/s10872-016-0404-y

Tsujimoto, A., Nomura, R., Yasuhara, M., Yamazaki, H., and Yoshikawa, S. (2006). Impact of eutrophication on shallow marine benthic foraminifers over the last 150 years in Osaka Bay, Japan. *Mar. Micropaleont.* 60, 258–268.

Uye, S., and Takamatsu, K. (1990). Feeding interactions between planktonic copepods and red-tide flagellates from Japanese coastal waters. *MEPS* 59, 97–107. doi: 10.3354/meps059097

van Geel, B. (2001). "non-pollen palynomorphs," in *Tracking Environmental Change Using Lake Sediments. Volumen 3: Terrestrial, Algal and Siliceous Indicators*, eds J. P. Smol, H. J. B. Birks, and W. M. Last (Netherlands: Kluwer Academic Publishers), 99–119.

van Waveren, I. M. (1993). Chitinous palynomorphs and palynodebris representing crustacean exoskeleton remains from sediments of the Banda Sea (Indonesia). *Geologica Ultraiectina Mededelingen van den Faculteit Aardwetenschappen Universiteit Utrecht* 104, 18–51.

Versteegh, G. J. M., Blokker, P., Bogus, K. A., Harding, I. C., Lewis, J., Oltmanns, S., et al. (2012). Infra red spectroscopy, flash pyrolysis, thermally assisted hydrolysis and methylation (THM) in the presence of tetramethylammonium hydroxide (TMAH) of cultured and sediment-derived *Lingulodinium polyedrum* (Dinoflagellata) cyst walls. *Org. Chem.* 43, 92–102. doi: 10.1016/j.orggeochem.2011.10.007

Wall, D. (1962). Evidence from Recent plankton regarding the biological affinities of *Tasmanites* Newton 1875 and *Leiosphaeridia* Eisenack 1958. *Geol. Mag.* 99:362.

Wall, D., and Dale, B. (1968). Modern dinoflagellate cysts and the evolution of the Peridiniales. *Micropaleont.* 14, 265–304.

Williams, G. L., Fensome, R. A., and MacRae, R. A. (2017). *DINOFLAJ3. American Association of Stratigraphic Palynologists, Data Series* 2. Available online at: http://dinoflaj.smu.ca/dinoflaj3 (accessed January 20, 2022).

Yamada, K., Takemura, K., Kuwae, M., Ikehara, K., and Yamamoto, M. (2016). Basin filling related to the Philippine Sea Plate motion in Beppu Bay, southwest Japan. *J. Asian Earth Sci.* 117, 13–22. doi: 10.1016/j.jseaes.2015.12.008

Yasuhara, M., Yamazaki, H., Irizuki, T., and Yoshikawa, S. (2003). Temporal changes of ostracode assemblages and anthropogenic pollution during the last 100 years, in sediment cores from Hiroshima Bay, Japan. *Holocene* 13, 527–536.

Zonneveld, K. A. F., Marret, F., Versteegh, G. J. M., Bonnet, S., Bouimetarhan, I., Crouch, E., et al. (2013). Atlas of modern dinoflagellate cyst distribution based on 2405 datapoints. *Rev. Palaeobotan. Palynol.* 191, 1–197.

Zonneveld, K. A. F., Versteegh, G. J. M., and De Lange, G. J. (1997). Preservation of organic walled dinoflagellate cysts in different oxygen regimes: a 10,000 years natural experiment. *Mar. Micropaleont.* 29, 393–405.

Conflict of Interest: The authors declare that the research was conducted in the absence of any commercial or financial relationships that could be construed as a potential conflict of interest.

frontiers | Frontiers in Marine Science

ORIGINAL RESEARCH
published: 04 April 2022
doi: 10.3389/fmars.2022.812622

A Multiparametric Approach to Unravelling the Geoenvironmental Conditions in Sediments of Bay of Koper (NE Adriatic Sea): Indicators of Benthic Foraminifera and Geochemistry

Petra Žvab Rožič[1], Jelena Vidović[2,3], Vlasta Ćosović[3], Ana Hlebec[3], Boštjan Rožič[1] and Matej Dolenec[1]*

[1] Department of Geology, Faculty of Natural Sciences and Engineering, University of Ljubljana, Ljubljana, Slovenia, [2] Joint Research Centre, European Commission, Brussels, Belgium, [3] Department of Geology, Faculty of Science, University of Zagreb, Zagreb, Croatia

OPEN ACCESS

Edited by:
Martina Orlando-Bonaca, Marine Biology Station Piran, National Institute of Biology, Slovenia

Reviewed by:
Luciana Ferraro, Institute of Marine Science (CNR), Italy
Alessandra Asioli, Institute of Marine Science (CNR), Italy

***Correspondence:**
Petra Žvab Rožič
petra.zvab@ntf.uni-lj.si

Specialty section:
This article was submitted to Marine Ecosystem Ecology, a section of the journal Frontiers in Marine Science

Received: *10 November 2021*
Accepted: *28 February 2022*
Published: *04 April 2022*

Citation:
Žvab Rožič P, Vidović J, Ćosović V, Hlebec A, Rožič B and Dolenec M (2022) A Multiparametric Approach to Unravelling the Geoenvironmental Conditions in Sediments of Bay of Koper (NE Adriatic Sea): Indicators of Benthic Foraminifera and Geochemistry. Front. Mar. Sci. 9:812622. doi: 10.3389/fmars.2022.812622

The Bay of Koper is influenced by agricultural, urban, and port activities, therefore pollution from trace metals is a concern. A total of 20 sediment samples obtained from four 10-cm sediment cores were analyzed. Element concentration in the sediment of the bay was determined spatially and temporally from the recent surface to depth. The results were correlated with the composition and diversity of the benthic foraminiferal assemblages. Major element concentrations indicate natural lithogenic origin (which is also confirmed by mineralogical features). The benthic foraminiferal assemblages in sediment samples, although mainly composed of representatives of the Rotaliida, show moderate to high species diversity and are dominated by the pollution tolerant species *Ammonia pakinsoniana*, *Haynesina* sp., *Valvulineria bradyana* and the non-keel *Elphidium* sp. and subordinated by *Ammonia tepida* and *Haynesina depressula*. Canonical correspondence analysis (CCA) on foraminiferal species and trace element concentrations shows a possible control of some potential toxic elements (i.e., Cu, Ni, Pb, Zr, Cr, As) on the diversity and taxonomic composition of foraminiferal assemblages. Nevertheless, foraminiferal diversity and dominance in the bay are related to sediment characteristics such as sediment grain size, and the amount of terrigenous inflow rather than to the element concentrations of sediments. This study evaluated ecological conditions by using the Foram-AMBi and EcoQS indices. The values of the Foram-AMBI index reflect the good to moderate quality of ecological conditions, whereas high to poor ecological statuses were interpreted by calculating EcoQS.

Keywords: marine sediments, major, minor and trace elements, benthic foraminifera, geoenvironmental assessment, Bay of Koper, Northern Adriatic

INTRODUCTION

The Adriatic Sea is one of the largest recent epicontinental seas in the world and a young marine ecosystem that was subject to various natural and anthropogenic processes during the Holocene: marine transgression (Trincardi et al., 1994; Correggiari et al., 1996), regional climate fluctuations (Giani et al., 2012; Appiotti et al., 2014), and urbanization and pollution (Lotze et al., 2006; Cozzi and Giani, 2011). The Bay of Koper in southern part of the Gulf of Trieste (north-eastern Adriatic Sea), represents an area of particular interest, where the most recent anthropogenic pressure was generated by industrial and domestic activities along the coast. The Bay of Koper is characterized by the Port of Koper, one of the most important ports in the northern Adriatic. Through its activities, the port covers a wide range of freight transport (Cepak and Marzi, 2009) and in recent years also international passenger transport, organized in 12 dedicated terminals along 2 piers. The port's annual cargo throughput is growing since the 90s of the 20^{th} century and has already counts some 20 million tonnes per year in 2015. With its activities, the port represents a potential source of pollution for different environmental matrices: air, water, sediments, and soil. Therefore, several studies have been carried out on this issue (Žitnik et al., 2005; David et al., 2007; Cepak and Marzi, 2009; Zuin et al., 2009; Mladenović et al., 2013; Zupančič and Skobe, 2014; Rogan Šmuc et al., 2018). The results of above mentioned studies show that the ecological quality status of the seafloor sediments and water is better than in other ports of the Eastern Adriatic, that the accumulation of pollutants in the sediments is less significant due to the sedimentological characteristics (i.e., mineralogy, grain size) and the advective transport of particles.

In addition, industrial and municipal wastewater damage the coastal area (the amount of wastewater rises considerably during the summer months). Rivers (especially those along the southern Slovenian coast) also contribute by delivering sediment loads from their catchments (Cozzi et al., 2020). Due to generally superficial clockwise (Malačič and Petelin, 2001) sea currents, the bay may also be threatened by pollutants from the northern parts of the Gulf of Trieste, which is also highly industrialized and urbanized (Adami et al., 1996; Barbieri et al., 1999; Cibic et al., 2008; Cepak and Marzi, 2009; Aquavita et al., 2010). All of these anthropogenic pressures may lead to the accumulation of pollutants in the coastal environment and affect the natural conditions of the area (Dassenakis et al., 2003).

Recent decades have seen increased concern over the management and protection of these nearshore marine areas, and considerable efforts have been made to develop tools to assess their environmental and ecological status (Borja et al., 2008; Birk et al., 2012). The main objective of these efforts is to use the pollutants, physico-chemical parameters, and biological elements of the ecosystem to assess the status in an integrated manner (Borja et al., 2008). Among the biological indicators, benthic species are preferred due to their main characteristics: reduced motility, high diversity, and a life span that allows for the monitoring of the short, medium or long-term effects of any discharged substances (Solis-Weiss et al., 2007 and references therein). The resulting species composition, replacements, eliminations, diversity, or changes in abundance may indicate the recent history of events affecting the area (Solis-Weiss et al., 2001).

Benthic foraminifera – protozoans that live as epiphytic, epifaunal, or infauna on soft sediments from transitional and coastal environments to the deep sea – are useful ecological indicators of depositional dynamics owing to their abundance and adaptations to different environmental conditions (i.e., Kaminski et al., 2002; Oldfield et al., 2003; Morigi et al., 2005; Bouchet et al., 2007; Gooday et al., 2021; Romano et al., 2021). The usefulness of foraminifera for such studies stems from their short life cycles, high biodiversity, and the ecological preferences of known species (Murray, 2006). Because benthic foraminifera are small and abundant compared to other hard-shelled taxa, they are easy to collect, and small sample sizes can provide a reliable database for statistical analysis (Frontalini and Coccioni, 2008). They are among the best tools to study human-induced marine degradation over long periods of time using sediment cores (Yasuhara et al., 2012). Several ecological studies on the effects of element content (trace metals) on modifications and changes in foraminifera (Jorissen, 1987; Alve, 1991, 1995; Yanko et al., 1998; Angel et al., 2000; Coccioni, 2000; Debenay et al., 2001; Armynot du Châtelet et al., 2004; Bergin et al., 2006; Burone et al., 2006; Ferraro et al., 2006; Frontalini and Coccioni, 2008; Frontalini et al., 2009; Rumolo et al., 2009; Vidović et al., 2009, 2014, 2016; Caruso et al., 2011; Yasuhara et al., 2012; Popadić et al., 2013; Romano et al., 2016) have been made, many of them in gulfs with port activities. Studies in the Gulf of Trieste show a minor increase in foraminiferal diversity in areas with intensive agricultural and maricultural activities (Vidović et al., 2016). Higher concentrations of trace elements due to industrial activities in the Gulf of Rijeka resulted in the dominance of stress-tolerant epifaunal foraminiferal species (Popadić et al., 2013).

Studies of benthic foraminifera in the Adriatic Sea have shown that organic matter is an important controlling factor for assemblage abundance and diversification (Jorissen, 1987, 1988; Coccioni et al., 2009; Melis et al., 2019). Thus, the foraminiferal distribution pattern follows the granulometric characteristics of the seafloor sediments (Jorissen, 1987, 1988).

In last decades, the sediment in the Gulf of Trieste has been intensively studied in numerous environmental studies focused on elemental (heavy metal) distribution in relation to anthropogenic impacts (Donazzolo et al., 1981; Brambati and Catani, 1988; Hohenegger et al., 1988, 1993; Faganeli et al., 1991; Ogorelec et al., 1991; Adami et al., 1996; Colizza et al., 1996; Covelli and Fontolan, 1997; Barbieri et al., 1999; Horvat et al., 1999; Covelli et al., 2006, 2012; Cibic et al., 2008; Aquavita et al., 2010; Vidović et al., 2016; Melis et al., 2019). Some studies showed positive correlations between abundances of tolerant taxa (especially *Ammonia* spp., *Bolivina* spp. and *Bulimina* spp.) and increased concentrations of Ni, Zn, and As (Frontalini and Coccioni, 2008; Melis et al., 2019). Sediment from Bay of Koper were classified as silty clay, rich in foraminiferal and molluscan fragments (Ogorelec et al., 1987, 1991; Rogan Šmuc et al., 2018). The grain-size of the sediment increases toward the central part of the bay (Ogorelec et al., 1987). Most of trace elements (such us Cr, Cu, Zn, Cd, Ni) are following the organic

matter content in sediment which was shown with the same distribution pattern of these two parameters (Ogorelec et al., 1987; Faganeli et al., 1991). The contents of trace elements in the surface sediments of the Bay of Koper are comparable to the geochemical background of this area (Ogorelec et al., 1987). To date, there is no study in the Bay of Koper that evaluates the impact of the anthropogenic influence on benthic foraminifera and geochemical proxies.

The integrative approach we propose to assess the potential anthropogenic impacts (port activities, industry, municipal activities, tourism) on the Bay of Koper is based on the benthic foraminifera assemblages. The study is focused on the spatio-temporal comparison of mineralogical and geochemical properties (element concentrations) of sediments and benthic foraminifera from four sites in the bay with different degrees of anthropogenic load. This work contributes to detect anthropogenic stress against a background of natural conditions in the southern part of the Gulf of Trieste. For ecological condition evaluation, Foram-AMBi and EcoQS indices were calculated.

STUDY AREA

The Bay of Koper on the Northern Adriatic Sea (**Figure 1A**) constitutes the enclosed south-eastern part of the Gulf of Trieste. The bay covers approximately 35 km^2 and stretches from Izola in the south to the cliffs of Debeli rtič in the north. Two rivers, the Rižana and the Badaševica, flow into the bay.

The Gulf of Trieste/Trst coast geologically consists mainly of Middle Eocene Flysch, whereas Cretaceous – Early Eocene limestone outcrops in its southern part along the Istra Peninsula, in the core of the Izola Anticline and north of the city of Trieste/Trst (**Figures 1A,B**; Pleničar et al., 1973; Pavšič and Peckmann, 1996; Placer et al., 2004, 2010; Vrabec and Rožič, 2014).

The base rock below Gulf of Trieste/Trst, and in areas north of the gulf, is covered by Pliocene-Pleistocene fluvial deposits (mainly sand, gravel, and silty clays) occasionally interrupted by marine and brackish sediments. These do not outcrop but are covered by two types of Holocene deposits. The first are fluvial/deltaic deposits found on the mainland: coarse-grained, carbonate-siliciclastic Soča/Isonzo River sediments characterize the northern rim of the gulf, whereas to the south the Rižana and Dragonja rivers contribute fine siliciclastic material with brackish environments at river mouths (Pleničar et al., 1973). The second are marine deposits found on the sea bottom in the gulf. These are fine-grained clastic sediments (sandy silt, clayish silt, silt and silty sands) with common foraminifera, bivalve and gastropod shells (Ogorelec et al., 1987, 1991, 1997). The Holocene transgression is dated with the radiocarbon method at 8.270 ± 50 yr BP - 9.160 ± 120 yr BP

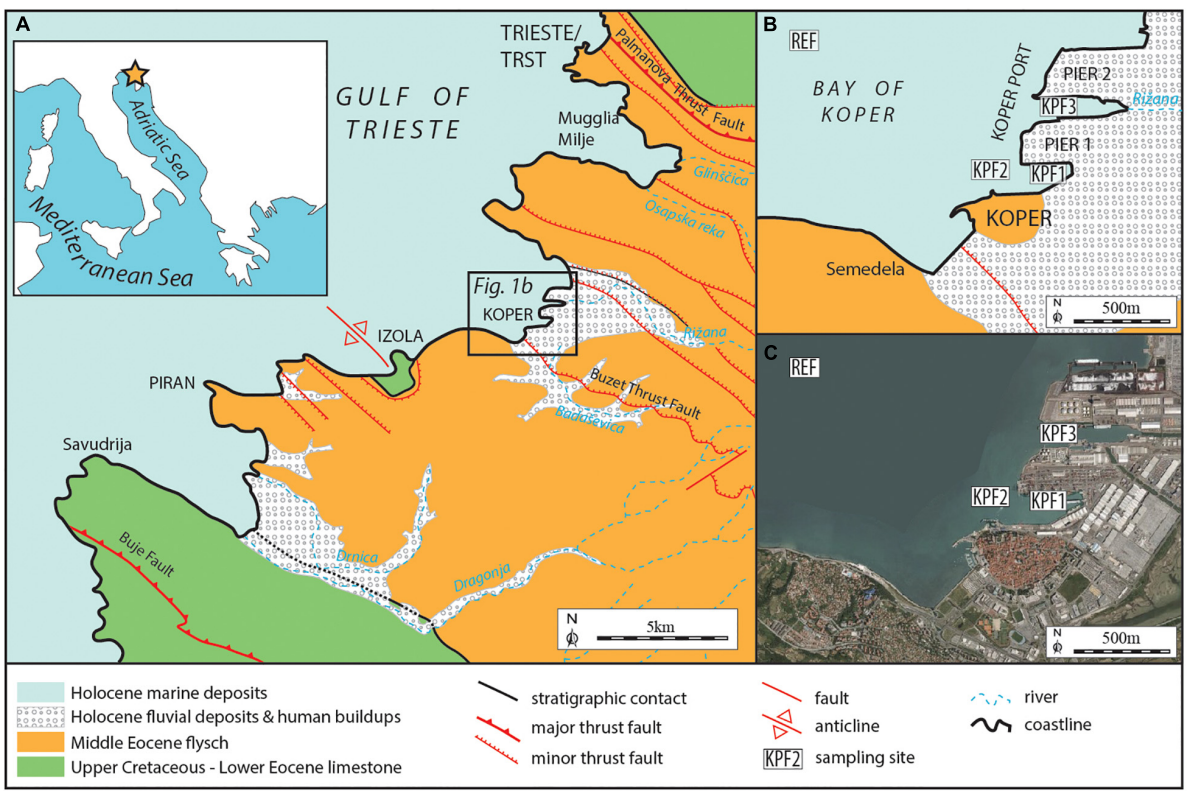

FIGURE 1 | (A) Geographical and geological map of investigated area. **(B)** Enlarged boxed area from **Figure 1A** with sampling locations. **(C)** Bay of Koper with sampling locations (http://gis.arso.gov.si/atlasokolja/).

(Ogorelec et al., 1981; Covelli et al., 2006). The thickness of the marine sedimentary cover varies from 0 meters in coastal areas to several tens of meters in the central part of the gulf (Romeo, 2009; Slavec, 2012; Vrabec et al., 2014; Trobec, 2015; Trobec et al., 2018). Specific sub-recent sedimentary environments are represented by the Sečovlje and Strunjan Salinas (Ogorelec et al., 1981).

MATERIALS AND METHODS

Sampling

Sediment samples were collected at four sites in Koper Bay during the summer of 2014 (**Figures 1B,C**). Three sampling sites were located in the Port of Koper, KPF1 (13°44021′E, 45°33,108′N, water depth 13.6 m) and KPF2 (13°43′51.10″E, 45°33′5.67″N, water depth 13 m) in the part of the port with the highest activity, and KPF3 (13°44,318′E, 45°33,489′N, water depth 13.2 m) near the outflow of Rižana River. The reference sampling sites REF (13°42,321′E, 45°34,320′N, water depth 18.5 m) were positioned outside the port near the anchorage in the fairway to the port and have been considered as reference sampling sites by the National Institute of Biology for decades.

The sediment samples were taken with a gravity sampler using plastic cores (10 cm diameter) to avoid metal contaminations. Two cores were collected at each location, one core was dedicated to meiofaunal analysis and other was used for geochemical and mineralogical studies. The upper 10 cm of the sediment was immediately sliced into 2-cm thick depth intervals and marked with numbers/1 = 0–2cm,/2 = 2–4cm,/3 = 4–6cm,/4 = 6–8cm,/5 = 8–10cm. The sediment samples were stored in clean plastic bags and immediately frozen. The sediment samples derived from the cores dedicated for the geochemical and mineralogical analysis were freeze-dried (lyophilized) until a constant weight was achieved. The samples were further homogenized and crushed to a fine powder using an agate mortar.

Mineralogical Analyses

The general mineral composition of the sediment samples was measured by X-ray powder diffraction using a Philips PW3710 X-ray diffractometer with $CuK\alpha_1$ radiation and a secondary graphite monochromator. The data was collected at 40 kV with a current of 30 mA at a speed of 3.4° 2θ per minute in a range from 2 to 70° (2θ). Oriented clay mineral aggregate was also performed using a household kitchen blender, an ultrasonic bath, ultracentrifugation, and the common glass slide method. In order to show the extent of expansion and/or concentration in the d-spacing that would indicate certain clay minerals, the oriented samples were air dried, glycolated with ethylene glycol, and heated to 550°C for 2 h. Diffraction patterns were identified using X'Perth Highscore Plus 4.6 diffraction software using the PAN-ICSD database and the full pattern fit method (Rietveld) for the quantitative mineral phase analysis.

Geochemical Analyses

Multi-elemental analyses of total elemental concentrations were performed using a portable handheld ThermoFisher Niton XL3t-GOLDD 900S-He X-ray fluorescence (XRF) analyzer. Approximately 3 g of powdered sediment samples were pressed into pellets using stainless steel capsules, a hammer and a pellet press tool. Two factory setting modes were used during the measurements: "Mining" mode for major elements and "Soil" mode for trace elements. When measuring with using "Mining" mode, helium (He) gas was purged in the analyzer, allowing better detection of light elements (Mg, Si, Al, S, and P). The measurement time on each sample was 210 s in "Mining" mode and 180 s in "Soil" mode. The accuracy and precision of the sediment analyses were evaluated using the pre-calibrated 24 reference standards (NIST, USGS) and the NIST-1d (limestone) and NIST-88b (dolomitic limestone) standards at the beginning and end of the measurement. According to the 2 replicate measurements of sediment samples and measured references analytical quality was satisfactory for almost all elements.

Foraminiferal Analyses

The sediment samples from the cores dedicated for foraminiferal analyses were stained in a 70% (ethanol/2g L^{-1}) Rose Bengal mixture (Walton, 1952). To obtain a good staining, the samples were treated with Rose Bengal for at least two weeks (Schönfeld et al., 2012). Specimens were considered "alive" when all chambers expect the last one or two were well stained (Caulle et al., 2015). In the laboratory, the samples were wet sieved, repeatedly rinsed with fresh water, through a 63 μm mesh sieve, and dried at room temperature. From each sample,

TABLE 1 | The list of 51 identified taxa that have been assigned to ecological groups from the most sensitive to organic enrichment (Group 1) to the 1st order opportunists (Group V) for the Foram-AMBI calculation.

Sensitive Taxa (Group I)	Indifferent taxa (Group II)	Opportunistic taxa (Groups III – V)
Adelosina spp.	*Quinqueloculina parvula*	*Reophax nana* – III
Adelosina cliarensis	*Triloculina marioni*	*Eggerelloides scaber* – III
Adelosina longostira	*Bolivina pseudoplicata*	*Textularia agglutinans* – III
Adelosina mediterranensis	*Bolivina variabilis*	*Textularia bocki* – III
Spiroloculina excavata	*Globocassidulina subglobosa*	*Quinqueloculina seminulum* – III
Siphonaperta aspera	*Ammonia beccarii*	*Bolivina spathulata*– III
Quinqueloculina laevigata	*Elphidium advenum*	*Bolivina striatula* – III
Miliolinella subrotunda	*Elphidium decipiens*	*Bulimina elongate* – III
Triloculina oblonga	*Elphidium translucens*	*Bulimina marginata* – III
Triloculina tricarinata	*Haynesina depressula*	*Rosalina bradyi* – III
Triloculina trigonula	*Nonion* sp.	*Asterigerinata adriatica* – III
Sigmoilinita costata		*Aubignyna perlucida* – III
Reussella spinulosa		*Eilohedra vitrea* – IV
Eponides concameratus		*Bolivina dilatata* – IV
Neoconorbina terquemi		*Bulimina aculeata* – IV
Rosalina floridensis		*Valvulineria bradyana* – IV
Rosalina macropora		*Nonionella opima* – IV
Lobatula lobatula		*Ammonia tepida* – IV
Asterigerinata mamilla		*Nonionides turgidus* - V
Ammonia parkinsoniana		
Elphidium crispum		
Elphidium macellum		

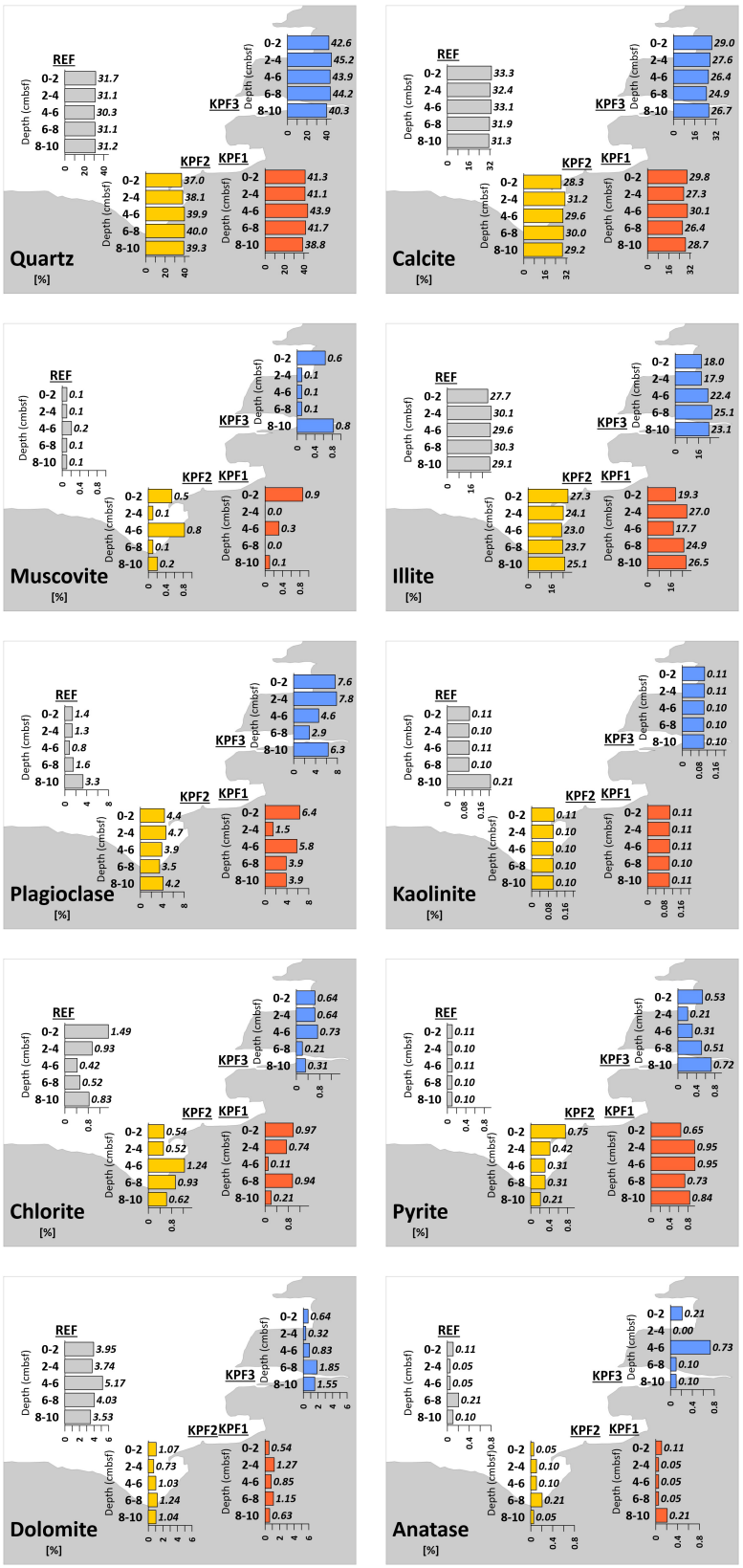

FIGURE 2 | Mineralogical composition (in%) of sediments of Bay of Koper.

using the Reich microsplitter, at least living + dead 200 - 300 foraminiferal tests (Murray, 2006; Martínez-Colón et al., 2018) were picked. The study of foraminiferal assemblages was carried out on the total assemblage instead of on the living assemblage. The total population is a more reliable indicator of assemblages because all of the seasonal variations are integrated into it, and no seasonal variation of living species will be overemphasized (Scott and Medioli, 1980). Considering the sedimentation rate of about 0.25 cm/year for the area in the immediate vicinity of the sampling area (Ogorelec et al., 1997), the collected cores probably provide information for the last 4-5 decades.

The specimens were examined under a stereomicroscope and identified according to the generic taxonomy Loeblich and Tappan (1987) and to species level when possible (due to size < 63 μm), following studies on Mediterranean and Adriatic foraminifera (Cimerman and Langer, 1991; Sgarrella and Moncharmont Zei, 1993; Ćosović et al., 2011; Hayward et al., 2021) and the species names follow the World Modern Foraminiferal Database (World Register of Marine Species, 2021).

Elpidium specimens that lack elements to be classified at the species level, were divided into two groups based on different life-strategies (have a keel or not, being infaunal and epifaunal, after Murray, 2006; Vidović et al., 2009, 2016).

Species with relative abundances greater than 10% are considered abundant, those between 5 and 10% are considered common, and those below 5% are considered rare (Lo Giudice Cappelli and Austin, 2019). For all studied assemblages, species diversity, expressed as Species richness (S), the Fisher α-index, the Shannon H-index (which considers both the abundance and evenness of species), and dominance (Simpson and Berger-Parker indices) were calculated. Species diversity is affected by salinity (Murray, 1991), values of Fisher α-index > 5 indicate normal marine salinity, while hyposaline and hypersaline conditions are characterized by low species diversity (index values < 5). These indices were computed for all assemblages using free statistical software PAST (PALentological Statistic; version 2.14; (Hammer et al., 2001).

The Foram-AMBI index was calculated (Foram-AMBI = [(0 *%GRI) + (1.5 *%GRII) + (3 *%GRIII) + (4.5 + %GRIV) + (6 *%GRV)]/100) according to Borja et al. (2000). Foraminiferal species are grouped in five ecological groups according to their sensitivity to organic matter enrichment (from the most sensitive GRI to the 1st order opportunists GRV, **Table 1**). For the calculation only species assigned to the ecological groups (Alve et al., 2016; Jorissen et al., 2018; Dubois et al., 2021; Parent et al., 2021) were used. The unassigned species are excluded from the data set before the proportion is calculated (Borja et al., 2000, 2008). The proportion of the five groups sums up to 1. The index ranges from 0 (100% of species GRI) to 6 (100% of species GRV) reflecting the degree of pollution and considers an individual species sensitivity to environmental stressor.

Five EcoQS categories (high, good, moderate, poor or bad) classify coastal waterbodies according to ecological quality statuses. The EcoQS was reconstructed (Bouchet et al., 2012) by applying diversity index exp (H'_{bc}). Species diversity index H' was calculated using the SpadeR program (version 2016, Chao and Shen, 2003; Chao et al., 2016; El Kateb et al., 2020). The classes boundaries are from Bouchet et al. (2012) and Hess et al. (2020). Sample KPF3/3 which contained < 100 foraminiferal tests were excluded from calculation).

Statistical Analyses

Statistica 13.3 software was used for basic statistical analyses (median, min., max.) for both mineralogical and geochemical data (**Supplementary Tables 1–3**). Canonical correspondence analysis (CCA) was applied to construct site/species matrix for 31 environmental variables (10 from X-ray diffraction analyses and 21 from the X-ray fluorescence analyses) and to identify correlations within and between the data sets. The free statistical software PAST package (Moore and Reynolds, 1997) was used for these analyses.

The strength of the correlation between the variables was measured using the correlation coefficient "r", also known as Pearson's r or the product-moment correlation coefficient. The values of the correlation coefficient r range from zero, indicating no correlation between variables, to + 1, indicating full positive or −1, indicating full negative correlations (Hammer et al., 2001). The Spearman Rank Order correlation coefficient was measured between the multivariate components (CCA) with the highest percentage of variance (axes 1 and 2) and the mineralogical and geochemical data.

To better define the relationships between the variability of foraminiferal species and environmental conditions, statistical analyses (canonical correspondence analysis, CCA) of the total foraminiferal assemblages were carried out using the PAST program package (Hammer et al., 2001). Prior to the analyses an additive logarithmic transformation log (x + 1) was performed on standardized data (relative abundances of foraminiferal species) in order to reduce the significance of extreme values, reduce the contributions of common species, increase the contributions of rare species and normalize the data (Hammer and Harper, 2006).

RESULTS

Mineralogy of Sediment

Mineralogical analysis of the sediments of the Bay of Koper revealed the following mineral composition (**Figure 2** and **Supplementary Table 1**): quartz (median 39.9%), calcite (median 29.4%), illite/muscovite (median 25.1%), Na-Ca-plagioclase (median 3.9%), dolomite (median 1.1%), chlorite group (median 0.6%), pyrite (median 0.4%) and kaolinite (median 0.1%). Certain differences in mineral composition between the sampling sites were found. Higher concentrations of minerals characteristic of siliciclastic rocks (quartz, plagioclase, muscovite) were encountered at coastal sites (KPF1, KPF2, KPF3). The offshore reference site (REF) was characterized by elevated concentrations of carbonate minerals (calcite, dolomite) were measured.

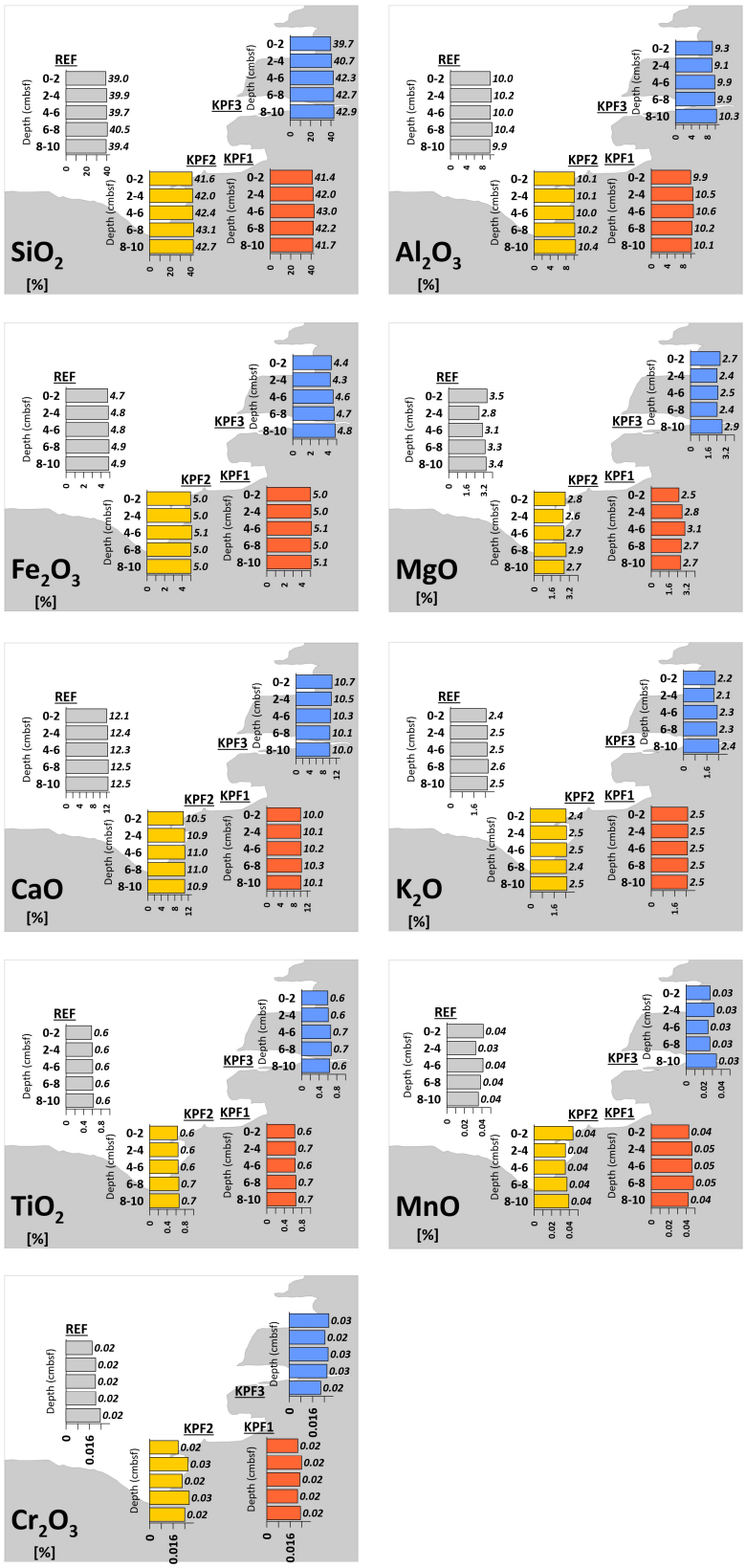

FIGURE 3 | Major oxides concentrations (%) of sediments of Bay of Koper (cmbsf = cm below sediment floor).

Geochemistry of Sediment

The results for major, minor and trace elements in sediment samples are presented in **Supplementary Tables 2**, **3**. The highest concentrations of major elements in sediment (**Figure 3**) show Si with higher concentrations in samples near the coast (KPF1, KPF2 and KPF3; 21.3-22.1%) and lower concentrations at offshore reference sites (REF; 19.7%). A reverse trend was observed for Ca (7.6-8.3% near the coast, 9.4% offshore) and Mg (1.5-2.0% near the coast, 2.11% offshore). Other major and minor elements (Si, Al, Fe, K, Ti, Mn, Cr) show a similar composition at all sampling sites with rather minimal differences (differences < 1%) at site KPF3 at the Rižana River inflow. Concentrations of elements over the entire depth in the sediment are practically constant (differences < 0.5%).

In general, concentrations of trace elements (As, Cr, Cu, Nb, Ni, Th, Zn, and Zr) were higher at coastal sampling sites (KPF1 and KPF2 in basin I, KPF3 in basin II) and lower at the reference site in the bay (REF) (**Figure 4**). For As, Ni, Nb and Th, the higher concentrations were observed at sites KPF1 or KPF2 in basin I and for Cr, Cu, Zr and Zn at site KPF3, where the Rižana River flows into the sea. Concentrations of other trace elements (Pb, Rb, Sr and V) were higher at the reference location (REF) and lower at coastal sites. The trace elements do not show any significant changes and trends at sediment depth (**Figure 4**).

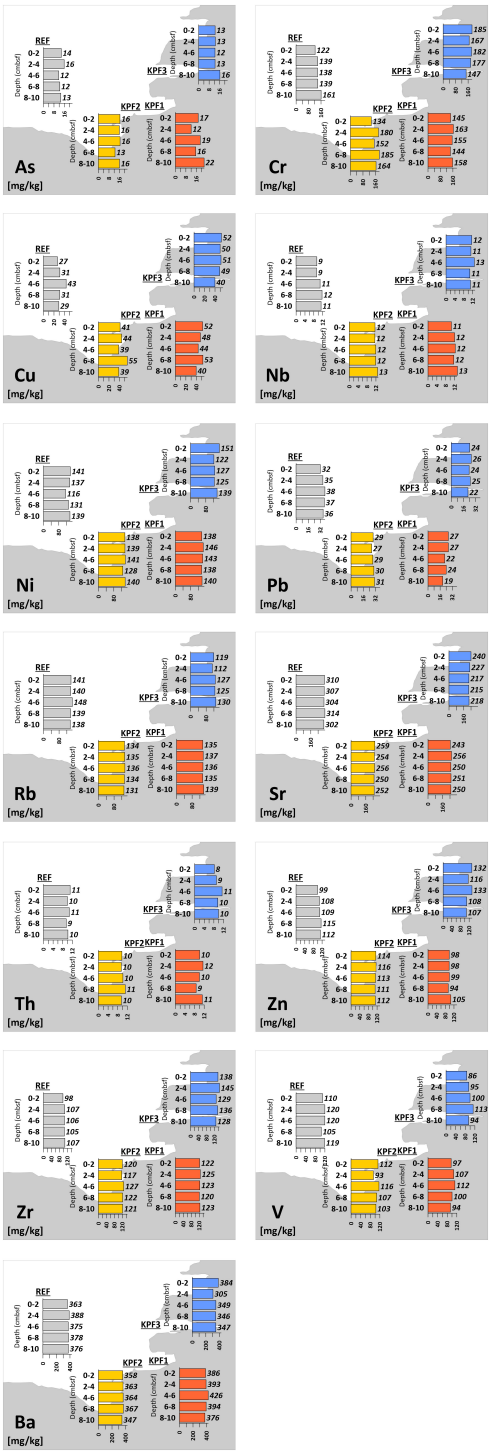

FIGURE 4 | Concentrations of trace elements (mg/kg) of sediments of Bay of Koper (cmbsf = cm below sediment floor).

Foraminifera

Diversity and Dominance

A total of 83 species belonging to 57 genera were identified (**Supplementary Table 4**), of which 18 taxa were agglutinated, 69 perforate-hyaline and 31 porcelaneous. Most foraminifera were rare and contributed less than 5% (**Table 2**) to the assemblages or were found in only a few samples (**Supplementary Table 4**). The low number of foraminiferal tests (N = 12) in the depth interval of 6–8 cm KPF3/3 (**Table 3**) excludes this interval from statistical interpretation. Unidentifiable miliolid fragments and reworked Eocene planktonic foraminifera were also listed (**Supplementary Table 4**) but are not included in any analysis.

The species richness (S) of the total assemblages (**Table 3** and **Supplementary Table 4**) ranges from 5 (KPF3/3) to 49 (KPF1/2). The number of species decreased from the top to the bottom of each studied core. The Shannon H-index (**Table 3**) ranges from 1.5 to 3.1, with the highest values indicated in the central parts of the cores. The Simpson 1-D values (**Table 3**) remained constant throughout each core. The values of Fisher's alpha index (**Table 3**) varied between stations (from 2.6 at station KPF3 to 17.0 at station KPF1) and along each core (exhibiting a down-core decreasing trend).

The percentage of tolerant species (Foram-AMBI assigned species; **Table 3**) varies among stations and also along individual core. The highest percentage of tolerant species is at REF (from 32.7% REF/1 to 47.4% at REF/5), and the lowest at KPF2 (from 21.2% to 27.6% at KPF2/2). At stations KPF1 and KPF2, the proportion of tolerant species within the total foraminiferal assemblages decreases downcore. The lowest values of the Foram-AMBI index are at KPF 2 (ranging from 1.46 to 3.19, **Tables 3**, **4**), followed by stations KPF1 (1.92-2.44) and REF with values between 2.6 and 3.2, while station KPF3 has the highest value (up to 3.9). The values of EcoQS indicate poor status in the REF1-REF3 samples and KPF2/1 and KPF2/5 and bad status for

TABLE 2 | Comparative status of the abundant and common species (> 5%) of total assemblages in at least one of studied interval and sample.

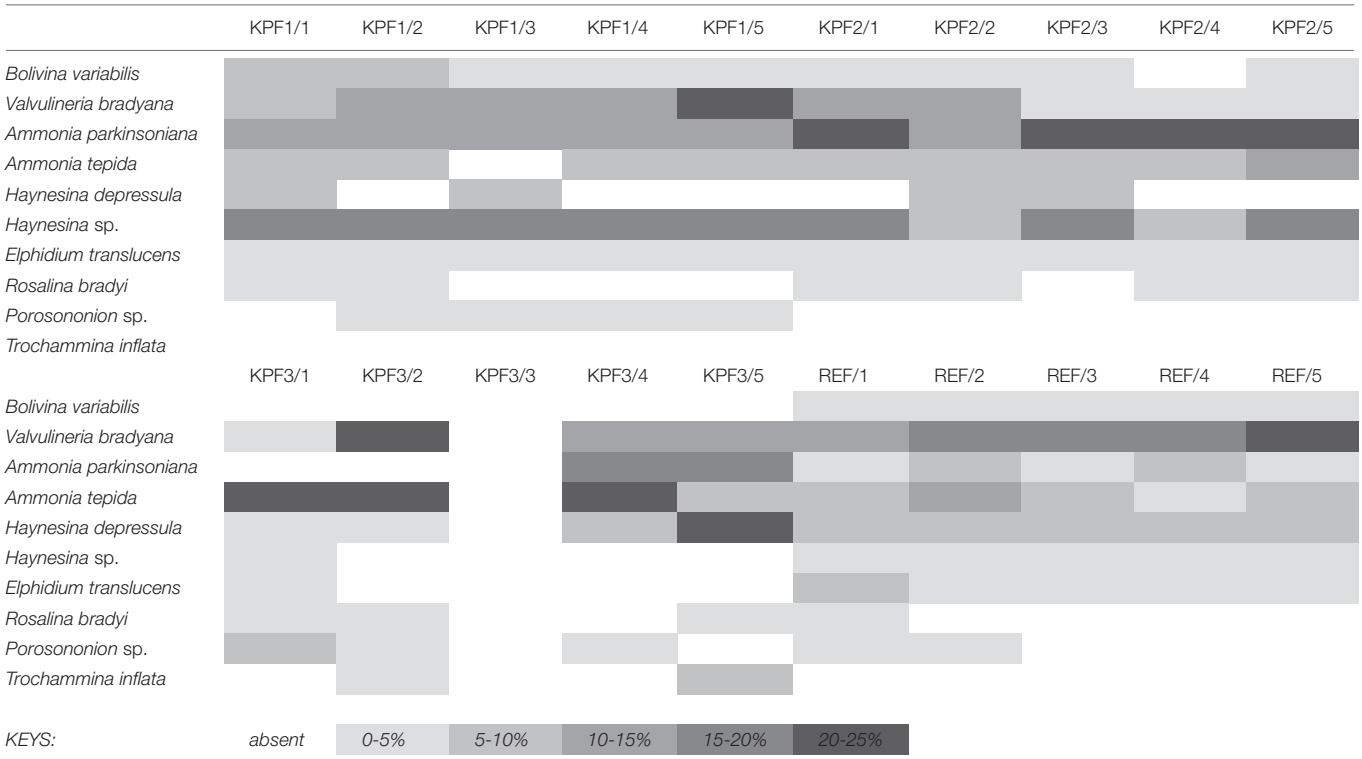

The numbers from/1 to/5 representing the sediment layers in depth (/1 = 0–2cm,/2 = 2–4cm,/3 = 4–6cm,/4 = 6–8cm,/5 = 8–10cm).

KPF1station, older part of the REF station and middle part of the KPF2 (**Table 4**).

Foraminiferal Distribution

The distribution of foraminiferal species in total assemblages showed variations between stations, while changes along the core at each station are less obvious (**Figure 5** and **Supplementary Table 4**).

At station KPF1, infaunal, planispiral *Haynesina* sp. (**Figures 6A,B**) and trochospiral *A. parkinsoniana* (**Figure 6F**) dominated with relative frequencies of 15.5–16.7% and 11.5–18.9%, while the other species contributing > 10% were *V. bradyana* (9.0-18.4%), *H. depressula* (2.9–8.7%), *A. tepida* (**Figures 6D,E,G**; 1.6–9.6%), *B. variabilis* (1.4–5.3%) and *Elphidium translucens* (2.8–4.0%). Miliolids constituted between 6.2 and 9.5% and agglutinated foraminifera between 1.2 and 3.4% to total assemblage.

The three co-dominant species of the foraminiferal assemblages from station KPF2 were *A. parkinsoniana* (18.15–28.77%), *Haynesina* sp. (**Figure 6C**; 8.63–17.63%) and *V. bradyana* (5.04–12.13%). Individuals of *A. tepida* and *H. depressula* were subordinate, but still contributed significantly to the assemblages (5.83–11.15% and 2.45–6.25%, respectively). Agglutinated and porcelaneous foraminifera were rare throughout the core, with the only representatives of *M. subrotunda* (1.44–2.21%), *Sigmolilinita* sp. (1.23–3.86%) and *P. lecalvezae* showing slightly greater abundances.

Significant decrease in the diversity of foraminiferal taxa were found in the sediments collected at station KPF3. The dominant species were *A. tepida* (5.99–24.7%) and *V. bradyana* (7.06–21.43%), while the subordinate species was *H. depressula* (4.7–28.14%). *H. depressula* was rare in the upper part (< 5%) and, then became more frequent until it reached the highest frequency at the bottom of the core. Non-keeled *Elphidium* sp. and *Porosononion* sp. occurred in significant amounts in the first two centimeters of the core, accounting for 10.59% and 9.02% of the assemblage, respectively. Large amounts of miliolid fragments and significant occurrences of reworked Eocene planktonic foraminifera (including pollen grains) characterized the station, especially the 4–6 cm depth interval (KPF3/3).

In the core of the REF station, tests of non-keeled *Elphidium* sp. predominated (20.69% in REF/1 and 38.79% in REF/4). Moreover, individuals of *V. bradyana* (**Figure 6H**) were subordinate with constant abundance throughout the core (14.66% in the depth interval of 0–2 cm to 20.39% in the depth interval of 8–10 cm). *H. depressula* (5.64–9.05%) and *A. tepida* (4.63–10.34%) were regularly present throughout the core, except for *A. tepida*, which was more abundant in the depth interval of 2–4 cm. The agglutinated foraminifera *Textularia bocki* contributed significantly to the assemblage (4.98% in REF/4).

Results of Statistical Analyses

Canonical correspondence analysis (CCA) of total species abundances (response) with the gradient of environmental variables (mineralogy and geochemistry) from four stations

TABLE 3 | Number of taxa (Species richness), number of individuals, diversity indices from standardized aliquots for total assemblages from four locations (KPF1, KPF2, KPF3 and REF) from the Bay of Koper.

	KPF1/1	KPF1/2	KPF1/3	KPF1/4	KPF1/5	KPF2/1	KPF2/2	KPF2/3	KPF2/4	KPF2/5
Taxa_S	47	49	41	37	35	37	48	38	45	32
Individuals	264	286	245	211	239	272	334	311	326	278
Dominance_D	0.09	0.09	0.093	0.092	0.103	0.106	0.075	0.108	0.096	0.137
Simpson 1-D	0.909	0.909	0.906	0.907	0.897	0.894	0.925	0.892	0.90	0.863
Shannon_H	2.96	2.96	2.89	2.85	2.75	2.77	3.10	2.77	2.96	2.56
Evenness e H/S	0.41	0.39	0.44	0.47	0.44	0.43	0.46	0.42	0.43	0.41
Equitability_J	0.77	0.76	0.78	0.79	0.77	0.777	0.80	0.76	0.78	0.74
Fisher_alpha	16.63	17.02	14.08	13	11.3	11.56	15.36	11.36	14.15	9.34
Foram_AMBI	1.98	2.18	1.91	2.07	2.44	1.86	3.19	1.64	1.62	1.46
% of NA species for Foram_AMBI	28	31	35	29.8	31	31	32	31	35	33
	KPF3/1	**KPF3/2**	**KPF3/3**	**KPF3/4**	**KPF3/5**	**REF/1**	**REF/2**	**REF/3**	**REF/4**	**REF/5**
Taxa_S	25	12	5	14	11	32	32	42	29	32
Individuals	237	144	12	133	167	232	319	337	281	255
Dominance_D	0.123	0.20	0.222	0.153	0.161	0.095	0.178	0.141	0.202	0.137
Simpson 1-D	0.876	0.799	0.778	0.847	0.833	0.904	0.821	0.858	0.797	0.863
Shannon_H	2.50	1.86	1.54	1.95	2.03	2.77	2.37	2.68	2.19	2.57
Evenness e H/S	0.49	0.53	0.94	0.56	0.69	0.50	0.33	0.35	0.31	0.41
Equitability_J	0.77	0.75	0.96	0.80	0.85	0.80	0.68	0.72	0.65	0.74
Fisher_alpha	7.05	3.11	3.22	3.95	2.64	10.06	8.86	12.65	8.11	9.67
Foram_AMBI	3.89	3.90		2.79	2.21	2.69	3.13	3.00	3.14	3.18
% of NA species for Foram_AMBI	50	37		27	16	38	47	43	42	36

The numbers from/1 to/5 representing the sediment layers in depth (/1 = 0–2cm,/2 = 2–4cm,/3 = 4–6cm,/4 = 6–8cm,/5 = 8–10cm). For each core interval the Foram-AMBI values are listed, along with the percentages of individuals assigned to the ecological groups in brackets.

TABLE 4 | Foram-AMBI indices and ecological quality statuses EcoQS at each studied interval obtained from the study of total assemblages.

	KPF1/1	KPF1/2	KPF1/3	KPF1/4	KPF1/5	KPF2/1	KPF2/2	KPF2/3	KPF2/4	KPF2/5
Foram-AMBI	1.98	2.18	1.91	2.07	2.44	1.86	3.19	1.64	1.62	1.46
Class										
H'_{bc}	3.15	3.14	3.04	3.01	2.88	2.89	3.24	2.85	3.08	2.66
EcoQS	23.4	23.2	20.9	20.3	17.8	17.9	25.7	17.3	21.7	14.2
Class	I	I	I	I	II	II	I	II	I	III
	KPF3/1	**KPF3/2**	**KPF3/3**	**KPF3/4**	**KPF3/5**	**REF1**	**REF2**	**REF3**	**REF4**	**REF5**
Foram-AMBI	3.89	3.9		2.79	2.21	2.69	3.13	3	3.14	3.18
Class										
H'_{bc}	2.58	1.92		2.18	1.96	2.88	2.47	2.8	2.33	2.69
EcoQS	13.2	6.9		8.8	7.1	17.8	11.8	16.4	10.3	14.7
Class	III	IV		IV	IV	II	III	II	II	III

Foram-AMBI indices			
UNPOLLUTED	SLIGHTLY POLLUTED	POLLUTED	HEAVILY POLLUTED
0.2 - 1.20	1.20-3.30	3.30-5.50	5.50-6.00

EcoQS status classification				
I – HIGH	II - GOOD	III - MODERATE	IV - POOR	V - BAD
>20	20-15	15-10	10-5	5-0

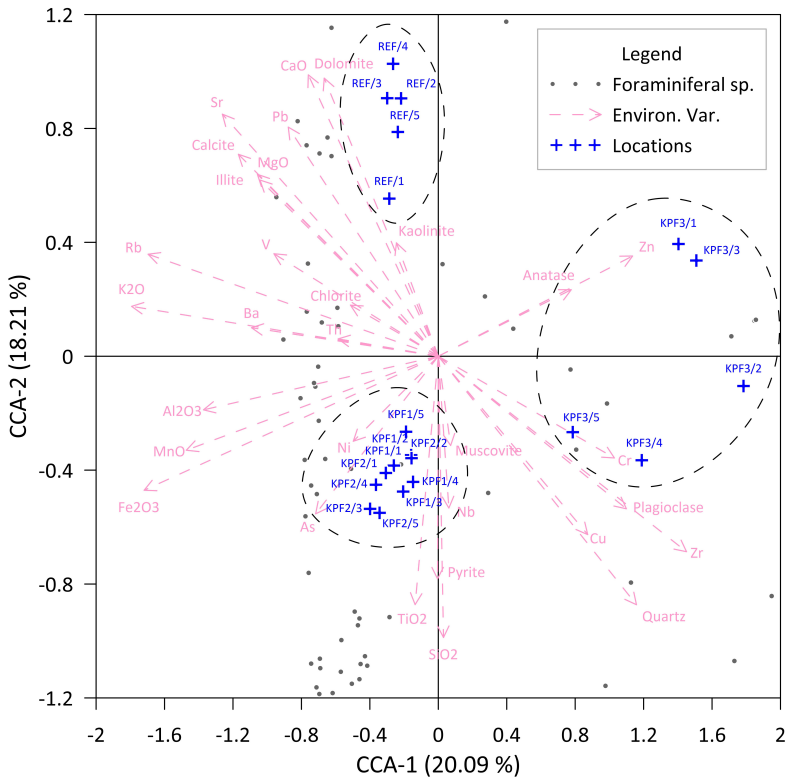

FIGURE 5 | Canonical correspondence analyses (CCA) of total foraminiferal assemblages, and mineralogical and geochemical data in sediment samples from four locations (KPF1, KPF2, KPF3, and REF) from Bay of Koper.

grouped the samples into three main groups: the first included the samples from stations KPF1, KPF2, the second included the samples from the REF site, while the third included only the samples from station KPF3 (**Figure 5**).

In addition, the CCA analyses show that stations KPF1 and KPF2 correlate with pyrite, As, Ni, Ti and Si, the REF station correlates with higher carbonates contents (calcite, dolomite), illite, kaolinite, Sr and Pb, and station KPF3 correlates with plagioclase, muscovite, quartz, Cu, Cr and Zn.

The measure of similarity accounted for the eigenvectors CCA-1 and CCA-2 is 20.09 and 18.21% respectively.

Correlation analysis of multivariate foraminiferal data (CCA axis 1 and 2) of the samples from all 4 stations with geochemical data did not show a strong or significant relationship between the community and the environmental parameters observed. However, due to the strong influence of station KPF3 on the plotting of the samples in multivariate space, a further correlation with geochemical results was carried out, now only on the CCA foraminiferal data of the other three stations. This analysis produced the following results: significant positive correlation of the CCA-1 axis with S and Zr, a strong positive correlation with Cu and Cr, as well as a significant negative correlation of the same axis with Fe, Mg, Ca, Rb, Sr, Pb and V. A significant positive correlation of the CCA-2 axis appears with Ca, Rb and Sr, and a strong positive correlation with Mg, Pb and Zn, while a significant negative correlation with Si, Fe and Ti is indicated (**Table 5**).

DISCUSSION

Based on study of four sediment cores we investigated the impact of increasing shipping and human-induced activities (i.e., industry, tourism) in the Bay of Koper on the geochemical element composition of sediments and benthic foraminiferal assemblages over the past 40 - 50 years. The study of the composition and diversity of foraminiferal assemblages were used to describe the ecological conditions by using Foram-AMBI and EcoQS indices.

Environmental Characterization Based on Mineralogical and Geochemical Data

The mineralogical composition and the content of major elements (**Figure 3**) reflect the geological characteristics of the wider area of the Gulf of Trieste/Trst coast. Higher concentrations of minerals characteristic of siliciclastic rocks (quartz, plagioclase, muscovite; **Figure 2** and **Supplementary Table 1**) can be explained by the geological siliciclastic properties of the hinterland of the bay, which is more influenced along the coast (KPF1-KPF3). The significant trend of increasing sediment carbonate content toward the central part of the bay can be observed, which is attributed to the considerably higher proportion of carbonate skeletons of various organisms in this part of the bay (REF). The same trend was already described by Ogorelec et al. (1987). Similar pattern was also indicated by the

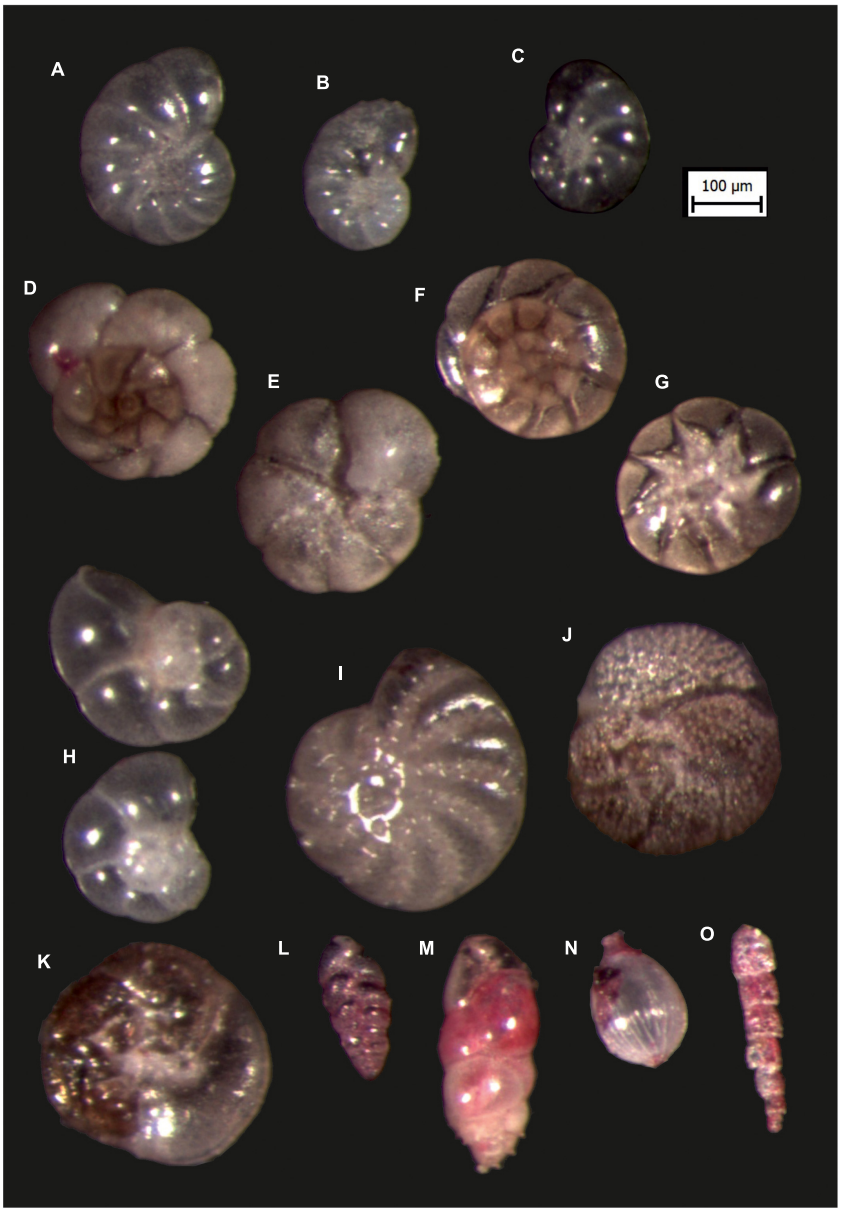

FIGURE 6 | Microphoto images (using Olympus U-TV1XC camera) of the selected foraminiferal species: **(A)** *Haynesina depressula* (Walker and Jacob, 1798), KPF1/5. **(B)** *Haynesina depressula* (Walker and Jacob, 1798), KPF1/5. **(C)** *Haynesina depressula* (Walker and Jacob, 1798), KPF2/5. **(D)** *Ammonia tepida* (Cushman, 1926): spiral side, KPF1/2, **(E)** *Ammonia tepida* (Cushman, 1926): umbilical side, KPF1/2. **(F)** *Ammonia parkinsoniana* (d' Orbigny, 1839): spiral side, KPF1/2. **(G)** *Ammonia parkinsoniana* (Cushman, 1926): umbilical side, KPF1/2. **(H)** *Aubignyna perlucida* (Heron-Allen and Earland, 1913): KPF2/2. **(I)** *Elphidium* sp., non-keeled, KPF1/4. **(J)** *Rosalina bradyi* (Cushman, 1926): spiral side, KPF1/1. **(K)** *Rosalina bradyi* (Cushman, 1926): umbilical side, KPF1/1. **(L)** *Bolivina variablis* (Williamson, 1858), KPF1/5. **(M)** *Bulimina elongata*, d' Orbigny, 1826, KPF1/3. **(N)** *Lagena striata* (d' Orbigny, 1839), KPF1/3. **(O)** *Reophax* sp., KPF1/1.

content level of major elements, with higher Si and Al levels along the coast, and higher Ca and Mg levels in the inner part of the bay, which can be also explained by the geogenic origin of the hinterland. The authigenic mineral pyrite indicates the reduction conditions in the sediment. Ogorelec et al. (1987) describe the reduction conditions already a few centimeters below the surface, which is favorable for pyrite formation. Slightly lower levels of Fe at the Rižana outflow (KPF3) can be explained by the stronger inflow of oxygenated river water into the bay and the oxidizing environment of the sedimentation (Ogorelec et al., 1987).

The concentrations of trace elements (As, Cr, Cu, Nb, Ni, Pb, Rb, Sr, Th, Zn, V, Ba) show spatial differences between the sampling sites, indicating a non-point source of potential pollutants into the environment. In general, As, Ni, Nb, and Th are highest at KPF1, Cr, Cu, Zn, and Zr at KPF3 and Pb, Rb, Sr, and V at the REF site. In addition, the Spearman correlation

TABLE 5 | Spearman Rank Order correlations analysis between total foraminiferal assemblages and geochemical data from three (KPF1, KPF2 and REF) sampling stations (marked correlations are significant at $p < 0.05$).

	Si	Al	Fe	Mg	Ca	K	Ti	S	Mn	Rb	Sr
CCA-1	0.12	–1.15	–1.49	–1.27	–1.09	–1.12	0.20	1.25	–1.32	–1.19	–1.31
CCA-2	–1.71	–0.91	–1.76	0.51	1.00	0.31	–1.60	–0.61	–1.08	0.54	0.45
	Ba	**As**	**Cu**	**Nb**	**Pb**	**Th**	**Zn**	**Zr**	**Cr**	**V**	**Ni**
CCA-1	–0.72	–0.84	1.10	–0.62	–1.33	–1.59	0.59	1.25	1.06	–1.45	–0.84
CCA-2	–0.21	–1.85	–0.75	–1.76	0.64	–0.08	0.89	–0.45	–0.41	0.12	–1.45

analyses confirms strong or moderately positive correlations between trace elements at the respective sampling site. The statistical grouping of the sites (**Figure 5**) can be explained by the geogenic origin, the different basic mineralogical characteristics of the sediment (carbonates at REF and siliciclastic at KPF1-KPF3) and the higher inflow of river water into the bay (between KPF3 and other sites). Although the minor positive signal of trace element concentrations might be recognized in the inner part of the port of Koper (KPF1 and KPF2), the values are generally within the background geological levels, which is in accordance with analyses previously published on the Bay of Koper (Ogorelec et al., 1987, 1991; Rogan Šmuc et al., 2018). Contrary some trace elements (i.e., As, Cd, Cr, Cu, Ni, Zn) show higher concentrations compared to other locations in the Adriatic Sea (Adami et al., 1996; Aquavita et al., 2010). Concentrations of elements over the entire depth in the sediment are practically constant which is certainly also affected by bioturbation.

While the element concentration in the sediment were described to be controlled by the natural conditions (mineralogical, grain size, organic matter) these should be considered in background evaluation as the basis for the assessment of anthropogenic pollution (Coccioni et al., 2009).

The Response of Foraminiferal Assemblages

The foraminiferal species from studied samples (one replica, **Table 2**), including the most common (*A. tepida*, *A. parkinsoniana*, *V. bradyana*, *Haynesina* sp., *H. depressula*, *B. variabilis* and *Elphidium* spp. (keeled and no-keeled) are characteristic of infra-circalittoral of Mediterranean and northern Adriatic (Jorissen, 1987; Hohenegger et al., 1988, 1993; Cimerman and Langer, 1991; Sgarrella and Moncharmont Zei, 1993; Coccioni et al., 2009; Vidović et al., 2009, 2014; Ćosović et al., 2011; Popadić et al., 2013; Jorissen et al., 2018; Melis et al., 2019).

Foraminiferal diversity parameters show clustering of stations, KPF1, KPF2 and REF with higher values and KPF3 has lower values. This trend is clearly visible in the multivariate biplots (**Figure 5**). Knowing that low diversity is related to highly variable conditions and/or stressful environmental conditions, we assume that the position of station KPF3 off the coast of the Rižana River caused a decrease in diversity (**Table 3**). The freshwater influence is confirmed by: (i) the significant content of reworked Eocene planktonic foraminifera (**Supplementary Table 4**, reaching frequency of 82% of total skeletal grains in sample KPF 3/3) transported as sediment load from the Eocene Flysch in the hinterland (Pleničar et al., 1973); (ii) the abundance of species *A. tepida* and *H. depressula* (including *Haynesina* sp.), known for their tolerance to salinity fluctuations, and their ability to survive in nutrient-rich conditions off river mounts (Murray, 2006; Barbieri et al., 2019). In coastal environments, parameters such as active bioturbation, current and wave regimes, and biotic interactions may be important to the distribution of benthic foraminifera (Murray, 2006 and references therein). Although almost all identified benthic species are considered opportunistic taxa, we hypothesize that river flow and sediment surge have caused certain physical disturbances in benthic microhabitats that some species cannot tolerate (elphidiids and infaunal representatives).

Several studies on the influence of trace metal concentrations on the distribution of foraminifera typically indicate a negative correlation between trace metal concentrations and foraminiferal diversity and abundance (Alve, 1991; Sharifi et al., 1991; Yanko et al., 1999; Coccioni, 2000; Carnahan et al., 2008; Frontalini and Coccioni, 2008; Coccioni et al., 2009; Frontalini et al., 2009; Li et al., 2013; Martins et al., 2013). Our results show that the highest values of species diversity were found in sediments with the highest concentration of Fe and Mn (KPF1 station). Also, no negative correlation was found between foraminiferal diversity and concentrations of Ni and Pb. It must be emphasized that some discrepancies were observed in the correlation of Fe concentrations with species diversity at certain depth-interval levels at each station. This may be due to sediment mixing at depth due to bioturbation and sediment mixing in Bay of Koper caused by waves induced by strong winds (Leder et al., 1998). Carnahan et al. (2008) showed that abundance of *Ammonia* decreases with increasing Pb concentrations, and *Elphidium* specimens are more numerous when the environment is enriched with Fe. Our data shows no correlation between the abundance of representatives of genera *Ammonia* and *Elphidium* (non-keeled in particular, *sensu* Murray, 2006; Vidović et al., 2009, 2014) and the concentration of Fe and Pb at each station (all depth intervals). The distribution of trace metals showed that As and Rb have similar distributions along the core, while concentrations of Pb, Cu, and Cr increase slightly downwards from the core, with these conditions associated with reduced biodiversity. Nevertheless, we can conclude that no significant changes occurred in the overall composition of the assemblages. The representatives of genus *Ammonia* are

tolerant to trace metal pollution (Armynot du Châtelet et al., 2004; Ferraro et al., 2006; Frontalini and Coccioni, 2008). In particular, *A. tepida* is tolerant of elevated trace metal pollution (Armynot du Châtelet et al., 2004; Barbieri et al., 2019) and the species abundance increases with increases in Ni, Cr, Cd, As, and Hg concentrations (Frontalini and Coccioni, 2008; Melis et al., 2019). As an opportunistic feeder *A. tepida* showed a strong response to phytodetrital input (Wukovits et al., 2018), and recorded phytoalgal bloom in the Northern Adriatic could cause the species abundance (Cabrini et al., 2012; Cozzi et al., 2020). The positive response of representatives of the genus *Ammonia* at KPF 3 and KPF 2 to slightly elevated concentrations of trace elements (but within normal levels) is consistent with the previous study in Gulf of Trieste (Melis et al., 2019). In general, a comparison of the distribution of the most abundant species indicates a moderate supply of organic matter at all sites because *H. depressula* in a case of increased organic supplies (Jorissen et al., 2018) would disappear. The positive correlation between abundance of *H. depressula* and Zn concentration (Melis et al., 2019) was recorded at KPF2.

The Foram-AMBI index reflects changes in organic matter concentrations (Jorissen et al., 2018; Parent et al., 2021). The presence and abundance of organic matter are related to mud content in sediments, and consequently affect the concentration of oxygen and pollutants (El Kateb et al., 2020). The calculated Foram-AMBI index values (**Table 4**) imply from good and slightly polluted (KPF1 and KPF2 assemblages) to moderate and polluted (KPF3 and REF assemblages) conditions. Our results are consistent with previous studies (Coccioni, 2000; Frontalini and Coccioni, 2008; Coccioni et al., 2009; Frontalini et al., 2009) suggesting that the decrease in diversity of foraminiferal assemblages correlates with the increase in abundance of tolerant species. The percentage of unassigned species ranged from 29 – 36% in KPF1, 30-34% in KPF2 and 38-43% in REF, which is well above the quality assurance threshold of 20% unassigned (Alve et al., 2016). Because of the high number of unassigned species, these indices are used to get trends in changes in the ecological status of stations only. For the REF station, the moderate to good EcoQS ecological status (**Table 4**) comes from the position of the station with ship traffic, where ballast water is openly discharged into the environment. Our study questioned the status of the REF site as the referral for further investigations of benthic habitats. The diversified assemblages of opportunistic detritivores (**Supplementary Table 4**) in the bay showed high (KPF1) and good to high (KPF2) ecological quality statuses (**Table 4**). The unstable condition at the KPF3 station due to vicinity of river input, resulted with moderate to poor ecological status. At all studies cores the better ecological quality for benthic foraminifera were observed in younger intervals, because of proliferation of opportunistic foraminifera.

Investigating anthropogenic impacts on foraminiferal abundances and taxonomic composition of assemblages in different enclosed shallow water settings (lagoons) in the Adriatic, especially in the Northern Adriatic (Donnici and Serandrei Barbero, 2002; Frontalini and Coccioni, 2008; Bergamin et al., 2009; Coccioni et al., 2009; Frontalini et al., 2009; Frontalini and Coccioni, 2011; Vidović et al., 2016; Bouchet et al., 2018; Barbieri et al., 2019; Melis et al., 2019), and in the Mediterranean Sea (Türkmen et al., 2011; El-Gamal et al., 2012; Dimiza et al., 2016; Jorissen et al., 2018) have recently intensified. Our results fit the distribution of benthic foraminifera recorded in these studies. Representatives of the stress-tolerant genus *Ammonia* dominate the sediments of most lagoons. In the studied samples the values of the Foram-AMBI indices, although considered with caution, indicate a good to moderate ecological conditions, which does not suggest the highest organic concentrations. It seems that for the dominance of *A. tepida* in the assemblages, together with *Haynesina* sp. and *H. depressula* the following factors are important: river inflow, eutrophication of the area (Giani et al., 2012), anthropogenic pressure and shallow-water and enclosed morphology of the area. Epiphytic forms which were common until the 1990s (Murray, 2006), are less common due to the disappearance of vegetation cover (Li et al., 2013).

Considering the sedimentary rates in the area (Ogorelec et al., 1997), it seems that more or less similar geochemical conditions prevailed in the last decades, despite the increased anthropogenic pressure from the activities in the Port of Koper, which favored the development of opportunistic benthic foraminifera. Normal marine conditions continued to prevail, reflected in moderate diversity along the shallow sedimentary cores. According to our interpretation, the environmental characteristics that contribute most to the distribution of foraminifera in Bay of Koper are shallow-water, semi-enclosed area with freshwater inflow, limited enrichment with trace elements despite anthropogenic pressure and low to moderate concentration of organic matter.

CONCLUSION

Coastal environments are often interesting for environmental studies in the light of various anthropogenic pressures. In Gulf of Trieste, and consequently in Bay of Koper, numerous investigations were done also due to specific natural characteristic of this area. Besides the intensive urbanization, tourism, and agriculture of the wider area, the port activity in the Bay of Koper represents an important factor in the study of marine environmental pollution. The main aim of this paper is to highlight, by means of statistical analysis, the correlation between the foraminiferal parameters (diversity, relative abundance and absolute abundance) and the possible natural and anthropogenic stressors due to intensify anthropogenic pressure in last three decades in the bay.

A total of 20 sediment samples (one replica) were analyzed at four sampling sites with a varying degree of anthropogenic input. The mineralogical characteristics and major element concentrations indicate the characteristics of a natural lithogenic origin, siliciclastic rocks on the coastline, and more carbonate components in the inner part of the bay. The trace metals, whose concentrations are higher at the location inside the port and at the inflow of the Rižana River (values of Fisher index, As, Cr, Cu, Nb, Ni, Zn, Zr, Th), can be of anthropogenic input. However, no

significantly increased concentrations of elements were observed, which means that the pollution of trace metal is still negligible.

The total benthic foraminiferal assemblages of moderate diversity are composed of opportunistic species. *Ammonia parkinsoniana*, *Haynesina* sp., *Valvulineria bradyana* and the non-keel *Elphidium* sp. dominate, while *A. tepida* and *Haynesina depressula* are subordinate. *A. tepida* proved to be the most tolerant taxa, whereas *H. depressula*, could be considered a less tolerant species, as it benefitted from the less stressful conditions documented at the KPF1 and KPF2 sites. Infaunal life strategists fit well with fluctuations in salinity caused by river supply (KPF3) and the possible higher amount of organic matter. The general geochemical preferences of dominant species are consistent with those from other studies.

The values of the Foram-AMBI index imply good to moderate ecological quality of the studied area in the Bay of Koper, with the most polluted area near to river mouth (KPF 3). The application of the index has to be treated with caution in order to assess the ecological conditions, as more than 20% of the species present are not assigned to any ecological group. The calculated ecological quality status (EcoQS) classified KPF 1 and KPF2 stations as of high and good conditions, REF as moderate to good, and KPF3 as of moderate to bad ecological conditions for benthic foraminifera.

DATA AVAILABILITY STATEMENT

The datasets presented in this study can be found in online repositories. The names of the repository/repositories and accession number(s) can be found in the article/ **Supplementary Material**.

AUTHOR CONTRIBUTIONS

PŽR and JV: conceptualization. PŽR, JV, VĆ, and MD: methodology. JV and MD: software. PŽR, JV, VĆ, AH, and MD: formal analysis. PŽR, JV, and VĆ: investigation. PŽR and JV: writing—original draft preparation. PŽR, VĆ, MD, and BR: writing—review and editing. MD and BR: visualization. All authors have read and agreed to the published version of the manuscript.

FUNDING

This research was financially supported by the Ministry of Higher Education, Science, and Technology of the Republic of Slovenia (Slovenian Research Agency); Program Group Geoenvironment and geomaterials (P1-0195) and the project record of environmental change and human impact in Holocene sediments, Gulf of Trieste (J1-1712). Sediment sampling was performed by the technical support of the National Institute of Biology, Marine Biology Station Piran. The last part of the work was executed in the frame of the Croatian Science Foundation project IP–2019–04-5775 BREEMECO. For grammar corrections we would like to thank Jeff Bickert. Many thanks also to the reviewers who make the manuscript significantly upgraded.

SUPPLEMENTARY MATERIAL

The Supplementary Material for this article can be found online at: https://www.frontiersin.org/articles/10.3389/fmars.2022.812622/full#supplementary-material

REFERENCES

Adami, G., Barbieri, P., Campisi, B., Predonzani, S., and Reisenhofer, E. (1996). Anthropogenic heavy metal distribution in sediments from an area exposed to industrial pollution (Harbour of Trieste, Northern Adriatic Sea). *Boll. Della Soc. Adriat. Sci.* 77, 5–18.

Alve, E. (1991). Benthic foraminifera in sediment cores reflecting heavy metal pollution in Sorfjord, Western Norway. *J. Foraminifer. Res.* 21, 1–19. doi: 10.2113/gsjfr.21.1.1

Alve, E. (1995). Benthic foraminiferal responses to estuarine pollution: a review. *J. Foraminifer. Res.* 25, 190–203. doi: 10.2113/gsjfr.25.3.190

Alve, E., Korsun, S., Schönfeld, J., Dijkstra, N., Golikova, E., Hess, S., et al. (2016). Foram-AMBI: a sensitivity index based on benthic foraminiferal faunas from North-East Atlantic and Arctic fjords, continental shelves and slopes. *Mar. Micropaleontol.* 122, 1–12. doi: 10.1016/j.marmicro.2015.11.001

Angel, D. L., Verghese, S., Lee, J. J., Saleh, A. M., Zuber, D., Lindell, D., et al. (2000). Impact of a net cage fish farm on the distribution of benthic foraminifera in the northern Gulf of Eilat (Aqaba, Red Sea). *J. Foraminifer. Res.* 30, 54–65. doi: 10.2113/0300054

Appiotti, F., Krželj, M., Russo, A., Feretti, M., Bastianini, M., and Marincioni, F. (2014). A multidisciplinary study on the effects of climate change in the northern Adriatic Sea and the Marche region. *Reg. Environ. Change* 14, 2007–2024. doi: 10.1007/s10113-013-0451-5

Aquavita, A., Predonzani, S., Mattassini, G., Rossin, P., Tamberlich, F., Falomo, J., et al. (2010). Heavy metals contents and distribution in coastal sediments of the gulf of Trieste (Northern Adriatic Sea, Italy). *Water Air Soil Pollut.* 211, 95–111. doi: 10.1016/j.jes.2017.12.009

Armynot du Châtelet, E., Debenay, J. P., and Soulard, R. (2004). Foraminiferal Proxies from pollution monitoring in moderately polluted harbours. *Environ. Pollut.* 127, 27–40. doi: 10.1016/s0269-7491(03)00256-2

Barbieri, G., Rossi, V., Vaiani, S. C., and Horton, B. P. (2019). Benthic ostracoda and foraminifera from the North Adriatic Sea (Italy, Mediterranean Sea): a proxy for the epositional characterization of river-influenced shelves. *Mar. Micropaleontol.* 153:101772. doi: 10.1016/j.marmicro.2019.101772

Barbieri, P., Adami, G., Predonzani, S., and Edoardo, R. (1999). Heavy metals in surface sediments near urban and industrial sewage discharges in the Gulf of Trieste. *Toxicol. Environ. Chem.* 71, 105–114. doi: 10.1080/02772249909358785

Bergamin, L., Romano, E., Finois, M. G., Venti, F., Bianchi, J., Colasanti, A., et al. (2009). Benthic foraminifera from the coastal zone of Baia (Naples, Italy): assemblage distribution and modification as tools from environmental characterisation. *Mar. Pollut. Bull.* 59, 234–244. doi: 10.1016/j.marpolbul.2009.09.015

Bergin, F., Kucuksezgin, F., Uluturham, E., Barut, I. F., Meric, E., Avsar, N., et al. (2006). The response of benthic foraminifera and ostracoda to heavy metal pollution in Gulf of Izmir (Eastern Aegean Sea). *Estuar. Coast. Shelf Sci.* 66, 368–386. doi: 10.1016/j.ecss.2005.09.013

Birk, S., Bonne, W., Borja, A., Brucet, S., Courrat, A., Poikane, S., et al. (2012). Three hundred ways to assess Europe's surface water: an almost complete overview of biological methods to implement the Water Framework Directive. *Ecol. Indic.* 18, 31–41. doi: 10.1016/j.ecolind.2011.10.009

Borja, A., Bricker, S. B., Dauer, D. M., Demetriades, N. T., Ferreira, J. G., Forbes, A. T., et al. (2008). Overview of integrative tools and methods in assessing

ecological integrity in estuarine and coastal systems worldwide. *Mar. Pollut. Bull.* 56, 1519–1537. doi: 10.1016/j.marpolbul.2008.07.005

Borja, A., Franco, J., and Pérez, V. (2000). A marine biotic index to establish the ecological quality of soft-bottom benthos within European estuarine and coastal environments. *Mar. Pollut. Bull.* 40, 1100–1114. doi: 10.1016/S0025-326X(03)00090-0

Bouchet, V. M. P., Alve, E., Rygg, B., and Telford, R. J. (2012). Benthic foraminifera provide a promising tool for ecological quality assessment of marine waters. *Ecol. Indic.* 23, 66–75. doi: 10.1016/j.ecolind.2012.03.011

Bouchet, V. M. P., Debenay, J.-P., Sauriau, P.-G., Radford-Knoery, J., and Soletchnik, P. (2007). Effects of short-term environmental disturbances on living benthic foraminifera during the Pacific oyster summer mortality in the Marennes-Oléron Bay (France). *Mar. Environ. Res.* 64, 358–383. doi: 10.1016/j.marenvres.2007.02.007

Bouchet, W. M. P., Goberville, E., and Frontalini, F. (2018). Benthic foraminifera to assess ecological quality statuses in Italian transitional waters. *Ecol. Indic.* 84, 130–139. doi: 10.1016/j.ecolind.2017.07.055

Brambati, A., and Catani, G. (1988). Le coste e I fondali del Golfo di Trieste dall'Isonzo a Punta Sottile: aspetti geologici, geomorfologici, sedimentologici e geotecnici. *Hydrores Trieste* 6, 13–28.

Burone, L., Venturini, N., Sprechmann, P., Valente, P., and Muniz, P. (2006). Foraminiferal responses to polluted sediments in the Montevideo coastal zone, Uruguay. *Mar. Pollut. Bull.* 52, 61–73. doi: 10.1016/j.marpolbul.2005.08.007

Cabrini, M., Fornasaro, D., Cossarini, G., Lipizer, M., and Virgilio, D. (2012). Phytoplankton temporal changes in a coastal northern Adriatic site during the last 25 years. *Estuar. Coast. Shelf Sci.* 115, 113–124. doi: 10.1016/j.ecss.2012.07.007

Carnahan, E. A., Hoare, A. M., Hallock, P., Lidz, B. H., and Reich, C. D. (2008). Distribution of heavy metals and foraminiferal assemblages in sediments of Biscayne Bay, Florida, USA. *J. Coast. Res.* 24, 159–169. doi: 10.2112/06-0666.1

Caruso, A., Cosentino, C., Tranchina, L., and Brai, M. (2011). Response of benthic foraminifera to heavy metal contamination in marine sediments (Sicilian coasts, Mediterranean Sea). *Chem. Ecol.* 27, 9–30. doi: 10.1080/02757540.2010.529076

Caulle, C., Mojtahid, M., Gooday, A. J., Jorissen, F. J., and Kitazato, H. (2015). Living (Rose – Bengal – stained) foraminiferal fauna along a strong bottom-water oxygen gradient on the Indian margin (Arabian Sea). *Biogeosciences* 12, 5005–5012. doi: 10.5194/bg-12-5005-2015

Cepak, F., and Marzi, B. (2009). Environmental impacts of the Port of Koper. *Varst. Narave* 22, 97–116.

Chao, A., Ma, K. H., Hsieh, T. C., and Chun-Hou, C. (2016). *Introduction to Online Program Spader (Species-Richness Prediction and Diversity Estimation in R)*. Available Online at: https://chao.shinyapps.io/SpadeR/, version [accessed September 2016].

Chao, A., and Shen, T. J. (2003). Nonparametric estimation of Shannon's index of diversity when there are unseen species in sample. *Environ. Ecol. Stat.* 10, 429–443.

Cibic, T., Acquavita, A., Aleffi, F., Bettoso, N., Blasutto, O., De Vittor, C., et al. (2008). Integrated approach to sediment pollution: a case study in the Gulf of Trieste. *Mar. Pollut. Bull.* 56, 1650–1667. doi: 10.1016/j.marpolbul.2008.05.009

Cimerman, F., and Langer, M. R. (1991). *Mediterranean Foraminifera. Razred za Naravoslovne Vede, Classis IV: Historia Naturalis, Dela-Opera 30*. Ljubljana: Slovenian academy of sciences and arts, 119.

Coccioni, R. (2000). "Benthic foraminifera as bioindicators of heavy metal pollution: a case study from the Goro Lagoon (Italy)," in *Environmental Micropaleontology*, ed. R. Martin (New York, NY: Kluwer Academic), 71–103. doi: 10.1007/978-1-4615-4167-7_4

Coccioni, R., Frontalini, F., Marsili, A., and Mana, D. (2009). Benthic foraminifera and trace element distribution: a case-study from the heavily polluted lagoon of Venice (Italy). *Mar. Pollut. Bull.* 59, 257–267. doi: 10.1016/j.marpolbul.2009.08.009

Colizza, E., Fontolan, G., and Brambati, A. (1996). Impact of a coastal disposal site for inert wastes on the physical marine environment, Barcola-Bovedo, Trieste, Italy. *Environ. Geol.* 27, 270–285. doi: 10.1007/bf00766697

Correggiari, A., Field, M., and Trincardi, F. (1996). "Late quaternary large dunes on the sediment-starved Adriatic shelf," in *Geology of Siliciclastic Shelf Seas*, Vol. 117, eds M. De Batist and P. Jacob (London: Geological Society), 155–169. doi: 10.1144/gsl.sp.1996.117.01.09

Ćosović, V., Zavodnik, D., Borčić, A., Vidović, J., Deak, S., and Moro, A. (2011). A checklist of foraminifera of the eastern shelf of the Adriatic Sea. *Zootaxa* 3035, 1–56. doi: 10.11646/zootaxa.3035.1.1

Covelli, S., and Fontolan, G. (1997). Application of a normalization procedure in determining regional geochemical baselines: Gulf of Trieste, Italy. *Environ. Geol.* 30, 34–45. doi: 10.1007/s002540050130

Covelli, S., Fontolan, G., Faganeli, J., and Ogrinc, N. (2006). Anthropogenic markers in the Holocene stratigraphic sequence of the Gulf of Trieste (northern Adriatic Sea). *Mar. Geol.* 230, 23–51.

Covelli, S., Langone, L., Aquavita, A., Piani, R., and Emili, A. (2012). Historical flux of mercury associated with mining and industrial sources in the Murano and Grado Lagoon (northern Adriatic Sea). *Estuar. Coast. Shelf Sci.* 113, 7–19. doi: 10.1016/j.ecss.2011.12.038

Cozzi, S., Cabrini, M., Kralj, M., De Vittor, C., Celio, M., and Giani, M. (2020). Climatic and anthropogenic impacts on environmental conditions and phytoplankton community in gulf of Trieste (Northern Adriatic Sea). *Water* 12:2652. doi: 10.3390/w12092652

Cozzi, S., and Giani, M. (2011). River water and nutrient discharges in the northern Adriatic Sea: current importance and long-term changes. *Cont. Shelf Res.* 31, 1881–1893. doi: 10.1016/j.csr.2011.08.010

Cushman, J. A. (1926). The foraminifera of the Velasco shale of the Tampico Embayment. *Bull. Am. Assoc. Pet. Geol.* 10, 581–612. doi: 10.1306/3D932728-16B1-11D7-8645000102C1865D

Dassenakis, M., Adrianos, H., Depiazi, G., Konstantas, A., Karabela, M., Sakellari, A., et al. (2003). The use of various methods for the study of metal pollution in marine sediments, the case of Euvoikos Gulf, Greece. *Appl. Geochem.* 18, 781–794. doi: 10.1016/s0883-2927(02)00186-5

David, M., Gollasch, S., Cabrini, M., Perkoviè, M., Bošnjak, D., and Virgilio, D. (2007). Results from the first ballast water sampling study in the Mediterranean Sea – the Port of Koper study. *Mar. Pollut. Bull.* 54, 53–65. doi: 10.1016/j.marpolbul.2006.08.041

Debenay, J. P., Tsakiridis, E., Soulard, R., and Grossel, H. (2001). Factors determining the distribution of foraminiferal assemblages in Port Joinville Harbor (Ile d'Yeu, France): the influence of pollution. *Mar. Micropaleontol.* 43, 75–118. doi: 10.1016/s0377-8398(01)00023-8

Dimiza, M. D., Triantaphyllou, M. V., Koukousioura, O., Hallock, P., Simboura, N., Karageorgis, A. P., et al. (2016). The foram stress index: a new tool for environmental assessment of soft-bottom environments using benthic foraminifera. A case study from the Saronikos Gulf, Greece, Eastern Mediterranean. *Ecol. Indic.* 60, 611–621. doi: 10.1016/j.ecolind.2015.07.030

Donazzolo, R., Hieke Merlin, O., MenegazzoVitturi, I., Orio, A. A., Pavoni, B., Perin, G., et al. (1981). Heavy metal contamination in surface sediments from the Gulf of Venice, Italy. *Mar. Pollut. Bull.* 12, 417–425. doi: 10.1016/0025-326x(81)90160-0

Donnici, S., and Serandrei Barbero, R. (2002). The benthic foraminiferal communities of the northern Adriatic continental shelf. *Mar. Micropalaeontol.* 44, 93–123. doi: 10.1016/s0377-8398(01)00043-3

d' Orbigny, A. D. (1826). Tableau méthodique de la classe des céphalopodes. *Ann. Sci. Nat.* 7, 245–314.

d' Orbigny, A. D. (1839). Voyage dans l'Amérique Méridionale. *Foraminifères* 5, 1–86.

Dubois, A., Barras, C., Pavard, J.-C., Donnay, A., Béatrix, M., and Bouchet, V. M. P. (2021). Distribution patterns of benthic foraminifera in fish farming areas (Corsica, France): implications for the Implementation of benthic Indices in Biomonitoring Studies. *Water* 13:2821. doi: 10.3390/w13202821

El Kateb, A., Stalder, C., Martinez-Colon, M., Mateu-Vinces, G., Francescangeli, F., Coletti, G., et al. (2020). Foraminiferal-based biotic indices to assess the ecological quality status of the Gulf of Gabes (Tunisia): present limitation and future perspective. *Ecol. Indic.* 111:105962. doi: 10.1016/j.ecolind.2019.105962

El-Gamal, A. A., Peterson, R. N., and Burnett, W. C. (2012). Detecting freshwater inputs via groundwater discharge to Marina Lagoon, Mediterranean Coast, Egypt. *Estuar. Coast.* 35, 1486–1499. doi: 10.1007/s12237-012-9539-2

Faganeli, J., Planinc, R., Pezdic, J., Smodis, B., Stegnar, P., and Ogorelec, B. (1991). Marine geology of the gulf of Trieste (North Adriatic): geochemical aspects. *Mar. Geol.* 99, 93–108. doi: 10.1016/0025-3227(91)90085-i

Ferraro, L., Sprovieri, M., Alberico, I., Lirer, F., Prevedello, L., and Marsella, E. (2006). Benthic foraminifera and heavy metals distribution: a case study from

the Naples Harbour (Tyrrhenian Sea, Southern Italy). *Environ. Pollut.* 142, 274–284. doi: 10.1016/j.envpol.2005.10.026

Frontalini, F., Buosi, C., Da Pelo, S., Coccioni, R., Cherchi, A., and Bucci, C. (2009). Benthic foraminifera as bio-indicators of trace element pollution in the heavily contaminated Santa Gilla Lagoon (Cagliari, Italy). *Mar. Pollut. Bull.* 58, 858–877. doi: 10.1016/j.marpolbul.2009.01.015

Frontalini, F., and Coccioni, R. (2008). Benthic foraminifera for heavy metal pollution monitoring: a case study from the central Adriatic Sea coast of Italy. *Estuar. Coast. Shelf Sci.* 76, 404–417. doi: 10.1016/j.ecss.2007.07.024

Frontalini, F., and Coccioni, R. (2011). Benthic foraminifera as bioindicators of pollution: a review of Italian research over the last three decades. *Rev. Micropaléontol.* 54, 115–127. doi: 10.1016/j.revmic.2011.03.001

Giani, M., Djakovac, T., Degobbis, D., Cozzi, D., Solidoro, C., and Fonda-Umani, S. (2012). Recent changes in the marine ecosystems of the northern Adriatic Sea. *Estuar. Coast. Shelf Sci.* 115, 1–13. doi: 10.1016/j.ecss.2012.08.023

Gooday, A. J., Lejzerowicz, F., Goineau, A., Holzmann, M., Kamenskaya, O., Kitizato, H., et al. (2021). The biodiversity and distribution of abyssal benthic foraminifera and their possible ecological roles: a synthesis across the clarion-clipperton zone. *Front. Mar. Sci.* 8:634726. doi: 10.3389/fmars.2021.634726

Hammer, Ø., and Harper, D. A. T. (2006). *Paleontological Data Analysis*. Hoboken, NJ: Wiley Online Library.

Hammer, Ø., Harper, D. A. T., and Ryan, P. D. (2001). PAST: paleontological statistics software package for education and data analysis. *Palaeontol. Electronica* 4, 1–9.

Hayward, B. C., Holzmann, M., Pawlowski, J., Parker, H. J., Kaushik, T., Toyofuku, M. S., et al. (2021). Molecular and morphological taxonomy of living *Ammonia* and related taxa (Foraminifera) and their biogeography. *Micropaleontology* 67, 109–313.

Heron-Allen, E., and Earland, A. (1913). Clare island survey: part 64. Foraminifera. *Proc. R. Ir. Acad.* 31, 1–188.

Hess, S., Alve, E., Andersen, T. J., and Joranger, T. (2020). Defining ecological reference conditions in naturally stressed environments – how difficult is it? *Mar. Environ. Res.* 156:104885. doi: 10.1016/j.marenvres.2020.104885

Hohenegger, J., Piller, W. E., and Baal, C. (1988). Reason for spatial micro distribution of foraminifers in an intertidal pool (northern Adriatic Sea). *Mar. Ecol.* 10, 43–78. doi: 10.1111/j.1439-0485.1989.tb00065.x

Hohenegger, J., Piller, W. E., and Baal, C. (1993). Horizontal and vertical spatial micro distribution of foraminifers in the shallow subtidal Gulf of Trieste, northern Adriatic Sea. *J. Foraminifer. Res.* 23, 79–101. doi: 10.2113/gsjfr.23.2.79

Horvat, M., Covelli, S., Faganeli, J., Logar, M., Mandic, V., and Rajar, R. (1999). Mercury in contaminated coastal environments; a case study: the Gulf of Trieste. *Sci. Total Environ.* 237, 43–56. doi: 10.1016/s0048-9697(99)00123-0

Jorissen, F., Nardelli, M. P., Almodgi-Labin, A., Barras, C., Bergamin, L., Bicchi, E., et al. (2018). Developing foram-AMBI for biomonitoring in the Mediterranean: species assignments to ecological categories. *Mar. Micropaleontol.* 140, 33–45. doi: 10.1016/j.marmicro.2017.12.006

Jorissen, F. J. (1987). The distribution of benthic foraminifera in the Adriatic Sea. *Mar. Micropaleontol.* 12, 21–48. doi: 10.1016/0377-8398(87)90012-0

Jorissen, F. J. (1988). Benthic foraminifera from the Adriatic Sea: principles of phenotypic variation. *Utrecht Micropaleontol. Bull.* 37, 1–174.

Kaminski, M. A., Aksu, A. E., Box, M., Hiscott, R. N., Filipescu, S., and Al-Salameen, M. (2002). Late glacial to holocene benthic foraminifera in the Marmara Sea: implications for Black Sea Mediterranean Sea connections following the last deglaciation. *Mar. Geol.* 190, 165–202. doi: 10.1016/s0025-3227(02)00347-x

Leder, N., Smirčić, A., and Vilibić, I. (1998). Extreme values of surface wave heights in the Northern Adriatic. *Geofizika* 15, 1–13.

Li, T., Xiang, R., and Li, T. (2013). Benthic foraminiferal assemblages and trace metals reveal the environment outside the Pearl River Estuary. *Mar. Pollut. Bull.* 75, 114–125. doi: 10.1016/j.marpolbul.2013.07.055

Lo Giudice Cappelli, E., and Austin, W. E. N. (2019). Size matters: analyses of benthic foraminiferal assemblages across differing size fraction. *Front. Mar. Sci.* 6:752. doi: 10.3389/fmars.2019.00752

Loeblich, A. R., and Tappan, H. (1987). *Foraminiferal Genera and their Classification*, Vol. 2. New York, NY: Van Nostrand Reinhold, 970.

Lotze, H. K., Lenihan, H. S., Bourque, B. J., Bradbury, R. H., Cooke, R. G., Kay, M. C., et al. (2006). Depletion, degradation, and recovery potential of estuaries and coastal seas. *Science* 312, 1806–1809. doi: 10.1126/science.1128035

Malačič, V., and Petelin, B. (2001). "Chapter 6, regional studies," in *Physical Oceanography of the Adriatic Sea, Past, Present, Future*, eds B. Cushman-Roisin, M. Gačić, P. M. Poulain, and A. Artegiani (Amsterdam: Kluwer Academic), 167–181.

Martínez-Colón, M., Hallock, P., Green-Ruíz, C. R., and Smoak, J. M. (2018). Benthic foraminifera as bioindicators of potentially toxic element (PTE) pollution: torrecillas lagoon (San Juan Bay Estuary), Puerto Rico. *Ecol. Indic.* 89, 516–527. doi: 10.1016/j.ecolind.2017.10.045

Martins, V. A., Frontalini, F., Tramonte, K. M., Figueira, R. C., Miranda, P., Sequeira, C., et al. (2013). Assessment of the health quality of Ria de Aveiro (Portugal): heavy metals and benthic foraminifera. *Mar. Pollut. Bull.* 70, 18–33. doi: 10.1016/j.marpolbul.2013.02.003

Melis, R., Celio, M., Bouchet, V., Varagona, G., Bazzaro, M., Crosera, M., et al. (2019). Seasonal response of benthic foraminifera to anthropogenic pressure in two stations of the Gulf of Trieste (northern Adriatic Sea, Italy): the marine protected area of Miramare versus the Servola water sewage outfall. *Mediterr. Mar. Sci.* 20, 120–141.

Mladenović, A., Pogačnik, Ž, Milačič, R., Petkovšek, A., and Cepak, F. (2013). Dredger mud from the Port of Koper – civil engineering applications. *Mater. Technol.* 47, 353–356.

Moore, D. M., and Reynolds, R. C. Jr. (1997). *X-Ray Diffraction and the Identification and Analysis of Clay Minerals*, 2nd Edn. Oxford: Oxford University Press, 332–378.

Morigi, C., Jorissen, F. J., Fraticelli, S., Horton, B. P., Principi, M., Sabbatini, A., et al. (2005). Benthic foraminiferal evidence for the formation of the Holocene mud-belt and bathymetrical evolution in the central Adriatic Sea. *Mar. Micropaleontol.* 57, 25–49. doi: 10.1016/j.marmicro.2005.06.001

Murray, J. W. (1991). *Ecology and Paleoecology of Benthic Foraminifera*. London: Longman Harlow, 397.

Murray, J. W. (2006). *Ecology and Applications of Benthic Foraminifera*. Cambridge: Cambridge University Press, 426.

Ogorelec, B., Faganeli, J., Mušič, M., and Èermelj, G. (1997). Reconstruction of paleoenvironment in the Bay of Koper: (Gulf of Trieste, northern Adriatic). *Ann. Ser. Hist. Nat.* 7, 187–200.

Ogorelec, B., Mišič, M., and Faganeli, J. (1991). Marine geology of the Gulf of Trieste (northern Adriatic): sedimentological aspects. *Mar. Geol.* 99, 79–92. doi: 10.1016/0025-3227(91)90084-h

Ogorelec, B., Mišič, M., Faganeli, J., Stegnar, P., Vrišer, B., and Vukovič, A. (1987). Recentni sediment Koprskega zaliva. *Geologija* 30, 87–121.

Ogorelec, B., Mišič, M., Šercelj, A., Cimerman, F., Faganeli, J., and Stegnar, P. (1981). Sediment seèoveljske soline (Sediment of the salt marsh of Sečovlje). *Geologija* 24, 179–216.

Oldfield, F., Asioli, A., Accorsi, C. A., Mercuri, A. M., Juggins, S., Langone, L., et al. (2003). A high resolution late Holocene palaeo environmental record from the central Adriatic Sea. *Quat. Sci. Rev.* 22, 319–342. doi: 10.1016/s0277-3791(02)00088-4

Parent, B., Hyams-Kaphzan, O., Barras, C., Lubinevsky, H., and Jorissen, F. (2021). Testing foraminiferal environmental quality indices along a well-defined organic matter gradient in the Eastern Mediterranean. *Ecol. Indic.* 125:107498. doi: 10.1016/j.ecolind.2021.107498

Pavšič, J., and Peckmann, J. (1996). Stratigraphy and sedimentology of the Piran flysch area (Slovenia). *Annales* 9, 123–138.

Placer, L., Košir, A., Popit, T., Šmuc, A., and Juvan, G. (2004). The buzet thrust fault in istria and overturned carbonate megabeds in the Eocene flysch in the Dragonja Valley (Slovenia). *Geologija* 47, 193–198. doi: 10.5474/geologija.2004.015

Placer, L., Vrabec, M., and Celarc, B. (2010). Osnove razumevanja tektonske zgradbe NW Dinaridov in polotoka Istre. *Geologija* 53, 55–86. doi: 10.5474/geologija.2010.005

Pleničar, M., Polšak, A., and Šikić, D. (1973). *Osnovna Geološka karta SFRJ. L 33-88, Trst [Kartografsko gradivo]. 1:100.000*. Beograd: Zvezni Geološki Zavod.

Popadić, A., Vidović, J., Ćosović, V., Medaković, D., Dolenec, M., and Felja, I. (2013). Impact evaluation of the industrial activities in the Bay of Bakar (Adriatic Sea, Croatia): recent benthic foraminifera and heavy metals. *Mar. Pollut. Bull.* 76, 333–348. doi: 10.1016/j.marpolbul.2013.09.039

Rogan Šmuc, N., Dolenec, M., Kramar, S., and Mladenović, A. (2018). Heavy metal signature and environmental assessment of nearshore sediments: port of Koper (Northern Adriatic Sea). *Geoscience* 8:398. doi: 10.3390/geosciences8110398

Romano, E., Bergamin, L., Ausili, A., Magni, M. C., and Gabellini, M. (2016). Evolution of the anthropogenic impact in the Augusta Harbor (Eastern Sicily, Italy) in the last decades: benthic foraminifera as indicator of the environmental status. *Environ. Sci. Pollut. Res.* 23, 10514–10528. doi: 10.1007/s11356-015-5783-x

Romano, E., Bergamin, L., Di Bella, L., Frezza, V., Pierfranceschi, G., Marassich, A., et al. (2021). Benthic foraminifera as environmental indicators in extreme environments: the marine cave of Bue Marino (Sardinia, Italy). *Ecol. Indic.* 120:106977. doi: 10.1016/j.ecolind.2020.106977

Romeo, R. (2009). *Studio Geofisico Integrato ad Alta Risoluzione dei Depositi Marini e Della Struttura del Substrato Della Riviera di Miramare (Golfo di Trieste)*. Ph.D. thesis. Trieste: University of Trieste.

Rumolo, P., Salvagio Manta, D., Sprovieri, M., Coccioni, R., Ferraro, L., and Marsella, E. (2009). Heavy metals in benthic foraminifera from the highly polluted sediments of the Naples harbor (Southern Tyrrhenian Sea, Italy). *Sci. Total Environ.* 407, 5795–5820. doi: 10.1016/j.scitotenv.2009.06.050

Schönfeld, J., Alve, E., Geslin, E., Jorissen, F., Korsun, S., and Spezzaferri, S. (2012). The FOBIMO (foraminiferal bio-monitoring) initiative — towards a standardised protocol for soft-bottom benthic foraminiferal monitoring studies. *Mar. Micropaleontol.* 94, 1–13. doi: 10.1016/j.marmicro.2012.06.001

Scott, D. B., and Medioli, F. (1980). Quantitative studies of marsh foraminiferal distributions in Nova Scotia and comparison with those in other parts of the world: implications for sea-level studies. *Spec. Publ. Cushman Found. Foraminifer. Res.* 17, 1–58.

Sgarrella, F., and Moncharmont Zei, M. (1993). Benthic foraminifera of the Gulf of Naples (Italy): systematics and autoecology. *Boll. Della Soc. Paleontol. Ital.* 32, 145–264.

Sharifi, A. R., Crouda, I. W., and Austin, R. L. (1991). Benthic foraminifera as pollution indicators in Southampton Water, Southern England, UK. *J. Micropaleontol.* 10, 109–113. doi: 10.1144/jm.10.1.109

Slavec, P. (2012). *Analiza Morfologije Morskega dna Slovenskega Morja = Slovenian Seafloor Morphology analysis*. Master thesis. Ljubljana: University of Ljubljana, 58.

Solis-Weiss, V., Aleffi, F., Bettoso, N., Rossin, P., and Orel, G. (2007). The benthic macrofauna at the outfalls of the underwater sewage discharges in the Gulf of Trieste (northern Adriatic Sea). *Ann. Ser. Hist. Nat*. 17, 1–16.

Solis-Weiss, V., Rossin, P., Aleffi, F., Bettoso, N., Orel, G., and Vriser, B. (2001). "Gulf of Trieste: sensitivity areas using benthos and GIS techniques," in *Proceedings of the MEDCOAST 01*, Hammamet.

Trincardi, F., Correggiari, A., and Roveri, M. (1994). Late-quaternary transgressive erosion and deposition in a modern continental shelf: the Adriatic semi enclosed basin. *Geomar. Lett.* 14, 41–51. doi: 10.1007/bf01204470

Trobec, A. (2015). *Raziskave Zgradbe Sedimentnega Morskega dna v Strunjanskem Zalivu s Podpovršinskim Sonarjem = Investigation of sea Bottom Sediment Structure in the Strunjan Bay with Sub-Bottom Sonar Profiler*. Master thesis. Ljubljana: University of Ljubljana, 63.

Trobec, A., Busetti, M., Zgur, F., Baradello, L., Babich, A., Cova, A., et al. (2018). Thickness of marine Holocene sediment in the Gulf of Trieste (northern Adriatic Sea). *Earth Syst. Sci. Data* 10, 1077–1092. doi: 10.5194/essd-10-1077-2018

Türkmen, M., Türkmen, A., and Tepe, Y. (2011). Comparison of metals in tissues of fish from Paradeniz Lagoon in the coastal area of Northern East Mediterranean. *Bull. Environ. Contam. Toxicol.* 87, 381–385. doi: 10.1007/s00128-011-0381-1

Vidović, J., Ćosović, V., JuraČić, M., and Petricioli, D. (2009). Impact of fish farming on foraminiferal community, Drvenik Veliki Island, Adriatic Sea, Croatia. *Mar. Pollut. Bull.* 58, 1297–1309. doi: 10.1016/j.marpolbul.2009.04.031

Vidović, J., Dolenec, M., Dolenec, T., Karamarko, V., and Žvab Rožič, P. (2014). Benthic foraminifera assemblages as elemental pollution bioindicator in marine sediments around fish farm (Vrgada Island, Central Adriatic, Croatia). *Mar. Pollut. Bull.* 83, 198–213. doi: 10.1016/j.marpolbul.2014.03.051

Vidović, J., Nawrot, R., Gallmetzer, I., Haselmair, A., Tomašových, A., Stachowitch, M., et al. (2016). Anthropogenically inducted environmental changes in the Northeastern Adriatic Sea in the last 400 years (Panzano Bay, Gulf of Trieste). *Biogeosciences* 13, 5965–5981. doi: 10.5194/bg-13-5965-2016

Vrabec, M., Busetti, M., Zgur, F., Facchin, L., Pelos, C., Romeo, R., et al. (2014). "Refleksijske seizmične raziskave v slovenskem morju SLOMARTEC 2013," in *Raziskave s Področja Geodezije in Geofizike 2013: Zbornik del*, ed. M. Kuhar (Ljubljana: Fakulteta za Gradbeništvo in Geodezijo), 97–101.

Vrabec, M., and Rožič, B. (2014). "Strukturne in sedimentološke posebnosti obalnih klifov. In: 4. slovenski geološki kongres, Ankaran, 8.-10. Oktober 2014," in *Povzetki in Ekskurzije = Abstracts and Field Trips*, eds B. Rožič, T. Verbovšek, and M. Vrabec (Ljubljana: Naravoslovnotehniška Fakulteta), 84–91.

Walton, W. R. (1952). Techniques for recognition of living foraminifera, contribution Cushman foundation. *J. Foraminifer. Res.* 3, 56–60.

Walker, G., and Jacob, E. (1798). "An arrangement and description of minute and rare shells," in *Essays on the Microscope. The Second Edition, with Considerable Additions and Improvements*, eds G. Adams and F. Kanmacher (London: Dillon & Keating), 629–645.

Williamson, W. C. (1858). *On the Recent Foraminifera of Great Britain*. London: The Ray Society, 1–107.

World Register of Marine Species (2021). *World Register of Marine Species*. Available Online at: http://www.marinespecies.org [accessed November 8, 2021].

Wukovits, J., Oberrauch, M., Enge, A. J., and Heinz, P. (2018). The distinct roles of two intertidal foraminiferal species in phytodetrital carbon and nitrogen fluxes – results from laboratory feeding experiments. *Biogeosciences* 15, 6185–6198. doi: 10.5194/bg-15-6185-2018

Yanko, V., Ahmad, M., and Kaminski, M. (1998). Morphological deformities of benthic foraminiferal tests in response to pollution by heavy metals: implications for pollution monitoring. *J. Foraminifer. Res.* 28, 177–200.

Yanko, V., Arnold, A. J., and Parker, W. C. (1999). "Effects of marine pollution on benthic foraminifera," in *Modern Foraminifera*, ed. B. K. Sen Gupta (Dordrecht: Kluwer Academic Publishers), 217–235. doi: 10.1007/0-306-48104-9_13

Yasuhara, M., Hunt, G., Breitburg, D., Tsujimoto, A., and Katsuki, K. (2012). Human-induced marine ecological degradation: micropaleontological perspectives. *Ecol. Evol.* 2, 3242–3268. doi: 10.1002/ece3.425

Žitnik, M., Jakomin, M., Pelicon, P., Rupnik, Z., Simèiè, J., Burdar, M., et al. (2005). Port of Koper – elemental concentration in aerosols by PIXE. *X-Ray Spectrom.* 34, 330–334. doi: 10.1002/xrs.828

Zuin, S., Belac, E., and Marzi, B. (2009). Life cycle assessment of ship-generated waste management of Luka Koper. *Waste Manag.* 29, 3036–3046. doi: 10.1016/j.wasman.2009.06.025

Zupančič, N., and Skobe, S. (2014). Anthropogenic environmental impact in the Mediterranean coastal area of Koper/Capodistria, Slovenia. *J. Soil Sediments* 14, 67–77. doi: 10.1007/s11368-013-0770-7

Conflict of Interest: The authors declare that the research was conducted in the absence of any commercial or financial relationships that could be construed as a potential conflict of interest.

Publisher's Note: All claims expressed in this article are solely those of the authors and do not necessarily represent those of their affiliated organizations, or those of the publisher, the editors and the reviewers. Any product that may be evaluated in this article, or claim that may be made by its manufacturer, is not guaranteed or endorsed by the publisher.

frontiers | Frontiers in Marine Science

ORIGINAL RESEARCH
published: 28 April 2022
doi: 10.3389/fmars.2022.864214

Distribution of Different *Scrippsiella acuminata* (Dinophyta) Cyst Morphotypes in Surface Sediments of the Black Sea: A Basin Scale Approach

*Nina Dzhembekova[1], Fernando Rubino[2], Manuela Belmonte[2], Ivelina Zlateva[1], Nataliya Slabakova[1], Petya Ivanova[1], Violeta Slabakova[1], Satoshi Nagai[3] and Snejana Moncheva[1]**

[1] Institute of Oceanology "Fridtjof Nansen" – Bulgarian Academy of Sciences, Varna, Bulgaria, [2] Water Research Institute, Unit Talassografico "A. Cerruti", National Research Council CNR-IRSA, Taranto, Italy, [3] National Research Institute of Fisheries Science, Yokohama, Japan

OPEN ACCESS

Edited by:
Alberto Basset, University of Salento, Italy

Reviewed by:
Haifeng Gu, State Oceanic Administration, China
Jelena Godrijan, Rudjer Boskovic Institute, Croatia

***Correspondence:**
Snejana Moncheva
snejanam@abv.bg

Specialty section:
This article was submitted to Marine Ecosystem Ecology, a section of the journal Frontiers in Marine Science

Received: *28 January 2022*
Accepted: *04 April 2022*
Published: *28 April 2022*

Citation:
Dzhembekova N, Rubino F, Belmonte M, Zlateva I, Slabakova N, Ivanova P, Slabakova V, Nagai S and Moncheva S (2022) Distribution of Different Scrippsiella acuminata (Dinophyta) Cyst Morphotypes in Surface Sediments of the Black Sea: A Basin Scale Approach. Front. Mar. Sci. 9:864214. doi: 10.3389/fmars.2022.864214

Plankton cyst abundance and distribution is controlled by multiple factors. The stress linked to the fluctuations and variations of the environmental conditions in the water column is a major vector of encystment and intraspecific variability is an important adaptive strategy. The present study aims to disclose a link between the spatial distribution and abundance of different cyst morphotypes of *Scrippsiella acuminata* complex in surface sediments collected in the Black Sea at 34 sites and selected environmental variables. With this purpose, a basin scale data set was analyzed for patterns of intraspecific spatial heterogeneity. Redundancy analysis (RDA) was implemented to identify explanatory environmental variables associated with the cyst morphotypes abundance. Environmental multiyear data were used to ensure better approximation of a model that links environmental gradients with cyst abundance. Our results show that all *S. acuminata* cysts morphotypes are significantly correlated to one or a combination of the environmental variables, i.e., salinity, temperature and nutrients (nitrates and phosphates). The geographical distribution of *Scrippsiella* blooms in the Black Sea indicates that the interplay between the planktonic and benthic habitat of the dinoflagellate gives to *S. acuminata* the advantage to dominate in the plankton communities.

Keywords: Black Sea, *Scrippsiella acuminata*, cyst abundance, cyst distribution, environmental variables, redundancy analysis

INTRODUCTION

Many dinoflagellates produce benthic cysts as a part of their life cycle (reviewed in Belmonte and Rubino, 2019). The resting cysts accumulate in the sediments and serve as potential seed banks that secure the survival of the species over time (Lundholm et al., 2011; Ribeiro et al., 2013). They also play a crucial role in bloom initiation, especially important in the case of harmful algal bloom

species (HABs) (Anderson et al., 2003; Garcés et al., 2004). Encystment is considered as an adaptive strategy the species play out to respond to environmental stresses driven by variations of environmental conditions, such as temperature, salinity, nutrient concentration or daylength. These variations can also influence the patterns of spatial distribution of dinocysts (Anderson et al., 1984; Devillers and de Vernal, 2000; Sgrosso et al., 2001; Grigorszky et al., 2006; Richter et al., 2007; Zonneveld and Susek, 2007; Kremp et al., 2009; Lundgren and Granéli, 2011; Shin et al., 2018). Furthermore, intraspecific morphological variability among cysts produced by some species, including dinoflagellates like *Scrippsiella* spp., has been associated to variations in environmental conditions, both in cultures (Kokinos and Anderson, 1995) and in the field (Olli and Anderson, 2002; Zonneveld and Susek, 2007; Mertens et al., 2009) and this intraspecific variability can be read as a quantitative measure of environmental variations (Mertens et al., 2009; Mertens et al., 2012a; Persson et al., 2013; Shin et al., 2013; Hoyle et al., 2019).

The cosmopolitan dinoflagellate *Scrippsiella acuminata* (Ehrenberg, 1836) Kretschmann, Elbrächter, Zinssmeister, S. Soehner, Kirsch, Kusber & Gottschling, 2015 (the currently accepted name of *Scrippsiella trochoidea* (Stein, 1883) Loeblich III, 1976), is one of the dominant species in the phytoplankton community in the Black Sea, responsible for bloom events in the coastal areas of this basin (Nesterova et al., 2008; Terenko and Terenko, 2009; Moncheva et al., 2019 and the references therein). Even the cysts of this species are widespread in the basin, being dominant in the western region off the Bulgarian coast (Rubino et al., 2010). Their presence is reported also from many sites in the South (Mudie et al., 2017) and in the Northwest off the Ukrainian coast where the abundance increases with the depth in the shelf zone (Nikonova, 2010; Nikonova, 2015; Mudie et al., 2021).

Many studies, aimed to clarify the taxonomic characters both of thecae and cysts of *S. acuminata* and the cyst-theca relationships, showed that actually this species should be considered as a member of a complex (Montresor et al., 2003; Gottschling et al., 2005) with cryptic species genetically differentiated but morphologically indistinguishable so far (Zinssmeister et al., 2011; Kretschmann et al., 2014).

Based on the high morphological variability of the *S. acuminata* cysts already observed in the Black Sea (Dzhembekova et al., 2020), and in the Mediterranean (Ferraro et al., 2017; Rubino et al., 2017) and reported also from the East China Sea (Gu et al., 2008), the aim of the present study was to clarify whether the geographic distribution of the different cyst morphotypes of *S. acuminata* in the surface sediments of many coastal and shelf sites of the Black Sea, could be related to other environmental variables, besides hypoxia and pH, as reported by Shin et al. (2013) and Ishikawa et al. (2019) from the Pacific Ocean. Accordingly, sea surface temperature (SST), sea surface salinity (SSS), currents speed (CS), station depth, nitrates (NO_3) and phosphates (PO_4) were analyzed as plausible drivers of the spatial distribution and abundance of *S. acuminata* cyst morphotypes.

MATERIALS AND METHODS

Sampling

The study area covers Ukrainian, Romanian, Bulgarian, Turkish and Georgian waters. Surface sediment samples (top 2 cm; N = 48) were collected during different campaigns carried out in spring and/or summer seasons, from April 2008 to June 2016, at 34 sites both at coastal (C), shelf (S) and open sea (O) areas (depth 13.1 – 2100 m), using a multicorer or a Van Veen Grab sampler. In addition, material collected by a sediment trap deployed at 1,000 m in the deep sea (bottom: 2,000 m depth) was analyzed (**Figure 1**; **Table 1**) (details about the sediment trap are given in Gogou et al., 2014). All the sediment samples were stored in the dark without preservatives at 4°C until processing.

Sediment Treatment, Qualitative and Quantitative Analysis of Cysts

From each sample, an aliquot of homogenized sediment (from 2.0 to 2.2 cm^3) was used for the analyses of cysts while a parallel aliquot (≈ 10 cm^3) was collected to calculate the water content. The wet aliquots were weighed and screened through a 10 μm mesh (Endecotts Limited steel sieves, ISO3310-1, London, England) using natural filtered (0.45 μm) seawater (Montresor et al., 2010). The material retained onto the sieve was ultrasonicated for 1 min at low frequency and screened again through a sieve battery (200, 75 and 20 μm mesh sizes). A fine-grained fraction (20–75 μm) mainly containing protistan cysts, was obtained. The material retained onto the 75 and 200 μm mesh was not considered in this study. No chemicals were used to dissolve sediment particles in order to preserve calcareous cyst walls.

Qualitative and quantitative analyses were carried out under an inverted microscope (Zeiss Axiovert 200M) equipped with a Leica MC170 HD digital camera at x320-400 magnification. Both full cysts with cytoplasmic content (i.e., presumably viable) and empty, already germinated cysts were enumerated; 200 viable cysts were counted at least for each sample to obtain abundance values as homogeneous as possible and evaluate rare species too. To estimate the water content of sediment an aliquot from each sample (≈ 10 cm^3) was weighed and dried out overnight at 70°C. Quantitative data are reported as cysts g^{-1} of dry sediment.

All resting stage morphotypes were identified based on published descriptions. For organic dinocysts, the images and the key provided in Appendix B by Mudie et al. (2017) were used. The different resting stage morphotypes of *S. acuminata* were identified based on published descriptions (Gu et al., 2008; Shin et al., 2013; Shin et al., 2014) and germination experiments (as described below). They are distinguished here based on their size and wall features (i.e., calcified or uncalcified walls, presence and type of processes) and named with acronyms considering these features as:

SaR= S. acuminata rough
SaU= *S. acuminata* uncalcified
SaL= *S. acuminata* large
SaM= *S. acuminata* medium
SaS= *S. acuminata* small.

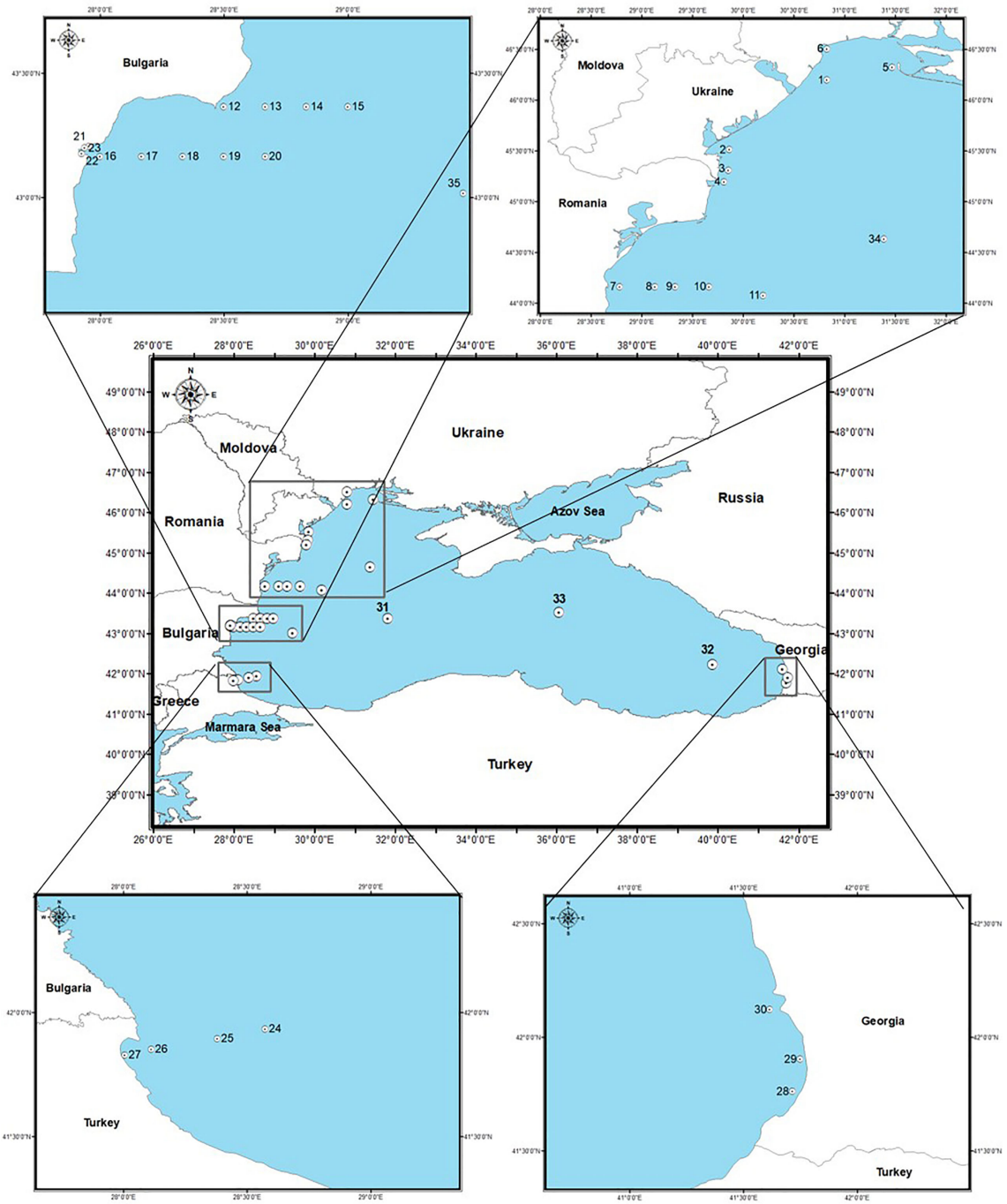

FIGURE 1 | Map of sampling sites and location of stations in the Black Sea.

To confirm the taxonomical identification, germination experiments were performed on single cysts isolated into Nunclon MicroWell plates (Nalge Nunc International, Roskilde, Denmark) containing ≈ 1 ml of natural sterilized seawater. Particular attention was given to the naked forms (i.e., without calcareous structures) with a smooth wall and those with a size smaller than that typical of *S. acuminata*. A total of more than 100 cysts of these types were isolated, considering the samples from all the campaigns, to obtain germination. All the isolated cysts were incubated at 20°C, equinoctial photoperiod and 80 μE m^{-2} s^{-1} irradiance and examined daily until germination. The choice of the incubation conditions was based on previous studies of *S. acuminata* excystment (Ferraro et al., 2017; Rubino et al., 2017).

TABLE 1 | Sampling stations (location, sampling date, season, geographic coordinates, depth).

Area		Station number	Station code	Sampling date	Season	Lat N (DD)	Lon E (DD)	Depth (m)
Ukraine	C	01	U01	May 2016	spring	46.202	30.827	28.6
	C	02	U05	May 2016	spring	45.516	29.862	20.4
	C	03	U06	May 2016	spring	45.311	29.853	22.8
	C	04	U07	May 2016	spring	45.200	29.810	20.5
	C	05	U12	May 2016	spring	46.325	31.467	16
	C	06	U15	May 2016	spring	46.509	30.824	13.1
Romania	C	07	R01	July 2013	summer	44.167	28.783	33.3
	C	08	R02	July 2013	summer	44.167	29.133	47
	S	09	R03	July 2013	summer	44.167	29.333	54
	S	10	R04	July 2013	summer	44.167	29.667	64.7
	S	11	R05	July 2013	summer	44.080	30.198	101
Bulgaria	S	12	B201	April 2008 June 2008	spring	43.367	28.500	32
	S	13	B202	April 2008 June 2008	spring	43.367	28.667	72
	S	14	B203	April 2008 June 2008	spring	43.367	28.833	80
	S	15	B204	June 2008	spring	43.367	29.000	96
	C	16	B301	April 2008 June 2008	spring	43.167	28.000	22
	C	16a	B301	July 2013	summer	43.167	28.000	22
	C	17	B302	April 2008 June 2008 April 2009	spring	43.167	28.167	22
	S	18	B303	April 2008 June 2008 April 2009	spring	43.167	28.333	41
	S	18a	B303	July 2013	summer	43.167	28.333	41
	S	19	B304	April 2008 June 2008 April 2009	spring	43.167	28.500	78
	S	19a	B304	July 2013	summer	43.167	28.500	78
	S	20	B305	June 2008	spring	43.167	28.667	93
	S	20a	B305	July 2013	summer	43.167	28.667	93
Bulgaria (Varna Bay)	C	21	VB	June 2008	spring	43.206	27.956	7.5
	C	22	VB1	June 2008	spring	43.169	27.925	16.4
	C	23	VB2	June 2008	spring	43.200	27.937	11
Turkey	S	24	T15	July 2013	summer	41.936	28.573	101
	S	25	T16	July 2013	summer	41.897	28.379	75.6
	S	26	T17	July 2013	summer	41.854	28.113	53.3
	S	27	T18	July 2013	summer	41.830	28.005	27.2
Georgia	S	28	G07	May 2016	spring	41.763	41.715	63
	S	29	G08	May 2016	spring	41.904	41.749	42
	S	30	G11	May 2016	spring	42.123	41.616	37
Open Sea	O	31	OS3	May 2016	spring	43.367	31.833	1933
	O	32	OS12	May 2016	spring	42.235	39.886	1904
	O	33	OS13	May 2016	spring	43.526	36.070	2100
	O	34	OS23	May 2016	spring	44.636	31.388	391
	O	35	Trap32	April 2009	spring	43.017	29.467	1000

C, coastal; S, shelf; O, open sea.

Environmental Data

A multiyear (1998-2016) data set of six environmental variables near surface temperature (SST), salinity (SSS), currents' speed (CS), station depth, nitrates (NO_3) and phosphates (PO_4) concentrations) was constructed based on monthly Black Sea reanalysis products available from the Copernicus Marine Environment Monitoring Service (CMEMS https://resources.marine.copernicus.eu/?option=com_csw&task=results). The time interval of the data set was calibrated considering the time span represented by the sediment surface layer collected for the cyst analysis. The physical parameters (CMEMS product id: BLKSEA_REANALYSIS_PHYS_007_004) were derived from a hydrodynamic model (NEMO, v3.6) implemented over the whole Black Sea basin (Madec, 2012). The horizontal grid resolution of the model is 1/36° in zonal resolution, 1/27° in meridional resolution. The latter provides data for temperature, salinity, horizontal velocity (zonal and meridional components) for the Black Sea domain since 1992. Nutrients (NO_3 and PO_4) were obtained from CMEMS product id: BLKSEA_REANALYSIS_BIO_007_005-BAMHBI, with the same grid resolution as NEMO model (Grégoire et al., 2008; Grégoire & Soetaert, 2010; Capet et al., 2016). A multiyear (1998–2016) environmental (explanatory) dataset covering the period from April to September, corresponding with the seasons of sediment sampling campaigns for cyst collection, was extracted.

Statistical Analyses

The data set for the analysis was based on the abundance of the different *Scrippsiella acuminata* cyst morphotypes as registered at each coastal and shelf sampling sites during the entire survey period (N = 34 samples excluding open sea stations and the trap data). For the stations with repetitive sampling (narrow Bulgarian coastal and shelf area – stations from 12 to 20) the data were averaged for the purpose of the analyses. Detrended canonical analysis (DCA) was employed for the estimation of gradient lengths and feasibility of linear or unimodal methods, respectively. Redundancy analysis (RDA) was implemented to identify explanatory environmental variables, associated with cyst morphotypes abundance (log-transformed data). Initially,

all the six environmental variables were explored by RDA to check their influence on the cyst abundance. The variables "depth" and "current" resulted not statistically significant from this preliminary analysis, so they were excluded to improve the overall model statistical significance. The variance inflection factors of the variables were calculated as a diagnostic tool for multicollinearity of data. Analysis of variance (ANOVA) was used as permutation test to assess the overall RDA model significance, RDA axes and the explanatory variables significance.

Bi-dimensional representation of the statistical comparison among the samples and the seasonal maxima of monthly mean values of environmental variables (SST, SSS, NO_3 and PO_4) was performed by means of non-parametric multidimensional scaling (NMDS). The analysis of similarities (ANOSIM) was carried out to statistically verify the segregation of the sampling sites in relation to the environmental variables.

All analyses and graphic representations were performed using the statistics and programming software R 3.6.2 (R Core Team, 2019), packages 'vegan' (Oksanen, 2015), available through the CRAN repository (www.r-project.org). All maps were produced using ArcGIS software version 10.2.2 (ESRI 2011).

RESULTS

Cyst Distribution and Concentrations

Total dinocyst abundance varied largely during the study period, ranging from 5 cysts g^{-1} (st. 13, June 2008) to 5,981 cysts g^{-1} (st. 1, May 2016) for viable forms and from 6 cysts g^{-1} (st. 21, June 2008) to 3,963 cysts g^{-1} (st. 31, May 2016) for empty forms. Cysts of *Scrippsiella* spp. (i.e., also including species different from *S. acuminata*) were recorded at all stations representing between 29 and 100% of the total abundance of viable cysts and between 30 and 94% of empty cysts total number, with viable cysts prevailing in the majority of the samples. Altogether, 13 different taxa were distinguished within the genus *Scrippsiella* with six identified to species level (*S. acuminata*, *S. kirschiae*, *S. lachrymosa*, *S. ramonii*, *S. spinifera*, *S. trifida*). *S. acuminata* cysts were widespread throughout the entire study area (**Figure 2**) and dominated in the sediments, with 46 to 100% of *Scrippsiella* viable forms.

Similar to total dinocysts, the cyst densities of *S. acuminata* complex were highly variable. The lowest values were registered in June 2008 at the Bulgarian shelf station 13 and at the coastal site 21, along the Varna transect, with 3 and 5 cysts g^{-1} respectively, while the highest densities were observed in May 2016 at the open sea station 31, with 4,275 cysts g^{-1} for full forms and 2,500 cysts g^{-1} for empty ones. Viable cyst proportions exceeded 50% (up to 100% – st. 14 in June 2008) of the total cyst abundance in about 68% of the samples, and in 58% of the samples for the empty cysts. Spatially, *S. acuminata* complex cysts were more abundant at open sea (347–4,275 cysts g^{-1}). In the shelf area, the abundance varied between 3 and 1,985 full cysts g^{-1}, and for coastal stations from 5 to 2,556 full cysts g^{-1}.

Finally, cysts of *S. acuminata* complex were abundant in the sediment trap deployed at a depth of 1,000 m as well, accounting up to 83% of the *Scrippsiella* cysts and 48% of the total dinocyst abundance.

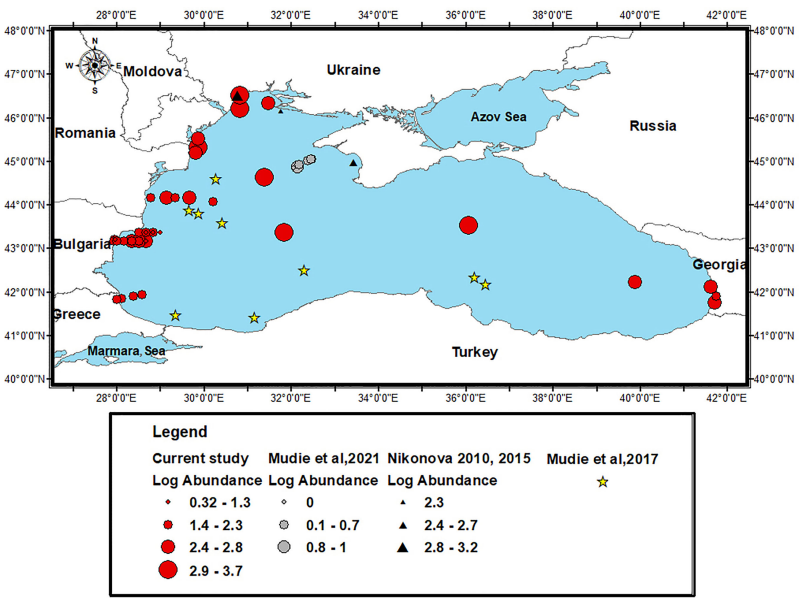

FIGURE 2 | Distribution of *S. acuminata* complex cysts in the Black Sea sediments (data according to Mudie et al., 2017 are not quantitative and are shown only as presence locations).

Scrippsiella acuminata Cysts Morphotypes – Identification and Distribution

Five cyst morphotypes of *Scrippsiella acuminata* were observed in the sediment samples (**Figure 3, 1a-7**; **Table 2**).

SaR (*Scrippsiella acuminata* rough type) (**Figure 3, 1a, b**)

Spherical, from light to dark brown in color, 30-40 μm in diameter. The calcareous layer has a rough surface with many irregular cobblestone-like crystals. A red body is always visible inside, with many other greenish granules. The archeopyle is chasmic and epicystal.

More than 70% of the incubated cysts (n = 11) germinated producing active stages identified as *Scrippsiella acuminata* by light microscopy.

SaU (*Scrippsiella acuminata* uncalcified type) (**Figure 3, 2a, b**)

Spherical, light brown in color, 32-38 μm in diameter. The wall is uncalcified, made by a thick organic layer, resistant to dissolution in HCl 10%. One or two large red or sometimes orange bodies are always well visible. The archeopyle is chasmic epicystal.

More than 75% of the incubated cysts (n = 23) germinated producing active stages identified as *Scrippsiella acuminata* by light microscopy.

SaL (*Scrippsiella acuminata* large type) (**Figure 3a, b**)

Spherical to mostly ovoid, dark brown, with a prominent red body clearly visible inside. The wall is covered by typical rod-like capitate or spiny calcareous processes. The body size ranges from 45 μm to 55 μm for the major axis and 30 μm to 40 μm for the minor axis (excluding processes). The archeopyle is chasmic epicystal, in form of a zig-zag split along some plate boundaries. The epicyst usually remains attached. More than 80% of the incubated cysts (n = 15) germinated producing active stages identified as *Scrippsiella acuminata* by light microscopy. This morphotype is similar to that produced by *Scrippsiella erinaceus*, recently signaled in the Black Sea, along the Romanian coast (Žerdoner Čalasan et al., 2019).

SaM (*Scrippsiella acuminata* medium type) (**Figure 3, 4a, b**)

Spherical to ovoid, dark brown, with a prominent red body clearly visible below the wall. This is covered by typical rod-like capitate or spiny calcareous processes. The body size ranges from 26 μm to 31 μm for the minor axis and 30 μm to 40 μm for the major axis (excluding processes). The archeopyle is meso-epicystal, in form of a zig-zag split. There is no detachable operculum.

More than 70% of the incubated cysts (n = 18) germinated producing active stages identified as *Scrippsiella acuminata* by light microscopy.

SaS (*Scrippsiella acuminata* small type) (**Figure 3, 5a, b**)

Spherical to ovoid, dark brown, with a prominent red body clearly visible below the wall. This is made by calcareous capitate, sometimes spiny, processes. The body size ranges from 20 μm to 26 μm in diameter (excluding processes). The archeopyle is epicystal, in form of a zig-zag split and without an operculum that can detach. Nearly 50% of the incubated cysts (n = 10) germinated producing active stages identified as *Scrippsiella acuminata* by light microscopy.

Generally, more than two different *S. acuminata* morphotypes co-occurred in the studied samples. The morphotypes SaM and SaS resulted the most abundant, accounting for 59% and 30% of the total density of *S. acuminata* cysts. The abundance of SaL was much lower (only 2%) while SaR and SaU densities resulted variable, but

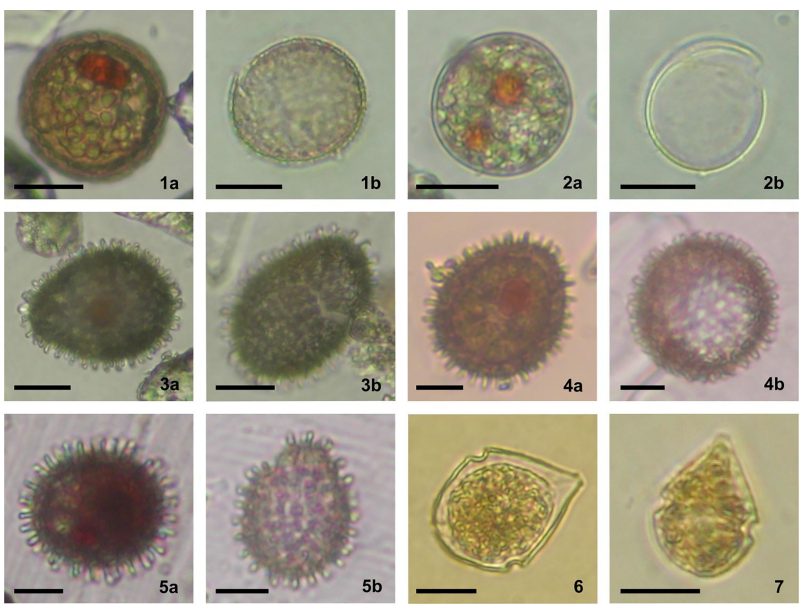

FIGURE 3 | Different cyst morphotypes produced by *Scrippsiella acuminata* complex, identified in the surface sediments of the Black Sea*; a* and *b* refer to viable and germinated cysts respectively; scale bars = 20 μm, except **4a, b** and **5a, b** scale bars = 10 μm. 1. SaR **(1a, b)** – *S. acuminata* rough type; 2. SaU **(2a, b)** – *S. acuminata* uncalcified type; 3. SaL **(3a, b)** – *S. acuminata* large type; 4. SaM **(4a, b)** *S. acuminata* medium type; 5. SaS **(5a, b)** – *S. acuminata* small type; 6. Vegetative stage produced by germination of SaR; 7. Vegetative stage produced by germination of SaM.

TABLE 2 | Environmental variables (sea surface temperature, SST; sea surface salinity, SSS; currents' speed, CS; station depth; nitrates, NO_3; and phosphates, PO_4) and abundance of viable *S. acuminata* cyst morphotypes (SaL, *S. acuminata* large; SaM, *S. acuminata* medium; SaS, *S. acuminata* small; SaR, *S. acuminata* rough; SaU, *S. acuminata* uncalcified; Tot , total).

St. No	Sampling date month year	SST °C	SSS psu	CS m s^{-1}	Station depth m	NO_3 mmol m^{-3}	PO_4 mmol m^{-3}	SaL cysts g^{-1}	SaM cysts g^{-1}	SaS cysts g^{-1}	SaR cysts g^{-1}	SaU cysts g^{-1}	Tot cysts g^{-1}
1	**May 2016**	22.94	15.85	0.0214	28.6	150.58	3.2	93	1074	630	426	333	2556
2	**May 2016**	22.9	16.73	0.0114	20.4	207.35	3.19	15	175	146	39	19	394
3	**May 2016**	22.59	16.86	0.0365	22.8	196.85	2.6	17	368	282	188	34	889
4	**May 2016**	22.59	16.58	0.0741	20.5	188.96	2.49	6	140	101	0	9	256
5	**May 2016**	22.05	15.3	0.0077	16	170.46	2.42	15	130	91	27	18	281
6	**May 2016**	23.05	15.31	0.0189	13.1	197.07	16.99	0	346	150	9	523	1028
7	**July 2013**	28.04	17.02	0.024	33.3	62.57	2.83	0	186	141	11	32	370
8	**July 2013**	28.09	17.77	0.0641	47	32.63	3.35	40	741	273	60	84	1198
9	**July 2013**	28.04	17.92	0.0873	54	22.33	3.58	7	162	113	28	16	326
10	**July 2013**	27.91	17.96	0.0325	64.7	16.85	3.91	4	470	355	37	52	918
11	**July 2013**	27.75	18.47	0.041	101	14.12	4.86	12	453	276	10	37	788
12	**April 2008**	22.31	17.34	0.1193	32	26.17	0.46	0	86	67	0	0	153
	June 2008							16	95	58	0	0	169
13	**April 2008**	22.38	17.6	0.0664	72	22.04	0.42	3	40	6	0	0	49
	June 2008							0	2	1	0	0	3
14	**April 2008**	22.47	18.26	0.0127	80	18.44	0.27	0	47	14	0	0	61
	June 2008							1	12	7	1	0	21
15	**June 2008**	22.47	18.37	-0.0088	96	7.62	0.29	1	8	2	0	1	12
16	**April 2008**	22.27	17.61	0.0011	22	16.89	0.43	6	93	44	0	0	143
	June 2008							0	40	10	0	0	50
	July 2013	27.85	17.73	0.0299		17.28	3.4	4	217	134	32	28	415
17	**April 2008**	22.39	17.64	0.039	22	18.54	0.43	0	46	26	0	0	72
	June 2008							5	101	51	0	3	160
	April 2009							1	42	12	7	5	67
18	**April 2008**	22.35	17.59	0.0069	41	16.89	0.98	0	23	4	0	4	31
	June 2008							7	182	97	0	0	286
	April 2009							0	196	170	78	85	529
	July 2013	27.88	17.71	-0.008		16.89	3.36	0	295	239	99	44	677
19	**April 2008**	22.55	17.7	0.0354	78	23.05	1.18	6	126	46	6	0	184
	June 2008							0	92	50	0	0	142
	April 2009							0	272	132	104	119	627
	July 2013	27.72	18	0.1489		21.11	3.45	7	338	276	89	58	768
20	**June 2008**	22.57	18.02	0.0487	93	18.2	0.31	0	11	3	0	0	14
	July 2013	27.62	18.2	0.1071		18.2	4.58	33	933	656	211	152	1985
21	**June 2008**	22.14	17.58	0.0094	7.5	16.89	0.43	0	4	1	0	0	5
22	**June 2008**	22.14	17.58	0.0094	16.4	16.89	0.43	0	75	53	0	0	128
23	**June 2008**	22.14	17.58	0.0094	11	16.89	0.43	5	98	52	0	0	155
24	**July 2013**	27.53	18.48	0.1624	101	15.00	4.92	13	280	168	4	6	471
25	**July 2013**	27.63	18.53	0.0897	75.6	13.52	3.34	13	288	161	74	25	561
26	**July 2013**	27.58	18.62	0.0057	53.3	12.65	3.34	15	342	166	24	17	564
27	**July 2013**	27.2	18.67	-0.000851	27.2	42.51	3.32	1	31	33	1	13	79
28	**May 2016**	21.59	16.05	0.0318	63	3.35	4.43	0	112	82	2	6	202
29	**May 2016**	23.86	16.93	0.008	42	6.88	4.39	2	82	45	2	8	139
30	**May 2016**	23.69	17.65	0.0092	37	41.69	4.18	10	130	60	2	0	202
31	**May 2016**	n/a	n/a	n/a	1933	n/a	n/a	75	2700	1450	0	50	4275
32	**May 2016**	n/a	n/a	n/a	1904	n/a	n/a	5	208	132	0	2	347
33	**May 2016**	n/a	n/a	n/a	2100	n/a	n/a	37	2037	1259	0	37	3370
34	**May 2016**	n/a	n/a	n/a	391	n/a	n/a	0	1900	767	0	0	2667
35	**April 2009**	n/a	n/a	n/a	1000	n/a	n/a	0	78	1127	1	492	1698

they were observed in a high number of sites, i.e., 57% and 67%, respectively.

Concerning the spatial distribution, the highest density of SaR viable cysts (426 cysts g^{-1}) was observed at the Ukrainian station 1, while it resulted less abundant in Georgian and Turkish areas. The range of abundance of this morphotype in coastal area was between 0 and 426 cysts g^{-1}, whereas at the deeper stations the maximum abundance was lower (between 0 and 211 cysts g^{-1} for shelf and between 0 and 1 cysts g^{-1} for open sea). Worth to note, SaR and SaU viable cysts were observed mainly during the summer surveys. Although its variable density at the sampling sites, SaU viable cysts were particularly abundant at the Ukrainian station 6 (523 cysts g^{-1}) (**Figure 4**). In the coastal area the SaU abundance was between 0 and 523 cysts g^{-1}, similarly in the open sea it varied from 0 to 496, while in the shelf the maximum value was lower (0 – 152 cysts g^{-1}).

For SaL type the maximum recorded abundance was lowest for shelf area (0 – 33 cysts g^{-1}) whereas the values for coastal and

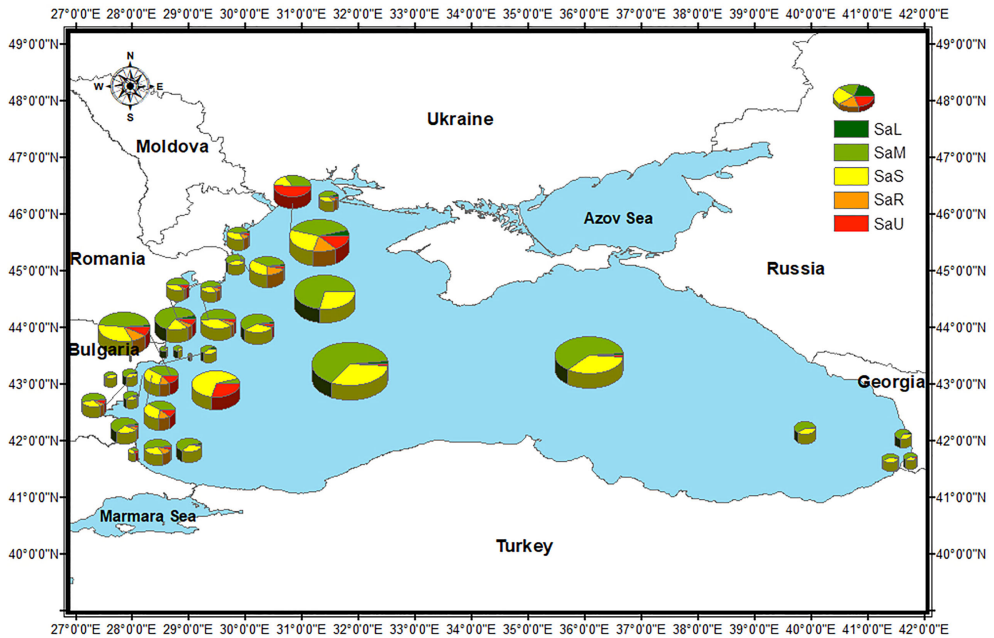

FIGURE 4 | *S. acuminata* morphotypes distribution and % of the total abundance of *S. acuminata* viable cysts in the Black Sea, by sampling stations (for the stations with repetitive sampling, the maximum abundance is shown). Size of the pies corresponds to total *S. acuminata* cyst abundance (**Table 2**).

open sea stations were close (0 – 93 cysts g^{-1} and 0 – 75 cysts g^{-1}, respectively). SaM and SaS tended to increase offshore (78 – 2700 cysts g^{-1} and 132 – 1450 cysts g^{-1}, respectively). At coastal stations, they ranged between 4 and 1074 cysts g^{-1} for SaM and from 1 to 630 cysts g^{-1} for SaS. In shelf area, SaM abundance varied between 2 and 933 cysts g^{-1} and SaS between 1 and 656 cysts g^{-1}.

Among the four different morphotypes collected in the trap, i.e., SaR, SaU, SaM and SaS, the "small type" was the dominant one (66% of all *S. acuminata* cysts), followed by the "uncalcified type" (29%) while the presence of the "medium" and "rough" types was much lower (5%).

Environmental Factors and Statistical Analyses

The summary of the environmental variables' statistics is presented in **Table 3**, showing rather limited ranges of variation of salinity and temperature.

According to the NMDS ordination (ANOSIM R = 0.69 and p = 0.0001), the sampling sites, together with the seasonal maxima of the monthly values of the considered environmental variables are segregated into three clearly differentiated clusters (C1, C2 and C3) (**Figure 5**).

Cluster C1 comprised Ukrainian stations only (1–5) where NO_3 concentrations were higher than all other sampling sites (150.6–207.3 mmol NO_3 m^{-3}). Station 6 (also located in the Ukrainian area) segregated alone due to high NO_3 concentration together with the highest PO_4 concentration (16.99 mmol PO_4 m^{-3}). Cluster C2 comprised all the Bulgarian sites sampled in spring and was defined by small ranges of variation of SST (22.14–22.94°C) and SSS (17.34–18.37 PSU) and relatively low NO_3 and PO_4 concentrations (7.62–22.04 mmol NO_3 m^{-3} and 0.27–1.18 mmol PO_4 m^{-3}). The third cluster (C3) comprised the Romanian, Turkish, Georgian and Open Sea sites, plus the three Bulgarian sites sampled in the summer of 2013 and was correlated to higher variability of SST (21.59–28.09°C), SSS (16.05-18.67 PSU), NO_3 (3.35–62.57 mmol NO_3 m^{-3}) and PO_4 (2.83–4.92 mmol PO_4 m^{-3}). The segregation of sites into clusters was more strongly related to the nutrient concentrations rather than SST and SSS, which fluctuated within relatively short ranges, suggesting that eutrophication level is most likely acting as a strong selective environmental driver.

TABLE 3 | Summary of the statistic of the environmental variables in the study area.

Variable	Minimum	Maximum	Average	Std. dev.	Variance	Range
Temperature, °C	21.59	28.09	24.54	2.61	6.8	6.5
Salinity, psu	15.3	18.67	17.51	0.88	0.77	3.37
Nitrates, mmol m^{-3}	3.35	207.35	49.63	65.13	4241.58	204
Phosphates, mmol m^{-3}	0.27	16.99	2.89	2.96	8.75	16.72

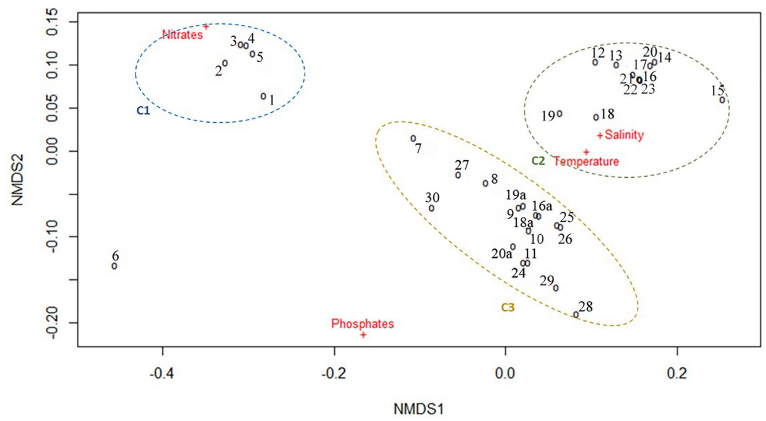

FIGURE 5 | NMDS plot of multiyear environmental data by sampling stations.

Detrended correspondence analysis (DCA) results proved that species abundance data are homogeneous and thus more suitable for linear ordination methods (1st ordination axis length is 1.21 in DC units or gradient length is < 3, respectively the most appropriate ordination method is RDA).

Variance Inflation Factors were estimated for environmental variables to test data for multicollinearity and avoid model misinterpretation. RDA provided a statistically significant model ($p = 0.001$, $R^2 = 0.43$, $R^2_{adj} = 0.35$) with the first two axes explaining roughly 35% of the total variance in morphotype concentrations (RDA1 – 26.21%, $p = 0.001$, and RDA2 – 7.14%. $p = 0.03$). Salinity ($p = 0.001$), temperature ($p = 0.010$), phosphates ($p = 0.022$) and nitrates ($p = 0.034$) were found to significantly contribute to the variance of cyst concentrations (SSS – 10.83%, SST – 4.18%, PO_4 and NO_3 with roughly 4% each to the variance explained by RDA1). The RDA triplot (**Figure 6**) shows that SaM and SaL abundance is strongly associated with SSS, SaS and SaR with SST and NO_3, while SaU is associated with NO_3 and PO_4 concentrations and SST.

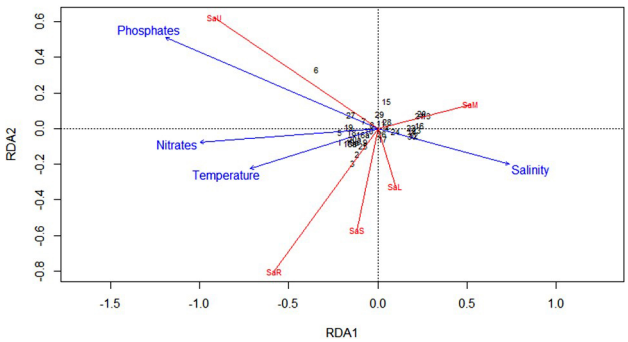

FIGURE 6 | RDA Correlation Triplot (scaling type 2 – lc) between environmental multiyear explanatory dataset and the corresponding response cysts matrix with fitted site scores.

DISCUSSION

The present study represents one of the largest basin-scale surveys (depth 13.1–2100 m) of *Scrippsiella acuminata* (the currently accepted name of *S. trochoidea*) cyst distribution in the Black Sea conducted to this date. As a consequence, a great variability in cysts abundance throughout the study area was observed, both for the whole dinoflagellate encysted community and the *S. acuminata* complex. Even considering the natural variability linked to the different seasons of sampling, the huge amplitude of densities observed (ranging from 5 to 5,981 cysts g^{-1} dry weight of sediment for viable forms), most likely could be associated with the different abiotic and biotic conditions occurring within the Black Sea study region, as demonstrated in the recent literature. In a comprehensive study of cysts distribution from 43 samples at water depths of 71–905 m on the outer Ukrainian Shelf and upper continental slope, Mudie et al. (2021) reported the presence of *Scrippsiella* spp. cysts at almost all the investigated sites with densities ranging between 2-89 cysts g^{-1} dry weight of sediment. The cysts of *S. acuminata* (as *S. trochoidea*) were recorded at 6 sites only with very low abundance (1–10 cysts g^{-1} dry weight of sediment) (**Figure 2**). Nikonova (2010; 2015) found much higher densities (190–1,690 cysts g^{-1} dry weight of sediment), at three stations in the same area close to those observed in our study (Stations 1, 5 and 6) (**Table 2**; **Figure 2**). Over the investigated 34 sites, our samples recorded a presence of the *S. acuminata* cysts widespread throughout the entire area and particularly higher relative abundance (46 to 100% of *Scrippsiella* viable forms) as compared to the data (less than 5%) documented by Mudie et al. (2017). The study of Mudie et al. (2017) was based on information from different datasets considering data from top 2 cm of sediment, similar to the current study. However, the use of hydrochloric acid impose difficulties in the differentiation of the cyst morphotypes of species with organic walls such as *S. trochoidea* (= *S. acuminata*), as highlighted in the paper (Mudie et al., 2017). Even if the highest densities were detected at the

deep open sea stations (up to 4,275 cysts g^{-1}), high values were also observed at the coastal stations (up to 2,556 cysts g^{-1}) and at some shelf stations, suggesting no distinct pattern of spatial distribution related to depth and/or distance from the coast. Similarly, Mudie et al. (2021) exploring the relationship to sediment grain size, abiotic and biotic oceanographic parameters, including methanogenesis, found that *Scrippsiella* cysts (mostly cysts of *S. acuminata*) tend to be more abundant at higher depths on the continental slope, but this species could be also dominant on the continental shelf-break around 200 m depth.

Cysts identified in surface sediment samples are usually assumed as recently produced in relation to the sedimentary regime of the area. Nevertheless, the natural encysted community represents an integration in time and space of the species encystment/excystment dynamics and consists of different "dormancy aged" assemblages (Kim and Han, 2000) expression of different time intervals with a succession of highly variable environmental conditions. They reflect the dominant ecological processes for plankton over several years rather than a seasonal signature (Dale, 1976), that imposes a further complication to explain dinocyst distribution patterns with environmental specific conditions at the time of sampling (Devillers and de Vernal, 2000). Taking into account various factors such as sedimentation, sampling method, and amount of bioturbation, Mudie et al. (2017) estimated that the time span represented by the Black Sea surface sediment samples is between less than five years to a few decades. Therefore, in the present study, environmental multiyear data were used in the statistical analysis, to account for the disparity between the time scale of the cyst record and the time scale of the environmental factors (Ribeiro and Amorim, 2008; García-Moreiras et al., 2021) and to ensure better approximation of the model linking environmental gradients with cysts abundance data.

In this study, Redundant discriminant analysis (RDA) helped to explore the relationships between the environmental variables and the *S. acuminata* cyst assemblages. All the cysts morphotypes were found to be associated to a single or a combination of environmental variables, confirming that cysts beds are repositories of ecophysiological diversity for the planktonic communities (Ribeiro et al., 2013). The links revealed by the applied multivariate analyses between temperature, salinity, phosphates, and nitrates and the spatial distribution of cyst morphotypes conform to findings in other studies (e.g., Sala-Pérez et al., 2020); salinity was generally reported to induce primarily variation in cyst process morphology of some Gonyaulacacean dinoflagellate species (e.g., Ellegaard, 2000; Mertens et al., 2009). In particular, process length variation has been observed to mostly change with water density (as a function of salinity and temperature) (Mertens et al., 2011; Mertens et al., 2012a; Mertens et al., 2012b). However, other variables have been mentioned as drivers of intraspecific variation, such as water column deoxygenation (Pross, 2001; Mudie et al., 2021), temperature and nutrients, associated with intraspecific cyst body size variation (Mertens, 2013; Mousing et al., 2017). In our study, the diagnostic of morphological variability of the cyst produced by *S. acuminata* was particularly related to the cyst wall surface structure (calcification and length of the processes), cyst body shape and size. The literature provides contradictory links between nutrients levels and *Scrippsiella* cyst morphotypes. Accordingly, the naked-type (i.e. non-calcified) cysts of *S. acuminata* were perceived as a morphological response to pH in the sediments and it has been suggested that they could be an indicator for eutrophication or acidification (Shin et al., 2013). On the contrary, Wang et al. (2007) reported high rates of formation of the naked cyst-type of *S. acuminata* during the bloom and shortly after the bloom, perceived to be related to the cellular nutrient limitation, while Gu et al. (2008) did not find any effect of nutrients on calcification in laboratory conditions.

Our results suggest that the formation of different morphotypes of cysts of *S. acuminata* complex within the water depths studied is regulated by specific environmental conditions (salinity, temperature, nitrates and phosphates) and even if some morphotypes appeared to have more confined geographical distribution, our data did not explain the existence of explicit ecological niches. The ecological niche theory (Pocheville, 2015) assumes that differences in species composition among communities are caused by heterogeneity in the environment or by limiting resources and environmental filtering of species according to their environmental requirements, such as climate, oceanographic conditions, both in pelagic and coastal areas, and competition for resources such as nutrients for marine algae, as a result of biotic interactions (Cadotte and Tucker, 2017).

In order to add new information about the relation between environmental drivers and *S. acuminata* morphotypes a very cautious approach should be used to interpret the data, considering the high cryptic diversity within the *Scrippsiella* species complex (Montresor et al., 2003). Essentially, the taxonomy of species within *S. acuminata* complex is still quite challenging and problematic. DNA-based results showed the presence of two *S. acuminata* ribotypes in the Romanian Black Sea assigned ambiguously as *S.* cf. *erinaceus* and *S.* aff. *acuminata* (Žerdoner Čalasan et al., 2019). Thus, additional molecular analyses would be vital (Žerdoner Čalasan et al., 2019) to clarify if the morphotypes are ecotypes, produced under distinctive environmental conditions, indicating different survival strategies of a single species (Sgrosso et al., 2001), or they represent a variety of cryptic species (Zinssmeister et al., 2011).

We found out that the Black Sea sediments harbor phenotypically diverse seed banks of *S. acuminata* complex as described also in other geographic areas (Montresor et al., 2003; Gu et al., 2008; Rubino et al., 2016; Rubino et al., 2017). Noteworthy, *S. acuminata* morphotypes dominated in the sediment trap sample, collected at 1,000 depth, confirming the high efficiency of the species in cyst production (Montresor et al., 1994; Wang et al., 2004; Morozova et al., 2016). The environmental and hydrodynamic conditions in the water column can influence the resting stage assemblages as species composition and abundance, and the resting stage encystment/

excystment dynamics, by coupling the bentho-pelagic compartments (Casabianca et al., 2020). The conditions leading to bloom seeding and initiation are still not fully understood, although seeding from planktonic populations is considered the most plausible hypothesis (García-Moreiras et al., 2021 and the references therein). The high *S. acuminata* complex cyst densities documented in our study suggest the build-up and growth in time of significant cyst beds. They play a crucial role in the dinoflagellate bloom dynamics, seeding the planktonic blooms and refueling the communities in the water column (Kremp, 2001; Rubino and Belmonte, 2021). Moreover, they ensure the persistence of the species in the environment, serving as a benthic reservoir of biodiversity (Belmonte and Rubino, 2019). The geographical spread of *Scrippsiella* blooms in the Black Sea indicates that most likely the interplay between the planktonic and benthic habitat is advantageous and common for *S. acuminata*, allowing it to dominate in the plankton communities and proliferating to bloom densities (Nesterova et al., 2008; Moncheva et al., 2019). Outbursts of *S. acuminata* have been observed basin-wide since the '70s in abundance ranging between 7.8 x 10^5–125.4 x 10^6 cells/L – in Odessa Bay (Ukraine) in 2005 (8.0 x 10^6 cells/L, Terenko and Terenko, 2009) and Crimea in 2011 (4.4 x 10^6 cells/L, Bryantseva and Gorbunov, 2012), in Romanian waters (25.8–125.4 x 10^6 cells/L in the period 1973–2005, Bodeanu, 2002; Nesterova et al., 2008), in Varna Bay (Bulgaria) (1.9 x 10^6 cells/L, Moncheva et al., 1995) in Turkish waters – Bay of Sinop (7.8 x 10^5 cells/L during 1995–1996, Turkoglu and Koray, 2002) and Trabson (1.34 x 10^6 cells/L in 2000, Feyzioğlu and Oğut, 2006), and in Russian waters (Novorosiysk) (8.6 x 10^6 cells/L in 2005–2006, Yasakova, 2010).

Although the new finding of different cyst morphotypes and ecological affinity to the environmental conditions and regional distribution advances our understanding of *S. acuminata* complex, many uncertainties remain about their ecological role in the benthic seed banks and plankton dynamics above all. Moreover, there are unanswered questions about the persistence and expansion of homogenous/heterogeneous vegetative populations in the water column in relation to the dynamics and distribution of cyst beds in the sediment. Further research focusing on the pelagic/benthic coupling however seems promising for large-scale monitoring and tracking phytoplankton community alterations and climate change effects.

DATA AVAILABILITY STATEMENT

The original contributions presented in the study are included in the article/supplementary material. Further inquiries can be directed to the corresponding author.

AUTHOR CONTRIBUTIONS

SM, ND, and IZ conceived the study. ND, SM, FR, and IZ wrote the manuscript. FR and MB analysed the cysts. SM and NS carried out the samplings and organized the research cruises. VS extracted and prepared the environmental data and maps. IZ carried out statistical analyses. All authors commented on the manuscript. All authors contributed to the article and approved the submitted version.

FUNDING

This study was supported by the National Science Fund, Ministry of Education and Science (MES), Bulgaria under project "Phytoplankton cysts – an intricacy between a "memory" or a "potential" for Black sea biodiversity and algal blooms" (Grant number DN01/8, 16.12.2016) and the National Science Program "Environmental Protection and Reduction of Risks of Adverse Events and Natural Disasters", approved by the Resolution of the Council of Ministers № 577/17.08.2018 and supported by the Ministry of Education and Science (MES) of Bulgaria (Agreement № D01-230/06.12.2018).

ACKNOWLEDGMENTS

We thank Peta Mudie (NRCan Geological Survey Canada Atlantic) for critically reading an earlier version of the ms, providing valuable comments and many useful suggestions that greatly improved this manuscript.

REFERENCES

Anderson, D. M., Fukuyo, Y., and Matsuoka, K. (2003). "Cyst Methodologies" in *Manual on Harmful Marine Microalgae*. Eds. G. M. Hallegraeff, D. M. Anderson and A. D. Cembella (Paris: UNESCO Publishing), 165–209.

Anderson, D. M., Kulis, D., and Binder, B. (1984). Sexuality and Cyst Formation in the Dinoflagellate *Gonyaulax Tamarensis*: Cyst Yield in Batch Cultures. *J. Phycol.* 20, 418–425. doi: 10.1111/j.0022-3646.1984.00418.x

Belmonte, G., and Rubino, F. (2019). "Resting Cysts From Coastal Marine Plankton" in *Oceanography and Marine Biology: An Annual Review*. Eds. S. J. Hawkins, A. L. Allcock, A. E. Bates, L. B. Firth, I. P. Smith, S. E. Swearer and P. A. Todd (Boca Raton:CRC Press), 1–88.

Bodeanu, N. (2002). Algal Blooms in Romanian Black Sea Waters in the Last Two Decades of the XXth Century. *Cercet. Mar.* 34, 7–22.

Bryantseva, Y., and Gorbunov, V. (2012). Spatial Distribution Phytoplankton Basic Parameters at the Northern Black Sea. *Optim. Prot. Ecosyst.* 7, 126–137.

Cadotte, M., and Tucker, C. (2017). Should Environmental Filtering be Abandoned? *Trends Ecol. Evol.* 32, 429–437. doi: 10.1016/j.tree.2017.03.004

Capet, A., Meysman, F. J. R., Akoumianaki, I., and Soetaert, K. (2016). Integrating Sediment Biogeochemistry Into 3D Oceanic Models: A Study of Benthic-Pelagic Coupling in the Black Sea. *Ocean. Modell.* 101, 83–100. doi: 10.1016/j.ocemod.2016.03.006

Casabianca, S., Capellacci, S., Ricci, F., Andreoni, F., Russo, T., Scardi, M., et al. (2020). Structure and Environmental Drivers of Phytoplanktonic Resting Stage Assemblages in the Central Mediterranean Sea. *Mar. Ecol. Prog. Ser.* 639, 73–89. doi: 10.3354/meps13244

Dale, B. (1976). Cyst Formation, Sedimentation, and Preservation, Factors Affecting Dinoflagellate Assemblages in Recent Sediments From Trondheimsfjord, Norway. *Rev. Palaeobot. Palynot.* 22, 39–60. doi: 10.1016/0034-6667(76)90010-5

Devillers, R., and de Vernal, A. (2000). Distribution of Dinoflagellate Cysts in Surface Sediments of the Northern North Atlantic in Relation to Nutrient

Content and Productivity in Surface Waters. *Mar. Geol.* 166, 103–124. doi: 10.1016/S0025-3227(00)00007-4

Dzhembekova, N., Rubino, F., Nagai, S., Zlateva, I., Slabakova, N., Ivanova, P., et al. (2020). Comparative Analysis of Morphological and Molecular Approaches Integrated Into the Study of the Dinoflagellate Biodiversity Within the Recently Deposited Black Sea Sediments – Benefits and Drawbacks. *Biodivers. Data J.* 8, e55172. doi: 10.3897/BDJ.8.e55172

Ellegaard, M. (2000). Variations in Dinoflagellate Cyst Morphology Under Conditions of Changing Salinity During the Last 2000 Years in the Limfjord, Denmark. *Rev. Palaeobot. Palynol.* 109, 65–81. doi: 10.1016/S0034-6667(99)00045-7

Ferraro, L., Rubino, F., Belmonte, M., Da Prato, S., Greco, M., and Frontalini, F. (2017). A Multidisciplinary Approach to Study Confined Marine Basins: The Holobenthic and Merobenthic Assemblages in the Mar Piccolo of Taranto (Ionian Sea, Mediterranean). *Mar. Biodivers.* 47, 887–911. doi: 10.1007/s12526-016-0523-0

Feyzioğlu, A. M., and Oğut, H. (2006). Red Tide Observations Along the Eastern Black Sea Coast of Turkey. *Turk. J. Bot.* 30, 375–379.

Garcés, E., Bravo, I., Vila, M., Figueroa, R. I., Masó, M., and Sampedro, N. (2004). Relationship Between Vegetative Cells and Cyst Production During *Alexandrium Minutum* Bloom in Arenys De Mar Harbour (NW Mediterranean). *J. Plankton. Res.* 26, 637–645. doi: 10.1093/plankt/fbh065

García-Moreiras, I., Oliveira, A., Santos, A. I., Oliveira, P. B., and Amorim, A. (2021). Environmental Factors Affecting Spatial Dinoflagellate Cyst Distribution in Surface Sediments Off Aveiro-Figueira Da Foz (Atlantic Iberian Margin). *Front. Mar. Sci.* 8. doi: 10.3389/fmars.2021.699483

Gogou, A., Sanchez-Vidal, A., Durrieu de Madron, X., Stavrakakis, S., Calafat, A. M., Stabholz, M., et al. (2014). Carbon Flux to the Deep in Three Open Sites of the Southern European Seas (SES). *J. Mar. Syst.* 129, 224–233. doi: 10.1016/j.jmarsys.2013.05.013

Gottschling, M., Knop, R., Plötner, J., Kirsch, M., Willems, H., and Keupp, H. (2005). A Molecular Phylogeny of *Scrippsiella* Sensu Lato (Calciodinellaceae, Dinophyta) With Interpretations on Morphology and Distribution. *Eur. J. Phycol.* 40, 207–220. doi: 10.1080/09670260500109046

Grégoire, M., Raick, C., and Soetaert, K. (2008). Numerical Modeling of the Deep Black Sea Ecosystem Functioning During the Late 80's (Eutrophication Phase). *Prog. Oceanogr.* 76, 286–333. doi: 10.1016/j.pocean.2008.01.002

Grégoire, M., and Soetaert, K. (2010). Carbon, Nitrogen, Oxygen and Sulfide Budgets in the Black Sea: A Biogeochemical Model of the Whole Water Column Coupling the Oxic and Anoxic Parts. *Ecol. Model.* 221, 2287–2301. doi: 10.1016/j.ecolmodel.2010.06.007

Grigorszky, I., Kiss, K. T., Beres, V., Bacsi, I., Márta, M., Máthé, C., et al. (2006). The Effects of Temperature, Nitrogen, and Phosphorus on the Encystment of *Peridinium Cinctum*, Stein (Dinophyta). *Hydrobiologia* 563, 527–535. doi: 10.1007/s10750-006-0037-z

Gu, H., Sun, J., Kooistra, W. H., and Zeng, R. (2008). Phylogenetic Position and Morphology of Thecae and Cysts of *Scrippsiella* (Dinophyceae) Species in the East China Sea 1. *J. Phycol.* 44, 478–494. doi: 10.1111/j.1529-8817.2008.00478.x

Hoyle, T. M., Sala-Pérez, M., and Sangiorgi, F. (2019). Where Should We Draw the Lines Between Dinocyst "Species"? Morphological Continua in Black Sea Dinocysts. *J. Micropalaeontol.* 38, 55–65. doi: 10.5194/jm-38-55-2019

Ishikawa, A., Wakabayashi, H., and Kim, Y. O. (2019). A Biological Tool for Indicating Hypoxia in Coastal Waters: Calcareous Walled-Type to Naked-Type Cysts of *Scrippsiella Trochoidea* (Dinophyceae). *Plankton. Benthos. Res.* 14, 161–169. doi: 10.3800/pbr.14.161

Kim, Y. O., and Han, M. S. (2000). Seasonal Relationships Between Cyst Germination and Vegetative Population of *Scrippsiella Trochoidea* (Dinophyceae). *Mar. Ecol. Prog. Ser.* 204, 111–118. doi: 10.3354/MEPS204111

Kokinos, J. P., and Anderson, D. M. (1995). Morphological Development of Resting Cysts in Cultures of the Marine Dinoflagellate *Lingulodinium Polyedrum (=L. Machaerophorum). Palynology* 19, 143–166. doi: 10.1080/01916122.1995.9989457

Kremp, A. (2001). Effects of Cyst Resuspension on Germination and Seeding of Two Bloom-Forming Dinoflagellates in the Baltic Sea. *Mar. Ecol. Prog. Ser.* 216, 57–66. doi: 10.3354/meps216057

Kremp, A., Rengefors, K., and Montresor, M. (2009). Species Specific Encystment Patterns in Three Baltic Cold-Water Dinoflagellates: The Role of Multiple Cues in Resting Cyst Formation. *Limnol. Oceanogr.* 54, 1125–1138. doi: 10.4319/lo.2009.54.4.1125

Kretschmann, J., Elbrächter, M., Zinssmeister, C., Soehner, S., Kirsch, M., Kusber, W. H., et al. (2015). Taxonomic Clarification of the Dinophyte *Peridinium Acuminatum* Ehrenb., ≡ *Scrippsiella Acuminata*, Comb. Nov. (Thoracosphaeraceae, Peridiniales). *Phytotaxa* 220, 239–256. doi: 10.11646/phytotaxa.220.3.3

Kretschmann, J., Zinssmeister, C., and Gottschling, M. (2014). Taxonomic Clarification of the Dinophyte *Rhabdosphaera Erinaceus* Kamptner, ≡ *Scrippsiella Erinaceus* Comb. Nov. (Thoracosphaeraceae, Peridiniales). *System. Biodivers.* 12, 393–404. doi: 10.1080/14772000.2014.934406

Lundgren, V., and Granéli, E. (2011). Influence of Altered Light Conditions and Grazers on *Scrippsiella Trochoidea* (Dinophyceae) Cyst Formation. *Aquat. Microb. Ecol.* 63, 231–243. doi: 10.3354/ame01497

Lundholm, N., Ribeiro, S., Andersen, T. J., Koch, T., Godhe, A., Ekelund, F., et al. (2011). Buried Alive – Germination of Up to a Century-Old Protist Resting Stages. *Phycologia* 50, 629–640. doi: 10.2216/11-16.1

Madec, G. (2012). *Nemo Ocean Engine* Vol. 27 (Paris: IPSL Note du Pole de Modélisation), 357.

Mertens, K. N. (2013). ""Morphological Variation in Dinoflagellate Cysts: Current Status and Future Challenges."," in *AASP-CAP-NAMS-CIMPDINO10 Joint Meeting* (San Francisco, USA: Canadian Association of Palynologists), 137–137.

Mertens, K. N., Bradley, L. R., Takano, Y., Mudie, P. J., Marret, F., Aksu, A. E., et al. (2012a). Quantitative Estimation of Holocene Surface Salinity Variation in the Black Sea Using Dinoflagellate Cyst Process Length. *Quater. Sci. Rev.* 39, 45–59. doi: 10.1016/j.quascirev.2012.01.026

Mertens, K. N., Bringué, M., Van Nieuwenhove, N., Takano, Y., Pospelova, V., Rochon, A., et al. (2012b). Process Length Variation of the Cyst of the Dinoflagellate *Protoceratium Reticulatum* in the North Pacific and Baltic-Skagerrak Region: Calibration as an Annual Density Proxy and First Evidence of Pseudo-Cryptic Speciation. *J. Quater. Sci.* 27, 734–744. doi: 10.1002/jqs.2564

Mertens, K. N., Dale, B., Ellegaard, M., Jansson, I., Godhe, A., Kremp, A., et al. (2011). Process Length Variation in Cysts of the Dinoflagellate *Protoceratium Reticulatum*, From Surface Sediments of the Baltic–Kattegat–Skagerrak Estuarine System: A Regional Salinity Proxy. *Boreas* 40, 242–255. doi: 10.1111/j.1502-3885.2010.00193.x

Mertens, K. N., Ribeiro, S., Bouimetarhan, I., Caner, H., Nebout, N. C., Dale, B., et al. (2009). Process Length Variation in Cysts of a Dinoflagellate, *Lingulodinium Machaerophorum*, in Surface Sediments: Investigating its Potential as Salinity Proxy. *Mar. Micropaleontol.* 70, 54–69. doi: 10.1016/j.marmicro.2008.10.004

Moncheva, S., Boicenco, L., Mikaelyan, A. S., Zotov, A., Dereziuk, N., Gvarishvili, C., et al. (2019). "Chapter 1.3.2. Phytoplankton," in *State of the Environment of the Black Se-2014/5)*. Ed. A. Krutov (Istanbul, Turkey: Publications of the Commission on the Protection of the Black Sea against Pollution (BSC) 2019), 225–284. Available at: http://www.blacksea-commission.org/Inf.%20and%20Resources/Publications/SOE2014/, ISBN: .

Moncheva, S., Petrova-Karadjova, V., and Palazov, A. (1995). "Harmful Algal Blooms Along the Bulgarian Black Sea Coast and Possible Patterns of Fish and Zoobenthic Mortalities" in *Harmful Marine Algal Blooms* . Ed. P. Lassus (Lavoisier, Paris: Harmful marine algal blooms), 193–298.

Montresor, M., Bastianini, M., Cucchiari, E., Giacobbe, M., Penna, A., Rubino, R., et al. (2010). "Capitolo 26. Stadi Di Resistenza Del Plankton" in *Metodologie Di Studio Del Plancton Marino*. Eds. G. Socal, I. Buttino, M. Cabrini, O. Mangoni, A. Penna and C. Totti (Rome: ISPRA - Istituto Superiore per la protezione e la ricerca ambientale), 258–273.

Montresor, M., Montesarchio, E., Marino, D., and Zingone, A. (1994). Calcareous Dinoflagellate Cysts in Marine Sediments of the Gulf of Naples (Mediterranean Sea). *Rev. Palaeobot. Palynol.* 84, 45–56. doi: 10.1016/0034-6667(94)90040-X

Montresor, M., Sgrosso, S., Procaccini, G., and Kooistra, W. H. (2003). Intraspecific Diversity in *Scrippsiella Trochoidea* (Dinophyceae): Evidence for Cryptic Species. *Phycologia* 42, 56–70. doi: 10.2216/i0031-8884-42-1-56.1

Morozova, T. V., Orlova, T. Y., Efimova, K. V., Lazaryuk, A. Y., and Burov, B. A. (2016). *Scrippsiella Trochoidea* Cysts in Recent Sediments From Amur Bay, Sea of Japan: Distribution and Phylogeny. *Bot. Mar.* 59, 159–172. doi: 10.1515/bot-2015-0057

Mousing, E. A., Ribeiro, S., Chisholm, C., Kuijpers, A., Moros, M., and Ellegaard, M. (2017). Size Differences of Arctic Marine Protists Between Two Climate Periods – Using the Paleoecological Record to Assess the Importance of Within-Species Trait Variation. *Ecol. Evol.* 7, 3–13. doi: 10.1002/ece3.2592.

Mudie, P. J., Marret, F., Mertens, K. N., Shumilovskikh, L., and Leroy, S. A. (2017). Atlas of Modern Dinoflagellate Cyst Distributions in the Black Sea Corridor: From Aegean to Aral Seas, Including Marmara, Black, Azov and Caspian Seas. *Mar. Micropaleontol.* 134, 1–152. doi: 10.1016/j.marmicro.2017.05.004

Mudie, P. J., Yanko-Hombach, V. V., and Mudryk, I. (2021). Palynomorphs in Surface Sediments of the North-Western Black Sea as Indicators of Environmental Conditions. *Quat. Int.* 590, 122–145. doi: 10.1016/j.quaint.2020.05.014

Nesterova, D., Moncheva, S., Mikaelyan, A., Vershinin, A., Akatov, V., Boicenco, L., et al. (2008). "Chapter 5.The State of Phytoplankton" in *State of the Environment of the Black Se-2006/7)*. Ed. T. Oguz (Istanbul, Turkey: Black Sea Commission Publications 2008-3), 133–167. Available at: http://www.blacksea-commission.org/_publ-SOE2009.asp.

Nikonova, S. (2010). The Dinoflagellate Cysts of Odessa and Tendra Regions of the Northwestern Part of the Black Sea. *Sci. Iss. Ternopil. Natl. Pedagogic. Univ. Series.: Biol.* 3, 190–192.

Nikonova, S. (2015). Spatial Distribution of Dinoflagellates Cysts in the Northern Part of the Black Sea. *Sci. Iss. Ternopil. Volody. Hnatiuk. Natl. Pedagogic. Univ. Series.: Biol.* 64, 3-4, 503–506.

Oksanen, J. (2015) *Vegan: An Introduction to Ordination*. Available at: http://cran.r-project.org/web/packages/vegan/vignettes/intro-vegan.pdf.

Olli, K., and Anderson, D. M. (2002). High Encystment Success of the Dinoflagellate *Scrippsiella* Cf. *Lachrymose* in Culture Experiment. *J. Phycol.* 38, 145–156. doi: 10.1046/j.1529-8817.2002.01113.x

Persson, A., Smith, B. C., Morton, S., Shuler, A., and Wikfors, G. H. (2013). Sexual Life Stages and Temperature Dependent Morphological Changes Allow Cryptic Occurrence of the Florida Red Tide Dinoflagellate *Karenia Brevis*. *Harm. Algae.* 30, 1–9. doi: 10.1016/j.hal.2013.08.004

Pocheville, A. (2015). "The Ecological Niche: History and Recent Controversies" in *Handbook of Evolutionary Thinking in the Sciences*. Eds. T. Heams, P. Huneman, G. Lecointre and M. Silberstein (Dordrecht: Springer Science +Business Media Dordrecht), 543–586. doi: 10.1007/978-94-017-9014-7_26

Pross, J. (2001). Paleo-Oxygenation in Tertiary Epeiric Seas: Evidence From Dinoflagellate Cysts. Palaeogeogr. *Palaeoclimatol. Palaeoecol.* 166, 369–381. doi: 10.1016/S0031-0182(00)00219-4

R Core Team (2019). *R: A Language and Environment for Statistical Computing* (Vienna, Austria: R Foundation for Statistical Computing). Available at: https://www.R-project.org/.

Ribeiro, S., and Amorim, A. (2008). Environmental Drivers of Temporal Succession in Recent Dinoflagellate Cyst Assemblages From a Coastal Site in the NorthEast Atlantic (Lisbon Bay, Portugal). *Mar. Micropaleontol.* 68, 156–178. doi: 10.1016/j.marmicro.2008.01.013

Ribeiro, S., Berge, T., Lundholm, N., and Ellegaard, M. (2013). Hundred Years of Environmental Change and Phytoplankton Ecophysiological Variability Archived in Coastal Sediments. *PloS One* 8, e61184. doi: 10.1371/journal.pone.0061184

Richter, D., Vink, A., Zonneveld, K. A., Kuhlmann, H., and Willems, H. (2007). Calcareous Dinoflagellate Cyst Distributions in Surface Sediments From Upwelling Areas Off NW Africa, and Their Relationships With Environmental Parameters of the Upper Water Column. *Mar. Micropaleontol.* 63, 201–228. doi: 10.1016/j.marmicro.2006.12.002

Rubino, F., and Belmonte, G. (2021). Habitat Shift for Plankton: The Living Side of Benthic-Pelagic Coupling in the Mar Piccolo of Taranto (Southern Italy, Ionian Sea). *Water* 13, 3619. doi: 10.3390/w13243619

Rubino, F., Cibic, T., Belmonte, M., and Rogelja, M. (2016). Microbenthic Community Structure and Trophic Status of Sediments in the Mar Piccolo of Taranto (Mediterranean, Ionian Sea). *Environ. Sci. Pollut. Res.* 23, 12624–12644. doi: 10.1007/s11356-015-5526-z

Rubino, F., Moncheva, S., Belmonte, M., Slabakova, N., and Kamburska, L. (2010). Resting Stages Produced by Plankton in the Black Sea — Biodiversity and Ecological Perspective. *Rap. Comm. Int. Pour. l'Exploration. Scientif. La. Mer. Mediter.* 39, 399.

Sala-Pérez, M., Lattuada, M., Flecker, R., Anesio, A., and Leroy, S. A. G. (2020). Dinoflagellate Cyst Assemblages as Indicators of Environmental Conditions and Shipping Activities in Coastal Areas of the Black and Caspian Seas. *Reg. Stud. Mar. Sci.* 39, 101472. doi: 10.1016/j.rsma.2020.101472

Sgrosso, S., Esposito, F., and Montresor, M. (2001). Temperature and Daylength Regulate Encystment in Calcareous Cyst-Forming Dinoflagellates. *Mar. Ecol. Prog. Ser.* 211, 77–87. doi: 10.3354/meps211077

Shin, H. H., Jung, S. W., Jang, M. C., and Kim, Y. O. (2013). Effect of pH on the Morphology and Viability of *Scrippsiella Trochoidea* Cysts in the Hypoxic Zone of a Eutrophied Area. *Harm. Algae.* 28, 37–45. doi: 10.1016/j.hal.2013.05.011

Shin, H. H., Li, Z., Kim, Y. O., Jung, S. W., and Han, M. S. (2014). Morphological Features and Viability of *Scrippsiella Trochoidea* Cysts Isolated From Fecal Pellets of the Polychaete. *Capitella Harm. Algae.* sp37, 47–52. doi: 10.1016/j.hal.2014.05.005

Shin, H. H., Li, Z., Lim, D., Lee, K. W., Seo, M. H., and Lim, W. A. (2018). Seasonal Production of Dinoflagellate Cysts in Relation to Environmental Characteristics in Jinhae-Masan Bay, Korea: One-Year Sediment Trap Observation. *Estuar. Coast. Shelf. Sci.* 215, 83–93. doi: 10.1016/j.ecss.2018.09.031

Terenko, L., and Terenko, G. (2009). Dynamics of *Scrippsiella Trochoidea* (Stein) Balech 1988 (Dinophyceae) Blooms in Odessa Bay of the Black Sea (Ukraine). *Oceanol. Hydrobiol. Stud.* 38, 107–112.

Turkoglu, M., and Koray, T. (2002). Phytoplankton Species' Succession and Nutrients in the Southern Black Sea (Bay of Sinop). *Turk. J. Bot.* 26, 235–252.

Wang, Z., Matsuoka, K., Qi, Y., Chen, J., and Lu, S. (2004). Dinoflagellate Cyst Records in Recent Sediments From Daya Bay, South China Sea. *Psychol. Res.* 52, 396–407. doi: 10.1111/j.1440-183.2004.00357.x

Wang, Z., Qi, Y., and Yang, Y. (2007). Cyst Formation: An Important Mechanism for the Termination of *Scrippsiella Trochoidea* (Dinophyceae) Bloom. *J. Plankton. Res.* 29, 209–218. doi: 10.1093/plankt/fbm008

Yasakova, O. N. (2010). "Annual Dynamics of Toxic Phytoplankton in Novorossiysk Bay" in *ICHA14 Conference Proceedings Crete. Crete, International Society for the Study of Harmful Algae and Intergovernmental Oceanographic Commission of UNESCO*, 132.

Žerdoner Čalasan, A., Kretschmann, J., Filipowicz, N. H., Irimia, R. E., Kirsch, M., and Gottschling, M. (2019). Towards Global Distribution Maps of Unicellular Organisms Such as Calcareous Dinophytes Based on DNA Sequence Information. *Mar. Biodivers.* 49 (2), 749–758. doi: 10.1007/s12526-018-0848-y

Zinssmeister, C., Soehner, S., Facher, E., Kirsch, M., Meier, K. S., and Gottschling, M. (2011). Catch Me If You can: The Taxonomic Identity of *Scrippsiella Trochoidea* (F. Stein) AR Loebl. (Thoracosphaeraceae, Dinophyceae). *System. Biodivers.* 9, 145–157. doi: 10.1080/14772000.2011.586071

Zonneveld, K. A., and Susek, E. (2007). Effects of Temperature, Light and Salinity on Cyst Production and Morphology of *Tuberculodinium Vancampoae* (the Resting Cyst of *Pyrophacus Steinii*). *Rev. Palaeobot. Palynol.* 145, 77–88. doi: 10.1016/j.revpalbo.2006.09.001

Conflict of Interest: The authors declare that the research was conducted in the absence of any commercial or financial relationships that could be construed as a potential conflict of interest.

Publisher's Note: All claims expressed in this article are solely those of the authors and do not necessarily represent those of their affiliated organizations, or those of the publisher, the editors and the reviewers. Any product that may be evaluated in this article, or claim that may be made by its manufacturer, is not guaranteed or endorsed by the publisher.

frontiers | Frontiers in Marine Science

ORIGINAL RESEARCH
published: 04 May 2022
doi: 10.3389/fmars.2022.887464

Contribution of Intermediate and High Trophic Level Species to Benthic-Pelagic Coupling: Insights From Modelling Analysis

Pasquale Ricci[1], Roberto Carlucci[1], Francesca Capezzuto[1], Angela Carluccio[1], Giulia Cipriano[1], Gianfranco D'Onghia[1], Porzia Maiorano[1], Letizia Sion[1], Angelo Tursi[1] and Simone Libralato[2]*

[1] Department of Biology, University of Bari, Bari, Italy, [2] Department of Oceanography, National Institute of Oceanography and Applied Geophysics - OGS, Trieste, Italy

Benthic-pelagic coupling (BPC) is a combination of downward (from pelagic to benthic) and upward (from benthic to pelagic) flows of organic matter and nutrients mediated by trophic interactions in the food web. Hydrological changes in marine ecosystems affect BPC patterns at several temporal and spatial scales. Thus, a food-web perspective help to to quantify and disentangle the role of ecosystem components and high trophic levels species in the BPC. This study investigated the spatio-temporal variability of energy and matter flows between the benthic and pelagic domains in two areas (Salento and Calabria) of the Northern Ionian Sea (Central Mediterranean Sea) during two different periods. The region is subject to large-scale oceanographic changes, e.g., the Adriatic-Ionian Bimodal Oscillating Systems (BiOS), that might result in relevant spatial and temporal BPC changes. Four food-web models describe the trophic structure, the role of ecosystem components and energy flows in the Salento and Calabrian areas, during two BiOS periods, the anticyclonic (1995-1997) and the cyclonic phases (2003-2005). The food webs are described by 58 functional groups obtained by aggregating species into ecological domains, depth gradients and biological traits. The role of species in the BPC has been quantified using a new Benthic-Pelagic Coupling Index calculated on the basis of food web flows estimated by models. The results highlight the pivotal role of deep faunal communities, in which demersal and benthopelagic species sustain upward energy flows towards the pelagic domain and shelf faunal communities. Temporal changes driven by BiOS affect the trophic state of the deep communities resulting in considerable variations in their amount of consumption flows. In addition, the presence of submarine canyons seems to better support the stability of the Calabrian food web in both investigated periods, whereas geomorphological traits of the Salento area seem to support greater pelagic production during the cyclonic period than the anticyclonic one. Benthopelagic species show an important role as couplers. In particular, *Aristaemorpha foliacea*, *Hoplostetus mediterraneus*, Macrourids and *Plesionika martia* are important couplers of bathyal communities in both areas.

Keywords: ecosystem functioning, consumption flows, food web modelling, Northern Ionian Sea, BiOS

OPEN ACCESS

Edited by:
Martina Orlando-Bonaca, National Institute of Biology (Slovenia), Slovenia

Reviewed by:
Francesco Cozzoli, National Research Council (CNR), Italy
Maria Flavia Gravina, University of Rome "Tor Vergata", Italy

***Correspondence:**
Roberto Carlucci
roberto.carlucci@uniba.it

Specialty section:
This article was submitted to Marine Ecosystem Ecology, a section of the journal Frontiers in Marine Science

Received: *01 March 2022*
Accepted: *31 March 2022*
Published: *04 May 2022*

Citation:
Ricci P, Carlucci R, Capezzuto F, Carluccio A, Cipriano G, D'Onghia G, Maiorano P, Sion L, Tursi A and Libralato S (2022) Contribution of Intermediate and High Trophic Level Species to Benthic-Pelagic Coupling: Insights From Modelling Analysis. Front. Mar. Sci. 9:887464. doi: 10.3389/fmars.2022.887464

INTRODUCTION

The functioning of marine ecosystems is mainly driven by the primary production in the pelagic domain, where the energy moves from phytoplanktonic organisms to large pelagic predators. The pelagic food chain is not isolated, but a part of the overall pelagic matter that sinks to the seabed, such as faecal material and the remains of dead individuals, while another part is consumed by organisms that take food from the water column, including benthic organisms (Kiljunen et al., 2020). Once pelagic matter reaches the bottom, it becomes available to benthic organisms and can be recycled back into the pelagic domain through physical mechanisms, such as resuspension processes, or through a "biological transport", this latter mediated by demersal and benthopelagic organisms (Griffiths et al., 2017). Therefore, benthic-pelagic coupling (BPC) results from the combination of downward (from pelagic to benthic) and upward (from benthic to pelagic) energy pathways. Trophic interactions connect the benthic domain to the pelagic domain in both direct (such as direct predation) and indirect ways (as trophic mediation by benthopelagic and demersal species). The term BPC is used to indicate all processes able to influence the pelagic and benthic domains without an effective distinction of the flow direction (Baustian et al., 2014).

BPC patterns in marine ecosystems concern the impacts of hydrological changes on the food web and the energy pathway mediated trophic interactions at several temporal and spatial scales (Coll et al., 2013; Cresson et al., 2020). In fact, temporal and spatial modifications to the water column structure influence the biological components with effects on the ecological community structure and trophic interactions patterns. Several studies have focused on seasonal variations in BPC mechanisms involving the pelagic or benthic domain (Pitt et al., 2008; Kiljunen et al., 2020), or on a mid-term scale exploring the relationships between nutrients, phytoplankton, and suspension feeders (Chauvaud et al., 2000). However, investigations aiming to explore the effects of these changes in the long-term (e.g., decadal scale) on the role of demersal and species in the ecosystems are very scarce, especially in the Mediterranean Sea (Agnetta et al., 2019). Yet, deepening the understanding of BPC could be very important from a fisheries management perspective, being able to provide information to address Ecosystem-Based Fishery Management (EBFM, Pikitch et al., 2004). One area highly influenced by mesoscale oceanographic features and where BPC patterns are supposed to importantly affect ecosystem dynamics in the Mediterranean basin is the Northern Ionian Sea (Menna et al., 2019).

The Northern Ionian Sea is the deepest basin in the Mediterranean Sea, where hydrography, geomorphology, temporal changes of environmental conditions and fishing impacts have shaped the structure of the demersal and benthopelagic assemblages (D'Onghia et al., 1998; Capezzuto et al., 2010; Civitarese et al., 2010; Maiorano et al., 2010; D'Onghia et al., 2012; Carlucci et al., 2018). In particular, the chemical and physical traits of the water column are affected by peculiar temporal events, which result in the reversal of the upper layer circulation in the Northern Ionian Gyre (NIG) over a decadal time scale, indicated with the term Bimodal Oscillating System (BiOS, Gačić et al., 2010). Little information exists, and few investigations have been carried out on the role of demersal and benthopelagic species in the BPC mechanisms and their relationships with hydrographic changes occurring during BiOS oscillations.

BPC patterns are mainly studied by means of stable isotope analysis (SIA) both in freshwater (Wang et al., 2020) and marine ecosystems (Duffill Telsnig et al., 2019; Kiljunen et al., 2020). Most BPC analyses focus on biogeochemical cycles, involving plankton and lower trophic level organisms (Mussap and Zavatarelli, 2017; Rodil et al., 2020). A few SIA studies in shallow seas (Kiljunen et al., 2020), and in deep habitats (Boyle et al., 2012; Trueman et al., 2014) have explored the role of intermediate and high trophic level species in BPC mechanisms. However, the use of the SIA technique is not properly suited for investigating the long-term dynamics of BPC mechanisms in complex ecosystem contexts with high numbers of species (Shiffman et al., 2012). In these contexts, the food web modelling approach could be a more efficient and less expensive way than the application of SIA protocols. In fact, food web modelling allows the quantification of energy flows and the BPC pattern in marine exploited ecosystems (Lassalle et al., 2011; Banaru et al., 2013; Agnetta et al., 2019; Carlucci et al., 2021) and it is possible to disentangle the role of species in the BPC.

The goal of this study is to identify the role of different species/groups from plankton to top predators in BPC mechanisms in the Salento and Calabria food webs previous investigated in (Ricci et al. 2019). Insights into BPC and its variability over space and time are analysed by looking at the properties and changes which occurred in the Northern Ionian Sea in two periods (the 1995-1997 anticyclonic phase, and the 2003-2005 cyclonic phase). Specifically, four mass-balance models have been realized to describe the trophic structure, species roles and energy flows in the Salento (north-eastern zone along the Apulian coast) and Calabrian (south-western zone). The role of species in coupling processes between the pelagic and benthic domains has been assessed using a new Benthic-Pelagic Coupling Index (BPCI) calculated thorough the consumption flows in the food webs estimated by a mass-balance model.

MATERIALS AND METHODS

Study Area

The Northern Ionian Sea lies between Cape Otranto and Cape Passero (Sicily) along a coastline of about 1000 km. This area is characterized by very deep zones (up to 4000 m in depth) with a complex geomorphology that results in different features between the western and eastern sector. In the western area, the Calabrian shelf platform is very narrow and shaped by active canyons transporting materials from the shelf break to the deep bottoms (Capezzuto et al., 2010). Conversely, in the eastern sector, corresponding to the Apulian region, the continental shelf is wider and abrasion terraces and bioclastic calcareous deposits

with several coral rocks are distributed from the shallowest to the deepest grounds (D'Onghia et al., 2016). These two sectors are divided by the Taranto Valley, a large NW-SE oriented submarine canyon with depths of over 2200 meters (Rossi and Gabbianelli, 1978). The geomorphological diversity of the basin is reflected in different habitat distribution along the coastline and in the deep grounds affecting the abundances of megafauna in benthic and pelagic domains (D'Onghia et al., 1998; Maiorano et al., 2010; D'Onghia et al., 2011; Capezzuto et al., 2018; Capezzuto et al., 2019; Carlucci et al., 2021b).

The entire basin is characterized by a complex system of water circulation both in the upper and deeper layers, showing reversals of the NIG direction affected by BiOS. The NIG inversion from anticyclonic to cyclonic, and vice versa, is influenced by the inlet of Atlantic Water (AW) eastward and salty Levantine waters westward (Civitarese et al., 2010; Liu et al., 2021). In addition, these oscillations are also influenced by the cold dense deep-water masses of the Adriatic Sea flowing in through the Otranto Channel (**Figures 1A, B**). BiOS induce strong impacts on biogeochemical cycles and transport of particulate organic matter (Klein et al., 1999; Boldrin et al., 2002), primary productivity (D'Ortenzio et al., 2003; Lavigne et al., 2018), the zooplankton community (Mazzocchi et al., 2003), the adaptation of allochthonous species and biodiversity (Civitarese et al., 2010), as well as the population dynamics of species at higher trophic levels (Capezzuto et al., 2010; Maiorano et al., 2010; D'Onghia et al., 2012; Carlucci et al., 2018; Ricci et al., 2021). Therefore, the complexity of these hydrological changes could be reflected in abundance changes of several species in the food web with modification to the trophic interactions and the BPC pattern. Furthermore, changes in the water column structure are not spatially homogeneous in the Ionian basin, but they show differences between the coastal areas in the western and eastern sectors (De Lazzari et al., 1999; Boldrin et al., 2002; Mazzocchi et al., 2003).

In this study, the food webs of two distinct areas, extending between 10–800 m in depth, were modelled (Ricci et al., 2019). Specifically, the Salento food-web model (SAL) represents the domain delimited by Capo Otranto and Capo San Vito (Taranto) and covers an area of approximately 6660 km^2. Whereas the domain of the Calabrian food-web model (CAL) extends from Punta Alice to Capo Spartivento for approximately 3469 km^2 (**Figure 1C**).

Modelling Approach

The mass-balance models were built by means the Ecopath with Ecosim approach (EwE, Christensen & Walters, 2004), which for over 30-years has been the most used modelling tool to study

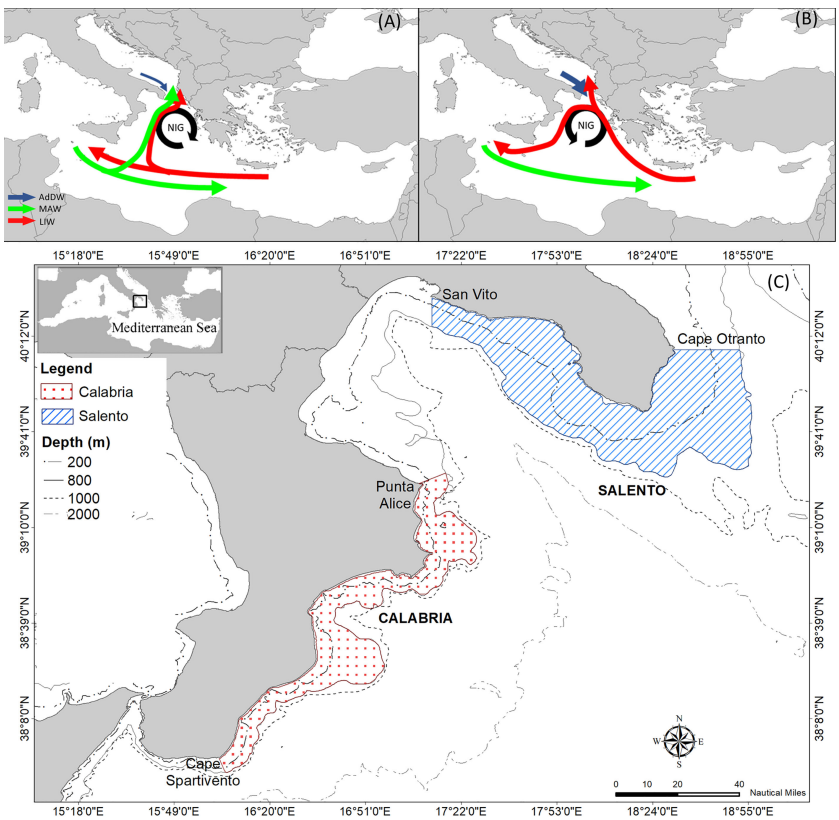

FIGURE 1 | Scheme of the Bimodal Oscillating System (BiOS) with the representation of hydrographic circulation during **(A)** anticyclonic and **(B)** cyclonic periods in the Ionian and Adriatic Seas (modified by Civitarese et al., 2010). Water current acronyms: MAW is Modified Atlantic Water, LIW is Levantine Intermediate Water, AdDW is Adriatic Dense Water and NIG is Northern Ionian Gyre. **(C)** Map of modelled study areas in the Northern Ionian Sea.

marine food web dynamics and fishing impacts (Coll and Libralato, 2012). The trophic structure is represented by Functional Groups (FGs) and trophic flows. The former, is represented by a single species, a life stage of a species, or a group of species with similar trophic, ecological, and physiological features. Trophic flows between FGs are formally described by a set of two linear equations for each FG (Christensen et al., 2008). The first equation represents the fate of production:

$$\left(\frac{P}{B}\right)_i B_i = Y_i + \sum_j B_j \left(\frac{Q}{B}\right)_j DC_{ji} + E_i + BA_i + \left(\frac{P}{B}\right)_i B_i(1 - EE_i) \quad \text{(eq.1)}$$

where (P/B) is the production to biomass ratio for a certain functional group (i), Bi is the biomass of a group (i), Yi the fishery catch of group (i), (Q/B)j is the consumption to biomass ratio for each predator (j), DCji is the proportion of the group (i) in the diet of predator (j), Ei is the net migration rate of a group from the modelled area, BAi is the biomass accumulation rate for the group (i), EEi is the ecotrophic efficiency, and the term (1 −EEi) represents other mortality different from predation and fishing. The second equation represents the consumption of a group:

$$\text{consumption} = \text{production} + \text{respiration} + \text{unassimilated food} \quad \text{(eq.2)}$$

Equation (1) and (2) for all functional groups make a system of equations that is solved by providing EwE routine information on three out of the four basic parameters Bi, (P/Bi), (Q/Bi) and EEi. Further details on the EwE modeling approach can be found in review literature (Christensen and Walters, 2004; Christensen et al., 2008; Heymans et al., 2016).

Model Structure and Data

The food web model in both investigated areas was described by means of the same functional groups obtained from the model realized by (Ricci et al. 2019). In particular, the nomenclature adopted for demersal and benthopelagic FGs have three components: the former indicates the bathymetric domain, the second the faunal category of the main taxa, and the last describes the feeding behaviour of the group (**Table 1**). Therefore, FGs were mainly classified according to their belonging to ecological domains and their depth layer distribution made explicit in **Table 1**. The former classification was based on 5 general domains: Pelagic (PEL, including the planktonic groups and particulate organic matter), Benthopelagic (BP), Demersal (DEM), Benthic (BENT, including the bottom detritus and discards). This classification was carried out using the information on the single species obtained from Fishbase (Froese and Pauly, 2021; www.fishbase.org, version 08/2021) and Sealifebase (Palomares and Pauly, 2021; www.sealifebase.org, version 12/2021), as well as information from video surveys (e.g., Lorance and Trenkel, 2006; D'Onghia et al., 2011; D'Onghia et al., 2015). The depth layer classification aggregates FGs into 5 categories: groups of shelf grounds (SH) and neritic zone (NER) distributed at depths < 200 m; groups of open waters (or off-shore, OFS); groups on sloping grounds (SL) distributed at depths > 200 m; ubiquitous groups (U) distributed throughout the entire depth gradient and in neritic and off-shore zones (e.g., macrobenthic invertebrates, suprabenthic crustaceans, planktonic groups). The classification based on the bathymetric gradient was driven by the Centre of Gravity (COG) calculated for the species of benthopelagic, demersal and benthic domains (see Ricci et al., 2019). Finally, the classifications for domain and depth layer were combined in a unique classification named Domain-depth (**Table 1**).

Input data (Biomass, P/B and Q/B rates, Landings and Discards) of the balancing models are reported in **Tables S1**, **S2** for the Salento and Calabrian food webs, respectively. Biomasses (kg/km^2) for a total of 276 benthopelagic and demersal species that were obtained from the experimental sampling of the "MEDiterranean International Trawl Survey" (MEDITS) research programme for all investigated periods (Spedicato et al., 2019). The biomass input of each FG was calculated as an average value for the 3-year period investigated in each model (Heymans et al., 2016). Biomass data of cetacean groups and Loggerhead turtle (1, 2, 3) were estimated by abundance data (N/km^2) obtained from the OBIS SeaMap (Halpin et al., 2009) and the local mean individual weight for the Ionian Sea (Ricci et al., 2020; Carlucci et al., 2021).

Biomasses of zooplankton and benthic groups were estimated fixing EE at a value of 0.90 for the polychaetes, macrobenthic invertebrate groups and gelatinous plankton, at 0.95 for the suprabenthic crustacean groups, and at a value of 0.99 for the macro and mesozooplankton (Heymans et al., 2016) FGs. Biomasses of phytoplankton and bacterioplankton groups for each modelled area were estimated using biogeochemical data of models available from 1998 (Lazzari et al., 2012). The lack of available data for the period 1995-1997 led to the choice of using an average value for the period 1998-1999, as adopted in the previous models realized for the area (Ricci et al., 2019).

P/B and Q/B rates were obtained from the previous model in (Ricci et al. 2019) collecting data from the literature or empirical relationships based on the total mortality (Z) as an equivalent of P/B rate (Allen, 1971).

Diet information was acquired from previous models realized for the same study areas (Ricci et al., 2019; Ricci et al., 2021), with some update inherent to *Engraulis encrasicolus* and *Sardina pilchardus* diet information in the Small pelagic group obtained from the literature (Zorica et al., 2017; Hure and Mustać, 2020). Further updates concern local diets of *Helicolenus dactylopterus* and *Pagellus bogaraveo* (Capezzuto et al., 2020; Capezzuto et al., 2021).

Official annual landings by species for GSA 19 were provided by the Fisheries and Aquaculture Economic Research for the Italian Ministry of Agricultural Food and Forestry Policies (MIPAAF) with data separated for the Calabria and Apulia regions by otter trawls (OTB), long lines (LL), passive nets (GND), purse seines (PS) and other gears (MIX, mainly small-

TABLE 1 | Functional groups (FG) used in both Ecopath models classified by domains (Pelagic, PEL; Benthopelagic, BP, Demersal, DEM; Benthic, BENT) and depth layers (Neritic, NER; Off-shore, OFS; Shelf, SH; Slope, SL, Shelf-Break, SHB only for FGs; Ubiquitarian, U).

FG	Domain	Depth	COG (var)	Main taxa	FG	Domain	Depth	COG (var)	Main taxa
1. Odontocetes	PEL	OFS	n.a.	*Stenella coeruleoalba, Tursiops truncatus, Grampus griseus, Physeter macrocephalus*	22. SHB_Fishes_planktivorous	DEM	SH	90 (60)	*Macroramphosus scolopax, Capros aper, Glossandon leioglossus*
2. Fin whale	PEL	OFS	n.a.	*Balaenoptera physalus*	23. Small pelagics	PEL	SH	n.a	Clupeidae
3. Loggerhead turtle	PEL	NER	n.a.	*Caretta caretta*	24. Medium pelagics	PEL	SH	n.a	Trachurus spp., Scomber spp.
4. Seabirds	PEL	NER	n.a.	*Larus* spp., *Puffinus puffinus*	25. Macrourids_Med. slimehead	DEM	SL	516 (119)	*Coelothynchus coelothynchus, Hymenocephalus italicus, Hoplostethus mediterraneus*
5. Large pelagics	PEL	OFS	n.a.	*Xiphias gladius, Thunnus* spp.	26. Myctophids	BP	SL	431 (123)	Micthophidae
6. SL_SharksRays_bent	DEM	SL	523 (95)	*Dipturus oxyrinchus, Centrophorus granulosus*	27. Red mullet	DEM	SH	38 (49)	*M. barbatus*
7. SH-SHB_SharksRays_BP	BP	SH	171 (28)	*Scyliorhinus canicula, Raja miraletus*	28. Hake	DEM	SH	131 (176)	*M. merluccius*
8. SH_SharksRays_bent	DEM	SH	29 (47)	*R. asterias, Mustelus mustelus, Dasyatis pastinaca*	29. Anglers	DEM	SL	232 (196)	*Lophius* spp.
9. SL_Sharks_BP	BP	SL	631 (79)	*Etmopterus spinax, Dalathias licha*	30. Roughtip grenadier	DEM	SL	549 (123)	*Nezumia sclerorhynchus*
10. B catshark	DEM	SL	546 (135)	*Galeus melastomus*	31. SL_Squids_BP	BP	SL	545 (85)	*Todarodes sagittatus, Histioteuthis* spp.
11. SL_DemFishes_opportunistic	DEM	SL	597 (154)	*Conger conger, Molva dipterygia*	32. SHB_Squids_BP	BP	SH	121 (85)	*Illex coindettii, Loligo* spp., *Todaropsis eblanae*
12. SL_DemFishes_gen	DEM	SL	204 (179)	*Pagellus bogaraveo, Trigla lyra*	33. SH_Cephalopds	DEM	SH	77 (64)	*Octopus vulgaris, Sepia* spp., *Eledone* spp.
13. SH-SHB_DemFishes_gen	DEM	SH	66 (47)	*Zeus faber, Pagellus erythrinus, Aspitrigla cuculus*	34. SL_Cephalopods	DEM	SL	430 (133)	*Pteroctopus tetracirrhus, Heteroteuthis dispar*
14. SH-SHB_DemFishes_pisc	DEM	SH	89 (66)	*Scorpaena* spp., *Micromesistius potassou*	35. SHB_BobSquids_BP	BP	SL	232 (98)	*Sepietta oweniana, Rossia macrosoma, Sepiola* spp.
15. SL_BathypelFishes_pisc	BP	SL	520 (104)	*Stomias boa, Chauliodus sloanii, Lampanyctus crocodilus*	36. Shrimps_BP	BP	SL	447 (92)	*Pasiphaea sivado, P. multidentata*, *Acanthephyra* spp., *Plesionika edwardsii, Sergia robusta*
16. SL_DemFishes_decapods	DEM	SL	388 (121	*Phycis blennoides, Helicolenus dactyloterus*, *Lepidorhombus boscii*	37. SL_Decapods_bent	BENT	SL	433 (104)	*N. norvegicus, Munida* spp., *P. heterocarpus*
17. SL_Fishes_BP crust	BP	SL	488 (137)	*Epigonus* spp., *Nemichthys scolopaceus, Argyropelecus hemigymnus*	38. SL_Crabs	BENT	SL	295 (87)	*Macropipus tuberculatus*, *Goneplax rhomboides*
18. SHB_Fishes_BP_crust	BP	SL	229 (100)	*Argentina sphyrena, Chlorophthalmus agassizii*	39. SHB_Crabs	BENT	SH	111 (83)	*Maia* spp., *Macropodia* spp., *P. narval*
19. SH_DemFishes_bent crust	DEM	SH	77 (40)	*Spicara* spp., *Boops boops, Chelidonichthys lucerna*	40. SH_Crabs	BENT	SH	32 (40)	*Liocarcinus depurator, Medorippe lanata, Inachus* spp.
20. SH_DemFishes_bent inv	DEM	SH	65 (40)	*Pagellus acarne, Mullus surmuletus, Bothus podas*	41. Deep-water Rose shrimp	DEM	SL	252 (96)	*Parapenaeus longirostris*
21. SL_Fishes_planktivorous	DEM	SL	556 (107)	*Mora moro*	42. Red Giant shrimp	DEM	SL	436 (152)	*Aristaemorpha foliacea*
43. Blue Red shrimp	DEM	SL	545 (126)	*Aristeus antennatus*					
44. Golden shrimp	DEM	SL	433 (128)	*P. martia*					
45. Polychaetes	BENT	U	n.a.	Polychaeta, Nematoda					
46. Macrobenthic invertebrates	BENT	U	n.a.	Bivalves, Gastropods, Cnidarians, Echinoderms, Porifera, Ascidians					

(Continued)

TABLE 1 | Continued

FG	Domain	Depth	COG (var)	Main taxa
47. Gelatinous plankton	PEL	U	n.a.	Scyphozoa, Siphonophora, Thaliacea
48. Suprabenthic crustaceans	BENT	U	n.a.	Cumacea, Ostracoda, Amphipoda, Isopoda,
49. Macrozooplankton	PEL	U	n.a.	Chetognata, Mysidiacea, Euphasiacea
50. Mesozooplankton	PEL	U	n.a.	Copepoda, Cladocera
51. Microzooplankton	PEL	U	n.a.	Foraminifera, Larvae
52. Bacterioplankton	PEL	U	n.a.	Bacteria
53. Seagrasses-algae	BENT	SH	n.a.	*Posidonia oceanica*, benthic algae
54. Large phytoplankton	PEL	U	n.a.	Diatoms, Dinoflagellates
55. Small phytoplankton	PEL	U	n.a.	Pico-phytoplankton
56. POM	PEL	Plank U	n.a.	Particulate organic matter
57. Discards	BENT	BENT U	n.a.	Discards
58. Detritus	BENT	BENT U	n.a.	Bottom detritus

COG and variance (in meters, m) are reported (n.a. indicates not available value). Feeding behaviour codes in FG names: generalist, gen; piscivorous, pisc; crustaceans, crust; invertebrates, inv.

scale fisheries) in the period 1995–2005. Landings and discards by FG, species, and fishing gears were estimated for the periods 1995-1997 and 2003-2005 as reported in Ricci et al. (2019).

Four mass-balance models were developed using an average of 3 years of data describing the CAL and SAL food webs in two distinct periods, which represent the anticyclonic and cyclonic phases of the BiOS. In particular, the anticyclonic phase referred to the years 1995–1997, whereas the cyclonic phase was represented in the years 2003–2005. Therefore, the final models adopted in the analysis were: 1) Salento 1995-1997 (named model SAL_1995 or anticyclonic); 2) Salento 2003-2005 (named model SAL_2005 or cyclonic); 3) Calabrian 1995-1997 (named model CAL_1995 or anticyclonic); 4) Calabrian 2003-2005 (named model CAL_2005 or cyclonic).

Balancing Steps

Both models belonging to the period 1995-1997 were balanced according to the standard pre-balancing analysis (PREBAL, Link, 2010) and a top-down strategy described in (Ricci et al. 2019). These models were manually balanced by means of modifications to the less reliable values identified in the DC matrix and P/B and Q/B rates through the Pedigree Index (Pauly et al., 2000). In addition, it was checked that Net food conversion efficiencies (P/Q [0.05–0.3]), respiration/assimilation (R/A [<1]), and production/respiration (P/R [<1]) ratios were within expected limits (Christensen et al., 2008). Cannibalism in the diet was decreased for hake, sharks, the demersal fish groups, squids, shrimps, and the decapod crustaceans' groups (Heymans et al., 2016).

Differently, the Salento and Calabrian models realized for the period 2003-2005 were balanced by adopting PREBAL analysis and a successive balancing step based on the Monte-Carlo routine (Ecoranger, developed in EwE, version 5, Christensen, 2008), in order to change the parameters in a progressive way following an automated procedure to improve model balancing and avoiding further manipulation of the input data. Specifically, the procedure was adopted exclusively for the diet matrix (10% changes for all elements in the diet matrix) given the higher uncertainty in the data, while the most important parameters (biomasses and catches) were kept fixed for each group during the automatic routine (Ricci et al., 2021). Therefore, the Ecoranger routine provided two balanced models (SAL_2005 and CAL_2005) by exploring the range of trophic uncertainty through a more objective procedure and adjusting the diet matrix to the estimated biomass at sea and the observed fishery catch in each period.

Analysis of BPC Patterns and Ecosytem Traits

The whole ecosystem traits selected from the Ecopath output were Total System Throughput (TST), Consumption (Q), Exports (E), Fluxes to Detritus (FD), Respiration (R), Production (P) and Net Primary Production of the system (NPP) (for details on these indicators see Heymans et al., 2014). All ecosystem traits are expressed as t km^{-2} y^{-1}. These

synthetic properties of the ecosystem permit a quick comparison and the detection of relevant overall differences.

BPC patterns were explored by Domain and Domain-depth classifications (**Table 1**). In particular, the latter classification was performed by merging the following categories between them: groups of neritic and shelf zones (Loggerhead Turtle, Seabirds, Small pelagics and Medium pelagics) were joined and named pelagic-shelf (PEL-SH); Odontocetes, Large pelagics and Fin whale represent the off-shore pelagic domain (PEL-OFS); the demersal and benthopelagic groups were in two different domains in the shelf zone (DEM_BP SH) and in the slope zone (DEM_BP SL), respectively. Seagrasses-algae, SH_Crabs and SHB_Crabs were combined in the shelf-benthic domain (BENT-SH), while SL_Crabs and SL_Decapods_bent were aggregated in the slope-benthic domain (BENT-SL). Polychaetes, Macrobenthic invertebrates and Suprabenthic crustaceans are ubiquitous groups representing a third benthic domain (BENT U). Finally, the zooplankton groups (representing the planktonic domain (PLANK), which were exclusively considered, together with the BENT U domain, as prey in the consumption flows system.

Analysis of Functional Groups' Role

Comparison between the four models (two areas in two investigated periods) was focusing on biomass changes, keystone species ranks and trophic impacts of FGs, as well as consumption flows in the investigated models.

Biomasses (t km^{-2} y^{-1}) of FGs with TL>3.0 (1-44 in **Table 1**) were aggregated and compared by faunistic categories, shelf and slope zones and domains. Moreover, Fishes/Invertebrates and Predator/Prey (Predators TL> 4.0) biomass ratios were calculated.

The importance of FGs as a keystone group/species in the investigated food webs was estimated by means of the Keystoness index (KSi) and Mixed Trophic Impact analysis (MTI, Ulanowicz and Puccia, 1990). MTI quantifies the relative impact of biomass change within a component (impacting group) on each of the other components (impacted groups) in the food web, including the fishing gears. Thus, positive/negative MTI values indicate an increase/decrease in biomass of group j due to a slight increase in biomass of the impacting group i. Therefore, negative impacts can be associated to prevailing top-down effects and positive ones to bottom-up effects (Libralato et al., 2006). The relative overall effect (OE) of an impacting group i represents all the direct or indirect MTI values of group i on all the other groups in the food web:

$$OE = \sqrt{\sum_{j\neq 1}^{n} m_{ij}^2} \quad \text{(eq.3)}$$

where the impact on the group itself (mij with $i = j$) is not considered, and OE is calculated as a relative value with respect to the maximum (Libralato et al., 2006). Therefore, the keystone groups/species are ranked using the following equation:

$$KS_i = \log[OE_i(1 - p_i)] \quad \text{(eq.4)}$$

where pi is the relative biomass of the group, excluding detritus biomass. Changes in the KSi rank composition between two investigated time periods were analysed in both the SAL and CAL food web models. Specifically, the most important KS groups in each food web model were identified by calculating the 3rd quartile on each KS rank. In addition, changes in rel OE of each group between the first and second periods were analysed in both the SAL and CAL models.

The analysis of consumption flows was carried out to classify the role of FGs as couplers of energy flows between pelagic and benthic domains (downward flows, dQf), or vice versa, between benthic and pelagic domains (upward flows, -uQf). A pelagic FG plays the role of direct coupler, for example, if it is effected by a trophic flow (as predator or prey) involving any benthic FG. Groups belonging to the pelagic or benthic domains having direct consumption on benthic or pelagic groups, respectively, contribute directly to the BPC. On the other hand, FGs can be mediating couplers (or two-step couplers) represented by the species of demersal and benthopelagic domains. Species/groups belonging to these domains can drive downward consumption flows by consuming pelagic prey and becoming prey for benthic consumers, or in the upward direction, exploiting benthic prey and becoming prey for pelagic predators. In the latter, some groups could perform partial energy transfers, consuming pelagic or benthic preys with the consequence of transferring part of the energy within the benthopelagic or demersal domains. Successively, these partial couplers could be consumed by other benthopelagic or demersal couplers following other energy transfer pathways towards the pelagic or benthic domains. The downward (dQf) and upward (uQf) consumption flows are identified and quantified through the detailed food webs. Thus, the dQf, indicated with a positive sign, and uQf, expressed with a negative sign can be used to quantify the importance of each FG in BPC mechanisms. To summarise the contribution of each group to the BPC, the Benthic-Pelagic Coupling Index (BPCI, t km^{-2} y^{-1}) was calculated as:

$$BPCI = |dQf - uQf| \quad \text{(eq.5)}$$

Therefore, dQf and uQf were calculated for each FG considered as both predators and prey (excluding non-living detritus groups 56-58 from the calculation, **Table 1**). To identify more important couplers, FGs with a BPCI value higher than 0.100 t km^{-2} y^{-1} are classified as direct (D), mediating (M) or partial (P) couplers, and successively, they were analysed using dQf and uQf (expressed as percentage values). High dQf values indicate the prevalence of downward flows (pelagic-benthic coupling), while high values of uQf indicate the predominance of upward flows (benthic-pelagic coupling). Lastly, the COG and variance of each demersal and benthopelagic couplers were analysed in function of BPCI.

RESULTS

Ecosystem Traits and Consumption Flow Patterns Between Domains

Ecosystem traits of the SAL food web models showed relevant temporal differences (**Figure 2** and **Table S3**). All indicators of

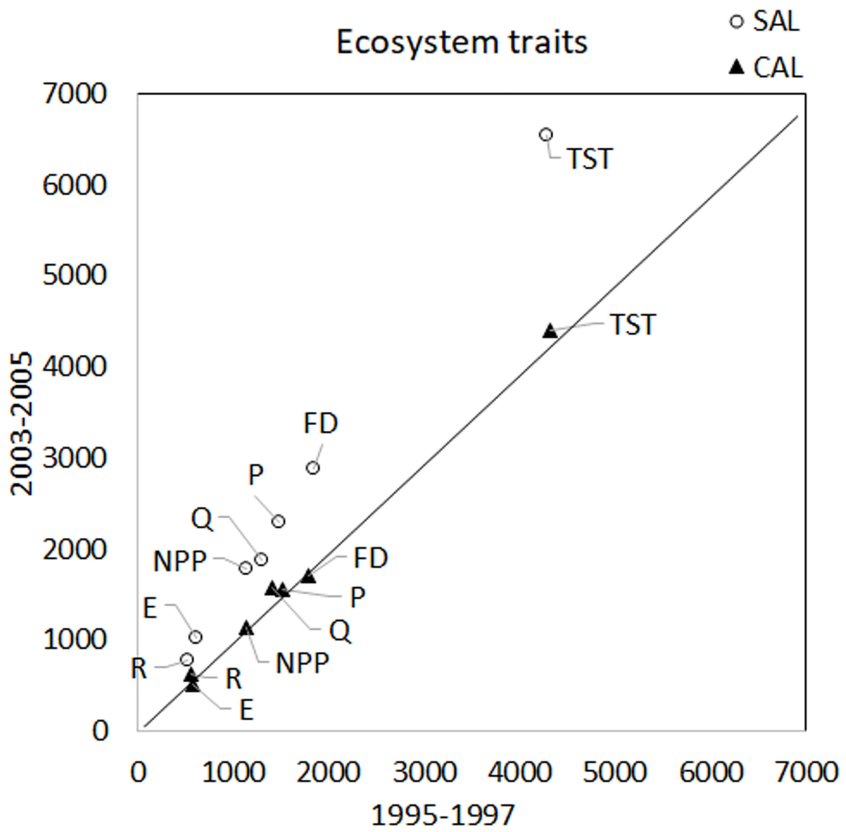

FIGURE 2 | Total System Throughput (TST), Fluxes to Detritus (FD), Sum of Production (P), Sum of Consumption (Q), Sum of Exports (E), Sum of Respiration (R) and Net Primary Production (NPP) estimated for SAL (white circle) and CAL (black triangle) models in 1995-1997 (x-axis) and in 2003-2005 (y-axis). All indicators are expressed as t km^{-2} y^{-1}.

flow showed values higher in the SAL 2005 models than the SAL 1995, with an increase of 22 and 21% for NPP and TST, respectively. In contrast, no relevant changes were observed in the CAL model between the two investigated periods, with the estimated NPP in 1995 (1137 t km^{-2} y^{-1}) being slightly lower than that in 2005 (1132 t km^{-2} y^{-1}). In addition, the CAL TST value in 2005 (4408 t km^{-2} y^{-1}) was lower than the SAL value in 2005 (6547 t km^{-2} y^{-1}).

The patterns of all consumption flows (including POM and Detritus in the pelagic and benthic domains, respectively) characterizing both food webs are shown in **Figure 3**. The highest consumptions were estimated in the pelagic domains of each model, with a higher increase observed in the SAL food web (3225 t km^{-2} y^{-1}) than the CAL one (2415 t km^{-2} y^{-1}) in the 2005 period. Similarly, consumption flows from the pelagic domain to the benthic, benthopelagic and demersal domains increased in 2005 in the SAL food web. In particular, the highest increase was estimated for the Pelagic-Benthic flow, which was equal to 729 t km^{-2} y^{-1} in 1995 and 1210 t km^{-2} y^{-1} in 2005. However, a slight increase in the consumption of pelagic groups by demersal groups was detected in the CAL model from 1995 (8 t km^{-2} y^{-1}) to 2005 (11 t km^{-2} y^{-1}), while the flows from the pelagic domain towards the benthic domain showed a decrease from 663 t km^{-2} y^{-1} in 1995 to 616 t km^{-2} y^{-1} in 2005. Considering exchanges between the BP and DEM domains, an increase in consumption of BP prey by DEM consumers was observed in the 2005 period for both SAL (4 t km^{-2} y^{-1}) and CAL (3 t km^{-2} y^{-1}). In the SAL model, consumptions in the BP domain increased in 2005, as well as consumption flows between BP and the Benthic domain, while in the CAL model this condition was observed only for the flows between the DEM and Benthic domains and an increase in the consumptions in the DEM domains was estimated.

The analysis of the flows according to the domains and depth layers distribution of FGs highlighted the pattern of energy and matter exchanges between shelf and deep zones (**Figure 4** and **Table S4**). In the SAL model, planktonic resources were mostly consumed by demersal and benthopelagic groups of the slope (12.7 t km^{-2} y^{-1}) and, secondarily, by pelagic neritic consumers (10.2 t km^{-2} y^{-1}) in 1995. In addition, the ubiquitous benthic groups were mainly exploited by bathyal demersal-benthopelagic groups (8.3 t km^{-2} y^{-1}), the shallowest benthic decapods (4.7 t km^{-2} y^{-1}) and the shelf demersal-benthopelagic groups (3.3 t km^{-2} y^{-1}). This pattern changed in the 2005 period, with the highest increases estimated for the bathyal demersal-benthopelagic groups by consuming planktonic prey (17.6 t km^{-2} y^{-1}) and the ubiquitous benthic groups (14.1 t km^{-2} y^{-1}). A very relevant increase in consumptions was estimated for the ubiquitous benthic groups exploited by

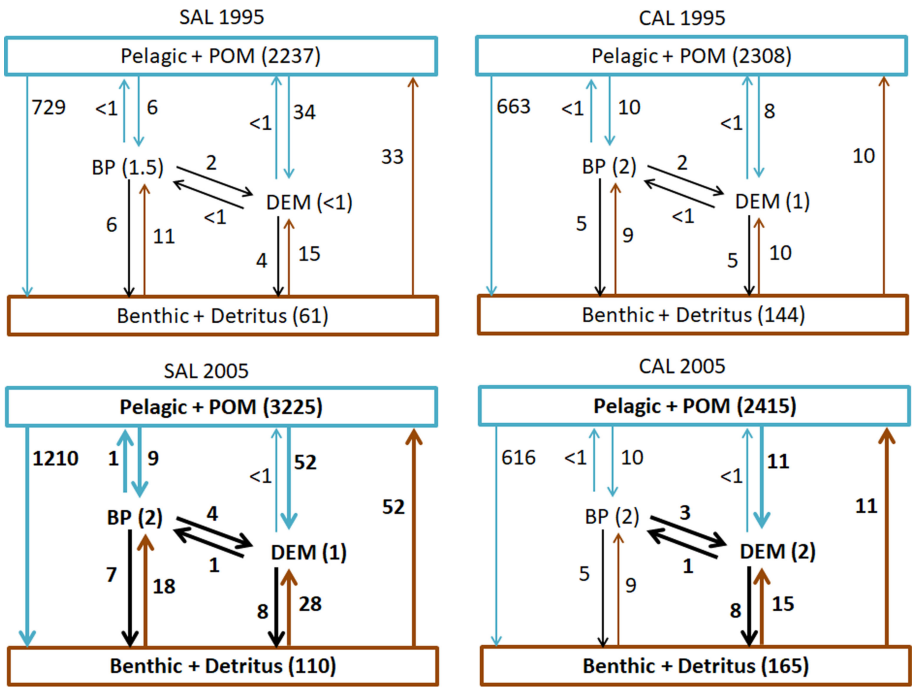

FIGURE 3 | Consumption flows (t km^{-2} y^{-1}) of groups aggregated into Pelagic+POM, Benthopelagic (BP), Demersal (DEM) and Benthic+Detritus domains analysed in the Salento (SAL) and Calabria (CAL) models for both investigated periods. Bold numbers and arrows indicate increased flows in 2005 and <1 indicate consumption flows lower than 1 t km^{-2} y^{-1}.

shallowest benthic decapods (11.4 t km^{-2} y^{-1}). In addition, shelf demersal-benthopelagic groups showed an increase in all consumptions, with the most relevant values estimated for planktonic prey (6.8 t km^{-2} y^{-1}) and ubiquitous benthic groups (4.7 t km^{-2} y^{-1}). Moreover, an increase in consumption values of up to 1.5 t km^{-2} y^{-1} was detected for bathyal demersal-benthopelagic groups towards shelf demersal-benthopelagic groups.

In the CAL model during 1995, the consumption flows from ubiquitous benthic organisms towards the shallowest benthic decapods (11.2 t km^{-2} y^{-1}), and from planktonic prey to bathyal demersal-benthopelagic groups (11.6 t km^{-2} y^{-1}) and shelf pelagic consumers (10.5 t km^{-2} y^{-1}) showed the highest values. In addition, the consumption of ubiquitous benthic organisms by bathyal demersal-benthopelagic groups was equal to 9.5 t km^{-2} y^{-1}. In 2005, similar increases in the consumption values on planktonic and benthic groups were estimated. The most relevant rises were estimated for the consumption of ubiquitous benthic organisms by both demersal-benthopelagic groups on shelf and slope bottoms (6.3 and 11.9 t km^{-2} y^{-1}, respectively). Similarly, the consumption of planktonic resources increased for both demersal-benthopelagic groups. These increases were lower than those estimated in the SAL model for the same period.

Finally, an increase in the consumption flows was observed from the shallowest benthic decapods and shelf pelagic organisms towards the shelf demersal-benthopelagic groups in both models during the cyclonic period.

Functional Groups Roles in the Investigated Food Web Models

Outputs estimated by Ecopath models for each FG are reported in **Table S1**. A general biomass increase was observed from 1995 to 2005 in both food webs, with the highest percentages observed in the SAL food web (**Figures 5A, B** and **Table S5**). Considering the faunistic categories, the highest biomass was estimated for bony fishes in both modelled areas. The largest percentage increases were found for decapod crustaceans, cephalopods, and elasmobranchs in the Salento model, whereas in Calabria they were for cephalopods, elasmobranchs, and bony fishes. Changes in shelf and slope grounds showed higher percentage increases in the SAL food web than in the CAL one. In addition, the estimated biomass on the shelf of the CAL area was slightly higher than that estimated on the slope. An inverse condition between biomass in the shelf and slope zones was observed in the SAL food web. The highest percentage increases were observed for groups of the demersal domain in both investigated food webs, with values higher in the SAL model than in the CAL one. In addition, a very slight decrease in the biomass of the pelagic groups was observed in the SAL model, whereas in the CAL model, decreases were observed for the groups in the benthopelagic and benthic domains. The Fish/Inv ratios showed a different condition between the investigated areas, with a decrease of 13% in the SAL food web, and an increase of 4% in the CAL food web (**Figure 5C**). In addition, the

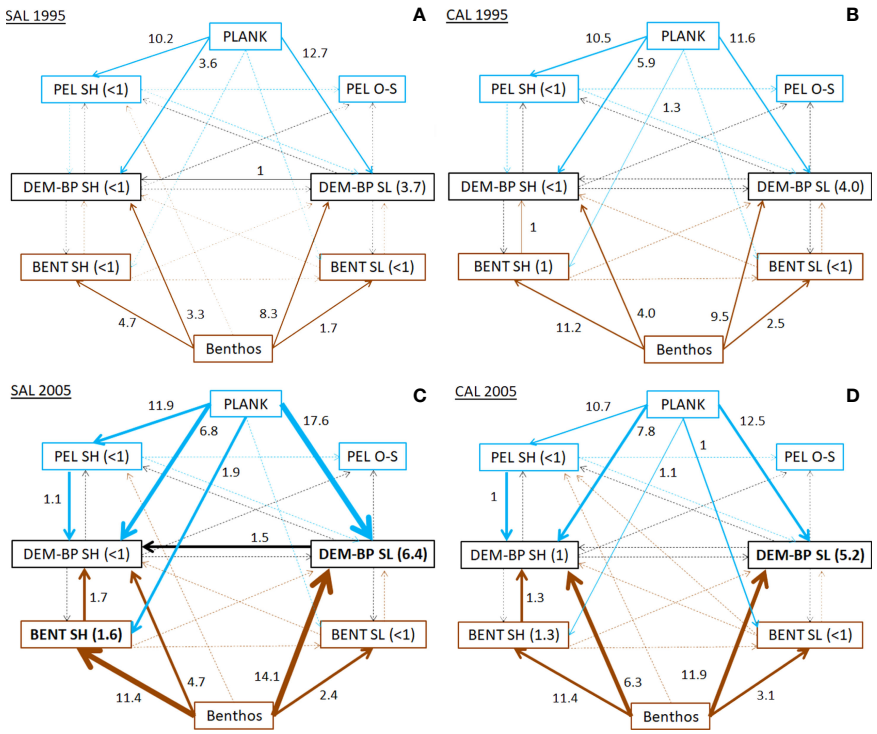

FIGURE 4 | Consumption flows (Q, t km^{-2} y^{-1}) between FGs aggregated in domains and depth layers for **(A)** SAL_1995, **(B)** CAL_1995, **(C)** SAL_2005 and **(D)** CAL_2005. Values in brackets indicate the consumption within the same domain. Lines indicate flows from pelagic (blue), benthic (brown) and other domains (black). Bold lines show Q values increases over time higher than 0.5, 2 and 4 t km^{-2} y^{-1}.

Predator/prey ratios showed similar increases in the SAL and CAL models (3% and 6%, respectively).

Macrozooplankton, Mesozoplankton and Macrobenthic invertebrates were the most impacting groups, showing the highest Overall Effect (OE) in both food webs during all investigated periods (**Table S6** and **Figures 6A, B**). In the SAL model, Odontocetes, Medium pelagics, *Parapenaeus longirostris* and SL_BathypelFishes_pisc showed the highest OE values in 1995-1997 (**Figure 6A**). Whereas, SH_Cephalopods, SL_Squids_BP, *Aristaemorpha foliacea*, and SHB_Squids_BP showed the highest values in the period 2003-2005. In the CAL model, Anglers, Odontocetes, Sl_Sharks_BP and SL_BathypelFishes_pisc showed the highest OE in the period 1995-1997, whileOE values increased in SL_Squids_BP, SH_Cephalopods, SL_Crabs and *A. foliacea* in the period 2005-2007 (**Figure 6B**). The main KS groups identified in the SAL model during both investigated periods were zooplankton groups (49-50-51), Macrobenthic invertebrates, Polychaetes (46-45), Shrimps BP (36), Small pelagics (23), the cephalopods groups SH_Cephalopods. SL_Squids_BP, SHB_Squids_BP, SHB_Crabs and Small phytoplankton (**Table S4** and **Figures 6C–E**). In addition, Medium pelagics, Odontocetes, and SL_BathypelFishes_pisc showed high KS values in 1995, but were later replaced by *A. foliacea*, and Suprabenthic crustaceans in 2005, and the importance of cephalopods increased as keystone groups. In the CAL model, all groups of zooplankton, SL_Squids_BP, Anglers, Medium pelagics, Macrobenthic invertebrates and Polychaetes, Shrimps BP, Small pelagics and SHB_Fishes_BP crust represented the most important keystone groups in both investigated periods (**Figures 6D–F**). Relevant changes in the KS rank were observed for SL_Sharks_BP, SL_BathypelFishes_pisc and Odontocetes, which showed high values in 1995. However, these groups were replaced by SH_Cephalopods, SHB_Squids_BP and Suprabenthic crustaceans during 2005.

Direct couplers supported the energy transfer from the pelagic to the benthic domain, such as Suprabenthic crustaceans, Macrobenthic invertebrates, Small phytoplankton, Macrozooplankton, Mesozooplankton, Polychaetes and Bacterioplankton, with dQf (downward) percentage values greater than 6%, while uQf (upward) were lacking for all these groups (**Tables 2**, **3** and **Figures 7A–D**). Differently, the upward flows from the benthic to the pelagic domain were supported by trophic interactions of demersal and benthopelagic FGs. In the deep benthopelagic domain, Shrimps BP (maximum BPCI= 11.69 t km^{-2} y^{-1}, in the SAL 2005 model) and Myctophids (BPCI= 6.85 t km^{-2} y^{-1}, in the SAL 2005 model) were identified as the most important mediating couplers of all the food webs models investigated. The former more predominantly supported upward flows (19-29%) than downward ones (1-3%), while the latter showed more similar percentage values between dQf (2-4%) and uQf (4-7%). Other minor benthopelagic

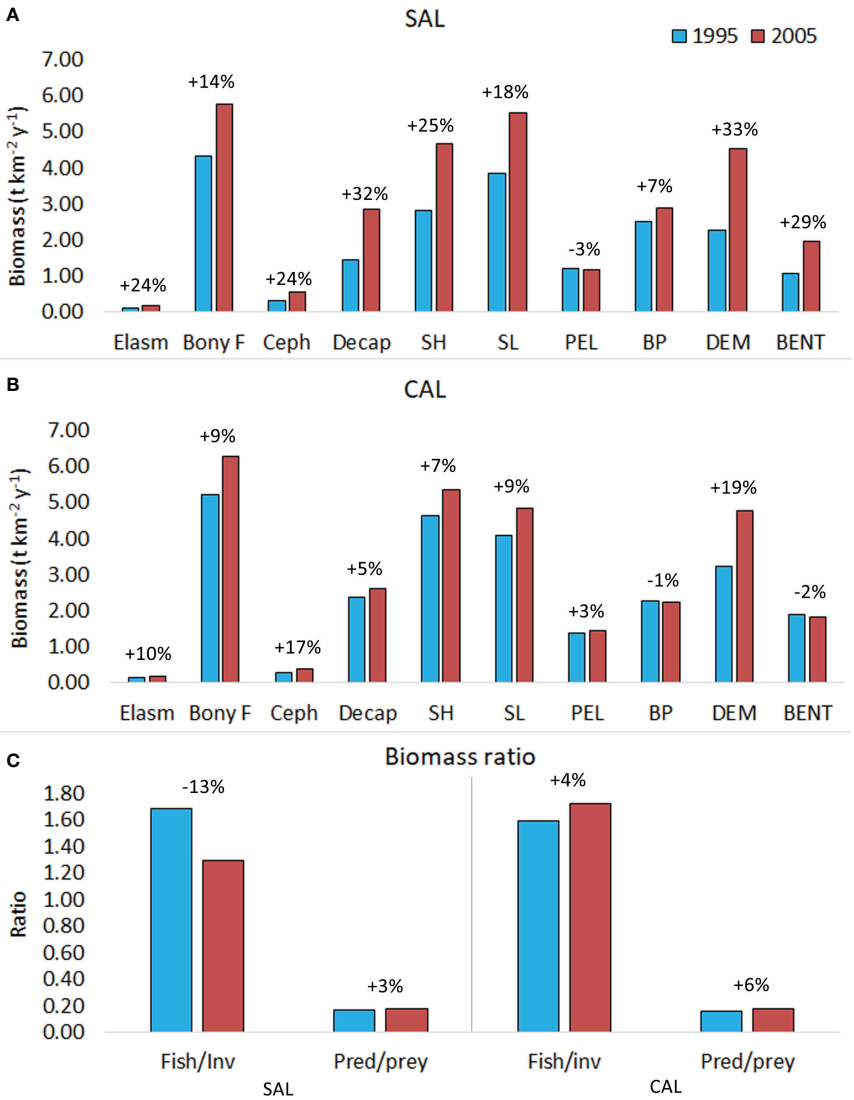

FIGURE 5 | Biomass estimated in all investigated periods for **(A)** SAL **(B)** CAL models for faunistic categories (Elasmobranchs, Elasm; bony fishes, Bony F; cephalopods, Ceph; Decapods, Decap); shelf (SH) and slope (SL) and domains. **(C)** Fish/invertebrates and Predator/prey biomass ratio. Percentages indicated increase (+) or decrease (-) from 1995 to 2005 for each indicator. FGs from 1 to 44 were considered.

couplers detected in both food webs are SHB_BobSquids_BP, SL_BathypelFishes_pisc, SHB_Squids_BP.

In all investigated models, demersal FGs were mediating or partial couplers characterized by uQf values that ranged between 1-13%. SHB_F_planktivorous (*Macroramphosus scolopax*, *Capros aper*) was the only group with dQf percentage values around 2%.

In the SAL food web, SH_Cephalopods were the most important demersal mediating coupler in 1995 and 2005 (BPCI=2.07 and 3.21t km^{-2} y^{-1}, respectively), with uQf values of 13% (**Table 2** and **Figures 7A, C**) In addition, SH_DemFishes_bent inv (uQf 9%), SH_DemFishes_bent crust (uQf 6%), SL_Fishes_BP crust, *Plesionika martia* and *P. longirostris* (all with uQf values of 4%) were relevant couplers in 1995. This rank changed in 2005, when the most important couplers were *P. martia* (uQf 10%), SH_DemFishes_bent crust (uQf 7%), *A. foliacea*, *Nezumia sclerorhynchus*, SH_DemFishes_bent inv and SL_Fishes_BP crust (all with a uQf value of 4%).

In the CAL food web, SH_DemFishes_bent inv, SH_Cephalopods and SH_DemFishes_bent crust were the most important mediating couplers of the demersal domain in both investigated periods, with the highest uQf values in 2005 (13%, 10% and 8%, respectively) (**Table 3** and **Figures 7B, D**). Moreover, *P. longirostris*, Macrourids_Med. slimehead and SL_Fishes_BP crust (all uQf values of 6%), *P. martia* (uQf 4%) and *Aristeus antennatus* (uQf 3%) were relevant couplers in 1995. Conversely, the rank changed in 2005, with *P. martia* (uQf 7%), Macrourids (uQf 6%), *P. longirostris* and *A. foliacea* (uQf

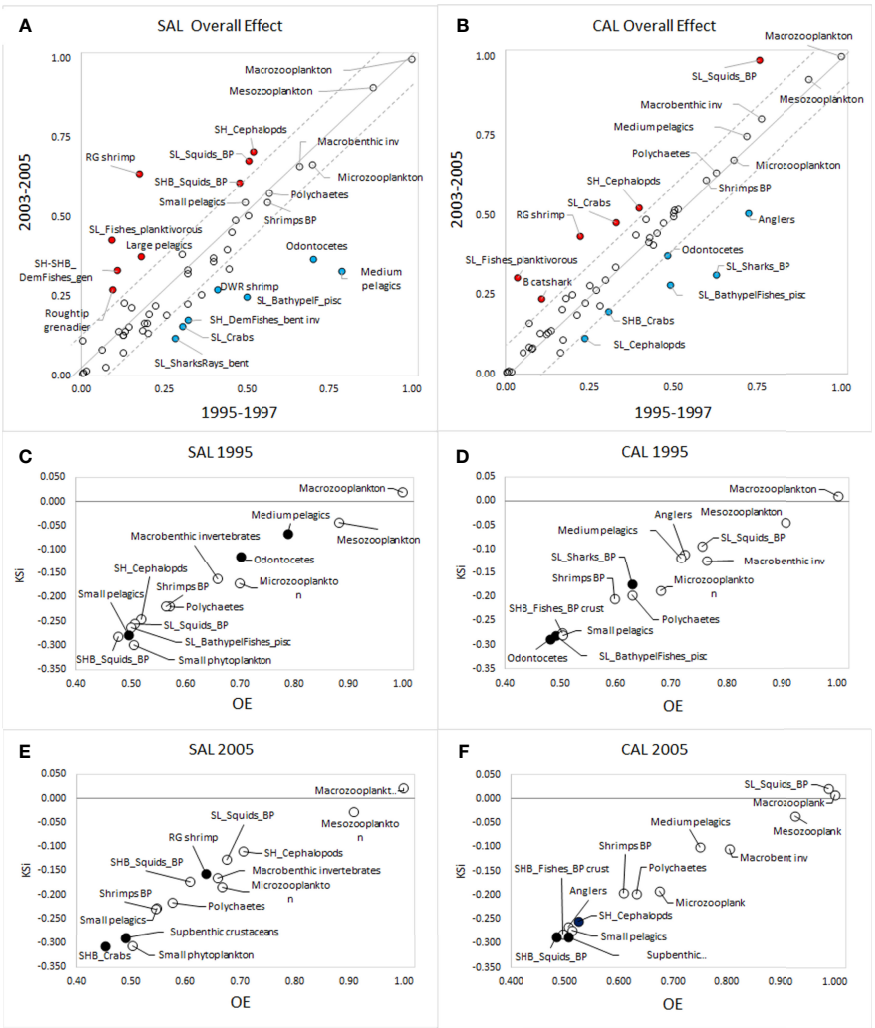

FIGURE 6 | Overall Effect estimated for all living FGs in the **(A)** SAL and **(B)** CAL models. Values higher in the period 1995-1997 (x-axis) are blue-coloured, while values higher in the period 2003-2005 (y-axis) are red-coloured. FGs ranked by KSI and OE in models **(C)** SAL 1995; **(D)** CAL 1995, **(E)** SAL 2005 and **(F)** CAL 2005. Black circles indicate FGs in 1995 replaced by others in 2005.

5%), *Mullus barbatus* and SL_Fishes_BP crust (uQf 3%) as the most relevant couplers.

The analysis of BPCI and COG highlights that the bathymetric position and its variance (indication of wide vertical movement of organisms) played an important role for benthopelagic and demersal couplers in the SAL and CAL models (**Figures 8A–D**, **9A–D**). In the benthopelagic domain, Myctophids and Shrimps support the highest energy flows in the upper and middle slope. From the shelf to the upper slope, SHB_Squids_BP, SHB_Fishes_BP crust and SHB_BSquids_BP supports the main energy exchanges. This pattern showed a temporal stability in both areas. On the contrary, the demersal domain showed spatial and temporal changes in the pattern of the couplers. SHB_Fishes_planktivorous showed a greater importance in the shelf of Calabrian area. In addition, a temporal increase in the number shelf and deep couplers and their bathymetric overlap in the SAL food web was observed in 2005. SH_Crabs, SHB_Crabs contributed to this overlap on the shelf, whereas SL_Decapods_bent, *A. foliacea*, *N. sclerorhynchus* and SL_Fishes_planktivorous contributed to that on the bathyal bottoms. In the Calabrian area, this overlap pattern was more evident in 1995, with the highest contribution to the flows coupling along the bathymetric gradient by SH_Crabs, SHB_Crabs, SL_Crabs, *P. longirostris*, *P. martia*, Macrourids_Med. slimehead and *A. antennatus*. In 2005, the pattern was the same, except for SHB_Crabs and *A. antennatus* being replaced by *M. barbatus* and *A. foliacea*.

DISCUSSIONS

A pivotal role in the southwestern and north-eastern Ionian areas is played by deep faunal communities (D'Onghia et al., 1998; Capezzuto et al., 2010; Carlucci et al., 2018), which

TABLE 2 | FGs classified as direct (D), mediating (M) and partial (P) couplers (Coup.) in the SAL food web with their respective estimated downward flow (dQf), upward flow (uQf) (expressed in t km^{-2} y^{-1} and %) and Benthic-Pelagic Coupling Index (BPCI, t km^{-2} y^{-1}).

1995	FG	dQf	uQf	BPCI	% dQf	% uQf	Coup.	2005	FG	dQf	uQf	BPCI	% dQf	% uQf	Coup.
Domain								**Domain**							
BENT	Supbrabenthic crustaceans	26.45	-0.15	26.60	19%	1%	D	BENT	Supbrabenthic crustaceans	43.39	-0.17	43.56	23%	1%	D
BENT	Macrobenthic invertebrates	19.06	-0.01	19.07	14%	0%	D	BENT	Macrobenthic invertebrates	35.70	-0.01	35.71	19%	0%	D
PEL	Small phytoplankton	14.79	0.00	14.79	11%	0%	D	BENT	Polychaetes	24.53	0.00	24.53	13%	0%	D
PEL	Mesozooplankton	13.94	0.00	13.94	10%	0%	D	PEL	Small phytoplankton	14.79	0.00	14.79	8%	0%	D
PEL	Macrozooplankton	13.89	0.00	13.89	10%	0%	D	PEL	Mesozooplankton	13.94	0.00	13.94	7%	0%	D
BENT	Polychaetes	12.78	0.00	12.78	9%	0%	D	PEL	Macrozooplankton	13.89	0.00	13.89	7%	0%	D
PEL	Bacterioplankton	11.87	0.00	11.87	9%	0%	D	PEL	Bacterioplankton	11.87	0.00	11.87	6%	0%	D
BP	Shrimps BP	3.43	-4.19	7.61	3%	29%	M	BP	Shrimps BP	5.26	-6.43	11.69	3%	29%	M
BP	Myctophids	5.07	-0.97	6.04	4%	7%	M	BP	Myctophids	5.80	-1.05	6.85	3%	5%	M
PEL	Microzooplankton	3.67	0.00	3.67	3%	0%	D	DEM	SHB_Fishes_planktivorous	4.68	-0.05	4.73	2%	0%	P
DEM	SHB_Fishes_planktivorous	2.58	-0.05	2.63	2%	0%	P	DEM	G shrimp	1.56	-2.22	3.78	1%	10%	M
DEM	SH_Cephalopods	0.21	-1.86	2.07	0%	13%	M	PEL	Microzooplankton	3.67	0.00	3.67	2%	0%	D
BP	SL_Fishes_BP crust	1.08	-0.64	1.72	1%	4%	P	DEM	SH_DemFishes_bent crust	1.63	-1.62	3.25	1%	7%	M
PEL	Large phytoplankton	1.70	0.00	1.70	1%	0%	D	DEM	SH_Cephalopods	0.34	-2.88	3.21	0%	13%	M
DEM	SH_DemFishes_bent crust	0.80	-0.81	1.61	1%	6%	M	BP	SL_Fishes_BP crust	1.42	-0.85	2.27	1%	4%	P
DEM	SH_DemFishes_bent inv	0.04	-1.27	1.30	0%	9%	P	PEL	Large phytoplankton	1.70	0.00	1.70	1%	0%	D
BP	SHB_BobSquids_BP	0.99	-0.10	1.08	1%	1%	M	DEM	RG shrimp	0.31	-0.84	1.16	0%	4%	P
DEM	G shrimp	0.39	-0.52	0.91	0%	4%	M	BP	SHB_BobSquids_BP	1.01	-0.10	1.11	1%	0%	M
BP	SHB_Fishes_BP crust	0.47	-0.40	0.87	0%	3%	M	BENT	SH_Crabs	1.06	0.00	1.06	1%	0%	D
DEM	DWR shrimp	0.28	-0.55	0.83	0%	4%	M	BP	SHB_Fishes_BP crust	0.56	-0.48	1.04	0%	2%	M
DEM	Macrourids_Med. slimehead	0.37	-0.35	0.72	0%	2%	M	BP	SHB_Squids_BP	0.62	-0.40	1.03	0%	2%	M
BP	SL_BathypelFishes_pisc	0.41	-0.21	0.62	0%	1%	M	DEM	Macrourids_Med. slimehead	0.53	-0.49	1.02	0%	2%	M
BP	SHB_Squids_BP	0.32	-0.27	0.59	0%	2%	M	DEM	Roughtip grenadier	0.09	-0.85	0.94	0%	4%	P
DEM	RB shrimp	0.17	-0.37	0.54	0%	3%	P	DEM	SH_DemFishes_bent inv	0.02	-0.90	0.92	0%	4%	P
BENT	SL_Crabs	0.47	0.00	0.47	0%	0%	D	BENT	SHB_Crabs	0.87	0.00	0.87	0%	0%	D
BENT	SHB_Crabs	0.46	0.00	0.46	0%	0%	D	DEM	SH-SHB_DemFishes_gen	0.29	-0.54	0.83	0%	2%	P
BENT	SH_Crabs	0.37	0.00	0.37	0%	0%	D	DEM	DWR shrimp	0.26	-0.49	0.75	0%	2%	M
DEM	Hake	0.31	-0.02	0.33	0%	0%	P	DEM	SL_Fishes_planktivorous	0.35	-0.26	0.61	0%	1%	P
DEM	SL_Cephalopods	0.01	-0.30	0.31	0%	2%	M	BENT	SL_Decapods_bent	0.57	0.00	0.57	0%	0%	D
BENT	SL_Decapods_bent	0.27	0.00	0.27	0%	0%	D	DEM	SL_Cephalopods	0.02	-0.50	0.52	0%	2%	M
DEM	SH-SHB_DemFishes_gen	0.07	-0.14	0.22	0%	1%	P	DEM	RB shrimp	0.16	-0.34	0.50	0%	2%	P
DEM	RG shrimp	0.06	-0.16	0.21	0%	1%	P	BP	SL_BathypelFishes_pisc	0.25	-0.12	0.37	0%	1%	M
DEM	Roughtip grenadier	0.02	-0.17	0.19	0%	1%	P	BENT	SL_Crabs	0.36	0.00	0.36	0%	0%	D
DEM	SL_DemFishes_decapods	0.07	-0.12	0.19	0%	1%	M	DEM	SL_DemFishes_decapods	0.13	-0.16	0.29	0%	1%	M
DEM	SH-SHB_DemFishes_pisc	0.06	-0.12	0.18	0%	1%	P	DEM	Hake	0.19	-0.01	0.21	0%	0%	P
PEL	Medium pelagics	0.00	-0.11	0.11	0%	1%	D	DEM	SH_SharksRays_bent	0.05	-0.13	0.18	0%	1%	P
								DEM	SH-SHB_DemFishes_pisc	0.06	-0.10	0.16	0%	0%	M
								DEM	R mullet	0.00	-0.12	0.12	0%	1%	P

are able to intercept the particulate organic matter through benthic organisms that are then exploited by demersal and benthopelagic species of higher trophic levels.

The differences between the Salento and Calabrian models related to the net primary production were estimated during the cyclonic period 2003-2005. The magnitude of the consumption and production flows, as well as the complexity of ecosystem indicate a higher pelagic production in the Salento food web than the Calabrian one. These differences could be explained by the NIG direction, which favours the inflow of Adriatic Dense Waters (flowing at depths between 200-800 m), as well as this area also being impacted by the Po River nutrient load transported along eastern Italian coasts in the Ionian Sea (Gačić et al., 2010; Taricco et al., 2015). Furthermore, Adriatic Dense Waters are considered to sustain upwelling currents able to increase primary productivity in the North-eastern Ionian region because they are enriched in nutrients (Lavigne et al., 2018). These cascading oceanographic effects promote higher productivity in the cyclonic period, and increased deep particulate fluxes, which can be evinced from the results showing higher consumption fluxes of deep benthic and demersal groups in both investigated areas. These conditions are explained by the hydrographic circulation in the basin, where the long-distance particle transport is supported by deep currents from east to west up to the Sicily channel (Berline et al., 2021). In this framework, a fundamental role could be

TABLE 3 | FGs classified as direct (D), mediating (M) and partial (P) couplers (Coup.) in the CAL food web with their respective estimated downward flow (dQf), upward flow (uQf) (expressed in t km^{-2} y^{-1} and %) and Benthic-Pelagic Coupling Index (BPCI, t km^{-2} y^{-1}).

1995	FG	dQf	uQf	BPCI	% dQf	% uQf	Coup.	2005	FG	dQf	uQf	BPCI	% dQf	% uQf	Coup.
Domain								**Domain**							
BENT	Macrobenthic invertebrates	34.52	-0.01	34.53	18%	0%	D	BENT	Macrobenthic invertebrates	39.31	-0.01	39.33	18%	0%	D
BENT	Suprabenthic crustaceans	28.05	-0.05	28.09	15%	0%	D	BENT	Suprabenthic crustaceans	32.90	-0.15	33.06	15%	1%	D
PEL	Small phytoplankton	23.86	0.00	23.86	12%	0%	D	PEL	Small phytoplankton	27.80	0.00	27.80	12%	0%	D
BENT	Polychaetes	21.69	-0.02	21.71	11%	0%	D	BENT	Polychaetes	27.16	-0.02	27.19	12%	0%	D
PEL	Mesozooplankton	20.98	0.00	20.98	11%	0%	D	PEL	Mesozooplankton	25.00	0.00	25.00	11%	0%	D
PEL	Bacterioplankton	17.78	0.00	17.78	9%	0%	D	PEL	Bacterioplankton	20.83	0.00	20.83	9%	0%	D
PEL	Macrozooplankton	14.25	0.00	14.25	7%	0%	D	PEL	Macrozooplankton	16.75	0.00	16.75	7%	0%	D
BP	Shrimps BP	3.06	-4.04	7.11	2%	25%	M	BP	Shrimps BP	3.27	-4.26	7.53	1%	19%	M
PEL	Microzooplankton	5.55	0.00	5.55	3%	0%	D	PEL	Microzooplankton	6.63	0.00	6.63	3%	0%	D
BP	Myctophids	4.40	-0.80	5.20	2%	5%	M	DEM	SHB_Fishes_planktivorous	5.99	-0.29	6.27	3%	1%	P
DEM	SHB_Fishes_planktivorous	4.49	-0.23	4.72	2%	1%	P	BP	Myctophids	4.34	-0.77	5.11	2%	4%	M
PEL	Large phytoplankton	3.92	0.00	3.92	2%	0%	D	PEL	Large phytoplankton	4.48	0.00	4.48	2%	0%	D
DEM	SH_DemFishes_bent crust	1.24	-1.23	2.47	1%	8%	M	DEM	SH_DemFishes_bent crust	1.67	-1.66	3.32	1%	8%	P
BP	SL_Fishes_BP crust	0.90	-0.91	1.81	0%	6%	P	DEM	SH_DemFishes_bent inv	0.03	-2.91	2.94	0%	13%	M
DEM	SH_DemFishes_bent inv	0.02	-1.73	1.75	0%	11%	M	DEM	SH_Cephalopods	0.21	-2.15	2.37	0%	10%	M
DEM	Macrourids_Med. slimehead	0.78	-0.96	1.74	0%	6%	M	DEM	Macrourids_Med. slimehead	0.97	-1.23	2.19	0%	6%	M
DEM	SH_Cephalopods	0.12	-1.26	1.38	0%	8%	M	DEM	G shrimp	0.58	-1.53	2.11	0%	7%	P
DEM	DWR shrimp	0.42	-0.94	1.36	0%	6%	M	DEM	DWR shrimp	0.53	-1.06	1.59	0%	5%	M
DEM	G shrimp	0.30	-0.65	0.95	0%	4%	P	DEM	RG shrimp	0.39	-1.19	1.58	0%	5%	P
BP	SHB_Fishes_BP crust	0.48	-0.30	0.78	0%	2%	P	BP	SL_Fishes_BP crust	0.69	-0.70	1.39	0%	3%	P
BENT	SH_Crabs	0.70	-0.02	0.72	0%	0%	D	BP	SHB_Fishes_BP crust	0.67	-0.42	1.10	0%	2%	P
BP	SL_BathypelFishes_pisc	0.42	-0.21	0.63	0%	1%	M	BENT	SH_Crabs	0.83	0.00	0.84	0%	0%	D
BENT	SHB_Crabs	0.60	-0.02	0.62	0%	0%	D	BP	SHB_Squids_BP	0.41	-0.36	0.78	0%	2%	M
BP	SHB_BobSquids_BP	0.56	-0.06	0.62	0%	0%	I	BENT	SL_Crabs	0.71	-0.07	0.78	0%	0%	D
BP	SHB_Squids_BP	0.32	-0.27	0.59	0%	2%	M	DEM	R mullet	0.01	-0.60	0.62	0%	3%	P
BENT	SL_Crabs	0.56	-0.02	0.58	0%	0%	D	DEM	RB shrimp	0.12	-0.36	0.48	0%	2%	P
DEM	RB shrimp	0.14	-0.42	0.56	0%	3%	P	DEM	Roughtip grenadier	0.02	-0.45	0.48	0%	2%	P
DEM	SH-SHB_DemFishes_pisc	0.18	-0.24	0.42	0%	1%	P	BP	SHB_BobSquids_BP	0.38	-0.04	0.42	0%	0%	M
DEM	SH-SHB_DemFishes_gen	0.13	-0.23	0.36	0%	1%	P	BP	SL_BathypelFishes_pisc	0.28	-0.14	0.42	0%	1%	M
DEM	RG shrimp	0.08	-0.23	0.31	0%	1%	P	DEM	SH-SHB_DemFishes_pisc	0.18	-0.24	0.42	0%	1%	P
DEM	R mullet	0.01	-0.30	0.30	0%	2%	P	DEM	SL_DemFishes_decapods	0.15	-0.19	0.35	0%	1%	P
DEM	Hake	0.24	-0.01	0.25	0%	0%	P	BENT	SHB_Crabs	0.31	0.00	0.31	0%	0%	D
DEM	SL_DemFishes_decapods	0.10	-0.14	0.24	0%	1%	P	DEM	SL_Fishes_planktivorous	0.15	-0.11	0.26	0%	1%	P
DEM	Roughtip grenadier	0.01	-0.22	0.23	0%	1%	P	BENT	SL_Decapods_bent	0.26	0.00	0.26	0%	0%	D
BENT	SL_Decapods_bent	0.22	0.00	0.22	0%	0%	D	DEM	SHB-SL_DemFishes_gen	0.05	-0.18	0.22	0%	1%	P
DEM	SL_Cephalopods	0.01	-0.19	0.20	0%	1%	M	DEM	SH-SHB_DemFishes_gen	0.08	-0.14	0.22	0%	1%	P
DEM	SH_SharksRays_bent	0.02	-0.11	0.13	0%	1%	P	DEM	Hake	0.20	-0.01	0.21	0%	0%	P
DEM	SHB-SL_DemFishes_gen	0.03	-0.10	0.13	0%	1%	P	PEL	M pelagics	0.00	-0.21	0.21	0%	1%	D
PEL	M pelagics	0.00	-0.09	0.09	0%	1%	D								
BP	SL_Squids_BP	0.00	-0.09	0.09	0%	1%	M								

played by submarine canyons along the Calabrian sectors, where upwelling currents and water cascading processes allow movement of the deep organic matter towards the upper slope (Canals et al., 2009). Furthermore, cold-water coral habitats are found on the Apulian slope (D'Onghia et al., 2016; Vassallo et al., 2017) and in the Sicily channel (Taviani et al., 2005; Freiwald et al., 2009) and this distribution supports the idea of an ecological connectivity between the eastern and western Ionian areas regulated by deep currents carrying nutrients and organic matter exploited by these organisms (Carlier et al., 2009). A further aspect that could explain the differences in pelagic production and downward particulate fluxes between the two areas is represented by the wider shelf platform in the Apulian area, which can positively affect the particulate matter sinks to the bottom, vertical mixing and the resuspension of large amount of nutrients in the upper layer of the water column (De Lazzari et al., 1999; Boldrin et al., 2002). Conversely, in the Calabrian sector, downward flows of particulate matter linked to surface production occurring in the photic layer (D'Ortenzio et al., 2003), sink to a depth that makes nutrients resulting from organic matter degradation largely inaccessible for the phytoplankton in the area itself. Rather, particulate sinking appears to supply the bottom detritus food chain in the Calabrian canyons, as observed from results on consumption fluxes between benthic and demersal domains.

If the cyclonic period stressed spatial differences in the pelagic production and consumption between the two food webs, these characteristics were not observed during the anticyclonic phase

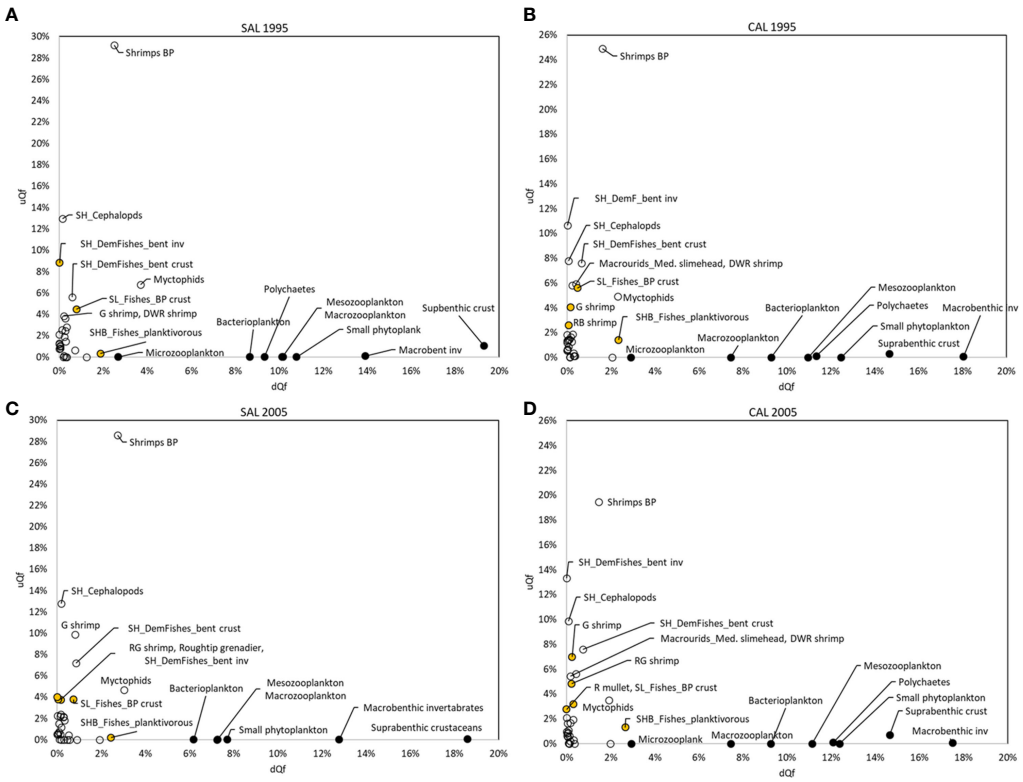

FIGURE 7 | Direct (black circle), mediating (white) and partial (orange) couplers by downward (dQf, x-axis) and upward (uQf, y-axis) flows (%), estimated for all investigated **(A–C)** SAL and **(B–D)** CAL models.

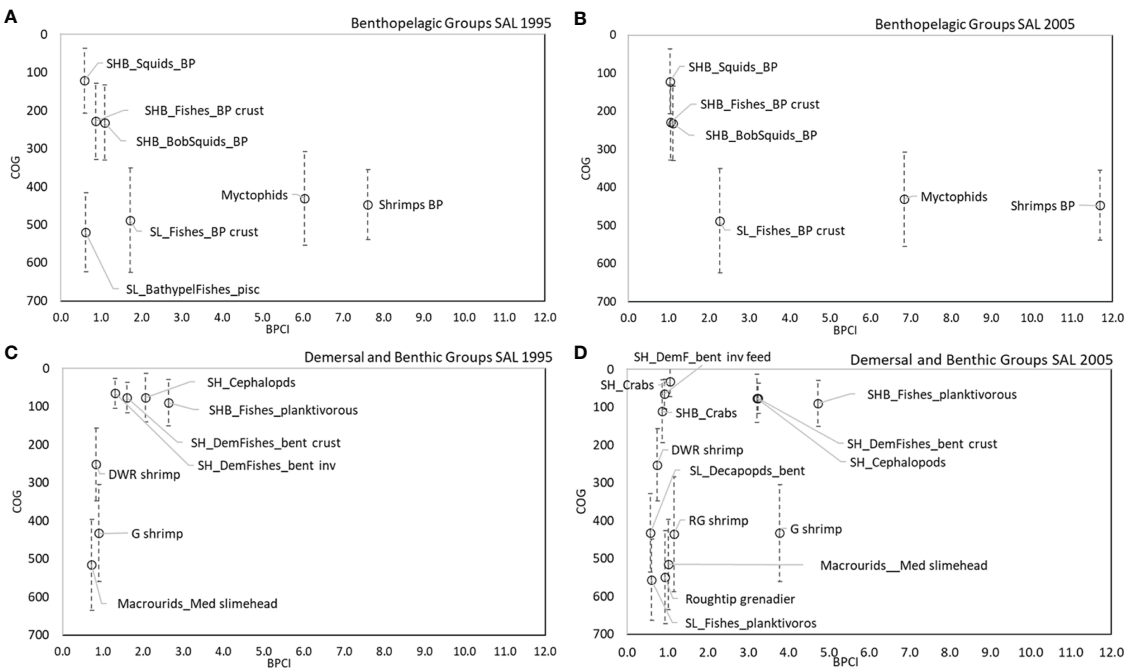

FIGURE 8 | COG (m) of main couplers by BPCI (>0.5 t km^{-2} y^{-1}) in all SAL models for **(A, B)** benthopelagic and **(C, D)** demersal domains.

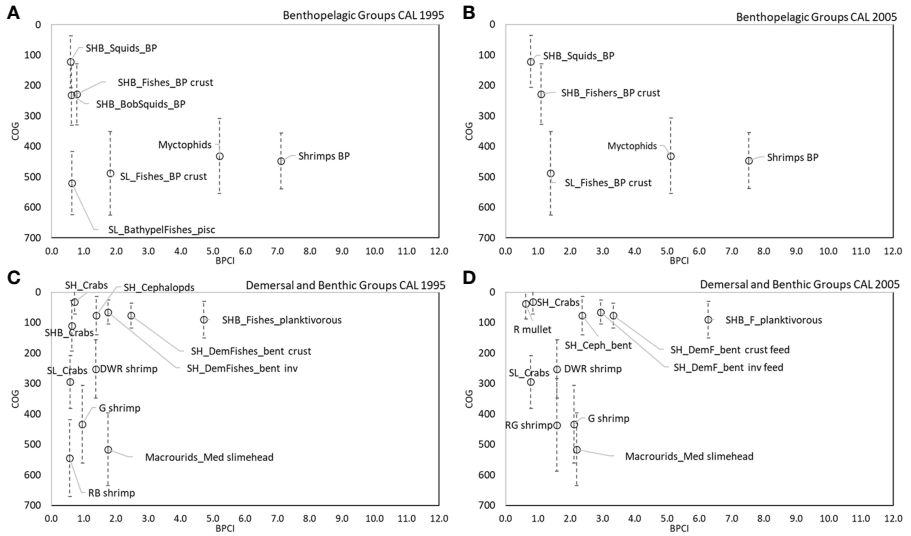

FIGURE 9 | COG (m) of main couplers by BPCI (>0.5 t km^{-2} y^{-1}) in all CAL models for **(A, B)** benthopelagic and **(C, D)** demersal domains.

(1995-1997). This could be due to the peculiar water circulation in this phase, when the Calabrian and Salento areas were impacted by Modified Atlantic Waters coming from the western Mediterranean Sea and they move in the upper layer of the water column (Klein et al., 1999). Thus, the absence of effects on the deep faunal communities is reasonable. Furthermore, a lower input of Adriatic Dense Waters occurred in the basin and the geostrophic circulation of the water masses was directed from the Calabrian area towards the Apulian one.

Functional Group's Role in the BPC Process

The differences in oceanographic conditions and their cascading food web effects are confirmed in our models, stressing an increase in biomass of the groups during 2003-2005. This estimated increase was higher on the north-eastern (Salento) than on the south-western slope (Calabria), especially for deep faunal assemblages. In both food webs, the contribution to the biomass increase is given by the demersal assemblage, with the highest value observed for shelf demersal assemblage in the Salento area. Moreover, benthopelagic groups also showed a greater biomass increase in the Salento food web. However, increases estimated in the Calabrian food web were smaller than the Salento one because, during the anticyclonic period, biomasses were higher in the former food web than the latter. These observations suggest maintenance of the biomass structure of the ecosystem in the Calabrian area in both periods investigated, probably due to a refuge effect of submarine canyons (Fernandez-Arcaya et al., 2017; Capezzuto et al., 2018; Sion et al., 2019) Although comparative studies on the temporal dynamics of species abundances between the two areas are very limited (D'Onghia et al., 1998), changes estimated by the models are consistent with fluctuations in abundance of demersal resources studied at the scale of the entire Northern Ionian basin (Capezzuto et al., 2010; Maiorano et al., 2010; Carlucci et al., 2018) and for the sharks and rays in the Calabrian area (Ricci et al., 2021).

Changes in biomass influence the trophic interactions between predators and prey, which affect trophic impacts detected by the models, as well as in the rank of keystone groups. In general, zooplankton groups assume a keystone role in the Ionian food web, being an important resource for several consumers in oligotrophic systems (Mazzocchi et al., 2003; Ricci et al., 2019). This role was maintained during the investigated periods, as were those of the Macrobenthic invertebrates and Suprabenthic crustaceans, which represent dominant structuring groups of the benthic domain. On the contrary, relevant temporal changes in the trophic impacts were mainly estimated for the groups of intermediate and high trophic levels (TL>3). Cephalopods increased in their importance as keystone groups in the cyclonic period. In particular, Shelf Cephalopods (*Octopus vulgaris*, *Sepia* spp., *Eledone* spp.) showed more importance in the Salento area, whereas Slope Benthopelagic Squids (*Todarodes sagittatus*, *Histioteuthis* spp.) was the most important keystone group in the CAL food web. This difference may be explained by the habitat distribution of the two groups: Shelf Cephalopods inhabit the shallowest grounds (Jereb et al., 2015), which widely extend in the Salento areas while Slope Benthopelagic Squids are distributed in the bathyal grounds exploiting several species at different levels in the water column (Rosas-Luis et al., 2014) and they can find suitable habitats in the submarine canyons. In addition, the biological traits of cephalopods, such as rapid growth, short lifespans, and plasticity, explain the faster response of these species to changes in productivity of the food web becoming a very highly impacting group in the trophic structure (Doubleday et al., 2016).

In both Northern Ionian Sea food webs, pelagic and benthic groups substantially drive energy transfer from pelagic to benthic

communities in a direct manner as direct couplers. In the benthopelagic domain, flux coupling is mainly performed by Benthopelagic Shrimps (*Pasiphaea* spp., *Acanthephyra* spp., *Plesionika edwardsii*) and Myctophids, which show a temporal stability in their role. It is worth noting that both Benthopelagic Shrimps and Myctophids appear to support downward and upward flows in a different way. Benthopelagic Shrimps mainly plays a role in sustaining flows towards the pelagic, improving to be an effective benthic-pelagic coupler, while Myctophids supports energy transfers in both directions. The COG analysis showed that this feature is connected to the vertical movement of these species along the upper slope (300-400 m) and middle slope (500-700 m), migrations that have been widely observed (Aguzzi et al., 2007; Simão et al., 2015; Drazen and Sutton, 2017). The different trophic strategies could explain the difference between Myctophids and Benthopelagic Shrimps in the BPC patterns. Indeed, Myctophids and other mesopelagic fishes perform extensive daily migrations along the water column, eating plankton and micronekton at multiple depths in the epipelagic layers at night (Bernal et al., 2015). Whereas, the group of benthopelagic shrimps is also characterized by several deep-water crustaceans decapods, which feed on benthic prey (such as polychaetas exploited by *P. edwardsii*) and their opportunistic behavior is affected by the availability of planktonic resources (Cartes, 1993; Cartes, 1998). The importance of these groups in the energy exchanges has been observed in previous local models (Ricci et al., 2019; Carlucci et al., 2021), and in models realized for nearby areas, such as the Strait of Sicily model (Agnetta et al., 2019).

Demersal groups mostly contribute to BPC mechanisms in an almost exclusive way, acting as an elevator in the sustaining of upwelling flows. Thus, these groups play a critical role in the transfer of energy towards the surface, supporting recycling of the matter available for pelagic organisms (Raffaelli et al., 2003; Baustian et al., 2014). Only Shelf-break Planktivorous Fishes (*M. scolopax*, *C. aper*) showed a higher BPCI values with a relevant contribution to downward flows in the Calabrian food web, indicating an exploitation of zooplanktonic prey. This result seems to be consistent with the structural importance of these species in the Calabrian demersal assemblage (D'Onghia et al., 1998) and their feeding strategy and rapid life cycles (Carpentieri et al., 2016).

In the shelf grounds of the Salento food web, Shelf Cephalopods and Shelf Demersal Fishes benthic crustacean feeders occupy an important position as mediating couplers of ascending consumption flows during both investigated periods. According to BPCI outputs, the former supports exclusively upward consumption flows, while the latter is also involved in the downward and upward energy transfer. Indeed, Shelf Cephalopods are characterized by species mainly linked to benthic prey and exploited by different predators, such as large pelagics and odontocetes (Clarke, 1996). However, Shelf Demersal Fishes benthic crustaceans feeders (Spicara spp., *Boops boops*) consist of species involved in the exploitation of zooplankton resources and benthopelagic crustaceans, as well as being prey of several fish predators and the common bottlenose dolphin (Pipitone and Andaloro, 1995; Riccioni et al., 2018; Ricci et al., 2020).

In bathyal grounds of the Salento area, *P. martia* and *P. longirostris* represent the main important couplers of energy flows from deep bottoms up to the upper slope in the anticyclonic period. Successively, the golden shrimp increased its consumption becoming the most important mediating coupler in the cyclonic periods, followed by *A. foliacea*, *N. sclerorhynchus* as partial couplers. *P. martia* represents an important species in the bathyal assemblage of the Northern Ionian Sea (Maiorano et al., 2002.; Capezzuto et al., 2010; D'Onghia et al., 2011), which is an important opportunistic predator of planktonic and benthic resources (Cartes, 1993). Its role as coupler became more relevant in the period 2003-2005 and this could be explained by its trophic strategy, favoured by a greater productivity during the cyclonic period (Mazzocchi et al., 2003; Lavigne et al., 2018). Similarly, *N. sclerorhynchus* and *A. foliacea* are characterized by a trophic strategy that could have been supported by the increase in mesopelagic prey during the cyclonic period (Madurell and Cartes, 2006; Kapiris et al., 2010).

In the Calabrian shelf area, energy flows in the BPC pattern are mainly supported by Shelf Demersal Fishes benthic invertebrates feeders (*Pagellus acarne, Mullus surmuletus*) in both investigated periods, followed by Shelf Cephalopods and Shelf Demersal Fishes benthic crustaceans feeders. In addition, the role of *M. barbatus* as a mediating coupler of the demersal domain emerged in 2005. These observations highlight the importance of benthic invertebrates (annelids, crustaceans, and molluscs) as prey in the Calabrian food web, where crabs also play a role in the BPC mechanisms in shelf and upper slope grounds.

In bathyal grounds, Macrourids and Mediterranean Slimehead (*Coelothynchus coelothynchus, Hymenocephalus italicus, Hoplostethus mediterraneus*), *P. longirostris*, *P. martia* and *A. antennatus* showed the main contribution to the energy flows coupling in the demersal domain. This condition was confirmed in 2005, but with *A. antennatus* replaced by *A. foliacea*. In addition, the role of *P. martia* emerged in the cyclonic period, as observed in the Salento area. Thanks to their ecological traits and trophic positions, Macrourids (*C. coelorhynchus*, *H. italicus*) and *H. mediterraneus* seem to be more able to respond to the trophic changes due to the BiOS. Indeed, these species feed on suprabenthic and mesopelagic prey (Madurell and Cartes, 2005; Madurell and Cartes, 2006), which are highly sensitive to water column changes. Concerning *P. longirostris*, its importance in the BPC pattern seems to be due its wide displacement in the shelf-break and upper slope grounds, its exploitation of prey on benthic and deposit feeders (Benallal et al., 2020), as well as its movements during the life cycle from nursery to spawning areas, as observed in the Strait of Sicily (Fortibuoni et al., 2010). The replacement of *A. antennatus* by *A. foliacea* with an inverted ratio between the two red shrimps during the cyclonic phase has been reported in several local studies (Capezzuto et al., 2010; Carlucci et al., 2018). This could be linked to changes in the deep-water direction which occurred in the cyclonic period by affecting the water cascading into the Calabrian canyons. Indeed, *A. antennatus* shows a great capability

in its vertical movement up and down canyons (Relini et al., 2000), and dense waters cascading facilitate its displacement in deep waters, where the species performs its important recruitment process (Company et al., 2008; D'Onghia et al., 2009). Moreover, changes in the thermohaline circulation seemed to favour *A. foliacea*, but not *A. antennatus*, which is more linked to colder and less saline waters. The best hydrodynamic conditions for *A. antennatus* appear to be a combination of relatively cold temperatures and high salinity, associated with moderate energy variability (Sardà et al., 2009).

Insights for Future Improvements and Analysis

The approach adopted has the potential to provide a holist view for the BPC. One of the main limitations of the approach is related to the poor biological resolution of processes involving for macrobenthic invertebrates. For the macrobenthic invertebrates, in fact, information on biomasses and diet are generally scant and also in these models the biomass of some of these groups was estimated by means the model (Heymans et al., 2016).

Another limitation is represented by the lack of data for phytoplankton biomasses before 1998-1999 (Lazzari et al, 2012) and the assumption used that the primary production condition of the period 1995-1997 was similar to the period 1998-1999 (Di Biagio et al., 2019; Cossarini et al., 2021). Nevertheless, the focus on the higher trophic level and by the integrated use of several independent information sources in the modelling approach, including details on benthopelagic and demersal species data obtained from the MEDITS surveys, partially mitigate the limitation.

The results stimulate future works on the hydrographic features and bioecological traits of deep species, which can provide some insights for future analysis. In particular, a quantification of the deep transport of particulate organic material from the north-western side to the south-western side of the Ionian Basin during the cyclonic period compared to the anticyclonic, with cascading effects on the energetic input to deep benthic and demersal communities, should be useful to shed light on spatially distributed BPC processes (Berline et al., 2021). The role of the deep and intermediate currents in this process could represent an interesting field of study to investigate particulate matter transport between these two areas of the Ionian basin.

Environmental changes driven by the water circulation inversion have relevant effects on the physical variables and as reported in several studies (Civitarese et al., 2010; Liu et al., 2021) are affecting the faunal community distributed in the slope grounds (Carlucci et al., 2018). Therefore, an important area of investigation is the effects of changes in environmental features on the growth and recruitment of several deep-sea species, such as the case of *A. foliacea*, which has shown large fluctuations in abundance and biomass (Capezzuto et al., 2010). In addition, the wide bathymetric displacement of several demersal and benthopelagic species, as observed for *A. antennatus* (D'Onghia et al., 2009), indicates population movements at depths greater than 1000 m, which are performed in response to environmental changes (Sardà et al., 2004; D'Onghia et al., 2005; Company et al., 2008; Maiorano et al., 2010; Capezzuto et al., 2010). Therefore, further modelling analysis could be addressed to include these vertical migrations, although this will not be easy given the scarcity of temporal information on deep faunal communities.

In conclusion, BPC flows analysed by means of a food web modelling approach and a new BPCI index allowed the quantification of the flow between the benthic and pelagic domains and to disentangle the contribution of species to the BPC mechanisms. In the Northern Ionian Sea, the BPC is affected by temporal changes during the BiOS phases, as well as by spatial differences between the two investigated areas, which are characterized by peculiar environmental conditions. These differences are mainly reflected in the role of some groups of benthopelagic and demersal species, which support the upward flows towards pelagic systems through their feeding behaviours and their wide variation along the bathymetric gradient in the shelf break and upper slope. Temporal changes driven by BiOS seem to have relevant influences on the trophic state of the deep communities, which showed important variations in the amount of consumption flows estimated by means of BPCI.

DATA AVAILABILITY STATEMENT

The original contributions presented in the study are included in the article/**Supplementary Material**. Further inquiries can be directed to the corresponding author.

AUTHOR CONTRIBUTIONS

Conceptualization, PR and SL; methodology, PR, SL, RC; formal analysis, PR, SL, GC; data investigation and sampling design, GD'O, PM, AC, FC, RC, LS, AT; writing—original draft preparation, PR, SL, RC; writing—review and editing, GD'O, PM, LS, FC; AT GC, AC, SL, PR; supervision, RC, SL. All authors contributed to the article and approved the submitted version.

SUPPLEMENTARY MATERIAL

The Supplementary Material for this article can be found online at: https://www.frontiersin.org/articles/10.3389/fmars.2022.887464/full#supplementary-material

REFERENCES

Agnetta, D., Badalamenti, F., Colloca, F., D'Anna, G., Di Lorenzo, M., Fiorentino, F., et al. (2019). Benthic-Pelagic Coupling Mediates Interactions in Mediterranean Mixed Fisheries: An Ecosystem Modeling Approach. *PloS One* 14 (1), e0210659. doi: 10.1371/journal.pone.0210659

Aguzzi, J., Company, J. B., Abelló, P., and García, J. A. (2007). Ontogenetic Changes in Vertical Migratory Rhythms of Benthopelagic Shrimps *Pasiphaea*

Multidentata and *P. Sivado*. *Mar. Ecol. Progr. Ser.* 335, 167–174. doi: 10.3354/meps335167

Allen, R. R. (1971). Relation Between Production and Biomass. *J. Fish. Res. Board Can.* 28, 1573–1581. doi: 10.1139/f71-236

Banaru, D., Mellon-Duval, C., Roos, D., Bigot, J. L., Souplet, A., Jadaud, A., et al. (2013). Trophic Structure in the Gulf of Lions Marine Ecosystem (North-Western Mediterranean Sea) and Fishing Impacts. *J. Mar. Syst.* 111, 45–68. doi: 10.1016/j.jmarsys.2012.09.010

Baustian, M. M., Hansen, G. J. A., de Kluijver, A., Robinson, K., Henry, E. N., Knoll, L. B., et al. (2014). "Linking the Bottom to the Top in Aquatic Ecosystems: Mechanisms and Stressors of Benthic-Pelagic Coupling," in *Eco-DAS X Symposium Proceedings Chapter: Chapter 3*. Ed. P. F. Kemp (Waco, Texas, USA:Association for the Sciences of Limnology and Oceanography), P.38–P.60. doi: 10.4319/ecodas.2014.978-0-9845591-4-5.38

Benallal, A. M., Baaloudj, A., Kerfouf, A., Bouzidi, M. A., and Belhadj Tahar, K. (2020). Natural Diet of Deep-Water Rose Shrimp in the Beni-Saf Bay (Western Algeria). *Ukr. J. Ecol.* 10 (4), 109–115. doi: 10.15421/2020_176

Berline, L., Doglioli, A. M., Petrenko, A., Barrillon, S., Espinasse, B., Le Moigne, F. A. C., et al. (2021). Long-Distance Particle Transport to the Central Ionian Sea. *Biogeosciences* 18, 6377–6392. doi: 10.5194/bg-18-6377-2021

Bernal, A., Pilar Olivar, M., Maynou, F., and Luz Fernández de Puelles, M. (2015). Diet and Feeding Strategies of Mesopelagic Fishes in the Western Mediterranean. *Prog. Oceanogr.* 135, 1–17. doi: 10.1016/j.pocean.2015.03.005

Boldrin, A., Miserocchi, S., Rabitti, S., Turchetto, M. M., Balboni, V., and Socal, G. (2002). Particulate Matter in the Southern Adriatic and Ionian Sea: Characterisation and Downward Fluxes. *J. Mar. Syst.* 33–34, 389–410. doi: 10.1016/S0924-7963(02)00068-4

Boyle, M. D., Ebert, D. A., and Cailliet, G. M. (2012). Stable-Isotope Analysis of a Deep-Sea Benthic-Fish Assemblage: Evidence of an Enriched Benthic Food Web. *J. Fish Biol.* 80, 1485–1507. doi: 10.1111/j.1095-8649.2012.03243.x

Canals, M., Danovaro, R., Heussner, S., Lykousis, V., Puig, P., Trincardi, F., et al. (2009). Cascades in Mediterranean Submarine Grand Canyons. *Oceanography* 22 (1), 26–43. doi: 10.5670/oceanog.2009.03

Capezzuto, F., Ancona, F., Calculli, C., Carlucci, R., Sion, L., Maiorano, P., et al. (2021). Comparison of Trophic Spectrum in the Blackspot Seabream, *Pagellus Bogaraveo* (Brünnich 1768), Between Cold-Water Coral Habitats and Muddy Bottoms in the Central Mediterranean. *Deep Sea Res. I* 169, 103474. doi: 10.1016/j.dsr.2021.103474

Capezzuto, F., Ancona, F., Calculli, C., Sion, L., Maiorano, P., and D'Onghia, G. (2020). Feeding of the Deep-Water Fish *Helicolenus Dactylopterus* (Delaroche 1809) in Different Habitats: From Muddy Bottoms to Cold-Water Coral Habitats. *Deep-Sea Res. I* 159, 103252. doi: 10.1016/j.dsr.2020.103252

Capezzuto, F., Ancona, F., Carlucci, R., Carluccio, A., Cornacchia, L., Maiorano, P., et al. (2018). Cold-Water Coral Communities in the Central Mediterranean: Aspects on Megafauna Diversity, Fishery Resources and Conservation Perspectives. *Rend. Lincei Sci. Fish. Nat.* 29, 589–597. doi: 10.1007/s12210-018-0724-5

Capezzuto, F., Calculli, C., Carlucci, R., Carluccio, A., Maiorano, P., Pollice, A., et al. (2019). Revealing the Coral Habitat Effect on Benthopelagic Fauna Diversity in the Santa Maria Di Leuca Cold-Water Coral Province Using Different Devices and Bayesian Hierarchical Modelling. *Aquat. Conserv: Mar Freshw Ecosyst.* 29, 1608–1622. doi: 10.1002/aqc.3144

Capezzuto, F., Carlucci, R., Maiorano, P., Sion, L., Battista, D., Giove, A., et al. (2010). The Bathyal Benthopelagic Fauna in the NW Ionian Sea: Structure, Patterns and Interactions. *Chem. Ecol.* 26, 199–217. doi: 10.1080/02757541003639188

Carlier, A., Le Guilloux, E., Olu, K., Sarrazin, J., Mastrototaro, F., Taviani, M., et al. (2009). Trophic Relationships in a Deep Mediterranean Cold-Water Coral Bank (Santa Maria Di Leuca, Ionian Sea). *Mar Ecol. Prog. Ser.* 397, 125–137. doi: 10.3354/meps08361

Carlucci, R., Bandelj, V., Ricci, P., Capezzuto, F., Sion, L., Maiorano, P., et al. (2018). Exploring Spatio-Temporal Changes of the Demersal and Benthopelagic Assemblages of the North-Western Ionian Sea (Central Mediterranean Sea). *Mar. Ecol. Prog. Ser.* 598, 1–19. doi: 10.3354/meps12613

Carlucci, R., Capezzuto, F., Cipriano, G., D'Onghia, G., Fanizza, C., Libralato, S., et al. (2021a). Assessment of Cetacean-Fishery Interactions in the Marine Food Web of the Gulf of Taranto (Northern Ionian Sea, Central Mediterranean Sea). *Rev. Fish Biol. Fish.* 31, 135–156. doi: 10.1007/s11160-020-09623-x

Carlucci, R., Manea, E., Ricci, P., Cipriano, G., Fanizza, C., Maglietta, R., et al. (2021b). Managing Multiple Pressures for Cetaceans' Conservation With an Ecosystem-Based Marine Spatial Planning Approach. *J. Environ. Manage.* 287, 112240. doi: 10.1016/j.jenvman.2021.112240

Carpentieri, P., Serpetti, N., Colloca, F., Criscoli, A., and Ardizzone, G. (2016) Food Preferences and Rhythms of Feeding Activity of Two Co-Existing Demersal Fish, the Longspine Snipefish, *Macroramphosus Scolopax* (Linnaeus 1758), and the Boarfish *Capros Aper* (Linnaeus 1758), on the Mediterranean Deep Shelf. *Mar. Ecol.* 37, 106–118. doi: 10.1111/maec.12265

Cartes, J. E. (1993). Diets of Deep-Water Pandalid Shrimps on the Western Mediterranean Slope. *Mar. Ecol. Prog. Ser.* 96, 49–61. doi: 10.3354/meps096049

Cartes, J. (1998). Feeding Strategies and Partition of Food Resources in Deep-Water Decapod Crustaceans (400–2300 M). *J. Mar. Biol. Ass. UK* 78 (2), 509–524. doi: 10.1017/S002531540004159X

Chauvaud, L., Jean, F., Ragueneau, O., and Thouzeau, G. (2000). Long-Term Variation of the Bay of Brest Ecosystem: Benthic-Pelagic Coupling Revisited. *Mar. Ecol. Prog. Ser.* 200, 35–48. doi: 10.3354/meps200035

Christensen, V., and Walters, R. (2004). Ecopath With Ecosim: Methods, Capabilities and Limitations. *Ecol. Modell.* 172 (2–4), 109–139. doi: 10.1016/j.ecolmodel.2003.09.003

Christensen, V., Walters, C., Pauly, D., and Forrest, R. (2008). *Ecopath With Ecosim 6: A User's Guide* (Vancouver, BC: Fisheries Centre. University of British Columbia).

Civitarese, G., Gačić, M., Lipizer, M., and Eusebi Borzelli, G. L. (2010). On the Impact of the Bimodal Oscillating System (BiOS) on the Biogeochemistry and Biology of the Adriatic and Ionian Seas (Eastern Mediterranean). *Biogeosciences* 7 (12), 3987–3997. doi: 10.5194/bg-7-3987-2010

Clarke, M. R. (1996). Cephalopods as Prey. III. *Cetaceans Phil. Trans. R. Soc. Lond.* B351, 1053–1065. doi: 10.1098/rstb.1996.0093

Coll, M., and Libralato, S. (2012). Contributions of Food-Web Modelling for an Ecosystem Approach of Marine Resource Management in the Mediterranean Sea. *Fish. Fish.* 13, 60–88. doi: 10.1111/j.1467-2979.2011.00420.x

Coll, M., Navarro, J., Olson, R. J., and Christensen, V. (2013). Assessing the Trophic Position and Ecological Role of Squids in Marine Ecosystems by Means of Food-Web Models. *Deep Sea Res. II* 95, 21–36. doi: 10.1016/j.dsr2.2012.08.020

Company, J. B., Puig, P., Sardà, F., Palanques, A., Latasa, M., and Scharek, R. (2008). Climate Influence on Deep Sea Populations. *PloS One* 3 (1), e1431. doi: 10.1371/journal.pone.0001431

Cossarini, G., Feudale, L., Teruzzi, A., Bolzon, G., Coidessa, G., Solidoro, C., et al. (2021). High-Resolution Reanalysis of the Mediterranean Sea Biogeochemistry, (1999–2019). *Front. Mar. Sci.* 8. doi: 10.3389/fmars.2021.741486

Cresson, P., Chouvelon, T., Bustamante, P., Bănaru, D., Baudrier, J., Le Loc'h, F., et al. (2020). Primary Production and Depth Drive Different Trophic Structure and Functioning of Fish Assemblages in French Marine Ecosystems. *Prog. Oceanogr.* 186, 102343. doi: 10.1016/j.pocean.2020.102343

De Lazzari, A., Boldrin, A., Rabitti, S., and Turchetto, M. M. (1999). Variability and Downward Fluxes of Particulate Matter in the Otranto Strait Area. *J. Mar. Syst.* 20, 399–413. doi: 10.1016/S0924-7963(98)00076-1

Di Biagio, V., Cossarini, G., Salon, S., Lazzari, P., Querin, S., Sannino, G., et al. (2019). Temporal Scales of Variability in the Mediterranean Sea Ecosystem: Insight From a Coupled Model. *J. Mar. Syst.* 197, 103176. doi: 10.1016/j.jmarsys.2019.05.002

D'Onghia, G., Calculli, E., Capezzuto, F., Carlucci, R., Carluccio, A., Maiorano, P., et al. (2016). New Records of Cold-Water Coral Sites and Fish Fauna Characterization of a Potential Network Existing in the Mediterranean Sea. *Mar. Ecol.* 37, 1398–1422. doi: 10.1111/maec.12356

D'Onghia, G., Capezzuto, F., Cardone, F., Carlucci, R., Carluccio, A., Chimienti, G., et al. (2015). Macro- and Megafauna Recorded in the Submarine Bari Canyon (Southern Adriatic, Mediterranean Sea) Using Different Tools. *Mediterr. Mar. Sci.* 16 (1), 180–196. doi: 10.12681/mms.1082

D'Onghia, G., Capezzuto, F., Mytilineou, Ch., Maiorano, P., Kapiris, K., Carlucci, R., et al. (2005). Comparison of the Population Structure and Dynamics of *Aristeus Antennatus* (Risso 1816) Between Exploited and Unexploited Areas in the Mediterranean Sea. *Fish Res.* 76 (1), 22–38. doi: 10.1016/j.fishres.2005.05.007

D'Onghia, G., Giove, A., Maiorano, P., Carlucci, R., Minerva, M., Capezzuto, F., et al. (2012). Exploring Relationships Between Demersal Resources and

Environmental Factors in the Ionian Sea (Central Mediterranean). *J. Mar. Biol.* 2012, 279406. doi: 10.1155/2012/279406

D'Onghia, G., Indennidate, A., Giove, A., Savini, A., Capezzuto, F., Sion, L., et al. (2011). Distribution and Behaviour of the Deep-Sea Benthopelagic Fauna Observed Using Towed Cameras in the Santa Maria Di Leuca Cold Water Coral Province. *Mar. Ecol. Prog. Ser.* 443, 95–110. doi: 10.3354/meps09432

D'Onghia, G., Maiorano, P., Capezzuto, F., Carlucci, R., Battista, D., Giove, A., et al. (2009). Further Evidences of Deep-Sea Recruitment of *Aristeus Antennatus* (Crustacea: Decapoda) and its Role in the Population Renewal on the Exploited Bottoms of the Mediterranean. *Fish. Res.* 95, 236–245. doi: 10.1016/j.fishres.2008.09.025

D'Onghia, G., Tursi, A., Maiorano, P., Matarrese, A., and Panza, M. (1998). Demersal Fish Assemblages From the Bathyal Grounds of the Ionian Sea (Middle-Eastern Mediterranean). *Ital. J. Zool.* 65, 287–292. doi: 10.1080/11250009809386834

D'Ortenzio, F., Ragni, M., Marullo, S., and Ribera d'Alcalà, M. (2003). Did Biological Activity in the Ionian Sea Change After the Eastern Mediterranean Transient? Results From the Analysis of Remote Sensing Observations. *J. Geophys Res.* 108 (9), 20. doi: 10.1029/2002JC001556

Doubleday, Z. A., Prowse, T. A. A., Arkhipkin, A., Pierce, G. J., Semmens, J., Steer, M., et al. (2016). Global Proliferation of Cephalopods. *Curr. Biol.* 26, R406–R407. doi: 10.1016/j.cub.2016.04.002

Drazen, J. C., and Sutton, T. T. (2017). Dining in the Deep: The Feeding Ecology of Deep-Sea Fishes. *Annu. Rev. Mar. Sci.* 9,1, 337–366. doi: 10.1146/annurev-marine-010816-060543

Duffill Telsnig, J. I., Jennings, S., Mill, A. C., Walker, N. D., Parnell, A. C., and Polunin, N. V. C. (2019). Estimating Contributions of Pelagic and Benthic Pathways to Consumer Production in Coupled Marine Food Webs. *J. Anim. Ecol.* 88, 405–415. doi: 10.1111/1365-2656.12929

Fernandez–Arcaya, U., Ramirez-Llodra, E., Aguzzi, J., Allcock, A. L., Davies, J. S., Dissanayake, A., et al. (2017). Ecological Role of Submarine Canyons and Need for Canyon Conservation: A Review. *Front. Mar. Sci.* 4. doi: 10.3389/fmars.2017.00005

Fortibuoni, T., Bahri, T., Camilleri, M., Garofalo, G., Gristina, M., and Fiorentino, F. (2010). Nursery and Spawning Areas of Deep-Water Rose Shrimp, *Parapenaeus Longirostris* (Decapoda: Penaeidae), in the Strait of Sicily (Central Mediterranean Sea). *J. Crustac. Biol.* 30, 167–174. doi: 10.1651/09-3167.1

Freiwald, A., Beuck, L., Rüggeberg, A., Taviani, M., and Hebbeln, D. (2009). The White Coral Community in the Central Mediterranean Sea Revealed by ROV Surveys. *Oceanography* 22, 58–74. doi: 10.5670/oceanog.2009.06

Froese, R., and Pauly, D. (2021). *FishBase. World Wide Web Electronic Publication*. Available at: www.fishbase.org.

Gačić, M., Borzelli, G. L. E., Civitarese, G., Cardin, V., and Yari, S. (2010). Can Internal Processes Sustain Reversals of the Ocean Upper Circulation? The Ionian Sea Example. *Geophys. Res. Lett.* 37, L09608. doi: 10.1029/2010GL043216

Griffiths, J. R., Kadin, M., Nascimento, F. J. A., Tamelander, T., Törnroos, A., Bonaglia, S., et al. (2017). The Importance of Benthic–Pelagic Coupling for Marine Ecosystem Functioning in a Changing World. *Glob Change Biol.* 23, 2179–2196. doi: 10.1111/gcb.13642

Halpin, P. N., Read, A. J., Fujioka, E., Best, B. D., Donnelly, B., Hazen, L. J., et al. (2009). OBIS-SEAMAP: The World Data Center for Marine Mammal, Sea Bird and Sea Turtle Distributions. *Oceanography* 22 (2), 104–115. doi: 10.5670/oceanog.2009.42

Heymans, J. J., Coll, M., Libralato, S., Morissette, L., and Christensen, V. (2014). Global Patterns in Ecological Indicators of Marine Food Webs: A Modelling Approach. *PloS One* 9 (4), e95845. doi: 10.1371/journal.pone.0095845

Heymans, J. J., Coll, M., Link, J. S., Mackinson, S., Steenbeek, J., Walters, C., et al. (2016). Best Practice in Ecopath With Ecosim Food-Web Models for Ecosystem-Based Management. *Ecol. Modell.* 331, 173–184. doi: 10.1016/j.ecolmodel.2015.12.007

Hure, M., and Mustać, B. (2020). Feeding Ecology of *Sardina Pilchardus* Considering Co-Occurring Small Pelagic Fish in the Eastern Adriatic Sea. *Mar. Biodivers.* 50, 40. doi: 10.1007/s12526-020-01067-7

Jereb, P., Allcock, A. L., Lefkaditou, E., Piatkowski, U., Hastie, L. C., and Pierce, G. J. (Eds.) (2015). "Cephalopod Biology and Fisheries in Europe: II. Species Accounts," in *ICES Cooperative Research Report No. 325*, (Copenaghen, Denmark), 360 pp. doi: 10.17895/ices.pub.5493

Kapiris, K., Thessalou-Legaki, M., Petrakis, G., and Conides, A. (2010). Ontogenetic Shifts and Temporal Changes the Trophic Patterns of Deep-Sea Red Shrimp A. Foliacea (Decapods, Aristeidae) in the E. Ionian Sea (E. Mediterranean). *Mar. Ecol.* 31 (2), 341–354. doi: 10.1111/j.1439-0485.2009.00344.x

Kiljunen, M., Peltonen, H., Lehtiniemi, M., Uusitalo, L., Sinisalo, T., Norkko, J., et al. (2020). Benthic-Pelagic Coupling and Trophic Relationships in Northern Baltic Sea Food Webs. *Limnol. Oceanogr.* 65, 1706–1722. doi: 10.1002/lno.11413

Klein, B., Roether, W., Manca, B. B., Bregant, D., Beitzel, V., Kovacevic, V., et al. (1999). The Large Deep Water Transient in the Eastern Mediterranean. *Deep Sea Res. I* 46 (3), 371–414. doi: 10.1016/S0967-0637(98)00075-2

Lassalle, G., Lobry, J., Le Loc'h, F., Bustamante, P., Certain, G., Delmas, D., et al. (2011). Lower Trophic Levels and Detrital Biomass Control the Bay of Biscay Continental Shelf Food Web: Implications for Ecosystem Management. *Progr. Oceanogr.* 91, 561–575. doi: 10.1016/j.pocean.2011.09.002

Lavigne, H., Civitarese, G., Gačić, M., and D'Ortenzio, F. (2018). Impact of Decadal Reversals of the North Ionian Circulation on Phytoplankton Phenology. *Biogeosciences* 15, 4431–4445. doi: 10.5194/bg-15-4431

Lazzari, P., Solidoro, C., Ibello, V., Salon, S., Teruzzi, A., Béranger, K., et al. (2012). Seasonal and Inter-Annual Variability of Plankton Chlorophyll and Primary Production in the Mediterranean Sea: A Modelling Approach. *Biogeosciences* 9, 217–233. doi: 10.5194/bg-9-217-2012

Libralato, S., Christensen, V., and Pauly, D. (2006). A Method for Identifying Keystone Species in Food Web Models. *Ecol. Modell.* 195 (3–4), 153–171. doi: 10.1016/j.ecolmodel.2005.11.029

Link, J. S. (2010). Adding Rigor to Ecological Network Models by Evaluating a Set of Pre-Balance Diagnostics: A Plea for PREBAL. *Ecol. Model.* 221, 1582–1593. doi: 10.1016/j.ecolmodel.2010.03.012

Liu, F., Mikolajewicz, U., and Six, K. D. (2021). Drivers of the Decadal Variability of the North Ionian Gyre Upper Layer Circulation During 1910–2010: A Regional Modelling Study. *Clim Dyn.* 58, 2065–2077. doi: 10.1007/s00382-021-05714-y

Lorance, P., and Trenkel, V. M. (2006). Variability in Natural Behaviour, and Observed Reactions to an ROV, by Mid-Slope Fish Species. *J. Exp. Mar. Biol. Ecol.* 332 (1), 106–119. doi: 10.1016/j.jembe.2005.11.007

Madurell, T., and Cartes, J. E. (2005). Trophodynamics of a Deep-Sea Demersal Fish Assemblage From the Bathyal Eastern Ionian Sea (Mediterranean Sea). *Deep Sea Res. I* 52, 2049–2064. doi: 10.1016/j.dsr.2005.06.013

Madurell, T., and Cartes, J. E. (2006). Trophic Relationships and Food Consumption of Slope Dwelling Macrourids From the Bathyal Ionian Sea (Eastern Mediterranean). *Mar. Biol.* 148 (6), 1325–1338. doi: 10.1007/s00227-005-0158-3

Maiorano, P., D'Onghia, G., Capezzuto, F., and Sion, L. (2002). Life History Traits of *Plesionika Martia* (Decapoda: Caridea) From the Eastern-Central Mediterranean Sea. *Mar Biol.* 141, 527–539. doi: 10.1007/s00227-002-0851-4

Maiorano, P., Sion, L., Carlucci, R., Capezzuto, F., Giove, A., Costantino, G., et al. (2010). The Demersal Faunal Assemblage of the North-Western Ionian Sea (Central Mediterranean): Current Knowledge and Perspectives. *Chem. Ecol.* 26, 219–240. doi: 10.1080/02757541003693987

Mazzocchi, M. G., Nervegna, D., D'Elia, G., Di Capua, I., Aguzzi, L., and Boldrin, A. (2003). Spring Mesozooplankton Communities in the Epipelagic Ionian Sea in Relation to the Eastern Mediterranean Transient. *J. Geophys. Res.* 108, 8114. doi: 10.1029/2002JC001640

Menna, M., Suarez, N. R., Civitarese, G., Gačić, M., Rubino, A., and Poulain, P. M. (2019). Decadal Variations of Circulation in the Central Mediterranean and its Interactions With Mesoscale Gyres. *Deep Sea Res. II* 164, 14–24. doi: 10.1016/j.dsr2.2019.02.004

Mussap, G., and Zavatarelli, M. (2017). A Numerical Study of the Benthic–Pelagic Coupling in a Shallow Shelf Sea (Gulf of Trieste). *Reg. Stud. Mar. Sci.* 9, 24–34. doi: 10.1016/j.rsma.2016.11.002

Palomares, M. L. D., and Pauly, D. (2021) *SeaLifeBase. World Wide Web Electronic Publication*. Available at: www.sealifebase.org.

Pauly, D., Christensen, V., and Walters, C. (2000). Ecopath, Ecosim, and Ecospace as Tools for Evaluating Ecosystem Impact of Fisheries. *ICES J. Mar. Sci.* 57, 697–706. doi: 10.1006/jmsc.2000.0726

Pikitch, E. K., Santora, C., Babcock, E. A., Bakun, A., Bonfil, R., Conover, D. O., et al. (2004). Ecology. Ecosystem-Based Fishery Management. *Science* 305, 346–347. doi: 10.1126/science.1098222

Pipitone, C., and Andaloro, F. (1995). Food and Feeding Habits of Juvenile Greater Amberjack, *Seriola Dumerili* Osteichthyes, Carangidae in Inshore Waters of the Central Mediterranean Sea. *Cybium* 193, 305–310.

Pitt, K. A., Clement, A.-L., Connolly, R. M., and Thibault-Botha, D. (2008). Predation by Jellyfish on Large and Emergent Zooplankton: Implications for Benthic-Pelagic Coupling. *Estuar. Coast. Shelf Sci.* 76, 827–833. doi: 10.1016/j.ecss.2007.08.011

Raffaelli, D., Bell, E., Weithoff, G., Matsumoto, A., Cruz-Motta, J. J., Kershaw, P., et al. (2003). The Ups and Downs of Benthic Ecology: Considerations of Scale, Heterogeneity, and Surveillance for Benthic–Pelagic Coupling. *J. Exp. Mar. Biol. Ecol.* 285–286, 191–203. doi: 10.1016/S0022-0981(02)00527-0

Relini, M., Maiorano, P., D'Onghia, G., Orsi Relini, L., Tursi, A., and Panza, M. (2000). A Pilot Experiment of Tagging the Deep Shrimp *Aristeus Antennatus* (Risso 1816). *Sci. Mar.* 64 (3), 357–361. doi: 10.3989/scimar.2000.64n3357

Ricci, P., Ingrosso, M., Carlucci, R., Fanizza, C., Maglietta, R., Santacesaria, F. C., et al. (2020). "Quantifying the Dolphins-Fishery Competition in the Gulf of Taranto (Northern Ionian Sea, Central Mediterranean Sea)," in *MetroSea 2020 - TC19 International Workshop on Metrology for the Sea* (Naples, Italy), pp.94–99.

Ricci, P., Libralato, S., Capezzuto, F., D'Onghia, G., Maiorano, P., Sion, L., et al. (2019). Ecosystem Functioning of Two Marine Food Webs in the North-Western Ionian Sea (Central Mediterranean Sea). *Ecol. Evol.* 9, 10198–10212. doi: 10.1002/ece3.552

Riccioni, G., Stagioni, M., Piccinetti, C., and Libralato, S. (2018). A Metabarcoding Approach for the Feeding Habits of European Hake in the Adriatic Sea. *Ecol. Evol.* 8, 10435–10447. doi: 10.1002/ece3.4500

Ricci, P., Sion, L., Capezzuto, F., Cipriano, G., D'Onghia, G., and Libralato, S. (2021). Modelling the Trophic Roles of the Demersal Chondrichthyes in the Northern Ionian Sea (Central Mediterranean Sea). *Ecol. Modell.* 444, 109468. doi: 10.1016/j.ecolmodel.2021.109468

Rodil, I. F., Lucena-Moya, P., Tamelander, T., Norkko, J., and Norkko, A. (2020). Seasonal Variability in Benthic–Pelagic Coupling: Quantifying Organic Matter Inputs to the Seafloor and Benthic Macrofauna Using a Multi-Marker Approach. *Front. Mar. Sci.* 7, 404. doi: 10.3389/fmars.2020.00404

Rosas-Luis, R., Villanueva, R., and Sánchez, P. (2014). Trophic Habits of the Ommastrephid Squid *Illex Coindetii* and *Todarodes Sagittatus* in the Northwestern Mediterranean Sea. *Fish. Res.* 152, 21–28. doi: 10.1016/j.fishres.2013.10.009

Rossi, S., and Gabbianelli, G. (1978). Geomorfologia Del Golfo Di Taranto. *Boll. Soc Geol. It.* 97, 423–437.

Sardà, F., Company, J. B., Bahamón, N., Rotllant, G., Flexas, M. M., Sánchez, J. D., et al. (2009). Relationship Between Environment and the Occurrence of the Deep-Water Rose Shrimp *Aristeus Antennatus* (Risso 1816) in the Blanes Submarine Canyon (NW Mediterranean). *Prog. Oceanogr.* 824, 227–238. doi: 10.1016/j.pocean.2009.07.001

Sardà, F., D'Onghia, G., Politou, C.-Y., Company, J. B., Maiorano, P., and Kapiris, K. (2004). Maximum Deep-Sea Distribution and Ecological Aspects of *Aristeus Antennatus* in the Western and Central Mediterranean Sea. *Sci. Mar.* 68 (3), 117–127. doi: 10.3989/scimar.2004.68s3117

Shiffman, D. S., Gallagher, A. J., Boyle, M. D., Hammerschlag-Peyer, C. M., and Hammerschlag, N. (2012). Stable Isotope Analysis as a Tool for Elasmobranch Conservation Research: A Primer for non-Specialists. *Mar. Freshw. Res.* 63, 635–643. doi: 10.1071/MF11235

Simão, D. S., Zas, E., Carbonell, A., and Abelló, P. (2015). Pasiphaeid Shrimps in the Western Mediterranean: Geographical Variability in Distribution and Population Patterns. *Sci. Mar.* 79 (2), 199–209. doi: 10.3989/scimar.04147.07A

Sion, L., Calculli, C., Capezzuto, F., Carlucci, R., Carluccio, A., Cornacchia, L., et al. (2019). Does the Bari Canyon (Central Mediterranean) Influence the Fish Distribution and Abundance? *Progr. Oceanogr.* 170, 81–92. doi: 10.1016/j.pocean.2018.10.015

Spedicato, M. T., Massutí, E., Mérigot, B., Tserpes, G., Jadaud, A., and Relini, G. (2019). The MEDITS Trawl Survey Specifications in an Ecosystem Approach to Fishery Management. *Sci. Mar.* 83 (S1), 9–20. doi: 10.3989/scimar.04915.11X

Taricco, C., Alessio, S., Rubinetti, S., Zanchettin, D., Cosoli, S., Gačić, M., et al. (2015). Marine Sediments Remotely Unveil Long-Term Climatic Variability Over Northern Italy. *Sci. Rep.* 5, 12111. doi: 10.1038/srep12111

Taviani, M., Freiwald, A., and Zibrowius, H. (2005). "Deep Coral Growth in the Mediterranean Sea: An Overview," in *Erlangen Earth Conference Series* (Berlin, Heidelberg: Springer). doi: 10.1007/3-540-27673-4_7

Trueman, C. N., Johnston, G., O'Hea, B., and MacKenzie, K. M. (2014). Trophic Interactions of Fish Communities at Midwater Depths Enhance Long-Term Carbon Storage and Benthic Production on Continental Slopes. *Proc. R. Soc B* 281, 20140669. doi: 10.1098/rspb.2014.0669

Ulanowicz, R. E., and Puccia, C. J. (1990). Mixed Trophic Impacts in Ecosystems. *Coenoses* 5, 7–16.

Vassallo, P., D'Onghia, G., Fabiano, M., Maiorano, P., Lionetti, A., Paoli, C., et al. (2017). A Trophic Model of the Benthopelagic Fauna Distributed in the Santa Maria Di Leuca Cold-Water Coral Province (Mediterranean Sea). *Energy Ecol. Environ.* 2, 114–124. doi: 10.1007/s40974-016-0047-2

Wang, S. C., Liu, X., Liu, Y., and Wang, H. Z. (2020). Benthic-Pelagic Coupling in Lake Energetic Food Webs. *Ecol. Model.* 417, 108928. doi: 10.1016/j.ecolmodel.2019.108928

Zorica, B., Čikeš Keč, V., Vidjak, O., Kraljević, V., and Krzulja, G. (2017). Seasonal Pattern of Population Dynamics, Spawning Activities, and Diet Composition of Sardine (*Sardina Pilchardus* Walbaum) in the Eastern Adriatic Sea. *Turk J. Zool* 41, 892–900. doi: 10.3906/zoo-1609-27

Conflict of Interest: The authors declare that the research was conducted in the absence of any commercial or financial relationships that could be construed as a potential conflict of interest.

frontiers | Frontiers in Marine Science

REVIEW
published: 19 May 2022
doi: 10.3389/fmars.2022.886335

Benthic–Pelagic Coupling in the Oligotrophic Eastern Mediterranean: A Synthesis of the HYPOXIA Project Results

Panagiotis D. Dimitriou[1]*, *Ioulia Santi*[2,3], *Manos L. Moraitis*[4], *Irini Tsikopoulou*[1,5], *Paraskevi Pitta*[2] *and Ioannis Karakassis*[1]

[1] Department of Biology, Marine Ecology Laboratory, University of Crete, Heraklion, Greece, [2] Hellenic Centre for Marine Research, Institute of Oceanography, Heraklion, Greece, [3] Hellenic Centre for Marine Research, Institute of Marine Biology, Biotechnology and Aquaculture, Heraklion, Greece, [4] Cyprus Marine and Maritime Institute, Larnaca, Cyprus, [5] Hellenic Centre for Marine Research, Institute of Marine Biological Resources and Inland Waters, Heraklion, Greece

OPEN ACCESS

Edited by:
Tamara Cibic, Istituto Nazionale di Oceanografia e di Geofisica Sperimentale, Italy

Reviewed by:
Christian Henri Nozais, Université du Québec à Rimouski, Canada
Vivianne Solis-Weiss, National Autonomous University of Mexico, Mexico

***Correspondence:**
Panagiotis D. Dimitriou
pdimitriou@uoc.gr

Specialty section:
This article was submitted to Marine Ecosystem Ecology, a section of the journal Frontiers in Marine Science

Received: *28 February 2022*
Accepted: *20 April 2022*
Published: *19 May 2022*

Citation:
Dimitriou PD, Santi I, Moraitis ML, Tsikopoulou I, Pitta P and Karakassis I (2022) Benthic–Pelagic Coupling in the Oligotrophic Eastern Mediterranean: A Synthesis of the HYPOXIA Project Results. Front. Mar. Sci. 9:886335. doi: 10.3389/fmars.2022.886335

Benthic–pelagic coupling studies have shown that the response of the benthic system to eutrophication is subject to complex nonlinear dynamics with specific thresholds beyond which abrupt changes in the response of the ecosystem occur and time lags between inputs and responses. The "HYPOXIA: *Benthic–pelagic coupling and regime shifts*" project aimed to investigate how nutrient input in the water column results in ecological processes of eutrophication, which may lead to significant, irreversible changes in the eastern Mediterranean marine ecosystems within a short period of time. The project included analysis of historical water and benthic data, field sampling, and mesocosm experiments. From the project results, it can be concluded that nutrient inputs are quickly capitalized by small phytoplankton species in the water column resulting in the bloom of specific species with high nutrient uptake capabilities. When Eutrophic Index values (calculated using nutrient and chlorophyll-*a* concentrations) cross the moderate-to-poor threshold, the precipitating organic matter can cause observable effects on the benthic system. Depending on eutrophication intensity and persistence, the effects can start from microbenthos, meiofauna, and macrofauna increase in abundance and biomass to significant changes in the community structure. The latter includes the proliferation of macrofaunal opportunistic species, an increase in deposit feeders, and the high risk of ecosystem quality degradation. However, contrary to other regions of the world, no water hypoxia or benthic dead zones were observed as chlorophyll-*a* and O_2 concentrations showed a positive correlation. This is caused by the high photosynthetic activity of the phytoplankton and microphytobenthos, the increased bioturbation of macrofauna, and the increased abundance of sediment deposit-feeding species, which quickly consume the excess organic matter. Eastern Mediterranean coastal ecosystems show high resilience to the adverse effects of eutrophication, preventing hypoxia and azoic conditions when eutrophication is the only source of environmental disturbance.

Keywords: benthic–pelagic coupling, eutrophication, macrofauna, ecosystem health, ecosystem processes, phytoplankton

INTRODUCTION

Traditionally, the research on eutrophication has focused mainly on phytoplankton, but it has now become obvious that eutrophication affects all components of coastal ecosystems, and it is therefore necessary to identify those impacts on both water and benthos (Duarte, 2009). Different regions around the globe show major differences regarding eutrophication effects on coastal ecosystems, with some regions being under significant pressure (i.e., Baltic Sea, the Northern gulf of Mexico, and regions in the North Atlantic) while others have localized problems (i.e., eastern Mediterranean or Australia) (Boesch, 2019). To address this issue, it is commonly accepted that management actions need to be taken to reduce nutrient loads and identify the status of the coastal ecosystems through environmental monitoring (Andersen et al., 2019).

After extensive effort in some regions facing periodic hypoxic events, a significant reduction of nutrient input has been recently reported, ranging from 25% (Chesapeake Bay) to 100% (Tampa Bay) (Duarte and Krause-Jensen, 2018). However, it is possible that even under an oligotrophication of a system, neither the chlorophyll-*a* (Chl-*a*) in the water column returns nor the benthos recovers fully to pre-conditions of hypoxia (Diaz and Rosenberg, 2008). Several studies have shown that the response of the ecosystem eutrophication is subject to complex nonlinear dynamics. According to Duarte (2009), causes for this nonlinearity are (a) occurrence of thresholds of nutrient inputs beyond which abrupt changes in the response of the ecosystem occur (e.g., hypoxia); (b) occurrence of time lags in the responses due to the accumulation and release of nutrients in the sediments or the long time spans involved in the recovery of some inherently slow-growing organisms, such as seagrasses; or (c) changes in the basis for comparison—shifting baselines (Duarte et al., 2009) altering the relationship between Chl-*a* and nutrient inputs over time.

In theory, high production of organic matter due to eutrophication in the water column causes sedimentation of particulate organic matter (POM) and increased oxygen demand, which gradually decreases the available dissolved oxygen (DO), therefore leading to benthic hypoxia. The first signs are a reduction of the layer with a positive redox potential (Eh), i.e., the depth of the Redox potential discontinuity (RPD) layer. Typically, the threshold for hypoxia used in the literature is 2 mg O_2 L^{-1} (Diaz, 2001; Diaz and Rosenberg, 2008). However, Vaquer-Sunyer and Duarte (2008), analyzing experimental data in a large number of studies for various species, found that there are significant differences between taxonomic groups regarding their tolerance to minimal oxygen availability and concluded that the number and extent of coastal ecosystems affected by hypoxia have been underestimated.

Attempts to develop quantitative benthic–pelagic coupling models are available in the literature from Graf (1992) focusing on organic carbon (Vaquer-Sunyer and Duarte, 2008) relating primary production to the rate of oxygen consumption in the sediment, organic matter (Brady et al., 2013), and different biogeochemical variables (Ubertini et al., 2012), and recently from Zhang et al. (2021) who highlighted the importance of bioturbation to benthic–pelagic coupling models. However, the most challenging issue is the identification of a eutrophication key point beyond which significant changes in the status of the benthic system are expected. Such a point has only been mentioned in Comprehensive Studies for the Purposes of Article 6 of Directive 91/271 EEC (CSTT, 1997), which states that a Chl-*a* concentration in the water column greater than 10 Mg L^{-1}, during the summer months, would be capable of causing anoxia conditions in the seabed. This value, although extensively republished, is essentially an expert judgement estimate that is not based on any published field or experimental data (Dimitriou et al., 2015).

In the water column, dissolved inorganic nutrient input (natural or anthropogenic) will likely result in a phytoplankton bloom (Bracken et al., 2015). Usually, micro-autotrophs will rapidly capitalize the available nutrients and increase their biomass, followed by species of slower metabolic dynamics (Lin et al., 2016). Furthermore, it is possible that different types of dissolved organic matter (DOM) may result in different bacterial communities (Teeling et al., 2012). Therefore, the response of different plankton communities to inorganic and/or organic nutrient addition may show significant variation (Santi et al., 2019).

Benthic macrofauna is possibly the most common biotic indicator characterizing the quality of marine ecosystems in environmental monitoring programs (Gray, 1981), because it integrates the effects that took place in time periods prior to the sampling event. The empirical model of hierarchical response to stress and the description of the succession pattern of macrofauna in gradients of organic enrichment (Pearson and Rosenberg, 1978) have been confirmed in hundreds of published papers worldwide. This general model was calibrated with values of total organic carbon (TOC) by Hyland et al. (2005) using a large global dataset. In recent years, in Europe, for the implementation of the Water Framework Directive and Marine Strategy Framework Directive, there is intense scientific interest for the study of eutrophication effects on benthos and the associated ecological status indicators in the eastern Mediterranean (ES) (Simboura and Argyrou, 2010; Pavlidou et al., 2015).

Except for macrofauna, which is now an established indicator of anthropogenic disturbance, other components of the benthic ecosystem have also been used to assess the effects of anthropogenic activities (including eutrophication) on ecosystem health, such as meiofauna (Schratzberger and Ingels, 2018) or microfauna (Aylagas et al., 2017). Furthermore, Apostolaki et al. (2007) have shown that in some habitats, the effects of disturbance on macrofauna may be limited, while at the same time (and at the same place), the impact on marine phanerogams, especially *Posidonia oceanica*, might be highly detrimental.

The "HYPOXIA: *Benthic–pelagic coupling and regime shifts*" project (2014–2016), funded by the Greek General Secretariat for Research and Technology (GSRT) in the framework of the Operational Program "Education and Lifelong Learning" of the

National Strategic Reference Framework (NSRF)—ARISTEIA II (HYPOXIA project, No. 5381), aimed to investigate how nutrient input in the water column results in ecological processes of eutrophication, which may lead to significant, irreversible changes in the benthic marine ecosystems within a short period of time. Following the suggestion of Duarte (2009), the project investigated the response of various components of the ecosystem to eutrophication and the consequently induced organic enrichment of the benthos. The inclusion of different groups of organisms and biogeochemical processes, particularly at various spatial and temporal scales, served to further shed light on different aspects of the problem.

DESCRIPTION OF THE PROJECT

The project included three independent approaches with different advantages and limitations: analysis of historical data, field sampling, and a mesocosm experiment (large enclosed experimental ecosystems). Within each approach, different components of the ecosystem were studied including plankton communities, microbial benthos, meiofaunal and macrofaunal communities, as well as environmental variables and ecological status indicators (**Table 1**).

The main objective of the analysis of historical data was to assemble a large dataset of stations, involving both water column and benthic data aiming to detect the response of the benthic system to a eutrophication gradient in the overlying water column. Overall, it included 126 sampling stations; 34 in the Ionian Sea, 68 in the Northern Aegean Sea, and 24 in the Southern Aegean or Cretan Sea (**Figure 1**). In order to reduce variability, specific inclusion criteria were set: Sediment and water had to be sampled simultaneously, with sampling taking place during spring or early summer, and more importantly, sites receiving allochthonous organic material (e.g., wastes from fish farms and sewage) were excluded from the analysis. The resulting stations were all sampled with a Niskin bottle in the water column and a 0.1 m^2 grab or a 0.05^2 box corer in the sediment. Depth ranged from 5 m to 70 m (MD = 27 ± 15 m). Chl-*a* needed to be filtered in a 0.2-Mm filter and macrofauna needed to be identified to the species level or the lowest possible taxon.

The field sampling campaign was carried out in areas with known high, medium, and low Chl-*a* concentration as classified using the Greek Chl-*a* scale (Simboura et al., 2015) and determined through remote sensing techniques. The objective was to sample different components of the marine ecosystem (benthic and planktonic) (**Table 1**), with the same sampling protocol (0.1 m^2 grab and Niskin bottles), same bottom depth (20 m), and at the same season (late spring). Overall, it included 59 sampling stations from gulfs in the Aegean Sea (**Figure 1**). The design included sampling of the water column at the surface (2 m) and bottom (20 m) depths as well as of the sediment, studying both water and benthic communities and environmental variables at the same time. The field sampling and the consecutive laboratory analyses for common variables were performed using the same sampling equipment and analytical protocols as with the historical samples.

Finally, the main objective of the mesocosm experiment was to induce a perturbation beyond the usually high levels found normally in the Aegean to assess the effects of possible extreme nutrient additions. This was achieved through a sudden and extremely high nutrient enrichment in the water column and subsequently by investigating the response (i) of prokaryotic and eukaryotic plankton to nutrient enrichment, and (ii) of different benthic communities and environmental variables to the increased OM precipitation, over a 60-day experimental duration. The mesocosms used were developed specifically for benthic–pelagic coupling experiments and included an enclosed water column part (4 m deep, total volume 1.5 m^3) and a sediment part in the bottom (0.3 m height, total volume 85 L). There were two levels of tion, codnutrient addienamed "low" (concentration after addition: 5 μM PO_4^{3-} and 30 μMNO_3^-) and "high" (concentration after addition: 10 μM PO_4^{3-} and 60 μM NO_3^-), as well as "control" mesocosms (no addition); both treatments and the control mesocosms were triplicated. The experiment took place in autumn 2014 (September–October),

TABLE 1 | Biotic and abiotic variables and communities studied in each approach of the HYPOXIA project.

		Meta-analysis	Field sampling	Mesocosm experiments	Data included in publication
Water Column	Prokaryotic plankton		+	+	(Santi et al., 2019; Santi et al., 2021)
	Eukaryotic plankton		+	+	(Santi et al., 2019; Santi et al., 2021)
	Environmental variables	+	+	+	(Dimitriou et al., 2015; Dimitriou et al., 2017b; Dimitriou et al., 2017a; Santi et al., 2019; Santi et al., 2021)
Sediment	Ecological status indicators	+	+	+	(Dimitriou et al., 2015; Dimitriou et al., 2017b; Dimitriou et al., 2017c)
	Microbenthos		+	+	(Tsikopoulou et al., 2020)
	Meiofauna			+	(Dimitriou et al., 2017b)
	Macrofauna	+	+	+	(Dimitriou et al., 2015; Moraitis et al., 2018; Moraitis et al., 2019; Moraitis and Karakassis, 2020)
	Micro-phytobenthos			+	(Tsikopoulou et al., 2020)
	Macroalgae		+		(Apostolaki et al., 2018)
	Environmental variables	+	+	+	(Dimitriou et al., 2015; Dimitriou et al., 2017b; Dimitriou et al., 2017a; Santi et al., 2019)

All data are published in the articles shown in the last column.

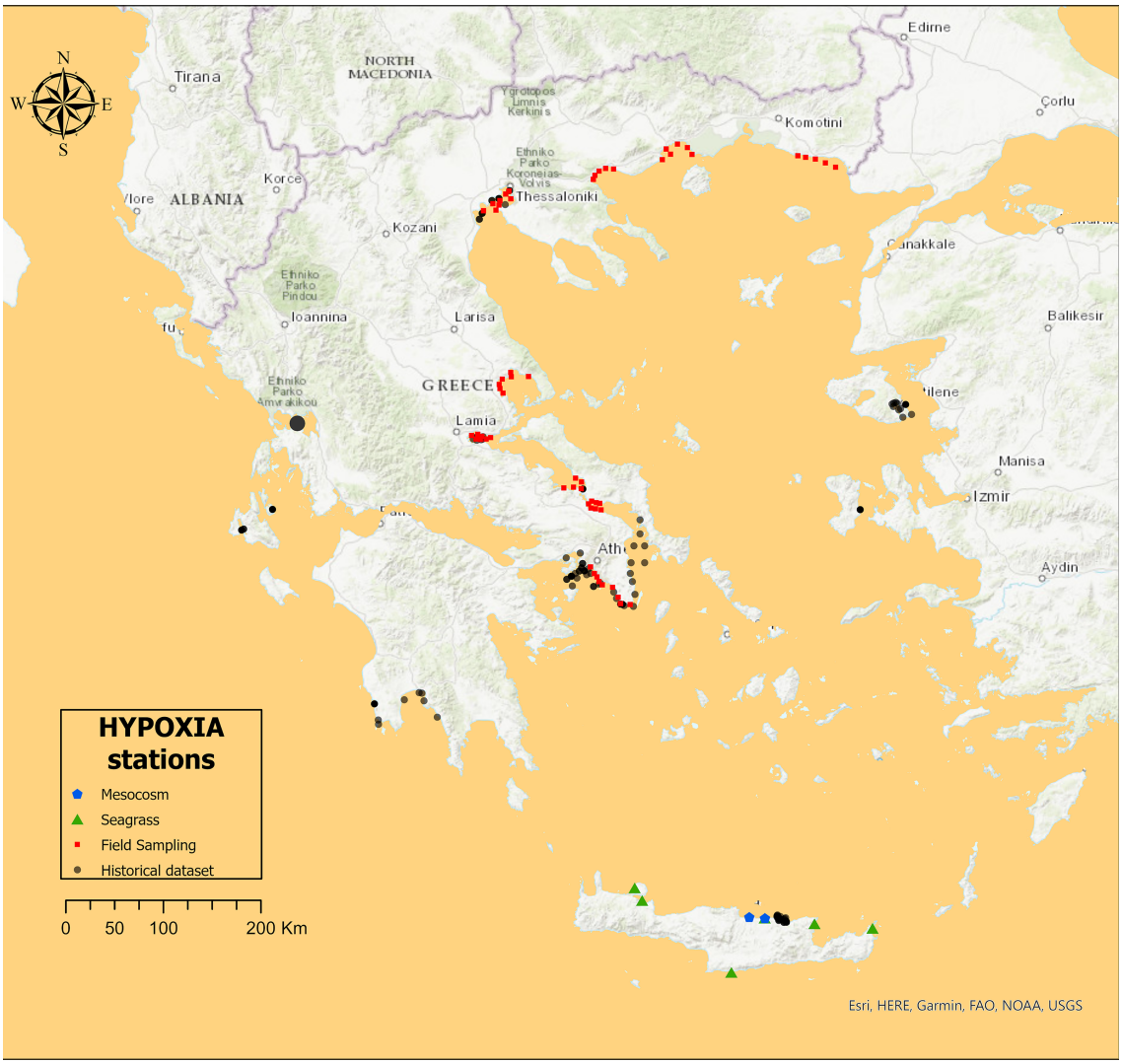

FIGURE 1 | The sampling stations included in the HYPOXIA project, in the Aegean Sea and the Ionian Sea of the east Mediterranean Sea.

in the CRETACOSM mesocosm facilities of the Hellenic Center for Marine Research in Crete. The mesocosms were filled with seawater pumped from a coastal area in the vicinity of the CRETACOSM facilities and used to fill the mesocosms. The sediment was collected from the leisure boat area of the port of Heraklion (**Figure 1**), where annual values of water column Chl-*a* concentration ranged from 0.4 Mg L^{-1} in spring to 1.4 Mg L^{-1} during autumn. Sediment was collected using a box corer, gently placed into the containers and transported to the mesocosm facilities. Water samples were collected every 3 or 6 days and sediment corers were collected every 6 days using a corer sampler design especially for this study. All laboratory analyses (**Table 1**) used the same protocols with the field sampling. See Dimitriou et al. (2017b) for more details about the mesocosm design and sampling methodology, and see Dimitriou et al. (2017a) and Santi et al. (2019) for laboratory protocols.

KEY FINDINGS IN EACH APPROACH

Historical Data Analysis

Analysis of historical data from 126 coastal sites in the Aegean Sea and the Ionian Sea (Greece) revealed a negative correlation of the water column variables measuring eutrophication Chl-*a* scale (Simboura et al., 2012) and Eutrophic Index (EI) (Primpas et al., 2010) with the Eh of underlying marine sediments as well as the ES, as measured by means of benthic macrofauna. Macrofaunal opportunistic species abruptly increased in abundance (the stations being classified as poor or bad ES) after the threshold of moderate to poor ES was crossed in the water column, using Chl-*a* or EI as indicators. The most important finding was that no hypoxia was detected in any of these stations and that DO was positively correlated to water Chl-*a* concentration [i.e., highly eutrophic stations had high DO availability in the benthic

boundary layer (BBL)]. Furthermore, despite the fact that Eh had a negative correlation to Chl-*a*, the lowest value recorded was −122 mV, a value suboxic but higher than Eh values recorded in studies focusing on organic enrichment with allochthonous OM from other sources such as aquaculture (Papageorgiou et al., 2010) or ports (Chatzinikolaou et al., 2018) in nearby regions.

Field Sampling

The results of the field sampling showed that despite the high Chl-*a* content in the water column (ranging from 0.06 to 2.04 Mg L^{-1}) and from poor to good ES using the EI index, the DO at the BBL was in all cases above standard hypoxia levels and again positively correlated to the Chl-*a* concentration (Moraitis et al., 2018). Measured Chl-*a* was within the range recorded in the east Mediterranean in the context of monitoring programs. The plankton community was dominated by pico- and micro-planktonic groups with high nutrient uptake capability (Santi, 2019). The composition of the microbial plankton community was significantly different between the high and low Chl-*a* areas and the high Chl-*a* areas were characterized by low diversity (Santi, 2019).

In the sediment, the majority of the stations were classified by high sand content (mud content ranged from 5% to 20%). The change in trophic conditions was reflected on sediment Eh (−20 to +380 mV) with a negative correlation to Chl-*a*. However, the benthic macrofaunal community ES classified using the BQI_Family index (Dimitriou et al., 2012) was found good in the vast majority of the sampling stations, with ES indications for benthos changing to unacceptable conditions again, only after EI values of the overlying water crossed to poor indication (Moraitis et al., 2015). Eutrophication affected the benthic community by favoring the settlement of certain species: The abundance of the bivalve *Corbula gibba*, a tolerant to disturbance deposit feeder with high bioturbation potential, increased in all eutrophic areas. Another bivalve, *Flexopecten hyalinus*, a sensitive species endemic to the Mediterranean Sea, was found only in oligotrophic conditions related mainly to other environmental variables like increased salinity (Moraitis et al., 2018) and temperature (Moraitis et al., 2019), indicating the close relation between eutrophication and climate change. To further support this point, Moraitis and Karakassis (2020) suggested that when studying the structure of macrofaunal communities under a eutrophication gradient, the replacement component was more important than the richness component, indicating that species substitution (i.e., replacement) rather than richness difference is the main driver defining the macrobenthic community structure along the gradient, mirroring the pelagic environmental conditions at each region.

Contrary to macrobenthos, *P. oceanica* meadows, a highly sensitive and protected ecosystem in the Mediterranean, was affected by eutrophication (Apostolaki et al., 2018). In more detail, nutrient availability and eutrophication conditions in the water column was found to be closely related to the sulfide intrusion in the shoot of *P. oceanica* and other seagrasses. However, under the pressure of moderate eutrophication, there is detectable sulfide intrusion, in the shoots of the plant, despite the fact that the structure of the plant did not seem to be affected. Seagrasses can minimize sulfide intrusion, *via* reoxidation of sulfide in the rhizosphere or in the plant aerenchyma, or tolerate sulfides, *via* incorporation of sulfur in the plant tissue (Hasler-Sheetal and Holmer, 2015). Notably, in those stations, the BBL was well oxygenated, as well as the upper layer of the sediment, indicating high levels of sulfide reoxidation. Similarly to macrofauna, the plants can tolerate medium eutrophication; however, they were under pressure, making them vulnerable to degradation.

Mesocosms

Over the experimental duration, water temperature ranged from 24 to 19°C and light illuminance ranged from 1,000 lx to 4,000 lx at 1-m depth and from 2,500 to 15,000 lx at 3.5-m depth measured at noon (Dimitriou et al., 2017b). After the initial addition, both nutrient concentrations were several times higher than the usual coastal concentrations. In both treatments, nutrients were quickly consumed by autotrophic plankton causing several blooms and Chl-*a* maxima (approximately 8 Mg L^{-1}, in both treatments). In the "low" treatment, nutrients were depleted after day 18. However, in the "high" treatment, concentrations of both nutrients did not fall below 0.5 MM until the end of the experiment (60 days). Chl-*a* and POC sedimentation rates were similar for both enriched treatments and maximized on day 24. However, after day 24, the rate was constantly higher in the high treatment, reaching a second maximum on day 24. DO concentration in the BBL at 4-m depth showed no water hypoxia during the whole experiment; DO was positively correlated to Chl-*a*. The EI showed constantly bad ES in the high treatment, whereas the low treatment started in bad ES, switched to poor (after day 21), and then to moderate (after day 30; (Dimitriou et al., 2017b).

Autotrophic nanoflagellates dominated the beginning of the first bloom, during the peak of nutrients (days 2–3), in both treatments. Later, during the second bloom (days 12–18), all autotrophic groups were present but pico- and nano-autotrophs dominated the community (Santi et al., 2019). Towards the end of the second bloom, the treatments clearly differentiated with micro-autotrophs (diatoms and dinoflagellates) increasing in the "low" treatment and nano-autotrophs prevailing in the Chl-*a* in the "high" treatment. A grazing effect on autotrophic nanoflagellates during the second bloom was hinted, and there was an important decrease of *Synechococcus* towards the end of the experiment (after day 21) in the "high" treatment (Santi et al., 2019).

In both enriched treatments, there was a transition from heterotrophic bacteria species of less-dynamic lifestyles, common in oligotrophic waters, like *Pelagibacter* (Teeling et al., 2016), to fast-growing species of the Bacteroidetes phylum, which are favored by phytoplankton-derived organic matter (Teeling et al., 2012). In addition, a Bacillariophyta-dominated community shifted to larger Dinoflagellata species and Haptophytes in both treatments. The high-nutrient treatment sustained for a prolonged time bacterial populations characterized by rapid metabolic rates, fast-growth capacities, and efficient nutrient uptake, such as Rhodobacteraceae and Flavobacteriaceae. The presence of Actinobacteria was also

distinctive to the "high" treatment, possibly due to their ability to effectively escape grazing (Santi et al., 2019).

Sediment OM started to respond to the increased precipitation of OM after a time lag of 12 and 18 days in low and high treatments, respectively, reaching a maximum on day 24, while redox potential (Eh) started to decrease after a time lag of 30 days with sulfide production recorded 5 cm deep within the sediment. The pattern was similar in both enriched treatments; however, the effect was stronger in the high mesocosms where the sediment became temporarily hypoxic after 50 experimental days and recovered on day 60 (Dimitriou et al., 2017a).

Sediment heterotrophic bacteria quickly increased in abundance at the beginning of the experiment, responding to the initial high availability of OM, in both treatments (Tsikopoulou et al., 2020). However, in the high treatment, bacterial abundance decreased after the maximum value recorded, as a result of predation by bacteria eating benthic meiofaunal species. Benthic meiofauna abundance and diversity steadily increased over the experimental duration, with the high addition showing higher values (Dimitriou et al., 2017b). Specific polychaete macrofaunal species (species *Paradoneis lyra, Chaetozone setosa, Leiochone leiopygos, Monticellina dorsobranchialis*, and *Notomastus latericeus*) responded to the increased sedimentation rate in the high treatment forming a community significantly different for the low treatment in terms of abundance species composition and functional traits. Those species were characterized by fast reproduction cycles, small body sizes, sediment eating traits, and high bioturbation capabilities, as quantified by Queirós et al. (2013) using mobility and sediment reworking capability. By the end of the 60-day experiment, the macrofaunal community of the high-nutrient addition treatment had a bioturbation potential (measured by the bioturbation index; Queirós et al., 2013) three times higher than the control or the low treatment. The higher bioturbation potential of the high treatment not only contributed to the oxygenation of the sediment, keeping the Eh in oxic conditions, but also resulted in continuous resuspension of inorganic nutrients from the sediment to the water column (Dimitriou et al., 2017c). The resuspended nutrients continued to feed the water phytoplankton, resulting in several blooms. The microphytobenthic community in all mesocosms contained algal groups with high resistance to nutrient addition. In the high-nutrient addition treatment, microphytobenthic community also contributed in keeping the oxic conditions, as a significant increase in total abundance and photosynthetic activity was recorded consuming nutrients and producing O_2 (Tsikopoulou et al., 2020).

DISCUSSION

The primary objective of the HYPOXIA project, to detect hypoxic conditions due to eutrophication in the oligotrophic eastern Mediterranean, was not met. No hypoxia was detected in the field, nor was it possible to induce hypoxic conditions under the experimental manipulation, no matter how unusually high was the addition of nutrients. Usual eutrophic conditions induced Chl-*a* concentrations of 2–4 Mg L^{-1}; the maximum values recorded in all cases did not exceed 8 Mg L^{-1}, and have never exceeded the theoretical value of 10 Mg L^{-1}, which could possibly induce hypoxia. The high water clarity found (common in Mediterranean waters) enabled high DO production from photosynthesis in both the water column and over the benthos, resulting in a positive correlation between DO and Chl-*a*. On the other hand, the project succeeded in providing critical values in nutrient concentration, which may result from observable changes in sediment geochemical variables to regime shifts in macrofaunal community structure. Such values could aid in designing interventions for reducing nutrients specific at the local level in east Mediterranean as highlighted by Duarte and Krause-Jensen (2018), since they can serve at measurable targets.

In phytoplankton, nutrient uptake is regulated by factors such as cell size and shape, nutrient uptake affinity, and rate of transport mechanisms of the phytoplankton community, especially when nutrients are in excess (Lin et al., 2016). All plankton samples analyzed from both the field and mesocosm studies showed high abundance of nano-, rather than micro-autotrophs; nano-autotrophs were the first to take advantage of the nutrient addition (Santi et al., 2019), while larger cell organisms such as diatoms were not found in the field or were observed much later in the succession in the mesocosm experiments. Small plankton species are known to be quickly grazed in the water column by heterotrophic nanoflagellates and micro-zooplankton in eutrophic gulfs or in aquaculture sites (Tsagaraki et al., 2013), therefore reducing sedimentation of OM to the sediment. Furthermore, the settled OM is highly bioavailable and may be quickly consumed not only by benthic bacteria (a fact that could increase oxygen demand) but also by meiofaunal and macrofaunal species, as concluded from the mesocosm experiments (Dimitriou et al., 2017b; Dimitriou et al., 2017c).

In the end, benthic macrofauna plays a very important role in regulating the benthic–pelagic coupling link through bioturbation. Settled OM and inorganic nutrients therein are constantly remineralized and released from the sediment to the water column providing up to 80% of the needed phytoplankton nutrient requirements (Zhang et al., 2021). This was clearly observed in the mesocosm experiment where nutrients were never entirely depleted from the water column, as they were constantly resuspended from the high bioturbation potential characterizing the benthic community. As a result, the water column was in a constant high productivity–high grazing–high OM sedimentation situation, further feeding benthic meiofauna and macrofauna, which are known to rely on OM sedimentation (Herman et al., 1999; Campanyà-Llovet et al., 2017).

Through bioturbation, the available OM is distributed within the sediment, along with oxygen contributing to macrofaunal subsistence and growth (Zhang et al., 2021). In the oligotrophic eastern Mediterranean, the surplus OM was quickly consumed in both the water column and sediment and transferred up the food web.

As the word "coupling" suggests, this link works both ways. While, as previously mentioned, the settling OM and nutrients are distributed, resuspended, and consumed by benthic fauna, the settling OM affects the benthic species composition by

favoring specific biological characteristics and life strategies. Deposit feeding species, tolerant or indifferent to disturbance, are favored according to the AMBI grouping (Borja et al., 2000), forming communities characterized as either moderate, poor, or bad ES (Moraitis and Karakassis, 2020). Only when the settling OM exceeds the assimilative capacity of the benthic community (e.g., prolonged nutrient supply and maintenance of eutrophication conditions in the water column), as recorded in some stations in Dimitriou et al. (2015) and Pavlidou et al. (2019), will the Eh in the sediment then drop, favoring opportunistic species and eventually a shift towards bad ES. However, even then, no water hypoxia was recorded, preventing the total collapse of the system and dramatic regime shifts. This was recorded in the study of Dimitriou et al. (2015), who included a time series of 6 stations in the Thermaikos gulf, which were sampled before and after the start of operation of a sewage treatment plant; over a period of 5 years, ES changed from bad to moderate in the water column and from poor to good in the benthos. However, the benthic–pelagic coupling can be affected by the spatial scale of the study, the environmental characteristics, and the diversity partition that is being examined as several studies in the Eastern Mediterranean conclude (Moraitis et al., 2019; Moraitis and Karakassis, 2020).

All taxa studied throughout the project contributed in maintaining ecosystem health and good environmental status. Tett et al. (2013) suggested that ecosystem health is the result of a system's resilience, which depends on organization and vigor, in other words, the system's ability to maintain its structure (organization) and function (vigor) over time, in the face of external stress (resilience). The studied oligotrophic ecosystems had both these elements and, more specifically, (a) the organization in terms of co-adapted species and alternative trophic pathways (i.e., smaller plankton species, meiofauna-eating bacteria, deposit-feeding macrofauna, and species with high bioturbation abilities) and (b) the vigor (i.e., high primary production capability, small plankton with fast metabolism, and constant DO flux due to bioturbation), therefore forming a system with high resilience to eutrophication (external, possible anthropogenic pressure) (**Figure 2**).

As long as the threshold of poor to moderate ES in the water column is not crossed for a prolonged period of time (i.e., year round and not just during a spring or autumn bloom), the ES of the benthic community remains good. However, under constant nutrient supply and eutrophication pressure, and after a considerable time lag of at least 2 months after the initial nutrient addition, it is possible to overcome resilience and lead to a system collapse, suddenly and abruptly. This abrupt change after crossing the system's resilience threshold was initially suggested by Elliott and Quintino (2007) and Tett et al. (2007) and called the "cliff metaphor", which was later modified by Tett et al. (2013) and found to be in agreement with the data presented here. It should be noted that two key components of the oligotrophic ecosystems play a significant role in preventing benthic hypoxia and the resulting dead

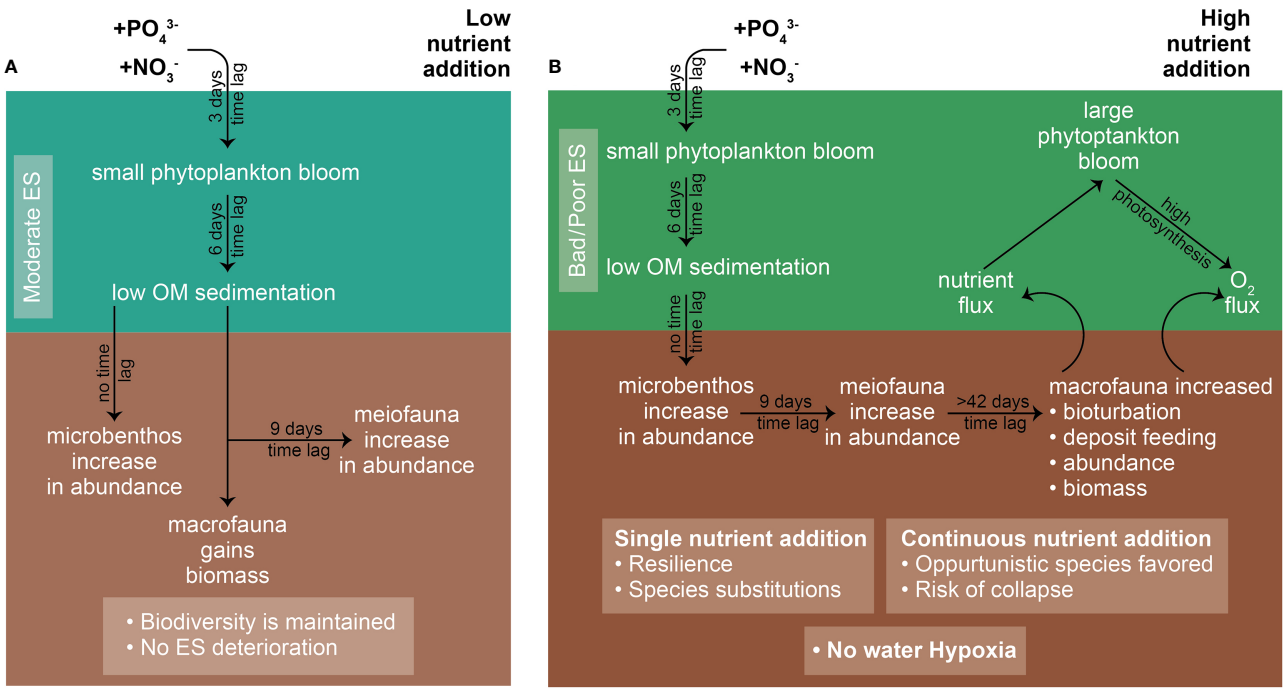

FIGURE 2 | Schematic representation of the benthic–pelagic succession pattern under two different scenarios. **(A)** Low nutrient addition. **(B)** High nutrient addition (single or continuous).

zones: the inability of the plankton system in the water column to reach Chl-*a* concentrations higher than 10 Mg L^{-1} and the high DO flux due to bioturbation, which keeps the BBL well oxygenated.

AUTHOR CONTRIBUTIONS

PD: conceptualization, investigation, writing – original draft, visualization. IS, MM, IT, VP: investigation and writing – review and editing. IK: resources, methodology, writing – review and editing

FUNDING

Thanks are due to the numerous colleagues involved in the field sampling campaign, the mesocosm experiment and the laboratory analyses. Helpful comments by two reviewers are gratefully acknowledged. The "HYPOXIA: Benthic-pelagic coupling and regime shifts" project (2014-2016), was funded by the Greek General Secretariat for Research and Technology (GSRT) in the framework of the Operational Program "Education and Lifelong Learning" of the National Strategic Reference Framework (NSRF) – ARISTEIA II (HYPOXIA project, No 5381).

REFERENCES

Andersen, J. H., Carstensen, J., Holmer, M., Krause-Jensen, D., and Richardson, K. (2019). Editorial: Research and Management of Eutrophication in Coastal Ecosystems. *Front. Mar. Sci.* 6. doi: 10.3389/fmars.2019.00768

Apostolaki, E. T., Holmer, M., Santinelli, V., and Karakassis, I. (2018). Species-Specific Response to Sulfide Intrusion in Native and Exotic Mediterranean Seagrasses Under Stress. *Mar. Environ. Res.* 134, 85–95. doi: 10.1016/j.marenvres.2017.12.006

Apostolaki, E. T., Tsagaraki, T., Tsapakis, M., and Karakassis, I. (2007). Fish Farming Impact on Sediments and Macrofauna Associated With Seagrass Meadows in the Mediterranean. *Estuar. Coast. Shelf. Sci.* 75 (3), 408–416. doi: 10.1016/j.ecss.2007.05.024

Aylagas, E., Borja, MÁ., Tangherlini, M., Dell'Anno, A., Corinaldesi, C., Michell, C. T., et al. (2017). A Bacterial Community-Based Index to Assess the Ecological Status of Estuarine and Coastal Environments. *Mar. Pollut. Bull.* 114 (2), 679–688. doi: 10.1016/j.marpolbul.2016.10.050

Boesch, D. F. (2019). Barriers and Bridges in Abating Coastal Eutrophication. *Front. in Mar. Sci.* 6. doi: 10.3389/fmars.2019.00123

Borja, A., Franco, J., and Perez, V. (2000). A Marine Biotic Index to Establish the Ecological Quality of Soft-Bottom Benthos Within European Estuarine and Coastal Environments. *Mar. Pollut Bull.* 40 (12), 1100–1114. doi: 10.1016/S0025-326X(00)00061-8

Bracken, M. E. S., Hillebrand, H., Borer, E. T., Seabloom, E. W., Cebrian, J., Cleland, E. E., et al. (2015). Signatures of Nutrient Limitation and Co-Limitation: Responses of Autotroph Internal Nutrient Concentrations to Nitrogen and Phosphorus Additions. *Oikos* 124 (2), 113–121. doi: 10.1111/oik.01215

Brady, D. C., Testa, J. M., Di Toro, D. M., Boynton, W. R., and Kemp, W. M. (2013). Sediment Flux Modeling: Calibration and Application for Coastal Systems. *Estuar. Coast. Shelf. Sci.* 117, 107–124. doi: 10.1016/j.ecss.2012.11.003

Campanyà-Llovet, N., Snelgrove, P. V. R., and Parrish, C. C. (2017). Rethinking the Importance of Food Quality in Marine Benthic Food Webs. *Prog. Oceanog.* 156, 240–251. doi: 10.1016/j.pocean.2017.07.006

Chatzinikolaou, E., Mandalakis, M., Damianidis, P., Dailianis, T., Gambineri, S., Rossano, C., et al. (2018). Spatio-Temporal Benthic Biodiversity Patterns and Pollution Pressure in Three Mediterranean Touristic Ports. *Sci. Tot. Environ.* 624, 648–660. doi: 10.1016/j.scitotenv.2017.12.111

CSTT (1997). "Comprehensive Studies for the Purposes of Article 6 of Directive 91/271 EEC). The Urban Waste Water Treatment Directive," in *Edinburgh: Scottish Environment Protection Agency (East Region)*. (Edinburgh: Scottish Environment Protection Agency (East Region)).

Diaz, R. J. (2001). Overview of Hypoxia Around the World. *J. Environ. Qual.* 30 (2), 275–281. doi: 10.2134/jeq2001.302275x

Diaz, R. J., and Rosenberg, R. (2008). Spreading Dead Zones and Consequences for Marine Ecosystems. *science* 321 (5891), 926–929. doi: 10.1126/science.1156401

Dimitriou, P. D., Apostolaki, E. T., Papageorgiou, N., Reizopoulou, S., Simboura, N., Arvanitidis, C., et al. (2012). Meta-Analysis of a Large Data Set With Water Framework Directive Indicators and Calibration of a Benthic Quality Index at the Family Level. *Ecol. Indic.* 20 (0), 101–107. doi: 10.1016/j.ecolind.2012.02.008

Dimitriou, P. D., Papageorgiou, N., Arvanitidis, C., Assimakopoulou, G., Pagou, K., Papadopoulou, K. N., et al. (2015). One Step Forward: Benthic Pelagic Coupling and Indicators for Environmental Status. *PLoS One* 10 (10), e0141071. doi: 10.1371/journal.pone.0141071

Dimitriou, P. D., Papageorgiou, N., Geropoulos, A., Kalogeropoulou, V., Moraitis, M., Santi, I., et al. (2017a). Benthic Pelagic Coupling in a Mesocosm Experiment: Delayed Sediment Responses and Regime Shifts. *Sci. Tot. Environ.* 605–606. doi: 10.1016/j.scitotenv.2017.06.239

Dimitriou, P. D., Papageorgiou, N., Geropoulos, A., Kalogeropoulou, V., Moraitis, M., Santi, I., et al. (2017b). A Novel Mesocosm Setup for Benthic-Pelagic Coupling Experiments. *Limnol. Oceanog.: Methods* 15 (4), 349–362. doi: 10.1002/lom3.10163

Dimitriou, P. D., Papageorgiou, N., and Karakassis, I. (2017c). Response of Benthic Macrofauna to Eutrophication in a Mesocosm Experiment: Ecosystem Resilience Prevents Hypoxic Conditions. *Front. Mar. Sci.* 4, 391. doi: 10.3389/fmars.2017.00391

Duarte, C. M. (2009). Coastal Eutrophication Research: A New Awareness. *Hydrobiologia* 629 (1), 263–269. doi: 10.1007/s10750-009-9795-8

Duarte, C. M., Conley, D. J., Carstensen, J., and Sánchez-Camacho, M. (2009). Return to Neverland: Shifting Baselines Affect Eutrophication Restoration Targets. *Estuar. Coast.* 32 (1), 29–36. doi: 10.1007/s12237-008-9111-2

Duarte, C. M., and Krause-Jensen, D. (2018). Intervention Options to Accelerate Ecosystem Recovery From Coastal Eutrophication. *Front. Mar. Sci.* 5. doi: 10.3389/fmars.2018.00470

Elliott, M., and Quintino, V. (2007). The Estuarine Quality Paradox, Environmental Homeostasis and the Difficulty of Detecting Anthropogenic Stress in Naturally Stressed Areas. *Mar. Pollut. Bull.* 54 (6), 640–645. doi: 10.1016/j.marpolbul.2007.02.003

Graf, G. (1992). Benthic-Pelagic Coupling: A Benthic View. *Oceanog. Mar. Biol.: Annu. Rev.* 30 (B), 149–190.

Gray, J. S. (1981). *The Ecology of Marine Sediments* (Cambridge: Cambridge University Press).

Hasler-Sheetal, H., and Holmer, M. (2015). Sulfide Intrusion and Detoxification in the Seagrass Zostera Marina. *PLoS One* 10 (6), e0129136. doi: 10.1371/journal.pone.0129136

Herman, P. M. J., Middelburg, J. J., Van De Koppel, J., and Heip, C. H. R. (1999). "Ecology of Estuarine Macrobenthos," in *Advances in Ecological Research*. Eds. D. B. Nedwell and D. G. Raffaelli (Academic Press) 29, 195–240. doi: 10.1016/S0065-2504(08)60194-4

Hyland, J., Balthis, L., Karakassis, I., Magni, P., Petrov, A., Shine, J., et al. (2005). Organic Carbon Content of Sediments as an Indicator of Stress in the Marine Benthos. *Mar. Ecol. Prog. Ser.* 295, 91–103. doi: 10.3354/meps295091

Lin, S., Litaker, R. W., and Sunda, W. G. (2016). Phosphorus Physiological Ecology and Molecular Mechanisms in Marine Phytoplankton. *J. Phycol.* 52 (1), 10–36. doi: 10.1111/jpy.12365

Moraitis, M. L., Dimitriou, P. D., Geropoulos, A., Tsikopoulou, I., and Karakassis, I. (2015). "Monitoring and evaluating the ecological status of coastal bays in the Aegean Sea: matching water column and benthic indicators", in: *DEVOTES-EUROMARINE. Integrative Assessment of Marine Systems: The Ecosystem Approach in Practice*). San Sebastian, Spain.

Moraitis, M. L., and Karakassis, I. (2020). Assessing Large-Scale Macrobenthic Community Shifts in the Aegean Sea Using Novel Beta Diversity Modelling

Methods. Ramifications on Environmental Assessment. *Sci. Tot. Environ.* 734, 139504. doi: 10.1016/j.scitotenv.2020.139504

Moraitis, M. L., Tsikopoulou, I., Geropoulos, A., Dimitriou, P. D., Papageorgiou, N., Giannoulaki, M., et al. (2018). Molluscan Indicator Species and Their Potential Use in Ecological Status Assessment Using Species Distribution Modeling. *Mar. Environ. Res.* 140,10–17. doi: 10.1016/j.marenvres.2018.05.020

Moraitis, M. L., Valavanis, V. D., and Karakassis, I. (2019). Modelling the Effects of Climate Change on the Distribution of Benthic Indicator Species in the Eastern Mediterranean Sea. *Sci. Tot. Environ.* 667, 16–24. doi: 10.1016/j.scitotenv.2019.02.338

Papageorgiou, N., Kalantzi, I., and Karakassis, I. (2010). Effects of Fish Farming on the Biological and Geochemical Properties of Muddy and Sandy Sediments in the Mediterranean Sea. *Mar. Environ. Res.* 69 (5), 326–336. doi: 10.1016/j.marenvres.2009.12.007

Pavlidou, A., Simboura, N., Pagou, MM., Assimakopoulou, G., Gerakaris, V., Hatzianestis, I., et al. (2019). Using a Holistic Ecosystem-Integrated Approach to Assess the Environmental Status of Saronikos Gulf, Eastern Mediterranean. *Ecol. Indic.* 96, 336–350. doi: 10.1016/j.ecolind.2018.09.007

Pavlidou, A., Simboura, N., Rousselaki, E., Tsapakis, M., Pagou, K., Drakopoulou, P., et al. (2015). Methods of Eutrophication Assessment in the Context of the Water Framework Directive: Examples From the Eastern Mediterranean Coastal Areas. *Continent. Shelf. Res.* 108, 156–168. doi: 10.1016/j.csr.2015.05.013

Pearson, T. H., and Rosenberg, R. (1978). Macrobenthic Succession in Relation to Organic Enrichment and Pollution of the Marine Environment. *Oceanog. Mar. Biol.: Annu. Rev.* 16, 229–311.

Primpas, I., Tsirtsis, G., Karydis, M., and Kokkoris, G. D. (2010). Principal Component Analysis: Development of a Multivariate Index for Assessing Eutrophication According to the European Water Framework Directive. *Ecol. Indic.* 10 (2), 178–183. doi: 10.1016/j.ecolind.2009.04.007

Queirós, A. M., Birchenough, S. N. R., Bremner, J., Godbold, J. A., Parker, R. E., Romero-Ramirez, A., et al. (2013). A Bioturbation Classification of European Marine Infaunal Invertebrates. *Ecol. Evol.* 3 (11), 3958–3985. doi: 10.1002/ece3.769

Santi, I. (2019). *Eukaryotic Microbial Plankton and Nutrient Supply in the Eastern Mediterranean Sea* (PhD, University of Crete).

Santi, I., Kasapidis, P., Karakassis, I., and Pitta, P. (2021). A Comparison of DNA Metabarcoding and Microscopy Methodologies for the Study of Aquatic Microbial Eukaryotes. *Diversity* 13 (5), 180. doi: 10.3390/d13050180

Santi, I., Tsiola, A., Dimitriou, P. D., Fodelianakis, S., Kasapidis, P., Papageorgiou, N., et al. (2019). Prokaryotic and Eukaryotic Microbial Community Responses to N and P Nutrient Addition in Oligotrophic Mediterranean Coastal Waters: Novel Insights From DNA Metabarcoding and Network Analysis. *Mar. Environ. Res.* 150, 104752. doi: 10.1016/j.marenvres.2019.104752

Schratzberger, M., and Ingels, J. (2018). Meiofauna Matters: The Roles of Meiofauna in Benthic Ecosystems. *J. Exp. Mar. Biol. Ecol.* 502, 12–25. doi: 10.1016/j.jembe.2017.01.007

Simboura, N., and Argyrou, M. (2010). An Insight Into the Performance of Benthic Classification Indices Tested in Eastern Mediterranean Coastal Waters. *Mar. Pollut. Bull.* 60 (5), 701–709. doi: 10.1016/j.marpolbul.2009.12.005

Simboura, N., Tsapakis, M., Pavlidou, A., Assimakopoulou, G., Pagou, K., Kontoyiannis, H., et al. (2015). Assessment of the Environmental Status in the Hellenic Coastal Waters (Eastern Mediterranean): From the Water Framework Directive to the Marine Strategy Framework Directive. *Mediterranean. Mar. Sci.* 16 (1), 46–64. doi: 10.12681/mms.960

Simboura, N., Zenetos, A., Pancucci-Papadopoulou, M. A., Reizopoulou, S., and Streftaris, N. (2012). Indicators for the Sea-Floor Integrity of the Hellenic Seas Under the European Marine Strategy Framework Directive: Establishing the Thresholds and Standards for Good Environmental Status. *Med. Mar. Sci.* 13 (1), 140–152. doi: 10.12681/mms.31

Teeling, H., Fuchs, B. M., Becher, D., Klockow, C., Gardebrecht, A., Bennke, C. M., et al (2012). Substrate-Controlled Succession of Marine Bacterioplankton Populations Induced by a Phytoplankton Bloom. *Science* 336, 608–611. doi: 10.1126/science.1218344

Teeling, H., Fuchs, B. M., Becher, D., Klockow, C., Gardebrecht, A., Bennke, C. M., et al. (2012). Substrate-Controlled Succession of Marine Bacterioplankton Populations Induced by a Phytoplankton Bloom. *Science* 336 (6081), 608–611. doi: 10.1126/science.1218344

Tett, P., Gowen, R., Mills, D., Fernandes, T., Gilpin, L., Huxham, M., et al. (2007). Defining and Detecting Undesirable Disturbance in the Context of Marine Eutrophication. *Mar. Pollut. Bull.* 55 (1), 282–297. doi: 10.1016/j.marpolbul.2006.08.028

Tett, P., Gowen, R. J., Painting, S. J., Elliott, M., Forster, R., Mills, D. K., et al. (2013). Framework for Understanding Marine Ecosystem Health. *Mar. Ecol. Prog. Ser.* 494, 1–27. doi: 10.3354/meps10539

Tsagaraki, T. M., Pitta, P., Frangoulis, C., Petihakis, G., and Karakassis, I. (2013). Plankton Response to Nutrient Enrichment is Maximized at Intermediate Distances From Fish Farms. *Mar. Ecol. Prog. Ser.* 493, 31–42. doi: 10.3354/meps10520

Tsikopoulou, I., Santi, I., Dimitriou, P. D., Papageorgiou, N., Pitta, P., and Karakassis, I. (2020). Response of Microphytobenthos and Benthic Bacteria Viability to Eutrophication in a Benthic–Pelagic Coupling Mesocosm Experiment. *Front. Mar. Sci.* 7, 270. doi: 10.3389/fmars.2020.00270

Ubertini, M., Lefebvre, S., Gangnery, A., Grangeré, K., Le Gendre, R., and Orvain, F. (2012). Spatial Variability of Benthic-Pelagic Coupling in an Estuary Ecosystem: Consequences for Microphytobenthos Resuspension Phenomenon. *PLoS One* 7 (8), e44155. doi: 10.1371/journal.pone.0044155

Vaquer-Sunyer, R., and Duarte, C. M. (2008). Thresholds of Hypoxia for Marine Biodiversity. *Proc. Natl. Acad. Sci. U. S. A.* 105 (40), 15452–15457. doi: 10.1073/pnas.0803833105

Zhang, W., Neumann, A., Daewel, U., Wirtz, K., van Beusekom, J. E., Eisele, A., et al. (2021). Quantifying Importance of Macrobenthos for Benthic-Pelagic Coupling in a Temperate Coastal Shelf Sea. *J. Geophys. Res.: Ocean* 126 (10), e2020JC016995. doi: 10.1029/2020JC016995

Conflict of Interest: The authors declare that the research was conducted in the absence of any commercial or financial relationships that could be construed as a potential conflict of interest.

frontiers | Frontiers in Marine Science

ORIGINAL RESEARCH
published: 31 May 2022
doi: 10.3389/fmars.2022.882463

Effect of Ecological Recovery on Macrophyte Dominance and Production in the Venice Lagoon

Adriano Sfriso[1], Alessandro Buosi[1], Katia Sciuto[1,2], Marion Wolf[1,2], Yari Tomio[1], Abdul-Salam Juhmani[1] and Andrea Augusto Sfriso[2]*

[1] Department of Environmental Sciences, Informatics and Statistics, University Ca' Foscari of Venice, Venice, Italy,
[2] Department of Chemical, Pharmaceutical and Agricultural Sciences, University of Ferrara, Ferrara, Italy

In the last decade, the Venice Lagoon showed a significant environmental recovery that changed the assemblages of macroalgal and aquatic angiosperm dominant species and significantly increased the primary production. The decreasing of anthropogenic impacts, such as eutrophication and clam harvesting, favored a strong reduction of Ulvaceae, replaced by species with higher ecological value, and the recolonization of aquatic angiosperms. Consequently, hypo-anoxic conditions, once frequently occurring in the lagoon, have been considerably reduced and aquatic angiosperms have recolonized the area, covering 94.8 km^2 in comparison to the 55.9 km^2 recorded in 2003 (+70%). *Cymodocea nodosa*, *Zostera marina*, and *Zostera noltei* expanded by 37.5%, 44.6%, and 191%, respectively, with a significant increase in biomass and primary production. In late spring 2018, angiosperms showed a standing crop of approximately 372 ktonnes (+77%) and a net primary production of approximately 1189 ktonnes FW (+67%). In the meantime, *Ruppia cirrhosa*, which since the 1980s had disappeared from the lagoon areas subjected to tidal expansion, but was still present in some fishing valleys, recolonized the bottoms of the northern lagoon with meadows of over 6 km^2; this accounted for a standing crop and net primary production of 8.9 and 18.0 ktonnes, respectively. Based on surveys carried out in 2021, ecological conditions are still improving, and this is increasing both the biodiversity and the production of macroalgae and aquatic angiosperms.

Keywords: aquatic angiosperms, biomass, environmental recovery, macroalgae, primary production, Venice Lagoon

OPEN ACCESS

Edited by:
Martina Orlando-Bonaca, National Institute of Biology (Slovenia), Slovenia

Reviewed by:
Vasillis Papathanasiou, Hellenic Agricultural Organization – ELGO, Greece
Sotiris Orfanidis, Institute of Fisheries Research, Greece

****Correspondence:***
Adriano Sfriso
sfrisoad@unive.it

Specialty section:
This article was submitted to Marine Ecosystem Ecology, a section of the journal Frontiers in Marine Science

Received: *23 February 2022*
Accepted: *11 April 2022*
Published: *31 May 2022*

Citation:
Sfriso A, Buosi A, Sciuto K, Wolf M, Tomio Y, Juhmani A-S and Sfriso AA (2022) Effect of Ecological Recovery on Macrophyte Dominance and Production in the Venice Lagoon. Front. Mar. Sci. 9:882463. doi: 10.3389/fmars.2022.882463

1 INTRODUCTION

The Venice Lagoon, with an area of 549 km^2, is the largest transitional water system (TWS) in the Mediterranean Sea (**Figure 1**). The number of TWS in the Mediterranean is very high; there are 209 basins with an area >0.25 km^2, for a total surface of approximately 2230 km^2. The Venice Lagoon alone occupies approximately 25% of this area and approximately 39% of the Italian TWS surface (1398 km^2) (Sfriso et al., 2017).

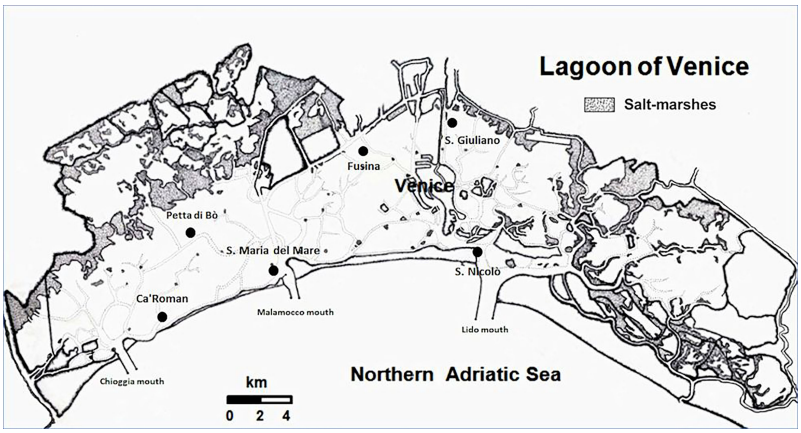

FIGURE 1 | Map of the Venice Lagoon and the 6 stations sampled bimonthly.

For its size, the extremely variable morphology [i.e., there are areas heavily influenced by seawater exchanges and choked areas where water renewal takes up to 30-40 days (Cucco and Umgiesser, 2006)] and its more than millenary mercantile history, the Venice Lagoon is a basin characterized by a very high biodiversity. Macrophytes (aquatic angiosperms and macroalgae) are among the most studied organisms. The first studies, generally extensive monographs, date back to the 18th and 19th centuries (Olivi, 1794; Naccari, 1828; Zanardini, 1847; De Toni and Levi, 1885; De Toni and Levi, 1888b; De Toni, 1889; De Toni, 1924) and continued in the 20th century (Schiffner and Vatova, 1938; Sighel, 1938; Vatova, 1940; Pignatti, 1962). These monographs are systematic studies that report lists of species along with their areas of discovery. Subsequently, in the 1980s, an abundant production of scientific papers regarding Venice Lagoon macrophyte biodiversity started. A complete review of this literature up to 2007 was reported by Sfriso and Curiel (2007), whereas information on the biomass changes and global production of macroalgae and seagrasses are shown by Sfriso and Facca (2007). In the following years, studies of macrophytes were mainly focused on their correlation with water and sediment parameters and on the discovery of new species, many of which are alien species (Sfriso et al., 2020a).

However, from the second half of the 20th century, the lagoon experienced continuous environmental changes. After the Second World War, the lagoon was affected by a pronounced chemical and organic pollution that caused replacements in the vegetation, until that period represented by aquatic angiosperms and sensitive macroalgae (Pavoni et al., 1992; Marcomini et al., 1995). Until the end of the 1980s, the lagoon was dominated by luxuriant growth of Ulvaceae (Sfriso and Facca, 2007), whose expansion declined in the 1990s (Sfriso and Marcomini, 1996). In the following years, the basin was affected by an intense fishing of the clam *Ruditapes philippinarum* Adams and Reeve, which peaked in the late 2010s with approximately 40,000 tonnes per year. This activity had a serious impact on the sediment resuspension and bottom erosion (Sfriso et al., 2005), the macrofauna (Pranovi and Giovanardi, 1994), and the aquatic vegetation (Sfriso and Facca, 2007).

Since the beginning of the 2010s, clam fishing has significantly been reduced due to overfishing of the resource and the lagoon has started a rapid ecological recovery (Sfriso et al., 2019; Sfriso et al., 2021a; Sfriso et al., 2021b).

In 2018 and 2019, an extensive study on the macrophytes of the entire Venice Lagoon was carried out, with the goal of investigating macroalgal and aquatic angiosperm changes on time and spatial scales. The performed analyses allowed us to update biomass and net primary production (NPP) data for macroalgae and single aquatic angiosperms and to compare these data with those obtained in 2003, when the Venice Lagoon was affected by an intense clam overexploitation. Furthermore, the simultaneous sampling of the main physico-chemical parameters and of the nutrient concentrations in the water column and in the surface sediments allowed us to discriminate their correlation with the main variables of both aquatic angiosperm and macroalgae.

2 MATERIALS AND METHODS

2.1 Study Area

The lagoon of Venice is a wide shallow basin of approximately 549 km^2 (432 km^2 of water surface), located in the northern Adriatic Sea (sexagesimal coordinates: 45° 35'-11'N; 12°08'-38'E) (**Figure 1**). The mean depth is approximately 1.2 m and tidal excursion is ±31 cm on the average tidal level, although there are seasonal tidal extremes of over 2 m. The lagoon is connected to the sea through three large (400–900 m) and deep (15–50 m) mouths (Lido, Malamocco, and Chioggia), which divide the area into three hydrological basins separated by watersheds that shift according to tides and winds.

To have well-defined boundaries, the lagoon was divided into three morphological basins (northern, central, and southern basins), which are separated at the North by Burano and

Torcello tidal marshes and at the South by the deep Malamocco-Marghera artificial canal. Of the three basins, the central one (ca. 132 km^2 of water surface) is the most anthropized and, in the past, was heavily affected by the impact of industrial waste, urban sewage, and other anthropogenic pressures, such as touristic and commercial activities and the illegal fishing of Manila clam (*Ruditapes philippinarum* Adams & Reeve) carried out by disruptive fishing gears (Pranovi and Giovanardi, 1994; Sfriso et al., 2003; Sfriso et al., 2005). In the last decade, these impacts have been greatly reduced and the lagoon has begun a progressive environmental recovery (Sfriso et al., 2019; Sfriso et al., 2021a). The southern and northern basins are less artificial but have different ecological conditions due to, respectively, a greater and lesser exchange with marine waters. Therefore, the southern basin has less trophy and is abundantly colonized by seagrasses, especially *C. nodosa* and *Z. marina* which cover a large part of the shallow bottoms. Although the anthropogenic impacts are not significant, the northern basin has conditions strongly affected by the low water turnover. It is mainly colonized by *Z. noltei* and *R. cirrhosa* while *Z. marina* and *C. nodosa* are present along the edges of the canals which have a higher water turnover. Since the 1980s all these species had almost completely disappeared due to high trophy, clam fishing, and a picocyanobacteria bloom which eliminated much of the remaining prairies in the summer of 2001 (Sorokin et al., 2004). Aquatic angiosperms were reintroduced into the choked areas with the Life SeResto Project (Life12 NAT/IT/000331) by transplanting more than 75,000 rhizomes that have now colonized extensive areas of this basin (Sfriso et al., 2021b).

The present study refers to biweekly samplings at 6 stations for one year and to late spring-early summer samplings carried out in the soft bottoms of 88 stations, spread in the whole lagoon, in 2018. Samplings were performed in the framework of the project MOVECO III (ecological monitoring of the Venice Lagoon), which aimed at assessing the ecological status of the lagoon by the determination of the biological element "Macrophytes" and the application of the Index MaQI (Macrophyte Quality Index by Sfriso et al., 2009; Sfriso et al., 2014). The 6 stations were selected to study the annual growth of aquatic angiosperms and macroalgae before and after the entry into operation of the MOSE (experimental electromechanical module) gates which took place in October 2020, to counteract the exceptional high tides that affect the Venice Lagoon. Three stations were placed near the lagoon mouth: San Nicolò (SN), Santa Maria del Mare (SMM), Ca' Roman (Ca'R), and three in the innermost areas: San Giuliano (SG), Fusina (Fus), and Petta di Bò (PBò) (**Figure 1**).

2.2 Physico-Chemical Parameters

In the six stations at each sampling campaign the physico-chemical parameters of the water column [%DO, salinity, pH, Eh, Chl-*a*, phaeopigments, reactive phosphorus (RP), ammonium (NH_4^+), nitrite (NO_2^-), nitrate (NO_3^-), silicate (Si)], and the 5-cm sediment top layer [fraction <63μm (Fines), density, moisture, porosity, total, inorganic and organic phosphorus (Ptot, Pinorg, Porg), total nitrogen (Ntot), total, inorganic and organic carbon (Ctot, Cinorg, Corg), sedimentation rates (SPM = Settled Particulate Matter)] where recorded. The analytical procedures have been reported in specific papers (Sfriso et al., 2017; Sfriso et al., 2019; Sfriso et al., 2021a).

2.3 Macrophyte Sampling

Following Sfriso et al. (1991), during each sampling campaigns the biomass of macroalgae was determined as the mean of 6 sub-samples using a frame of 50x50 cm. A selection of the different taxa was stored in 4% formaldehyde solution until taxonomic determination. When present, 6 samples of aquatic angiosperms were also collected by using a frame of 20x25 cm, to determine the biomass of shoots, rhizomes, and dead parts (blackened, no longer vital parts), the shoot density, the shoot height, and the number of leaves, according to Sfriso and Ghetti (1998). Each sample was collected manually by taking the plants inside the square. The rhizomes were cut with a blade along the edge of the square and the samples with sediments were collected up to 20-30 cm deep, placed in a 0.5-cm mesh basket and washed to remove sediments, shell fragments, and live organisms. Each sample was then collected in a bag and kept in the refrigerator at 4°C until the morphological analysis took place within 2-3 days. During the analyses, each sample was washed with tap water to remove salts and sediment residues and carefully dried with laboratory paper. Then each plant was divided into three parts (rhizomes+roots, leaf bundles, and dead parts), which were weighed separately for each sample with a technical balance (precision 0.01 g). The final value was the average weight of the 6 samples, whose values were then extrapolated to the square meter. The average measurement of the 20 longest leaf bundles provided the height of the prairie while the average of the number of leaves allowed us to have the average number of leaves. The dry weight of the samples was determined after sample lyophilization.

The study on spatial basis was carried out by sampling 88 stations, equally distributed throughout the lagoon, in late spring-early summer 2018. The sexagesimal coordinates are reported in **Supplementary Table S1** together with those of the 6 stations. At each station, the cover and biomass of macroalgae and the cover of aquatic angiosperms were determined by collecting samples for the taxonomic determination.

The distribution of macroalgae throughout the whole lagoon was reported in biomass ranges (0.01-0.1, 0.1-0.5, 0.5-1.0, 1.0-5.0, 5.0-10.0 kg m^{-2}) of fresh weight (FW) biomass, marking in a map the boundaries of the distribution ranges with a GPS when reference morphological structures were not available. Then the area of each biomass range was calculated in a map with a scale of 1:50,000 (1 cm^2 = 500*500 m = 250,000 m^2) by reporting the mean and maximum surface for each biomass range. The sum of the areas and biomasses of the individual ranges provides the lagoon surface covered by macroalgae and the total biomass. These calculations were made for each of the lagoon basins and then added together to obtain the total values.

The distribution of each aquatic angiosperm in the whole lagoon was obtained by drawing biomass distribution maps in the same way. For each species, the biomass was reported into 4 ranges (0-25, 25-50, 50-75, 75-100%) of cover. A biomass range was then associated with each cover range using the maximum

value obtained during the annual sampling in the 6 stations studied in this paper or those previously found in other stations (Sfriso and Facca, 2007).

2.4 Primary Production Determination

2.4.1 Aquatic Angiosperms

At each station, the NPP of the aboveground part of the aquatic angiosperms (shoots) was determined by piercing the leaf bundles above the basal meristem with a needle in accordance with Dennison (1990a) and Dennison (1990b). At each campaign, approximately 20 leaf bundles were drilled and, at the subsequent sampling, the leaf growth of 10 leaf bundles was determined. The growth of each bundle was assessed bimonthly by adding the displacement of the hole from the basal meristem of the single leaves. These data were transformed into a linear leaf production for square meter considering the mean leaf bundles per square meter (sum of the leaf increase of each shoot * number of shoots m^{-2}) and biomass production by mean fresh (FW) weight and dry weight (DW) of 10 linear meters of leaves.

The NPP of the belowground part (rhizomes+roots, hereinafter referred to as rhizomes) of the plants was obtained monthly by sampling all rhizomes with the biomass variation method within dense and uniform prairies (Sfriso and Ghetti, 1998). Indeed, the drilling of the rhizomes could only be applied to *Zostera marina* Linnaeus, but not to *Zostera noltei* Hornemann and with difficulty to *Cymodocea nodosa* (Ucria) Ascherson. In fact, *Z. marina* rhizomes can be perforated above the basal meristem, but the operation is complex and subjected to a high margin of error; *Z. noltei* has rhizomes that are too thin, and the drilling could compromise their growth; *C. nodosa* has very elongated rhizomes and only the apical bundles can be pierced. Therefore, for all three species it was preferred to apply the biomass variation method. Sfriso and Ghetti (1998) showed that 6 replicated subsamples with a frame of 20x25 (0.05 m^2) cm are sufficient to obtain an accurate biomass measurement with an error of less than 5%. The sum of the rhizome biomass increases recorded monthly for 1 year, excluding the values found not significant by one-way ANOVA, supplies the NPP of the underground part. This value added to that of shoots gives the total production of each species.

Following Sfriso and Facca (2007), the NPP of the whole lagoon was estimated based on the production/biomass ratios (P/B) (i.e., the ratios between the annual NPP and the annual maximum biomass) determined for each species, sampled during the year in the framework of different projects and characterized by different biomass intervals in accordance with the following calculation:

$$\text{Standing Crop(SC)} = \text{Sum of the mean biomass} \star \text{lagoon surface of each biomass range}$$

$$\text{Net Primary Production (NPP)} = \text{Sum of the maximum biomass} \star \text{lagoon surface} \star \text{P/B ratio of each biomass range}$$

2.4.2 Macroalgae

In the 6 stations macroalgae were sampled twice a month determining the cover, the biomass, the total number of taxa, the number of sensitive taxa according to ISPRA (2011), and the parameters for the application of the index of ecological status MaQI (Macrophyte Quality Index of Sfriso et al., 2009, Sfriso et al., 2014). It was not possible to calculate the P/B ratios because macroalgae require a higher number of samplings, especially in the period of greatest growth of the dominant species. Therefore, the NPP of macroalgae was determined by using the P/B ratios reported in Sfriso and Facca (2007). They were calculated in stations characterized by different biomass ranges (0-2 kg FW m^{-2}, 5-8 kg FW m^{-2}, 8-12 kg FW m^{-2}) because the P/B ratio increased with the decreasing biomass. Indeed, macroalgae have a higher growth rate in the presence of smaller biomass as they are not self-limited.

For macroalgae, it was also possible to determine the gross primary production (GPP) by using the GPP/NPP ratios reported in Sfriso and Facca (2007) and calculated from the balance of phosphorus, an element that completes its cycle between sediments, water, and biota, in stations placed in the lagoon watershed or without water exchanges (Sfriso and Marcomini, 1994). In brief, the ratio of all phosphorus recycled annually from macroalgae to that recycled from NPP provided the GPP/PPN ratio. For the calculation we used the average value of phosphorus in the annual macroalgal biomass, the minimum winter value of phosphorus retained by the surface sediments, and the average value of the phosphorus in the particles captured annually with sedimentation traps (SPM = settled particulate matter). The system reported below:

$$\begin{cases} Ax + By = C \\ x + y = 100 \end{cases}$$

A = mean value of P in macroalgae
B = winter background of P in surface sediment
C = mean value of P in SPM
x = fraction of macroalgae in SPM
y = fraction of sediment in SPM

Taking into account the total amount of SPM collected by traps during the year made it possible to separate the contributions of phosphorus due to the degradation of macroalgae produced during 1 year from that contained in the resuspended surface sediments settling into the traps in the same period of time. Since phosphorus is a sedimentary element with negligible losses as phosphines, which occur only in the case of anoxic events, it was possible to calculate the total amount of this element recycled by macroalgae and released in the particulate collected by traps during their degradation.

2.5 Statistical Procedures

All the data of physico-chemical parameters of the water column, surface sediments, sedimentation rates (29 parameters), and some macrophyte variables (angiosperm cover, macroalgal biomass, macroalgal cover, total macroalgal taxa, number of sensitive taxa, number of calcareous taxa) collected in the 6 stations were analyzed together in a PCA analysis to highlight their associations and grouping. In addition, the analysis of the transposed matrix allowed us to see the associations between stations discriminating the stations characterized by good high ecological conditions from those of poor ecological conditions.

3 RESULTS

3.1 Environmental Parameters

In **Figure 2**, some parameters of the water column and surface sediments highlight the main differences between the 6 stations. SG and Fus showed the highest concentrations of reactive phosphorus (RP: 1.36 and 0.96 μM, respectively) and inorganic dissolved nitrogen (DIN = sum of ammonium, nitrite, and nitrate: 19.0 and 10.1 μM, respectively) in the water column. The same stations also showed the highest values of total Chl-*a* (7.73 and 3.91 μg L^{-1}, respectively) and SG the highest amount of TSS (89.2 mg L^{-1}). Similarly, the number of fines was higher at SG (90.0%) and Fus (66.7%). Consequently, SG exhibited the highest concentrations of Porg (141 μg g^{-1}) and Corg (15.51 mg g^{-1}) followed by Ca'R (100 μg g^{-1} and 15.47 mg g^{-1}, respectively) that also had the highest concentration of Ntot (1.49 mg g^{-1}).

3.2 Macrophyte Variables

The macrophytes variables recorded in the 6 stations [San Nicolò (SN), Santa Maria del Mare (SMM), Ca' Roman (Ca'R), San Giuliano (SG), Fusina (Fus), Petta di Bò (PBò)] in 2019 are reported in **Table 1**. The number of total taxa was 130 (44 Chlorophyceae, 67 Rhodophyceae, 19 Phaeophyceae). The highest biodiversity was recorded at SN (86 taxa) and the lowest at Fus (17). Out of them, 25 were sensitive taxa and 3 crustose calcareous taxa. The highest number of sensitive taxa

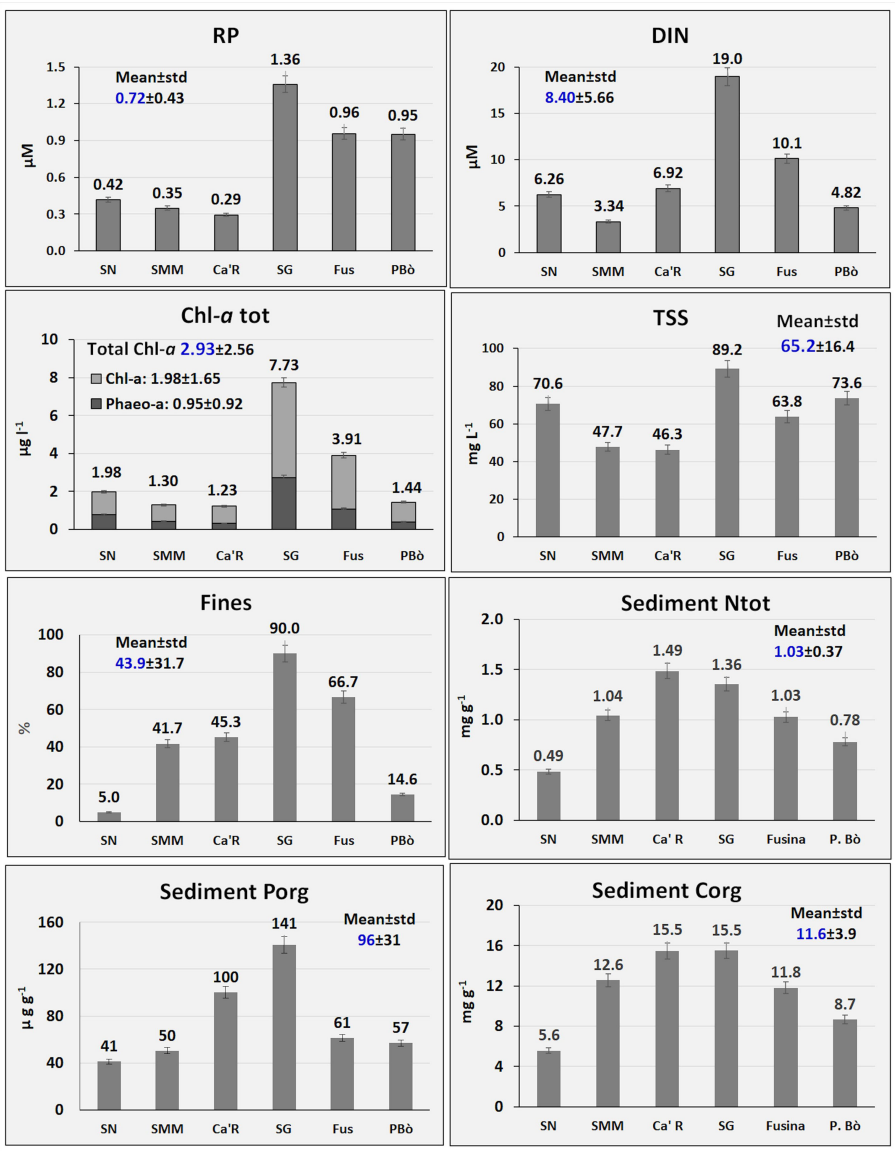

FIGURE 2 | Main ecological parameters.

TABLE 1 | Macrophyte variables.

Macrophyte variables	Ca' R	SMM	SN	PBò	Fus	SG
N° of Samples	24	24	24	24	24	24
N° Taxa (max)	73	71	86	56	17	25
N° Sensitive taxa (tot)	10	15	12	8	0	0
% Sensitive taxa	13.7	21.1	14	14.3	0	0
N° Calcareus taxa	2	3	2	3	0	0
Chlorophyta N°	22	20	24	21	7	10
Rhodophyta N°	41	40	51	30	7	12
Ochrophyta N°	10	11	11	5	3	3
Rhodophyta/Chlorophyta (R/C)	1.9	2	2.1	1.4	1	1.2
Cover %	78	66	53	30	82	45
Chlorophyta %	68	70	38	38	33	27
Rhodophyta %	32	30	62	62	67	73
Mean Macroalgal Biomass (g FW m^{-2})	593	415	146	161	2422	397
Max Macroalgal Biomass (g FW m^{-2})	3448	1546	505	1383	4650	2525
Macroalgae NPP (g FW m^{-2} y^{-1})*	12068	5411	2273	4841	16275	8838
C. nodosa cover %	0	100	100	+	0	0
C. nodosa NPP (g FW m^{-2} y^{-1})	0	12554	12274	+	0	0
Z. marina cover %	90	0	0	+	0	0
Z. marina NPP (g FW m^{-2} y^{-1})	12981	0	0	+	0	0
Z. noltei cover %	+	0	0	90	0	0
Z. noltei NPP (g FW m^{-2} y^{-1})	+	0	0	6647	0	0
Total Macrophyte NPP (g FW m^{-2} y^{-1})	25049	17955	14547	11488	16275	8838
MaQI	0.85	1	0.85	0.85	0.35	0.35

**According to Sfriso and Facca (2007), the P/B value for macroalgal biomass ranging from 1 to 5 Kg FW m^{-2} is 3.5. For lower biomass the P/B ratio is 4.5.*

was recorded at SMM (15, i.e., 21.1%) whereas at SG and at Fus sensitive taxa were missing.

The Rhodophyta/Chlorophyta (R/C) ratio ranged from 1.0 at Fus to 2.1 at SN. The mean macroalgal cover range was 30-82% with the highest value at Fus and the lowest at PBò.

The NPP recorded by applying the P/B reported by Sfriso and Facca (2007) for different levels of biomass ranged from 2273 g FW m^{-2} y^{-1} at SN to 16,275 g FW m^{-2} y^{-1} at Fus.

The mean annual macroalgal biomass was the highest at Fus (2422 g FW m^{-2}) where no aquatic angiosperms were present. In the same station, the highest biomass (4650 g FW m^{-2}) was also recorded.

By considering the total NPP of macroalgae and aquatic angiosperms, the highest production was recorded at Ca'R (25049 g FW m^{-2} y^{-1}) where macroalgae and *Z. marina* contributed with a quite similar biomass (**Table 1**). The lowest NPP was recorded at SG (8838 g m^{-2} y^{-1}) where no angiosperms were recorded. The other stations showed intermediate values with different macrophyte contributions. However, at Fus, where only macroalgae were present, the NPP was higher than at PBò colonized by the angiosperm *Z. noltei*.

The application of the Macrophyte Ecological Index (MaQI) assessed SMM, Ca'R, PBò, and SNN as "High" quality and Fus and SG as "Poor" quality.

Aquatic angiosperms were represented by the species *Cymodocea nodosa* at SMM and SN (cover 100%), *Zostera marina* at Ca'R (cover 90%), and *Zostera noltei* at PBò (cover 90%). The annual biomass variation of these plants is reported in **Figure 3**.

C. nodosa was recorded at SMM in a shallow area (ca. 0.6 m depth) and at SN near the border of Lido port entrance at the same depth. At SMM *C. nodosa* showed both the highest mean biomass (3095 g FW m^{-2}) and the biomass peak (7067 g FW m^{-2}) in July. On average, rhizomes contributed with 1920 g FW m^{-2} (62% of the total), whereas shoots reached 1032 g FW m^{-2} only. The presence of dead parts was lower than 5% 143 g FW m^{-2}. This species started to grow in May and sharply declined in September. At SN the mean biomass was lower (2816 g FW m^{-2}) as well as the biomass peak (4474 g FW m^{-2}).

Z. marina showed a slightly smaller mean biomass (2399 g FW m^{-2}) with a peak of 4830 g FW m^{-2} in June. This species, which grows all year round, had a minimum biomass in September. The mean biomass of shoots (975 g FW m^{-2}) was slightly greater than that of rhizomes (950 g FW m^{-2}) but in this species the dead parts reached almost 20% of the total biomass (474 g FW m^{-2}).

Z. noltei biomass was significantly lower (1991 g FW m^{-2}). The mean biomass peak value was recorded in July (3628 g FW m^{-2}), whereas the minimum was in March. Rhizomes of this species, as for *C. nodosa*, showed the maximum contribution reaching even 70% of the total biomass.

The number of shoots per square meter is reported in **Figure 4A**. *Z. noltei*, the smallest species, and *Z. marina* showed the highest (5502 m^{-2}) and the lowest (696 m^{-2}) mean number of shoots, respectively. Both these species peaked in June with 13,021 and 1327 shoots m^{-2}. *C. nodosa* showed almost twice as many shoots as *Z. marina* with a mean value ranging from 1273 m^{-2} at SMM to 1373 m^{-2} at SN. The highest values were recorded in June both at SMM and SN (2747 and 2333 shoots m^{-2}, respectively).

On average shoot height was the highest for *C. nodosa* at SMM with a peak in August (86.6 cm, **Figure 4B**) whereas at SN the mean value was slightly smaller (36.4 cm) but with a peak of 89.4 cm in July. *Z. marina* showed an intermediate mean value (37.7 cm), and the peak was 53.1 cm only. *Z. noltei* peaked in August (29.3 cm) with a mean value of 19.1 cm.

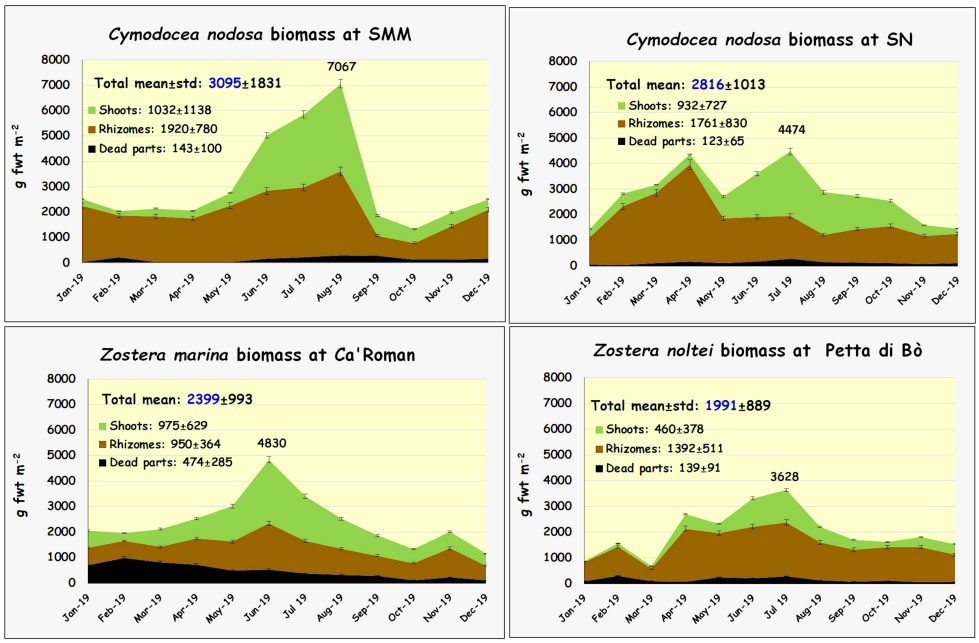

FIGURE 3 | Biomass changes of *C. nodosa, Z. marina*, and *Z. noltei* during the year.

The number of leaves was average between 2.45 for *C. nodosa* at SMM and 3.35 for *Z. marina* at Ca'R. (**Figure 4C**). In autumn and winter *C. nodosa* showed 1-2 small sleeping leaves that started to grow only in May.

The growth of shoots was measured about twice a month and scaled monthly (**Figure 4D**). *Z. marina* showed a mean value (2.73 cm d^{-1}) almost double than that of *C. nodosa* (1.26-1.39 *cm* d^{-1}) and over three times higher than that of *Z. noltei* (0.82 *cm* d^{-1}). The highest shoot increase was recorded at Ca'R for *Z. marina* in the last two weeks of May (6.88 cm d^{-1}, i.e., 5.69 cm d^{-1} monthly) and at SN in the first week of July for *C. nodosa* (6.18 cm d^{-1}, i.e., 5.47 cm d^{-1} monthly).

The NPP of the aquatic angiosperms in 2018 is reported in **Table 2**. It is sorted in the production of shoots and rhizomes. The NPP of *C. nodosa* and *Z. marina* in the three stations was very similar ranging from 12,274 to 12,981 g FW m^{-2} y^{-1}, whereas that of *Z. noltei* was about half (6647 g FW m^{-2} y^{-1}).

On average, the production of shoots was significantly higher than that of rhizomes ranging from 61.3% in *Z. noltei* to (83.7%) in *Z. marina*. The percentage of shoot production in *C. nodosa* in both stations was very similar ranging from 73.2 to 73.9%.

By considering these values and the highest biomass of the single species recorded during the year it was possible to calculate the P/B ratios. They were 1.78 and 2.74 for *C. nodosa* (mean value: 2.26), 2.69 for *Z. marina*, and 1.83 for *Z. noltei*.

3.3 Biomass Maps and Total Macrophyte NPP

3.3.1 Aquatic Angiosperms

The data of macrophyte biomass of the entire lagoon, collected as part of the MOVECO III project, allowed us to calculate the cover, standing crop (SC), and NPP throughout the lagoon and draw the biomass distribution. For macroalgae it was also possible to determine the GPP. An example of the procedure used to define these variables is shown in **Supplementary Table S2**. The three basins were analyzed separately and globally.

Maps report the biomass of each angiosperm species in the three Venice basins (southern, central, northern, **Supplementary Figures S1** and **S2**) in 4 cover ranges with the corresponding biomass (**Supplementary Figure S1**).

Overall, the angiosperms *C. nodosa, Z. marina*, and *Z. noltei* together with the rarer species *Ruppia cirrhosa* that was present only in the northern basin (**Supplementary Figure S2**), colonized approximately 94.8 km^2 (**Table 3**), although in many cases they overlapped. The southern basin presented the highest cover (63.5 km^2) followed by the central basin (18.4 km^2) and the northern basin (12.9 km^2). The total standing crop (SC) was 372 ktonnes FW, of which 298 (ca. 80%) were in the southern basin.

The NPP reached 1189 ktonnes FW with 954 ktonnes produced in the southern lagoon whereas 157 and 77 ktonnes FW were produced in the central and northern lagoons, respectively.

The highest cover was displayed by *Z. marina* (38.2 km^2, 40%), whereas *C. nodosa* covered 32.4 km^2 (34%). *Z. noltei* and *R. cirrhosa* covered 18.1 km^2 (19%) and 6.0 km^2 (6.4%), respectively.

Conversely, the highest SC was that of *C. nodosa* (181 ktonnes, 49%) followed by *Z. marina* (145 ktonnes, 39%), and *Z. noltei* and *R. cirrhosa* showed 37 ktonnes (10%) and 8.9 ktonnes (2.4%), respectively.

The NPP of *C. nodosa* and *Z. marina* were quite similar: 539 and 545 ktonnes, respectively, accounting for 45% and 46% of

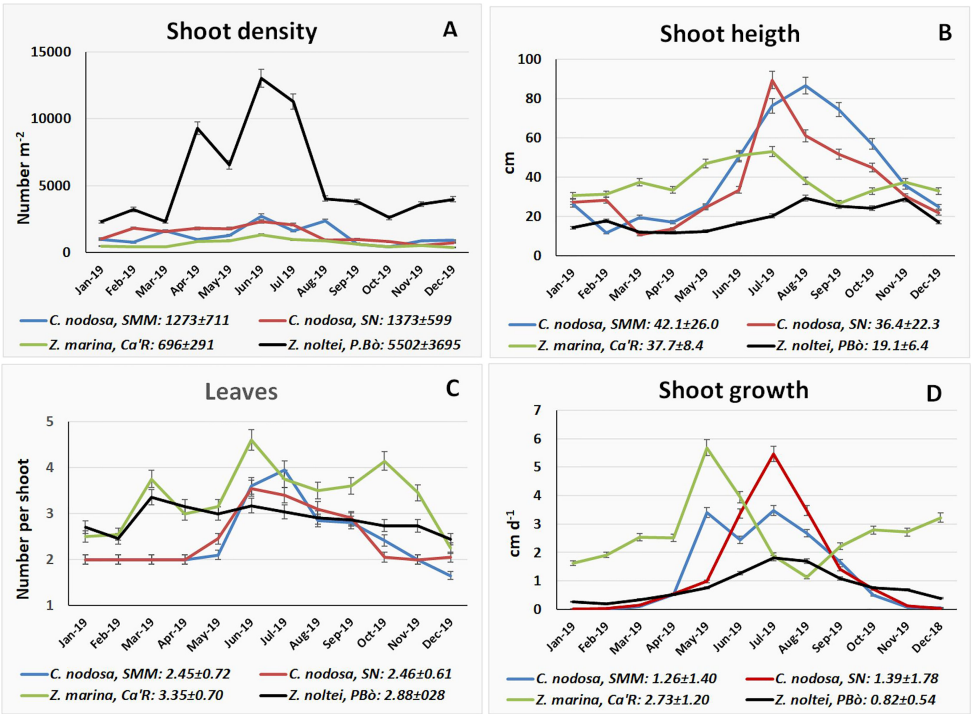

FIGURE 4 | **(A)** Shoot density, **(B)** shoot height, **(C)** leaf number, and **(D)** shoot growth of aquatic angiosperms monthly for 1 year.

the total. *Z. noltei* and *R. cirrhosa* contributed with 86 ktonnes (7.3%) and 18 ktonnes (1.5%), respectively.

3.3.2 Macroalgae

Total macroalgal species covered approximately 133 km^2 with a biomass ranging from 0.01 to 10.0 kg FW m^{-2} and 214 km^2 with a biomass >0.001 kg FW m^{-2}. The highest cover (ca. 100.3 km^2) was recorded in the southern lagoon where the SC reached 59.5 ktonnes FW, that is, approximately 57% of the biomass recorded in the whole lagoon (104 ktonnes FW) (**Table 3**; **Supplementary Figure S3**).

However, in the southern basin the SC reached a maximum of 5 kg FW m^{-2} (**Supplementary Figure S3**), whereas in the central lagoon SC up to 10 kg FW m^{-2}, composed mainly by Gracilariaceae, was also recorded.

The macroalgal NPP reached 648 ktonnes FW and 369 (57%) of them were produced in the southern lagoon. The total GPP reached approximately 3014 ktonnes FW of which 1705 ktonnes were produced in the southern lagoon (**Supplementary Table S2**).

3.4 Statistical Analyses

The PCA (principal component analysis) between the main environmental parameters and macrophyte variables (36 in total) is plotted in **Figure 5**. The first two components explain 76.5% of the total variance. This value increases to 87.9% and

TABLE 2 | Angiosperm production.

Net Primary Production (NPP) of aquatic angiosperms								
	C. nodosa				*Z. marina*		*Z. noltei*	
	SMM		SN		Ca'R		PBò	
	g FW m^{-2} y^{-1}	%	g FW m^{-2} y^{-1}	%	g FW m^{-2} y^{-1}	%	g FW m^{-2} y^{-1}	%
Shoots	9278	73.9	8984	73.2	10864	83.7	4073	61.3
Rhizomes	3276	26.1	3290	26.8	2117	16.3	2574	38.7
Total	12554		12274		12981		6647	
Max Biom	7067		4474		4830		3628	
P/B	1.78		2.74		2.69		1.83	

TABLE 3 | Macrophyte cover, SC and NPP .

Total macrophytes 2018.					
Species	**Cover**				
	Basins			**Total**	
	South	**Central**	**North**		
		km²		**km²**	**%**
C. nodosa	30.1	1.28	1.07	32.4	34
Z. marina	22.6	12.7	2.91	38.2	40
Z. noltei	10.8	4.36	2.86	18.1	19
R. cirrhosa	0.0	0.0	6.03	6.03	6.4
Total angiosperms	63.5	18.4	12.9	94.8	100
Total macroalgae	100.3	82.0	31.9	214	
Species	**Standing Crop**				
	Basins			**Total**	
	Southern	**Central**	**Northern**		
		ktonnes FW		**ktonnes FW**	**%**
C. nodosa	171	5.5	4.2	181	49
Z. marina	105	33	7.4	145	39
Z. noltei	22	6.7	7.5	37	10
R. cirrhosa	0.0	0.0	8.9	8.9	2.4
Total angiosperms	298	45.2	28.1	372	100
Total macroalgae	59.5	29.2	15.7	104	
Total macrophytes	358	74	44	476	
Species	**Net Primary Production**				
	Basins			**Total**	
	Southern	**Central**	**Northern**		
		ktonnes FW		**ktonnes FW**	**%**
C. nodosa	504	20.3	15.2	539	45
Z. marina	398	119	28.4	545	46
Z. noltei	53	17.1	16.2	86	7.3
R. cirrhosa	0.0	0.0	17.2	18	1.5
Total angiosperms	954	157	77	1189	100
Total macroalgae	369	178	101	648	
Total macrophytes	1323	335	178	1837	

96.9% by considering three and four components, respectively. All parameters/variables are mainly plotted in two main groups associated to bad or high ecological conditions. The ecological value of each parameter/variable is shown by the orthogonal projection on the line that connects the extreme conditions. By **Figure 5A**, the parameters/variables associated with the highest ecological conditions are the pH of the water column (pHw) and the index MaQI followed by the number of sensitive taxa (Sens), the angiosperm cover (AngCOV), the total number of taxa (Taxa), water transparency (Trans), the water redox potential (Ehw), and the number of calcareous macroalgae. On the other side, the parameters/variables associated with the worst conditions are silicates (Si) and nitrites (NO_2^-) followed by all the nutrients in the water column, total suspended solids (TSS), Chl-*a*, and phaeopigments (Phaeo-*a*). All the other parameters/variables are placed in intermediate positions.

The transposed matrix (**Figure 5B**) with two components explains 86.6% of the total variance highlighting two groups of stations, associated to high (SMM, PBò, Ca'R, SN) or bad (Fus, SG) ecological conditions, respectively. The first group groups the stations colonized by seagrasses. Out of them, SMM showed the highest conditions. The second group had no seagrasses or sensitive macroalgae and Fus showed the worst conditions.

4 DISCUSSION

There is a conspicuous literature on the degradation of transitional environments both from the point of view of pollution and of the trophic status (Smith, 2003; Viaroli and Christian, 2003; Gamito et al., 2005; Howarth et al., 2011; Pérez-Ruzafa et al., 2012; Vybernaite-Lubiene et al., 2017;

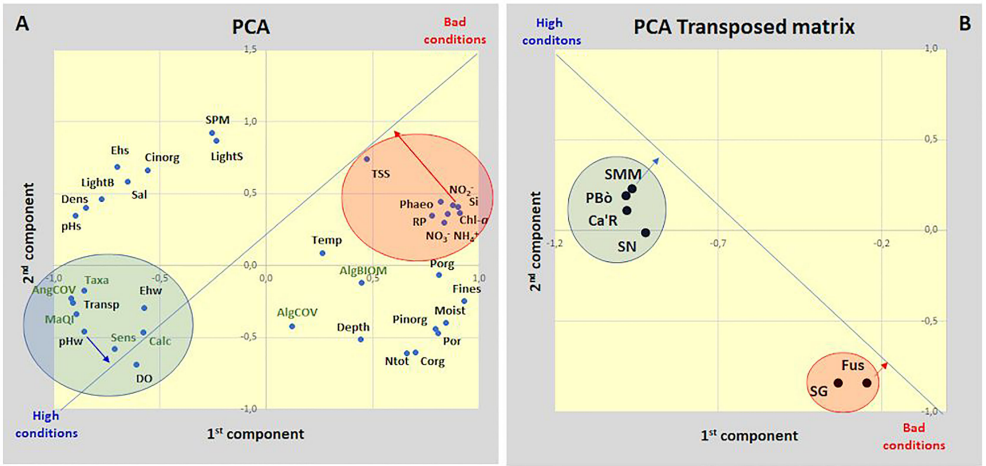

FIGURE 5 | PCA analysis of **(A)** plot of environmental parameters and macrophyte variables; **(B)** plot of the 6 stations in the transposed matrix.

Hsieh et al., 2021) but relatively fewer articles are about the possibility of a reversal of this trend and on the consequent environmental recovery (Carstensen et al., 2006; Rodrigo et al., 2013; Kralj et al., 2016; McCrackin et al., 2016). Recent studies reported that the Venice Lagoon can be taken as an example of quick environmental recovery due to a marked nutrient decrease (Sfriso et al., 2019; Sfriso et al., 2021a; Sfriso et al., 2021b) with a significant impact on the aquatic vegetation. Indeed, the decrease of the macroalgal biomass and production which occurred in the 1980s allowed the recovery of aquatic angiosperms whose biomasses increased markedly. This was the effect of several policies that were adopted in the framework of EU legislation to prevent or attenuate the impacts of nutrient pollution and its consequences on the aquatic ecosystems. Among them, the Nitrates Directive (ND, 91/676/EEC), dealing with diffuse pollution of nitrogen from agriculture, the Urban Wastewater Treatment Directive (UWWT, 91/271/EEC), addressed to the major point sources, and the Water Framework Directive (2000/60/EC) (European Commission, 2000) that prompted Member States of the European Union to enact new laws to reduce major pollutant resources because the impacts on the biota were of particular importance.

The result of these new policies on the vegetation of the Venice Lagoon was relevant. Data comparison of the cover, SC, and NPP values recorded in 2018 with those found in 2003 for macroalgae and aquatic angiosperms is reported in **Table 4** (macroalgae data from 1980 are also available).

In 1980 macroalgae, mainly represented by *Ulva rigida* C. Agardh and *Ulva australis* Areschoug ex *U. laetevirens* Areschoug (>90%) showed a luxuriant growth colonizing 202 km^2 with an SC and an NPP of approximately 841 and 2912 ktonnes FW, respectively (**Table 4**). Macroalgae reduced significantly in 2003 (Sfriso and Facca, 2007) due to the synergistic effect of many factors including climatic changes (Sfriso and Marcomini, 1996). Indeed, in this period the total SC and NPP were approximately 10 and 6 times lower than in 1980, respectively. Moreover, the dominant species changed from Ulvaceae to Gracilariaceae or other Rhodophyceae. At present Ulvaceae, mainly *U. rigida* and *U. australis* Areschoug, are frequent but usually have a negligible biomass whereas *Gracilaria gracilis* (Stackhouse) Steentoft et al., *Gracilaria bursa-pastoris* (S.G. Gmelin) P.C. Silva, *Gracilariopsis longissimima* (S. G. Gmelin) Steentoft et al., *Gracilariopsis vermiculophylla* Ohmi, *Hypnea cervicornis* J. Agardh are absolutely dominant.

The result of the decrease of macroalgal biomass and production was significant growth of all aquatic angiosperms. In fact, their cover increased from 55.9 to 94.8 km^2, the SC from 209 to 372 ktonnes FW and NPP from 714 to 1189 ktonnes FW. *Ruppia cirrhosa* was the species that in the past suffered most the effects of eutrophication and anthropogenic impacts, such as clam fishing (Pranovi and Giovanardi, 1994; Sfriso et al., 2005). However, after its disappearance in the 1980s (Mannino et al., 2015) the species recolonized the northern lagoon covering 6.0 km^2 with a SC of 8.9 ktonnes FW and an NPP of 18 ktonnes FW. *Zostera noltei*, that in 2003 covered about 6.2 km^2 with an SC of 9.8 ktonnes FW and an NPP of 25 ktonnes FW, in 2018 increased its growing values even by 191% (cover), 272% (SC), and 249% (NPP) (**Table 4**). *Zostera marina* cover increased by 12.2 km^2 (+46.6%) from 26.1 to 38.2 km^2 whereas the SC and NPP increased by 61 and 59%, respectively. Finally, *C. nodosa* from 2003 to 2018 increased its cover from 23.6 to 32.4 km^2 (+37.5%).

With exception of *C. nodosa*, a significant growth of the angiosperm species was also favored by transplant activities carried out in the northern basin of the Venice Lagoon in the framework of the project Life SERESTO (LIFE12 NAT/IT/000331) (Project LIFE12 NAT/IT/000331, 2012; Sfriso et al., 2021b). Indeed, between 2014 and 2018 more than 75,000 rhizomes were transplanted forming wide meadows of *Z. noltei*, *Z. marina*, and *R. cirrhosa* that colonized approximately 15 km^2 of lagoon bottoms with a mean density of 40%. This contributed significantly to explain the increase of these species in the northern

TABLE 4 | Macrophyte comparison in different years.

Species	Year	Area	SC	NPP
		km^2	ktonnes	
C. nodosa	2003	23.6	109	346
	2018	32.4	181	539
Increase		8.8	72	193
	%	37.5	66	56
Z.marina	2003	26.1	91	343
	2018	38.2	145	545
Increase		12.2	55	203
	%	46.6	61	59
Z. noltei	2003	6.2	9.8	25
	2018	18.1	36.5	86
Increase		11.8	27	62
	%	191	272	249
R. cirrhosa	2003	0	0	0
	2018	6.0	8.9	18.0
Total angiosperms	2003	55.9	209	714
	2018	94.8	372	1189
Increase		39	162	475
	%	70	77	67
Total macroalgae	1980	202	841	2912
	2003	97	89	472
	2018	134	104	647
Increase		37	15	175
2003-18	%	38	17	37

basin where they had almost completely disappeared. But a strong natural recruitment was also recorded in the central and southern lagoon, mainly due to the almost total disappearance of clam fishing activities caused by overexploitation. Therefore, transplantation activities in areas where the nutrient reduction hinders the bloom of thionitrophilic macroalgae or phytoplankton and there are no other significant anthropogenic impacts are an excellent tool to accelerate a quick recovery of ecological conditions. Widespread manual transplants of small sods or single rhizomes of aquatic angiosperms are the simplest, rapid, and least expensive tool to favor the formation of prairies and the recolonization of sensitive macroalgae with a strong reduction of Ulvaceae. Indeed, at present the Venice Lagoon is dominated by angiosperms and macroalgae less dangerous than Ulvaceae for the environment because they withstand higher water temperatures and are unlikely to trigger hypo-anoxic conditions (Sfriso and Sfriso, 2017).

The strong inverse relationships between nutrient concentrations and aquatic angiosperms and sensitive macroalgae is well highlighted by the results recorded in the 6 stations sampled in the lagoon in 2019 on an annual basis. The stations characterized by a higher trophic level (SG and FUS) were only colonized by macroalgae of low ecological value and no sensitive species or aquatic angiosperm were present. Conversely, the areas characterized by a lower concentration of nutrients both in the water column and in the surface sediments (SMM, PBò, Ca'R, SN) had dense seagrass meadows and many sensitive macroalgae, especially the small calcareous macroalgae of the genus *Hydrolithon*, *Pneophyllum*, and *Melobesia* (Sfriso et al., 2020b). The latter are more sensitive than seagrasses to respond

TABLE 5 | Comparison of angiosperm biomass and Net Primary Production (NPP).

	Highest biomass		NPP		References
	g DW m^{-2}		g DW m^{-2} d^{-1}		
	shoots	rhizomes	shoots	rhizomes	
Mean of 30 Seagrasses	224	237	3.84	1.21	Duarte and Chiscano (1999).
C. nodosa	147	280	1.3	0.17	Duarte and Chiscano (1999).
	674	694	4.94	1.88	SMM, this paper
	594	355	5.79	1.92	SN, this paper
Z. marina	298	150	5.2	1.7	Duarte and Chiscano (1999).
	425	265	5.08	0.85	Ca'R, this paper
Z. noltei	83	66	1.1	ND	Duarte and Chiscano (1999).
	296	305	2.64	1.02	PBò, this paper

ND, Not Determined.

to an improvement in ecological conditions and their discovery is an excellent indicator to predict the possibility of a recolonization of angiosperms or the success of transplant activities.

Extensive literature is available on the biomass and production of the angiosperms treated in this paper, but an exhaustive summary has been made by Duarte and Chiscano (1999) who reported information on the highest biomass and production of 30 different species of seagrasses (**Table 5**). On average, the mean values of the above- and belowground highest biomass and production were 224 ± 18 and 237 ± 28 g DW m^{-2}, respectively. In addition, these authors also reported the values of *C. nodosa*, *Z. marina*, and *Z. noltei*. In general, the highest biomass and the production recorded in the Venice Lagoon were higher both for the above- and belowground of all three species. Shoots and rhizomes were 2-4 times higher for *C. nodosa* and *Z. noltei*, and 2 times for *Z. marina*. The production was 3-4 times higher for shoots of *C. nodosa*, 2 times for Z. *noltei*, and very similar for *Z. marina*. The production of rhizomes was markedly higher for *C. nodosa* whereas for *Z. marina* it was almost half. No information for the rhizomes of *Z. noltei* is available. The greater biomass recorded in the Venice Lagoon probably depends on the choice to study compact prairies to obtain information under optimal growth conditions. However, higher biomass and production data were also recorded by Sfriso and Ghetti (1998) who studied the annual growth of the same species in different areas of the Venice Lagoon. In addition, studies in progress show that in 2021 angiosperm biomass and production increased further.

Moreover, the recovery of angiosperm meadows contributed to a further environmental recovery accelerating the recolonization of fish species both of commercial and conservation interest (Jackson et al., 2001; Blandon and Zu Ermgassen, 2014; Bonometto et al., 2018; Scapin et al., 2018; Scapin et al., 2019) and is changing the composition of the benthic macrofauna (Orth et al., 1984; Sfriso et al., 2001; Leopardas et al., 2014; Lin et al., 2018; Mariño et al., 2018) living in these underwater forests.

These results confirm that the recovery of highly degraded TWS, such as the Venice Lagoon was up to the early 2000s, is easily achievable provided there is low trophy and clear waters. Indeed, even small reductions in anthropogenic impacts, especially in basins with high tidal exchange, can favor a rapid or progressive environmental recovery thanks to the high resilience of these environments.

DATA AVAILABILITY STATEMENT

The raw data supporting the conclusions of this article will be made available by the authors, without undue reservation.

AUTHOR CONTRIBUTIONS

AS: funding acquisition, conceptualization, methodology, formal analysis, writing–original draft; AB, AAS: methodology, formal analysis, writing–review and editing; KS, MW, YT, A-SJ: formal analysis, writing–review and editing. All authors contributed to the article and approved the submitted version.

ACKNOWLEDGMENTS

Scientific activity was performed in the following research programs: Venezia2021, coordinated by CORILA (consortium for coordination of research activities concerning the Venice Lagoon system), with the contribution of the Provveditorato for the Public Works of Veneto, Trentino Alto Adige and Friuli Venezia Giulia and MoVEco III (ecological monitoring of the Venice Lagoon), between ARPA (Regional Agency for Environmental Protection) Veneto and Ca' Foscari University of Venice - Department of Environmental Sciences, Informatics and Statistics.

SUPPLEMENTARY MATERIAL

The Supplementary Material for this article can be found online at: https://www.frontiersin.org/articles/10.3389/fmars.2022.882463/full#supplementary-material

REFERENCES

Blandon, A., and Zu Ermgassen, P. S. E. (2014). Quantitative Estimate of Commercial Fish Enhancement by Seagrass Habitat in Southern Australia. *Estuar. Coast. Shelf. Sci.* 141, 1–8. doi: 10.1016/j.ecss.2014.01.009

Bonometto, A., Sfriso, A., Oselladore, F., Ponis, E., Cornello, M., and Facca, C. (2018). "Il Trapianto Di Fanerogame Acquatiche Come Misura Per Il Ripristino Delle Lagune Costiere," in *Quaderni – Ricerca Marina*, vol. 12/2018. (Roma: ISPRA), 1–52.

Carstensen, J., Conley, D., Andersen, J., and Aertebjerg, G. (2006). Coastal Eutrophication and Trend Reversal: A Danish Case Study. *Limnol. Oceanogr.* 1 (2), 398–408. doi: 10.4319/lo.2006.51.1_part_2.0398

Cucco, A., and Umgiesser, G. (2006). Modeling the Venice Lagoon Residence Time. *Ecol. Model.* 193, 34–51. doi: 10.1016/j.ecolmodel.2005.07.043

Dennison, W. C. (1990a). "Leaf Production," in *Seagrass Research Methods*. Eds. R. C. Phillips and C. P. McRoy (Mayenne, France: UNESCO, Imprimerie de la Manutention), 77–79.

Dennison, W. C. (1990b). "Rhizome-Root Production," in *Seagrass Research Methods*. Eds. R. C. Phillips and C. P. McRoy (Mayenne, France: UNESCO, Imprimerie de la Manutention), 81–82.

De Toni, G. B. (1889). "Sylloge Algarum Omnium Hucusque Cognitarum," in *Chlorophyceae. Sectio I–II*, Vol I. (Patavii: Patavii, Padua), CXXXIX + 1315.

De Toni, G. B. (1895). "Sylloge Algarum Omnium Hucusque Cognitarum," in *Fucoideae. Sectio III*, Vol. III. (Patavii: Patavii, Padua), XVI + 638.

De Toni, G. B. (1897). "Sylloge Algarum Omnium Hucusque Cognitarum," in *Florideae, Sectio I*, Vol. IV. (Patavii: Patavii, Padua), ILXI + 338.

De Toni, G. B. (1900). "Sylloge Algarum Omnium Hucusque Cognitarum," in *Florideae, Sectio Ii*, Vol. IV. (Patavii: Patavii, Padua), 387–776.

De Toni, G. B. (1903). "Sylloge Algarum Omnium Hucusque Cognitarum," in *Florideae, Sectio III*, Vol. IV. (Patavii: Patavii, Padua), 775–1525.

De Toni, G. B. (1905). "Sylloge Algarum Omnium Hucusque Cognitarum," in *Florideae, Sectio Iv*, Vol. IV. (Patavii: Patavii, Padua), 1523–1973.

De Toni, G. B. (1907). Sopra Alcune Polysiphonia Inedite O Rare. *Nuova. Notarisia.* (Patavii: Patavii, Padua) 18, 153–168.

De Toni, G. B. (1924). "Sylloge Algarum Omnium Hucusque Cognitarum," in *Florideae, Sectio V*, Vol. IV. (Patavini: Patavii, Padua), XI + 767.

De Toni, G. B., and Levi, D. (1885). "Flora Algologia Della Venezia," in *Le Floridee* (Venezia: Tip. Antonelli), 182.

De Toni, G. B., and Levi, D. (1886). "Flora Algologia Della Venezia," in *Le Melanoficee* (Venezia: Tip. Antonelli), 107.

De Toni, G. B., and Levi, D. (1888a). "Flora Algologia Della Venezia," in *Le Cloroficee* (Venezia: Tip. Antonelli), 206.

De Toni, G. B., and Levi, D. (1888b). *Collezioni Botaniche, L'algarium Zanardini. Catalogo Alfabetico-Geografico Dell'algarium Del Civico Museo E Raccolta Correr in Venezia* (Venezia: Tip. Fontana), 144.

Duarte, C., and Chiscano, C. L. (1999). Seagrass Biomass and Production: A Reassessment. *Aquat. Bot.* 65, 159–174. doi: 10.1016/S0304-3770(99)00038-8

European Commission. (2000). Directive 2000/60/EC of the European Parliament and of the Council of 23 October 2000 Establishing a Framework for Community Action in the Field of Water Policy. *Off. J. Eur. Communities.* 327, 1–72.

Gamito, S., Gilabert, J., Marcos, C., and Pérez-Ruzafa, A. (2005). "Effects of Changing Environmental Conditions on Lagoon Ecology," in *Coastal Lagoons: Ecosystem Processes and Modeling for Sustainable Use and Development*. Eds. I. E. Gönenç and J. P. Wolflin (Boca Ratón, FL: CRC Press), 193–229.

Howarth, R., Chan, F., Conley, D. J., Garnier, J., Doney, S. C., Marino, R., et al. (2011). Coupled Biogeochemical Cycles: Eutrophication and Hypoxia in Temperate Estuaries and Coastal Marine Ecosystems. *Front. Ecol. Environ.* 9, 18–26. doi: 10.1890/100008

Hsieh, H.-H., Chuang, M.-H., Shih, Y.-Y., Weerakkody, W. S., Huang, W.-J., Hung, C. C., et al. (2021). Eutrophication and Hypoxia in Tropical Negombo Lagoon, Sri Lanka. *Front. Mar. Sci.* 8 (1-13), 678832. doi: 10.3389/fmars.2021.678832

ISPRA. (2011). *Protocolli Per Il Campionamento E La Determinazione Degli Elementi Di Qualità Biologica E Fisico-Chimica Nell'ambito Dei Programmi Di Monitoraggio Ex 2000/60/CE Delle Acque Di Transizione. El-Pr-TW-Protocolli Monitoraggio- 03.06* (Roma: ISPRA).

Jackson, E. L., Rowden, A. A., Attrill, M. J., Bossey, S. J., and Jones, M. B. (2001). The Importance of Seagrass Beds as a Habitat for Fishery Species. *Oceanogr. Mar. Biol. Annu. Rev.* 39, 269–303. doi: 10.4236/ns.2012.48069

Kralj, M., De Vittor, C., Comici, C., Relitti, F., Auriemma, R., Alabiso, G., et al. (2016). Recent Evolution of the Physical-Chemical Characteristics of a Site of National Interest – The Mar Piccolo of Taranto (Ionian Sea) – and Changes Over the Last 20 Years. *Environ. Sci. Pollut. Res.* 23, 12675–12690. doi: 10.1007/s11356-015-5198-8

Leopardas, V., Uy, W., and Nakaoka, M. (2014). Benthic Macrofaunal Assemblages in Multispecific Seagrass Meadows of the Southern Philippines: Variation Among Vegetation Dominated by Different Seagrass Species. *J. Exp. Mar. Biol. Ecol.* 457, 71–80. doi: 10.1016/j.jembe.2014.04.006

Lin, J., Huang, Y., Arbi, U. Y., Lin, H., Azkab, M. H., Wang, J., et al. (2018). An Ecological Survey of the Abundance and Diversity of Benthic Macrofauna in Indonesian Multispecific Seagrass Beds. *Acta Oceanol. Sin.* 37, 82–89. doi: 10.1007/s13131-018-1181-9

Mannino, A. M., Menéndez, M., Obrador, B., Sfriso, A., and Triest, L. (2015). The Genus *Ruppia* L. (Ruppiaceae) in the Mediterranean Region: An Overview. *Aquat. Bot.* 124, 1–9. doi: 10.1016/j.aquabot.2015.02.005

Marcomini, A., Sfriso, A., Pavoni, B., and Orio, A. A. (1995). "Eutrophication of the Lagoon of Venice: Nutrient Loads and Exchanges," in *Eutrophic Shallow Estuaries and Lagoons*. Ed. A. JMc Comb (Boca Raton, FL., U.S.A: CRC Press), 59–80.

Mariño, J., Mendoza, M. D., and Sánchez, B. L. (2018). Composition and Abundance of Decapod Crustaceans in Mixed Seagrass Meadows in the Paraguaná Peninsula, Venezuela. *Iheringia. Série. Zool.* 108, 2018004. doi: 10.1590/1678.4766e2018004

McCrackin, M. L., Jones, H. P., Jones, P. C., and Moreno-Mateos, D. (2016). Recovery of Lakes and Coastal Marine Ecosystems From Eutrophication: A Global Meta-Analysis. *Limnol. Oceanogr.* 62, 507–518. doi: 10.1002/lno.10441

Naccari, F. L. (1828). Algologia Adriatica. *Stamperia Cardinali E. frulli: Bologna* 157. doi: 10.5962/bhl.title.68746

Olivi, G. (1794). Sopra Una Nuova Specie Di *Ulva* Delle Lagune Venete. Saggi Scientifici E Letterari Dell'Accademia Di Padova. *Padova* 3, 1.

Orth, R., Heck, K. L., and Van Montfrans, J. (1984). Faunal Communities in Seagrass Beds. A Review of the Influence of Plant Structure and Prey Characteristics on Predator Prey Relationships. *Estuaries* 7 (4), 339–350.

Pavoni, B., Marcomini, A., Sfriso, A., Donazzolo, R., and Orio, A. A. (1992). "Changes in an Estuarine Ecosystem. The Lagoon of Venice as a Case Study," in *The Science of Global Change*. Eds. D. A. Dunnette and R. J. O'Brien (Washington, D.C., U.S.A: American Chemical Society), 287–305.

Pérez-Ruzafa, A., Marcos, C., Bernal, C. M., Quintino, V., Freitas, R., Rodrigues, A. M., et al. (2012). *Cymodocea Nodosa* vs. *Caulerpa Prolifera*: Causes and Consequences of a Long-Term History of Interaction in Macrophyte Meadows in the Mar Menor Coastal Lagoon (Spain, Southwestern Mediterranean). *Estuar. Coast. Shelf. Sci.* 110, 101–115. doi: 10.1016/j.ecss.2012.04.004

Pignatti, S. (1962). "Associazioni Di Alghe Marine Sulla Costa Veneziana. Mem," vol. 32, Fasc. 3. (Ist. Veneto Sci, Lett. Arti, Cl. Sci. Mat. Nat), 1–134.

Pranovi, F., and Giovanardi, O. (1994). The Impact of Hydraulic Dredging for Shortnecked Clams, Tapes Spp, on an Infaunal Community in the Lagoon of Venice. *Sci. Mar.* 58, 345–53.

Project LIFE12 NAT/IT/000331. (2012). Habitat 1150* (Coastal lagoon) recovery by SEagrass RESTOration. *A New Strategic Approach to Meet HD & WFD Objectives*. Available at: http://www.lifeseresto.eu.

Rodrigo, M. A., Martin, M., Rojo, C., Gargallo, S., Matilde Segura, M., and Oliver, N. (2013). The Role of Eutrophication Reduction of Two Small Man-Made Mediterranean Lagoons in the Context of a Broader Remediation System: Effects on Water Quality and Plankton Contribution. *Ecol. Eng.* 61, 371–382. doi: 10.1016/j.ecoleng.2013.09.038

Scapin, L., Zucchetta, M., Sfriso, A., and Franzoi, P. (2018). Local Habitat and Seascape Structure Influence Seagrass Fish Assemblages in the Venice Lagoon: The Value of Conservation at Multiple Spatial Scales. *Estuar. Coast.* 41, 2410–2425. doi: 10.1007/s12237-018-0434-3

Scapin, L., Zucchetta, M., Sfriso, A., and Franzoi, P. (2019). Predicting the Response of Nekton Assemblages to Seagrass Transplantations in the Venice Lagoon: An Approach to Assess Ecological Restoration. *Aquat. Conserv.: Mar. Freshw. Ecosyst.* 29, 849–864. doi: 10.1002/aqc.3071

Schiffner, C., and Vatova, A. (1938). "Le Alghe Della Laguna: Chlorophyceae, Phaeophyceae, Rhodophyceae, Myxophyceae," in *La Laguna Di Venezia*, Vol. 3. Ed. M. Minio (Venezia: Ferrari) 250.

Sfriso, A., Birkemeyer, T., and Ghetti, P. F. (2001). Benthic Macrofauna Changes in Areas of Venice Lagoon Populated by Seagrasses or Seaweeds. *Mar. Environ. Res.* 52, 323–349. doi: 10.1016/S0141-1136(01)00089-7

Sfriso, A., Buosi, A., Facca, C., and Sfriso, A. A. (2017). Role of Environmental Factors in Affecting Macrophyte Dominance in Transitional Environments: The Italian Lagoons as a Study Case. *Mar. Ecol.* 38 (2), e12414. doi: 10.1111/maec.12414

Sfriso, A., Buosi, A., Mistri, M., Munari, C., Franzoi, P., and Sfriso, A. A. (2019). "Long-Term Changes of the Trophic Status in Transitional Ecosystems of the Northern Adriatic Sea, Key Parameters and Future Expectations: The Lagoon of Venice as a Study Case," in *Italian Long-Term Ecological Research for Understanding Ecosystem Diversity and Functioning. Case Studies From Aquatic, Terrestrial and Transitional Domains*, vol. 34. Eds. M. G. Mazzocchi, L. Capotondi, M. Freppaz, A. Lugliè and A. Campanaro, 193–215.

Sfriso, A., Buosi, A., Tomio, Y., Juhmani, A.-S., Facca, C., Wolf, M., et al. (2021b). Environmental Restoration by Aquatic Angiosperm Transplants in Transitional Water Systems: The Venice Lagoon as a Case Study. *Sci. Tot. Environ.* 795, 148859. doi: 10.1016/j.scitotenv.2021.148859

Sfriso, A., Buosi, A., Tomio, Y., Juhmani, A.-S., Mistri, M., Munari, C., et al. (2021a). Nitrogen and Phosphorus Trends in Surface Sediments, a Litmus Paper of Anthropogenic Impacts. The Lagoons of the Northern Northern Adriatic Sea as a Study Case. *Water* 13, 2914. doi: 10.3390/w13202914

Sfriso, A., Buosi, A., Wolf, M. A., Sciuto, K., Molinaroli, E., Mistri, M., et al. (2020b). Microcalcareus Seaweeds a Sentinel of Trophic Changes and CO_2 Trapping in Transitional Waters. *Ecol. Indic.* 118, 1–10. doi: 10.1016/j.ecolind.2020.106692

Sfriso, A., Buosi, A., Wolf, M. A., and Sfriso, A. A. (2020a). Invasion of Alien Macroalgae in the Venice Lagoon, a Pest or a Resource? *Aquat. Invasion.* 15 (2), 245–270. doi: 10.3391/ai.2020.15.2.03

Sfriso, A., and Curiel, D. (2007). Check-List of Marine Seaweeds Recorded in the Last 20 Years in Venice Lagoon and a Comparison With the Previous Records. *Bot. Mar.* 50, 22–58. doi: 10.1515/BOT.2007.004

Sfriso, A., and Facca, C. (2007). Distribution and Production of Macrophytes in the Lagoon of Venice. Comparison of Actual and Past Abundance. *Hydrobiologia* 577, 71–85. doi: 10.1007/s10750-006-0418-3

Sfriso, A., Facca, C., Bonometto, A., and Boscolo, R. (2014). Compliance of the Macrophyte Quality Index (MaQI) With the WF/60/EC) and Ecological Status Assessment in Transitional Areas: The Venice Lagoon as Study Case. *Ecol. Indic.* 46, 536–547. doi: 10.1016/j.ecolind.2014.07.012

Sfriso, A., Facca, C., Ceoldo, S., Silvestri, S., and Ghetti, P. F. (2003). Role of Macroalgal Biomass and Clam Fishing on Spatial and Temporal Changes in N and P Sedimentary Pools in the Central Part of the Venice Lagoon. *Oceanol. Acta* 26 (1), 3–13. doi: 10.1016/S0399-1784(02)00008-7

Sfriso, A., Facca, C., and Ghetti, P. F. (2009). Validation of the Macrophyte Quality Index (MaQI) Set Up To Assess the Ecological Status of Italian Marine Transitional Environments. *Hydrobiologia* 617, 117–141. doi: 10.1007/s10750-008-9540-8

Sfriso, A., Facca, C., and Marcomini, A. (2005). Sedimentation Rates and Erosion Processes in the Lagoon of Venice. *Environ. Int.* 31 (7), 983–992. doi: 10.1016/j.envint.2005.05.008

Sfriso, A., and Ghetti, P. F. (1998). Seasonal Variation in the Biomass, Morphometric Parameters and Production of Rhizophytes in the Lagoon of Venice. *Aquat. Bot.* 61, 207–223. doi: 10.1016/S0304-3770(98)00064-3

Sfriso, A., and Marcomini, A. (1994). Gross Primary Production and Nutrient Behaviours in Shallow Lagoon Waters. *Bioresour. Technol.* 47, 59–66. doi: 10.1016/0960-8524(94)90029-9

Sfriso, A., and Marcomini, A. (1996). Decline of *Ulva* Growth in the Lagoon of Venice. *Bioresour. Technol.* 58, 299–307. doi: 10.1016/S0960-8524(96)00120-4

Sfriso, A., Raccanelli, S., Pavoni, B., and Marcomini, A. (1991). Sampling Strategies for Measuring Macroalgal Biomass in the Shallow Waters of the Venice Lagoon. *Environ. Technol.* 12, 263–269. doi: 10.1080/09593339109385004

Sfriso, A. A., and Sfriso, A. (2017). *In Situ* Biomass Production of Gracilariaceae and *Ulva Rigida*: The Venice Lagoon as Study Case. *Bot. Mar.* 60 (3), 271–283. doi: 10.1515/bot-2016-0061

Sighel, A. (1938). La Distribuzione Stazionale E Stagionale Delle Alghe Nella Laguna Di Venezia. Mem. Comit. Talass. Ital. Officine Grafiche Ferrari. *Memoria. CCL.*, 123.

Smith, V. H. (2003). Eutrophication of Freshwater and Coastal Marine Ecosystems a Global Problem. *Environ. Sci. Pollut. Res.* 10, 126–139. doi: 10.1065/espr2002.12.142

Sorokin, P., Yu, S. 1., Yu, I., Boscolo, R., and Giovanardi, O. (2004). Bloom of Picocyanobacteria in the Venice Lagoon During Summer–Autumn 2001: Ecological Sequences. *Hydrobiologia* 523, 71–85. doi: 10.1023/B:HYDR.0000033096.14267.43

Vatova, A. (1940). Distribuzione Geografica Delle Alghe Nella Laguna Veneta E Fattori Che La Determinano. *Thalassia* 4, 1–36.

Viaroli, P., and Christian, R. R. (2003). Description of Trophic Status, Hyperautotrophy and Dystrophy of a Coastal Lagoon Through a Potential Oxygen Production and Consumption Index - TOSI: Trophic Oxygen Status Index. *Ecol. Indic.* 3, 237–250. doi: 10.1016/j.ecolind.2003.11.001

Vybernaite-Lubiene, I., Zilius, M., Giordani, G., Petkuviene, J., Vaiciute, D., Bukaveckas, P. A., et al. (2017). Effect of Algal Blooms on Retention of N, Si and P in Europe's Largest Coastal Lagoon. *Estuar. Coast. Shelf. Sci.* 194, 217–228. doi: 10.1016/j.ecss.2017.06.020

Zanardini, G. (1847). Notizie Intorno Alle Cellulari Marine Delle Lagune E De' Litorali Di Venezia. *Atti. Reale. Ist. Veneto. Sci. Lett. Arti. Ser.* 1, 185–262.

Conflict of Interest: The authors declare that the research was conducted in the absence of any commercial or financial relationships that could be construed as a potential conflict of interest.

Publisher's Note: All claims expressed in this article are solely those of the authors and do not necessarily represent those of their affiliated organizations, or those of the publisher, the editors and the reviewers. Any product that may be evaluated in this article, or claim that may be made by its manufacturer, is not guaranteed or endorsed by the publisher.

frontiers | Frontiers in Marine Science

ORIGINAL RESEARCH
published: 09 June 2022
doi: 10.3389/fmars.2022.877935

Benthic and Pelagic Contributions to Primary Production: Experimental Insights From the Gulf of Trieste (Northern Adriatic Sea)

Tamara Cibic, Laura Baldassarre, Federica Cerino, Cinzia Comici, Daniela Fornasaro, Martina Kralj and Michele Giani*

Oceanography Section, Istituto Nazionale di Oceanografia e di Geofisica Sperimentale – OGS, Trieste, Italy

Although the ^{14}C-method remains one of the most sensitive measures of primary production in marine ecosystems, few data from coastal sublittoral areas are available. We applied an integrated approach to quantify the benthic (PPs) and pelagic (PPw) contributions to total primary production (PPt) in a 17-m deep coastal site. From March 2015 to March 2019, we carried out 16 *in situ* experiments on a seasonal basis, at the LTER site C1, whereas benthic rates were estimated in the laboratory. To relate PP to seawater physical features and to the water column stability, the Brunt-Väisälä frequency was calculated. We further related our PP rates to the abundance, biomass, main taxonomic groups and diversity of eukaryotic phytoplankton and microphytobenthos (MPB). In November 2018, the maximum PPw (6.71 ± 0.82 μgC L^{-1} h^{-1}) was estimated at the surface layer, in correspondence to the highest value of dinoflagellates biomass (29.35 μgC L^{-1}), on the account of small (<20 μm) naked and thecate forms. PPi, integrated over the water column, displayed the highest values in July 2017 and July 2018. In sediments, negative PPs values were estimated in late autumn/winter, when minima of MPB abundance occurred. The highest rates were displayed in January 2018 and October 2016 (28.50 and 17.55 mgC m^{-2} h^{-1}), due to the presence of dominant diatoms *Paralia sulcata* and *Nitzschia sigma* var. *sigmatella*, respectively. The PPs contribution to PPt was negligible (<2%) in 6 out of 16 experiments, with a mean value of 11.3% (excluding negative PPs values) over the study period, while it reached up to 43% in January 2018. The principal component analyses revealed that nutrients availability affected the seasonal development of pelagic and benthic phototrophs and primary production more than the physical variables, except for the surface layer of the water column where temperature and salinity were the main drivers. Our results add on the limited database on primary production in sublittoral areas and represent one of the few attempts, on a global scale, of integrating pelagic and benthic primary production using the ^{14}C method to quantify the overall ecosystem productivity.

Keywords: primary production, benthic-pelagic coupling, ^{14}C-uptake, phytoplankton, microphytobenthos, nutrient availability

OPEN ACCESS

Edited by:
Paolo Magni,
National Research Council (CNR), Italy

Reviewed by:
Peter Anton Upadhyay Staehr,
Aarhus University, Denmark
Conrad Pilditch,
University of Waikato, New Zealand

****Correspondence:***
Tamara Cibic
tcibic@inogs.it

Specialty section:
This article was submitted to Marine Ecosystem Ecology, a section of the journal Frontiers in Marine Science

Received: *17 February 2022*
Accepted: *05 May 2022*
Published: *09 June 2022*

Citation:
Cibic T, Baldassarre L, Cerino F, Comici C, Fornasaro D, Kralj M and Giani M (2022) Benthic and Pelagic Contributions to Primary Production: Experimental Insights From the Gulf of Trieste (Northern Adriatic Sea). Front. Mar. Sci. 9:877935. doi: 10.3389/fmars.2022.877935

INTRODUCTION

Shallow coastal photic systems are among the most productive on the planet (Odum, 1983). In these environments, light penetration to the bottom fuels multiple primary producers, including phytoplankton and benthic microalgae that develop on unvegetated soft bottoms (Sundbäck et al., 2000). Primary production measurement in marine waters is one of the most important tools to understand ecosystem functioning and the transport of inorganic/organic matter through the food web (Williams PJB et al., 2002). In shallow oligotrophic systems, pelagic production largely depends on rivers and freshwater-borne nutrient inputs (Mozetič et al., 2012), and internal recycling of nutrients particularly from sediments under seasonally elevated temperatures (Kemp et al., 1997). Aside from nutrients, coastal processes are largely influenced by physical factors such as light, temperature, stratification, winds and local currents that are key parameters regulating pelagic processes. On the other hand, rapid sinking of phytoplankton blooms and an efficient filtration of the water column by benthic fauna can determine a tight benthic-pelagic coupling that leads to a high local benthic production. Further, microbial mediated processes in sediments can enhance nutrient availability for primary production in both benthic and pelagic habitats and become important in regulating the relative magnitude of benthic versus pelagic primary production (Kennish et al., 2014).

Since the introduction of the radiolabelled carbon uptake method (Steemann Nielsen, 1952; Sorokin, 1958), the ^{14}C technique has become the standard method for measuring primary production in seawater and thousands of measurements of pelagic primary production have been made at discrete locations throughout the world's oceans. In contrast, several methodologies have been applied to estimate the benthic primary production in subtidal ecosystems. Among the ^{14}C methods applied to the sediment matrix, the slurry technique is still largely used (Sundbäck et al., 2011; van der Molen and Perisinotto, 2011; Jacobs et al., 2021). Although the existing microgradients in the sediment are destroyed, if no nutrients are limiting in the surface sediments, the measured potential photosynthetic rates still reflect real rates (Barranguet et al., 1998; Kromkamp and Forster, 2006).

Regardless of the methodology, despite the large body of literature on primary production estimated from intertidal (Barranguet and Kromkamp, 2000; Serodio et al., 2008; Migné et al., 2009) and shallow subtidal/lagoon ecosystems (Blasutto et al., 2005; Murrell et al., 2009; Bartoli et al., 2012), corresponding studies of ecosystems at depths higher than 15 m are limited (Jahnke et al., 2008; Lehrter et al., 2014; Santema and Huettel, 2018; Cesbron et al., 2019). Moreover, very few microphytobenthic primary production estimates, using the ^{14}C uptake, have been carried out in deeper subtidal areas (Sundbäck and Jönsson, 1988; Rogelja et al., 2016; Rubino et al., 2016). The importance of benthic microalgae for ecosystem primary production was first evaluated by Martin et al. (1987) and Longhurst et al. (1995) who estimated that 0.7% of the total oceanic production and 2.4-3.7% of the continental shelf production, respectively, is due to benthic microalgae. However, according to more recent estimates, the microphytobenthos may contribute for more than 50% to the total primary production in shallow coastal systems (Lehrter et al., 2014; Cesbron et al., 2019).

The Gulf of Trieste, located in the northern part of the Adriatic Sea, is a semi-enclosed basin with a maximum depth of 25 m. In this area, the phytoplankton development, in terms of microalgal blooms, community succession (Cabrini et al., 2012; Mozetič et al., 2012) and photosynthetic activity (Fonda Umani et al., 2004; Fonda Umani et al., 2007; Ingrosso et al., 2016; Cibic et al., 2018b; Talaber et al., 2018) is highly dependent on nutrient availability originating from freshwater discharges, and therefore responds to seasonal and interannual variations of riverine fluxes. On a seasonal basis, the pelagic ecosystem of the gulf shifts from a more nutrient enriched condition, typical of the late winter-spring season, when sufficient inorganic nutrients are available to sustain the main diatom bloom of the year, to an oligotrophic condition in summer-autumn, dominated by small-sized photoautotrophs (Fonda Umani et al., 2012). Focusing on the benthic domain, the microphytobenthic community at a 17-m deep site is not photosynthetically active throughout the year. From late summer to early winter, low or negative values are recorded in correspondence with low light and/or high temperature at the bottom (Cibic et al., 2008; Franzo et al., 2016). Although in the Gulf of Trieste primary production has been investigated both in the pelagic (Malej et al., 1995; Fonda-Umani et al., 2004; Fonda-Umani et al., 2007; Talaber et al., 2014; Ingrosso et al., 2016; Cibic et al., 2018b; Talaber et al., 2018) and benthic (Herndl et al., 1989; Cibic et al., 2008; Franzo et al., 2016; Rogelja et al., 2018) ecosystems over the last decades, estimates of the total (pelagic + benthic) rates are still very scarce (Testa et al., 2021).

Also on a global scale, very little information is available on combined benthic-pelagic primary production measurements (Lake and Brush, 2011; Cesbron et al., 2019; Frankenbach et al., 2020), even less considering the ^{14}C incorporation method (Anandraj et al., 2007; van der Molen and Perissinotto, 2011). To the best of our knowledge, excluding the few estimates published in these shallow estuarine or semi-enclosed ecosystems (Cibic et al., 2016), there is no literature on integrated, quasi-synchronous benthic-pelagic primary production from subtidal, not enclosed marine areas using the ^{14}C incubation technique. Therefore, to fill this knowledge gap, the aims of this study were to: i) investigate the pelagic and benthic primary production by performing quasi-synoptic estimates; ii) quantify the benthic contribution to total (pelagic + benthic) PP rates in an oligotrophic open coastal area; iii) highlight the most important physical and chemical drivers of the phototrophs' development and their photosynthetic rates in both domains. Our guiding questions and hypotheses were: Q1) To what extent is pelagic PP controlled by nutrient conditions and water column stability? H1) We expect pelagic PP to be mostly P-limited during summer, and to obtain the highest rates in stable water column conditions. Q2) To what extent is benthic PP controlled by

temperature and light conditions? H2) We expect benthic PP to be mostly inhibited by high temperatures during summer, and light limited during winter months. Q3) What is the relative importance of benthic PP in this system and how does it vary seasonally? H3) We expect total PP to be dominated by pelagic PP given the low light availability at the seafloor, except for clear water periods and during periods when pelagic PP is strongly nutrient depleted. Q4) Do the same abiotic factors equally affect the structure and function of the phototrophic communities along the water column and at the sediment surface? H4) We expect photosynthetic available radiation (PAR) availability to strongly affect the phototrophic development and PP at the lower layers of the water column and sediments, whereas temperature and salinity to be important drivers of the structure and function at the upper part of the water column. To test these hypotheses, between March 2015 and March 2019 we performed 16 *in situ* experiments on a seasonal basis, at four water depths of the sublittoral LTER site C1, whereas benthic rates were estimated in the laboratory within a few days. To relate PP to the water column stability, we calculated the Brunt-Väisälä frequency. We further computed monthly mean seawater temperature, salinity and PAR during the study period and compared them to climatological (1998 - 2019) mean data. To link our PP rates to phototrophs' dynamics, we further considered the abundance, biomass, main taxonomic groups and diversity of eukaryotic phytoplankton and microphytobenthos (MPB). Finally, we highlighted which abiotic factors are the most important drivers in influencing the development of the phototrophs and their photosynthetic rates at the four water depths and surface sediments, separately, and comprehensively discussed the integrated results.

MATERIAL AND METHODS

Study Area

The Gulf of Trieste is a small (~ 500 km^2) and shallow (maximum depth 25 m) basin in the northern part of the Adriatic Sea. In this area, freshwater inputs and atmospheric forcing greatly influence seawater temperature, salinity and water column stratification (Malačič and Petelin, 2001). The area is characterised by a marked seasonal cycle of seawater temperature (from winter minima of 8°C to summer maxima of 28.4°C) and strong salinity gradients (from 24.0, in spring during high riverine discharge, to 38.3) (Celio et al., 2006; Kralj et al., 2019). Typically, in winter, the water column is well-mixed, whereas during spring, freshwater input and surface heating lead to thermohaline stratification. The period between May and September is characterised by strong density gradients and the prevalence of respiration processes at the bottom layer, which determine low oxygen concentration and occasionally hypoxia events (Faganeli et al., 1985; Malej and Malačič, 1995; Kralj et al., 2019). In autumn, convective and mechanical mixing, induced by water cooling and wind, disrupt the vertical stratification, oxygenate the bottom water and distribute the re-generated nutrients to the entire water column.

The main riverine input in the Gulf of Trieste derives from Isonzo/Soča River on the north-western coast (Cozzi et al., 2012), which controls the salinity and nutrient concentration of the system with a highly variable outflow. On a seasonal scale, however, spring and autumn are generally characterised by the highest river discharges (due to snowmelt and rain, respectively), while drought periods occur during winter and summer (Comici and Bussani, 2007).

The trophic status of the gulf also depends on the prevailing circulation patterns and not only on the intensity of the Isonzo River discharge rate. Circulation in the gulf is mainly cyclonic at the transitional and lower layer (10 m – bottom), while the surface layer (0 – 4 m) is affected by wind conditions (Stravisi, 1983). There are mainly two dominant winds: the SE Scirocco and the NE Bora (Stravisi, 1977; Stravis, 1983). Bora-induced circulation is more frequent in autumn and winter, and it generates a cyclonic gyre at the surface layer, which causes a fast outflow of riverine waters from the gulf. When the Scirocco wind blows, instead, anticyclonic surface circulation favours eastward spreading of nutrient-enriched freshwater, which increases primary production (Cantoni et al., 2003; Querin et al., 2006).

The Gulf of Trieste is also influenced by the Eastern Adriatic Current (EAC), a current flowing northward along the Croatian coast and advecting warmer, saltier, and more oligotrophic waters coming from the Ionian Sea (Poulain et al., 2001). The ingression of EAC is more frequent in the cold seasons, when a cyclonic circulation is present, which can lead to oligotrophic conditions of the gulf.

Sampling and Environmental Data Collection

Sampling was performed at the Long-Term Ecological Research (LTER) station C1 (45°42'2" N and 13°42'36" E, maximum depth 17.5 m) located in the Gulf of Trieste (**Figure 1**). From March 2015 to March 2019, discrete seawater samples were collected on a seasonal basis with 5-L Niskin bottles at four depths (0.5, 5, 10, 15 m) for nutrient, phytoplankton and primary production analyses.

Seawater temperature and salinity were recorded monthly by a CTD probe model Sea-Bird Electronics SBE 19plus SeaCAT profiler. These data were compared to the monthly means (1998 - 2019) that were recorded with the following probes: from January 1998 to October 1999 with an Idronaut mod. 401 probe; from November 1999 to September 2003 with an Idronaut mod. 316 probe. These CTD probes were calibrated with an interval of 6 - 12 months. From October 2003 onwards, a Sea Bird Electronics SBE 19 plus SeaCAT was used that was calibrated every year.

To have an indication of the water column stability the Brunt-Väisälä (B-V) frequency was applied. This frequency is a measure of the natural oscillation resulting from vertical displacement of a neutrally buoyant body. Higher values indicate a large density gradient and a strong stratification, while near-zero and negative values indicate unstable conditions. For the calculation, the Matlab routine called

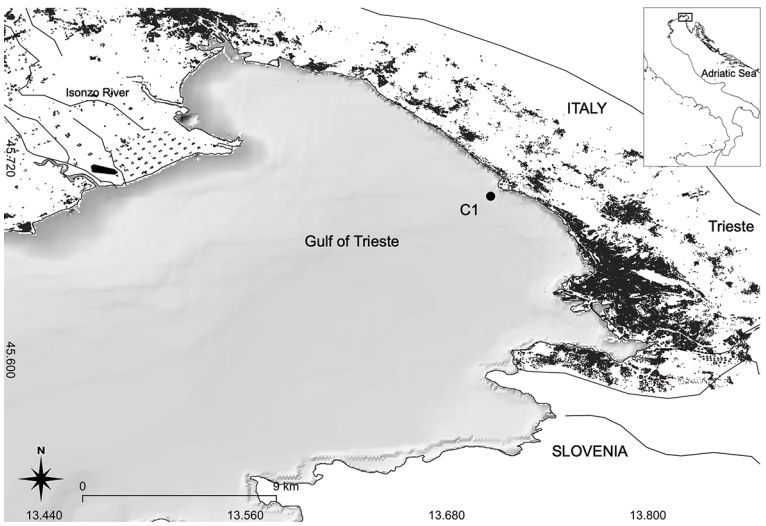

FIGURE 1 | Study area.

sw_bfrq (Revision 1.12, dated 1994/11/15, Copyright CSIRO, Phil Morgan 1993) contained in the SEAWATER package was used. This routine requires as input temperature (ITS-90), salinity and pressure (dbar) data and returns the Brunt-Väisälä square frequency (N^2) at mid-latitudes. Results were plotted using ODV (Schlitzer, 2021) and weighted-average gridding (Ocean Data View User's Guide, Version 5.6.0, 2022).

From March 2015 to September 2016, Photosynthetic available radiation (PAR) was recorded monthly by a PNF-300 Profiling Natural Fluorometer (Biospherical Instruments Inc., San Diego, USA), whereas from October 2016 onwards, a BNF-2102P S/N 1020 was used. These data were compared to the monthly means (November 1999 – September 2019) that were recorded with the above-mentioned probes. In 2015 the probe was sent to the USA for calibration and several monthly PAR data were missing, therefore we chose to exclude the year 2015 from the graphical representation of the monthly data.

Samples for the determination of dissolved inorganic nutrient concentrations (nitrite, $N\text{-}NO_2$; nitrate, $N\text{-}NO_3$; ammonium, $N\text{-}NH_4$; phosphate, $P\text{-}PO_4$; and silicate, $Si\text{-}Si(OH)_4$) were pre-filtered through glass-fibre filters, pore size 0.7 µm (Whatmann GF/F), stored at -20°C and analysed on a four-channel continuous segmented flow analyser (QuAAtro, Seal Analytical), using standard colorimetric methods (Hansen and Koroleff, 1999). To highlight nutrient limitation for microalgal growth we applied the following inequalities to our ratios: Si:N < 0.80 indicates Si limitation (Brzezinski, 1985), N:P > 22 indicates P limitation and N:P < 13 indicates N limitation (Hillebrand and Sommer, 1999). We also applied the Redfield ratio N:P < 16 to highlight a slight N limitation (Redfield, 1958). With the exception of January 2017, sediment sampling was carried out within a few days (-2/+2) from water sampling. Due to bad weather conditions, in January 2016 and April 2017 up to 9 days passed between the two samplings.

Virtually undisturbed sediment cores were collected by an automatic KC Haps bottom corer (KC-Denmark) using polycarbonate sample tubes (13.3 cm i.d. with a sample area of 127 cm^2); from one sediment core, in a N_2-filled chamber the overlying water was sampled with a syringe, filtered through Millipore Millex HA 0.45 µm pore size cellulose acetate filters and collected in acid-precleaned vials which were stored at -20°C until nutrient analysis, while from other 3 sediment cores, the uppermost oxic layer (<1 cm) was sampled, pooled, homogenised and subsampled for the analysis of microphytobenthos and benthic primary production. At the moment of sampling, PAR, sea water temperature and salinity were measured as already specified for the water sampling.

Phytoplankton Abundance, Biomass and Community Structure

For phytoplankton (2-200 µm) analysis, samples were collected in 500 mL-dark bottles and preserved with pre-filtered and neutralized 1.6% formaldehyde (Throndsen, 1978). Cell counts were performed following the Utermöhl method (Utermöhl, 1958). A variable volume of seawater (10-50 mL) was settled depending on cell concentrations. Cell counts were performed using an inverted light microscope (Olympus IX71 and LEICA BMI3000B) equipped with phase contrast. Cells (minimum 200) were counted along transects (1–2) at a magnification of 400×. In addition, one half of the Utermöhl chamber was also examined at a magnification of 200×, to obtain a more correct evaluation of less abundant phytoplankton taxa. Phytoplankton specimens were identified to the lowest possible taxonomic level referring to Tomas (1997); Bérard-Therriault et al. (1999); Horner (2002); Young et al. (2003) and Malinverno et al. (2008). Species/genus names were checked for validity against AlgaeBase (Guiry and Guiry, 2022). The biovolume of phytoplankton cells was calculated according to Edler (1979) and Hillebrand et al.

(1999). Cell volumes were converted to carbon content using the formula introduced by Menden-Deuer and Lessard (2000).

Cyanobacteria were not included in this study, however on average (over a 12-month study) they accounted for 13.3% of the total phytoplankton biomass in the same site (Cibic et al., 2018a), and their contribution to PP was previously presented and thoroughly discussed (Cibic et al., 2018b). Phytoplankton community loss factors (grazing pressure, viral infection) were not considered in this study.

Abundance, Biomass and Community Structure of Microphytobenthos

In this study, with the term microphytobenthos – MPB, we refer to the microscopic eukaryotic algae (diatoms, dinoflagellates, flagellates, etc.), and prokaryotic photosynthetic organisms, such as filamentous cyanobacteria. For MPB analyses, three aliquots of homogenized sediment (2 cm^3) were withdrawn using a syringe and directly fixed with 10 mL of formaldehyde (4% final concentration) buffered solution $CaMg(CO_3)_2$, in pre-filtered bottom seawater (0.2 μm filters). After manual stirring, 20 μL aliquots of the sediment suspension were drawn off from the slurries and placed into a counting chamber. Only cells containing pigments and not empty frustules were counted under a Leitz inverted light microscope (Leica Microsystems AG, Wetzlar, Germany) using a 32× or 40× objective (320× or 400× final magnification) (Utermöhl, 1958). When possible, at least 200 cells were counted per sample to evaluate rare species, too. The microalgal taxonomy was based on AlgaeBase (Guiry and Guiry, 2022) and WoRMS (WoRMS Editorial Board, 2022) websites. The qualitative identification of MPB assemblages was carried out using floras listed in Cibic and Blasutto (2011). Quantitative data are reported as cells cm^{-3} of wet sediment (cells cm^{-3}) and as Relative Abundance (RA). To estimate the biomass (expressed as μg cm^{-3}), the biovolume of MPB cells was calculated according to Hillebrand et al. (1999). Afterwards, the MPB biomass was obtained multiplying the abundance (cells cm^{-3}) by the carbon content of each counted cell using the formulas introduced by Menden-Deuer and Lessard (2000).

Pelagic and Benthic Primary Production

We estimated gross primary production (GPP) in water samples and in surface sediments by the ^{14}C uptake (Steeman Nielsen, 1952). GPP represents the sum of net primary production (NPP) and community respiration (CR). The ^{14}C technique measures values between GPP and NPP, depending on the incubation time: shorter incubation times are closer to GPP whereas incubation times ≥ 6 h are closer to NPP (Gazeau et al., 2004). In our study, the incubation time was about 2 hours for the water samples and 45 minutes for the sediment slurries, therefore in both cases a GPP rate was measured. From March 2015 to March 2019, pelagic primary production (PPw) was estimated *in situ*. Water samples were poured into three light and one dark 70 mL polycarbonate carboys (Nalgene) per each depth (0.5-5-10-15 m). The samples were kept in the dark for 30 minutes to stop residual photosynthetic activity. Subsequently, 0.22 MBq (6 μCi) of $NaH^{14}CO_3$ (DHI, Denmark) was added to each carboy. The samples were then fixed on a rosette, lowered to the corresponding sampling depth, and incubated for 2 h around noon. At the end of the incubation, the samples were stored in dark and cold conditions, and immediately transferred to the laboratory. From each sample, an aliquot of 25 mL was filtered through 0.2 μm polycarbonate filters (Nuclepore) applying low vacuum pressure (100 mmHg) in order to avoid cell damage. The filters were placed in 6 mL plastic scintillation vials (Perkin Elmer), acidified with 200 μL of HCl 0.5 M (Cibic and Virgilio, 2011) to remove the residual ^{14}C-bicarbonate not assimilated by the phytoplankton, and an aliquot of 5 mL of scintillation cocktail (Filter Count; Perkin-Elmer) was added to each vial.

Benthic primary production (PPs) was estimated in the laboratory from ^{14}C-incubation of slurries. An aliquot of 10 cm^3 of homogenised surface sediment was withdrawn with a syringe, resuspended in 190 mL of overlying filtered seawater (0.2 μm filter), withdrawn from undisturbed sediment cores, and inoculated with 20 μCi (0.74 MBq) of $NaH^{14}CO_3$ (DHI, Denmark) (Steemann Nielsen, 1952). After stirring, the slurry was transferred into 21 glass vials containing 9 mL which were divided as follows: 3 replicates to assess the sediment matrix effect, 3 dark replicates and 3 replicates for each of the 5 light intensities used. In a thermostatic chamber the samples were incubated at the *in situ* temperature under a gradient of light intensities (20–50–100–200–500 μE m^{-2} s^{-1}) and after 45 min carbon incorporation was stopped by adding 200 μL of HCl 5 N (final HCl concentration 0.11 N) (Cibic and Virgilio, 2010). Subsequently, samples were treated as described by Cibic et al. (2008). In this study only PPs rates, referred to data obtained at *in situ* light conditions, are presented and discussed.

Disintegrations per minute (DPM) were measured by a QuantaSmart TRI-CARB 2900 TR Liquid Scintillation Analyzer (Packard BioScience, USA) including quenching correction, obtained using internal standards. Assimilation of carbon was calculated as described by Gargas (1975), assuming 5% isotope discrimination. Activities of the added $NaH^{14}CO_3$ and inorganic carbon concentration (tCO_2) were calculated on the basis of total alkalinity measured in the same samples. Standard deviation (SD) of three replicate values was below 25% except for rates close to zero for which SD was over 50%.

Volumetric PPw data were converted to areal data using standard trapezoidal integration over the top 15 m of the water column. Total incident photosynthetically active radiation was continuously recorded at the OGS laboratory at S. Croce using the scalar PAR surface reference sensor QSR2100 (Biospherical Instruments). PP hourly rates were then converted into daily rates considering the amount of light during incubation *in situ*, and the total amount of light during the sampling day computed by integrating the PAR data over the hours of daylight.

Statistical Analyses

Physical data (sea water temperature, salinity and PAR) of the sampling period were compared to the monthly mean climatology. The latter was computed on seawater temperature and salinity data recorded between 1998 and 2019, and on PAR data measured from November 1999 to September 2019. The monthly mean climatology was computed for each parameter at four sampling depths (0.5, 5, 10 and 15 m), except for surface

PAR measurements that were carried out at 1 m instead of 0.5 m in order to reduce light scattering in the coastal waters. Whenever CTD and PAR measurements were performed with different sampling frequency (weekly and biweekly), data were averaged to a monthly value.

All statistical analyses, except for the correlations, were performed using PRIMER 7.0.21 (Clarke et al., 2014). To infer the temporal changes, the samples were grouped based on the sampling season considering the meteorological calendar. To highlight seasonal variability in the distribution of the phytoplankton and MPB biomass, a PERMANOVA test was used. "Season" was applied as a fixed factor in a one-way analysis. Unrestricted permutation of raw data, 9999 permutations and Monte Carlo pairwise comparisons were applied. To highlight relationships between abiotic and biotic variables, a Spearman rank correlation analysis (r) was performed using the software Past 4 (Hammer et al., 2001). Only statistically significant ($p < 0.05$) results are presented and discussed. For each water depth and for the sediment, the biological data were divided into two separated matrices, with the abundances and biomasses of phytoplankton and MPB taxa respectively. For each sampling layer, an additional matrix with the abiotic parameters (temperature, salinity, PAR, inorganic nutrients) was constructed. Univariate diversity analysis was applied to phytoplankton and benthic diatom abundances, after removing undetermined forms, considering richness (d, Margalef, 1986), equitability (J′, Pielou, 1966), diversity (H'(log_2), Shannon and Weaver, 1949) and dominance (λ, Simpson, 1949). Before the multivariate analysis, each biotic matrix was log (x + 1) transformed. The data were then analyzed using cluster analysis (performed with the complete linkage clustering algorithm) and for the biotic matrices, a Bray-Curtis similarity was applied.

A Principal Component Analysis (PCA) was carried out on environmental data of each sampling layer (or sediment) in order to visualize the temporal distribution of main abiotic variables (salinity, temperature and nutrients).

To visualize differences in taxa assemblages among the different samplings, a non-metric multidimensional scaling ordination (nMDS) (Kruskal and Wish, 1978) was performed separately on the Bray-Curtis similarity matrix of phytoplankton at each sampled depth (0.5, 5, 10 and 15 m) and of MPB, after log (x + 1) transformation of the data. To highlight which taxa mainly contributed to the temporal variation of the assemblages, the taxa with the highest relative biomass (average ≥ 1% for the phytoplankton and ≥ 2% for the MPB, over the study period), were overlaid on the nMDS plot. The normalized (z-standardization) environmental variables (i.e. temperature, salinity, PAR and dissolved inorganic nutrients: $N\text{-}NO_2$, $N\text{-}NO_3$, $N\text{-}NH_4$, $P\text{-}PO_4$ and $Si\text{-}Si(OH)_4$; for sediments also TOC and TN data presented in Franzo et al. (2019) were used) were fitted as supplementary variables (vectors) onto ordination spaces to investigate their effects on community structure, using an Euclidean distance matrix for physical-chemical data. The analyses were carried out on biomass values, since is the biomass, over the abundance that drives the primary production rate. On all the communities, we performed multivariate analyses to examine seasonal composition changes in relation to environmental factors. The following abiotic variables were considered for each sampling layer: i) physical parameters (temperature, salinity and light intensity); ii) inorganic nutrients ($N\text{-}NH_4$, $N\text{-}NO_2$, $N\text{-}NO_3$, $P\text{-}PO_4$, $Si\text{-}Si(OH)_4$); and TOC and TN for sediments only. The significancy of differences among *a priori*-fixed seasons (winter: December, January, February; spring: March, April, May; summer: June, July, August; autumn: September, October, November) was tested by ANOSIM (ANalysis Of SIMilarity) (Clarke et al., 2014). The resulting pair-wise R-values give an absolute measure of separation among groups with zero (0) indicating no difference among groups, while one (1) indicating that all the samples within groups are more similar to one another than any samples from different groups.

RESULTS

Physical-Chemical Properties of the Water Column

Comparing the seawater temperature to climatological (1998 - 2019) data, much lower values than the monthly means were recorded particularly in August 2015 (up to -4.73°C at the surface) and July 2018 (up to -2.16°C at the surface), and much higher values in May 2018 (up to +6.16°C at the bottom) and July 2015 (up to +4.30°C at the 5-m layer). (**Figures S1A–D**) In the sediment overlying water, the temperature, measured during seasonal samplings, ranged between a minimum of 9.45°C in January 2016 and a maximum of 22.16°C in July 2016 (**Table S1**).

The minimum of salinity recorded in May 2016 at the surface was -6.76 lower than the climatological (1998-2019) monthly mean and lower salinity persisted in the water column also in the following month. Higher values than the climatological monthly means were recorded at the surface particularly in spring-summer of 2018 (**Figures S1E–H**). In the sediment overlying water, the salinity, measured during seasonal samplings, ranged between a minimum of 36.99 in October 2015 and a maximum of 38.06 recorded in March 2019 (**Table S1**).

The degree of the water column stability was obtained by the Brunt-Väisälä (B-V) frequency that allows to identify the position of the seasonal pycnocline and further determine periods of substantial vertical gradients in water properties. The maximum B-V frequency along the water column was generally observed in late spring-summer, indicating the predominance of the thermal effect (**Figure 2**). However, marked differences among the investigated years were noticed. In particular, in 2016 a strong water stratification established at the surface in May, while a minimum B-V frequency was recorded in July. In 2017 maxima interested almost the whole water column both in June and July, with a minimum in July at -5m. The year 2018 was characterized by peaks at mid-water column from April to September, while in November 2018 a pycnocline appeared at about 2.5-m depth.

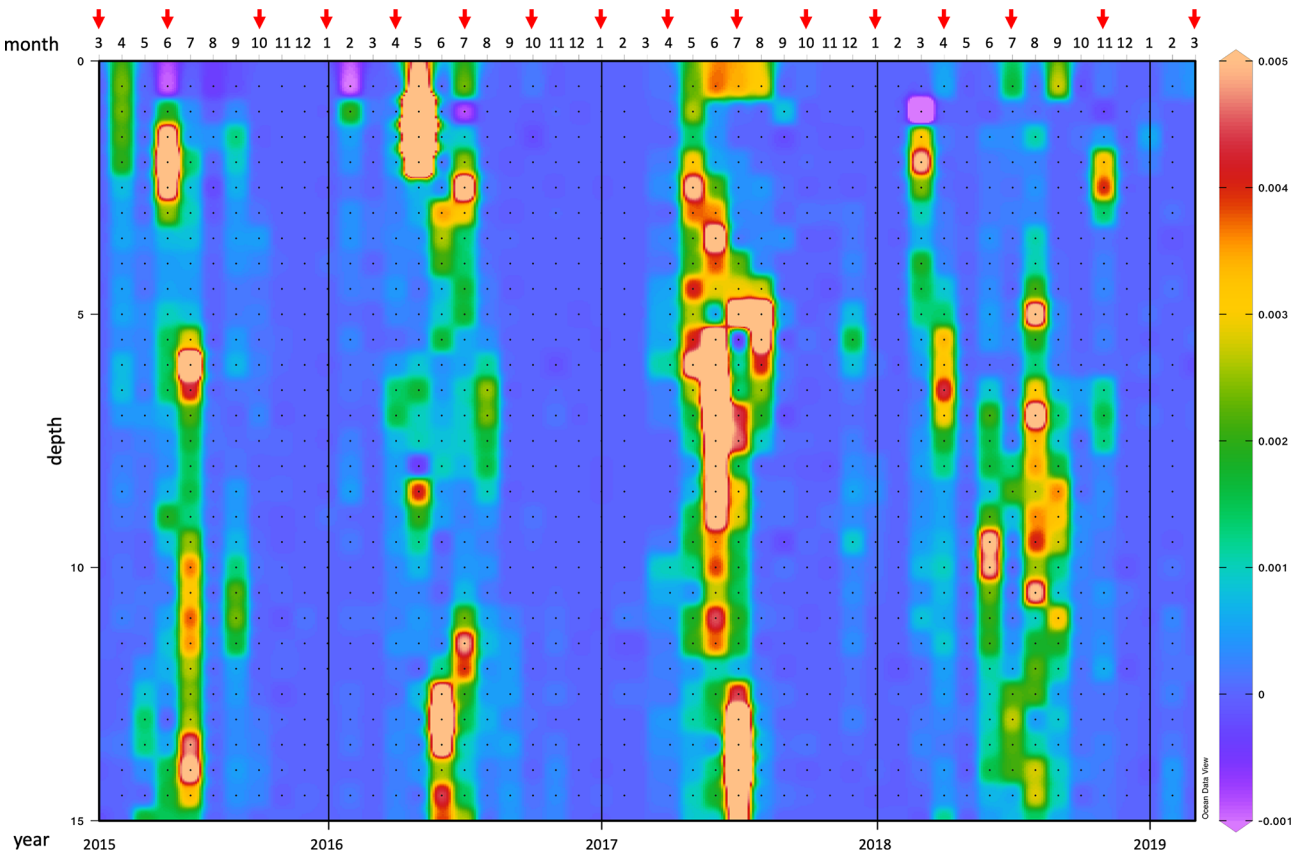

FIGURE 2 | Graphical representation of the Brunt-Väisälä frequency, expressed in units of hertz (Hz), in the water column from March 2015 to March 2019. Red arrows indicate the 16 samplings during the study period. For more details see the text.

PAR reached the maximum (1654.8 μE m^{-2} s^{-1}) of the study period at the surface in May 2017, while the minimum (2.5 μE m^{-2} s^{-1}) was recorded at the bottom in January 2019 (**Figures S2A–D**). Except for the surface, PAR was, on average, lower than the monthly mean at the other sampling depths. In the sediment overlying water, PAR, registered during seasonal samplings, was at its lowest (6.0 μE m^{-2} s^{-1}) in October 2016, while it reached the maximum (126.3 μE m^{-2} s^{-1}) in June 2015 (**Table S1**).

Nutrient concentrations analysed at the four water depths and in the overlying water, and N:P and Si:N ratios are shown in **Table S2**. N-NH_4 displayed two peaks (5.0 and 2.6 μM) in October 2015 at -5 m and in November 2018 at -15 m, respectively, and three peaks (5.6, 4.9 and 5.9 μM) in the overlying water in October 2017, April 2018 and November 2018, respectively (**Figure S3A**). Also N-NO_2 displayed high concentrations along the water column and in the sediment overlying water in January 2016, 2017, and 2018 (**Figure S3B**) whereas N-NO_3 in the overlying water in January 2016, and in November 2018 (**Figure S3C**). Similarly to N-NH_4, P-PO_4 reached its maximum (1.1 μM) in October 2015 at -5 m and in July 2017 (0.5 μM) in the overlying water (**Figure S3D**). Si-Si$(OH)_4$ reached the highest concentrations in November 2018 along the entire water column, while the minimum was recorded at -5 m in October 2015. In the overlying water, Si-Si$(OH)_4$ displayed three major peaks in July and October 2017, and in November 2018 (**Figure S3E**).

Applying the ratios (Redfield, 1958) as proposed by Hillebrand and Sommer (1999), and the Si:N ratio reported by Brzezinski (1985) to our data, we found Si limitation at the top 10 m-layer in October 2015, in April 2017, at the surface layer in January 2016 and in the overlying water in April 2018. N-depleted conditions were observed particularly in June 2015, April 2017, July 2018 and March 2019, whereas a slight N-limitation occurred in the overlying water in October 2016 and July 2017 (**Table S2**). When N was not depleted, P became the limiting nutrient for the phytoplankton growth in most of the other samplings or water layers.

Phytoplankton Density and Community Structure

Considering the whole study period, the phytoplankton community was dominated by flagellates in terms of absolute abundance, and by diatoms in terms of biomass. The average abundance of the whole study period was equal to $1.0{\cdot}10^6$ ± $8.3{\cdot}10^5$ cells L^{-1} for flagellates and to $3.0{\cdot}10^5$ ± $3.8{\cdot}10^5$ cells L^{-1} for diatoms. Three peaks in abundance were reached in June 2015 at

the surface, when the flagellates accounted for $3.4{\cdot}10^6$ cells L^{-1}, and in July 2017 and 2018, when this group reached $4.3{\cdot}10^6$ and $2.9{\cdot}10^6$ cells L^{-1}, respectively (**Figure S4A**). In July 2018, a peak was observed also at -10 m when flagellates and diatoms were co-dominant displaying similar abundances (**Figure S4C**). In addition, diatoms reached other two peaks in July 2018 at -5 m (**Figure S4B**) and April 2016 at -10 m (**Figure S4C**). Compared to the other two groups, dinoflagellates and coccolithophores represented a negligible portion of the phytoplankton community (**Figures S4A–D**).

In terms of biomass, the composition of the phytoplankton community differed substantially compared to what emerged from the abundance data. The diatoms dominated the community with an average biomass (considering the whole study period and all sampling depths) equal to 31.2 ± 45.4 µg C L^{-1} while that of flagellates was 19.5 ± 14.2 µg C L^{-1}. Diatom maxima were observed over the whole water column in April 2017 and January 2018 (**Figures S4E-H**), while the maxima of flagellates and dinoflagellates were recorded at the surface in June 2015 and November 2018, respectively (**Figure S4E**). A significant seasonal variability in the distribution of the phytoplankton biomass was highlighted by PERMANOVA at all depths, except for the 15-m layer (**Table 1**).

To have an indication of the community composition over the study period, the phytoplankton abundance and structure at the four depths were integrated over the water column and the relative abundance of taxa was calculated. On average, small flagellates (<10 µm) of uncertain taxonomic identification dominated the phytoplankton community (60.60%), followed by small (< 20 µm) diatom species belonging to the genus *Chaetoceros* (9.87%), undetermined cryptophyceae (5.89%) and the coccolithophore *Emiliania huxleyi* (3.47%) (**Figure 3A**). A very different picture was obtained considering the phytoplankton biomass. When large diatoms occurred in the water column, particularly *Lauderia annulata* and *Leptocylindrus* spp., but also *Chaetoceros*, they prevailed over the other groups in terms of carbon content (**Figure 3B**).

Univariate diversity indices applied to the phytoplankton community, integrated over the water column, revealed that the highest value of richness (d = 4.441) was observed in November 2018 when the highest number of species was identified in the water column (S = 78). The second maximum of richness was obtained in October 2016 (d = 4.389, S = 73), while the highest values of diversity and equitability were calculated in January 2018 (H' = 3.452, J' = 0.561) in correspondence to the lowest value of dominance (λ = 0.182) (**Table 2**).

TABLE 1 | Output of the one-way PERMANOVA tests on the phytoplankton and MPB biomass at the investigated layers where season was applied as a fixed factor. The significance values of the Monte Carlo pairwise comparisons are also reported (p-MC).

Season on BIOM			
Water	**pseudo-F**	**p-value**	**p-MC**
0.5m	3.596	0.012	0.019
5m	2.931	0.008	0.041
10m	2.238	0.020	0.085
15m	1.716	0.069	0.185
integrated	3.687	0.003	0.016
Sediment	1.492	0.048	0.182

Microphytobenthos (MPB) Abundance and Community Structure

Over the study period, MPB displayed two abundance peaks ($1.6{\cdot}10^5$ and $1.4{\cdot}10^5$ cells cm^{-3}) in March and June 2015, respectively, while two minima ($3.0{\cdot}10^4$ and $2.9{\cdot}10^4$ cells cm^{-3}) were recorded in October 2015 and December 2016, respectively. In contrast to the phytoplankton community, the MPB biomass dynamics were consistent with those of the abundances (**Figure S5A**). Two biomass peaks (50.8 and 48.9 µg C cm^{-3}) were reached in March and June 2015, while the minima (9.3 and 8.4 µg C cm^{-3}) were detected in October 2015 and December 2016 (**Figure S5B**). The MPB biomass significantly differed among seasons but not when the pairwise comparisons were considered (Monte Carlo test, **Table 1**).

Considering the whole study period, the MPB community was dominated by diatoms (94.78%), whereas diatom spores (2.27%), cyanobacteria (2.02%), undetermined flagellates (0.63%), dinoflagellates and their resting stages (0.30%) represented minor fractions of the benthic microalgal community. Focusing on diatoms only, *Nitzschia* was the most abundant genus over the study period (29.34%), followed by *Paralia* (15.49%) and *Gyrosigma* (11.28%). The tychopelagic diatom species *Paralia sulcata* was the most represented over the study (15.41%), *Nitzschia fasciculata* (5.73%) was particularly abundant in summer, other well represented species were *Gyrosigma acuminatum* (5.40%), *G. spencerii* (3.32%) and *Nitzschia sigma* var. *sigmatella* (3.01%) (**Figure 4**).

Univariate diversity indices applied to the benthic diatom community revealed that the highest value of richness (d= 3.368) and diversity (H'=4.217) were observed in July 2018 in correspondence to the highest number of species (S= 36). In October 2016 the highest value of dominance (λ = 0.222) and the lowest equitability (J' = 0.692) were obtained in correspondence to a major density of *Nitzschia sigma* var. *sigmatella*. Similarly, the second maximum of dominance (λ = 0.191) and the second minimum of equitability (J' = 0.701) were obtained in January 2018 due to a high relative abundance of *Paralia sulcata* (**Table 2**).

Primary Production in the Water Column (PPw) and in Surface Sediments (PPs)

The absolute PPw maximum of the study period was estimated at the surface in November 2018 (6.71 ± 0.82 µg C L^{-1} h^{-1}) (**Figure 5A**) in low light conditions, while a second maximum was obtained in July 2017 at -5 m (6.46 ± 0.52 µg C L^{-1} h^{-1}) (**Figure 5B**). Other three relative maxima were estimated at the surface in January 2018 (5.13 ± 0.07 µg C L^{-1} h^{-1}) and July 2017 (4.76 ± 0.74 µg C L^{-1} h^{-1}), and at -5 m in October 2016 (4.74 ± 0.85 µg C L^{-1} h^{-1}). In general, at the surface and -5 m PP dynamics were uncoupled with the light intensity, whereas at -10 m and -15 m the relative PP peaks were more in line with the PAR availability at these depths (**Figures 5C, D**, **S2**). PP minima (<0.2 µg C L^{-1} h^{-1}) were reached in April 2017 at the surface and in October 2017 at the bottom (**Figures 5A, D**).

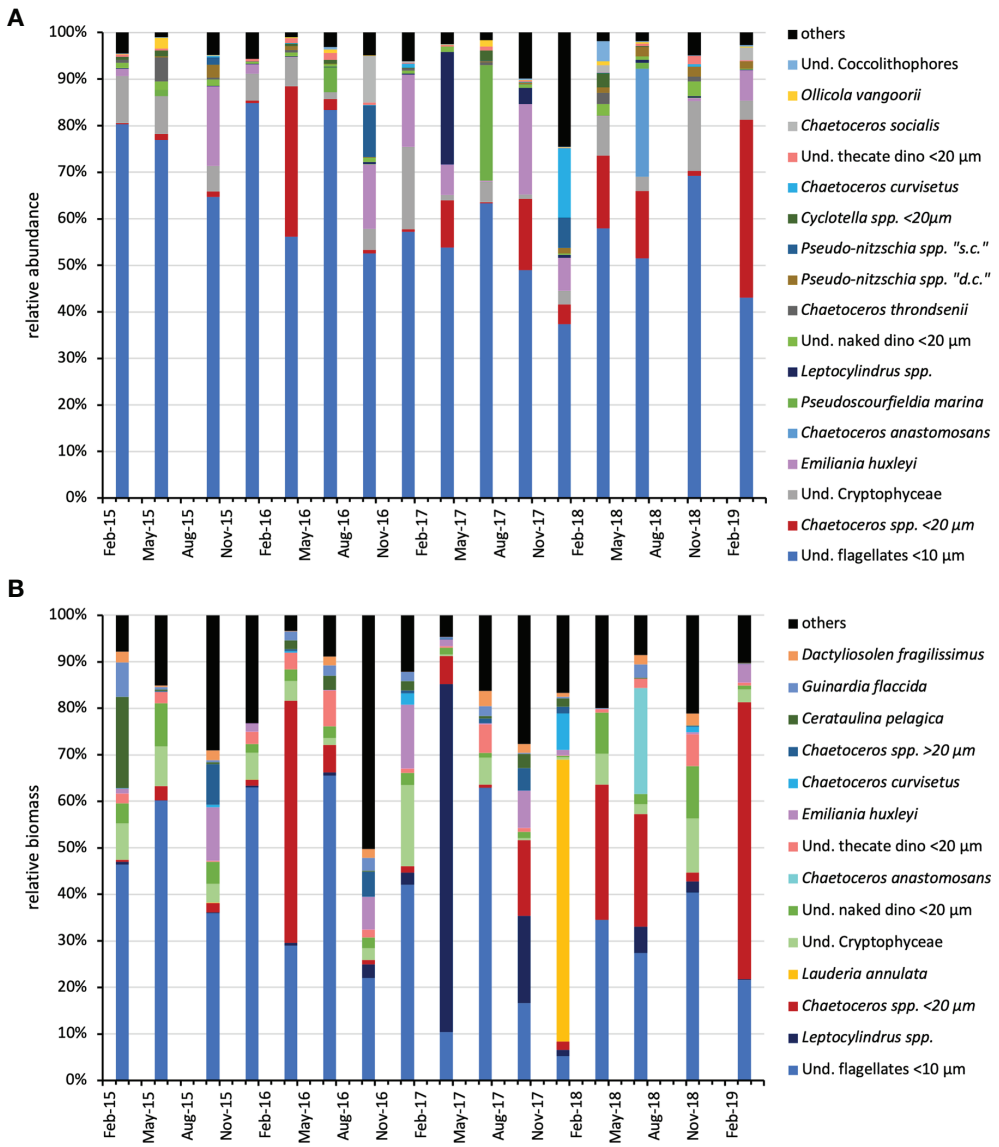

FIGURE 3 | Relative abundance **(A)** and relative biomass **(B)** of the main (≥ 1% of the total) phytoplankton taxa over the water column (integrated data) during the study period. dino, Dinoflagellates; und, undetermined; d.c., delicatissima complex; s.c., seriata complex.

The primary production depth-integrated rates (PPi) displayed the absolute maximum in July 2017 (69.30 mg C m^{-2} h^{-1}) and the second highest value in July 2018 (55.89 mg C m^{-2} h^{-1}), while the minima were obtained in March 2019 and April 2018 (11.47 and 13.17 mg C m^{-2} h^{-1}, respectively) (**Figure 6**).

The highest PPs rate was estimated in January 2018 (28.50 ± 2.08 mg C m^{-2} h^{-1}), a second maximum was reached in October 2016 (17.55 ± 1.17 mg C m^{-2} h-^{1}) while negative values were obtained in October 2015 (-20.88 ± 3.93 mg C m^{-2} h^{-1}), December and January 2016 (-7.58 ± 1.67 and -1.20 ± 0.30 mg C m^{-2} h^{-1} respectively) in low light conditions (**Figure 6**).

We made an estimate of the total primary production (PPt) rate per m^2. Therefore, PPs rates were added to PPi values. Even when PPs values were highly negative, the sum of PPs + PPi was consistently > 12 mg C m^{-2} h^{-1}, except for winter 2016 - 17 when the water sampling was much delayed compared to the sediment sampling (**Table 3**). To obtain an estimate of PPs to PPt rate, we first excluded the 3 negative PPs values then calculated the percentage of the benthic contribution to the overall primary production. The highest benthic contribution was obtained in January 2018 (43.2%) and October 2016 (28.3%), while the mean PPs value over the study period was 11.3% (**Table 3**).

TABLE 2 | Diversity indices applied to the phytoplankton community over the water column (integrated data) and to the microphytobenthic community in the sediments.

W_integrated	S	N	d	J'	H'(log2)	λ
Mar-15	39	7388733	2.403	0.238	1.256	0.656
Jun-15	60	28572020	3.437	0.246	1.454	0.603
Oct-15	69	13214160	4.147	0.318	1.943	0.453
Jan-16	35	*4724893*	2.212	*0.214*	*1.097*	**0.724**
Apr-16	49	32506945	2.775	0.296	1.66	0.424
Jul-16	45	22668173	2.598	0.216	1.186	0.699
Oct-16	73	13318373	4.389	0.384	2.376	0.321
Jan-17	54	7320155	3.353	0.352	2.026	0.383
Apr-17	*34*	30611103	*1.915*	0.387	1.968	0.363
Jul-17	45	32299765	2.545	0.301	1.65	0.465
Oct-17	65	13011713	3.907	0.413	2.487	0.303
Jan-18	71	13946655	4.255	**0.561**	**3.452**	*0.182*
Apr-18	46	31790575	2.605	0.398	2.199	0.372
Jul-18	67	**48714620**	3.728	0.348	2.109	0.342
Nov-18	**78**	33894748	**4.441**	0.294	1.849	0.504
Mar-19	39	11007193	2.344	0.383	2.026	0.339
Sediment	**S**	**N**	**d**	**J'**	**H'(log2)**	**λ**
Mar-15	24	**125333**	1.959	0.752	3.448	0.129
Jun-15	32	111900	2.667	0.735	3.674	0.123
Oct-15	27	21450	2.607	0.715	3.398	0.188
Jan-16	*18*	47400	*1.579*	0.780	3.252	0.156
Apr-16	27	43200	2.436	0.727	3.456	0.174
Jul-16	28	37500	2.564	0.843	4.055	0.092
Oct-16	22	48000	1.948	*0.692*	*3.087*	**0.222**
Dec-16	25	*20400*	2.419	0.704	3.271	0.179
Apr-17	31	37050	2.852	0.796	3.942	0.109
Jul-17	26	44400	2.336	0.788	3.704	0.111
Oct-17	30	31650	2.799	0.740	3.631	0.126
Jan-18	24	40200	2.169	0.701	3.213	0.191
Apr-18	28	25200	2.664	**0.859**	4.131	*0.079*
Jul-18	**36**	32550	**3.368**	0.816	**4.217**	0.085
Nov-18	21	25350	1.972	0.772	3.391	0.142
Mar-19	30	39300	2.741	0.817	4.007	0.091

S, number of species; N, total number of cells; d, richness; J', equitability; H'(log2), diversity; λ, dominance; (Bold = maxima; italics = minima).

Influence of Abiotic Variables on the Structure and Function of Phototrophic Communities

To highlight how the physical and chemical features of the water column and surface sediments affected the seasonal development of pelagic and benthic phototrophs and the overall primary production, a Principal Component Analysis (PCA) was first carried out on the five abiotic data matrices, separately. The total variance explained by the first two PC axis displayed increasing values from the surface to the 15-m depth layer, accounting for 64.2%, 69.6%, 70.0% and 73.8% of total variance for the 0.5 m, 5 m, 10 m and 15 m layer, respectively, whereas for the sediment PC1 + PC2 explained 63.3% of the total variance (data not graphically shown). For the PCA performed on the 0.5-m data, temperature (0.60) and salinity (-0.50) were the predominant elements of the first factor, while the major contributors to the second one were N-NO_3 (-0.66) and silicates (-0.64). For the PCA performed on the 5-m data, N-NO_3 (-0.47) and silicates (-0.46) were the predominant elements of the first factor, while the major contributors to the second one were P-PO_4 (-0.53) and N-NH_4 (-0.51). For the PCA performed on the 10-m data, N-NO_3 (0.53) and N-NO_2 (0.48) were the predominant elements of the first factor, while the major contributors to the second one were temperature (-0.56) and salinity (0.54). For the PCA performed on the 15-m data, N-NH_4 (0.53) and salinity (-0.43) were the predominant elements of the first factor, while the major contributors to the second one were N-NO_2 (0.59) and N-NO_3 (0.51). Finally, for the PCA performed on sediment data, silicates (0.47) and P-PO_4 (0.44) were the predominant elements of the first factor, while the major contributors to the second one were N-NO_2 (0.57) and N-NO_3 (0.45). On all PCA plots, the four groups of seasonal samplings significantly differed (R_{ANOSIM} varying from 0.366; p = 0.2% for the 5-m layer to R = 0.611; p = 0.1% for the sediment).

The nMDS analysis based on the biomass of either the phytoplankton (separately for each layer) or MPB revealed temporal differences among samplings (**Figures 7A–E**). The superimposed PP and abiotic variables indicated the main discriminating factors responsible for the separation of samplings. At the surface layer, the phytoplankton assemblages significantly differed among seasons (R_{ANOSIM} = 0.571; p = 0.1%) (**Figure 7A**). During spring, the diatom biomass prevailed in April 2017 but mostly it was co-dominant with that of flagellates, and the measured photosynthetic rates were quite low (1.13 ± 0.99 μg C L^{-1} h^{-1}). In summer, flagellates were consistently dominant and higher mean PP rates were estimated (3.30 ± 1.50 μg C L^{-1} h^{-1}). In autumn, diatoms contributed to higher PP (October16 and October17), whereas the absolute maximum PP (6.71 μg C L^{-1} h^{-1}) obtained in November 2018 was due to the highest biomass of small dinoflagellates which co-occurred with flagellates. In January 2018, the second maximum PP (5.13 μg C L^{-1} h^{-1}) was estimated on the account of the diatoms *Lauderia annulata* and several *Chaetoceros* species. In the other two winter samplings, PP rates were low due to a minor overall phytoplankton biomass and low light availability.

Similarly, at the 5-m layer, the phytoplankton assemblages significantly differed among seasons (R_{ANOSIM}=0.443; p=0.2%) (**Figure 7B**). Except for March 2015, in the other spring samplings the diatom biomass dominated over the other phytoplankton groups, particularly in April 2017 when a remarkable diatom biomass was obtained on the account of *Leptocylindrus* spp. However, not particularly high PP rates (1.66 ± 1.08 μg C L^{-1} h^{-1}) were estimated in this season at the 5-m depth layer. With the exception of July 2018, when the diatom biomass prevailed at this depth, in the other summer samplings the flagellates dominated the phytoplankton biomass as for instance in July 2017, when the second maximum PP rate of the study period was estimated (6.46 μg C L^{-1} h^{-1}). In autumn, diatoms and flagellates equally contributed to the phytoplankton biomass (October15 and October17), whereas in October 2016, when a relative PP maximum was reached (4.74 μg C L^{-1} h^{-1}) several diatom species co-occurred (*Pseudo-nitzschia* "seriata complex", *Chaetoceros socialis*, *Guinardia flaccida* and others). Overall, higher PP rates were estimated during the autumn samplings (3.47 ± 0.95 μg C L^{-1} h^{-1}). In January 2018, the phytoplankton biomass was dominated mostly by *Lauderia annulata*, but also *Chaetoceros curvisetus* and other diatom species contributed to PP, while in the other winter samplings a scarce phytoplankton biomass was present at this water depth.

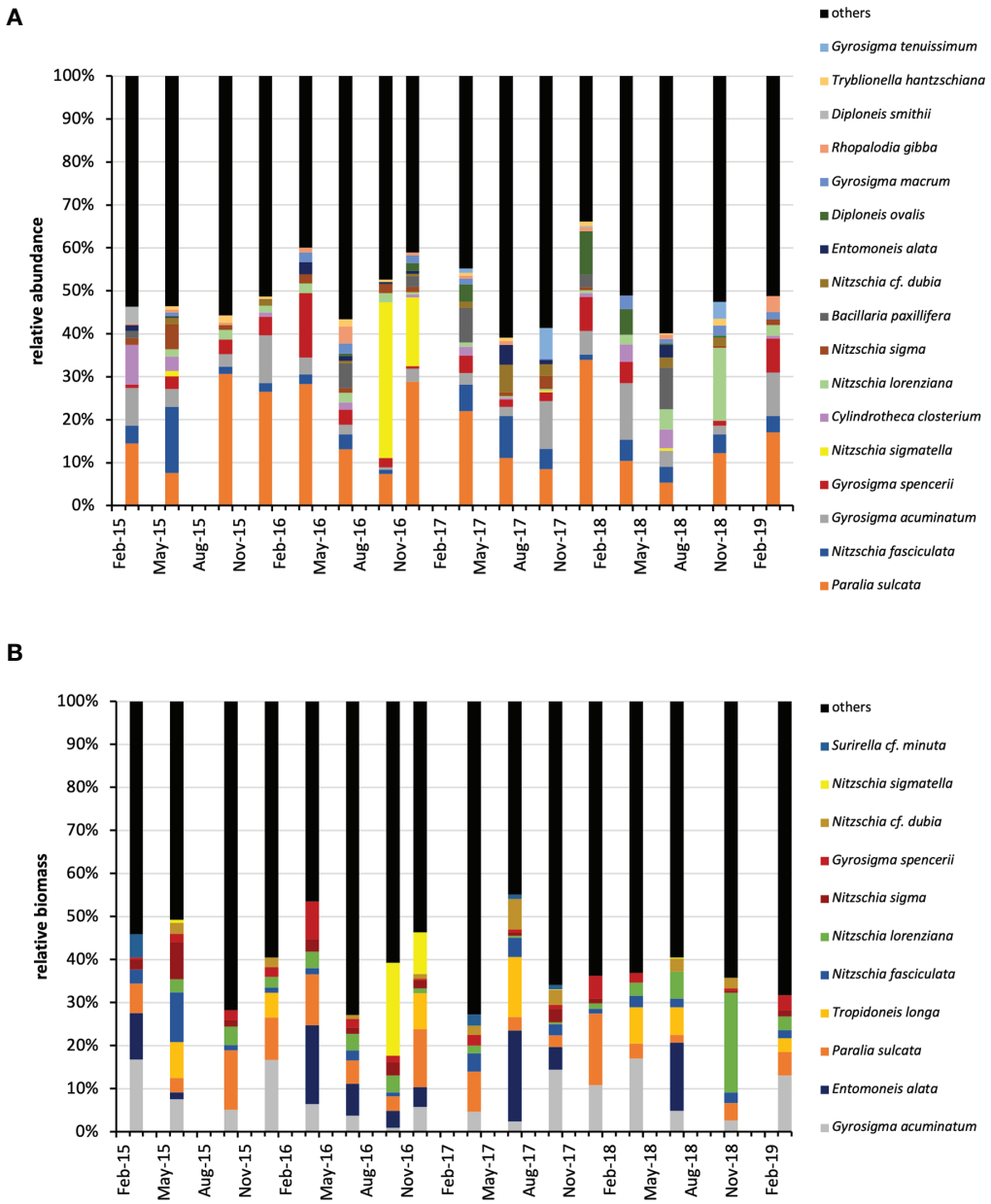

FIGURE 4 | Relative abundance **(A)** and relative biomass **(B)** of the main (≥ 0.5% of the total abundance and ≥ 1% of the total biomass) microphytobenthic species during the study period. *Nitzschia sigmatella*, *Nitzschia sigma* var. *sigmatella*.

Also at the 10-m layer, the phytoplankton assemblages significantly differed among seasons (R_{ANOSIM} = 0.432; p = 0.2%) (**Figure 7C**). The highest PP values estimated in spring at 10 m depth were observed in April 2016 (3.43 μg C L^{-1} h^{-1}) and April 2017 (1.93 μg C L^{-1} h^{-1}) when the phototrophic biomass was dominated by diatoms. In the former sampling, small *Chaetoceros* forms prevailed whereas in the latter a large *Leptocylindrus* species contributed to the maximum biomass obtained at this water layer. In summer, the highest PP rates were reached in July 2017 (3.87 μg C L^{-1} h^{-1}) and July 2018 (3.37 μg C L^{-1} h^{-1}), in the first case with a dominance of flagellates, in the second case with a major diatom biomass (*Chaetoceros anastomosans*, *Chaetoceros* spp. < 20 μm). In autumn, flagellates, diatoms, dinoflagellates and coccolithophores co-occurred at this layer and an average PP rate of 1.96 ± 0.74 μg C L^{-1} h^{-1} was obtained. *Lauderia annulata* was present also at this layer and contributed to PP in January 2018.

At the 15-m layer, the phytoplankton assemblages significantly differed among seasons (R_{ANOSIM} = 0.414; p = 0.1%) (**Figure 7D**). In spring 2015 and 2016, higher PP rates were estimated at this layer compared to spring 2017, although a major diatom biomass, mostly on the account of *Leptocylindrus* spp. persisted at the bottom layer in April 2017. A remarkable PP rate (4.46 μg C L^{-1} h^{-1}) was

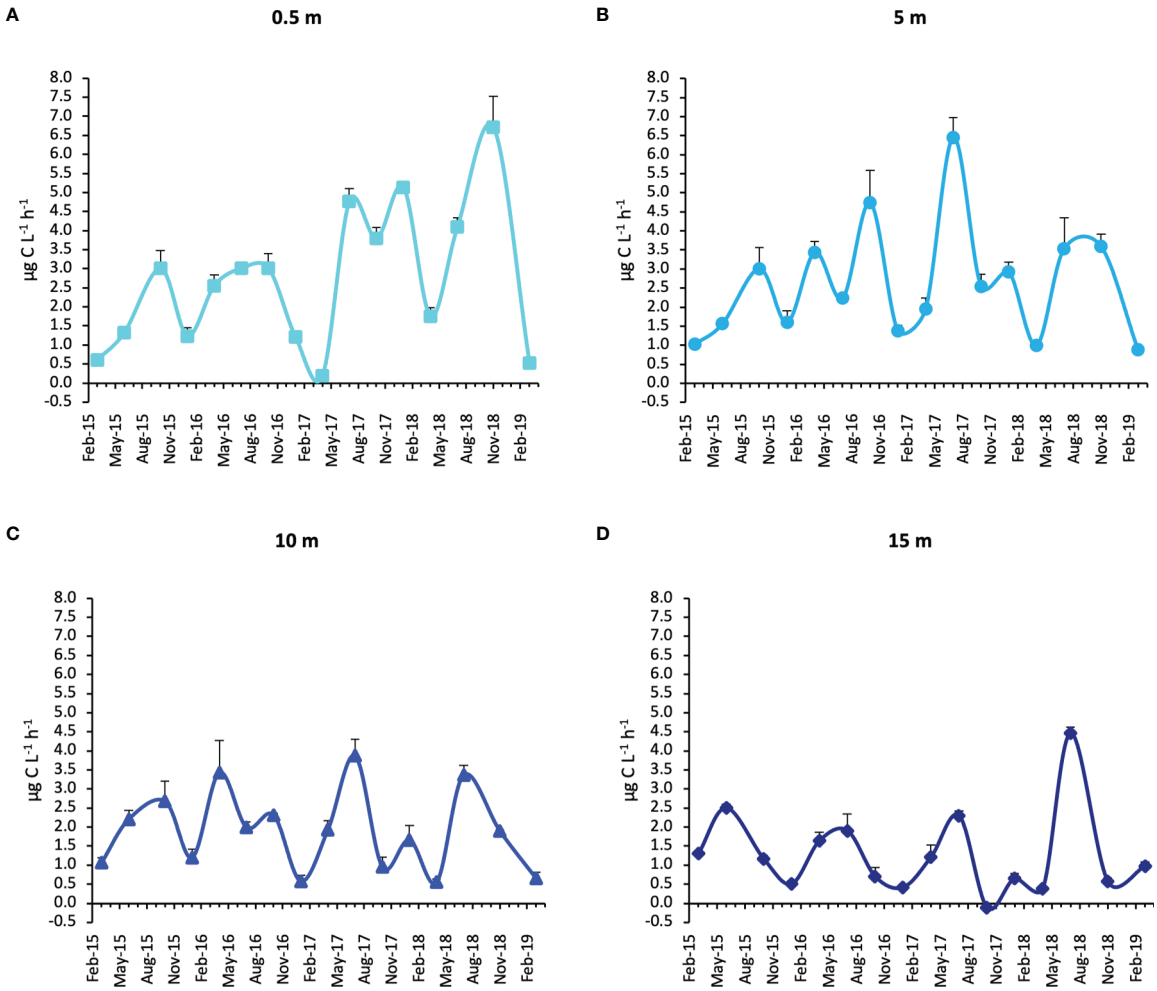

FIGURE 5 | Primary production rates during the study period at the four water column depths. (Whiskers represent SD). (**A** = 0.5 m; **B** = 5 m; **C** = 10 m; **D** = 15 m).

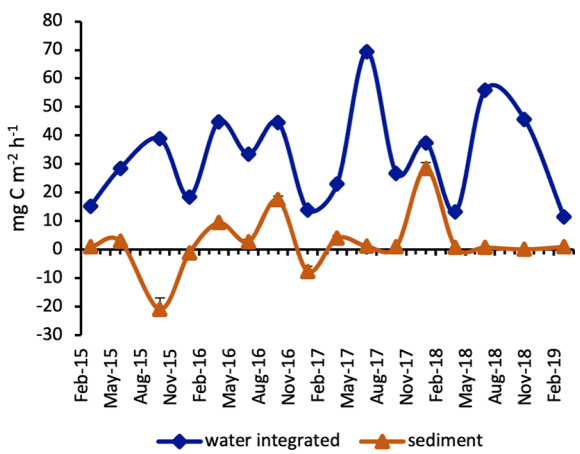

FIGURE 6 | Primary production rates in surface sediments and integrated over the water column. (Whiskers represent SD).

measured at the bottom layer in July 2018, in correspondence to a photosynthetically active phytoplankton assemblage (mostly *Leptocylindrus* spp., *Chaetoceros anastomosans*, small flagellates). In the other summer samplings, lower PP rates were obtained (1.91 to 2.50 µg C L^{-1} h^{-1}) when flagellates were the major contributors to the phototrophic biomass. Low PP rates, often close to zero (0.56 ± 0.38 µg C L^{-1} h^{-1}) were estimated in autumn and winter due to light depletion at 15 m depth.

At the surface sediment, the MPB biomass did not significantly differ among seasons (R_{ANOSIM} = 0.208; p = 5.5%). The maximum PP rate (28.50 µg C L^{-1} h^{-1}) was estimated in January 2018, in correspondence to a major contribution of *Paralia sulcata* (16.6%) and *Pinnularia* spp. (16.4%) to the benthic phototrophic biomass (**Figure 7E**). The second maximum was obtained in October 2016 mostly on the account of *Nitzschia sigma* var. *sigmatella* (21.4%). High PP values were further measured in April 2016 (9.42 mg C m^{-2} h^{-1}) and April 2017 (4.12 mg C m^{-2} h^{-1}). The highest benthic PP rates were consistently obtained in late winter-early spring or early autumn, i.e. in not excessively high temperature and light

TABLE 3 | Integrated primary production (PPi), primary production daily rates (PPd), primary production volumetric daily rates (PPwd), total primary production (PPt = the sum of primary production estimated in the water column, PPi, and in the sediments, PPs) and contribution of PPs to PPt during the study period.

Date	PPi (mg C m^{-2} h^{-1})	PPd (mg C m^{-2} d^{-1})	PPwd (µg C L^{-1} d^{-1})	PPt (mg C m^{-2} h^{-1})	PPs/PPt (%)
Mar-15	15.25	166.14	11.08	16.19	5.8
Jun-15	28.44	297.58	19.84	31.44	9.5
Oct-15	38.90	413.56	27.57	18.02	NC
Jan-16	18.35	108.13	7.21	17.15	NC
Apr-16	44.85	421.40	28.09	54.27	17.4
Jul-16	33.43	352.95	23.53	36.21	7.7
Oct-16	44.56	368.33	24.56	62.11	28.3
Jan-17 (*)	13.88	83.19	5.55	6.30	NC
Apr-17	22.96	216.96	14.46	27.08	15.2
Jul-17	69.30	767.40	51.16	70.52	1.7
Oct-17	26.70	325.35	21.69	27.67	3.5
Jan-18	37.47	252.08	16.81	65.97	43.2
Apr-18	13.17	381.90	25.46	13.98	5.78
Jul-18	55.89	556.70	37.11	56.68	1.40
Nov-18	45.62	248.43	16.56	45.73	0.25
Mar-19	11.47	98.11	6.54	12.44	7.82

Negative values recorded in the sediments (Oct-15, Jan-16, Jan-17) were removed from the calculation. (*): PPs was estimated in Dec-16 and PPw in Jan-17; because of the time lapse between the two samplings, the contribution of PPs to PPt was not calculated.

conditions. In contrast, the lowest PP rates were estimated in correspondence to the minima of MPB biomass, in October 2015 and December 2016, and in low light conditions. In each summer sampling, although a major MPB biomass was reached, the photosynthetic rates did not display high values. In June 2015, the benthic community was dominated by several *Nitzschia* species (*N. fasciculata, N. sigma, N. lorenziana*) and the large *Gyrosigma acuminatum*, but an uncoupling between the autotrophic biomass and PP occurred. Some of these taxa, namely *N. fasciculata*, *Nitzschia* spp., but also larger Naviculacea, seemed to be driven by higher concentrations of TOC and TN (Spearman R: *Nitzschia* spp. *vs* TN, $p = 0.001$; *N. fasciculata vs* TN, $p = 0.013$, and *vs* TOC, $p = 0.007$; *Navicula* sp.2 *vs* TN, $p = 0.010$, and *vs* TOC, $p = 0.012$). Similarly, in July 2017, the presence of very large diatom species (*Tropidoneis longa, Entomoneis alata, Nitzschia dubia*) and their high biomass was not mirrored in an equally high PP rate. The same pattern was observed on 30 March 2015, when the highest MPB biomass of the study period, due to the co-occurrence of taxa belonging to both winter (e.g. *Pinnularia* spp.) and spring (e.g. *Gyrosigma acuminatum*) assemblages, was uncoupled with the benthic photosynthetic rate.

DISCUSSION

Pelagic Primary Production in Relation to Nutrient Conditions and Water Column Stability

In the oligotrophic Gulf of Trieste, the phytoplankton density and structure are mostly driven by the nutrient availability (Mozetič et al., 2010; Cibic et al., 2018b; Cozzi et al., 2020). This was confirmed by our results that highlighted a persistent P-limitation for the phytoplankton development regardless of the degree of the water column stability. Indeed, the nutrient ratios applied to our data revealed P-limitation indiscriminately during both stratification and mixing of the water column. This was replaced by Si-limitation during a diatom bloom, as occurred in April 2017 (**Figure S4**), and coupled with N-limitation. N-depleted conditions were further observed in July 2018 and March 2019, when the diatom biomass prevailed over the other phytoplankton groups in the water column (**Figures 3**, **S4**). The N/P ratios higher than the Redfield one are a common feature not only for the gulf of Trieste (Lipizer et al., 2012) but also for the northern Adriatic Sea (Giani et al., 2012). However, the anomalous thermohaline conditions of the water column (extreme deviations in temperature and salinity compared to the climatological monthly means, **Figure S1**), particularly evident at the surface layer, seemed to influence greatly the phytoplankton development, as already observed in the area (Cerino et al., 2019) and in other shallow coastal waters (e.g. Trombetta et al., 2019). This clearly emerged in the PCA built on surface abiotic data, in which temperature and salinity were the predominant elements of the first factor, while in the other PCAs, dissolved inorganic nutrients were the major contributors to the total variance.

Focusing on the photosynthetic rates, we did not find a clear relationship between PPw and the stability of the water column (Spearman test $p > 0.05$, data not shown), neither considering the integrated rates. Indeed, only the highest PPi values of July 2017 and 2018 were obtained with a strong stratification of the water column, in typical summer conditions, whereas the other relative PPi peaks (November 2018, April and October 2016) were estimated in unstable or weak stratification conditions. During the other two summer samplings (June 2015 and July 2016), abiotic factors other than PAR availability (**Figure S2**) likely affected the phytoplankton productivity. As a general rule, major autotrophic densities observed in the summer period were not mirrored in exceptionally high PPw rates. Indeed, phytoplankton constantly adjust their photosynthetic

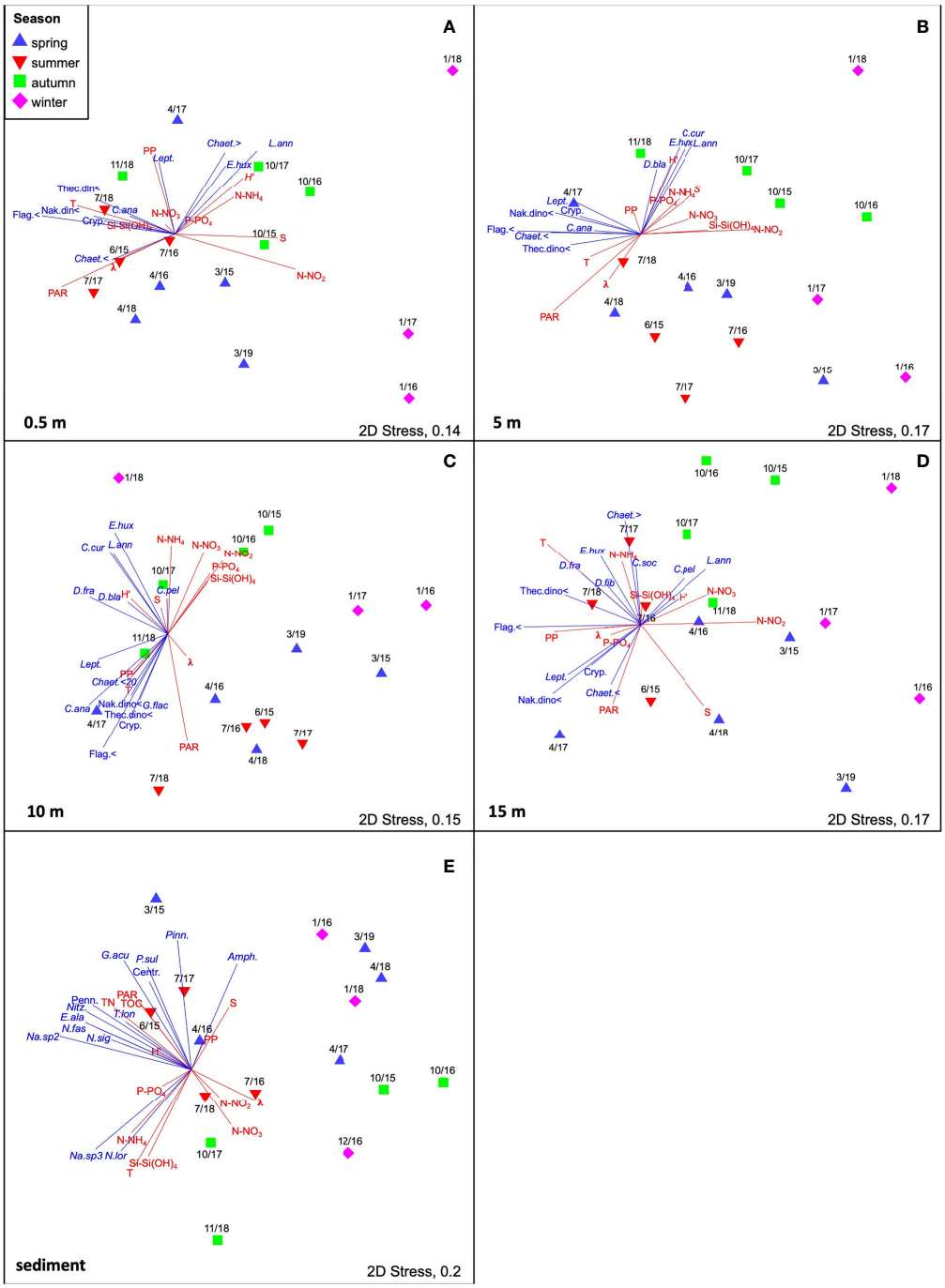

FIGURE 7 | Non-metric multidimensional scaling ordination (nMDS) performed on Bray-Curtis similarity matrices of **(A–D)** phytoplankton assemblages for each water column layer and **(E)** of MPB assemblage for the sediments. Data were log (x + 1) transformed before the analysis. Vectors (blue) represent the taxa constituting ≥ 1% of the total biomass for the water samples and ≥ 2% of the total biomass for the sediments. The environmental variables (T, temperature; S, salinity; PAR; TOC, Total Organic C; TN, Total N; N-NH4, ammonium; N-NO2, nitrite; N-NO3, nitrate; P-PO4, phosphate; Si-Si(OH)4, silicate.) and the diversity indices (diversity: H'; dominance: λ) were normalized (z-standardized), ordered in an Euclidean distance matrix and fitted as supplementary vectors (red) onto the ordination space. (*Amph., Amphora spp.; C. pel, Ceratulina pelagica; C. ana, Chaetoceros anastomosans; C. cur, Chaetoceros curvisetus; C. soc, Chaetoceros socialis; Chaet.*, < *Chaetoceros spp*. < 20μm; *Chaet*. >, *Chaetoceros spp*. > 20μm; *D. bla, Dactyliosolen blavyanus; D. fra, Dactyliosolen fragilissimus; D. fib, Dictyocha fibula; E. hux, Emiliania huxleyi; E. ala, Entomoneis alata; G. acu, Gyrosigma acuminatum; L.ann, Lauderia annulata; Lept., Leptocylindrus; Na.sp2, Navicula sp.2; Na.sp3, Navicula sp.3; N. fas, Nitzschia fasciculata; N. lor, Nitzschia lorenziana; N. sig, Nitzschia sigma; Nitz., Nitzschia spp.; P. sul, Paralia sulcata; Pinn, Pinnularia spp.; T. lon, Tropidoneis longa*; Centr., Undertermined Centrales; Cryp, Undetermined Cryptophycheae. Undetermined flagellates < 10μm, Flag.<; Undetermined naked dinoflagellates < 2μm, Nak.din<; Undetermined Pennales: Penn.; Undetermined thecate dinoflagellates < 20 μm, Thec.din<).

output to match environmental constrains and optimize their growth (Talaber et al., 2014). Moreover, the maximum PPw of the study occurred in November 2018, when a pycnocline was observed at -2.5 m depth, established after a freshwater input from the Isonzo River following the autumnal precipitations (flow rate obtained from the hydrometric height provided by: Regione Autonoma FVG, Water resources management service). This freshwater-induced pycnocline, likely triggered the not exceptionally abundant phototrophic community (**Figure S4**), leading to this major PPw. Our PPw rates were in line with previous results from the same site (Cibic et al., 2018 b). This could suggest that the trophic conditions at this coastal site have not changed after more than a decade. Interestingly, the maximum of the study period (November 2018) was consistent with that observed in November 2006 at the surface, and the high values recorded below 5 m in summer. Our PPi rates also displayed a very similar pattern to those calculated in 2006 - 07, with the highest values recorded in July 2017 and July 2018. Further, they were similar to the values estimated in the middle of the gulf from March 2011 to March 2013 (Ingrosso et al., 2016) and the south-eastern part of the gulf in the period 2010-2011 (Talaber et al., 2018). However, our mean PPi rate was about half of that estimated by Fonda Umani et al. (2007) from January 1999 to December 2001 at the same station (C1). Our daily rates (**Table 3**) were comparable or slightly lower than those obtained by Pugnetti et al. (2005) using the ^{14}C uptake in the northern Adriatic Sea; lower than those estimated by Decembrini et al. (2009) in the southern Tyrrhenian Sea in December (429 mg C m^{-2} d^{-1}) but higher than their rates in July (273 mg C m^{-2} d^{-1}); and much higher than those measured in the Mar Piccolo of Taranto (Ionian Sea) by the same ^{14}C technique (Cibic et al., 2016).

Benthic Primary Production in Relation to Physical-Chemical Features at the Seafloor

The maximum MPB abundances were observed in spring/early summer 2015, in correspondence to the highest light availability at the bottom (**Table S1**), in accordance with previous results (Cibic et al., 2012). However, the highest PPs rates were obtained in late winter - early spring or early autumn, with MPB abundances close to the average value of the study period. It is widely accepted that not all the viable cells present in sediments are likely to be active at once (Cahoon and Cooke, 1992). In contrast, the lowest or negative PP rates were estimated in correspondence to the minima of MPB density, and in low light conditions. The productivity of the microalgal community inhabiting surface sediments is known to be strongly dependent upon the light availability at the bottom (Miles and Sundbäck, 2000), especially in subtidal areas. Negative PPs values were previously reported, particularly from sublittoral sites worldwide (Meyercordt and Meyer-Reil, 1999; Gillespie et al., 2000; Forster et al., 2006). Overall, our PPs values are comparable to monthly data obtained from the same site in 2003-04 (Cibic et al., 2008), and to seasonal data reported from July 2010 to July 2012 (Franzo et al., 2016) as well as to those estimated in the port of Trieste at similar depths in June 2013 (Rogelja et al., 2018). In all these studies, with a few exceptions, the same pattern in primary production was observed, with higher rates from late winter to early summer, in correspondence with low temperature and increasing light conditions, and low or negative rates from late summer to early winter. As for the water column, the results in this study suggest that the trophic state of the benthic ecosystem has remained unaltered after more than 12 years.

The nutrient ratios applied to our data revealed that the MPB community was mostly P-depleted. When minima of all nutrients occurred in the overlying water (April 2016, 2017, 2018 and March 2019), the MPB abundances were consistently slightly lower, ranging from $4.5{\cdot}10^4$ to $5.7{\cdot}10^4$ cells cm^{-3}, than the average value ($6.1{\cdot}10^4 \pm 3.7{\cdot}10^4$ cells cm^{-3}). Notwithstanding, in those months the MPB community was photosynthetically active (PPs ranging from ~ 1 to 9.42 mg C $m^{-2}h^{-1}$). Very large diatom cells (length >100 μm: *Entomoneis alata, Gyrosigma acuminatum, G. attenuatum, Pinnularia* spp., *Tropidoneis longa*) represented a considerable fraction of the MPB biomass in these sampling months. Large diatoms have relatively larger nutrient storage vacuoles that allow them to achieve a slow but steady growth rate in pulsed-nutrient or nutrient-depleted environments and use the stored nutrients when needed (Finkel et al., 2005).

Benthic Contribution to Total Primary Production

At this sublittoral site, the benthic-pelagic coupling is not so tight as it might be in an estuarine or lagoon environment. The benthic microalgae occasionally enter the pelagic domain, mostly due to sediment resuspension and, on the other hand, the settlement of planktonic forms at the seafloor can increase the microphytobenthic biodiversity and the overall benthic photosynthetic activity. The mean annual contribution of benthic diatoms to the microphytoplankton (cells > 20 μm) was estimated to be 9.9% (Cibic et al., 2018b). Pennate diatoms (mostly *Nitzschia, Navicula, Pleurosigma* and *Diploneis*) were temporarily present in the phytoplankton assemblage following strong wind events that resuspended them from the bottom. However, in October 2006 when the microphytoplankton was quite scarce in the water column, *Nitzschia* alone reached up to 36% of this assemblage. We further calculated the mean benthic contribution to the total eukaryotic phytoplankton (2-200 μm), presented in this study, and in this case, it accounted for less than 1%, therefore it could be considered negligible.

From the benthic point of view, a two-year study focused on the MPB biodiversity carried out in the same site, identified 8 planktonic species out of 103 diatom taxa (Cibic et al., 2007 b) and found that on average 9% of the species in the sediment were planktonic. However, they were mostly in appalling condition and only species with a hardy frustule, e.g. *Pseudo-nitzschia seriata*, could be recognized (Cibic et al., 2007a), and were likely still photosynthetically active.

Our PPt rate per m^2, obtained adding PPs to PPi rates, displayed values varying from 12.44 to 70.52 mg C m^{-2} h^{-1}, indicating that the Gulf of Trieste, although oligotrophic (Mozetič et al., 2012; Cozzi

et al., 2020) is a productive ecosystem throughout the year. When the photosynthetic rates are lower along the water column, i.e. in late winter/early spring, they are compensated, to some extent, by higher rates of an active MPB community, once sufficient light reaches the surface sediments. In contrast, in summer and autumn much higher rates occur along the water column, when the benthic primary production is inhibited by low light or supra-optimal temperatures (Guarini et al., 1997; Kirk, 2000). Of course, to some degree there is an overlapping, particularly when a late winter phytoplankton bloom is triggered by favourable conditions and an abundant and photosynthetically active MPB community has already developed at the seafloor; or in summer when the water column is very clear and high PAR irradiance is available at the sea bottom. In any case, the pelagic contribution to total PP is consistently predominant in this coastal site. Indeed, excluding negative PPs values, the mean PPs contribution to PPt was 11.3%, while it reached up to 43% in January 2018. Although these results were obtained at a 17-m deep sublittoral site, they are in line with the literature, since the microphytobenthos have been reported to contribute up to 50% of the total PP in shallow coastal systems (Perissinotto et al., 2002; Montani et al., 2003). Only a few studies, mostly carried out in estuaries, investigated simultaneously the PPw and PPs (using the ^{14}C method), and calculated the PPs contribution to PPt. Perissinotto et al. (2003) and Anandraj et al. (2007) reported that the pelagic production was much higher than the microphytobenthic one in a river-dominated temporarily open/closed estuary in South Africa (up to 64x in the closed phase) as a direct consequence of the light availability at the bottom. van der Molen and Perissionotto (2011) found that in St. Lucia Estuary (South Africa, average depth about 2 m) the pelagic contribution to the total production varied greatly, from 2% to 100% and was below 15% in 4 out of 20 sampling dates/points. In the shallow (<12 m) semi-enclosed Mar Piccolo of Taranto (Ionian Sea) the PPs contribution to PPt was very low as it varied from 1% to 10% due to high concentration of contaminants (e.g. PCBs, PAHs, Hg) accumulated in the surface sediments (Cibic et al., 2016).

Influence of Abiotic Variables on the Structure and Function of Eukaryotic Phototrophic Communities

To detect which abiotic factors were most related with the occurrence and density of phytoplankton groups and the

TABLE 4 | Summary of the significant pairwise comparisons performed on the whole dataset applying the Spearman correlation test.

W - 0.5m		***r***	**p-value**	**W - 5m**		***r***	**p-value**
PP	sal	-0.56	0.024	PP	sal	-0.518	0.040
PP	T	0.593	0.015	PP	T	0.609	0.012
PP	d	0.519	0.039	PP	N	0.509	0.044
PP	d	0.519	0.039	Dino(ABU)	sal	-0.797	0.000
Dino(ABU)	sal	0.653	0.006	Dino(ABU)	T	0.524	0.037
Flag(ABU)	sal	-0.841	0	Flag(ABU)	sal	-0.744	0.001
Flag(ABU)	T	0.747	0.001	Flag(ABU)	T	0.576	0.019
Tot(ABU)	sal	-0.785	0	PAR	S	-0.175	0.045
Tot(ABU)	T	0.709	0.002	PAR	d	-0.004	0.043
Flag(ABU)	$N\text{-}NO_2$	-0.629	0.009	Dino(ABU)	$N\text{-}NO_2$	-0.447	0.023
Tot(ABU)	$N\text{-}NO_2$	-0.55	0.027	Flag(ABU)	$N\text{-}NO_2$	-0.606	0.003
H'	$N\text{-}NO_2$	0.729	0.001	Tot(ABU)	$N\text{-}NO_2$	-0.303	0.006
W - 10m		***r***	***p-value***	**W - 15m**		***r***	***p-value***
PP	sal	-0.699	0.003	PP	$N\text{-}NO_2$	-0.62	0.01
PP	T	0.644	0.007	PP	Cocco(ABU)	-0.621	0.01
PP	$N\text{-}NO_2$	-0.537	0.032	Flag(ABU)	$N\text{-}NO_2$	-0.53	0.035
Dino(ABU)	$N\text{-}NO_2$	-0.566	0.022	Tot(ABU)	$N\text{-}NO_2$	-0.595	0.015
Flag(ABU)	$N\text{-}NO_2$	-0.555	0.026	Dino(BIOM)	$N\text{-}NO_2$	-0.552	0.027
Tot(ABU)	$N\text{-}NO_2$	0.581	0.018	Tot(ABU)	T	0.597	0.015
$N\text{-}NH_4$	d	0.563	0.023	Flag(BIOM)	T	0.509	0.044
$N\text{-}NO_3$	d	0.504	0.046	$N\text{-}NH_4$	S	0.548	0.019
PAR	S	-0.542	0.037	$N\text{-}NH_4$	d	0.579	0.028
PAR	d	-0.568	0.027	PAR	N	-0.421	0.046
Sediment		***r***	***p-value***				
PP	Diato(ABU)	0.514	0.042				
PP	N	0.55	0.027				
$N\text{-}NO_2$	S	-0.517	0.04				
$N\text{-}NO_3$	S	-0.683	0.004				
$P\text{-}PO_4$	S	-0.53	0.035				
PAR	S	0.628	0.009				
PAR	H'	0.668	0.005				
TN	N	0.608	0.013				
TN	Tot(ABU)	0.752	0.001				
TN	Diato(BIOM)	0.598	0.015				
TOC	Tot(ABU)	0.55	0.027				
TOC	Diato(BIOM)	0.591	0.016				

(Abundance: ABU; biomass: BIOM; dinophyte: Dino; flagellates: Flag; coccolithophores: Cocco).

overall photosynthetic rate, an exploratory approach based on the Spearman rank correlation analysis was applied separately to samples from the four water depths and sediment. Only the significant relationships were extrapolated from the five matrices and shown in **Table 4**. Salinity and temperature highly affected the abundance of the main phytoplankton groups, i.e. undetermined flagellates and dinoflagellates, at the top 5 m of the water column, whereas their influence was less marked below the 10-m layer and not relevant at the sediment surface. This was also confirmed by the PCA. In contrast, light availability, which was not a limiting factor at the water surface, did not affect the phytoplankton density and photosynthetic rate but became an important driver of species richness below the 5-m layer, and particularly at the sediment surface, where a clear relation between PAR and biodiversity emerged. Among the considered inorganic nutrients, $N\text{-}NO_2$ highly influenced the abundance of flagellates along the water column, and of dinoflagellates below the 5-m layer. However, neither $N\text{-}NO_2$ nor other nutrients showed to directly affect the MPB total numbers and overall biomass that seemed to be rather influenced by TOC and TC concentrations. Yet, the nutrient availability showed to affect the number of species at the sediment surface. Indeed, changes in the relative availability of N and Si may influence the relative as well as absolute abundance of various diatom species (Gilpin et al., 2004). Interestingly, the significance of $N\text{-}NH_4$ on shaping the structure of the phytoplankton community increased particularly at the lower layers of the water column (<10 m) where this nutrient is regenerated from the microbial activity, particularly in summer (Souza et al., 2011; Cossarini et al., 2012), or become available after sediment resuspension. Primary production seemed to be directly influenced by salinity and temperature at the upper 10-m layer of the water column, only. PP was also dependent upon the community richness at the first 5-m layer, but a direct relation between PP and the overall abundance emerged only for the benthic community.

In conclusion, in this study, for the first time, pelagic and benthic primary production were estimated quasi-synchronously in the northern Adriatic Sea. Although the Gulf of Trieste is persistently P-limited, it is still a productive ecosystem throughout the year. We did not find a clear relationship between PP and the water column stability; however, the absolute maximum was obtained in a weak pycnocline at the surface in autumn whereas the highest integrated rates in stratified waters in typical summer conditions. We found higher benthic PP rates from late winter to early summer, in correspondence with low temperature and increasing light conditions, and low or negative rates from late summer, when PP was inhibited by supra-optimal temperature, to early winter when PP was light limited. The benthic contribution to total PP was generally low but it increased in clear water periods and/or when pelagic PP was strongly nutrient-depleted. We found PP to be influenced by salinity and temperature at the upper 10-m layer of the water column, and mostly by the $N\text{-}NO_2$-availability at the lower water layers. Light availability influenced the structure of the community at the sediment surface. $N\text{-}NO_2$ also emerged as the driving factor of the abundance of flagellates and dinoflagellates along the water column.

On a global scale, this study represents one of the few attempts of integrating pelagic and benthic primary production using the ^{14}C technique to quantify the ecosystem productivity. The main findings, obtained in the Gulf of Trieste, could be extended beyond the geographical limits of this particular ecosystem. Our results add on the limited database on primary production from sublittoral areas and could be used as proxy of ecosystem functioning in future studies on climate change impacts.

DATA AVAILABILITY STATEMENT

The original contributions presented in the study are included in the article/**Supplementary Material**. Further inquiries can be directed to the corresponding author.

AUTHOR CONTRIBUTIONS

TC: conceptualization, manuscript preparation, primary production analysis and interpretation. LB: statistical analysis and interpretation, manuscript preparation. FC: Phytoplankton analysis and interpretation, manuscript preparation. CC: physical data acquisition, climatological data production and interpretation. DF: field sampling, phytoplankton, and primary production analyses. MK: nutrients analyses and interpretation, manuscript revision. MG: field sampling, data interpretation, and manuscript critical revision. All authors contributed to the article and approved the submitted version.

ACKNOWLEDGMENTS

The authors thank the crew and all colleagues who participated to the sampling campaigns. We are very grateful to C. De Vittor for nutrient data from the sediment overlying water.

SUPPLEMENTARY MATERIAL

The Supplementary Material for this article can be found online at: https://www.frontiersin.org/articles/10.3389/fmars.2022.877935/full#supplementary-material

REFERENCES

Anandraj, A., Perissinotto, R., and Nozais, C. (2007). A Comparative Study of Microalgal Production in a Marine Versus a River-Dominated Temporarily Open/Closed Estuary, South Africa. *Estuar. Coast. She.lf Sci.* 73, 768–780. doi: 10.1016/j.ecss.2007.03.020

Barranguet, C., and Kromkamp, J. (2000). Estimating Primary Production Rates From Photosynthetic Electron Transport in Estuarine Microphytobenthos. *Mar. Ecol. Prog. Ser.* 204, 39–52. doi: 10.3354/meps204039

Barranguet, C., Kromkamp, J., and Peene, J. (1998). Factors Controlling Primary Production and Photosynthetic Characteristics of Intertidal Microphytobenthos. *Mar. Ecol. Prog. Ser.* 173, 117–126. doi: 10.3354/meps173117

Bartoli, M., Castaldelli, G., Nizzoli, D., and Viaroli, P. (2012). Benthic Primary Production and Bacterial Denitrification in a Mediterranean Eutrophic Coastal Lagoon. *J. Exp. Mar. Biol. Ecol.* 438, 41–51. doi: 10.1016/j.jembe.2012.09.011

Bérard-Therriault, L., Poulin, M., and Bossè, L. (1999). "Guide D'identification Du Phyto- Plankton Marin De L'estuarie Et Du Golfe Du Saint-Laurent Incluant Également Certains Protozoaires," in *CNRC-NRC*, vol. vol. 128. (Ottawa: Publication spéciale canadienne de sciences halieutiques et aquatiques), 387 pp.

Blasutto, O., Cibic, T., De Vittor, C., and Fonda Umani, S. (2005). Microphytobenthic Primary Production and Sedimentary Carbohydrates Along Salinity Gradients in the Lagoons of Grado and Marano (Northern Adriatic Sea). *Hydrobiologia* 550, 47–55. doi: 10.1007/s10750-005-4361-5

Brzezinski, M. A. (1985). The Si:C:N Ratio of Marine Diatoms: Interspecific Variability and the Effect of Some Environmental Variables. *J. Phycol.* 21, 347–357. doi: 10.1111/j.0022-3646.1985.00347.x

Cabrini, M., Fornasaro, D., Cossarini, G., Lipizer, M., and Virgilio, D. (2012). Phytoplankton Temporal Changes in a Coastal Northern Adriatic Site During the Last 25 Years. *Estuar. Coast. She.lf Sci.* 115, 113–124. doi: 10.1016/j.ecss.2012.07.007

Cahoon, L. B., and Cooke, J. E. (1992). Benthic Microalgal Production in Onslow Bay, North Carolina, USA. *Mar. Ecol. Prog. Ser.* 84, 185–196. doi: 10.3354/meps084185

Cantoni, C., Cozzi, S., Pecchiar, I., Cabrini, M., Mozetič, P., Catalano, G., et al. (2003). Short-Term Variability of Primary Production and Inorganic Nitrogen Uptake Related to the Environmental Conditions in a Shallow Coastal Area (Gulf of Trieste, N Adriatic Sea). *Oceanologica. Acta* 26, 565–575. doi: 10.1016/S0399-1784(03)00050-1

Celio, M., Malačič, V., Bussani, A., Čermelj, B., Comici, C., and Petelin, B. (2006). The Coastal Scale Observing System Component of ADRICOSM: Gulf of Trieste Network. *Acta Adriatica.* 47, 65–79.

Cerino, F., Fornasaro, D., Kralj, M., Giani, M., and Cabrini, M. (2019). Phytoplankton Temporal Dynamics in the Coastal Waters of the North-Eastern Adriatic Sea (Mediterranean Sea) From 2010 to 2017. *Nat. Conserv.* 34, 343–372. doi: 10.3897/natureconservation.34.30720

Cesbron, F., Murrell, M. C., Ederington Hagy, M., Jeffrey, W. H., Patterson, W. F., and Caffrey, J. M. (2019). Patterns in Phytoplankton and Benthic Production on the Shallow Continental Shelf in the Northeastern Gulf of Mexico. *Continental. She.lf Res.* 179, 105–114. doi: 10.1016/j.csr.2019.04.003

Cibic, T., and Blasutto, O. (2011). "Living Marine Benthic Diatoms as Indicators of Nutrient Enrichment: A Case Study in the Gulf of Trieste," in *Diatoms: Classification, Ecology and Life Cycle*. Ed. J. C. Compton (New York, USA: Nova Science Publishers, Inc), pp 169–pp 184.

Cibic, T., Blasutto, O., Burba, N., and Fonda Umani, S. (2008). Microphytobenthic Primary Production as ^{14}C Uptake in Sublittoral Sediments of the Gulf of Trieste (Northern Adriatic Sea): Methodological Aspects and Data Analyses. *Estuar. Coast. She.lf Sci.* 77, 113–122. doi: 10.1016/j.ecss.2007.09.005

Cibic, T., Blasutto, O., Falconi, C., and Fonda Umani, S. (2007b). Microphytobenthic Biomass, Species Composition and Nutrient Availability in Sublittoral Sediments of the Gulf of Trieste (Northern Adriatic Sea). *Estuar. Coast. She.lf Sci.* 75, 50–62. doi: 10.1016/j.ecss.2007.01.020

Cibic, T., Blasutto, O., and Fonda Umani, S. (2007a). Biodiversity of Settled Material in a Sediment Trap in the Gulf of Trieste (Northern Adriatic Sea). *Hydrobiologia* 580, 57–75. doi: 10.1007/s10750-006-0465-9

Cibic, T., Bongiorni, L., Borfecchia, F., Di Leo, A., Franzo, A., Giandomenico, S., et al. (2016). Ecosystem Functioning Approach Applied to a Large Contaminated Coastal Site: The Study Case of the Mar Piccolo of Taranto (Ionian Sea). *Environ. Sci. Pollution. Res.* 23, 12739–12754. doi: 10.1007/s11356-015-4997-2

Cibic, T., Cerino, F., Karuza, A., Fornasaro, D., Comici, C., and Cabrini, M. (2018b). Structural and Functional Response of Phytoplankton to Reduced River Inputs and Anomalous Physical-Chemical Conditions in the Gulf of Trieste (Northern Adriatic Sea). *Sci. Total Environ.* 636, 838–853. doi: 10.1016/j.scitotenv.2018.04.205

Cibic, T., Comici, C., Bussani, A., and Del Negro, P. (2012). Benthic Diatom Response to Changing Environmental Conditions. *Estuar. Coast. She.lf Sci.* 115, 158–169. doi: 10.1016/j.ecss.2012.03.033

Cibic, T., Comici, C., Falconi, C., Fornasaro, D., Karuza, A., and Lipizer, M. (2018a). Phytoplankton Community and Physical-Chemical Data Measured in the Gulf of Trieste (Northern Adriatic Sea) Over the Period March 2006-February 2007. *Data Brief* 19, 586–593. doi: 10.1016/j.dib.2018.05.054

Cibic, T., and Virgilio, D. (2010). Different Fixatives and HCl Concentrations in Microphytobenthic Primary Production Estimates Using Radiolabeled Carbon: Their Use and Misuse. *Limnol. Oceanogr.: Methods* (New York, USA: NOVA Science Publishers) 8, 453–461. doi: 10.4319/lom.2010.8.453

Cibic, T., and Virgilio, D. (2011). "In Situ Primary Production Measurements as an Analytical Support to Remote Sensing - An Experimental Approach to Standardize the 14C Incorporation Technique," in *Biomass and Remote Sensing of Biomass*. Ed. I. Atazadeh, pp 249–pp 262.

Clarke, K. R., Gorley, R. N., Somerfield, P. J., and Warwick, R. M. (2014). "Change in Marine Communities," in *An Approach to Statistical Analysis and Interpretation* (Plymouth: PRIMER-E), 260 pp.

Comici, C., and Bussani, A. (2007). Analysis of the River Isonzo Discharge, (1998-2005). *Bollettino. di. Geofisica. Teorica. ed. Applicata.* 48, 435–454.

Cossarini, G., Solidoro, C., and Fonda Umani, S. (2012). Dynamics of Biogeochemical Properties in Temperate Coastal Areas of Freshwater Influence: Lessons From the Northern Adriatic Sea (Gulf of Trieste). *Estuar. Coast. She.lf Sci.* 115, 63–74. doi: 10.1016/j.ecss.2012.02.006

Cozzi, S., Cabrini, M., Kralj, M., De Vittor, C., Celio, M., and Giani, M. (2020). Climatic and Anthropogenic Impacts on Environmental Conditions and Phytoplankton Community in the Gulf of Trieste (Northern Adriatic Sea). *Water* 12, 2652. doi: 10.3390/w12092652

Cozzi, S., Falconi, C., Comici, C., Čermelj, B., Kovac, N., Turk, V., et al. (2012). Recent Evolution of River Discharges in the Gulf of Trieste and Their Potential Response to Climate Changes and Anthropogenic Pressure. *Estuar. Coast. She.lf Sci.* 115, 1–11. doi: 10.1016/j.ecss.2012.03.005

Edler, L. (1979). Recommendations for Marine Biological Studies in the Baltic Sea. Phytoplankton and Chlorophyll. *Baltic. Mar. Biologist.* 5, 1–38.

Faganeli, J., Avcin, A., Fanuko, N., Malej, A., Turk, V., Tusnik, P., et al. (1985). Bottom Layer Anoxia in the Central Part of the Gulf of Trieste in the Late Summer 1983. *Mar. Pollution. Bull.* 16, 75–78. doi: 10.1016/0025-326X(85)90127-4

Finkel, Z. V., Katz, M. E., Wright, J. D., Schofield, O. M. E., and Falkowski, P. G. (2005). Climatically Driven Macroevolutionary Patterns in the Size of Marine Diatoms Over the Cenozoic. *Proc. Natl. Acad. Sci. U.S.A.* 102, 8927–8932. doi: 10.1073/pnas.0409907102

Fonda Umani, S., Beran, A., Parlato, S., Virgilio, D., Zollet, A., De Olazabal, A., et al. (2004). Noctiluca Scintillans MACARTNEY in the Northern Adriatic Sea: Long-Term Dynamics, Relationships With Temperature and Eutrophication, and Role in the Food Web. *J. Plankton. Reserach.* 26, 545–561. doi: 10.1093/plankt/fbh045

Fonda Umani, S., Del Negro, P., Larato, C., De Vittor, C., Cabrini, M., Celio, M., et al. (2007). Major Inter-Annual Variations in Microbial Dynamics in the Gulf of Trieste (Northern Adriatic Sea) and Their Ecosystem Implications. *Aquat. Microb. Ecol.* 46, 163–175. doi: 10.3354/ame046163

Fonda Umani, S., Malfatti, F., and Del Negro, P. (2012). Carbon Fluxes in the Pelagic Ecosystem of the Gulf of Trieste. *Estuar. Coast. She.lf Sci.* 115, 170–185. doi: 10.1016/j.ecss.2012.04.006

Forster, R. M., Créach, V., Sabbe, K., Vyverman, W., and Stal, L. J. (2006). Biodiversity-Ecosystem Function Relationship in Microphytobenthic Diatoms of the Westerschelde Estuary. *Mar. Ecol. Prog. Ser.* 311, 191–201. doi: 10.3354/meps311191

Frankenbach, S., Ezequiel, J., Plecha, S., Goessling, J. W., Vaz, L., Kühl, M., et al. (2020). Synoptic Spatio-Temporal Variability of the Photosynthetic Productivity of Microphytobenthos and Phytoplankton in a Tidal Estuary. *Front. Mar. Sci.* 7. doi: 10.3389/fmars.2020.00170

Franzo, A., Celussi, M., Bazzaro, M., Relitti, F., and Del Negro, P. (2019). Microbial Processing of Sedimentary Organic Matter at a Shallow LTER Site in the Northern Adriatic Sea: An 8-Year Case Study. *Nat. Conserv.* 34, 397–415. doi: 10.3897/natureconservation.34.30099

Franzo, A., Cibic, T., and Del Negro, P. (2016). Assessment of the Benthic Ecosystem Functioning in an Integrative Way: The Case Study of a Marine Protected Area in the Northern Adriatic Sea. *Continental. She.lf Res.* 121, 35–47. doi: 10.1016/j.csr.2015.12.005

Gargas, E. (1975). "A Manual for Phytoplankton Primary Production Studies in the Baltic," in *The Baltic Marine Biologist*. Ed. E. Gargas (Hørsholm, Denmark: Water Quality Institute), pp 1–pp18.

Gazeau, F., Smith, S. V., Gentili, B., Frankignoulle, M., and Gattuso, J. P. (2004). The European Coastal Zone: Characterization and First Assessment of Ecosystem Metabolism. *Estuar. Coast. She.lf Sci.* 60, 673–694. doi: 10.1016/j.ecss.2004.03.007

Giani, M., Djakovac, T., Degobbis, D., Cozzi, S., Solidoro, C., and Fonda Umani, S. (2012). Recent Changes in the Marine Ecosystems of the Northern Adriatic Sea. *Estuar. Coast. She.lf Sci.* 115, 1–13. doi: 10.1016/j.ecss.2012.08.023

Gillespie, P. A., Maxwell, P. D., and Rhodes, L. L. (2000). Microphytobenthic Communities of Subtidal Locations in New Zealand: Taxonomy, Biomass, Production, and Food-Web Implications. *New Z. J. Mar. Freshwater. Res.* 34, 41–53. doi: 10.1080/00288330.2000.9516914

Gilpin, L. C., Davidson, K., and Roberts, E. (2004). The Influence of Changes in Nitrogen: Silicon Ratios on Diatom Growth Dynamics. *J. Sea. Res.* 51, 21–35. doi: 10.1016/j.seares.2003.05.005

Guarini, J.-M., Blanchard, G. F., Gros, P., and Harrison, S. J. (1997). Modelling the Mud Surface Temperature on Intertidal Flats to Investigate the Spatio-Temporal Dynamic of the Benthic Microalgal Photosynthetic Capacity. *Mar. Ecol. Prog. Ser.* 153, 25–36. doi: 10.3354/meps153025

Guiry, M. D., and Guiry, G. M. (2022)AlgaeBase. In: *World-Wide Electronic Publication* (Galway: National University of Ireland) (Accessed 15 February 2022).

Hammer, Ø, Harper, D. A. T., and Ryan, P. D. (2001). PAST: Paleontological Statistics Software Package for Education and Data Analysis. *Palaeontologia. Electronica.* 4 (1), 9.

Hansen, H. P., and Koroleff, F. (1999). "Determination of Nutrients," in *Methods of Seawater Analysis*. Eds. K. Grasshof, K. Kremling and M. Ehrhardt (Weilheim: WILEY-VCH), pp 159–pp 228.

Herndl, G. J., Peduzzi, P., and Fanuko, N. (1989). Benthic Community Metabolism and Microbial Dynamics in the Gulf of Trieste (Northern Adriatic Sea). *Mar. Ecol. Prog. Ser.* 53, 169–178. doi: 10.3354/meps053169

Hillebrand, H., Dürselen, C. D., Kirschtel, D., Pollingher, U., and Zohary, T. (1999). Biovolume Calculation for Pelagic and Benthic Microalgae. *Jounal. Phycol.* 35, 403–424. doi: 10.1046/j.1529-8817.1999.3520403.x

Hillebrand, H., and Sommer, U. (1999). The Nutrient Stoichiometry of Benthic Microalgal Growth: Redfield Proportions are Optimal. *Limnol. Oceanogr.* 44, 440–446. doi: 10.4319/lo.1999.44.2.0440

Horner, R. A. (2002). *A Taxonomic Guide to Some Common Marine Phytoplankton* (Bristol: Biopress Ltd), 195 pp.

Ingrosso, G., Giani, M., Cibic, T., Karuza, A., Kralj, M., and Del Negro, P. (2016). Carbonate Chemistry Dynamics and Biological Processes Along a River-Sea Gradient (Gulf of Trieste, Northern Adriatic Sea). *J. Mar. Syst.* 155, 35–49. doi: 10.1016/j.jmarsys.2015.10.013

Jacobs, P., Pitarch, J., Kromkamp, J. C., and Philippart, C. J. M. (2021). Assessing Biomass and Primary Production of Microphytobenthos in Depositional Coastal Systems Using Spectral Information. *PloS One* 16 (7), e0246012. doi: 10.1371/journal.pone.0246012

Jahnke, R. A., Nelson, J. R., Richards, M. E., Robertson, C. Y., Rao, A. M. F., and Jahnke, D. B. (2008). Benthic Primary Productivity on the Georgia Midcontinental Shelf: Benthic Flux Measurements and High-Resolution, Continuous *in Situ* PAR Records. *J. Geophys. Res.* 113. doi: 10.1029/2008JC004745

Kemp, W. M., Smith, E. M., Marvin-DiPasquale, M., and Boynton, W. R. (1997). Organic Carbon Balance and Net Ecosystem Metabolism in Chesapeake Bay. *Mar. Ecol. Prog. Ser.* 150, 229–248. doi: 10.3354/meps150229

Kennish, M., Brush, M., and Moore, K. (2014). Drivers of Change in Shallow Coastal Photic Systems: An Introduction to a Special Issue. *Estuar. Coasts.* 37, 3–19. doi: 10.1007/s12237-014-9779-4

Kirk, J. T. O. (2000). *Light & Photosynthesis in Aquatic Ecosystems. Second Edition* (UK: Cambridge University Press), 509 pp.

Kralj, M., Lipizer, M., Čermelj, B., Celio, M., Fabbro, C., Brunetti, F., et al. (2019). Hypoxia and Dissolved Oxygen Trends in the Northeastern Adriatic Sea (Gulf of Trieste). *Deep. Sea. Res. Part II: Topical. Stud. Oceanogr.* 164, 74–88. doi: 10.1016/j.dsr2.2019.06.002

Kromkamp, J. C., and Forster, R. M. (2006). "Estimating Primary Production: Scaling Up From Point Measurements to the Whole Estuary," in *Functioning of Microphytobenthos in Estuaries*. Eds. J. C. Kromkamp, J. F. C. De Brouwer, G. F. Blanchard, R. M. Forster and V. Créach (Amsterdam: Proceedings of the Colloquium), pp 9–pp 30.

Kruskal, J. B., and Wish, M. (1978). *Multidimensional Scaling* (Beverly Hills: Sage), 96 pp.

Lake, S. J., and Brush, M. J. (2011). The Contribution of Microphytobenthos to Total Productivity in Upper Narragansett Bay, Rhode Island. *Estuar. Coast. She.lf Sci.* 95, 289–297. doi: 10.1016/j.ecss.2011.09.005

Lehrter, J. C., Fry, B., and Murrell, M. C. (2014). Microphytobenthos Production Potential and Contribution to Bottom Layer Oxygen Dynamics on the Inner Louisiana Continental Shelf. *Bull. Mar. Sci.* 90, 765. doi: 10.5343/bms.2013.1050

Lipizer, M., De Vittor, C., Falconi, C., Comici, C., Tamberlich, F., and Giani, M. (2012). Effects of Intense Meteorological and Biological Forcing Factors on Biogeochemical Properties of Coastal Waters (Gulf of Trieste, Northern Adriatic Sea). *Estuar. Coast. She.lf Sci.* 115, 40–50. doi: 10.1016/j.ecss.2012.03.024

Longhurst, A., Sathyendrenath, S., Platt, T., and Caverhill, C. (1995). An Estimate of Global Production in the Ocean From Satellite Radiometer Data. *J. Plankton. Res.* 17, 1245–1271. doi: 10.1093/plankt/17.6.1245

Malačič, V., and Petelin, B. (2001). "Regional Studies: Gulf of Trieste," in *Physical Oceanography of the Adriatic Sea: Past, Present and Future*. Eds. B. Cushman-Roisin, M. Gačić, P.-M. Poulain and A. Artegiani (Dordrecht, Netherlands: Kluwer Academic Publishers), pp 167–pp 181.

Malej, A., and Malačič, V. (1995). Factors Affecting Bottom Layer Oxygen Depletion in the Gulf of Trieste (Adriatic Sea). *Ann. Istrian. Mediterranean. Stud.* 6, 33–42.

Malej, A., Mozetič, P., Malačič, V., Terzić, S., and Ahel, M. (1995). Phytoplankton Responses to Freshwater Inputs in a Small Semi-Enclosed Gulf (Gulf of Trieste, Adriatic Sea). *Mar. Ecol. Prog. Ser.* 120, 111–121. doi: 10.3354/meps120111

Malinverno, E., Dimiza, M. D., Triantaphylou, M., Dermitzkis, M. D., and Corselli, C. (2008). "Coccolithophores of the Eastern Mediterranean Sea," in *A Look Into the Marine Microworld* (Peristeri: Ion Publishing Group), 188 pp.

Margalef, R. (1986). *Ecologia* (Barcellona: Omega).

Martin, J. H., Knauer, G. A., Karl, D. M., and Broenkow, W. W. (1987). VERTEX: Carbon Cycling in the Northeast Pacific. *Deep-Sea. Res.* 34, 267–285. doi: 10.1016/0198-0149(87)90086-0

Menden-Deuer, S., and Lessard, E. J. (2000). Carbon to Volume Relationships for Dinoflagellates, Diatoms and Other Protest Plankton. *Limnol. Oceanogr.* 45, 569–579. doi: 10.4319/lo.2000.45.3.0569

Meyercordt, J., and Meyer-Reil, L.-A. (1999). Primary Production of Benthic Microalgae in Two Shallow Coastal Lagoons of Different Trophic Status in the Southern Baltic Sea. *Mar. Ecol. Prog. Ser.* 178, 179–191. doi: 10.3354/meps178179

Migné, A., Spilmont, N., Boucher, G., Denis, L., Hubas, C., Janquin, M. A., et al. (2009). Annual Budget of Benthic Production in Mont Saint-Michel Bay Considering Cloudiness, Microphytobenthos Migration, and Variability of Respiration Rates With Tidal Conditions. *Continental. She.lf Res.* 29, 2280–2285. doi: 10.1016/j.csr.2009.09.004

Miles, A., and Sundbäck, K. (2000). Diel Variation in Microphytobenthic Productivity in Areas of Different Tidal Amplitude. *Mar. Ecol. Prog. Ser.* 205, 11–22. doi: 10.3354/meps205011

Montani, S., Magni, P., and Abe, N. (2003). Seasonal and Interannual Patterns of Intertidal Microphytobenthos in Combination With Laboratory and Areal Production Estimates. *Mar. Ecol. Prog. Ser.* 249, 79–91. doi: 10.3354/meps249079

Mozetič, P., Solidoro, C., Cossarini, G., Socal, G., Pyrecali, R., France, J, et al (2010). Recent Trends Towards Oligotrophication of the Northern Adriatic: Evidence from Chlorophyll a Time Series. . *Estuaries Coasts* 33, 362–375. doi: 10.1007/s12237-009-9191-7

Mozetič, P., Francé, J., Kogovšek, T., Talaber, I., and Malej, A. (2012). Plankton Trends and Community Changes in a Coastal Sea (Northern Adriatic): Bottom-Up *vs.* Top-Down Control in Relation to Environmental Drivers. *Estuar. Coast. She.lf Sci.* 115, 138–148. doi: 10.1016/j.ecss.2012.02.009

Murrell, M. C., Campbell, J. G., Hagy, J. D.III, and Caffrey, J. M. (2009). Effects of Irradiance on Benthic and Water Column Processes in a Gulf of Mexico Estuary: Pensacola Bay, Florida, USA. *Estuar. Coast. She.lf Sci.* 81, 501–512. doi: 10.1016/j.ecss.2008.12.002

Odum, E. P. (1983). *Basic Ecology* (Philadelphia: Saunders College Publishing).

Perissinotto, R., Nozais, C., and Kibirige, I. (2002). Spatio-Temporal Dynamics of Phytoplankton and Microphytobenthos in a South African Temporarily Open Estuary. *Estuar. Coast. She.lf Sci.* 54, 363–374. doi: 10.1006/ecss.2001.0885

Perissinotto, R., Nozais, C., Kibirige, I., and Anandraj, A. (2003). Planktonic Food Webs and Benthic-Pelagic Coupling in South African Temporarily-Open Estuaries. *Acta Oecologica.* 24, S307–S316. doi: 10.1016/S1146-609X(03)00028-6

Pielou, E. C. (1966). Shannon's Formula as a Measure of Species Diversity: Its Use and Misuse. *Am. Nat.* 118, 463–465. doi: 10.1086/282439

Poulain, P.-M., Kourafalou, V. H., and Cushman-Roisin, B. (2001). "Northern Adriatic Sea," in *Physical Oceanography of the Adriatic Sea Past, Present and Future*. Eds. B. Cushman-Roisin, M. Gačić, P.-M. Poulain and A. Artegiani (Dordrecht, Netherlands: Kluwer Academic Publishers), pp 143–pp 165.

Querin, S., Crise, A., Deponte, D., and Solidoro, C. (2006). Numerical Study of the Role of Wind Forcing and Freshwater Buoyancy Input on the Circulation in a Shallow Embayment (Gulf of Trieste, Northern Adriatic Sea). *J. Geophysical. Res.* 111, C03S16. doi: 10.1029/2006JC003611

Redfield, A. C. (1958). The Biological Control of the Chemical Factors in the Environment. *Am. Sci.* 46, 205–221.

Rogelja, M., Cibic, T., Pennesi, C., and De Vittor, C. (2016). Microphytobenthic Community Composition and Primary Production at Gas and Thermal Vents in the Aeolian Islands (Tyrrhenian Sea, Italy). *Mar. Environ. Res.* 118, 31–44. doi: 10.1016/j.marenvres.2016.04.009

Rogelja, M., Cibic, T., Rubino, F., Belmonte, M., and Del Negro, P. (2018). Active and Resting Microbenthos in Differently Contaminated Marine Coastal Areas: Insights From the Gulf of Trieste (Northern Adriatic, Mediterranean Sea). *Hydrobiologia* 806, 283–301. doi: 10.1007/s10750-017-3366-1

Rubino, F., Cibic, T., Belmonte, M., and Rogelja, M. (2016). Microbenthic Community Structure and Trophic Status of Sediments in the Mar Piccolo of Taranto (Mediterranean, Ionian Sea). *Environ. Sci. Pollution. Res.* 23, 12624–12644. doi: 10.1007/s11356-015-5526-z

Santema, M., and Huettel, M. (2018). Dynamics of Microphytobenthos Photosynthetic Activity Along a Depth Transect in the Sandy Northeastern Gulf of Mexico Shelf. *Estuar. Coast. She.lf Sci.* 212, 273–285. doi: 10.1016/j.ecss.2018.07.016

Schlitzer, R. (2021). *Ocean Data View*. Available at: https://odv.awi.de.

Serodio, J., Vieira, S., and Cruz, S. (2008). Photosynthetic Activity, Photoprotection and Photoinhibition in Intertidal Microphytobenthos as Studied *in Situ* Using Variable Chlorophyll Fluorescence. *Continental. She.lf Res.* 28, 1363–1375. doi: 10.1016/j.csr.2008.03.019

Shannon, C. E., and Weaver, W. (1949). *The Mathematical Theory of Communication* (Urbana, Illinois: Illinois Press).

Simpson, E. H. (1949). Measurement of Diversity. *Nature* 163, 688. doi: 10.1038/163688a0

Sorokin, Y. I. (1958). Results and Prospects of Using Isotopic Carbon for the Investigation of Carbon Cycle in Water Basins. *Int. Conf. Radioisotopes.* 4, 633–648.

Souza, A. C., Pease, T. K., and Gardner, W. S. (2011). The Direct Role of Enzyme Hydrolysis on Ammonium Regeneration Rates in Estuarine Sediments. *Aquat. Microb. Ecol.* 65, 159–168. doi: 10.3354/ame01541

Steeman Nielsen, E. (1952). The Use of Radioactive ^{14}C for Measuring Organic Production in the Sea. *J. du. Conseil. Permanent. Int. pour. l'exploitation. la. Mer* 18, 117–140. doi: 10.1093/icesjms/18.2.117

Stravisi, F. (1977). Bora Driven Circulation in Northern Adriatic. *Bollettino. di. Geofisica. Teorica. e Applicata.* 19, 73–74.

Stravisi, F. (1983). Some Characteristics of the Circulation in the Gulf of Trieste. *Thalassia. Jugoslavica.* 19, 355–363.

Sundbäck, K., and Jönsson, B. (1988). Microphytobenthic Productivity and Biomass in Sublittoral Sediments of a Stratified Bay, Southeastern Kattegat. *J. Exp. Mar. Biol. Ecol.* 122, 63–81. doi: 10.1016/0022-0981(88)90212-2

Sundbäck, K., Lindehoff, E., and Graneli, E. (2011). Dissolved Organic Nitrogen: An Important Source of Nitrogen for the Microphytobenthos in Sandy Sediment. *Aquat. Microb. Ecol.* 63, 89–100. doi: 10.3354/ame01479

Sundbäck, K., Miles, A., and Gőrnasson, E. (2000). Nitrogen Fluxes, Denitrification and the Role of Microphytobenthos in Microtidal Shallow-Water Sediments: An Annual Study. *Mar. Ecol. Prog. Ser.* 200, 59–76. doi: 10.3354/meps200059

Talaber, I., Francé, J., Flander-Putrle, V., and Mozetič, P. (2018). Primary Production and Community Structure of Coastal Phytoplankton in the Adriatic Sea: Insights on Taxon-Specific Productivity. *Mar. Ecol. Prog. Ser.* 604, 65–81. doi: 10.3354/meps12721

Talaber, I., Francé, J., and Mozetič, P. (2014). How Phytoplankton Physiology and Community Structure Adjust to Physical Forcing in a Coastal Ecosystem (Northern Adriatic Sea). *Phycologia* 53, 74–85. doi: 10.2216/13-196.1

Testa, J., Faganeli, J., Giani, M., Brush, M., De Vittor, C., Boynton, W., et al. (2021). "Advances in Our Understanding of Pelagic-Benthic Coupling," in *Coastal Ecosystems in Transition: A Comparative Analysis of the Northern Adriatic and Chesapeake Bay, Geophysical Monograph*, *1st Edition*, vol. 256 . Eds. T. Malone, A. Malej and J. Faganeli (New York, USA: Wiley & Sons Ltd), pp 147–pp 175.

Throndsen, J. (1978). "Preservation and Storage," in *Phytoplankton Manual*. Ed. A. Sournia (Paris: UNESCO), pp 69–pp 74.

Tomas, C. R. (1997). *Identifying Marine Phytoplankton* (San Diego, CA: Academic Press), 858 pp.

Trombetta, T., Vidussi, F., Mas, S., Parin, D., Simier, M., and Mostajir, B. (2019). Water Temperature Drives Phytoplankton Blooms in Coastal Waters. *PloS One* 14 (4), e0214933. doi: 10.1371/journal.pone.0214933

Utermöhl (1958). Zur Vervollkommnung Der Quantitativen Phytoplankton-Methodik. *Mitteilungen. Internationale. Vereiningung. für Theoretische. und Angewandte. Limnologie.* 9, 1–38. doi: 10.1080/05384680.1958.11904091

van der Molen, J. S., and Perissinotto, R. (2011). Microalgal Productivity in an Estuarine Lake During a Drought Cycle: The St. Lucia Estuary, South Africa. Estuarine. *Coast. She.lf Sci.* 92, 1–9. doi: 10.1016/j.ecss.2010.12.002

Williams PJ le, B., Thomas, D. N., and Reynolds, C. S. (2002). *Phytoplankton Productivity* (Oxford, UK: Blackwell Science).

WoRMS Editorial Board (2022) *World Register of Marine Species*. Available at: https://www.marinespecies.org (Accessed 2022-02-15).

Young, J., Geisen, M., Cros, L., Kleijne, A., Sprengel, C., and Probert, I. (2003). Guide to Extant Calcareous Nanoplankton Taxonomy. *J. Nanoplankton. Res.* 1, 125.

Conflict of Interest:: The authors declare that the research was conducted in the absence of any commercial or financial relationships that could be construed as a potential conflict of interest.

Publisher's Note: All claims expressed in this article are solely those of the authors and do not necessarily represent those of their affiliated organizations, or those of the publisher, the editors and the reviewers. Any product that may be evaluated in this article, or claim that may be made by its manufacturer, is not guaranteed or endorsed by the publisher.

frontiers | Frontiers in Marine Science

ORIGINAL RESEARCH
published: 13 June 2022
doi: 10.3389/fmars.2022.909927

Benthic-Pelagic Coupling of Marine Primary Producers Under Different Natural and Human-Induced Pressures' Regimes

Vasilis Gerakaris[1], Ioanna Varkitzi[1], Martina Orlando-Bonaca[2], Katerina Kikaki[1,3], Patricija Mozetič[2], Polytimi-Ioli Lardi[1], Konstantinos Tsiamis[1] and Janja Francé[2]*

[1] Institute of Oceanography, Hellenic Centre for Marine Research (HCMR), Anavyssos, Greece, [2] Marine Biology Station, National Institute of Biology (NIB), Piran, Slovenia, [3] Remote Sensing Laboratory, National Technical University of Athens (NTUA), Zographou, Greece

OPEN ACCESS

Edited by:
Christian GRENZ, UMR7294, Institut Méditerranéen d'océanographie (MIO), France

Reviewed by:
Pierre Boissery, Agence de l'eau Rhône Méditerranée Corse, France
Maria Flavia Gravina, University of Rome "Tor Vergata", Italy

***Correspondence:**
Vasilis Gerakaris
vgerakaris@hcmr.gr

Specialty section:
This article was submitted to Marine Ecosystem Ecology, a section of the journal Frontiers in Marine Science

Received: *31 March 2022*
Accepted: *10 May 2022*
Published: *13 June 2022*

Citation:
Gerakaris V, Varkitzi I, Orlando-Bonaca M, Kikaki K, Mozetič P, Lardi P-I, Tsiamis K and Francé J (2022) Benthic-Pelagic Coupling of Marine Primary Producers Under Different Natural and Human-Induced Pressures' Regimes. Front. Mar. Sci. 9:909927. doi: 10.3389/fmars.2022.909927

Marine primary producers are highly sensitive to environmental deterioration caused by natural and human-induced stressors. Following the Water Framework Directive and the Marine Strategy Framework Directive requirements, the importance of using the different primary producers of the coastal marine ecosystem (pelagic: phytoplankton and benthic: macroalgae and angiosperms) as appropriate tools for an integrated assessment of the ecological status of the coastal environment has been recognized. However, the processes by which water column characteristics and phytobenthic indicators are linked have not been systematically studied. Based on a large dataset from three Mediterranean sub-basins (Adriatic, Ionian and Aegean Seas) with different trophic conditions, this study aims to explore the coupled responses of benthic and pelagic primary producers to eutrophication pressures on a large scale, focusing on the structural and functional traits of benthic macroalgal and angiosperm communities, and to investigate the key drivers among the different eutrophication-related pelagic indicators (such as nutrient and Chl-a concentrations, water transparency, etc.) that can force the benthic system indicators to low ecological quality levels. In addition to the effects of high nutrient loading on phytoplankton biomass, our results also show that increased nutrient concentrations in seawater have a similar effect on macroalgal communities. Indeed, increasing nutrient concentrations lead to increased coverage of opportunistic macroalgal species at the expense of canopy-forming species. Most structural traits of *Posidonia oceanica* (expressed either as individual metrics: shoot density, lower limit depth and lower limit type, or in the context of PREI index) show opposite trends to increasing levels of pressure indicators such as ammonium, nitrate, phosphate, Chl-a and light attenuation. Furthermore, our results highlight the regulating effect of light availability on the ecological

status of seagrass meadows (*Posidonia oceanica* and *Cymodocea nodosa*). Increasing leaf length values of *C. nodosa* are closely associated with higher turbidity values linked to higher phytoplankton biomass (expressed as Chl-a). Overall, the coupling of pelagic and benthic primary producers showed consistent patterns across trophic gradients at the subregional scale.

Keywords: macroalgae, seagrasses, phytoplankton, eutrophication, Mediterranean Sea

INTRODUCTION

The use of biological indicators to monitor the status and trends of aquatic ecosystems has attracted much attention in recent decades (Martínez-Crego et al., 2010; Pawlowski et al., 2018). In the context of European directives, i.e., the Water Framework Directive (WFD, 2000/60/EC) and the Marine Strategy Framework Directive (MSFD, 2008/56/EC), biological indicators have been recognized as valuable monitoring tools as they enable ecosystem integrity by focusing on biological communities and not on only chemical and physical characteristics (Orfanidis et al., 2020).

Marine primary producers (phytoplankton and macrophytes) are very sensitive to environmental deterioration caused by natural and human-induced stressors. Therefore, both pelagic (phytoplankton) and benthic communities (macroalgae and angiosperms) are considered reliable ecological indicators that can integrate and adequately reflect natural and anthropogenic pressures in the coastal marine ecosystem (Orlando-Bonaca et al., 2015; Gerakaris et al., 2017; Varkitzi et al., 2018a; Rombouts et al., 2019; Orfanidis et al., 2001; Orfanidis et al., 2020). The importance of using the various marine primary producers as valuable indicators of coastal ecosystems' health is widely recognized (Orfanidis et al., 2001; Devlin et al., 2007; Orfanidis et al., 2007; Tweddle et al., 2018).

In accordance with WFD and MSFD requirements, phytoplankton, macroalgae and marine angiosperms are used as biological quality elements (BQEs) or indicators for the assessment of ecological and environmental status (ES) of EU coastal waters. In particular, in the context of the WFD, the Mediterranean water types, reference conditions and boundaries for each BQE were defined during the intercalibration process for Mediterranean coastal waters in European Member States (MS). For the Mediterranean pelagic habitats, only Chlorophyll-a (Chl-a) concentrations have been identified as an operational intercalibrated indicator so far (UNEP/MAP, 2017; Varkitzi et al., 2018a). On the contrary, several indices were intercalibrated for the macrophyte communities: two biotic indices for macroalgae, namely the EEI-c index (Orfanidis et al., 2001; Orfanidis et al., 2011) and the CARLIT index (Ballesteros et al., 2007) and a few biotic indices for seagrasses, namely POMI (Romero et al., 2007a; Romero et al., 2007b), PREI (Gobert et al., 2009) and Valencian CS (Fernadez-Torquemada et al., 2008) for *Posidonia oceanica* (L.) Delile and CymoSkew (Orfanidis et al., 2007; Orfanidis et al., 2010; Orfanidis et al., 2020) and MediSkew (Orlando-Bonaca et al., 2015; Orlando-Bonaca et al., 2016) for *Cymodocea nodosa* (Ucria) Ascherson.

The efficiency of the proposed indicators and biotic indices for the pelagic and benthic ecosystem for robust environmental assessments is well-documented (e.g., Orfanidis et al., 2001; Orlando-Bonaca et al., 2015; Gerakaris et al., 2017; Varkitzi et al., 2018a; Orfanidis et al., 2020). Most phytoplankton indicators (Chl-a and diversity) are able to discriminate between the highest and lowest pressure levels and maintain this sensitivity across latitudinal and longitudinal gradients; thus, their use at broad spatial scales has been recommended to cover broader gradients of natural and anthropogenic stress (Varkitzi et al., 2018a; Magliozzi et al., 2021; Magliozzi et al., 2021; Francé et al., 2021). The two indices for *C. nodosa* (CymoSkew and MediSkew) take advantage of the high phenotypic plasticity of the species (e.g., asymmetry of leaf length distribution) attributed to limiting resources such as nutrient availability (Mvungi and Mamboya, 2012; Marbà et al., 2013) and light (Abal et al., 1994; Orfanidis et al., 2010) and successfully use it as an early warning indicator of coastal ecosystem status and trends. Regarding macroalgal communities, EEI-c has been selected as the most appropriate index for assessing the ES of coastal waters in the eastern Mediterranean and northern Adriatic basins (MED-GIG, 2011). It takes into account the functional characteristics of the species in order to indicate changes in resource availability (mainly nutrients and light) that can alter species composition and abundance (Orfanidis et al., 2011). Finally, the proposed indices for *P. oceanica* are more complex and use different metrics that provide information at different organization levels (i.e., individual, population, and community), on different types of pressures (e.g., water transparency, nutrient concentrations and eutrophication, sediment dynamics), and with different response times (Gobert et al., 2009; Martínez-Crego et al., 2010).

If eutrophication is the main driving factor of environmental quality, the associated pelagic indicators (such as nutrient and Chl-a concentrations, water transparency, etc.) are expected to drive the benthic system indicators to low ecological quality levels (Graf, 1992). To date, the literature has mainly reported modelling approaches to describe the relationships between pelagic primary production and oxygen demand in sediments (Hargrave, 1973; Vaquer-Sunyer and Duarte, 2008), organic matter content in sediments (Brady et al., 2013), and sediment biogeochemical features (Grangeré et al., 2012). Sparse attempts to quantify the impacts of pelagic parameters on benthic communities suggest some concentrations of Chl-a and dissolved oxygen in the seawater column as thresholds above which zoobenthos in Scottish lochs is suggested to deteriorate (CSTT, 1997; Tett et al., 2008). Another study from the

oligotrophic eastern Mediterranean Sea investigated the quantitative relationship between benthic macrofaunal communities (macroinvertebrates) and seawater column variables and showed a strong link between pelagic indicators (Chl-a and Eutrophication Index - EI) and various benthic indicators describing macrofaunal diversity (Dimitriou et al., 2015).

To the best of our knowledge, the processes by which water column characteristics and phytobenthic indicators are linked have not been systematically studied. In the eastern Mediterranean, primary producers, such as macroalgae and phytoplankton, generally appear to be more sensitive to nitrogen and particulate matter in seawater, while benthic macroinvertebrate indicators are more sensitive to phosphate in seawater (Simboura et al., 2016). A follow-up study reported that nutrients in seawater and macroalgae are components with a stronger temporal response to mitigation measures taken (Pavlidou et al., 2019). However, how changes in trophic conditions in pelagic habitats may affect the structural and functional traits of macroalgal and angiosperm communities has not been studied in detail.

Based on the analysis of a pooled dataset of sampling sites in three Mediterranean sub-basins (northern Adriatic, eastern Ionian and Aegean Seas) reflecting different trophic conditions, this study aims to improve our understanding of how different benthic and pelagic primary producers are linked under natural and human-induced pressure gradients in coastal ecosystems. To this end, the main objectives of this study were (i) to explore the coupled responses of benthic and pelagic primary producers (macroalgae, angiosperms, and phytoplankton) to eutrophication pressure at large scales, (ii) to examine how different trophic conditions of the pelagic habitat may affect the structural and functional traits of benthic macroalgal and angiosperm communities, and (iii) to investigate which are the key drivers among the various eutrophication-related pelagic indicators (such as nutrient and Chl-a concentrations, water transparency, etc.) that can force the benthic system indicators to low ecological quality levels.

MATERIALS & METHODS

Dataset Description

Three different datasets were used, consisting of samples collected in different scientific and monitoring programmes in different sub-regions of the Mediterranean Sea (northern (N.) Adriatic, Eastern (E.) Ionian and Aegean Seas) (**Figure 1**). The dataset used in the present study includes 65 sampling sites from Greece (25 in the Ionian Sea, 40 in the Aegean Sea) and 26 sampling sites from the Slovenian part of the Gulf of Trieste (N. Adriatic). The dataset is based on a compilation of published data (Orlando-Bonaca et al., 2008; Orlando-Bonaca et al., 2015; Giovanardi et al., 2018; Orlando-Bonaca and Rotter, 2018; Orlando-Bonaca et al., 2019; Gerakaris et al., 2021; Orlando-Bonaca et al., 2021) and unpublished data from the Hellenic Centre of Marine Research and the National Institute of Biology (**Table 1**).

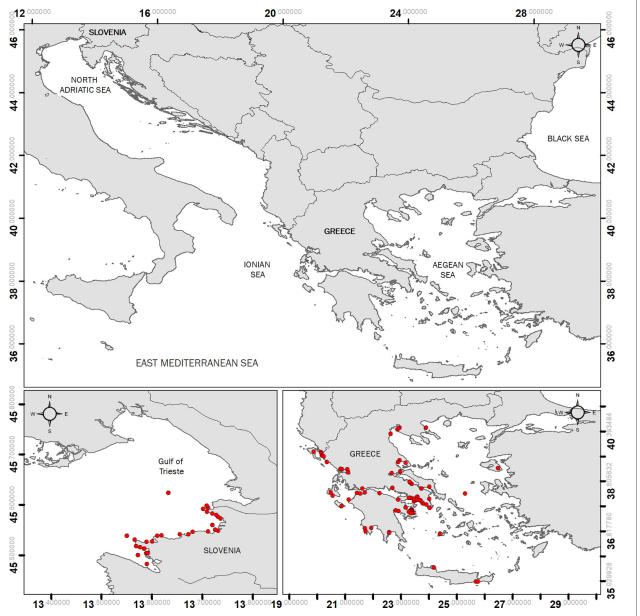

FIGURE 1 | Map of the study area with the three Mediterranean sub-regions (upper panel) and the distribution of the sampling sites on local scale (lower panels).

The dataset for the study of macroalgae was collected in the Greek and Slovenian coastal areas and includes two subsets (**Figure 1**). The first subset includes data (111 observations) collected in the Greek coastal areas, while the second subset (111 observations) is from the Slovenian coastal waters. The dataset for the study of the seagrass *C. nodosa* was collected in the Greek and Slovenian coastal areas and includes two subsets. The first subset includes data (16 observations) collected in the Greek coastal areas, while the second (16 observations) is from the Slovenian coastal waters. The dataset for the study on seagrass *P. oceanica* was collected only in the Greek coastal areas. The dataset includes data (50 observations) from the E. Ionian and the Aegean Seas.

Pelagic Indicators

Pelagic variables (seawater column) and indicators included concentrations of inorganic nutrients (phosphate, nitrate, ammonium), *Chlorophyll-a* (Chl-*a)* and dissolved oxygen (DO), temperature, salinity, pH, and diffuse attenuation coefficient (Kd). Data for the pelagic variables were obtained from the open access data repository Copernicus Marine Environment Monitoring Service (CMEMS). **Table 2** summarizes the pelagic variables studied with the corresponding CMEMS products we used. For each sampling station, in the case of products with a resolution of 0.042° x 0.042°, we used a 3 x 3 km pixel window to estimate the mean values of the variables studied and then calculate the annual mean values or the means for the previous three months (see also Data analysis below). For Kd and Chl-a products with 1 km resolution, an 11 x 11 km pixel window was used to keep the same study region (pixel area) for all variables. Experiments with pixel

TABLE 1 | List of benthic and pelagic indicators and variables used in the study.

Pelagic variables and indicators		Benthic variables and indicators	
Temperature	**Chl-a**	**Macroalgae**	**Biotic Indices**
Salinity	Concentrations in seawater	Species composition	EEI-c
pH			(Orfanidis et al., 2011)
Dissolved Oxygen (DO)		***Cymodocea nodosa***	Cymoskew
Kd		Leaf length	(Orfanidis et al., 2020)
Phosphate		Leaf length skewness	Mediskew
Nitrate			(Orlando-Bonaca et al., 2015)
Ammonium		***Posidonia oceanica***	PREI
		Lower Limit depth,	(Gobert et al., 2009)
		Lower Limit type,	
		Shoot density,	
		Shoot Leaf Surface, Epiphytic/Leaf Biomass	

windows smaller than 11 x 11 km, such as 5 x 5 km, yielded similar results for Kd and Chl-a products.

Pelagic variables from the Slovenian dataset were obtained during the National Monitoring Program campaigns from 2007 to 2020. Seawater samples for Chl-a and nutrients were collected monthly using Niskin bottles, while *temperature*, *salinity* and *dissolved oxygen* concentration were obtained using a CTD probe (Sea & Sun Technology GmbH, Germany). Chl-a concentrations were analyzed fluorimetrically with a Turner Designs Trilogy fluorimeter (Holm-Hansen et al., 1965). For the period 2007 - 2013, concentrations of inorganic nutrients were measured using standard colorimetric methods (Grasshoff et al., 1999). For the period 2014 - 2020, nutrient concentrations were determined spectrophotometrically using the QuAAtro autoanalyzer (Seal Analytical).

Benthic Indicators

A suite of indicators was selected for the benthic ecosystem to assess the status of coastal waters using macroalgae and seagrasses (*C. nodosa* and *P. oceanica*).

The Ecological Evaluation Index continuous formula (EEI-c) provides information on the response of benthic macrophytes to anthropogenic pressures (Orfanidis et al., 2011). This method divides macrophyte taxa into two Ecological State Groups (ESGs). ESG I includes thick perennial (IA), thick plastic (IB) and shade-adapted plastic (IC) species in coastal waters and angiosperm plastic (IA), thick plastic (IB) and shade-adapted plastic (IC) species in transitional waters. ESG II includes fleshy opportunistic (IIB) and filamentous leafy opportunistic (IIA) species in both coastal and transitional waters (Orfanidis et al., 2011). The relative abundance (%) of opportunistic species was also examined.

Two indices were used to assess the status of *C. nodosa* meadows: CymoSkew for the assessment of the data from the E. Ionian and the Aegean Sea and MediSkew for the data from the N. Adriatic Sea. The CymoSkew index is a quantitative expression of photosynthetic leaf length asymmetry of *C. nodosa* used as an index of early warning response (Orfanidis et al., 2010; Orfanidis et al., 2020) and calibrated against the anthropogenic stress index MA-LUSI (Papathanasiou and Orfanidis, 2018). The MediSkew index is a combination of two metrics, both based on *C. nodosa* leaf length: Deviation from the reference median length (Medi-) and Skewness of length-frequency distribution (-Skew), with greater importance given to the first, and was calibrated with a Pressure Index for Seagrass Meadows (Orlando-Bonaca et al., 2015). Median Leaf length of *C. nodosa* was used as an additional metric in the analysis.

The PREI (*Posidonia oceanica* Rapid Easy Index) is a multimetric index based on the integration of five individual metrics of *P. oceanica*: Shoot density, Shoot leaf surface, Epiphytic biomass/Leaf biomass ratio, Depth of Lower Limit, and type of the Lower Limit (Gobert et al., 2009). The *P. oceanica* metrics (indicators) used in the PREI index provide information on the vitality of the meadow (at the individual and population level) for a wide range of disturbances, including light deprivation, nutrient concentrations, and eutrophication (Gobert et al., 2009; Martínez-Crego et al., 2010).

Ecological quality ratio (EQR) values were calculated for the EEI-c, Cymoskew, Mediskew, and PREI biotic indices and used in the analyses. EQR values for all of these indices range from 0 for worst status to 1 for the best status. For the *C. nodosa* dataset (hereafter referred to as *CymodoceaEQR*), EQR values for the E. Ionian and Aegean Seas were calculated following the conversion formula of Orfanidis et al. (2020), while the equation EQR = 1 –

TABLE 2 | The collected CMEMS products for the pelagic variables, with the temporal and spatial resolutions of each product.

CMEMS Product	Temporal Resolution	Spatial Resolution	Pelagic Variable(s)
OCEANCOLOUR_MED_OPTICS_L3_REP_OBSERVATIONS_009_095	Daily	1 km	Diffuse attenuation coefficient (Kd)
OCEANCOLOUR_MED_CHL_L4_REP_OBSERVATIONS_009_078	Monthly	1 km	Chlorophyll-a
MEDSEA_MULTIYEAR_BGC_006_008	Monthly	0.042°x 0.042°	Phosphate, Nitrate, Ammonium, Oxygen, pH
MEDSEA_MULTIYEAR_PHY_006_004	Monthly	0.042°x 0.042°	Salinity, Temperature

MediSkew was used for the N. Adriatic data (Orlando-Bonaca et al., 2015).

Data Analysis

Prior to statistical analyses, all pelagic variables were averaged for the three months preceding the sampling of macroalgae and seagrass *C. nodosa*, while annual means were used for P. *oceanica*.

Multivariate analysis was performed in the R Environment (R Core Team, 2021). Prior to analysis, data were tested for normality using the shapiro.test() function. If normality was not achieved, the bestNormalize() function was used to find the best transformation of the data. The Kaiser–Meyer–Olkin measure (KMO) checked the sampling adequacy for the analysis. All KMO values for each item were > 0.70, which is well above the acceptable threshold of 0.6. Principal Component Analysis (PCA) was performed for both benthic and pelagic indicators and variables to check for the presence of common patterns. Prior to ordination, a Kendall's Tau correlation coefficient matrix was created between benthic and pelagic indicators and variables to highlight parameters with high and statistically significant correlation. All plots were created using the package "ggplot2" (Wickham, 2016).

RESULTS

Macroalgae Indicators vs Pelagic Indicators

When benthic and pelagic variables and indicators were considered for the macroalgae dataset (**Table 3**), significant negative correlations ($p < 0.01$) were found between the benthic index EEI-c and the pelagic eutrophication variables of nutrients (phosphate, nitrate), Chl-a and oxygen, according to Kendall's Tau correlation coefficient. The abundance of opportunistic species (%) of macroalgae showed a strong negative correlation with EEI-c and a positive correlation with Chl-a, phosphate, ammonium and pH. Chl-a was significantly correlated with all other pelagic variables ($p < 0.01$), negatively with temperature and salinity, and positively with nutrients, oxygen, and pH.

Principal component analysis (PCA) of the pelagic variables and benthic indicators EEI-c and Opportunistic Species (%) considered for the macroalgae dataset revealed two significant principal components (PCs; i.e., eigenvalues>1) that together account for 68.3% (PCA for EEI-c) and 66.8% (PCA for Opportunistic Species %) of the total variance in the dataset (**Table 4**). This is due to the fact that all other pelagic indicators (with the exception of ammonium) have strong loadings (>0.70) that fall under these two components.

Looking at the EEI-c index, the studied macroalgal sites can be divided into two major clusters (ordination biplot, **Figure 2A**): the cluster of sites in N. Adriatic Sea, which is mainly located in the positive part of PC1, and the cluster of sites in the E. Aegean and Ionian Seas, which is mainly located in the negative part of PC1. The Aegean - Ionian Sea cluster is better associated with increasing trends of EEI-c, salinity and temperature towards the negative PC1. In contrast, most of the N. Adriatic cluster is better associated with increasing trends of Chl-a, nutrients (phosphate, nitrate, ammonium), oxygen, and pH on the positive PC1. EEI-c contributed similarly to both PCs (see **Table 4** for PC1 and PC2), while pointing in the opposite direction to the pelagic eutrophication indicators (Chl-a, nutrients, and oxygen).

When considering Opportunistic Species (%), the studied sites are divided into the same two clusters (ordination biplot, **Figure 2B**) already highlighted for EEI-c. Furthermore, the vectors of pelagic indicators and variables showed a very similar ordination and trend as the PCA biplot for EEI-c; however, the vector of Opportunistic Species (%) is reversely ordinated. Opportunistic Species (%) seemed to be mainly associated with nutrients and pH.

Cymodocea nodosa Indicators vs Pelagic Indicators

The results of Kendall's Tau correlation coefficient calculated between pelagic and benthic indicators for the *C. nodosa* dataset (**Table 5**) showed a significant negative correlation ($p < 0.01$ and $p < 0.05$) between CymodoceaEQR and Leaf Length. Among all pelagic variables, Leaf Length values are significantly correlated only with nitrate, while CymodoceaEQR is not correlated with any pelagic variable. Chl-a is significantly correlated with all pelagic variables and showed strong positive correlations with phosphate, Kd, pH and a strong negative correlation with salinity.

TABLE 3 | Kendall's Tau correlation coefficient matrix between pelagic and benthic indicators and variables for macroalgae dataset.

	EEI-c	% Op. Species	Chl-a	Phosphate	Nitrate	Ammonium	Temperature	Salinity	Oxygen	pH
EEI-c	1									
% Op. Species	-0.332**	1								
Chl-a	-0.257**	0.160**	1							
Phosphate	-0.138**	0.145**	0.404**	1						
Nitrate	-0.207**	ns	0.270**	0.601**	1					
Ammonium	ns	0.109*	0.142**	0.484**	0.274**	1				
Temperature	0.266**	ns	-0.290**	-0.164**	-0.365**	ns	1			
Salinity	ns	ns	-0.498**	-0.411**	-0.241**	-0.323**	ns	1		
Oxygen	-0.218**	ns	0.233**	0.124*	0.324**	-0.105*	-0.636**	-0.093*	1	
pH	-0.172**	0.126**	0.583**	0.401**	0.369**	0.179**	-0.414**	-0.510**	0.366**	1

$^{**}p < 0.01$, $^{*}p < 0.05$.
ns, non significant.

TABLE 4 | Results of the PCA applied on pelagic and benthic indicators for macroalgae (EEI-c as EQR and % Opportunistic species).

Principal components	Eigenvalues	% Variance Explained	Cum. % Variance
1	4.21	46.83	46.83
2	1.93	21.47	68.30
3	0.86	9.54	77.84
4	0.80	8.89	86.73
5	0.48	5.29	92.02
Eigenvectors			
Variable	**PC1**	**PC2**	**PC3**
EEI-c	-0.446	0.314	0.602
Chl-a	0.830	0.091	0.230
Phosphate	0.765	0.313	-0.284
Nitrate	0.794	0.008	-0.143
Ammonium	0.594	0.461	-0.314
Temperature	-0.478	0.827	-0.028
Salinity	-0.738	-0.540	-0.264
Oxygen	0.548	-0.731	0.093
pH	0.828	-0.069	0.405

Principal components	Eigenvalues	% Variance Explained	Cum. % Variance
1	4.13	45.89	45.89
2	1.89	20.95	66.84
3	0.96	10.66	77.50
4	0.81	8.95	86.45
5	0.47	5.25	91.70
Eigenvectors			
Variable	**PC1**	**PC2**	**PC3**
% Opp.Species	0.307	0.173	0.869
Chl-a	0.831	0.059	0.166
Phosphate	0.776	0.275	-0.162
Nitrate	0.791	-0.064	-0.286
Ammonium	0.613	0.429	-0.185
Temperature	-0.435	0.853	-0.068
Salinity	-0.770	-0.469	0.068
Oxygen	0.511	-0.789	-0.071
pH	0.835	-0.136	0.144

Principal component analysis (PCA) of the pelagic variables and benthic indicator CymodoceaEQR, considered for the *C. nodosa* dataset, revealed three significant principal components (PCs; i.e., eigenvalues>1) that together account for 80.6% of the total variance in the dataset; with PC1 and PC2 accounting for > 65% of the total variance (**Table 6**). This is because 75% of the pelagic indicators analyzed have a strong loading (> 0.75) that falls under these two components.

The studied sites are divided into three clusters (ordination biplot, **Figure 3**). Cluster 1, on the negative part of PC1, is characterized mainly by higher values of temperature and salinity, while cluster 2, on the positive part of PC1, is characterized by higher values of pelagic eutrophication indicators (nutrients, Chl-a, Kd) and pH. Cluster 3, formed remotely from some sites in the Aegean Sea on the positive part of PC2, is characterized by higher oxygen values.

Attempting to elucidate further this clustering, the Ecological Status (ES) of the studied sites, as assessed by the biotic indices CymoSkew and MediSkew and expressed as CymodoceaEQR was introduced to the ordination biplot (**Figure 4**). The sites in the positive part of PC2 have lower CymodoceaEQR values (i.e., poor, bad and most moderate ES), while the remaining sites in the negative part of PC2 have higher CymodoceaEQR values (high and good ES).

Posidonia oceanica Indicators vs Pelagic Indicators

The results of Kendall's Tau correlation coefficients calculated between pelagic and benthic indicators for the *P. oceanica* dataset (**Table 7**) show significant correlations ($p < 0.01$ and $p < 0.05$) between Chl-a and LL depth and most pelagic indicators and variables. The PREI index is positively correlated with all *P. oceanica* metrics (except E/L Biomass) and nitrate while negatively correlated with Chl-a and Kd. As for nutrients, Chl-a showed a strong negative correlation with phosphate and nitrate but a non-significant correlation with ammonium. Kd and Chl-a showed a strong positive correlation as expected, because suspended particulate matter, including phytoplankton, contributes to high Kd.

Principal component analysis (PCA) of the pelagic and benthic indicators considered for the *P. oceanica* dataset revealed three significant principal components (PCs; i.e., eigenvalues>1) that together account for 90.5% (PCA for PREI) and 79% (PCA for *P. oceanica* metrics-indicators) of the total variance in the dataset; with PC1 and PC2 accounting for > 60% of the total variance (**Table 8**). This is due to the fact that > 80% of the analyzed pelagic indicators have strong loadings (>0.5) that fall under these two components.

Looking at the *P. oceanica* metrics, the studied sites can be divided into three clusters (ordination biplot, **Figure 5A**). Cluster 1, in the positive part of PC1, is characterized by high values for nutrients, temperature, salinity, oxygen, pH, Kd, Chl-a, and E/L Biomass and low values for Shoot density. Cluster 2, in the negative part of PC2, is characterized by high values for Chl-a, Kd, and Leaf Surface and low values for nutrients, LL Depth, LL type, and Shoot density. Cluster 3, in the negative part of PC1, is characterized by high values for Shoot density, LL Depth, LL type and low values for Kd, oxygen, Chl-a, pH, salinity, temperature, E/L Biomass, Leaf Surface and ammonium.

Focusing on the PREI index, the studied sites can also be divided into three clusters, with the total explained variance increasing to 77.3% (ordination biplot, **Figure 5B**). Cluster 1, in the negative part of PC1, is characterized by high values for PREI and low values for Chl-a, Kd, oxygen, pH, salinity, temperature, and ammonium. Cluster 2, in the positive part of PC1, is characterized by high values for nutrients, temperature, salinity, oxygen, pH, Kd, and Chl-a, and low values for PREI. Cluster 3, in the negative part of PC2, is characterized by high values for Chl-a, and Kd, and low values for nutrients.

DISCUSSION

Pelagic (phytoplankton) and benthic communities (macroalgae and angiosperms) are considered robust bioindicators that efficiently reflect natural and human-induced pressures in the coastal marine ecosystem (Orfanidis et al., 2007; Orlando-

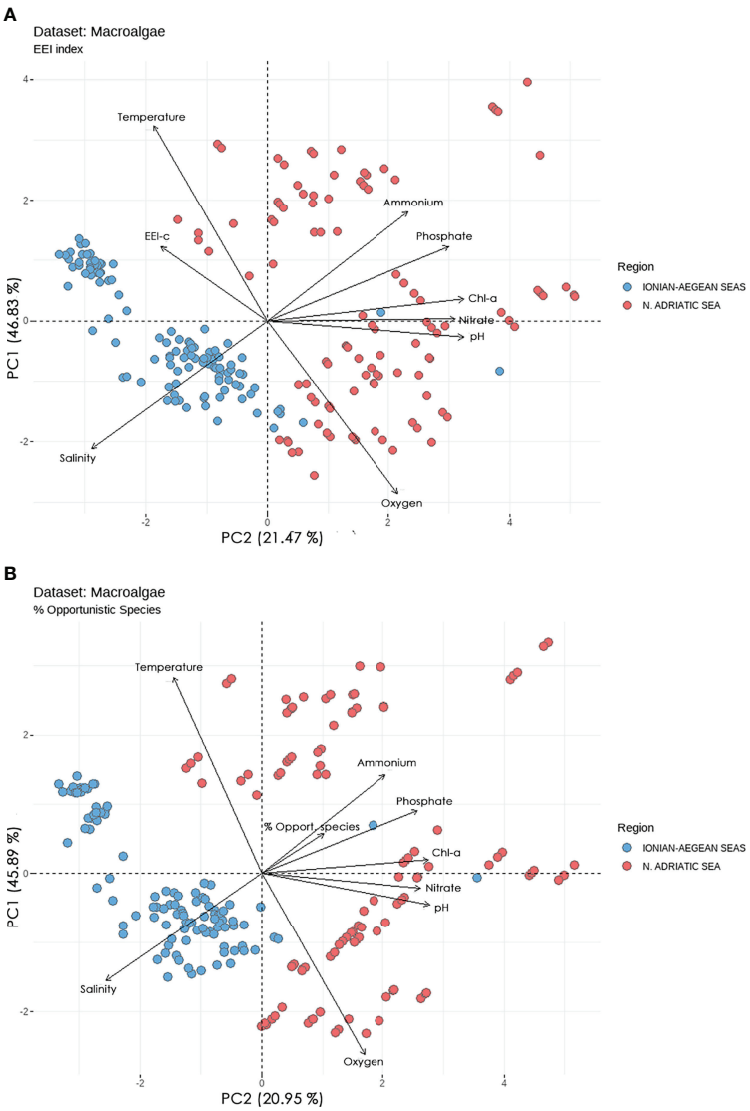

FIGURE 2 | Principal component analysis (PCA) biplots of studied sites and pelagic and benthic indicators **(A)** EEI-c index, and **(B)** Opportunistic Species (%). The biplot shows the PCA scores of the indicators as vectors (in black) and sites as circles (blue circles = Ionian-Aegean seas, red circles = N. Adriatic Sea).

TABLE 5 | Kendall's Tau correlation matrix between the benthic and pelagic indicators from the *Cymodocea nodosa* dataset.

	CymodoceaEQR	Leaf Length	Chl-a	Phosphate	Nitrate	Ammonium	Oxygen	Temperature	Salinity	pH	Kd
CymodoceaEQR	1										
Leaf Length	-0.397**	1									
Chl-a	ns	ns	1								
Phosphate	ns	ns	0.475**	1							
Nitrate	ns	-0.273*	ns	0.365**	1						
Ammonium	ns	ns	0.276*	0.348**	0.680**	1					
Oxygen	ns	ns	0.259*	ns	-0.270*	ns	1				
Temperature	ns	ns	-0.251*	ns	-0.402**	-0.459**	ns	1			
Salinity	ns	ns	-0.432**	-0.453**	-0.402**	-0.525**	ns	0.311*	1		
pH	ns	ns	0.504**	0.297*	0.457**	0.506**	ns	-0.296*	-0.708**	1	
Kd	ns	ns	0.625**	0.509**	ns	ns	0.266*	ns	-0.490**	0.488**	1

$^{**}p < 0.01$, $^{*}p < 0.05$.
ns, non significant.

TABLE 6 | Results of the PCA applied on pelagic and benthic indicators for *C. nodosa* (EQR, and median Leaf Length).

Principal components	Eigenvalues	% Variance Explained	Cum. % Variance
1	5.04	45.82	45.82
2	2.38	21.59	67.41
3	1.46	13.24	80.65
4	0.66	5.96	86.61
5	0.52	4.73	91.35
Eigenvectors			
Variable	**PC1**	**PC2**	**PC3**
CymodoceaEQR	0.175	-0.558	0.619
Leaf Length	-0.321	0.550	-0.530
Chl-a	0.778	0.481	0.124
Phosphate	0.568	0.496	0.487
Nitrate	0.754	-0.545	-0.104
Ammonium	0.822	-0.314	-0.333
Oxygen	0.049	0.810	0.072
Temperature	-0.600	0.041	0.597
Salinity	-0.925	0.012	-0.075
pH	0.921	-0.108	-0.158
Kd	0.818	0.467	0.159

Bonaca et al., 2008; Orfanidis et al., 2010; Orfanidis et al, 2011; Orlando-Bonaca et al., 2015; Varkitzi et al., 2018a; Rombouts et al., 2019; Orfanidis et al., 2020; Orlando-Bonaca et al., 2021); however, their response to stressors is related to their structural complexity and specificity (e.g., Adams and Greeley, 2000). To this end, much of the research has focused on the biology and ecology of pelagic and benthic primary producers and their responses to different stressors or impacts at different scales (physiology, population dynamics, community composition trends).

Relationships between benthic and pelagic primary producers are mainly associated with competition for light and nutrients in relatively shallow coastal ecosystems (Krause-Jensen et al., 2012; Orfanidis et al., 2020). Phytoplankton can take advantage of favorable light conditions in the upper water layers but is exposed to unstable nutrient supply, while benthic vegetation can benefit from the vast reservoir of nutrients in the sediment but is often light-limited (e.g., Duarte, 1991; Cloern et al., 2014). Excessive nutrient enrichment in the pelagic habitat stimulates rapid growth of phytoplankton and opportunistic macroalgae at the expense of seagrasses and perennial macroalgae, which are eventually eliminated by increasing light attenuation (i.e., shading) and other eutrophication effects such as hypoxia and anoxia (e.g., Valiela et al., 1992; Harlin, 1995; Schramm and Nienhuis, 1996; McGlathery et al., 2007).

Correlations between benthic primary producers and pelagic pressure indicators (nutrients) almost consistently show that the link between these stressors and the benthic community of primary producers is challenging to demonstrate. The data pooling conducted in this study was

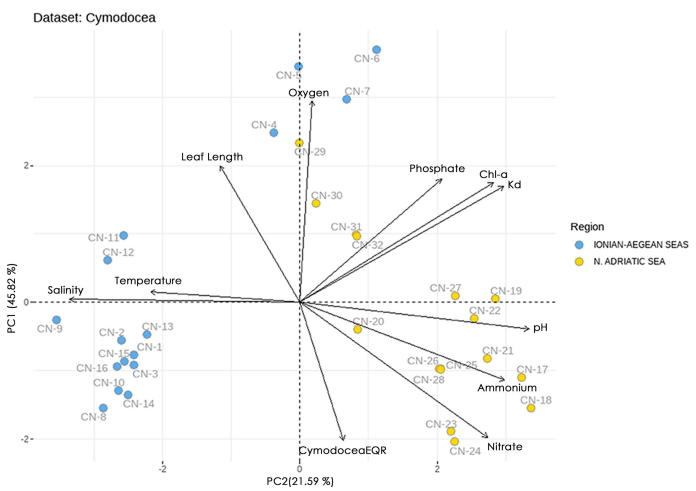

FIGURE 3 | Principal component analysis (PCA) biplots of studied sites and pelagic and benthic indicators for *C. nodosa* dataset. The biplot shows the PCA scores of the indicators as vectors (in black) and sites (blue circles = Ionian-Aegean seas, yellow circles = N. Adriatic Sea).

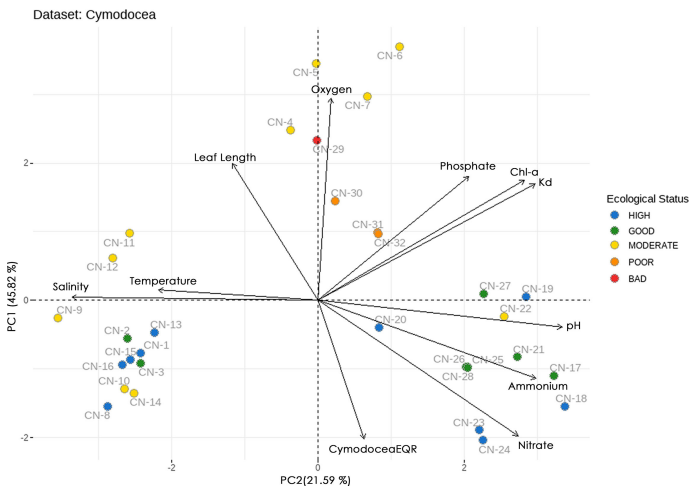

FIGURE 4 | Principal component analysis (PCA) biplots of studied sites and pelagic and benthic indicators for *C. nodosa* dataset. The biplot shows the PCA scores of the indicators as vectors (in black) and sites (coloured based on their ecological status assessment).

designed to improve our understanding of the effects of stressors and to facilitate the interpretation of the linkages between benthic and pelagic primary producers under complex natural and human-induced pressure gradients in the coastal ecosystems of three Mediterranean sub-basins (N. Adriatic, E. Ionian, and Aegean Seas). According to our results, Chlorophyll a (Chl-a) was significantly correlated with all other pelagic variables, such as nutrients, oxygen, pH, temperature and salinity, in all analyzed datasets for macroalgae and seagrass (*C. nodosa*, *P. oceanica*) indicators in all studied coastal waters. Apart from the fact that Chl-a measurements are simple, reproducible and time- and cost-effective, and the results are easily comparable, ensuring high data availability (Domingues et al., 2008), there is also a well-documented pressure-impact relationship between nutrient enrichment and response of phytoplankton biomass (e.g., Håkanson and Eklund 2010; Giovanardi et al., 2018). In contrast, the relationship between pressures and phytoplankton biodiversity parameters is much looser and often masked by the high complexity and dynamics of phytoplankton assemblages (Rombouts et al., 2019).

In addition to the effects of high nutrient loads on the phytoplankton community, our results also show that increased nutrient concentrations in seawater have a similar effect on the macroalgal community. Indeed, our analysis revealed that increasing nutrient levels lead to increased coverage of opportunistic macroalgal species at the expense of canopy-forming species, as previously suggested (Orfanidis et al., 2011; Orlando-Bonaca and Rotter, 2018). Opportunistic species (characterized by Orfanidis et al. (2011) as ESG II: species with high growth rates and short life history) were found to be significantly associated with eutrophication indicators (e.g., Chl-a, phosphate, ammonium), confirming that anthropogenic pressure shifts the ecosystem from a pristine state, where late-successional species (such as Cystoseira s.l. spp.) predominate, to a degraded state, where opportunistic, nitrophilous species are dominant (Orfanidis et al., 2001; Orfanidis et al., 2011). Given the above results, it is not surprising that opportunistic macroalgal species were negatively correlated with EEI-c values. Since the EEI-c index was developed to assess the impact of chronic pressures such as eutrophication and organic matter pollution (Orfanidis et al., 2001; Orfanidis et al., 2011), the significant negative correlation between this index, nutrients and Chl-a further confirms these properties of the EEI-c.

The regulating effect of light availability on the growth and depth distribution of the *P. oceanica* meadows studied is further supported by our results. Indeed, the clusters of sites with meadows that share higher shoot densities, LL depths, and LL type (i.e., progressive limit) show higher values of PREI index, i.e., better ecological status. In contrast, the clusters of sites with meadows that have higher values of E/L Biomass (the case of epiphytes overgrowth due to nutrient enrichment), Shoot Leaf Surface (leaves elongation as an acclimation response), along with higher values of light attenuation coefficient Kd, Chl-a, and nutrients, show lower ecological status.

As with all seagrass species, light is considered the most critical factor in regulating the distribution and growth dynamics of *P. oceanica* meadows (Ralph et al., 2007; Gerakaris et al., 2021). Fluctuations in light attenuation in the coastal marine environment due to direct (e.g., high turbidity due to abiotic and biotic factors) or indirect causes (e.g., shading by epiphytes/macroalgal overgrowth due to nutrient enrichment) results in specific photoadaptive physiological and morphological responses (e.g., elongation of leaves, thinning of shoot density, reduction in depth distribution, e.g., Greve and Binzer, 2004).

The *P. oceanica* metrics (indicators) considered in this study are the same as metrics used in the PREI index. Therefore, it is not surprising that both the PREI and the other metrics share

TABLE 7 | Kendall's Tau correlation matrix between the benthic and pelagic indicators for *P. oceanica* dataset.

	LL Depth	LL type	Shoot Density	Leaf Surface	E/L Biomass	PREI	Chl-a	Phosphate	Nitrate	Ammonium	Oxygen	Temperature	Salinity	pH	Kd
LL Depth	1														
LL Type	0.559**	1													
Shoot density	0.394**	0.448**	1												
Leaf Surface	ns	ns	ns	1											
E/L Biomass	ns	-0.254*	ns	ns	1										
PREI	0.616**	0.684**	0.607**	0.206*	ns	1									
Chl-a	-0.551**	-0.274*	-0.348**	ns	ns	-0.392**	1								
Phosphate	0.314**	ns	ns	ns	ns	ns	-0.325**	1							
Nitrate	0.369**	ns	0.218*	ns	ns	0.200*	-0.414**	0.553**	1						
Ammonium	ns	ns	ns	ns	ns	ns	ns	0.397**	0.537**	1					
Oxygen	-0.205*	ns	ns	ns	ns	ns	0.488**	ns	-0.319**	ns	1				
Temperature	-0.203*	ns	ns	ns	ns	ns	ns	-0.324**	ns	ns	-0.418**	1			
Salinity	ns	ns	ns	ns	ns	ns	-0.219*	ns	ns	ns	-0.544**	0.587**	1		
pH	ns	ns	ns	ns	ns	ns	0.377**	ns	ns	0.231*	0.683**	-0.542**	-0.617**	1	
Kd	-0.610**	-0.347**	-0.331**	ns	ns	-0.427**	0.870**	-0.262*	-0.381**	ns	0.478**	ns	ns	0.426**	1

*$p < 0.01$, *$p < 0.05$.
ns, non significant.

common patterns of variation when examined in the context of the pelagic indicators. In fact, all *P. oceanica* indicators exhibited the expected covariance (positive or negative depending on the indicator) with the pelagic indicators examined and adequately reflected the increasing magnitude of human-induced pressures. This is particularly evident with increasing levels of the pressure indicators, such as ammonium, nitrate, phosphate, Chl-a and Kd, along which the *P. oceanica* indicators (PREI, Shoot density, LL depth and LL type) show the opposite trend of decreasing values.

Cymodocea nodosa is a perennial leaf self-shading species with high light requirements (Kenworthy and Fonseca, 1996; Sand-Jensen and Borum, 1991), which, as with most seagrass species, are much higher than those of macroalgae and phytoplankton (Duarte, 1991). Indeed, seagrasses exhibit photoadaptive responses under light-deficient conditions that vary widely among seagrass taxa (Ralph et al., 2007). Our results show that increasing Leaf Length values of *C. nodosa* are closely associated with higher turbidity levels (expressed as Kd), which could be due to higher phytoplankton biomass (expressed as Chl-a). This implies that photoacclimation of the studied *C. nodosa* populations is expressed with increasing leaf size to maximize the amount of captured light (Goldberg, 1996; Touchette and Burkholder, 2000; Lee et al., 2007; Orfanidis et al., 2020). The fact that CymodoceaEQR values were correlated only with Leaf Length values (negative correlation) and with none of the pelagic variables examined suggests that CymodoceaEQR responses to such pelagic stressors are not straightforward. However, PCA showed that low CymodoceaEQR were associated with increasing trends in pelagic eutrophication indicators (phosphate, Chl-a, and Kd), highlighting them as significant drivers that may force *C. nodosa* benthic system indicators to deteriorate in ecological quality. Moreover, the observed negative correlation between Leaf Length and nitrate concentration suggests that in our case, the increased productivity and biomass of *C. nodosa* leaves are not the linear result of nutrient enrichment (Lee et al., 2007).

Cymodocea nodosa thrives in highly variable environments that receive fresh water and nutrient pulses. However, the increased amounts of nutrients in the water column are not taken up by *C. nodosa* directly, but are trapped in sedimented particulate matter and become available to angiosperms when released in sediment pore water (Tyerman, 1989; Hemminga and Duarte, 2000). Other factors are also known to have important effects on the health of *C. nodosa* meadows. High sedimentation and resuspension rates (both natural and due to anthropogenic activities) are known to limit light availability and are among the main factors leading to longer seagrass leaves and lower ecological status (Orlando-Bonaca et al., 2015).

Another interesting result of the analyses of the *C. nodosa* dataset was the formation of a distinct group with sites in the Aegean associated with higher oxygen levels. These sampling sites are located close to Thermaikos Gulf (N. Aegean Sea), an area with direct influence of oxygen-rich freshwater inputs from five rivers, well-documented eutrophication problems, and frequent harmful algal blooms (Pagou, 2005; Ignatiades and Gotsis-Skretas, 2010; Varkitzi et al., 2013).

TABLE 8 | Results of the PCA applied on pelagic and benthic seagrass indicators (*P. oceanica* metrics, and PREI, respectively).

Principal components	Eigenvalues	% Variance Explained	Cum. % Variance	Principal components	Eigenvalues	% Variance Explained	Cum. % Variance
1	6.16	44.02	44.02	1	5.51	55.12	55.12
2	2.69	19.24	63.26	2	2.22	22.17	77.29
3	2.21	15.78	79.04	3	1.32	13.17	90.46
4	1.14	8.16	87.20	4	0.58	5.80	96.26
5	0.82	5.84	93.04	5	0.25	2.50	98.76
Eigenvectors				**Eigenvectors**			
Variable	**PC1**	**PC2**	**PC3**	**Variable**	**PC1**	**PC2**	**PC3**
LL Depth	0.042	0.632	0.668	***PREI***	-0.633	0.335	-0.329
LL Type	-0.064	0.302	0.797	Chl-a	0.628	-0.448	0.579
Shoot density	-0.838	0.361	-0.023	Phosphate	0.410	0.752	0.179
Leaf Surface	0.190	-0.662	-0.300	Nitrate	0.181	0.916	0.146
E/L Biomass	0.595	0.272	-0.493	Ammonium	0.618	0.595	0.414
Chl-a	0.581	-0.505	-0.032	Temperature	0.911	-0.011	-0.400
Phosphate	0.443	0.623	-0.322	Salinity	0.921	0.010	-0.389
Nitrate	0.214	0.753	-0.501	Oxygen	0.959	-0.048	-0.261
Ammonium	0.628	0.411	-0.460	pH	0.951	-0.002	-0.305
Oxygen	0.913	0.049	0.248	Kd	0.795	-0.378	0.420
Temperature	0.927	0.071	0.244				
Salinity	0.960	0.007	0.234				
pH	0.955	0.052	0.225				
Kd	0.750	-0.414	0.027				

The sampling sites in the Aegean and Ionian Seas were distributed mainly on the positive side of the vectors for salinity and temperature, while the sampling sites in the N. Adriatic were mainly distributed around the positive sides of the vectors for the pelagic eutrophication indicators (Chl-a, nutrients, Kd). On this basis, a clear distribution pattern emerged with two distinct groups of sampling sites in the N. Adriatic and the Ionian-Aegean, which persisted for three of the benthic indicators EEI-c, Cymoskew and Mediskew (expressed as CymodoceaEQR). We hypothesize that these trends are driven by the characteristics and trophic conditions of the N. Adriatic Sea, which is colder, less saline and has higher nutrient inputs from rivers and higher concentrations of Chl-a (Brush et al., 2021; Zhang et al., 2021) compared to the waters of the Ionian-Aegean (Pavlidou et al., 2015; Varkitzi et al., 2018b; Varkitzi et al., 2020). As we move from the N. Adriatic to the Ionian and Aegean waters, this decreasing trophic gradient in pelagic habitats is well coupled with the responses and sensitivity of the benthic indices EEI-c, Cymoskew, and Mediskew in our dataset analyses.

In the N. Adriatic, the relationship between phytoplankton biomass and nutrients is evidenced by the process of oligotrophication observed from the beginning of this century onwards (Mozetič et al., 2010; Brush et al., 2021). Persistent low trophic conditions have been associated with a nutrient imbalance in the N. Adriatic, particularly due to severely reduced phosphate concentrations in the coastal waters of the N. Adriatic (Grilli et al., 2020). Nonetheless, there is recent evidence of a reversal in the trend toward increasing Chl-a at the southern edge of the N. Adriatic (Grilli et al., 2020). The decline in the trophic status of the Gulf of Trieste, the study area of the N. Adriatic, is reflected not only in the decrease in phytoplankton biomass but also in the increasing dominance of the nano- and picoplankton size classes (Flander-Putrle et al., 2022). However, while Chl-a concentrations in the Gulf of Trieste remain low nowadays, macroalgae have shown signs of deterioration (Orlando-Bonaca et al., 2021).

Despite the typical oligotrophic conditions in the waters of the Aegean and Ionian Seas, some coastal areas are hot spots of eutrophication, such as the well-studied Saronikos Gulf in the Aegean Sea. Thanks to the operation of a wastewater treatment plant for almost three decades, dissolved inorganic nitrogen and soluble reactive phosphorus loads in the waters of Saronikos Gulf have decreased, leading to an improvement in trophic status in the pelagic habitat (Pavlidou et al., 2019). Long-term data analyses have shown that the response of macroalgal communities to this improvement is the reduction in percent coverage of nitrophilous algae (Tsiamis et al., 2013). In addition, other studies indicate that macroalgae exhibit high divergence in status assessment relative to overall status resulting from different integration methods due to high spatial and temporal variability and localized pressures on rocky shores (Simboura et al., 2015).

The response of primary producers in the pelagic and benthic habitats of the study areas to eutrophication parameters is consistent with the findings of Elser et al. (2007), who conducted a large-scale meta-analysis of the response of primary producers to nutrient enrichment. On the global scale, phytoplankton responds most strongly to nutrient enrichment of marine environments, followed by hard-bottom macroalgae, while soft-bottom seagrasses show the weakest response to the enrichment (Elser et al., 2007). Our study shows that the coupling of pelagic and benthic primary producers across trophic gradients exhibits consistent patterns at the subregional scale.

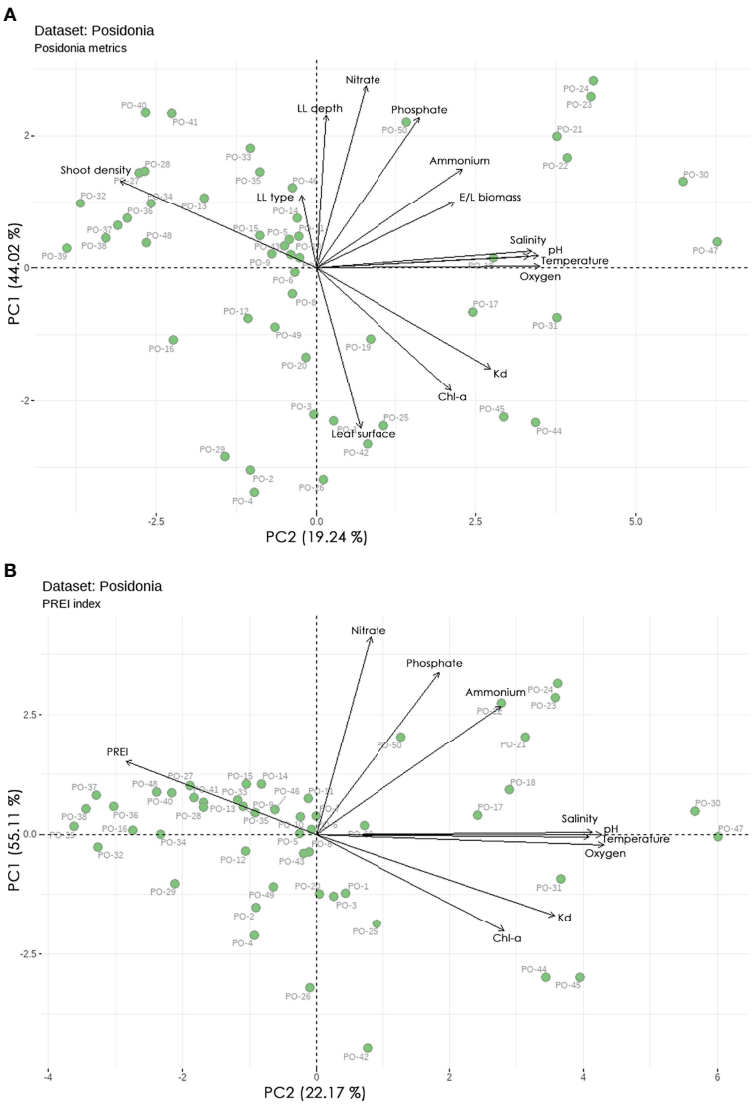

FIGURE 5 | Principal component analysis (PCA) biplot of studied sites and pelagic and benthic indicators **(A)** *P. oceanica* metrics, and **(B)** PREI index. The biplot shows the PCA scores of the indicators as vectors (in black) and sites (green circles).

CONCLUSIONS

Based on the outcomes of the present study, the responses of phytoplankton and macroalgal primary producers were coupled against all or most pelagic stressors/drivers. It is well known that phytoplankton is closely linked to water column turnovers. However, macroalgal communities may also include species that respond rapidly to nutrient inputs or other drivers in the pelagic habitat. Responses of *P. oceanica* traits to some of the pelagic drivers were coupled with the responses of phytoplankton, whereas the responses of *C. nodosa* traits were more loose. The relations between benthic primary producers and pelagic pressure indicators (nutrients) almost consistently indicate that it is difficult to demonstrate the link between these stressors and the benthic primary producers. The reasons for this may be multiple. Angiosperms do not respond directly to the availability of nutrients in the water column since nutrients released from the sediments are a luxurious pool for benthic vegetation (Duarte, 1991). On the other hand, with its shorter response time scales, phytoplankton is better associated with nutrient availability in the water column (Giovanardi et al., 2018). In addition, the documented oligotrophication of formerly nutrient-rich waters in some Mediterranean gulfs, such as the Gulf of Trieste in the N. Adriatic (Mozetič et al., 2010; Mozetič et al., 2012) and the Saronikos Gulf in the Aegean Sea (Tsiamis et al., 2013; Pavlidou et al., 2019), may indicate that the improvement in pelagic trophic status is slowly driving benthic vegetation status to higher levels in the absence of

other pressures. Furthermore, benthic primary producers are sampled near the coast, but rarely are stressors assessed at the same site so close to the coast. Typically, stressors are measured at a distance and then generalized to the entire water body, as in this study. However, all seagrass indicators sampled were closely associated with light attenuation and phytoplankton biomass, confirming the key role of light availability in the distribution and status of benthic primary producers. In the context of EU directives (WFD and MSFD), phytoplankton, macroalgae and marine angiosperms are known to be designed as biological quality elements (BQEs) or indicators that are complementary. Therefore, they can be used in combination to assess the ecological and environmental status (ES) of different marine habitats and processes related to ecological deterioration, thus showing the effects of different pressures and not duplicating the assessment outcomes. Although phytoplankton and macroalgae react to increased nutrient inputs, the impact may be localized and highlighted by only one of the two BQEs (for example, in-shore and off-shore areas). Moreover, the response time is generally different, capturing the deterioration in different time windows, if needed.

DATA AVAILABILITY STATEMENT

The raw data supporting the conclusions of this article will be made available by the authors, without undue reservation.

AUTHOR CONTRIBUTIONS

VG: Conceptualization, Investigation, Data curation, Methodology, Formal analysis, Writing - original draft, Writing - review & editing. IV: Conceptualization, Investigation, Methodology, Formal analysis, Writing - original draft, Writing - review & editing. MO-B: Conceptualization, Investigation, Data curation, Writing - original draft, Writing - review & editing. KK: Satellite data analyses, Writing - original draft, Writing - review & editing. PM: Data curation, Writing - review & editing. PI-L: Data curation, Writing - review & editing. KT: Data curation, Writing - review & editing. JF: Conceptualization, Investigation, Data curation, Writing - original draft, Writing - review & editing. All authors contributed to the article and approved the submitted version.

ACKNOWLEDGMENTS

The authors gratefully acknowledge financial support from the Operational Programme "Competitiveness, Entrepreneurship and Innovation 2014-2020 (EPAnEK)" (MIS 5045792) "DRESSAGE". VG would also like to thank Dr. Yiannis Issaris, and Dr. Maria Salomidi for their assistance during the fieldwork and data collection. IV and KK acknowledge support from the EU Horizon 2020 project "Marine-EO: Bridging Innovative Downstream Earth Observation and Copernicus enabled Services for Integrated maritime environment, surveillance and security" (Grant agreement ID: 730098). MOB, JF and PM gratefully acknowledge financial support from the Slovenian Research Agency (research core funding No. P1-0237), the Slovenian Environment Agency, and the Ministry of Environment and Spatial Planning of the Republic of Slovenia. In addition, MO-B, JF and PM would like to thank all colleagues involved in the fieldwork, laboratory work, and nutrient analyses. The authors would also like to thank the two anonymous reviewers for their constructive comments.

REFERENCES

Abal, E. G., Loneragan, N., Bowen, P., Perry, C. J., Udy, J. W., and Dennison, W. C. (1994). Physiological and Morphological Responses of the Seagrass Zostera Capricorni Aschers, to Light Intensity. *J. Exp. Mar. Biol. Ecol.* 178, 113–129. doi: 10.1016/0022-0981(94)90228-3

Adams, S. M., and Greeley, M. S. (2000). Ecotoxicological Indicators of Water Quality: Using Multi-Response Indicators to Assess the Heath of Aquatic Ecosystems. *Water Air Soil Pollut.* 123, 103–115. doi: 10.1023/A:1005217622959

Ballesteros, E., Torras, X., Pinedo, S., García, M., Mangialajo, L., and de Torres, M. (2007). A New Methodology Based on Littoral Community Cartography Dominated by Macroalgae for the Implementation of the European Water Framework Directive. *Mar. Pollution Bull.* 55, 172–180. doi: 10.1016/j.marpolbul.2006.08.038

Brady, D. C., Testa, J. M., Di Toro, D. M., Boynton, W. R., and Kemp, W. M. (2013). Sediment Flux Modeling: Calibration and Application for Coastal Systems. *Estuar Coast Shelf Sci.* 117, 107–124. doi: 10.1016/j.ecss.2012.11.003

Brush, M. J., Mozetič, P., Francé, J., Bernardi Aubry, F., Djakovac, T., Faganeli, J., et al. (2021). "Phytoplankton Dynamics in a Changing Environment," in *Coastal Ecosystems in Transition: A Comparative Analysis of the Northern Adriatic and Chesapeake Bay*. Eds. T. C. Malone, A. Malej and J. Faganeli (Hoboken: American Geophysical Union), 49–74. doi: 10.1002/9781119543626.ch4

Cloern, J. E., Foster, S. Q., and Kleckner, A. E. (2014). Phytoplankton Primary Production in the World's Estuarine-Coastal Ecosystems. *Biogeosciences* 11, 2477–2501. doi: 10.5194/bg-11-2477-2014

CSTT (1997). "Comprehensive Studies for the Purposes of Article 6 of Directive 91/271 EEC)," in *The Urban Waste Water Treatment Directive* (Edinburgh: Forth River Purification Board).

Devlin, M., Besyt, M., and Haynes, D. (2007). Implementation of the Water Framework Directive in European Marine Waters. *Mar. Pollut. Bull.* 55 (1–6), 1–2. doi: 10.1016/j.marpolbul.2006.09.020

Dimitriou, P. D., Papageorgiou, N., Arvanitidis, C., Assimakopoulou, G., Pagou, K., Papadopoulou, K. N., et al (2015). One Step Forward: Benthic Pelagic Coupling and Indicators for Environmental Status. *PLoS ONE* 10, e0141071. doi: 10.1371/journal.pone.0141071

Domingues, R. B., Barbosa, A., and Galvão, H. (2008). Constraints on the Use of Phytoplankton as a Biological Quality Element Within the Water Framework Directive in Portuguese Waters. *Mar. Pollut. Bull.* 56 (8), 1389–95. doi: 10.1016/j.marpolbul.2008.05.006.

Duarte, C. M. (1991). Seagrass Depth Limits. *Aquat Bot.* 40, 363–377. doi: 10.1016/0304-3770(91)90081-F

Elser, J. J., Bracken, M. E. S., Cleland, E. E., Gruner, D. S., Harpole, W. S., Hillebrand, H., et al. (2007). Global Analysis of Nitrogen and Phosphorus Limitation of Primary Producers in Freshwater, Marine and Terrestrial Ecosystems. *Ecol. Lett.* 10, 1135–1142. doi: 10.1111/j.1461-0248.2007.01113.x

Fernández-Torquemada, Y., Díaz-Valdés, M., Colilla, F., Luna, B., Sánchez-Lizaso, J. L., and Ramos-Esplá, A. A. (2008). Descriptors From Posidonia Oceanica (L.) Delile Meadows in Coastal Waters of Valencia, Spain, in the Context of the EU Water Framework Directive. *ICES J. Mar. Sci.* 65 (8), 1492–1497. doi: 10.1093/icesjms/fsn146

Flander-Putrle, V., Francé, J., and Mozetič, P. (2022). Phytoplankton Pigments Reveal Size Structure and Interannual Variability of the Coastal Phytoplankton Community (Adriatic Sea). *Water* 14, 23. doi: 10.3390/w14010023

Francé, J., Varkitzi, I., Stanca, E., Cozzoli, F., Skejić, S., Ungaro, N., et al. (2021). Large-Scale Testing of Phytoplankton Diversity Indices for Environmental Assessment in Mediterranean Sub-Regions (Adriatic, Ionian and Aegean Seas). *Ecol. Indic.* 126, 107630. doi: 10.1016/j.ecolind.2021.107630

Gerakaris, V., Panayotidis, P., Vizzini, S., and Nicolaidou, A. (2017). Effectiveness of Posidonia Oceanica Biotic Indices for Assessing the Ecological Status of Coastal Waters in the Saronikos Gulf (Aegean Sea, Eastern Mediterranean). *Mediterranean Mar. Sci.* 18, 161–178. doi: 10.12681/mms.1893

Gerakaris, V., Papathanasiou, V., Salomidi, M., Issaris, Y., and Panayotidis, P. (2021). Spatial Patterns of Posidonia Oceanica Structural and Functional Features in the Eastern Mediterranean (Aegean and E. Ionian Seas) in Relation to Large-Scale Environmental Factors. *Marine Environ. Res.* 165, 1–13. doi: 10.1016/j.marenvres.2020.105222

Giovanardi, F., Francé, J., Mozetič, P., and Precali, R. (2018).). Development of Ecological Classification Criteria for the Biological Quality Element Phytoplankton for Adriatic and Tyrrhenian Coastal Waters by Means of Chlorophyll a, (2000/60/EC WFD). *Ecol. Indic.* 93, 316–332. doi: 10.1016/j.ecolind.2018.05.015

Gobert, S., Sartoretto, S., Rico-Raimondino, V., Andral, B., Chery, A., Lejeune, P., et al. (2009). Assessment of the Ecological Status of Mediterranean French Coastal Waters as Required by the Water Framework Directive Using the Posidonia Oceanica Rapid Easy Index: PREI. *Mar. Pollut. Bull.* 58 (11), 1727–1733. doi: 10.1016/j.marpolbul.2009.06.012

Goldberg, D. (1996). Competitive Ability: Definitions, Contingency and Correlated Traits. *Philos. Trans. Biol. Sci.* 351, 1377–1385.

Graf, G. (1992). Benthic-Pelagic Coupling: A Benthic View. *Oceanogr. Mar. Biol. Annu. Rev. Vol* 30, 149–190.

Grangeré, K., Lefebvre, S., and Blin, J. L. (2012). Spatial and Temporal Dynamics of Biotic and Abiotic Features of Temperate Coastal Ecosystems as Revealed by a Combination of Ecological Indicators. *Estuar Coast Shelf Sci.* 108, 109–118. doi: 10.1016/j.ecss.2012.02.020

Grasshoff, K., Ehrhardt, M., and Kremling, K. (1999). Methods of Seawater Analysis, Third, Completely Revised and Extended Edition. Ed. W.-V. Weinheim. doi: 10.1002/9783527613984

Greve, T. M., and Binzer, T.. (2004). Which Factors Regulate Seagrass Growth and Distribution. In: *The Four European Seagrass Species* J. Borum, C. M. Duarte, D. Krause-Jensen and T. M. Greve Eds., European Seagrasses: An Introduction to Monitoring and Management, EU Project Monitoring and Managing of European Seagrasses (M&MS), 88.

Grilli, F., Accoroni, S., Acri, F., Bernardi Aubry, F., Bergami, C., Cabrini, M., et al. (2020). Seasonal and Interannual Trends of Oceanographic Parameters Over 40 Years in the Northern Adriatic Sea in Relation to Nutrient Loadings Using the EMODnet Chemistry Data Portal. *Water* 12, 2280. doi: 10.3390/w12082280

Håkanson, L., and Eklund, J. M. (2010). Relationships Between Chlorophyll, Salinity, Phosphorus, and Nitrogen in Lakes and Marine Areas. *J Coast Res*, 412–23. doi: 10.2112/08-1121.1

Hargrave, B. T. (1973). Coupling Carbon Flow Though Some Pelagic and Benthic Communities. *J. Fish Res. Board Can.* 30, 1317–1326. doi: 10.1139/f73-212

Harlin, M. M. (1995). "Changes in Major Plant Groups Following Nutrient Enrich- Ment," in *Eutrophic Shallow Estuaries and Lagoons*. Ed. A. J. MC Comb (Murdoch, Australia: Institute for Environmental Science, Murdoch University, CRC Press), p.173–p.187.

Hemminga, M. A., and Duarte, C. M. (2000). *Seagrass Ecology* (Cambridge: Cambridge University Press). doi: 10.1017/CBO9780511525551

Holm-Hansen, O., Lorenzen, C. J., Holmes, R. W., and Strickland, J. D. H. (1965). Fluorometric Determination of Chlorophyll. *J. Cons. Perm. Int. Expl. Mer.* 30, 3–15. doi: 10.1093/icesjms/30.1.3

Ignatiades, L., and Gotsis-Skretas, O. (2010). A Review on Toxic and Harmful Algae in Greek Coastal Waters (E. Mediterranean Sea). *Toxins* 2 (5), 1019–1037. doi: 10.3390/toxins2051019

Ignatiades, L., Gotsis-Skretas, O., Pagou, K., and Krasakopoulou, E. (2009). Diversification of Phytoplankton Community Structure and Related Parameters Along a Large-Scale Longitudinal East–West Transect of the Mediterranean Sea. *J. Plankton Res.* 31, 411–428. doi: 10.1093/plankt/fbn124

Kenworthy, W. J., and Fonseca, M. S. (1996). Light Requirements of seagrassesHalodule Wrightii and Syringodium Filiforme Derived From the Relationship Between Diffuse Light Attenuation and Maximum Depth Distribution. *Estuaries* 19, 740–750.

Krause-Jensen, D., Markager, S., and Dalsgaard, T. (2012). Benthic and Pelagic Primary Production in Different Nutrient Regimes. *Estuaries Coasts* 35, 527–545. doi: 10.1007/s12237-011-9443-1

Lee, K.-S., Park, S. R., and Kim, Y. K. (2007). Effects of Irradiance, Temperature, and Nutrients on Growth Dynamics of Seagrasses: A Review. *J. Exp. Mar. Biol. Ecol.* 350 (1-2), 144–175. doi: 10.1016/j.jembe.2007.06.016

Magliozzi, C., Druon, J. N., Palialexis, A., Aguzzi, L., Alexande, B., Antoniadis, K., et al. (2021). *Pelagic Habitats Under the MSFD D1: Scientific Advice of Policy Relevance* (Luxembourg: EUR 30671 EN, Publications Office of the European Union), ISBN: . doi: 10.2760/081368

Magliozzi, C., Druon, J.-N., Palialexis, A., Artigas, L. F., Boicenco, L., González-Quirós, R., et al. (2021). *Pelagic Habitats Under MSFD D1: Current Approaches and Priorities* (Luxembourg: EUR 30619 ENPublications Office of the European Union), ISBN: . doi: 10.2760/942589

Marbà, N., Krause-Jensen, D., Alcoverro, T., Birk, S., Pedersen, A., Neto, J. M., et al. (2013). Diversity of European Seagrass Indicators: Patterns Within and Across Regions. *Hydrobiologia* 704 (1), 265–278. doi: 10.1007/s10750-012-1403-7

Martínez-Crego, B., Alcoverro, T., and Romero, J. (2010). Biotic Indices for Assessing the Status of Coastal Waters: A Review of Strengths and Weaknesses. *J. Environ. Monitoring* 12 (5), 1013–1028. doi: 10.1039/b920937a

McGlathery, K. J., Sundback, K., and Anderson, I. C. (2007). Eutrophication in Shallow Coastal Bays and Lagoons: The Role of Plants in the Coastal Filter. *Mar. Ecol. Prog. Ser.* 348, 1–18. doi: 10.3354/meps07132

MED-GIG (2011). "WFD Intercalibration Phase 2: Milestone 6 Report," in *Coastal Waters, Mediterranean Sea GIG, Macroalgae*, 25 pp.

Mozetič, P., France, J., Kogovšek, T., Talaber, I., and Malej, A. (2012). Plankton Trends and Community Changes in a Coastal Sea (Northern Adriatic): Bottom-Up *vs.* Top-Down Control in Relation to Environmental Drivers. *Estuarine Coastal Shelf Sci.* 115, 138–148. doi: 10.1016/j.ecss.2012.02.009

Mozetič, P., Solidoro, C., Cossarini, G., Socal, G., Precali, R., France, J., et al. (2010). Recent Trends Towards Oligotrophication of the Northern Adriatic: Evidence From Chlorophyll a Time Series. *Estuaries Coasts* 33, 362–375. doi: 10.1007/s12237-009-9191-7

Mvungi, E. F., and Mamboya, F. A. (2012). Photosynthetic Performance, Epiphyte Biomass and Nutrient Content of Two Seagrass Species in Two Areas With Different Level of Nutrients Along the Dar Es Salaam Coast. *Afr. J. Marine Sci.* 34 (3), 323–330. doi: 10.2989/1814232X.2012.709957

Orfanidis, S., Panayotidis, P., and Stamatis, N. (2001). Ecological Evaluation of Transitional and Coastal Waters: A Marine Benthic Macrophytes-Based Model. *Mediterranean Mar. Sci.* 2 (2), 45–65. doi: 10.12681/mms.266

Orfanidis, S., Panayotidis, P., and Ugland, K. I. (2011). Ecological Evaluation Index Continuous Formula (EEI-C) Application: A Step Forward for Functional Groups, the Formula and Reference Condition Values. *Mediterr. Mar. Sci.* 12 (1), 199–231. doi: 10.12681/mms.60

Orfanidis, S., Papathanasiou, V., and Gounaris, S. (2007). Body Size Descriptor of Cymodocea Nodosa Indicates Anthropogenic Stress in Coastal Ecosystem. *Transitional Waters Bull.* 2, 1–7. doi: 10.1285/i1825229Xv1n2p1

Orfanidis, S., Papathanasiou, V., Gounaris, S., and Theodosiou, T. (2010). Size Distribution Approaches for Monitoring and Conservation of Coastal Cymodocea Habitats. *Aquat. Conservation: Marine Freshwater Ecosystems* 20, 177–188. doi: 10.1002/aqc.1069

Orfanidis, S., Papathanasiou, V., Mittas, N., Theodosiou, T., Ramfos, A., Tsioli, S., et al. (2020). Further Improvement, Validation, and Application of CymoSkew Biotic Index for the Ecological Status Assessment of the Greek Coastal and Transitional Waters. *Ecol. Indic.* 118, 106727. doi: 10.1016/j.ecolind.2020.106727

Orlando-Bonaca, M., Francé, J., Mavrič, B., Grego, M., Lipej, L., Flander-Putrle, V., et al. (2015). A New Index (MediSkew) for the Assessment of the Cymodocea Nodosa (Ucria) Ascherson Meadow's Status. *Marine Environ. Res.* 110, 132–141. doi: 10.1016/j.marenvres.2015.08.009

Orlando-Bonaca, M., Francé, J., Mavrič, B., and Lipej, L. (2019). Impact of the Port of Koper on Cymodocea Nodosa Meadow. *Annales Ser. Hist. Naturalis* 29 (2), 187–194. doi: 10.19233/ASHN.2019.18

Orlando-Bonaca, M., Lipej, L., and Francé, J. (2016). The Most Suitable Time and Depth to Sample Cymodocea Nodosa (Ucria) Ascherson Meadows in the

Shallow Coastal Area. *Experiences northern Adriatic Sea Acta Adriatica* 57 (2), 251–262.

Orlando-Bonaca, M., Lipej, L., and Orfanidis, S. (2008). Benthic Macrophytes as a Tool for Delineating, Monitoring and Assessing Ecological Status: The Case of Slovenian Coastal Waters. *Mar. Pollut. Bull.* 56 (4), 666–676. doi: 10.1016/j.marpolbul.2007.12.018

Orlando-Bonaca, M., Pitacco, V., and Lipej, L. (2021). Loss of Canopy-Forming Algal Richness and Coverage in the Northern Adriatic Sea. *Ecol. Indic.* 125, 107501. doi: 10.1016/j.ecolind.2021.107501

Orlando-Bonaca, M., and Rotter, A. (2018). Any Signs of Replacement of Canopy-Forming Algae by Turf-Forming Algae in the Northern Adriatic Sea? *Ecol. Indic.* 87, 272–284. doi: 10.1016/j.ecolind.2017.12.059

Pagou, K. (2005). "Eutrophication in Hellenic Coastal Areas," in *State of the Hellenic Marine Environment. Inst. Oceanography*. Eds. E. Papathanassiou and A. Zenetos (Athens: HCMR publ.), 311–317.

Papathanasiou, V., and Orfanidis, S. (2018). Anthropogenic Eutrophication Affects the Body Size of Cymodocea Nodosa in the North Aegean Sea: A Long-Term, Scale-Based Approach. *Mar. Pollut. Bull.* 134, 38–48. doi: 10.1016/j.marpolbul.2017.12.009

Pavlidou, A., Simboura, N., Pagou, K., Assimakopoulou, G., Gerakaris, V., Hatzianestis, I., et al. (2019). Using a Holistic Ecosystem-Integrated Approach to Assess the Environmental Status of Saronikos Gulf, Eastern Mediterranean. *Ecol. Indic* 96, 336–350. doi: 10.1016/j.ecolind.2018.09.007

Pavlidou, A., Simboura, N., Rousselaki, E., Tsapakis, M., Pagou, K., Drakopoulou, P., et al. (2015). Methods of Eutrophication Assessment in the Context of the Water Framework Directive: Examples From the Eastern Mediterranean Coastal Areas. *Cont Shelf Res.* 108, 156–168. doi: 10.1016/j.csr.2015.05.013

Pawlowski, J., Kelly-Quinn, M., Altermatt, F., Apothéloz-Perret-Gentil, L., Beja, P., Boggero, A., et al. (2018). The Future of Biotic Indices in the Ecogenomic Era: Integrating (E) DNA Metabarcoding in Biological Assessment of Aquatic Ecosystems. *Sci. Total Environ.* 637, 1295–1310. doi: 10.1016/j.scitotenv.2018.05.002

R Core Team (2021). R: A Language and Environment for Statistical Computing. Vienna, Austria: R Foundation for Statistical Computing. URL https://www.R-project.org/

Ralph, P. J., Durako, M. J., Enríquez, S., Collier, C. J., and Doblin, M. A. (2007). Impact of Light Limitation on Seagrasses. *J. Exp. Marine Biol. Ecol.* 350 (1-2), 176–193. doi: 10.1016/j.jembe.2007.06.017

Rombouts, I., Simon, N., Aubert, A., Cariou, T., Feunteun, E., Guérin, L., et al (2019). Changes in Marine Phytoplankton Diversity: Assessment Under the Marine Strategy Framework Directive. *Ecol. Indic.* 102, 265–77. doi: 10.1016/j.ecolind.2019.02.009

Romero, J., Martinez-Crego, B., Alcoverro, T., and Perez, M. (2007a). A Multivariate Index Based on the Seagrass Podidonia Oceanica (POMI) to Assess Ecological Status of Coastal Waters Under the Water Framework Directive (WFD). *Marine Pollution Bull.* 55, 196–204. doi: 10.1016/j.marpolbul.2006.08.032

Romero, J., Martinez-Crego, B., Alcoverro, T., and Perez, M. (2007b). Corrigendum of: "A Multivariate Index Based on the Seagrass Podidonia Oceanica (POMI) to Assess Ecological Status of Coastal Waters Under the Water Framework Directive (WFD) in Marine Pollution Bulletin 55, 196–204". *Marine Pollution Bull.* 54, 631. doi: 10.1016/j.marpolbul.2007.02.008

Sand-Jensen, K., and Borum, J. (1991). Interactions Among Phytoplankton, Periphyton, and Macrophytes in Temperate Freshwaters and Estuaries. *Aquatic Botany* 41 (1–3), 137–175. doi: 10.1016/0304-3770(91)90042-4

Schramm, W., and Nienhuis, P. H. (1996). "Marine Benthic Vegetation," in *Recent Changes and the Effects of Eutrophica- Tion* (New York: Springer), 470 pp.

Simboura, N., Tsapakis, M., Pavlidou, A., Assimakopoulou, G., Pagou, K., Kontoyiannis, H., et al. (2015). Assessment of the Environmental Status in Hellenic Coastal Waters (Eastern Mediterranean): From the Water Framework Directive to the Marine Strategy Water Framework Directive. *Mediterranean Mar. Sci.* 16 (1), 46–64. doi: 10.12681/MMS.960

Simboura, N., Pavlidou, A., Bald, J., Tsapakis, M., Pagou, K., Zeri, C., et al. (2016). Response of Ecological Indices to Nutrient and Chemical Contaminant Stress Factors in Eastern Mediterranean Coastal Waters. *Ecol. Ind.* 70, 89–105. doi: 10.1016/j.ecolind.2016.05.018

Tett, P., Carreira, C., Mills, D. K., Van Leeuwen, S., Foden, J., Bresnan, E., et al. (2008). Use of a Phytoplankton Community Index to Assess the Health of Coastal Waters. *ICES J. Mar. Sci.* 65, 1475–1482. doi: 10.1093/icesjms/fsn161

Touchette, B. W., and Burkholder, J. M. (2000). Overview of the Physiological Ecology of Carbon Metabolism in Seagrasses. *J. Exp. Marine Biol. Ecol.* 250, 169–205. doi: 10.1016/S0022-0981(00)00196-9

Tsiamis, K., Balanika, K., Kleinteich, J., Salomidi, M., Pavlidou, A., Küpper, F. C., et al. (2013). Macroalgal Community Response to Re-Oligotrophication: A Case Study From Saronikos Gulf (Eastern Mediterranean, Greece). *Mar. Ecol. Prog. Ser.* 472, 73–85. doi: 10.3354/meps10060

Tweddle, J. F., Gubbins, M., and Scott, B. E. (2018). Should Phytoplankton be a Key Consideration for Marine Management? *Mar. Policy* 97, 1–9. doi: 10.1016/j.marpol.2018.08.026

Tyerman, S. D. (1989). "Solute and Water Relations of Seagrasses," in *Biology of Seagrasses: A Treatise on the Biology of Seagrasses With Special Reference to the Australian Region*. Ed. A. W. D. Larkum (Amsterdam, The Netherlands: Elsevier), 723–759.

UNEP/MAP. (2017). Integrated Monitoring and Assessment Programme of theMediterranean Sea and Coast and Related Assessment Criteria. United NationsEnvironment Programme / Mediterranean Action Plan, Athens, Greece.

Valiela, I., Foreman, K., LaMontagne, M., Hersh, D., Costa, J., Peckol, P., et al. (1992). Couplings of Watersheds and Coastal Waters: Sources and Consequences of Nutrient Enrichment in Waquoit Bay, Massachusetts. *Estuaries* 15, 443–457. doi: 10.2307/1352389

Vaquer-Sunyer, R., and Duarte, C. M. (2008). Thresholds of Hypoxia for Marine Biodiversity. *Proc. Natl. Acad. Sci. U.S.A* 105, 15452–15457. doi: 10.1073/pnas.0803833105

Varkitzi, I., Francé, J., Basset, A., Cozzoli, F., Stanca, E., Zervoudaki, S., et al. (2018a). Pelagic Habitats in the Mediterranean Sea: A Review of Good Environmental Status (GES) Determination for Plankton Components and Identification of Gaps and Priority Needs to Improve Coherence for the MSFD Implementation. *Ecol. Ind.* 95, 203–218. doi: 10.1016/j.ecolind.2018.07.036

Varkitzi, I., Markogianni, V., Pantazi, M., Pagou, K., Pavlidou, A., and Dimitriou, E. (2018b). Effect of River Inputs on Environmental Status and Potentially Harmful Phytoplankton in a Coastal Area of Eastern Mediterranean (Maliakos Gulf, Greece). *Mediterranean Mar. Sci.* 19 (2), 326–343. doi: 10.12681/mms.14591

Varkitzi, I., Pagou, K., Granéli, E., Hatzianestis, I., Krasakopoulou, E., and Pavlidou, A. (2013). "Spatio-Temporal Distribution of Dinophysis Spp. In Relation to Organic Matter Availability and Other Parameters in Thermaikos Gulf, Greece (Eastern Mediterranean)," in *Proceedings of the 14th International Conference on Harmful Algae, International Society for the Study of Harmful Algae and Intergovernmental Oceanographic Commission of UNESCO*, 1-5 November 2013 (Greece: Hersonissos-Crete), 269.

Varkitzi, I., Psarra, S., Assimakopoulou, G., Pavlidou, A., Krasakopoulou, E., Velaoras, D., et al. (2020). Phytoplankton Dynamics and Bloom Formation in the Oligotrophic Eastern Mediterranean: Field Studies in the Aegean, Levantine and Ionian Seas. *Deep Sea Res. Part II* 171, 104662. doi: 10.1016/j.dsr2.2019.104662

Wickham, H. (2016). *Ggplot2: Elegant Graphics for Data Analysis*. (New York: Springer-Verlag).

Zhang, Q., Cozzi, S., Palinkas, S., and Giani, M. (2021). "Recent Status and Long-Term Trends in Freshwater Discharge and Nutrient Inputs," in *Coastal Ecosystems in Transition: A Comparative Analysis of the Northern Adriatic and Chesapeake Bay*. Eds. T. C. Malone, A. Malej and J. Faganeli (Hoboken: American Geophysical Union), 7–20. doi: 10.1002/9781119543626.ch2

Conflict of Interest: The authors declare that the research was conducted in the absence of any commercial or financial relationships that could be construed as a potential conflict of interest.

frontiers | Frontiers in Marine Science

ORIGINAL RESEARCH
published: 18 July 2022
doi: 10.3389/fmars.2022.889633

Life Cycle Strategies of the Centric Diatoms in a Shallow Embayment Revealed by the Plankton Emergence Trap/Chamber (PET Chamber) Experiments

Ken-Ichiro Ishii[1*†], *Kazumi Matsuoka*[2], *Ichiro Imai*[3] *and Akira Ishikawa*[4*]

[1] Graduate School of Agriculture, Kyoto University, Kyoto, Japan, [2] Osaka Museum of Natural History and C/O Institute for East China Sea, Nagasaki University, Nagasaki, Japan, [3] Graduate School of Fisheries Science, Hokkaido University, Hakodate, Hokkaido, Japan, [4] Graduate School of Bioresources, Mie University, Tsu, Japan

OPEN ACCESS

Edited by:
Tamara Cibic, Istituto Nazionale di Oceanografia e di Geofisica Sperimentale, Italy

Reviewed by:
David U. Hernández-Becerril, National Autonomous University of Mexico, Mexico
Genuario Belmonte, University of Salento, Italy

***Correspondence:**
Akira Ishikawa
ishikawa@bio.mie-u.ac.jp
Ken-Ichiro Ishii
restingspore@gmail.com

†Present address:
Ken-Ichiro Ishii, SeedBank Co. Ltd., Kyoto, Japan

Specialty section:
This article was submitted to Marine Ecosystem Ecology, a section of the journal Frontiers in Marine Science

Received: *04 March 2022*
Accepted: *21 April 2022*
Published: *18 July 2022*

Citation:
Ishii K, Matsuoka K, Imai I and Ishikawa A (2022) Life Cycle Strategies of the Centric Diatoms in a Shallow Embayment Revealed by the Plankton Emergence Trap/Chamber (PET Chamber) Experiments. Front. Mar. Sci. 9:889633. doi: 10.3389/fmars.2022.889633

In situ emergence of the centric diatoms from the surface sediment, along with the occurrence of the vegetative cells in the water column, were monitored monthly in a shallow embayment, Ago Bay, of central Japan, where light penetrated to the seafloor. The *in situ* emergence flux (cells m^{-2} day^{-1}) was measured by experiments using a 'plankton emergence trap/chamber (PET chamber)'. During the study period from July 2006 to May 2008, germinating and rejuvenating cells of centric diatoms were successfully collected by the PET chamber. Furthermore, vegetative cells forming long-chain colonies, including the species which have not been known to form resting stage cells, were also found, indicating that these cells already inhabited the surface sediment prior to the start of the PET chamber experiments. The vegetative cells could be cells that grew after germination/rejuvenation and/or cells deposited from the upper layer in the water column. When comparing emergence flux in the PET chamber and the integrated abundance of the vegetative cells in the water column for the diatoms frequently observed, significant positive relationships were found for some diatom taxa. However, even for these taxa that showed a clear relationship, the magnitude of the vegetative population in the water column did not necessarily correlate with that of the emergence flux. These observations indicate that the magnitude of the vegetative population was not regulated directly by the emergence flux. The magnitude of the vegetative population could be dependent on the vegetative growth itself. This implies that the presence of vegetative cells in the water column is important at the time when environmental conditions become suitable for vegetative growth. In this context, the presence of various types of cells, such as germinating, rejuvenating, and vegetative cells, in the sediment is essential as seeds waiting for recruitment into the water column. Consequently, the seafloor in Ago Bay may act as a 'refuge and nursery' for centric diatoms. Based on the above, we demonstrated various patterns of life cycle strategies of the diatoms in a shallow coastal water/embayment.

Keywords: diatom, resting stage cell, vegetative cell, emergence, PET chamber, shallow embayment, life cycle strategy

INTRODUCTION

Among phytoplankton, diatoms and dinoflagellates are the major primary producers in coastal areas. Diatoms and dinoflagellates show species successions in response to drastic changes in the coastal environments (Margalef, 1958; Smayda, 1980; Reynolds, 1984). Many species of both diatoms and dinoflagellates can produce dormant benthic cells possessing the ability to survive adverse environments for vegetative growth (Dale, 1983; Hargraves and French, 1983; Belmonte and Rubino, 2019).

Dormant benthic cells for most species of dinoflagellates are known to be produced through sexual reproduction (von Stosch, 1967; Dale, 1983; Pfiester and Anderson, 1987) and for most species of centric diatoms through asexual reproduction (Hargraves and French, 1983; Hasle and Sims, 1985; Rines and Hargraves, 1988; Hargraves, 1990). Such dormant benthic cells are named 'cysts' for dinoflagellates, and 'resting spores' or 'resting cells' for diatoms, depending on their morphological/physiological features. The resting spore, characterized by a different shape from its vegetative cell and by a thick cell wall, is formed in the frustule of a vegetative cell and possesses high tolerance to adverse conditions for the vegetative growth. In contrast, the resting cell is one in which the physiological status of the vegetative cell becomes dormant without any morphological differences from the vegetative cell (McQuoid and Hobson, 1996). These dormant benthic cells are collectively called 'resting stage cells' but the reproduction modes of these two types of cells are separately referred to as 'germination' for resting spores and 'rejuvenation' for resting cells (Sicko-Goad, 1986; McQuoid and Hobson, 1996).

The life cycle of such resting stage cell forming centric diatoms has generally been explained as a conceptual diagram shown in **Figure 1**, which was drawn with reference to the reviews (McQuoid and Hobson, 1996; Belmonte and Rubino, 2019). The resting stage cells are formed under unfavorable conditions, such as nutrient depletion or low light conditions, for vegetative growth. When the benthic environmental conditions become favorable, the cells germinate (from resting spores) and rejuvenate (from resting cells), forming the vegetative population in the water column (McQuoid and Hobson, 1996; Itakura et al., 1997). Therefore, it is widely accepted that the resting stage cells act as 'seed populations' in their population dynamics (Hargraves and French, 1983; Pitcher, 1990), as is the case of dinoflagellates(Wall, 1971; Steidinger, 1975).

Accordingly, to understand the population dynamics of diatoms, the biology and ecology, with reference to germination/rejuvenation, of the resting stage cells have been studied under laboratory conditions (e.g., Imai et al., 1996; Itakura, 2000; Ueno and Ishikawa, 2009; Montresor et al., 2013). However, the conditions of the *in situ* environment are extremely complex and impossible to be mimicked in the laboratory. Therefore, to get a better understanding of the population dynamics in the natural environment, it is necessary to investigate the "germination" of the resting stage cells *in situ*.

Given the above circumstances, the 'plankton emergence trap/chamber (PET chamber)' has been developed to collect

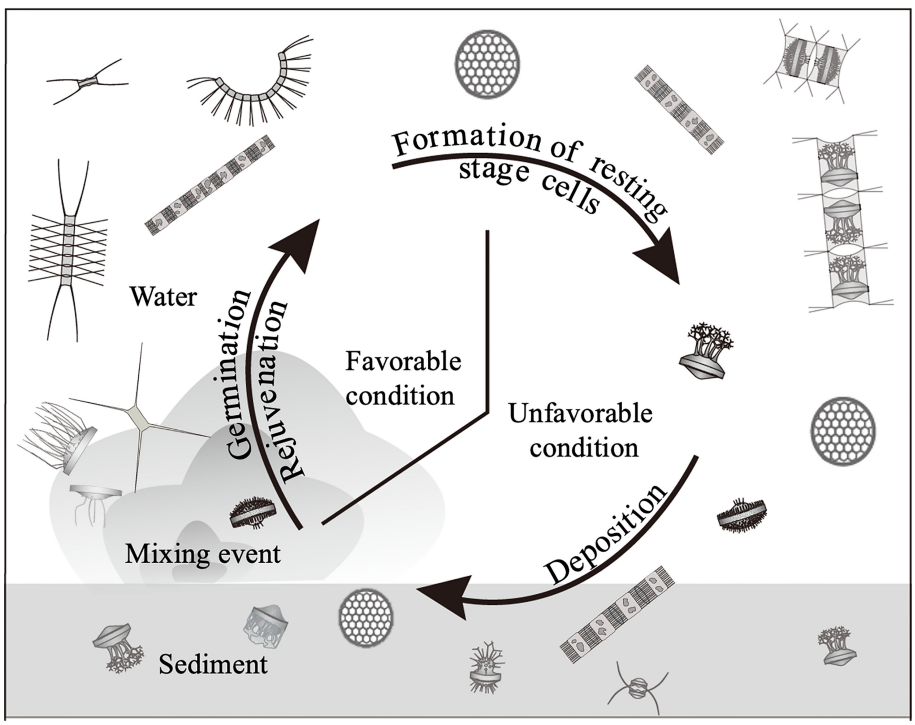

FIGURE 1 | Conceptual diagram of life cycle of the centric diatoms forming the resting stage cells (resting spores and resting cells).

germinating cells (the vegetative cells just after germination) from the microalgal cysts in the surface sediments (Ishikawa et al., 2007). Subsequent study using the PET chamber successfully elucidated the mechanism of population dynamics of a toxic dinoflagellate of *Alexandrium catenella* (present name *A. pacificum*) (Ishikawa et al., 2014). However, there are no reported investigations that applied the PET chamber to diatoms or other microalgae that form resting stage cells/cysts.

In this study, we investigated the germination/rejuvenation of centric diatoms by using the PET chamber in order to elucidate the mechanisms of their population dynamics in a temperate shallow embayment. Based on the results of this investigation, we discuss the life cycle strategies of diatoms in such shallow coastal waters.

MATERIALS AND METHODS

For this study, we selected Ago Bay, located on the southeast coast of Kii Peninsula, central Japan, as a model area of a typical coastal environment in the temperate zone (**Figure 2**). This bay is semi-enclosed with an area of 25 km^2 and is connected to the Pacific Ocean through a narrow bay mouth of ca. 2 km width. There are no major rivers in the bay, so freshwater inflow is limited. The average water depth of the bay is shallow at about 10 m, implying that light penetrates to the seafloor throughout the year. Sampling was conducted at a site (34° 16.30' N; 136° 48.40' E), located at the southern extent of the bay at a frequency of once a month for about two years from July 2006 to May 2008 (**Figure 2**). The average depth at the site is 11 m. This is the same site where the study of *A. catenella* was conducted before, by using the PET chamber (Ishikawa et al., 2014).

Measurements of Environmental Conditions

Water temperature and salinity were measured at three depths of 0, 4, and 1 m above the bottom (hereafter: b-1 m) at the sampling site, using a Multi-probe (Hach-Hydrolab, QUANTA). In addition, dissolved oxygen (DO) concentration and light intensity (PAR) at 0.3 m above the bottom (hereafter: b-0.3 m) were recorded every 20 minutes throughout the study period, using a compact memory oxygen meter (JFE Advantec, COMPACT-DOW) and a light quantum memory meter (JFE Advantec, COMPACT- LW), respectively. However, during the monitoring of the light, recording of its data occasionally failed due to the breakdown of the sensor.

Water Sampling and Treatments

Water samples were collected at different depths in the water column, using a Van-Dorn sampler. Samples (ca. 1,000 mL) collected from each depth were used to analyze nutrients and to count vegetative cells of centric diatoms.

A 100 mL aliquot of each water sample collected at 0 and b-1 m was filtered through a glass fiber filter (Whatman, GF/F) and the filtrate was frozen at -30°C until analysis of the following nutrients: dissolved inorganic nitrogen (NO_3-N + NO_2-N + NH_4-N: DIN), phosphate (PO_4-P; DIP), and silicate (SiO_4-Si). The concentrations of these nutrients were measured with an autoanalyzer (BL TEC, swAAt) by the method of Strickland and Parsons (1972). Dissolved silicate was measured starting on a later date, February 2007.

To count the vegetative cells of the diatoms, 500 mL water samples collected at 0, 2, 4, 6, 8 and b-1 m were immediately fixed by adding borax-buffered formaldehyde at a final concentration of 1% (v/v). After allowing the preserved

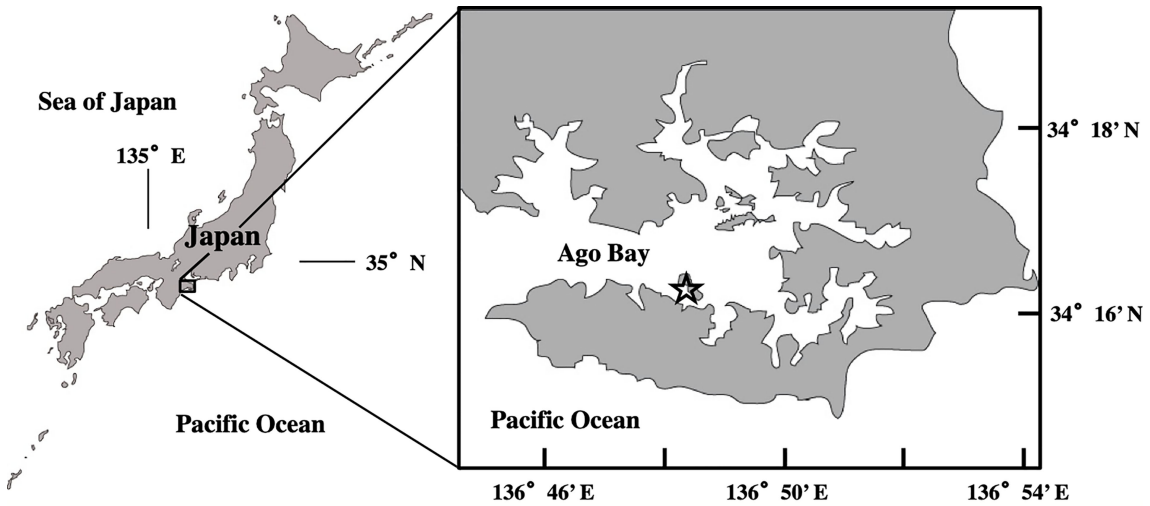

FIGURE 2 | Location of the sampling site (open star) in Ago Bay, central Japan.

samples to settle for at least 24 h in the laboratory, the supernatant was removed by siphoning and concentrated to 10 mL. From this concentrated sample, a 1 mL of aliquot was spread onto a Sedgewick-Rafter chamber, and all of the vegetative cells of diatoms that appeared were identified and counted usually at 200 X magnification (400 or 600 X when needed) under an inverted epifluorescence microscope (Nikon, ECLIPSE TE200), along with confirming the viability of cells. The identification of the species was mainly referred to Rines and Hargraves (1988); Hasle and Syvertsen (1997) and Jensen and Moestrup (1998). In this microscopy, the counting was conducted until the total number of the vegetative cells was more than 200 cells. All cell counts were made in triplicate and the cell abundance was obtained as the average value (cells L^{-1}). These cell abundances were finally integrated to obtain the total abundance of vegetative cells in the water column per m^2 (cells m^{-2}) by plotting the abundances (cells L^{-1}) against their respective depths.

Sediment Sampling and PET Chamber Experiment

The sediment core samples were collected without disturbance using the method of Yokoyama and Ueda (1997), in which an acrylic core tube (6.4 cm diameter, 23 cm length) was set in the bucket of an Ekman grab (see Ishikawa et al., 2007). A total of six sediment core samples were obtained randomly within a 10 m radius at the sampling site. Among them, five core samples were used for the PET chamber experiments to collect *in situ* germinating/rejuvenating cells from the surface sediment and the remaining one for measuring the temperature of the sediment at a depth of 1 cm with a mercury thermometer immediately after the core sample was obtained.

A schematic diagram of the PET chamber used in the present study is shown in **Figure 3**. The chamber consists of a top cylinder and a bottom cylinder. The top cylinder is designed to contain filtered seawater and the bottom cylinder to contain sediments collected at the sampling site. In every experiment, we employed five such units and set them all together on a stainless-steel incubation platform (**Figure 3**). In addition to the above units, one unit was placed on the platform as a control chamber filled with filtered seawater at the sampling site but without sediment inside of the bottom cylinder, in order to check the contamination (i.e., invasion) of diatoms from outside the cylinder (i.e., ambient seawater). The six PET chambers were set at a bottom depth of ~11 m at the sampling site. After 24 h, the chambers were retrieved and the seawater in the top cylinder of the chamber was carefully collected. All of the above handling procedures using PET chambers were described in Ishikawa et al. (2007).

The water samples (ca. 500 mL) collected from the top cylinder were immediately fixed with borax-buffered formaldehyde at a final concentration of 1% (v/v). The fixed samples were brought back to the laboratory and allowed to settle for at least 24 h. Thereafter, the supernatant in the sample was removed by siphoning and concentrated to 100 mL. This concentrated sample was finally poured into the "combined plate chamber" (see Hasle, 1978) and allowed to settle again for at least 24 h before microscopy. All of the vegetative cells that appeared in the sample of a PET chamber were identified and counted at usually 200 X magnification (400 or 600 X when needed) using an inverted epifluorescence microscope (Nikon, ECLIPSE TE200) under blue light excitation, making it possible to detect the viable vegetative cells easily by observing their autofluorescence, even though the samples occasionally contained sediment silt and clay particles which were derived from resuspension of the surface sediment at the time when the water sample in the top cylinder of the PET chamber was collected. The vegetative cell numbers in the five PET chambers were first averaged and finally converted to daily 'emergence flux' per m^2 (i.e., cells m^{-2} day^{-1}) by taking the sediment surface exposed area on the base plate of the PET chamber (i.e., 32.2 cm^2, see Ishikawa et al., 2007). It was assumed that grazing by zooplankton on the emerged cells during the PET chamber experiment was negligible, since large zooplankton were rarely observed in the samples, as was the case in a previous study of the dinoflagellate *A. catenella* conducted at this same site (Ishikawa et al., 2014).

In order to clarify the relationship between the emergence flux (cells m^{-2} day^{-1}) and the abundance of vegetative cells in the water column (cells m^{-2}), Spearman's rank test was conducted using the software SPSS (ver. 22).

After the above series of studies, sediment cores were additionally collected without disturbance by the same method using Ekman grab as described above at the same sampling site in July 2020. The water sample containing fine sediment particles in the flocculent layer (sediment/water interface) was obtained by sucking with a dropper. The contents in the sample were directly observed under the microscope.

RESULTS

Environmental Conditions

The water column was thermally stratified in the summer from July to September in 2006 and from June to September in 2007. During these periods, the temperatures at the surface (0 m) and the bottom (b-1 m) were in the range of 24.6 – 27.1°C and 19.1 – 23.4°C, respectively (**Figure 4A**). In contrast, the water column in other periods was vertically mixed, except in January 2007. The water temperatures in the water column were generally lower than 15°C from December to March in both 2006/2007 and 2007/2008, with minima of 9.0°C at 0 m and 8.7°C at b-1 m in January 2008. The temporal change in temperature of the sediment showed a similar trend to that in the water column, with a maximum of 25.2°C in July 2007 and a minimum of 10.0°C in January 2008.

Salinity in the water column showed no clear temporal changes, being almost always in the range of 30 – 35 during the study period, although it occasionally decreased to 23.9 at 0 m in July 2007 and about 16 throughout the water column in April 2008 (**Figure 4B**). Such lower values of salinity were due to heavy rain fall (Japan Meteorological Agency, data available at https://www.data.jma.go.jp/gmd/risk/obsdl/).

Concentrations of DO at b-0.3 m showed a clear temporal change, with relatively low and high values when the water column was stratified or vertically mixed, respectively (**Figure 5A**). DO was

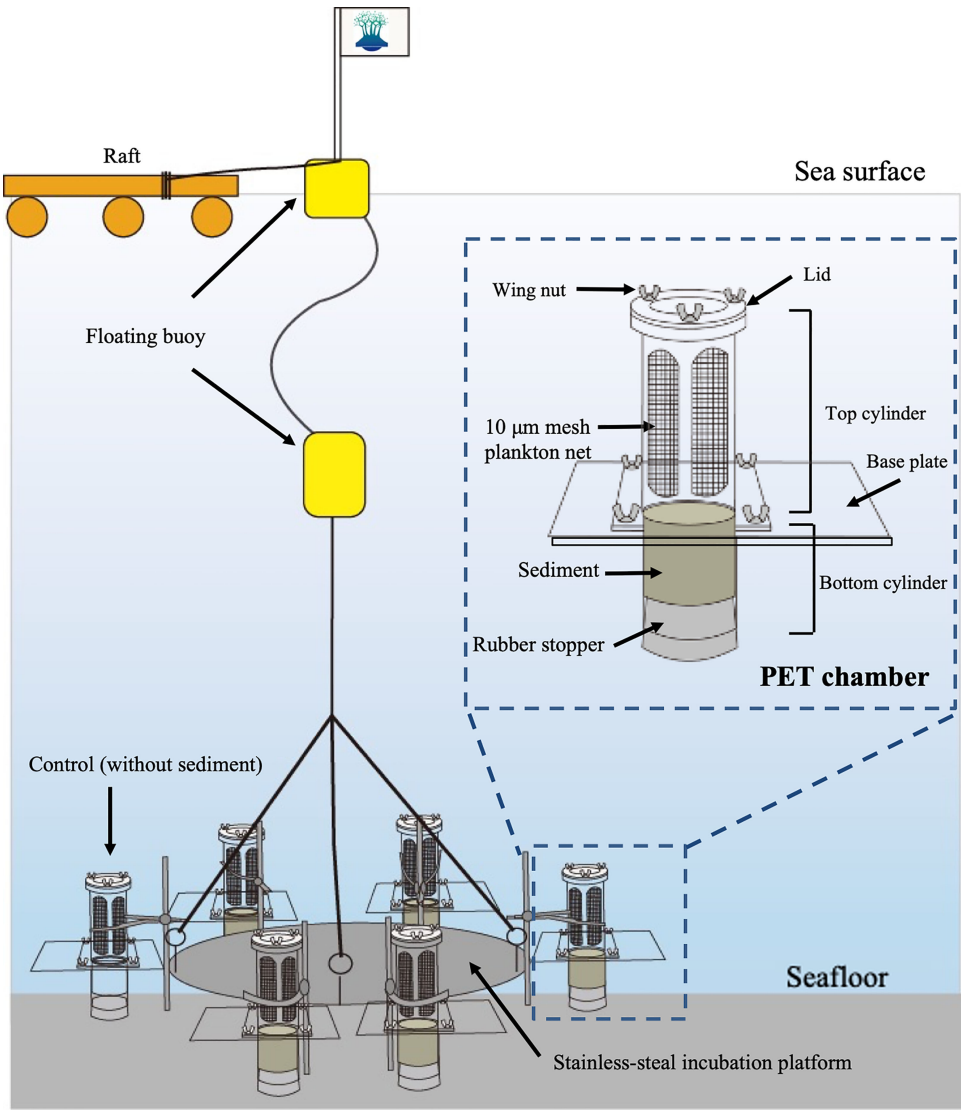

FIGURE 3 | Schematic diagram showing plankton emergence trap/chamber (PET chamber) experiment.

often lower than 2 mg L^{-1} in the warmer seasons (from July to September) but generally higher than 4 mg L^{-1} in other seasons.

The light intensity at b-0.3 m during daytime changed notably, not only seasonally but also daily, in the range of 1.3 – 187.0 µmol photons m^{-2} s^{-1} (**Figure 5B**). Throughout the study period, the light almost always penetrated to the bottom at intensities > 10 µmol photons m^{-2} s^{-1}, and although there were cases when intensity was < 10 µmol photons m^{-2} s^{-1}, it did not continue for more than 2 successive days. The average light intensity over the periods when the PET chamber experiment was conducted was 27.3 µmol photons m^{-2} s^{-1} (data not shown).

Concentrations of DIN (**Figure 6A**) and DIP (**Figure 6B**) changed temporally in a similar manner, being generally high at both depths (0 m and b-1 m) in the warm seasons from June/July to September/October in both years, 2006 and 2007, and low in cold seasons (January to March). During the study, the concentration of DIN fluctuated in the range of 1.4 -7.3 µM and 1.1 – 13.0 µM at 0 m and b-1 m, respectively, and DIP fluctuated in the range of 0.1-0.6 µM and 0.1-1.2 µM at 0 m and b-1 m, respectively. The concentration of SiO_4 (**Figure 6C**) changed over a wider range between 1.7 and 32.2 µM in the water column, although no obvious temporal change was observed in the concentrations.

As a whole, the environmental conditions measured at the sampling site tended to show changes with the seasons, like those in a typical temperate embayment.

Diatoms Observed in Water Column and PET Chamber

Over the course of this study, from July 2006 to May 2008, more than 79 species grouped in 34 genera, including unidentified

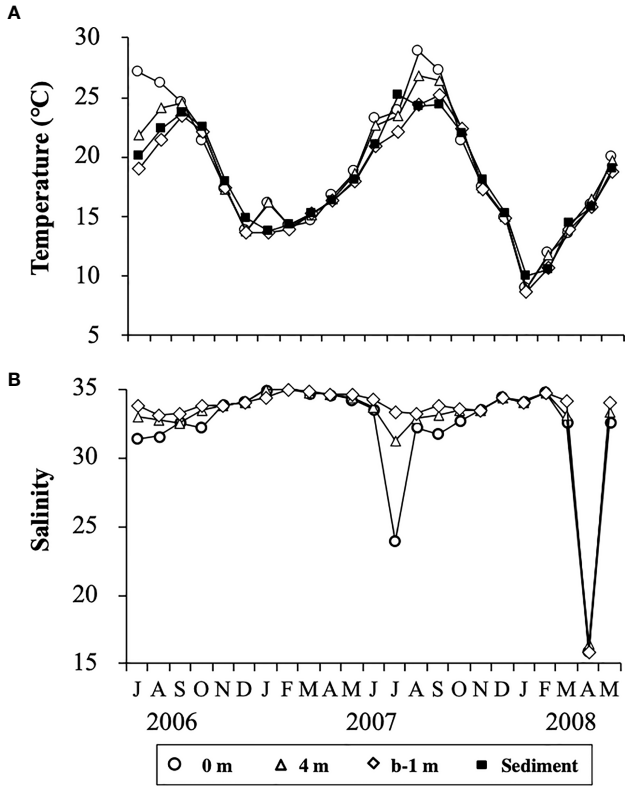

FIGURE 4 | Temporal changes in temperature **(A)** at different depths in the water column and at 1 cm depth in the sediment, and salinity **(B)** at different depths in the water column at the sampling site in Ago Bay. b-1 m denotes the depth at 1 m above the bottom.

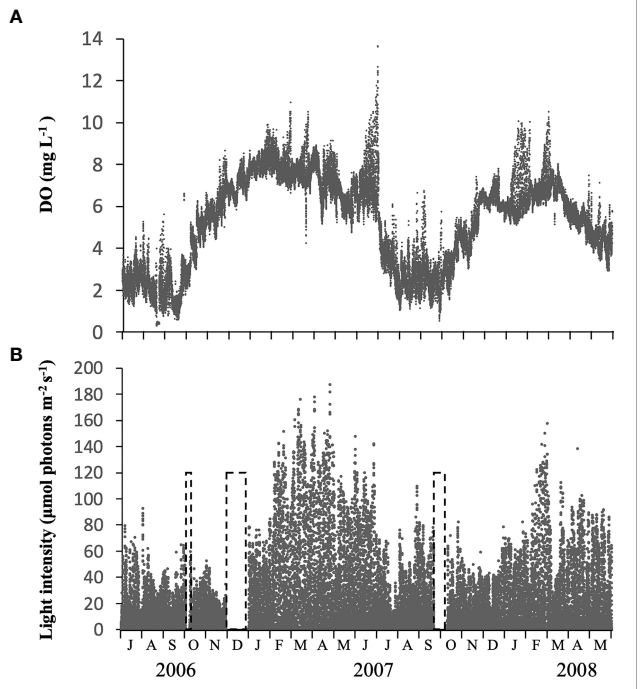

FIGURE 5 | Temporal changes in concentration of dissolved oxygen (DO) **(A)** and light intensity **(B)** measured at 0.3 m above the bottom, using memory meters, at the sampling site in Ago Bay. The periods in the dashed frame indicate that no data was recorded.

species, and more than 55 species grouped in 28 genera were observed in samples representing the water column and the PET chamber, respectively (**Table 1**): all of the 55 species in the PET chamber appeared in the water column.

Vegetative cells that frequently emerged in the PET chamber are shown in **Figure 7**. Among these vegetative cells, different types were found as follows. Vegetative cells with chloroplasts were observed beside a valve which was shed from a resting spore (**Figure 7G**). In addition, long chains of vegetative cells containing distinct chloroplasts were often observed for species of the genera *Chaetoceros* (e.g., **Figures 7J, M**), *Skeletonema* (**Figure 7Ab**) and *Thalassiosira* (**Figure 7Af**). Among the 55 species recognized in the PET chambers, 24 species have not been known to form the resting stage cells so far (**Table 1**).

The top five of the most frequently detected species were common in both the water column and the PET chamber. Those species were *Cerataulina pelagica*, *Chaetoceros debilis*, *Ch. didymus*, *Ch. distans* and *Leptocylindrus danicus*. Furthermore, the genus *Skeletonema* also occurred quite frequently. Since identification of species of the genus *Skeletonema* is very difficult under an optical microscope in a routine observation (see Sarno et al., 2005), they are collectively referred to as *Skeletonema* spp. in this study. No obvious trend of temporal change in either the abundance of the vegetative cells or the emergence flux of the frequently observed diatoms was found during the study (**Figure 8**). This was also true for other diatoms detected in this study (data not shown). The maximum abundance of the vegetative cells in the water column reached between 10^9- 10^{10} cells m^{-2} for *Ch. debilis* and *Skeletonema* spp., between 10^8 – 10^9 cells m^{-2} for *Ch. didymus* and between 10^7 – 10^8 cells m^{-2} for *Ce. Pelagica*, *Ch. distans*, and *Le. danicus*. In the PET chamber, the emergence flux exceeded 1.0×10^5 cells m^{-2} day^{-1} for *Ch. debilis* and *Skeletonema* spp. For other species, the maximum flux was in the range between 10^2-10^4 cells m^{-2} day^{-1}. The abundance of the vegetative cells in the water column and the emergence flux in the PET chamber for each of these five species and *Skeletonema* spp. varied notably during the study period, but no clear relationships were found in the temporal changes between either of them (the abundance of the vegetative cells or the emergence flux) and any of the environmental parameters, such as water temperature, salinity, DO, light intensity and concentrations of nutrients.

For these diatom taxa, in many cases their vegetative cells occurred in the water column when their cells emerged in the PET chamber. Analysis of the relationship between the abundance of the vegetative cells and the emergence flux by Spearman's rank test revealed a significant positive relationship for *Ch. debilis* (r = 0.50, n = 23, $p < 0.05$), *Ch. didymus* (r = 0.47, n = 23, $p < 0.05$) and *Skeletonema* spp. (r = 0.76, n = 23, $p < 0.01$), but not for *Ch. distans* (r = 0.41, n = 23, $p > 0.05$), *Le. danicus* (r = 0.38, n = 23, $p > 0.05$) and *Ce. pelagica* (r = 0.36, n = 23, $p > 0.05$) (**Table 2**).

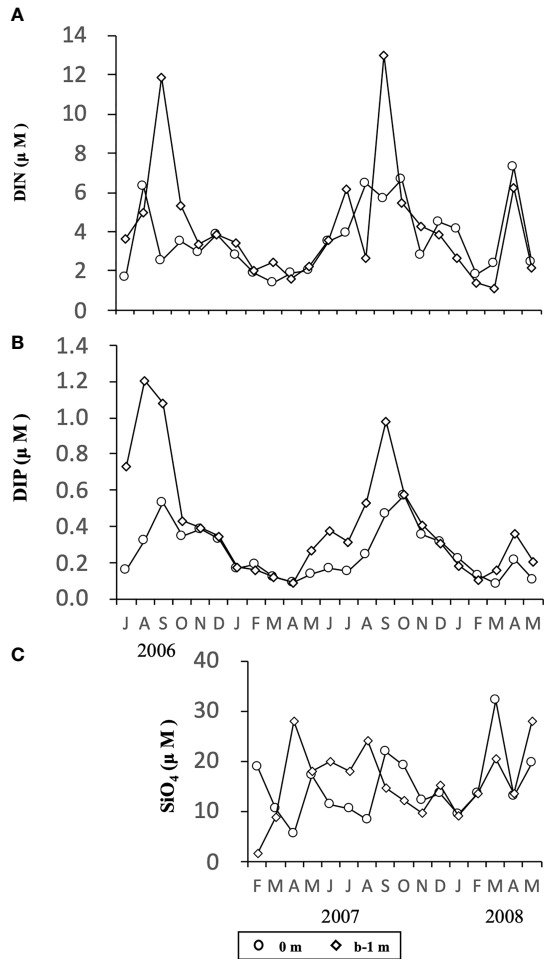

FIGURE 6 | Temporal changes in concentrations of DIN **(A)**, DIP **(B)** and SiO_4 **(C)** at the depth of 0 m and b-1 m at the sampling site in Ago Bay. b-1 m denotes the depth at 1 m above the bottom.

Throughout the PET chamber experiments, vegetative cells were not observed in the chamber employed as a control, confirming that there was no contamination from outside the PET chamber.

In the water samples of the flocculent layer obtained in July 2020, many diatom species forming long chains of vegetative cells with distinct chloroplasts in each cell were observed. *Chaetoceros* species dominated, but other genera (*Bacteriastrum* and *Skeletonema*) were also observed (**Figure 9**).

DISCUSSION

Vegetative Cells Emerged in the PET Chamber

In one of the samples of the PET chamber, a single vegetative cell with chloroplasts was observed just beside the valve of the resting spore (**Figure 7G**). Following the identification criteria for the species of the resting spores of diatoms presented by Ishii et al. (2011), the valve was morphologically identified as that of *Ch. debilis*, indicating that this single cell should have been a cell that germinated from a resting spore of the species during the 24 h of the PET chamber experiment. Similar cells were also observed for other species (photographs not shown). In addition, no contaminations of vegetative cells were observed in the PET chamber used as a control. These support that the monitoring of germinated/rejuvenated cells in the *in situ* sediment using the PET chamber was successful in this study.

Apart from the germinating cells, a large number of vegetative cells of diatom species which have not been known to form resting stage cells were observed in the PET chamber. The number of such species was 24, constituting about half of the total species that emerged in the PET chamber during the study period (**Table 1**). However, as suggested by Lewis et al. (1999) and Ueno and Ishikawa (2009), many unknown species of diatoms that form resting stage cells might exist. In this context, it is noteworthy that the resting stage cells of six species (*Actinoptycus senarius*, *Biddulphia alternans*, *Detonula pumila*, *Lithodesmium variabile*, *Odontella longicruris* and *O. mobiliensis*) were reported in the sediments collected in Ago Bay (Ishii et al., 2012) and the vegetative cells of all of these species emerged in the PET chamber in this study (**Table 1**). Therefore, it is possible that some additional species that emerged in the PET chamber can form resting stage cells.

It is intriguing that many long chains consisting of 4 or more cells were observed in the samples of the PET chamber (e.g., **Figures 7J, Ab, Af**). Considering that the cell division rate of diatoms is known to generally be one to two times per day, even for the fastest dividing species (Eppley, 1977; Frunas, 1990; Itakura et al., 1993), it is unlikely that those chains were formed after germination/rejuvenation of the resting stage cells within 24 h in the PET chamber experiments, suggesting that the vegetative cells consisting of the long chains had existed originally on the surface sediment before the experiment of the PET chamber started. Indeed, in the samples of the flocculent layer, many diatom species forming long chains of vegetative cells with distinct chloroplasts in each cell were observed (**Figure 9**). Vegetative cells were also found in the water of the benthic boundary layer (flocculent layer) off Oregon, U.S.A. (Wetz et al., 2004).

Vegetative cells could grow at light intensities > 9.4 μmol photons m^{-2} s^{-1} for *Skeletonema costatum* (sensu lato) (Itakura, 2000) and > 10 μmol photons m^{-2} s^{-1} for *Coscinodiscus wailesii* (Nishikawa and Yamaguchi, 2006) and *Eucampia zodiacus* (Nishikawa and Yamaguchi, 2008). This suggests that the two types of the living diatoms forming long chains in the flocculent layer of the surface sediment at the sampling site, where light almost always penetrated to the bottom (average depth 11 m) at intensities of > 10 μmol photons m^{-2} s^{-1} (**Figure 5B**), were present, although they could not be differentiated, as follows:

(1) the vegetative cells reproduced in the flocculent layer after germination/rejuvenation prior to the PET chamber experiment

TABLE 1 | Compiled list of species (genus) of centric diatoms observed in the water column and PET chamber at the sampling site in Ago Bay, during the period from July 2006 to May 2008.

Diatom species (genus)	Appearance		Type of resting stage cells	References**
	Water column	PET		
Actinocyclus spp.	○	○	–	
Actinoptychus senarius Ehrenberg	○	○	RC	Ishii et al., 2012; Belmonte and Rubino, 2019
Asteromphalus hyalinus Karsten*	○	○		
Bacteriastrum delicatulum Cleve	○		RS	Hargraves, 1976; Belmonte and Rubino, 2019
Ba. elongatum Cleve*	○	○		
Ba. furcatum Shadbolt	○	○	RS	Karsten, 1905; Belmonte and Rubino, 2019
Ba. hyalinum Lauder	○	○	RS	Cupp, 1943; Belmonte and Rubino, 2019
Biddulphia alternans (Bailey) Van Heurck	○	○	RC	Ishii et al., 2012; Belmonte and Rubino, 2019
Cerataulina dentata Hasle*	○	○		
Ce. pelagica (Cleve) Hendey	○	○	RS	Saunders, 1968
Chaetoceros affinis Lauder	○	○	RS	Gran and Yendo, 1914; Stockwell and Hargraves, 1986; Belmonte and Rubino, 2019; Saunders, 1968
Ch. anastomosans Grunow	○		RS	Stockwell and Hargraves, 1986; Belmonte and Rubino, 2019
Ch. borealis Bailey*	○			
Ch. brevis Schütt	○		RS	Cupp, 1943; Stockwell and Hargraves, 1986; Belmonte and Rubino, 2019
Ch. constrictus Gran	○		RS	Gran, 1912; Cupp, 1943; Stockwell and Hargraves, 1986; Belmonte and Rubino, 2019
Ch. contortus Schütt	○	○	RS	Jensen and Moestrup, 1998; Belmonte and Rubino, 2019
Ch. coronatus Gran	○	○	RS	Stockwell and Hargraves, 1986; Belmonte and Rubino, 2019
Ch. curvisetus Cleve	○	○	RS	Cupp, 1943; Rines and Hargraves, 1990; Belmonte and Rubino, 2019
Ch. danicus Cleve*	○	○		
Ch. debilis Cleve	○	○	RS	Cupp, 1943; Garrison, 1981; Belmonte and Rubino, 2019
Ch. decipiens Cleve*	○	○		
Ch. densus (Cleve) Cleve*	○			
Ch. diadema (Ehrenberg) Gran	○	○	RS	Gran and Yendo, 1914; Hargraves, 1972; Belmonte and Rubino, 2019
Ch. didymus Ehrenberg	○	○	RS	Karsten, 1905; Garrison, 1981; Belmonte and Rubino, 2019
Ch. distans Cleve	○	○	RS	Gran and Yendo, 1914; Stockwell and Hargraves, 1986; Belmonte and Rubino, 2019
Ch. eibenii Grunow	○		RS	Pavillard, 1921; Stockwell and Hargraves, 1986; Belmonte and Rubino, 2019
Ch. laciniosus Schütt	○	○	RS	Cupp, 1943; Stockwell and Hargraves, 1986; Belmonte and Rubino, 2019
Ch. lauderi Ralfs and Lauder	○	○	RS	Gran and Yendo, 1914; Stockwell and Hargraves, 1986; Belmonte and Rubino, 2019
Ch. lorenzianus Grunow	○	○	RS	Gran and Yendo, 1914; Stockwell and Hargraves, 1986; Belmonte and Rubino, 2019
Ch. pelagicus Cleve*	○			
Ch. peruvianus Brightwell*	○	○		
Ch. pseudocurvisetus Mangin	○	○	RS	Stockwell and Hargraves, 1986; Belmonte and Rubino, 2019
Ch. radicans Schütt	○	○	RS	Cupp, 1943; Garrison, 1981; Belmonte and Rubino, 2019
Ch. rostratus Ralfs*	○	○		
Ch. seiracanthus Gran	○	○	RS	Karsten, 1905; Stockwell and Hargraves, 1986; Belmonte and Rubino, 2019
Ch. siamense Ostenfeld	○		RS	Stockwell and Hargraves, 1986; Belmonte and Rubino, 2019
Ch. socialis Lauder	○	○	RS	Cupp, 1943; Stockwell and Hargraves, 1986; Belmonte and Rubino, 2019
Ch. tortissimus Gran*	○	○		
Ch. wighamii Brightwell	○	○	RS	Cupp, 1943; Stockwell and Hargraves, 1986; Belmonte and Rubino, 2019
Chaetoceros spp.	○	○	–	
Climacodium frauenfeldianum Grunow*	○			
Corethron pennatum (Grunow) Ostenfeld*	○	○		
Coscinodiscus gigas Ehrenberg*	○	○		
Cos. granii Gough*	○	○		
Cos. wailesii Gran and Angst	○	○	RC	Nagai et al., 1995
Coscinodiscus spp.	○	○	–	
Cyclotella spp.	○	○	–	
Dactyliosolen fragilissimus (Bergon) Hasle*	○	○		
Da. tenuijunctus (Manguin) Hasle*	○	○		
Detonula pumila (Castracane) Gran	○	○	RC	Ishii et al., 2012; Belmonte and Rubino, 2019
Ditylum brightwellii (West) Grunow	○	○	RS	Cupp, 1943; Hargraves, 1976; Hargraves, 1984; Belmonte and Rubino, 2019
Di. sol (Grunow) De Toni*	○			
Eucampia cornuta (Cleve) Grunow*	○			
Eu. zodiacus Ehrenberg*	○	○		
Guinardia delicatula (Cleve) Hasle*	○	○		
Gu. flaccida (Castracane) Peragallo*	○	○		
Gu. striata (Stolterfoth) Hasle*	○	○		

(Continued)

TABLE 1 | Continued

Diatom species (genus)	Appearance		Type of resting stage cells	References**
	Water column	PET		
Helicotheca tamesis (Shrubsole) Ricard*	○	○		
Hemiaulus hauckii Grunow and Van Heurck*	○			
Hem. sinensis Greville*	○			
Hyalodiscus subtilis Bailey*	○	○		
Lauderia annulata Cleve*	○	○		
Leptocylindrus danicus Cleve	○	○	RS	Gran, 1912; Cupp, 1943; Hargraves, 1976; Belmonte and Rubino, 2019
Lithodesmium undulatum Ehrenberg*	○	○		
Li. variabile Takano	○	○	RC	Ishii et al., 2012; Belmonte and Rubino, 2019
Melosira nummuloides Agardh*	○	○		
Neocalyptrella robusta (Norman and Ralfs) Hernández-Becerril and Meave del Castillo*	○			
Odontella aurita (Lyngbye) Agardh	○		RC	McQuoid and Hobson, 1996; Belmonte and Rubino, 2019
Od. longicruris (Greville) Hoban	○	○	RC	Ishii et al., 2012; Belmonte and Rubino, 2019
Paralia sulcata (Ehrenberg) Cleve	○	○	RS	Cupp, 1943; McQuoid and Hobson, 1996; Belmonte and Rubino, 2019
Proboscia alata (Brightwell) Sundström	○		RS	Cupp, 1943; McQuoid and Hobson, 1996; Belmonte and Rubino, 2019
Pr. indica (Peragallo) Hernández-Becerril*	○			
Pseudosolenia calcar-avis (Schultze) Sundström*	○			
Rhizosolenia crassispina Schröder*	○			
Rh. formosa Peragallo	○		RS	von Stosch, 1967; Belmonte and Rubino, 2019
Rh. hyalina Ostenfeld*	○	○		
Rh. setigera Brightwell	○	○	RS	Cupp, 1943; von Stosch, 1967; Belmonte and Rubino, 2019
Rh. striata Greville*	○	○		
Rh. styliformis Brightwell*	○			
Skeletonema spp.	○	○	–	
Stephanopyxis nipponica Gran and Yendo	○		RS	Haga, 1997; Belmonte and Rubino, 2019
St. palmeriana (Greville) Grunow	○	○	RS	Gran and Angst, 1931; Drebes, 1966; Belmonte and Rubino, 2019
Trieres mobiliensis (Bailey) Ashworth and Theriot	○		RC	Ishii et al., 2012 (as *Odontella mobiliensis*); Belmonte and Rubino, 2019
Trigonium alternans (Bailey) Mann	○	○	RC	Ishii et al., 2012
Thalassiosira spp.	○	○	–	

*Formation of the resting stage cells is unknown.

Open circles denote species (genus) which were observed in the water/PET samples. RS and RC in the column of 'Type of resting stage cells' indicate resting spore and resting cell, respectively.

**Representative references reporting RS/RC.*

(2) the vegetative cells had been deposited from the water column into the flocculent layer prior to the PET chamber experiment

In this study, the presence of diatom cells forming long chains in the flocculent layer was revealed by the PET chamber experiment. This is the reason why we used the term 'emergence' for the flux measured by the PET chamber rather than 'germination/rejuvenation'.

Relationship Between Emergence of the Vegetative Cells and Environmental Factors

Throughout the study period, the emergence flux of the diatoms fluctuated largely but no clear trends of temporal changes appeared (**Figure 8**). Itakura (2000) reported, on the basis of laboratory culture experiments, that the resting stage cells of diatoms (*Sk. costatum* (sl), *Chaetoceros* spp. and *Thalassiosira* spp.) could germinate/rejuvenate from the sediments collected at Hiroshima Bay, Japan, at temperatures from 10 – 28°C and suggested that temperature is not a limiting factor on the germination/rejuvenation of their resting stage cells. Meanwhile, the vegetative cells that emerged in the PET chamber included not only the vegetative cells that germinated/rejuvenated from the sediment but also two types of cells forming long chains, as described above. The vegetative cells of the diatoms generally grow at a wide range of temperatures in laboratory experiments (Eppley, 1977). Furthermore, it has been reported that no obvious trends of temporal changes in the occurrence of vegetative cells in the water column were observed (Itakura et al., 1997; Itakura, 2000). These findings indicate that the temporal change of emergence flux could not be determined by the temporal change of temperature. In addition, there seemed to be no clear relationships between any environmental condition (salinity, DO, light intensity, or nutrients) and emergence flux in this study. On the other hand, it is well known that light is a primary factor to induce germination/rejuvenation of diatom resting stage cells (Hollibaugh et al., 1981; Imai et al., 1996).

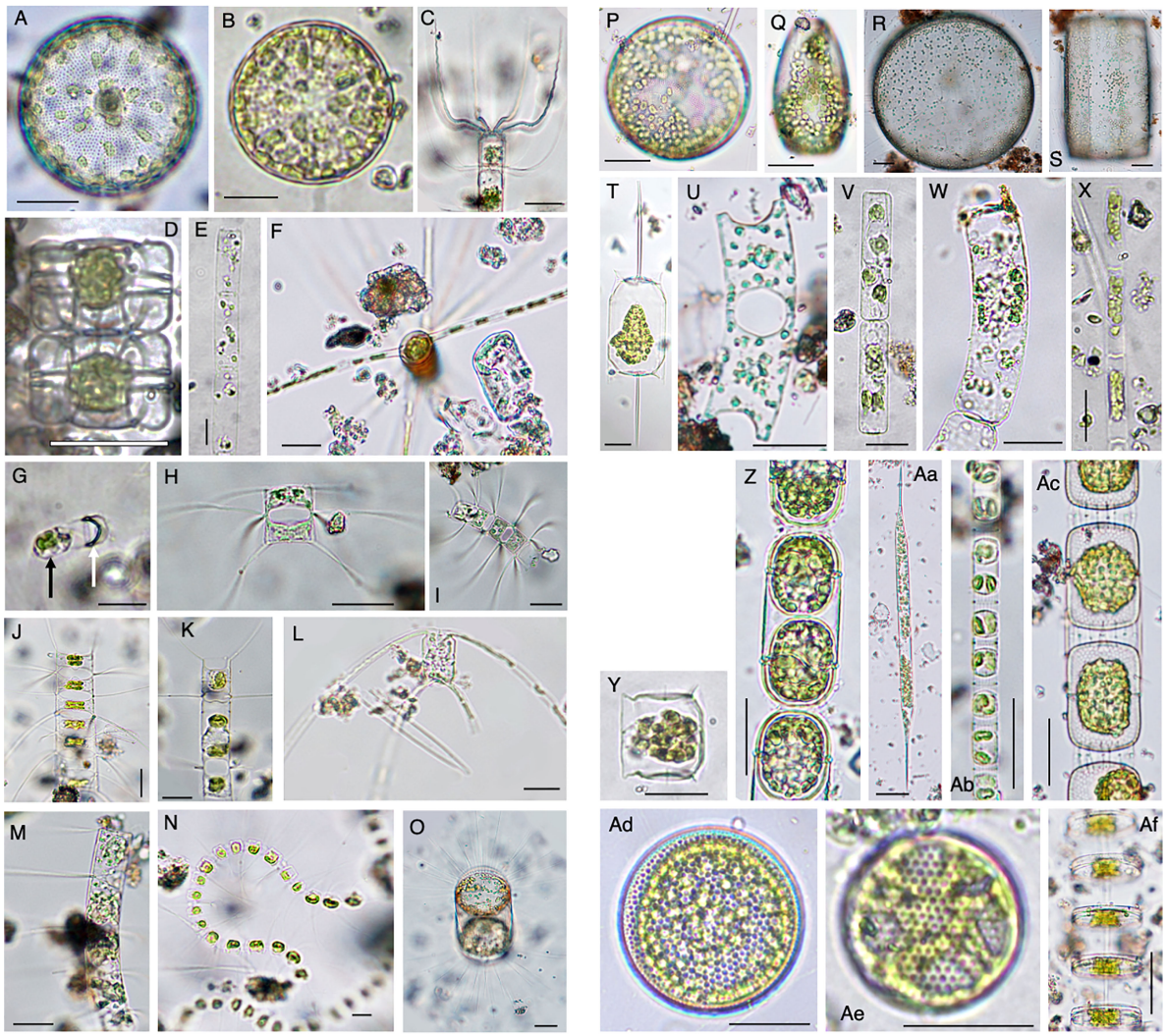

FIGURE 7 | Photomicrographs showing representative centric diatoms that emerged in the PET chamber. *Actinocyclus* sp. **(A)**, *Actinoptychus senarius* **(B)**, *Bacteriastrum elongatum* **(C)**, *Biddulphia alternans* **(D)**, *Cerataulina pelagica* **(E)**, *Chaetoceros danicus* **(F)**, *Chaetoceros debilis* **(G–I)**, *Chaetoceros didymus* **(J)**, *Chaetoceros distans* **(K)**, *Chaetoceros peruvianus* **(L)**, *Chaetoceros pseudocurvisetus* **(M)**, *Chaetoceros socialis* **(N)**, *Corethron pennatum* **(O)**, *Coscinodiscus granii* **(P, Q)**, *Coscinodiscus wailesii* **(R, S)**, *Ditylum brightwellii* **(T)**, *Eucampia zodiacus* **(U)**, *Guinardia delicatula* **(V)**, *Guinardia striata* **(W)**, *Leptocylindrus danicus* **(X)**, *Lithodesmium variabile* **(Y)**, *Melosira nummuloides* **(Z)**, *Rhizosolenia setigera* **(Aa)**, *Skeletonema* sp. **(Ab)**, *Stephanopyxis palmeriana* **(Ac)**, *Thalassiosira* spp. **(Ad–Af)**. In **(G)**, black and white arrows indicate a vegetative cell just after germination and a valve of the resting spore, respectively. Scale bars: 50 μm.

Hollibaugh et al. (1981) reported that resting stage cells of three species of the genus *Chaetoceros* did not germinate at a light intensity of 1.3 μmol photons m^{-2} s^{-1} or less. Itakura (2000) also reported that resting stage cells of *Ch. didymus* could not germinate under a low light intensity of 0.25 μmol photons m^{-2} s^{-1} or less, but could actively do so at a light intensity of 12 μmol photons m^{-2} s^{-1} or over. Furthermore, Imai et al. (1996) revealed that resting stage cells of *Sk. costatum* (sl) and *Chaetoceros* spp. needed a light intensity of about 4 μmol photons m^{-2} s^{-1} or over for germination/rejuvenation. Since the light during daytime almost always penetrated to the bottom at intensities > 10 μmol photons m^{-2} s^{-1} throughout the study period at the present study site and its average intensity during the period of PET chamber experiments was 27.3 μmol photons m^{-2} s^{-1}, it should not be considered that light was a limiting factor on the germination/rejuvenation of resting stage cells of the diatoms that emerged in the PET chamber and on the maintenance of the two types of vegetative cells mentioned above. Therefore, unlike in deeper seas with lower light intensity, such as the Seto Inland Sea of Japan (Imai et al., 1996) and the East China Sea (Ishikawa and Furuya, 2004), where the resting stage cells in the sediment cannot germinate/rejuvenate unless those cells reach the

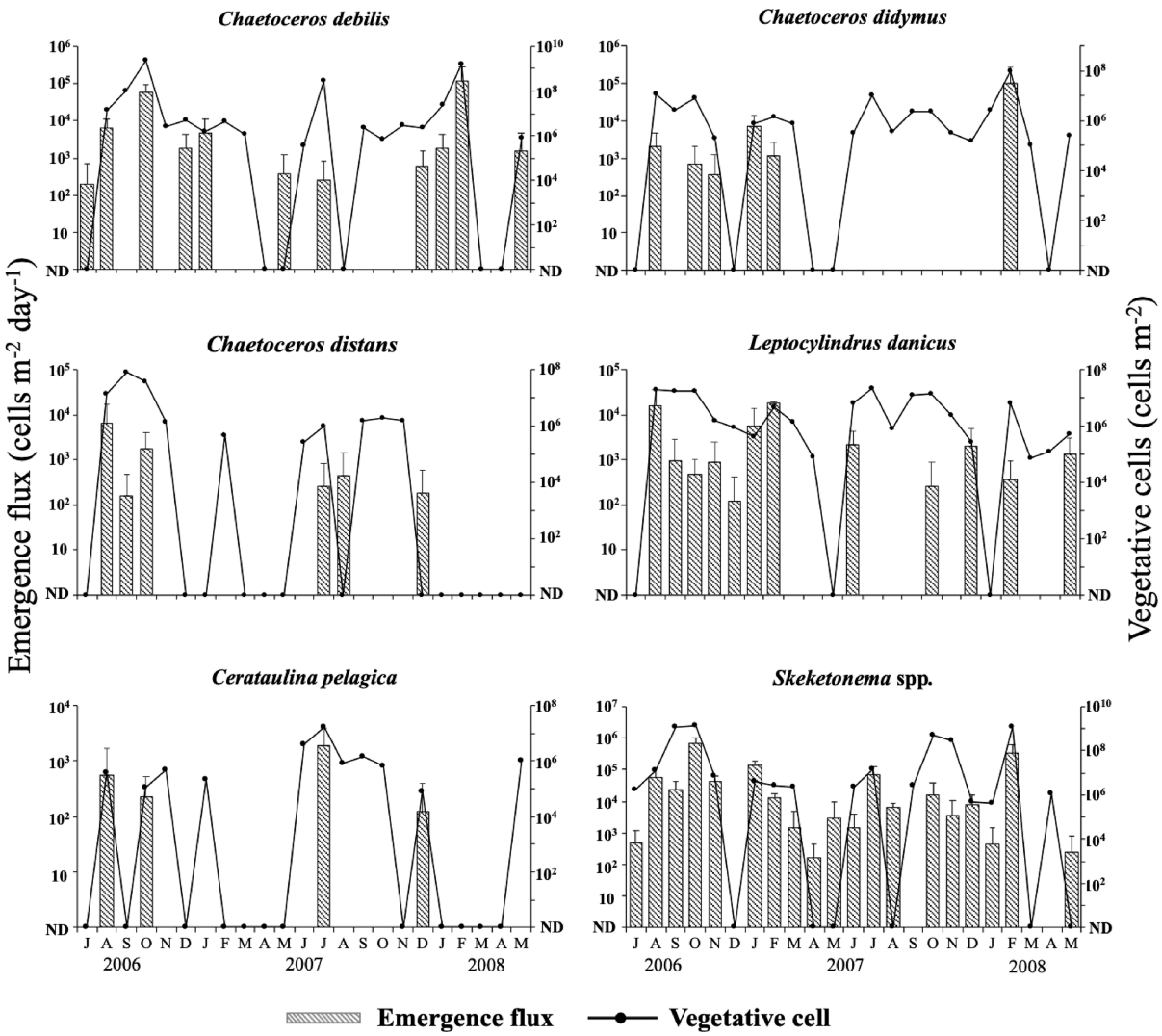

FIGURE 8 | Temporal changes in the integrated abundance of the vegetative cells in the water column and the emergence flux in the PET chamber for six diatom taxa at the sampling site in Ago Bay. ND denotes that the cells were not detected. Bars represent standard deviations (+SD).

euphotic layer as a result of mixing of the water column, the seafloor in a shallow embayment such as Ago Bay could provide an advantageous environment for diatoms to maintain their vegetative cells in the flocculent layer on the surface sediment even if there were no mixing of the water column.

TABLE 2 | Correlations between the integrated abundance of the vegetative cells (cells m^{-2}) in the water column and the emergence flux (cells m^{-2} day^{-1}) revealed by the Spearman's rank test.

Species	Spearman	Significance
Cerataulina pelagica	0.36	
Chatoceros debilis	0.50	*
Ch. didymus	0.47	*
Ch. distans	0.41	
Leptocylindrus danicus	0.38	
Skeletonema spp.	0.76	**

*Significance level: *p < 0.05, **p < 0.01.*

Quantitative Relationships Between Both the Vegetative Cells in the Water Column and Those in the PET Chamber

Since the cells that emerged in the PET chamber consisted of various types of vegetative cells, careful interpretation is needed to quantitatively compare the relationships between the abundance of the vegetative cells in the water column and emergence flux. However, even if it is assumed that all the vegetative cells in the PET chamber were resuspended into the water column at the same time, the level of statistical significance varied depending on the diatom taxa (**Table 2**).

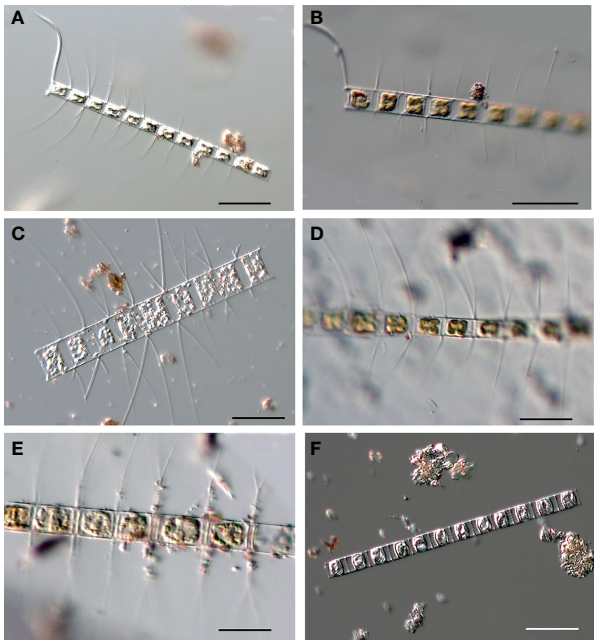

FIGURE 9 | Photomicrographs, as examples, of the diatoms forming long chains observed in the flocculent layer of the sediment core sample collected at the PET chamber experiment site in Ago Bay. *Chaetoceros affinis* **(A, B)**, *Chaetoceros lorenzianus* **(C)**, *Chaetoceros compressus* **(D)**, *Bacteriastrum* sp. **(E)**, *Skeletonema* sp. **(F)**. Scale bars: 50 μm.

Furthermore, several cases of disagreement were found for the relationships between the abundance of the vegetative cells and the emergence flux, even for the species (i.e., *Ch. debilis* and *Ch. didymus*) that showed a significant positive relationship. Namely, there were some cases when a large population of the vegetative cells occurred in the water column despite small emergence flux in the PET chamber (e.g., *Ch. debilis* in July 2007, *Ch. didymus* in October 2006 and February 2007). This was true for *Skeletonema* spp. (e.g., in October and November 2007), although it is necessary to pay attention to the statistical interpretation of the significant result due to the possibility of the content of multiple species. As pointed out for the case of dinoflagellates whose germination rate/flux was monitored (Ishikawa and Taniguchi, 1996; Ishikawa et al., 2014), these above considerations demonstrated that the magnitude of the emergence flux does not determine that of the vegetative populations in the water column, since the growth of the vegetative cells is largely dependent on complex factors, such as water temperature, light intensity, concentration of nutrients, competition with other phytoplankton species and predation by zooplankton. Namely, like to cyst-forming dinoflagellates (e.g., Ishikawa and Taniguchi, 1996; Ishikawa et al., 2014), the presence of vegetative cells, even in small numbers, in the water column by recruitment of the vegetative cells on the surface sediment (flocculent layer) as 'seeds' is important for proliferation of the diatoms at the time when environmental conditions become favorable for vegetative growth.

On the seafloor in a shallow embayment, such as Ago Bay, where the light always penetrates, various types of the vegetative cells demonstrated above wait for recruitment into the water column as seeds. This means that the flocculent layer on the seafloor acts as a 'refuge and nursery' for the vegetative population in the water column.

Life Cycle Strategies of Diatoms in a Shallow Coastal Waters

It has generally been suggested that the resting stage cells require resuspension, for their germination/rejuvenation, into the euphotic layer from the surface sediment by water mixing, as summarized in **Figure 1**. However, resuspension might be a dispensable condition for the cells to germinate/rejuvenate in a shallow embayment, such as Ago Bay, since the light penetrates to the seafloor. In addition, even the vegetative cells germinated/rejuvenated from the surface sediment and/or deposited from the water column could be alive on the surface sediment, as mentioned above. Based on this point of view, we propose three patterns of life cycle strategies for the diatoms in the bay (**Figure 10**);

Pattern 1: the resting stage cells, which are resuspended from the surface sediment into the upper layer where the light condition is more favorable for their vegetative growth, germinate/rejuvenate (**Figure 10A**).

Pattern 2: the resting stage cells germinated/rejuvenated on the surface sediment remain as the forms of the vegetative cells in the flocculent layer of the surface sediment, waiting for the opportunity to be resuspended into the upper layer (**Figure 10B**).

Pattern 3: the vegetative cells once deposited from the water column in the flocculent layer of the surface sediment remain there until being resuspended into the upper layer (**Figure 10C**).

Consequently, the seafloor in a shallow embayment, where the light penetrates, enables the diatoms to possess not only a simple life cycle strategy that proceeds from the resting stage cells to the vegetative cells, but also unique strategies that proceed from the vegetative cells to the vegetative cells. These links between the planktonic forms and the benthic forms might be recognized as complex life cycle strategies of the diatoms. In conclusion, such complex life cycle strategies could promote the thriving of the diatoms in the temperate coastal waters/embayment where the environmental conditions vary widely throughout the seasons.

Further investigations of the emergence of the diatoms using the PET chamber are needed to get a better understanding of their population dynamics in different locations, including deep sea areas.

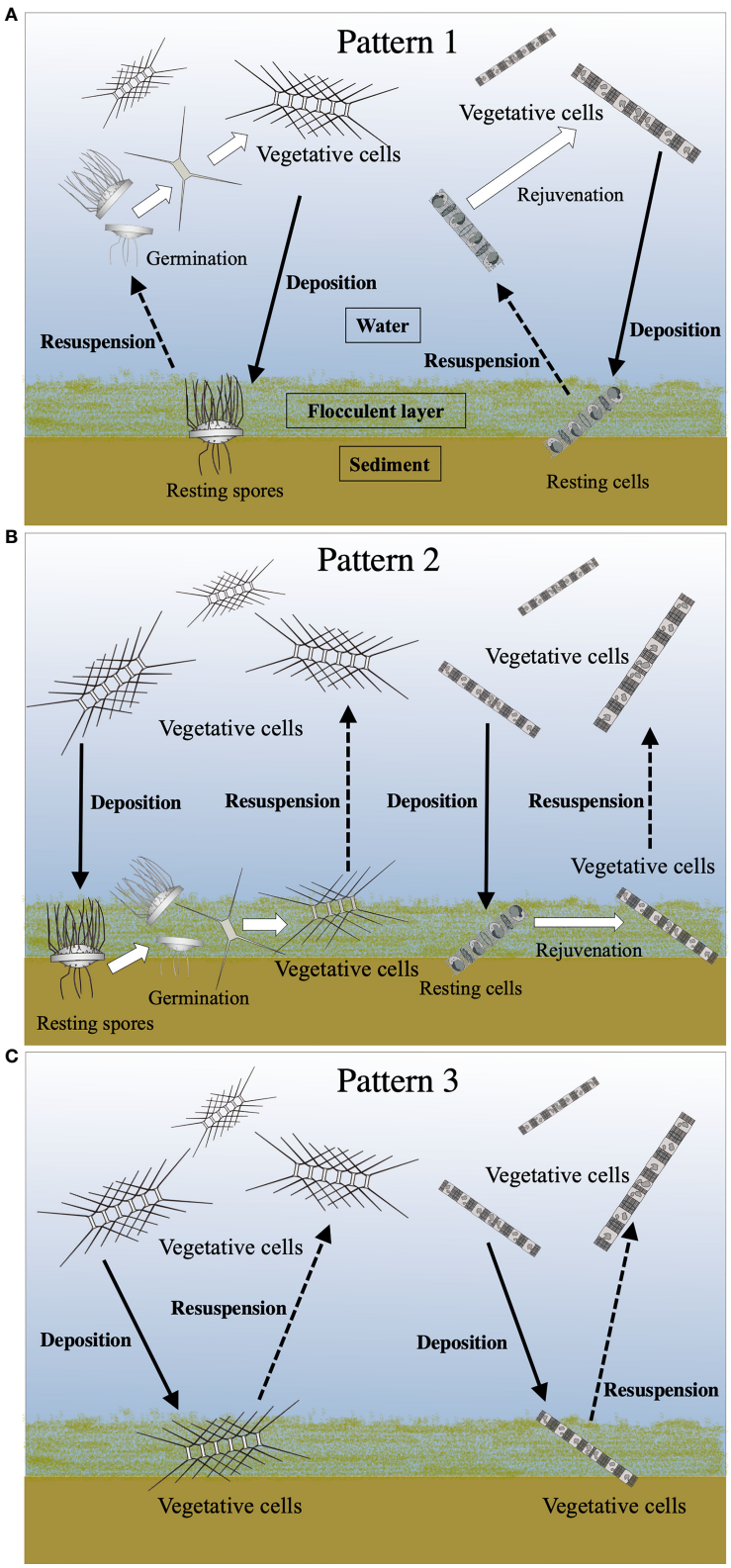

FIGURE 10 | Conceptual diagrams of various life cycle patterns of the centric diatoms. See the text for details of Pattern 1 **(A)**, Pattern 2 **(B)** and Pattern 3 **(C)**. Solid and dotted lines indicate the movement (deposition and resuspension, respectively) of the cells between the water column and the surface sediment. White arrows denote transformations of the cell stage.

DATA AVAILABILITY STATEMENT

The raw data supporting the conclusions of this article will be made available by the authors, without undue reservation.

AUTHOR CONTRIBUTIONS

AI and KI designed and conducted the research, and collected the data. All authors contributed to data interpretation. KI wrote the first version of the manuscript and AI edited it. KM and II reviewed the manuscript. All authors approved the submitted version.

FUNDING

This study was supported by a Grant-in-Aid for Scientific Research (C) (18580180) from the Japan Society for the Promotion of Science.

ACKNOWLEDGMENTS

We are grateful to Dr. Keigo Yamamoto of the Research Institute of Environment, Agriculture and Fisheries, Osaka Prefecture, for his kind cooperation in nutrient analysis. We also express our sincere thanks to Dr. Taisuke Otsuka of the Lake Biwa Museum, Shiga Prefecture, for his kind guidance in statistical analysis of the data. Our special thanks are extended to the staff members of the Fisheries Research Laboratory of Mie University and our colleagues at the university for their help in the field work.

REFERENCES

Belmonte, G., and Rubino, F. (2019). "Resting cysts from coastal marine plankton", in *Oceanography and Marine Biology, An Annual Review,*. Eds. S. J. Hawkins, A. L. Allcock, A. E. Bates, L. B. Firth, I. P. Smith, S. E. Swearer and P. A. Todd (Boca Raton: CRC Press), 57, 1–88.

Cupp, E. E. (1943). *Marine Plankton Diatoms of the West Coast of North America* (Berkeley: University of California Press).

Dale, B. (1983). "Dinoflagellate Resting Cysts: Benthic Plankton", in *Survival Strategies of the Algae*. Ed. G. A. Frexell (Cambridge: Cambridge University Press), 69–136.

Drebes, G. (1966). On the Life History of the Marine Plankton Diatom *Stephanopyxis Palmeriana*. *Helgol. Wiss. Meeresunters* 13, 101–114. doi: 10.1007/BF01612659

Eppley, R. W. (1977). "The Growth and Culture of Diatoms", in *The Biology of Diatom*. Ed. D. Werner (Oxford: Blackwell Scientific Publications), 24–64.

Furnas, M. J. (1990). *In situ* growth rate of marine phytoplankton: approached to measurement, community and species growth rates. *J. Plankton Res.* 12, 1117–1151. doi: 10.1093/plankt/12.6.1117

Garrison, D. L. (1981). Monterey Bay Phytoplankton. II. Resting Spore Cycles in Coastal Diatom Populations. *J. Plankton Res.* 3, 137–156. doi: 10.1093/plankt/3.1.137

Gran, H. H. (1912). "Pelagic Plant Life", in *The Depths of the Ocean*. Eds. J. Murray and J. Hijort (London: Macmillan & Co., Ltd), 307–386.

Gran, H. H., and Angst, E. C. (1931). Plankton Diatoms of Puget Sound. *Publ. Puget Sound Biol. Sta. Univ. Wash.* 7, 417–519.

Gran, H. H., and Yendo, K. (1914). *Japanese Diatoms. I. On Chaetoceras. II. On Stephanopyxia (Videnskapsselskapets Skrifter. I. Mat.-Naturu. Klasse. 1913. No. 8)* (Christiania: Utgit for Friftjof Nansens Fond).

Haga, M. (1997). Morphology of Vegetative and Resting Spore Valves of. *Stephanopyxis Nipponica. Diatom Res.* 12, 217–228. doi: 10.1080/0269249X.1997.9705416

Hargraves, P. E. (1972). Studies on Marine Plankton Diatom. I. *Chaetoceros Diadema* (Ehr.) Gran: Life Cycle, Structural Morphology, and Regional Distribution. *Phycologia* 11, 247–257. doi: 10.2216/i0031-8884-11-3-247.1

Hargraves, P. E. (1976). Studies on Marine Plankton Diatoms.II. Resting Spore Morphology. *J. Phycol.* 12, 118–128. doi: 10.1111/j.1529-8817.1976.tb02838.x

Hargraves, P. E. (1984). "Resting Spore Formation in the Marine Diatom *Ditylum Brightwellii* (West) Gran", in *Proceedings of the Seventh International Diatom Symposium*. Ed. D. G. Mann (Koenigstein: O. Koeltz Science Publishers), 33–46.

Hargraves, P. E. (1990). Studies on Marine Plankton Diatoms. V. Morphology and Distribution on *Leptocylindrus Minimus* Gran. *Beihefte zur Nova Hedwigia* 100, 47–60.

Hargraves, P. E., and French, F. W. (1983). "Diatom Resting Spores: Significance and Strategies", in *Survival Strategies of the Algae*. Ed. G. A. Fryxell (New York: Cambridge University Press), 49–68.

Hasle, G. R. (1978). "The Inverted-Microscope Method", in *Phytoplankton Manual*. Ed. A. Sournia (Paris: UNESCO), 88–96.

Hasle, G. R., and Sims, P. A. (1985). The Morphology of the Diatom Resting Spores *Syringidium Bicorne* and *Syringidium Simplex*. *Bri. Phycol. J.* 20, 219–225. doi: 10.1080/00071618500650231

Hasle, G. R., and Syvertsen, E. E. (1997). "Marine Diatoms", in *Identifying Marine Phytoplankton*. Ed. C. R. Tomas (San Diego: Academic press), 5–385.

Hollibaugh, J. T., Seibert, D. L. R., and Thomas, W. H. (1981). Observations on the Survival and Germination of Resting Spores of Three *Chaetoceros* (Bacillariophyceae) Species. *J. Phycol.* 17, 1–9. doi: 10.1111/j.1529-8817.1981.tb00812.x

Imai, I., Itakura, S., Yamaguchi, M., and Honjo, T. (1996). "Selective Germination of *Heterosigma Akashiwo* (Raphidophyceae) Cysts in Bottom Sediments Under Low Light Condition: A Possible Mechanism of Red Tide Initiation", in *Harmful and Toxic Algal Blooms*. Eds. T. Yasumoto, Y. Oshima and Y. Fukuyo (Paris: UNESCO), 197–200.

Ishii, K., Ishikawa, A., and Imai, I. (2012). Newly Identified Resting Stage Cells of Diatoms From Sediments Collected in Ago Bay, Central Part of Japan. *Plankton Benthos Res.* 7, 1–7. doi: 10.3800/pbr.7.1

Ishii, K., Iwataki, M., Matsuoka, K., and Imai, I. (2011). Proposal of Identification Criteria for Resting Spores of *Chaetoceros* Species (Bacillariophyceae) From a Temperate Coastal Sea. *Phycologia* 50, 351–362. doi: 10.2216/10-36.1

Ishikawa, A., and Furuya, K. (2004). The Role of Diatom Resting Stages in the Onset of the Spring Bloom in the East China Sea. *Mar. Biol.* 145, 633–639. doi: 10.1007/s00227-004-1331-9

Ishikawa, A., Hattori, M., and Imai, I. (2007). Development of the "Plankton Emergence Trap/Chamber (PET Chamber)", A New Sampling Device to Collect *in Situ* Germinating Cells From Cysts of Microalgae in Surface Sediments of Coastal Waters. *Harmful Algae* 6, 301–307. doi: 10.1016/j.hal.2006.04.005

Ishikawa, A., Hattori, M., Ishii, K., Kulis, D. M., Anderson, D. M., and Imai, I. (2014). *In Situ* Dynamics of Cyst and Vegetative Cell Population of the Toxic Dinoflagellate *Alexandrium Catenella* in Ago Bay, Central Japan. *J. Plankton Res.* 36, 1333–1343. doi: 10.1093/plankt/fbu048

Ishikawa, A., and Taniguchi, A. (1996). Contribution of Benthic Cysts to the Population Dynamics of *Scrippsiella* Spp. (Dinophyceae) in Onagawa Bay, Northeast Japan. *Mar. Ecol. Prog. Ser.* 140, 169–178. doi: 10.3354/meps140169

Itakura, S. (2000). Physiological Ecology of the Resting Stage Cells of Coastal Planktonic Diatoms. *Bull. Fish. Environ. Inland Sea* 2, 67–130.

Itakura, S., Imai, I., and Itoh, K. (1997). "Seed Bank" of Coastal Planktonic Diatoms in Bottom Sediments of Hiroshima Bay, Seto Inland Sea, Japan. *Mar. Biol.* 128, 497–508. doi: 10.1007/s002270050116

Itakura, S., Yamaguchi, M., and Imai, I. (1993). Resting Spore Formation and Germination of *Chaetoceros Didymus* Var. *Protuberans* (Bacillariophyceae) in Clonal Culture. *Nippon Suisan Gakkaishi* 59, 807–813. doi: 10.2331/suisan.59.807

Japan Meteorological Agency (2008) *Precipitation*. Available at: https://www.data.jma.go.jp/gmd/risk/obsdl/ (Accessed on August 2021).

Jensen, K. G., and Moestrup, Ø. (1998). The Genus *Chaetoceros* (Bacillariophyceae) in Inner Danish Coastal Waters. *Opera Bot.* 133, 5–68. doi: 10.1111/j.1756-1051.1998.tb01103.x

Karsten, G. (1905). Das Phytoplankton Des Antarktischen Meeres Nach Dem Material Der Deutschen Tiefsee-Expedition 1898-1899. *Dtsch. Tiefsee Exped.* 2, 1–136.

Lewis, J., Haris, A. S. D., Jones, K. J., and Edmonds, R. L. (1999). Long-Term Survival of Marine Planktonic Diatoms and Dinoflagellates in Stored Sediment Samples. *J. Plankton Res.* 21, 343–354. doi: 10.1093/plankt/21.2.343

Margalef, R. (1958). "Temporal Succession and Spatial Heterogeneity in Natural Phytoplankton", in *Perspectives in Marine Biology*, Ed. A. A. Buzzati-Traverso (Barkley: University of California Press), 323–349.

McQuoid, M. R., and Hobson, L. A. (1996). Diatom Resting Stages. *J. Phycol.* 32, 889–902. doi: 10.1111/j.0022-3646.1996.00889.x

Montresor, M., Di Prisco, C., Sarno, D., Margiotta, F., and Zingone, A. (2013). Diversity and Germination Patterns of Diatom Resting Stages at a Coastal Mediterranean Site. *Mar. Ecol. Prog. Ser.* 484, 79–95. doi: 10.3354/meps10236

Nagai, S., Hori, Y., Manabe, T., and Imai, I. (1995). Morphology and Rejuvenation of *Coscinodiscus Wailesii* Gran (Bacillariophyceae) Resting Cells Found in Bottom Sediments of Harima-Nada, Seto Inland Sea, Japan. *Nippon Suisan Gakkaishi* 61, 179–185. doi: 10.2331/suisan.61.179

Nishikawa, T., and Yamaguchi, M. (2006). Effect of Temperature on Light-Limited Growth of the Harmful Diatom *Coscinodiscus Wailesii*, a Causative Organism in the Bleaching of Aqua-Cultured *Porphyra Thalli*. *Harmful Algae* 7, 561–566. doi: 10.1016/j.hal.2007.12.021

Nishikawa, T., and Yamaguchi, M. (2008). Effect of Temperature on Light-Limited Growth of the Harmful Diatom *Eucampia Zodiacus* Ehrenberg, a Causative Organism in the Discoloration of *Porphyra Thalli*. *Harmful Algae* 5, 141–147. doi: 10.1016/j.hal.2005.06.007

Pavillard, J. (1921). Sur La Reproduction Du *Chaetoceros Eibenii* Meunier. *Compt. Rend. Séanc. l'Acad. Sci.* 172, 469–471.

Pfiester, L. A., and Anderson, D. M. (1987). "Dinoflagellate Reproduction", in *The Biology of Dinoflagellates*. Ed. F. J. R. Taylor (Oxford: Blackwell), 611–648.

Pitcher, G. C. (1990). Phytoplankton Seed Populations of the Cape Peninsula Upwelling Plume, With Particular Reference to Resting Spores of *Chaetoceros* (Bacillariophyceae) and Their Role in Seeding Upwelling Waters. *Estuar. Coast. Shelf Sci.* 31, 283–301. doi: 10.1016/0272-7714(90)90105-Z

Reynolds, C. S. (1984). Phytoplankton Periodicity: The Interactions of Form, Function and Environmental Variability. *Freshw. Biol.* 14, 111–142. doi: 10.1111/j.1365-2427.1984.tb00027.x

Rines, J. E. B., and Hargraves, P. E. (1988). The *Chaetoceros* Ehrenberg (Bacillariophyceae) Flora of Narragansett Bay, Rhode Island, U.S.A. *Bibl. Psychiat.* 79, 1–196.

Rines, J. E. B., and Hargraves, P. E. (1990). Morphology and Taxonomy of *Chaetoceros Compressus* Lauder Var. *Hirtisetus* Var. Nova, With Preliminary Consideration of Closely Related Taxa. *Diatom Res.* 5, 113–127. doi: 10.1080/0269249X.1990.9705097

Sarno, D., Kooistra, W. H., Medlin, L. K., Percopo, I., and Zingone, A. (2005). Diversity in the Genus *Skeletonema* (Bacillariophyceae). II. An Assessment of the Taxonomy of *S. Costatum*-Like Species With the Description of Four New Species. *J. Phycol.* 41, 151–176. doi: 10.1111/j.1529-8817.2005.04067.x

Saunders, R. P. (1968). *Cerataulina Pelagica* (Cleve) Hendey. *Florida Board Conserv. Leaflet* 1 (Pt. 2, No. 5), 1–11.

Sicko-Goad, L. (1986). Rejuvenation of *Melosira Granulata* (Bacillariophyceae) Resting Cells From the Anoxic Sediments of Douglas Lake, Michigan. II. Electron Microscopy. *J. Phycol.* 22, 28–35. doi: 10.1111/j.1529-8817.1986.tb02510.x

Smayda, T. J. (1980). "Phytoplankton Species Succession", in *The Physiological Ecology of Phytoplakton*. Ed. I. Morris (Oxford: Blackwell), 493–570.

Stedinger, K. A. (1975). "Basic Factors Influencing Red Tides", in *Proceedings of the First International Conference on Toxic Dinoflagellate Blooms*. Ed. V. R. Lo-Cicero (Wakefield: Mass Sci Tech Found), 153–162.

Stockwell, D. A., and Hargraves, P. E. (1986). "Morphological Variability Within Resting Spores of the Marine Diatom Genus Chaetoceros Ehrenberg", in *Proceedings of the Eighth International Diatom Symposium*. Ed. M. Richard (Koenigstein: Koeltz Scientific Books), 81–95.

Strickland, J. D. H., and Parsons, T. R. (1972). A Practical Handbook of Seawater Analysis. *Fish. Res. Bd. Can. Bull.* 167, 1–310.

Ueno, R., and Ishikawa, A. (2009). Evaluation of Functionality as a Seed Population of Resting Stage Cells of Centric Diatoms in Surface Sediments of Ago Bay, Central Part of Japan. *Bull. Plankton Soc. Jpn.* 56, 1–12.

von Stosch, H. A. (1967). "Diatomeen", in *Vegetative Fortpflanzung, Parthenogense Und Apogamie Bei Algen, Handbuch Der Pflanzenphysiologie*. Ed. W. Rhuland (Berlin: Springer-Verlag), 657–681.

Wall, D. (1971). Biological Problems Concerning Fossilizable Dinoflagellates. *Geosci. Man.* 3, 1–15. doi: 10.1080/00721395.1971.9989704

Wetz, M. S., Wheeler, P. A., and Letelier, R. M. (2004). Light-Induced Growth of Phytoplankton Collected During the Winter From the Benthic Boundary Layer Off Oregon, USA. *Mar. Ecol. Prog. Ser.* 280, 95–104. doi: 10.3354/meps280095

Yokoyama, H., and Ueda, H. (1997). A Simple Corer Set Inside an Ekman Grab to Sample Intact Sediments With the Overlying Water. *Benthos Res.* 52, 119–122. doi: 10.5179/benthos1996.52.2_119

Conflict of Interest: The authors declare that the research was conducted in the absence of any commercial or financial relationships that could be construed as a potential conflict of interest.

Advantages of publishing in Frontiers

OPEN ACCESS
Articles are free to read for greatest visibility and readership

FAST PUBLICATION
Around 90 days from submission to decision

HIGH QUALITY PEER-REVIEW
Rigorous, collaborative, and constructive peer-review

TRANSPARENT PEER-REVIEW
Editors and reviewers acknowledged by name on published articles

Frontiers
Avenue du Tribunal-Fédéral 34
1005 Lausanne | Switzerland

Visit us: www.frontiersin.org
Contact us: frontiersin.org/about/contact

REPRODUCIBILITY OF RESEARCH
Support open data and methods to enhance research reproducibility

DIGITAL PUBLISHING
Articles designed for optimal readership across devices

FOLLOW US
@frontiersin

IMPACT METRICS
Advanced article metrics track visibility across digital media

EXTENSIVE PROMOTION
Marketing and promotion of impactful research

LOOP RESEARCH NETWORK
Our network increases your article's readership